Rapporter och meddelanden 144

Synthesis of the bedrock geology in southern Norrbotten County, northern Sweden

Editors: Stefan Bergman & Benno Kathol

SGU
Sveriges geologiska undersökning
Geological Survey of Sweden

Rapporter och meddelanden 144

Synthesis of the bedrock geology in southern Norrbotten County, northern Sweden

Editors: Stefan Bergman & Benno Kathol

Sveriges geologiska undersökning
2018

ISSN 0349-2176
ISBN 978-91-7403-410-3

Cover photo: Archaean rocks on the northern shore of Stora Luleälven at Rimostugan.
Photographer: Benno Kathol

Head of department, Mineral Resources, Geological Survey of Sweden: Kaj Lax
Editors: Stefan Bergman & Benno Kathol
Layout: Tone Gellerstedt

Print: Elanders Sverige AB

Geological Survey of Sweden
Box 670, 751 28 Uppsala
phone: 018-17 90 00
fax: 018-17 92 10
e-mail: sgu@sgu.se
www.sgu.se

Table of Contents

1. Introduktion ... **4**

1. Introduction ... **5**

2. Methods ... **7**

3. Base data ... **9**
Bedrock geological maps, bedrock observations and outcrop distribution ... 9
Airborne geophysical data ... 9
Bouguer gravity field ... 14
Petrophysical and gamma radiation (gamma ray) data ... 16
Ground geophysical surveys ... 17
Lithogeochemistry ... 17
Sm-Nd isotopic analyses ... 18
Radiometric age determinations ... 21
Cored boreholes ... 27
Geophysical modelling ... 27

4. Regional tectonic framework ... **28**

5. Geological units ... **29**
Introduction ... 29
Svecokarelian orogen ... 29
Mesoproterozoic rocks ... 98
Ediacaran–Cambrian sedimentary cover ... 98
Caledonian orogen ... 99
Lithogeochemistry in the Svecokarelian orogen ... 104
Petrophysical and gamma radiation (gamma ray) data in the Svecokarelian orogen ... 118

6. Structure and metamorphism ... **131**
Introduction ... 131
Ductile structures ... 131
Brittle deformation zones ... 154
Metamorphism ... 155

7. Mineral resources ... **173**
Mining history ... 173
Classification of deposits ... 173
Ore deposits related to magmatic activity ... 174
Stratiform-stratabound ore deposits (base metals and iron) ... 183
Sulphide deposits hosted by supracrustal rocks ... 194
Epigenetic base metal deposits and gold-silver veins ... 206
Other metal deposits ... 207
Industrial mineral deposits ... 213
Dimension stone ... 219
Bedrock deposits for construction aggregates ... 219

8. Tectonic evolution of southern Norrbotten County ... **221**

9. Key issues for future work ... **223**

Acknowledgements ... **224**

References ... **225**
Manuscripts in preparation ... 243

1. Introduktion

Stefan Bergman & Benno Kathol

Den södra delen av Norrbottens län är ett geologiskt sett föga undersökt område. Det ligger mellan två av Sveriges stora malmproducerande regioner, nämligen malmfälten i norra Norrbottens län och Skelleftefältet i Västerbottens län (fig. 1). Berggrunden i området består huvudsakligen av paleoproterozoiska kristallina bergarter tillhörande den fennoskandiska skölden, som utgör huvudämnet i den här rapporten. Mindre utrymme har ägnats åt bergarterna i den ediacariska till kambriska sedimentära pålagringen och i den överskjutna skollberggrunden i den kaledoniska orogenen i områdets västligaste del. Undersökningsområdet i södra Norrbottens län, i den engelska texten kallat *the project area*, motsvarar det område som täcks av de topografiska kartbladen i kartvåderna 25 till 27 och H till M i det svenska indexeringssystemet RT 90 (fig. 2).

I den här rapporten presenterar vi resultaten från ett delprojekt inom Barentsprojektet, vilket var ett större geologiskt undersökningsprogram i norra Sverige. Det tvärvetenskapliga Barentsprojektet initierades av Sveriges geologiska undersökning (SGU) som ett första steg i genomförandet av den svenska mineralstrategin. SGU fick under en fyraårsperiod (2012–2015) extra medel utöver den reguljära budgeten från Näringsdepartementet för insamling av geologiska, geofysiska och geokemiska data samt för att öka den geologiska kunskapen om norra Sverige. Det statsägda gruvbolaget Luossavaara-Kiirunavaara AB (LKAB) bidrog också till finanseringen av projektet. Projektets strategiska mål var att genom utökad undersökning av naturresurserna stödja prospekterings- och gruvindustrin för utvecklingen av ett mer ansvarstagande och hållbart samhälle. Ny, offentligt tillgänglig geovetenskaplig information om det här området bidrar förhoppningsvis till att prospekterings- och gruvföretag kan reducera sina risker och prospekteringskostnader och därmed leda till ekonomisk utveckling.

Syftet med delprojektet i södra Norrbotten var att sammanställa och förenhetliga befintlig geologisk information samt att presentera uppdaterade databaser och en samstämmig tolkning av berggrunden i området. Tyngdpunkten i undersökningen lades på revidering och uppdatering av 1) ytbergarternas stratigrafi, 2) underindelningen av intrusiva bergartsled, 3) information om och klassificering av mineralförekomster, 4) kunskapen om det regionala strukturmönstret, 5) kunskapen om de metamorfa förhållandena och 6) den geofysiska informationen.

Den här rapporten beskriver och presenterar ytterligare information om de berggrundsgeologiska förhållandena inom undersökningsområdet i södra Norrbottens län. En tvådimensionell modell av berggrunden visas i en separat tryckt berggrundskarta i skala 1:250 000. Kartan och olika databaser finns tillgängliga på SGU.

1. Introduction

Stefan Bergman & Benno Kathol

Southern Norrbotten County is a geologically underexplored area located between two of Sweden's major ore-producing regions: the Northern Norrbotten ore district and the Skellefte district. The area of investigation (Fig. 1) is located in northern Sweden and comprises mainly Palaeoproterozoic crystalline bedrock of the Fennoscandian Shield, which is the main subject of the present description. Less attention has been paid to the Ediacaran to Cambrian sedimentary cover rocks and allochthonous units of the Caledonian orogen, which form the bedrock in the westernmost parts of the area. The investigated area of southern Norrbotten County, referred to below as the project area, corresponds to the topographic map sheets with row numbers 25 to 27 and columns H to M in the Swedish index system RT 90 (Fig. 2).

This report presents the results from a subproject within the Barents Project, which was a major geological investigation programme in northern Sweden. The multidisciplinary Barents Project was initiated by the Geological Survey of Sweden (SGU), as a first step in implementing the Swedish National Mineral Strategy. SGU obtained additional funding from the Ministry of Enterprise and Innovation to gather new geological, geophysical and till geochemistry data, and generally enhance geological knowledge of northern Sweden over a four-year period (2012–2015). Luossavaara-Kiirunavaara AB (LKAB), the state-owned iron mining company, co-funded the project. The strategic goal of the project was to support the exploration and mining industry by increasing exploration of natural resources for more responsible and sustainable resource development. New publicly accessible geoscientific information from this region helps exploration and mining companies to reduce their risks and exploration costs and thus encourages economic development.

The aim of this subproject was to compile and synthesise existing information, and present updated databases and coherent interpretations of the project area. Emphasis was placed on revising and updating 1) the stratigraphy of supracrustal rocks; 2) the subdivision of intrusive suites; 3) mineral deposit information and classification; 4) the regional structural framework; 5) information on metamorphic conditions; and 6) geophysical information.

This report describes and gives additional information on the geological features of the project area in southern Norrbotten County, which are shown on a separate printed bedrock map at a scale of 1:250 000. All maps and databases are available at SGU.

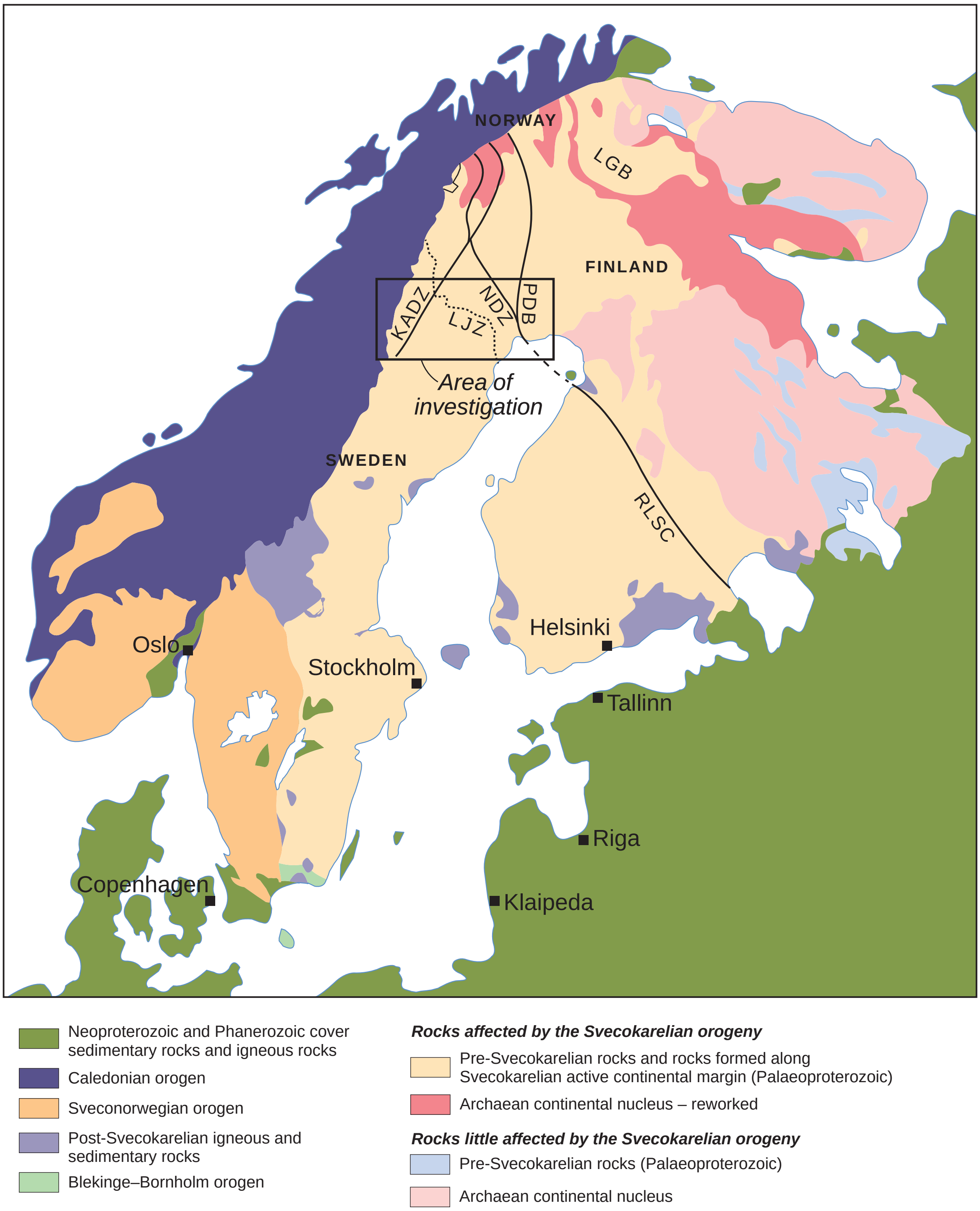

Figure 1. Major geological units in the Fennoscandian Shield (modified after Koistinen et al. 2001 and Stephens et al. 2009). The location of the northernmost parts of the shear zones (thick black lines) is from Henderson et al. (2015). The location of the area of investigation, referred to in the text as southern Norrbotten County, or the project area, is also indicated. KADZ = Karesuando–Arjeplog deformation zone, NDZ = Nautanen deformation zone, PDB = Pajala deformation belt, RLSC = Raahe–Ladoga shear complex, LGB = Lapland Granulite Belt. The dotted line shows the Luleå–Jokkmokk zone (LJZ), which is the boundary between the Norrbotten and Bothnia–Skellefteå lithotectonic units. The Överkalix lithotectonic unit is located east of the PDB.

2. Methods

Stefan Bergman, Martiya Sadeghi, Ildikó Antal Lundin & Claes Mellqvist

The project area (Fig. 1) has a size of approximately 44 000 km^2. The bedrock in the entire area has been mapped by SGU, two-thirds for compilation at a scale of 1:50 000, and one-third at a scale of 1:250 000 (Fig. 2). The geological observations on outcrops comprise determination of rock types and their type of occurrence, as well as description of textures and structures, including structural measurements. The occurrence of inclusions and dykes has been noted. The magnetic susceptibility of the different rock types has been measured on most outcrops. In crucial cases, field observations have been supplemented by thin sections, lithogeochemical analyses and radiometric dating. Information about outcrop locations has been obtained from earlier investigations and acquired by interpretation of aerial photographs and elevation data. Geological information has been correlated with geophysical data obtained by both airborne and ground measurements.

The bedrock map of the project area is a compilation of data from the mapping campaign referred to above. During the compilation process geological information has been adapted for presentation at the final map scale. This means that some important thin marker horizons have been somewhat exaggerated, while other small objects have been omitted. Form lines represent general structural trends that are interpolated from measured planar structures in the field. However, the lines prepared for the present area largely rely on magnetic connections interpreted in magnetic anomaly data. Structural data were plotted on stereograms and rose diagrams using Stereonet 9.5 software (Cardozo & Allmendinger 2013).

Most of the mapping was done when the former RT90 reference system was used, and for convenience that system is still used in this document when referring to map sheets. However, coordinates are always given in the modern reference system SWEREF99 TM.

Except for information gained during the mapping campaign, the information in this report is mainly a synthesis of map descriptions (Table 1). This is supplemented by information from published scientific papers, field reports and other documents. References to these are given in the text. Lithostratigraphic and lithodemic unit names have not yet been formalised in Sweden, and are therefore indicated in this document as informal, in accordance with the recently published *Guide for geological nomenclature in Sweden* (Kumpulainen 2017).

Most of the lithogeochemical analyses in the project area were conducted during 2002–2015 at ALS Minerals and at ACME labs in Vancouver (Canada) using major and trace lithogeochemical analysis packages, with a combination of methods. The methods are described in detail in chapter 5 in the section *Lithogeochemistry in the Svecokarelian orogen*. Briefly, however, analyses were made using Inductively Coupled Plasma Atomic Emission spectroscopy (ICP-AES) and Inductively Coupled Plasma Mass Spectrometry (ICP-MS), following lithium metaborate/tetraborate fusion or various types of acid digestion.

In addition to its use for age determination, the Sm-Nd isotope system is a useful means of indicating the source of a rock. The $\varepsilon_{Nd\,(T)}$ notation is commonly used in petrogenetic studies, in line with the methodology thoroughly described by DePaolo (1988). In general, the ε_{Nd} values at time T=1.9 Ga show strongly negative values (approximately -10) for Archaean rocks (>2.5 Ga), whereas juvenile mantle-derived rocks with an age of c. 1.9 Ga show positive values (approximately +3). In northern Sweden, most Palaeoproterozoic plutonic rocks with negative $\varepsilon_{Nd\,(T=1.9\,Ga)}$ values are interpreted to be products of mixing between the two constituents, mainly by partial melting of Archaean crust. The Sm-Nd isotopes are particularly useful in southern Norrbotten County in order to distinguish the influence in the bedrock of older Archaean (at present mainly hidden and reworked) from Palaeoproterozoic juvenile crust. Various SGU mapping projects over the past decades have contributed more Sm-Nd data points covering the areas in between the more densely sampled areas in Luleå–Boden and Jokkmokk.

The Archaean–Proterozoic boundary zone in southern Norrbotten can be defined in at least two different ways using the Sm-Nd isotope system. One way is to identify the shift for c. 1.9 Ga rocks from positive $\varepsilon_{Nd\,(T)}$ values in the southwest to negative $\varepsilon_{Nd\,(T)}$ values in the northeast. These 1.9 Ga rocks represent the pre-amalgamation phase, when the rocks were formed in island arc and continental arc (with Archaean basement) environments, respectively. The other way is to use the data from 1.8 Ga intrusions, which are interpreted to have been formed after amalgamation of the two crustal terranes (Öhlander et al. 1999). In this case the Archaean crust can be traced at depth to the south. The former way is used in this study to define the boundary at the ground surface.

Airborne geophysical data, comprising magnetic, electromagnetic and gamma-ray spectrometry, and gravity data have been used systematically in bedrock mapping. Potential field information such as the magnetic and the gravity field has been processed, and different geophysical filters have been used to enhance both shallow and deep source anomalies. Resistivity and current density of the ground was derived from electromagnetic (VLF) data. Geophysical fieldwork was carried out over the entire project area, with more extensive follow-up of anomalies in areas where 1:50 000 scale mapping was carried out and sparser in areas mapped at a scale of 1:250 000. Ground magnetic and electromagnetic profiling, and sampling for petrophysical analyses were conducted, and 8 susceptibility measurements were made on each rock type in the outcrops visited. Gamma-ray measurements were taken on selected outcrops to obtain concentrations of potassium (%), uranium (ppm) and thorium (ppm). Field observations were positioned using hand-held GPS. The aim of the anomaly follow-ups is to link the different types of anomaly to the causative bedrock.

Qualitative and quantitative interpretations of geophysical data have been made and implemented in compiling the bedrock map. Quantitative modelling of data from the ground measurements and field data is used mainly to improve the accuracy of qualitative interpretations. Electrical resistivity, magnetic anomaly field data and digital terrain models were used to interpret lineaments, which are inferred to represent different types of deformation zone. Deformation zones commonly appear as low-magnetic linear anomalies due to oxidation of magnetite, and brittle zones often appear as low-resistivity anomalies because of their water and clay content. Magnetic connections have been interpreted from narrow, high-magnetic and banded anomaly patterns to enhance the structural trends.

Geophysical 3D modelling was also carried out in certain areas to image subsurface conditions and gain a better understanding of the depth of known geological units. The models were generated by either "inverse" or "forward" techniques, using Voxi (Geosoft Inc.) and ModelVision (Tensor Research Pty Ltd) software. Forward modelling uses a priori knowledge about the physical properties of the bedrock in the study area. Forward modelling is parameter-driven, which assumes a property and finds the geometry of structures to fit the measured data. In inverse modelling, measured data determine the geometry and physical properties of geological structures. The space is divided into cells of known geometry, and the physical properties of each cell are estimated using an iterative mathematical method. The models can be constrained by factors such as known physical properties of the bedrock.

3. Base data

Fredrik Hellström, Martiya Sadeghi, Ildikó Antal Lundin, Carl-Axel Triumf & Claes Mellqvist

BEDROCK GEOLOGICAL MAPS, BEDROCK OBSERVATIONS AND OUTCROP DISTRIBUTION

The main sources of geological information in the project area have been obtained from bedrock mapping by SGU between 2002 and 2015, except for the Kalix area, which was mapped mainly between 1967 and 1974, with revision and map publication in the 1990s, (Fig. 2, Table 1). The published maps at a scale of 1:50 000, referred to as local maps, are accompanied by brief geological descriptions, including geophysical interpretations. Overview regional bedrock mapping intended for a scale of 1:250 000 was carried out under the Barents Project (2012–2015) in the remaining areas not covered by local 1:50 000 scale mapping (Fig. 2, Table 1).

Extensive material from earlier investigations, including exploration work and other geological studies, has been used in compiling bedrock maps; for references see the SGU publication search services: Georegister, Exploration reports and Geolagret at www.sgu.se. Earlier regional bedrock geological maps covering the project area include a 1:400 000 scale map of Precambrian rocks of Norrbotten County by Ödman (1957), 1:1 million scale geological compilation maps of northern Fennoscandia (Silvennoinen et al. 1987), as well as a digital bedrock compilation map of northern Sweden at a scale of 1:250 000, prepared in the late 1980s (NB-dig, T. Sjöstrand & H. Henkel, SGU).

During bedrock mapping between 2002 and 2015, approximately 50 000 bedrock observations were documented (Fig. 3a). Of these, 45 000 are located in areas of local-scale mapping, where almost all outcrops have been visited. The observation density (1.6 observations/km^2) is thus mainly governed by available outcrops (Fig. 3b), but to some degree also by the complexity of the geology. The degree of rock exposure is estimated to be c. 1% of the project area, and the 2D bedrock geological model (bedrock map) relies heavily on interpretation of geophysical data. The observation density is much less, c. 0.4 observations/km^2, for areas of regional-scale mapping.

AIRBORNE GEOPHYSICAL DATA

Airborne geophysical measurements in southern Norrbotten County were carried out systematically between 1961 and 2015 by SGU and LKAB (Fig. 4). Before 1995 the ground clearance was maintained at 30 m and the sampling interval at 40 m. From 1995 and onwards, all data were collected with a ground clearance of 60 m and a sampling interval of 16 m. The sampling interval for the gamma-ray measurements was approximately 65 m. Today, positioning is maintained with a radar altimeter and GPS. The survey direction was east–west over the entire project area, except for four measurements collected by private companies and outsourcers. Those measurements cover mainly small areas.

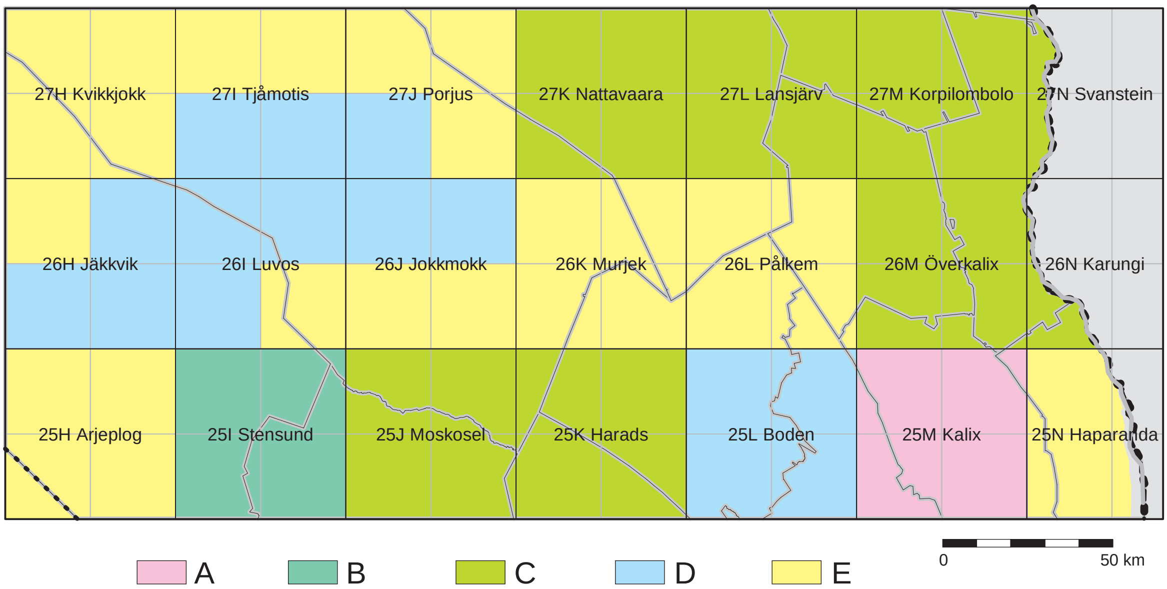

Figure 2. Bedrock geological maps in the project area of southern Norrbotten County (see also Table 1). A: Area mapped 1967–1974 at a scale of 1:50 000, maps with short descriptions compiled 1989–1994. B: Area mapped 2002–2003 at a scale of 1:50 000, maps with short description. C: Area mapped 2004–2013 at a scale of 1:50 000, maps and separate descriptions. D: Area mapped 2008–2013 at a scale of 1:50 000, maps and descriptions to be published. E: Area mapped 2012–2015 at a scale of 1:250 000, no published maps or descriptions.

Table 1. Map areas in the project area in southern Norrbotten County with their respective SGU bedrock geological maps (1:50 000 and 1:250 000) and descriptions.

Map area (RT90 index)	SGU map	Scale	Year	Map description
25H Arjeplog NO		1:250 000		
25H Arjeplog NV		1:250 000		
25H Arjeplog SO		1:250 000		
25H Arjeplog SV		1:250 000		
25I Stensund NO	SGU K 52	1:50 000	2006	Kathol & Aaro 2006a
25I Stensund NV	SGU K 51	1:50 000	2006	Mellqvist & Aaro 2006a
25I Stensund SO	SGU K 54	1:50 000	2006	Kathol & Aaro 2006b
25I Stensund SV	SGU K 53	1:50 000	2006	Mellqvist & Aaro 2006b
25J Moskosel NO	SGU K 402	1:50 000	2012	Kathol et al. 2012a
25J Moskosel NV	SGU K 403	1:50 000	2012	Kathol et al. 2012a
25J Moskosel SO	SGU K 405	1:50 000	2012	Kathol et al. 2012a
25J Moskosel SV	SGU K 404	1:50 000	2012	Kathol et al. 2012a
25K Harads NO	SGU K 407	1:50 000	2012	Kathol et al. 2012b
25K Harads NV	SGU K 406	1:50 000	2012	Kathol et al. 2012b
25K Harads SO	SGU K 409	1:50 000	2012	Kathol et al. 2012b
25K Harads SV	SGU K 408	1:50 000	2012	Kathol et al. 2012b
25L Boden NO		1:50 000		Sadeghi et al. in press
25L Boden NV		1:50 000		Sadeghi et al. in press
25L Boden SO		1:50 000		Sadeghi et al. in press
25L Boden SV		1:50 000		Sadeghi et al. in press
25M Kalix NO	SGU Ai 80	1:50 000	1996	Wikström 1996
25M Kalix NV	SGU Ai 79	1:50 000	1995	Wikström 1995
25M Kalix SO	SGU Ai 45	1:50 000	1990	Åhman et al. 1990
25M Kalix SV	SGU Ai 81	1:50 000	1993	Wikström et al. 1993
25N Haparanda NO		1:250 000		
25N Haparanda NV		1:250 000		

Table 1, continued.

Map area (RT90 index)	SGU map	Scale	Year	Map description
25N Haparanda SO		1:250 000		
25N Haparanda SV		1:250 000		
26H Jäkkvik NO		1:50 000		Kathol et al. in prep.
26H Jäkkvik NV		1:250 000		
26H Jäkkvik SO		1:50 000		Kathol et al. in prep.
26H Jäkkvik SV		1:50 000		Kathol et al. in prep.
26I Luvos NO		1:50 000		Hellström & Berggren in press
26I Luvos NV		1:50 000		Hellström & Berggren in press
26I Luvos SO		1:250 000		
26I Luvos SV		1:50 000		Hellström & Berggren in press
26J Jokkmokk NO		1:50 000		Claeson & Antal Lundin in press-a
26J Jokkmokk NV		1:50 000		Claeson & Antal Lundin in press-a
26J Jokkmokk SO		1:250 000		
26J Jokkmokk SV		1:250 000		
26K Murjek NO		1:250 000		
26K Murjek NV		1:250 000		
26K Murjek SO		1:250 000		
26K Murjek SV		1:250 000		
26L Pålkem NO		1:250 000		
26L Pålkem NV		1:250 000		
26L Pålkem SO		1:250 000		
26L Pålkem SV		1:250 000		
26M Överkalix NO	SGU K 396	1:50 000	2012	Åkerman & Kero 2012e
26M Överkalix NV	SGU K 395	1:50 000	2012	Åkerman & Kero 2012e
26M Överkalix SO	SGU K 398	1:50 000	2012	Åkerman & Kero 2012e
26M Överkalix SV	SGU K 397	1:50 000	2012	Åkerman & Kero 2012e
26N Karungi NV	SGU K 396	1:50 000	2012	Åkerman & Kero 2012e
26N Karungi SV	SGU K 399	1:50 000	2012	Åkerman & Kero 2012e
27H Kvikkjokk NO		1:250 000		
27H Kvikkjokk NV		1:250 000		
27H Kvikkjokk SO		1:250 000		
27H Kvikkjokk SV		1:250 000		
27I Tjåmotis NO		1:250 000		
27I Tjåmotis NV		1:250 000		
27I Tjåmotis SO		1:50 000		Claeson & Antal Lundin in press-b
27I Tjåmotis SV		1:50 000		Claeson & Antal Lundin in press-b
27J Porjus NO		1:250 000		
27J Porjus NV		1:250 000		
27J Porjus SO		1:250 000		
27J Porjus SV		1:50 000		Claeson & Antal Lundin in press-c
27K Nattavaara NO	SGU K 384	1:50 000	2012	Claeson & Antal Lundin 2012c
27K Nattavaara NV	SGU K 383	1:50 000	2012	Claeson & Antal Lundin 2012c
27K Nattavaara SO	SGU K 386	1:50 000	2012	Claeson & Antal Lundin 2012c
27K Nattavaara SV	SGU K 385	1:50 000	2012	Claeson & Antal Lundin 2012c
27L Lansjärv NO	SGU K 388	1:50 000	2012	Hellström et al. 2012d
27L Lansjärv NV	SGU K 387	1:50 000	2012	Hellström et al. 2012d
27L Lansjärv SO	SGU K 390	1:50 000	2012	Hellström et al. 2012d
27L Lansjärv SV	SGU K 389	1:50 000	2012	Hellström et al. 2012d
27M Korpilombolo NO	SGU K 392	1:50 000	2013	Jonsson & Kero 2013d
27M Korpilombolo NV	SGU K 391	1:50 000	2013	Jonsson & Kero 2013d
27M Korpilombolo SO	SGU K 394	1:50 000	2013	Jonsson & Kero 2013d
27M Korpilombolo SV	SGU K 393	1:50 000	2013	Jonsson & Kero 2013d
27N Svanstein NV	SGU K 392	1:50 000	2013	Jonsson & Kero 2013d
27N Svanstein SV	SGU K 394	1:50 000	2013	Jonsson & Kero 2013d

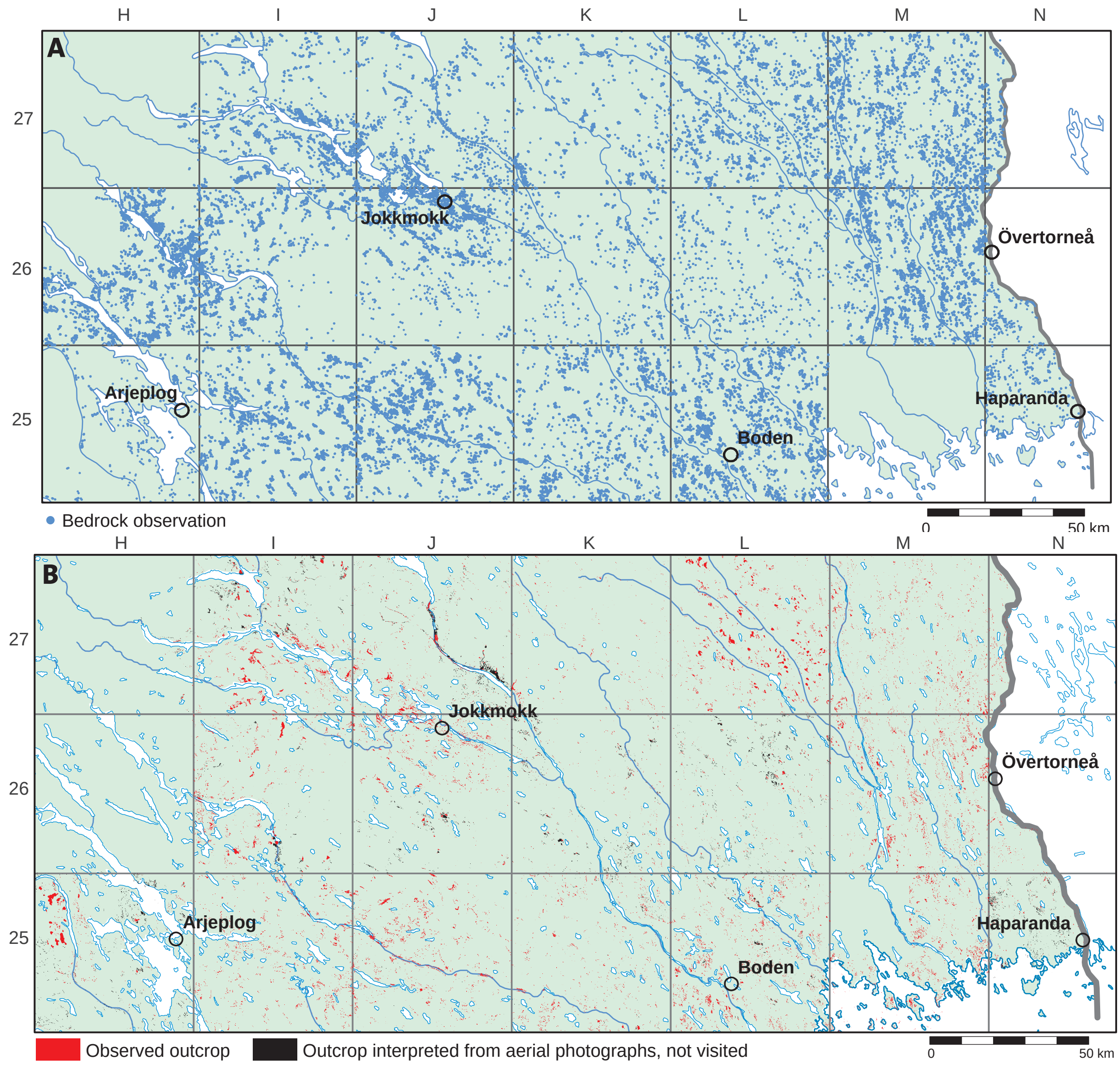

Figure 3. **A.** Location of bedrock observations (points from the SGU database, Bedrock observations). **B.** Coverage of bedrock outcrops (polygons in the SGU bedrock map database), including outcrops observed during bedrock mapping and outcrops interpreted from aerial photographs.

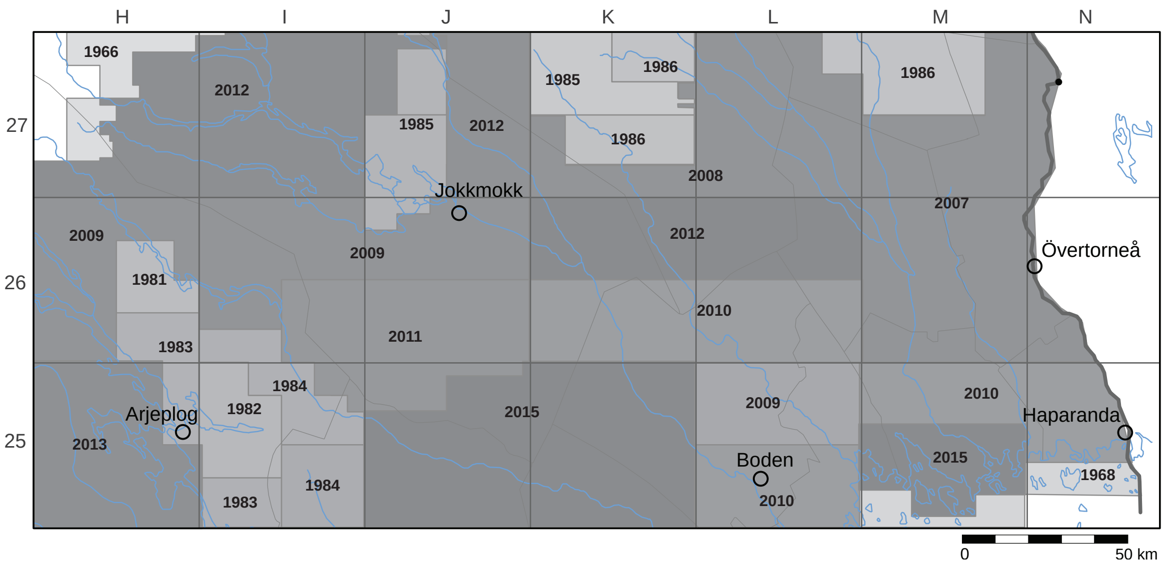

Figure 4. Coverage of airborne geophysical data. Grey scales show different periods when measurements have been made. Current measurements, i.e. those after 2009, were collected with a ground clearance of 60 m by SGU; earlier measurements were collected at an altitude of 30 metres by LKAB and SGU.

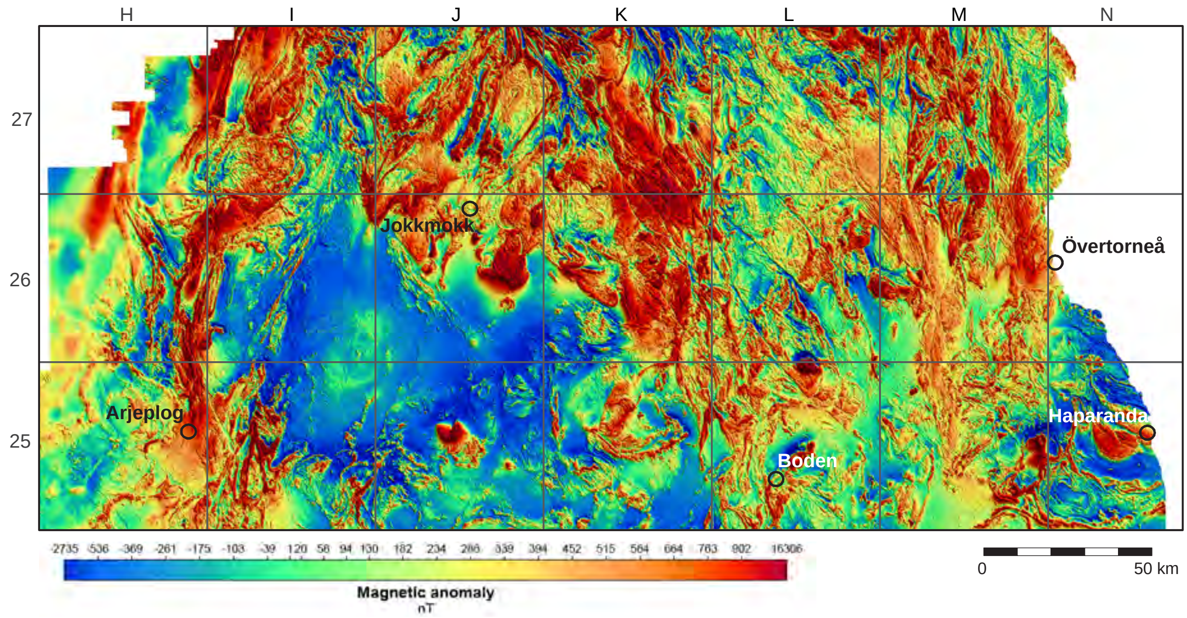

Figure 5. Magnetic anomaly map of southern Norrbotten County.

Magnetic anomaly field

Airborne geophysical measurements of the earth's magnetic field in southern Norrbotten County were carried out as early as 1961 by SGU as a part of the iron inventory programme. In the 1960s the relative accuracy of the measurements was approximately 10–15 nT, which later was improved to 5 and 1 nT. From 2007 the accuracy is 0.3 nT.

The magnetic anomaly map (Fig. 5) shows variations in the magnetic total field after subtracting the geomagnetic reference field (DGRF 1965.0). The data have been processed using a grid cell size of 50 m × 50 m.

Gamma-ray spectrometry

The map of the airborne gamma-ray spectrometry (Fig. 6) was produced using a grid cell size of 200 m. It gives information on the content of potassium (K), uranium (U), and thorium (Th) in the uppermost part of the ground, i.e. in the bedrock or in the Quaternary cover. Virtually all the data used were gathered by SGU between 2007 and 2015 using modern equipment. Some scattered parts of the project area were covered by LKAB during 1981–1986. Data quality varies, older data potentially being more negatively influenced by radon content and background radiation.

As outcrops are sparse, the Quaternary cover significantly affects the results. However, taking glacial drift into account, the composition of the cover reflects the bedrock composition of the region, which is why airborne gamma-ray spectrometry data can be used as an aid in bedrock mapping. The calculations of uranium and thorium content are based on assumed radioactive equilibrium. The relative content of the three elements in the uppermost part of the ground is presented as a colour composite (Fig. 6).

Electrical resistivity

Ground electrical resistivity is derived from airborne electromagnetic (VLF) measurements using two transmitters (Fig. 7). The data used in the map were collected by SGU and LKAB between 1981 and 2015. The whole project area is covered by resistivity data except two areas: one in the northwest of map area 27H and one around map area 27M NV and the northeastern part of 27L NO, where data are missing.

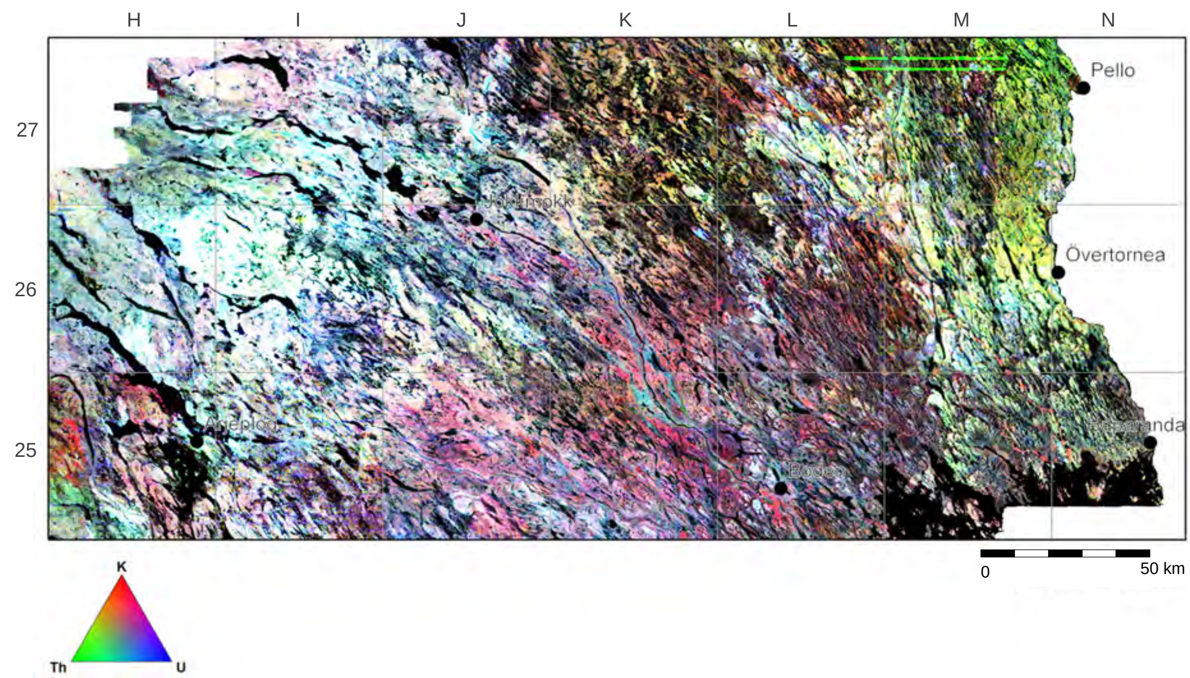

Figure 6. Radiometric map based on airborne measurements; red = potassium, blue = uranium, green = thorium.

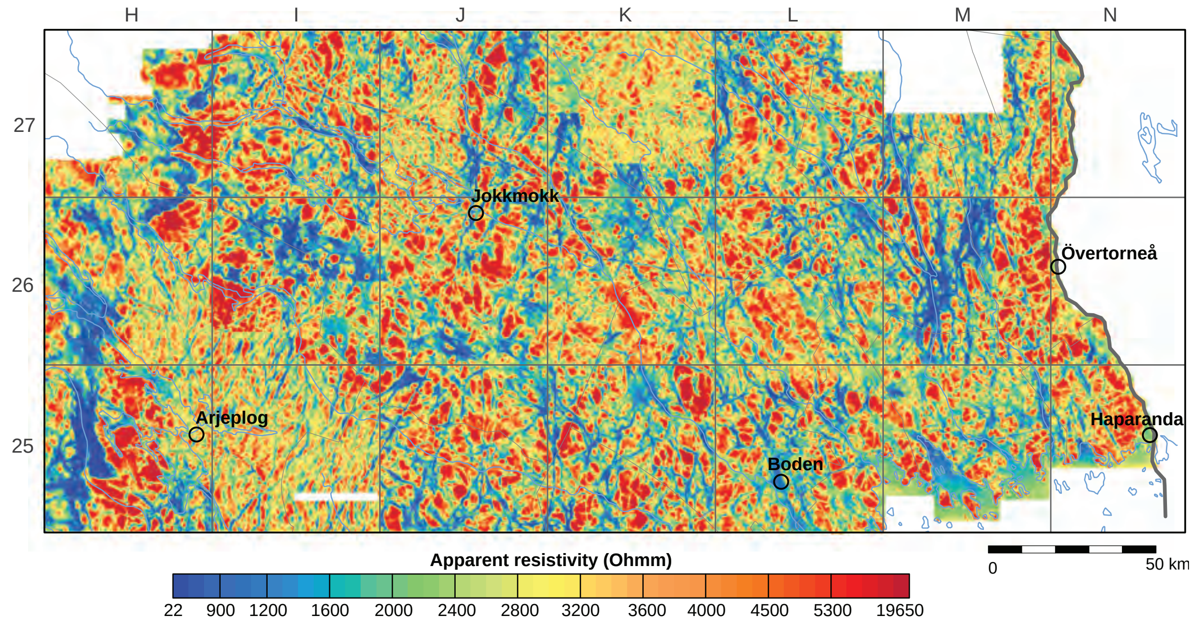

Figure 7. Map of resistivity based on airborne VLF measurements.

BOUGUER GRAVITY FIELD

Regional gravity measurements were made by SGU and LMV during different periods, most intensively between 1960 and 1985. Gravity measurements in areas with sparse data coverage were made from 2006 onwards. The distance between the measurement points varies between 300 and 3 000 metres, in the west of the project area up to 6 km. Gravity data are usually shown in the form of a Bouguer anomaly map (Fig. 8). The measurements were mainly acquired along roads. Transport between measurement points in areas with sparse road coverage was by helicopter and snowmobile. Measurements in the northernmost Gulf of Bothnia were made by SGU on the ice during the winter of 2014.

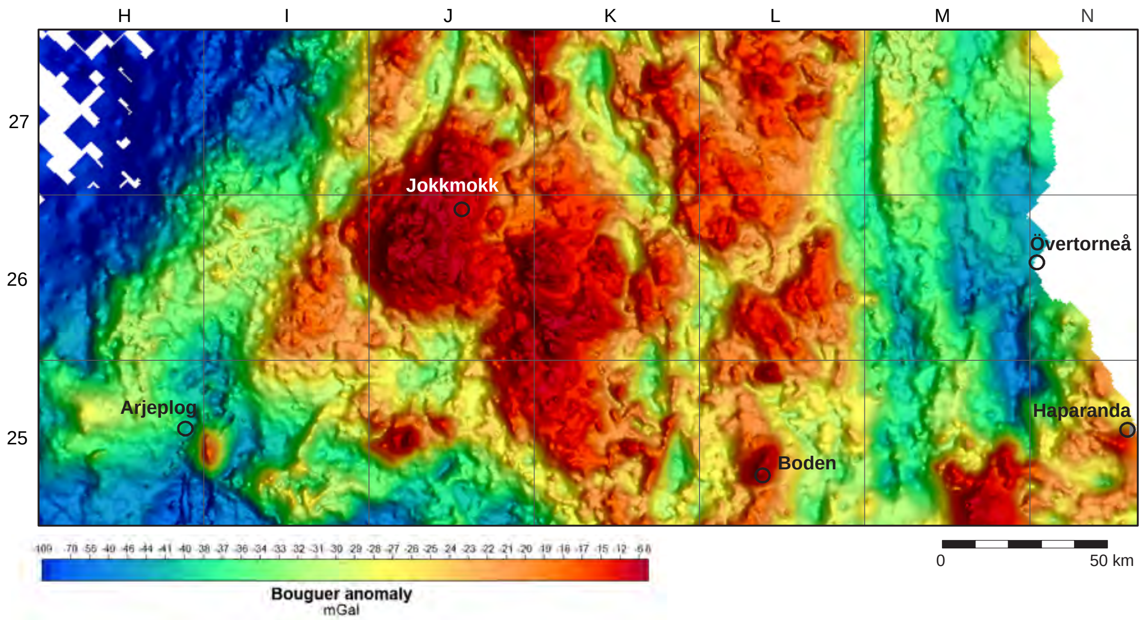

Figure 8. Bouguer gravity anomaly map of southern Norrbotten County.

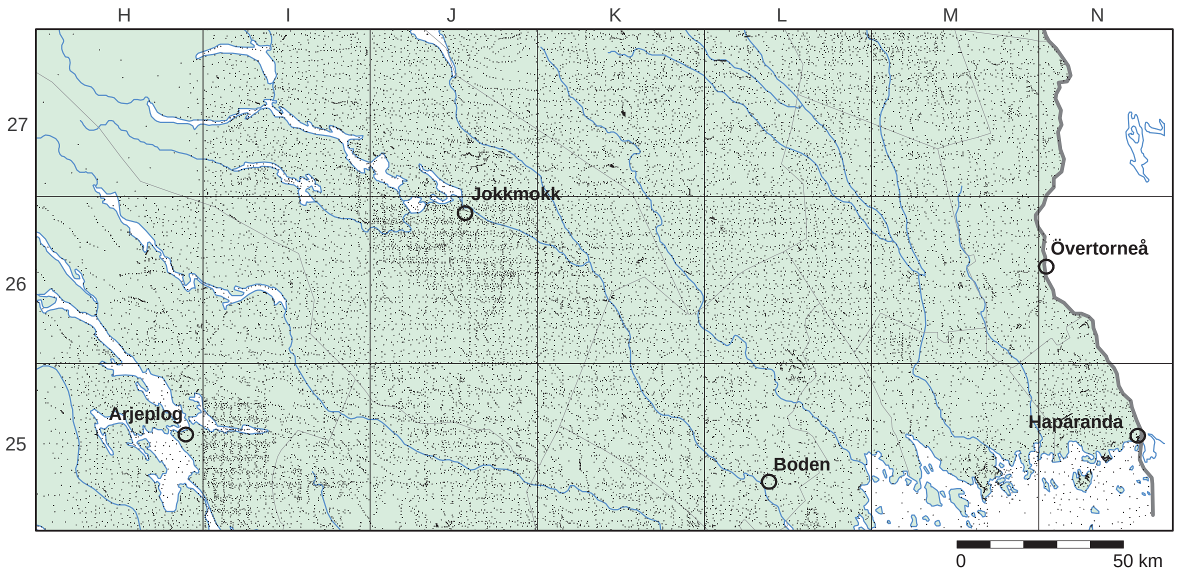

Figure 9. Location of gravity measurement sites.

The accuracy of gravity deviations, or Bouguer anomalies, very much depends on the quality of levelling. SGU is currently using network-RTK GNSS and altimeters to determine the elevation of each gravity measurement. The mean accuracy of the older measurements was approximately 0.6 mGal, but modern techniques have improved this to 0.1 mGal. The Bouguer anomaly is based upon the reference field RG82 (Regional Gravity Standard Network, 1982), the gravity formula from 1982, Bouguer density of 2 670 kg/m^3 and gravity database SW1510. The data were processed using a grid cell size of 500 m × 500 m, based on 31 872 measurement points (Fig. 9).

PETROPHYSICAL AND GAMMA RADIATION (GAMMA RAY) DATA

Rock samples for determining density and magnetic properties have been collected from outcrops and boulders in southern Norrbotten County over a long period. The first samples in the project area were collected more than 40 years ago, and the database at SGU includes petrophysical properties from more than 17 000 samples from the area. The quality of documentation of coordinates, rock type, source etc. is not uniform. In practice, this means that the samples to be included in statistical treatment of petrophysical data must be carefully considered. Even so, some erroneous values will probably remain, but since these data are sporadic, the authors consider the negative influence to be negligible. The spatial distribution of all collected samples can be seen in Figure 10. Gamma-ray spectrometry on

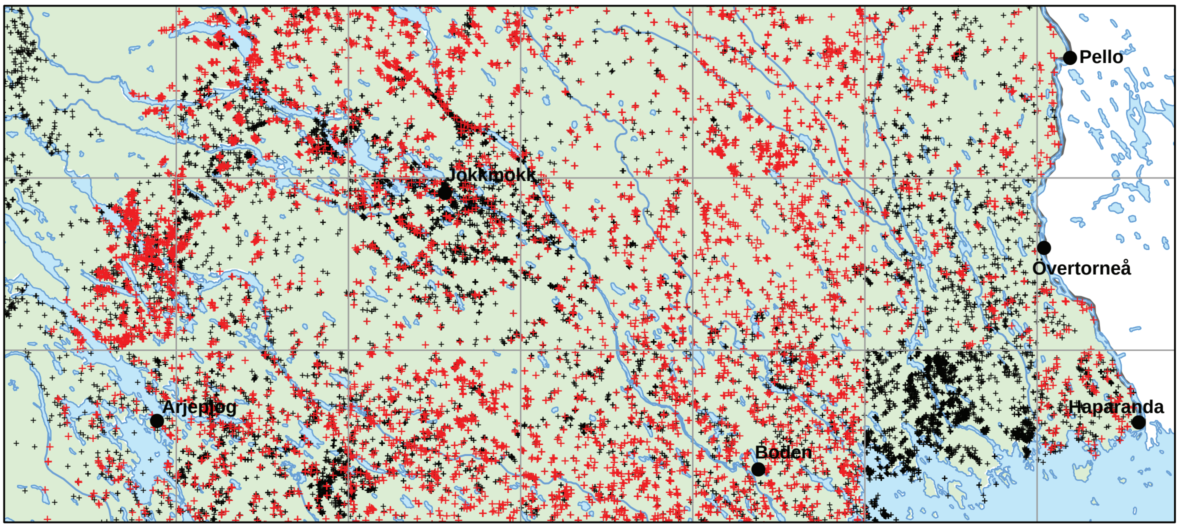

Rock samples for determination of petrophysical properties
+ Sampling from ca. 1990, with rock classification according to the current classification system
+ Sampling to ca. 1990, with rock classification according to the SURE classification system

0 50 km

Figure 10. Location of rock samples for determination of petrophysical properties.

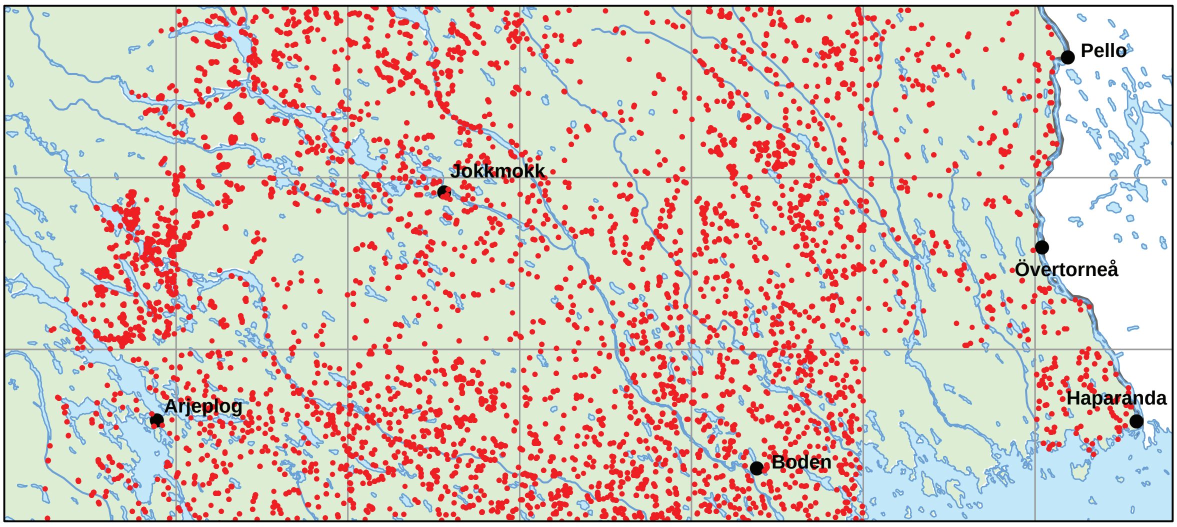

Gamma ray spectrometry on outcrops
• Position of measurements

0 50 km

Figure 11. Location of gamma ray spectrometry measurements on outcrops.

outcrops is currently performed in the SGU bedrock mapping programmes. The spatial distribution of measurements in the project area can be seen in Figure 11. The quality of documentation on the measuring sites is considered reliable and uniform. No gamma radiation measurements have been made in the area covered by map sheet 25M Kalix.

GROUND GEOPHYSICAL SURVEYS

Over the past 70 years, various exploration-oriented, ground-based profile measurements have been made in southern Norrbotten County, most intensively between 1970 and 1987. Measurements of the magnetic field, electromagnetic and electric field using different methods (slingram, VLF, resistivity and induced polarisation) and measurements of the gravity field have been made with a line separation of 20, 40, 80 or 100 m and a point distance of 10, 20 or 40m. The distribution of the detailed geophysical measurements can be seen on the SGU website: <http://apps.sgu.se/kartvisare/kartvisare-markgeofysik-sv.html>. More information can be obtained from SGUs Mineral resources information office. Several exploration permits have been granted in the project area, however, and new geophysical data with new methods are being added all the time.

LITHOGEOCHEMISTRY

In southern Norrbotten County, 1951 geochemical bedrock samples have been collected and analysed under SGU bedrock mapping programmes. The samples were chosen mainly for rock classification and as an aid in assigning rocks to different intrusive and extrusive suites, but in part also to characterise hydrothermal alterations and mineralisations. The distribution of the samples analysed is shown in Figure 12. The results of these analyses are stored in the lithogeochemistry database at SGU.

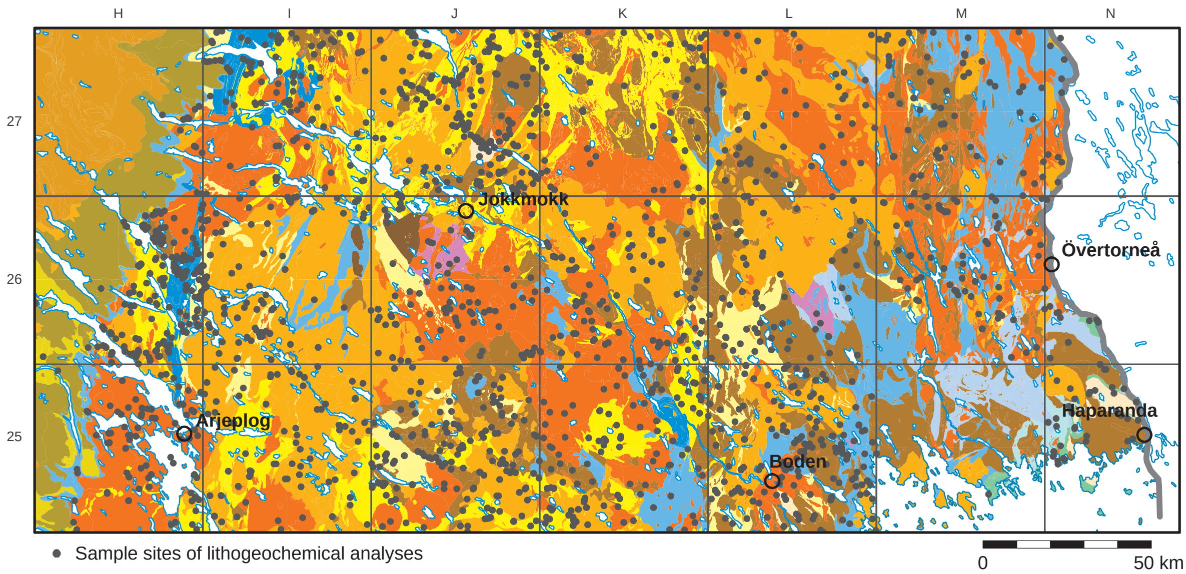

Figure 12. Sample sites for lithogeochemical analyses. Geological units as in Figure 17b.

Sm-Nd ISOTOPIC ANALYSES

SGU has 130 Sm-Nd isotopic whole-rock analyses in the project area, including 46 previously unpublished analyses (Fig. 13, Table 2). Sm-Nd isotopic analyses of Proterozoic granitoids and metavolcanic rocks roughly delineate the Archaean palaeoboundary zone between reworked Archaean rocks in the north and more juvenile Palaeoproterozoic rocks to the south of the Luleå–Jokkmokk zone in Sweden and the continuation along the Raahe–Ladoga zone in Finland (Huhma 1986, Öhlander et al. 1993, Mellqvist et al. 1999a, b, Vaasjoki & Sakko 1988, Nironen 1997).

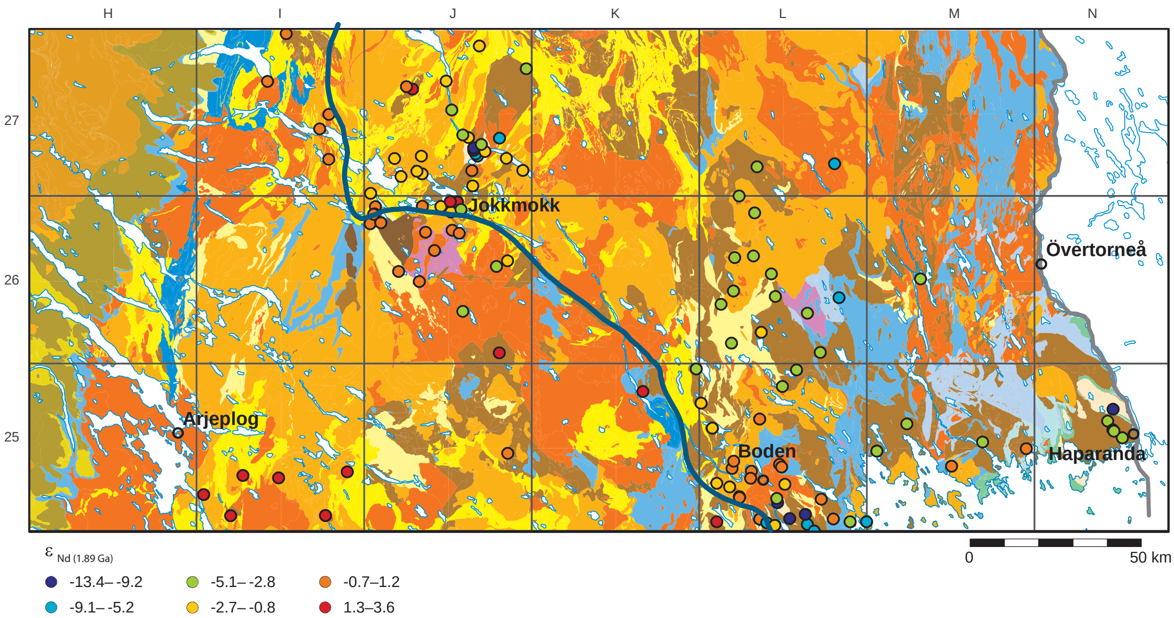

Figure 13. Sample sites for Sm-Nd isotopic analyses (see Table 2 for references to data). The Sm-Nd data delineate the Archaean–Proterozoic boundary zone (Luleå–Jokkmokk zone, (dark blue line)) between the reworked Archaean craton in the north (negative $\varepsilon_{Nd\ (T=1.89\ Ga)}$ values) and more juvenile Palaeoproterozoic domains to the south (positive $\varepsilon_{Nd\ (T=1.89\ Ga)}$ values) along the Luleå–Jokkmokk zone. Geological units as in Figure 17b.

Table 2. Compilation of Sm-Nd isotopic data in order of decreasing $\varepsilon_{Nd\ (T=1890\ Ma)}$.

ε_{Nd} (T=1890 Ma)	Sm (ppm)	Nd (ppm)	$^{147}Sm/^{144}Nd$	$^{143}Nd/^{144}Nd$ korr.	T_{CHUR} (Ma)	T_{DM} (Ma)	Sample No.	N (SR99)	E (SR99)	Reference*
-13.4	1.18	8.84	0.0806	0.510509	2779	2903	84074	7339183	909682	3
-12.0	4.60	33.68	0.0825	0.510607	2697	2833	RKN100114K	7303260	809224	13
-10.4	7.88	57.85	0.0824	0.510687	2587	2733	98005	7413832	717989	2
-10.3	7.97	46.26	0.1041	0.510961	2745	2904	MSI100202	7306667	818309	13
-10.2	8.57	54.38	0.0953	0.510854	2666	2821	CHB100334	7305326	813641	13
-9.9	8.28	47.12	0.1062	0.511006	2734	2896	96015	7310050	809959	1
-9.2	5.37	27.96	0.1161	0.511167	2765	2941	98006	7414551	717920	2
-7.8	8.86	43.44	0.1233	0.511325	2710	2906	96102	7413652	717982	2
-7.0	5.14	29.90	0.1039	0.511126	2471	2662	UJB130240A	7371330	827527	13
-6.4	2.42	11.98	0.1222	0.511385	2552	2769	96105	7303959	806787	1
-6.3	8.46	37.71	0.1356	0.511555	2685	2921	98004	7412809	718543	2
-6.0	1.40	10.40	0.0813	0.510895	2292	2466	88015	7411247	825702	3
-6.0	2.20	10.80	0.1198	0.511375	2491	2710	D18	7304642	836577	4
-6.0	6.55	34.45	0.1150	0.511317	2453	2667	98003	7412117	719101	2
-5.9	3.32	19.60	0.1023	0.511164	2369	2568	96014	7303665	818891	1
-5.7	3.55	21.15	0.1015	0.511165	2349	2551	MSI100060	7301720	821012	13

Table 2, continued.

ε_{Nd} (T=1890 Ma)	Sm (ppm)	Nd (ppm)	$^{147}Sm/^{144}Nd$	$^{143}Nd/^{144}Nd$ korr.	T_{CHUR} (Ma)	T_{DM} (Ma)	Sample No.	N (SR99)	E (SR99)	Reference*
-5.2	4.10	24.89	0.0997	0.511168	2299	2502	98012	7417600	725630	2
-4.8	8.56	46.00	0.1126	0.511346	2331	2556	88017	7379351	725224	3
-4.8	4.80	27.08	0.1072	0.511281	2300	2520	MSI 140146A	7396325	801995	13
-4.7	5.38	29.70	0.1097	0.511315	2308	2529	65096	7333083	909711	3
-4.6	4.38	24.97	0.1059	0.511272	2282	2502	MSI140202A	7401275	797290	13
-4.6	2.40	13.90	0.1044	0.511257	2271	2486	D17	7304579	831678	4
-4.5	4.78	22.50	0.1285	0.511559	2400	2658	89004	7377285	851740	3
-4.4	5.27	29.79	0.1069	0.511299	2265	2489	RKN100134	7311306	809719	13
-4.3	5.60	33.88	0.0999	0.511213	2234	2445	98013	7438367	733299	2
-4.2	5.89	29.71	0.1199	0.511466	2315	2563	STB141098A	7354983	822092	13
-4.2	4.40	24.40	0.1088	0.511331	2257	2483	89003	7334041	848198	3
-4.1	4.66	25.91	0.1086	0.511332	2251	2478	94027	7325727	839356	1
-4.1	5.93	34.80	0.1030	0.511265	2224	2442	84072	7332637	910017	3
-4.1	4.82	26.61	0.1095	0.511347	2248	2478	98016	7415711	720245	2
-4.0	3.90	21.00	0.1147	0.511413	2267	2506	88016	7365824	715300	3
-4.0	4.33	21.71	0.1205	0.511489	2290	2544	UJB130208A	7366607	818116	13
-4.0	7.55	43.10	0.1059	0.511307	2225	2449	84070	7330621	912593	3
-3.8	5.12	28.00	0.1105	0.511373	2228	2462	65093	7335613	908128	3
-3.8	1.16	6.96	0.1005	0.511250	2190	2408	98008	7396208	714358	2
-3.5	6.21	35.40	0.1061	0.511334	2185	2415	84071	7330621	912593	3
-3.5	6.45	36.07	0.1081	0.511359	2191	2427	STB 141011A	7368915	792310	13
-3.4	4.76	26.55	0.1083	0.511363	2190	2427	MSI 140130A	7382898	796170	13
-3.4	4.70	25.22	0.1127	0.511419	2203	2449	UJB 140407A	7357355	795558	13
-3.4	5.43	34.28	0.0957	0.511211	2146	2362	STB 141043A	7372883	795964	13
-3.3	1.51	6.35	0.1438	0.511812	2368	2695	MSI110040	7349649	815091	13
-3.2	6.89	34.42	0.1210	0.511531	2219	2485	STB141058A	7371450	808506	13
-3.2	4.41	25.10	0.1060	0.511349	2158	2391	88109	7410047	802569	3
-3.1	3.87	20.97	0.1115	0.511420	2170	2418	MSI090179	7344660	810978	13
-3.1	3.87	20.97	0.1115	0.511420	2169	2416	MSI090179	7344660	810978	13
-3.0	6.54	32.18	0.1228	0.511568	2198	2473	MSI140206A	7378225	807258	13
-2.9	4.42	23.99	0.1113	0.511425	2156	2402	90091	7375697	790764	13
-2.9	9.49	55.90	0.1025	0.511320	2126	2359	MSI 140134A	7383483	801817	13
-2.8	4.72	23.26	0.1227	0.511573	2183	2458	SPN070190K	7349565	785196	12
-2.8	5.05	25.80	0.1186	0.511523	2168	2431	88112	7425813	711225	3
-2.8	3.31	15.10	0.1324	0.511695	2226	2526	65105	7328833	870865	3
-2.8	2.98	17.20	0.1046	0.511351	2122	2357	88111	7418458	714620	3
-2.6	11.10	62.50	0.1068	0.511385	2116	2357	88110	7381093	728501	3
-2.5	5.00	22.99	0.1316	0.511702	2183	2488	90092	7360705	804457	13
-2.5	13.45	90.40	0.0899	0.511185	2067	2280	90084	7408043	732702	2
-2.4	3.59	16.88	0.1287	0.511668	2166	2466	MSI090056	7339414	786752	13
-2.4	3.59	16.88	0.1287	0.511668	2165	2465	MSI090056	7339414	786752	13
-2.4	5.18	27.17	0.1152	0.511504	2113	2376	98001	7403251	717766	2
-2.3	5.28	30.00	0.1063	0.511397	2085	2328	96120	7314514	795552	1
-2.1	3.45	19.00	0.1097	0.511450	2074	2327	84064	7315565	791739	3
-2.0	5.54	30.02	0.1114	0.511477	2068	2330	RKN100114L	7303260	809224	13
-2.0	12.68	61.18	0.1254	0.511651	2101	2397	96006	7434438	709464	2
-1.9	6.44	26.28	0.1482	0.511937	2193	2581	STB 141043B	7372883	795964	13
-1.8	4.52	23.63	0.1156	0.511535	2065	2337	98007	7397030	708348	2
-1.8	5.69	30.46	0.1128	0.511503	2055	2323	MSI090022	7331997	790183	13
-1.8	5.69	30.46	0.1128	0.511503	2055	2322	MSI090022	7331997	790183	13
-1.8	5.28	27.64	0.1155	0.511538	2056	2328	96104	7315476	812039	1
-1.6	11.06	57.51	0.1163	0.511557	2042	2318	98011	7413546	721363	2

Table 2, continued.

ε_{Nd} (T=1890 Ma)	Sm (ppm)	Nd (ppm)	$^{147}Sm/^{144}Nd$	$^{143}Nd/^{144}Nd$ korr.	T_{CHUR} (Ma)	T_{DM} (Ma)	Sample No.	N (SR99)	E (SR99)	Reference*
-1.5	13.76	98.56	0.0844	0.511166	1991	2203	96096	7405774	696387	2
-1.3	4.46	23.50	0.1150	0.511554	2016	2292	96125	7411578	727707	2
-1.3	8.85	46.65	0.1147	0.511554	2009	2285	90088	7406655	702675	2
-1.3	16.83	82.49	0.1233	0.511661	2022	2324	98015	7417660	716320	2
-1.3	3.80	19.64	0.1170	0.511583	2012	2295	96003	7400658	687355	2
-1.2	5.43	28.17	0.1165	0.511578	2007	2289	96010	7395369	711369	2
-1.0	8.15	38.25	0.1289	0.511742	2006	2331	96005	7411097	694419	2
-0.9	7.97	42.78	0.1126	0.511548	1968	2245	96095	7411900	702357	2
-0.8	10.80	59.90	0.1088	0.511502	1963	2230	89149	7445013	719175	3
-0.8	6.58	37.20	0.1070	0.511480	1961	2227	96011	7407385	701116	2
-0.8	4.62	29.10	0.0959	0.511346	1947	2187	88106	7394421	688335	3
-0.7	6.73	45.41	0.0897	0.511272	1939	2167	96101	7432585	697640	2
-0.4	6.67	35.54	0.1135	0.511581	1931	2216	98002	7407796	717458	2
-0.4	8.80	45.58	0.1167	0.511621	1932	2229	PEV090197	7320675	811056	13
-0.4	7.45	47.39	0.0951	0.511354	1921	2164	RKN090110	7334874	804303	13
-0.4	7.45	47.39	0.0951	0.511354	1920	2164	RKN090110	7334874	804303	13
-0.3	1.08	6.51	0.1007	0.511427	1917	2173	MSI090171	7321437	810411	13
-0.3	5.35	30.70	0.1054	0.511489	1912	2178	84067	7317195	801868	3
-0.2	12.51	80.18	0.0943	0.511354	1906	2149	MSI100081	7305387	826641	13
0.0	6.08	33.57	0.1094	0.511550	1894	2173	98009	7397009	702849	2
0.0	2.19	8.27	0.1599	0.512178	1899	2453	89150	7389103	713950	3
0.0	7.07	40.17	0.1064	0.511517	1887	2158	90085	7419654	671912	2
0.0	6.04	33.14	0.1102	0.511565	1886	2168	96004	7396728	688855	2
0.1	9.66	49.80	0.1173	0.511654	1884	2188	96127	7447915	661548	13
0.1	5.02	28.80	0.1054	0.511506	1884	2154	96124	7389976	711839	2
0.1	7.23	39.40	0.1109	0.511577	1879	2164	84060	7311403	798542	3
0.1	2.83	17.70	0.0964	0.511397	1880	2129	71269	7391999	690466	3
0.1	9.49	56.70	0.1012	0.511457	1879	2139	76241	7394525	688584	3
0.2	9.85	55.07	0.1082	0.511546	1875	2153	96099	7424039	674655	2
0.2	13.05	66.80	0.1181	0.511669	1873	2180	96098	7433648	656184	13
0.2	2.93	12.00	0.1473	0.512036	1852	2305	89152	7389274	703899	3
0.3	3.60	18.42	0.1181	0.511675	1862	2172	SPN050405L	7323665	729301	10
0.3	7.99	42.78	0.1129	0.511612	1861	2155	96013	7305032	804674	1
0.3	4.60	25.01	0.1113	0.511593	1859	2149	98014	7391560	687373	2
0.4	2.24	14.40	0.0942	0.511382	1862	2109	71271	7391950	690517	3
0.4	4.68	27.40	0.1032	0.511494	1859	2127	84069	7321565	861709	3
0.4	7.19	40.50	0.1072	0.511545	1856	2134	84059	7311652	798489	3
0.4	17.53	106.36	0.0996	0.511452	1857	2119	MSI100169	7311193	822969	13
0.5	3.96	19.50	0.1224	0.511737	1843	2171	96122	7374554	702240	2
0.6	6.27	35.27	0.1074	0.511557	1841	2122	96106	7319297	802040	1
0.6	6.77	39.40	0.1042	0.511517	1842	2114	96118	7320022	796232	1
0.8	6.10	32.93	0.1120	0.511626	1816	2113	96100	7410593	674729	2
1.0	4.22	24.62	0.1037	0.511532	1808	2084	98010	7377474	696053	2
1.0	7.21	45.60	0.0956	0.511432	1813	2069	96119	7322178	796704	1
1.2	5.81	36.40	0.0966	0.511454	1798	2059	96123	7383860	706619	2
1.2	16.60	98.50	0.1018	0.511521	1789	2063	65099	7327052	883988	3
1.4	8.95	41.71	0.1298	0.511876	1730	2109	CHB070318	7342654	769299	11
1.5	4.39	26.20	0.1012	0.511525	1772	2047	96121	7353619	726356	2
1.7	3.55	18.05	0.1190	0.511757	1724	2061	96097	7431910	699498	2
1.8	7.16	28.25	0.1532	0.512191	1565	2142	96026	7398343	713281	13
2.1	4.88	26.65	0.1107	0.511674	1703	2014	CHB020195L	7304441	675191	13
2.4	8.19	41.08	0.1205	0.511814	1644	1998	CHB020227K	7317546	681487	13

Table 2, continued.

ε_{Nd} (T=1890 Ma)	Sm (ppm)	Nd (ppm)	$^{147}Sm/^{144}Nd$	$^{143}Nd/^{144}Nd$ korr.	T_{CHUR} (Ma)	T_{DM} (Ma)	Sample No.	N (SR99)	E (SR99)	Reference*
2.6	7.49	34.95	0.1295	0.511936	1590	1997	CMT020032A	7316081	650352	13
2.6	4.20	21.66	0.1172	0.511783	1635	1978	CHB020195K	7304441	675191	13
2.9	11.48	54.75	0.1267	0.511915	1571	1968	CMT020022A	7315468	661015	13
2.9	1.85	10.17	0.1097	0.511704	1633	1952	CL0117	7398496	711199	5
2.9	6.31	35.73	0.1067	0.511668	1639	1951	EOG020086A	7310211	638692	13
3.1	4.40	23.23	0.1146	0.511777	1596	1940	CMT020067A	7304024	646883	13
3.4	1.63	8.67	0.1136	0.511777	1577	1917	96012	7398443	713279	13
3.6	1.74	10.41	0.1013	0.511635	1600	1899	96023	7304068	791887	1

* Reference numbers refer to the following publications: 1: Mellqvist et al. (1999b), 2: Mellqvist et al. (1999a), 3: Öhlander et al. (1993), 4: Öhlander & Skiöld (1994), 5: Lundmark et al. (2005a), 6: Öhlander et al. (1987b), 7: Skiöld et al. (1988), 8: Skiöld & Öhlander (1989), 9: Öhlander et al. (1987a), 10: Kathol & Persson (2007c), 11: Kathol & Persson (2008b), 12: Kathol & Persson (2008a), 13: SGU, unpublished.

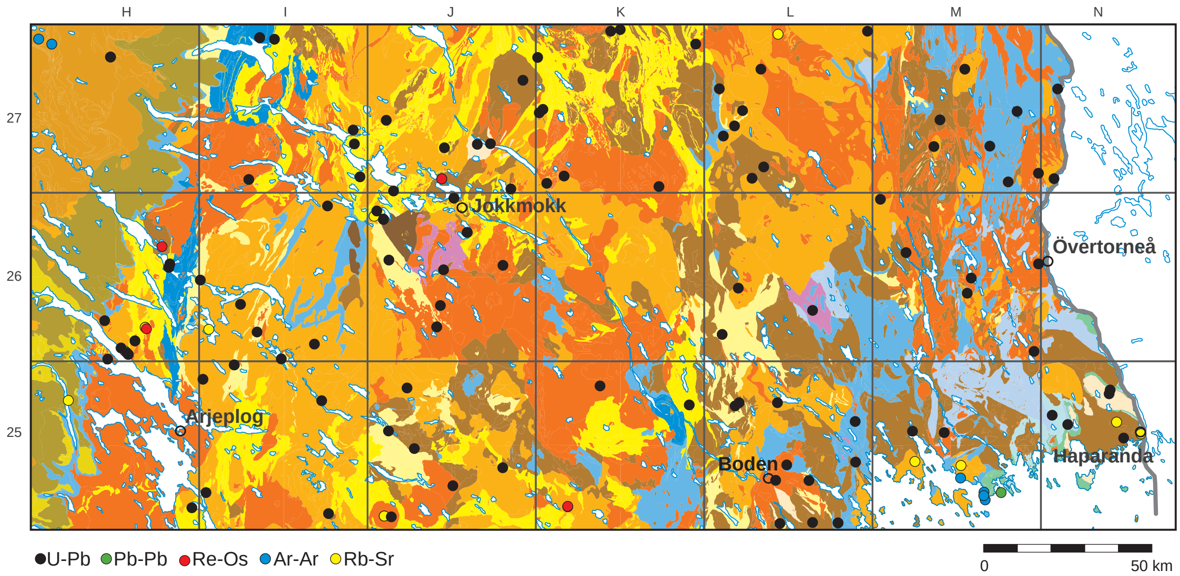

Figure 14. Sample sites for radiometric age determinations symbolised after isotopic system (from SGU database: Bedrock age database). Geological units as in Figure 17b.

RADIOMETRIC AGE DETERMINATIONS

Geochronological data have been compiled from the SGU database for radiometric age determinations. There were 123 radiometric age determinations in the project area, including 32 unpublished ages by SGU, at the end of 2017 (Fig. 14,). Most ages are from uranium-lead (U-Pb) isotopic analyses (109), some (14) being from other isotopic systems, such as rhenium-osmium (Re-Os), argon-argon (Ar-Ar) and lead-lead (Pb-Pb). The U-Pb ages are mainly from analyses of zircon (102); most of these are interpreted to date the magmatic age of the rock. Other analyses address the age of detrital zircons in metasedimentary rocks and the age of metamorphic events. Recently determined U-Pb ages are from in situ measurements within single grains of zircons using secondary ion mass spectrometer (SIMS) or laser ablation inductively coupled plasma mass spectrometry (LA-ICP-MS). Earlier U-Pb analyses were mainly made by isotope dilution thermal ionisation mass spectrometry (TIMS), analysing fractions of multiple grains.

Table 3. Radiometric age determinations in the project area in southern Norrbotten County.

Number	Lithology	Locality	Lithological unit	N (SR99)	E (SR99)	Map (RT90)	Tectonic subunit	Age (Ma)	Age Interpretation	Isotopic system	Method	Material	Reference
1	Tonalite	Pitkäjärvi	Archaean rocks	7344125	906769	25N8e	Ö	2689±3	Magmatic	U-Pb	SIMS	Zircon	Bergström et al. 2015a
2	Orthogneiss	Kukkola, Vesijänkkä	Archaean rocks	7344449	906891	25N8e	Ö	2670±18	Magmatic	U-Pb	TIMS	Zircon	Öhlander et al. 1987b
3	Granodioritic gneiss	Rimokojan	Archaean rocks	7414837	721822	27J2h	N	2668±3	Magmatic	U-Pb	SIMS	Zircon	Kathol et al. in press
4	Granodioritic gneiss	Lilllberget-Unbyn	Archaean rocks	7303260	809224	25L0e	N	2661±3	Magmatic	U-Pb	SIMS	Zircon	Sadeghi & Hellström 2018b
5	Granite	Anavare	Archaean rocks	7414551	717920	27J2g	N	2642±38	Uncertain	U-Pb	TIMS	Zircon	Mellqvist et al. 1999a
6	Migmatitic sandstone	Järvenkorvenjänkkä	Karelian supracrustal rock	7333712	894311	25N6b	Ö	2700-2670	Detrital	U-Pb	SIMS	Zircon	SGU unpublished
7	Arkose	Paskavaara	Karelian supracrustal rock	7408188	884662	27M1j	Ö	2690	Max depositional	U-Pb	Laser ICP-MS	Zircon	Lahtinen et al. 2015a
8	Dolomite	Trutskär	Karelian supracrustal rock	7313283	874765	25M2h	Ö	2119±243	not known	Pb-Pb	TIMS	Whole rock	Öhlander et al. 1992
9	Rhyolite	Risujärvi	Martimo suite	7336390	889652	25N6a	Ö	1930	Uncertain	U-Pb	SIMS	Zircon	Bergström et al. in prep.-b
10	Granodiorite	Norvijaur	Norvijaur intrusion	7392041	690272	26J8a	N	1930±6	Magmatic	U-Pb	SIMS	Zircon	Hellström 2015
11	Gneiss-tonalite	Norvijaur	Norvijaur intrusion	7392041	690272	26J8a	BS	1926+13/-11	Magmatic	U-Pb	TIMS	Zircon	Skiöld et al. 1993
12	Migmatite	Rutvik, quarry	Bothnian supergroup	7303669	826489	25L0h	N	1930	Max depositional	U-Pb	SIMS	Zircon	Sadeghi & Hellström 2018a
13	Arkose	Mettäjärvi	Bothnian supergroup	7426400	878080	<Null>	Ö	1920	Max depositional	U-Pb	Laser ICP-MS	Zircon	Lahtinen et al. 2015a
14	Arkose	Uusivirka	Bothnian supergroup	7416000	870120	<Null>	Ö	1920	Max depositional	U-Pb	Laser ICP-MS	Zircon	Lahtinen et al. 2015a
15	Migmatite	Sandkölen	Bothnian supergroup	7333801	831172	25L6i	N	1890	Max depositional	U-Pb	SIMS	Zircon	SGU unpublished
16	Migmatitic paragneiss	Kannusjärvi	Bothnian supergroup	7405500	875720	27M0i	Ö	1890	Detrital	U-Pb	SIMS	Zircon	SGU unpublished
17	Migmatite	Rutvik, quarry	Bothnian supergroup	7303669	826489	25L0h	N	1878±4	Metamorphic	U-Pb	SIMS	Zircon	Sadeghi & Hellström 2018a
18	Rhyolite	Skuppesavon	Porphyrite group	7373267	636223	26I4a	BS	1890	Magmatic	U-Pb	SIMS	Zircon	Hellström in prep.-a
19	Migmatite (dacitic)	Snierraudden	Porphyrite group	7350165	660519	26I0e	BS	1890	Magmatic	U-Pb	SIMS	Zircon	Hellström in prep.-b
20	Dacite	Kesaträsket	Porphyrite group	7359124	791321	26L1b	N	1890	Magmatic	U-Pb	SIMS	Zircon	SGU unpublished
21	Rhyolite	Lagmansgraven	Porphyrite group	7379927	692113	26J5b	BS	1890-1880	Magmatic	U-Pb	SIMS	Zircon	Claeson et al. in prep.
22	Rhyolite	Stasskölhuvudet	Porphyrite group	7337964	795484	25L7b	N	1886±4	Magmatic	U-Pb	SIMS	Zircon	Sadeghi & Hellström 2015
23	Felsic volcanic rock	Grassmyrberget	Porphyrite group	7316089	817673	25L2g	N	1884±5	Magmatic	U-Pb	SIMS	Zircon	Sadeghi & Hellström 2015
24	Rhyolite	Junitjåkåtj	Porphyrite group	7358073	653267	26I1d	BS	1880	Magmatic	U-Pb	SIMS	Zircon	Hellström in prep.-c
25	Migmatite (andesite)	Alep Tjåkkålis	Porphyrite group	7348221	646619	25I9c	BS	1880	Magmatic	U-Pb	SIMS	Zircon	SGU unpublished
26	Rhyolite	Trollforsen	Porphyrite group	7329219	692668	25J5b	BS	1880±6	Magmatic	U-Pb	SIMS	Zircon	Kathol et al. 2008a
27	Dacite	Mäntyvaara	Porphyrite group	7425632	796571	27L4c	N	1879±10	Magmatic	U-Pb	SIMS	Zircon	Hellström et al. 2012c
28	Migmatite (andesite)	Alep Tjåkkålis	Porphyrite group	7348221	646619	25I9c	BS	1780	Metamorphic	U-Pb	SIMS	Zircon	SGU unpublished

Table 3, continued.

Number	Lithology	Locality	Lithological unit	N (SR99)	E (SR99)	Map (RT90)	Tectonic subunit	Age (Ma)	Age Interpretation	Isotopic system	Method	Material	Reference
29	Granite	Tårrajaur	Jörn GI suite	7377242	708368	26J5e	BS	1890	Magmatic	U-Pb	SIMS	Zircon	SGU unpublished
30	Granodiorite	Övre Ljusselet	Jörn GI suite	7324060	700412	25J4c	BS	1882±8	Magmatic	U-Pb	TIMS	Zircon	Kathol & Persson 2007a
31	Molybdenum mineralisation	Vaikijaur	Haparanda suite	7404218	707505	27J0e	N	1899-1862	Mineralisation	Re-Os	N-TIMS	Molybdenite	Lundmark et al. 2005b
32	Granodiorite	S Sunderbyn	Haparanda suite	7303665	818891	25L0g	N	1891±32	Magmatic	U-Pb	TIMS	Zircon	Mellqvist et al. 2003
33	Granite	Jacksberget	Haparanda suite	7338933	796626	25L7c	N	1890	Magmatic	U-Pb	SIMS	Zircon	SGU unpublished
34	Quartz diorite	Paturijärvi	Haparanda suite	7423612	855227	27M4e	Ö	1890±20	Magmatic	U-Pb	TIMS	Zircon	Jonsson & Kero 2013c
35	Granodiorite	Unna Kielas	Haparanda suite	7433738	731235	27J6j	N	1889±5	Magmatic	U-Pb	SIMS	Zircon	Nysten et al. 2018
36	Granodiorite	Huhtirova	Haparanda suite	7408975	803084	27L1d	N	1885±18	Magmatic	U-Pb	SIMS	Zircon	Hellström et al. 2012c
37	Granite	SW of Aitik mine	Haparanda suite	7448672	757120	27K9e	N	1885±4	Magmatic	U-Pb	SIMS	Zircon	Sarlus et al. 2016
38	Tonalite	Slättberget	Haparanda suite	7384121	845651	26M6b	N	1885±7	Magmatic	U-Pb	TIMS	Zircon	Åkerman & Kero 2012b
39	Quartz monzonite	Kurkijänkkä	Haparanda suite	7329900	910975	25N5e	Ö	1884±7	Magmatic	U-Pb	SIMS	Zircon	Bergman et al. 2015a
40	Granodiorite	Jokkmokk	Haparanda suite	7398499	711196	26J9f	N	1883±15	Magmatic	U-Pb	TIMS	Zircon	Lundmark et al. 2005a
41	Granodiorite	Töre	Haparanda suite	7331141	848236	25M5c	N	1883±6	Magmatic	U-Pb	TIMS	Zircon	Wikström & Persson 1997a
42	Tonalite	Koutojärvi	Haparanda suite	7355252	884021	26M0j	Ö	1881±6	Magmatic	U-Pb	SIMS	Zircon	Åkerman & Kero 2012c
43	Granite	Linavare	Haparanda suite	7424193	736193	27K4a	N	1876±8	Magmatic	U-Pb	TIMS	Zircon	Claeson & Antal Lundin 2012b
44	Molybdenum mineralisation	Vaikijaur	Haparanda suite	7404218	707505	27J0e	N	1762-1742	Metamorphic	Re-Os	TIMS	Molybdenite	Lundmark et al. 2005b
45	Intermediate volcanic rock	Sammakkovaara	Arvidsjaur group	7445143	782397	27K8j	N	1882±6	Magmatic	U-Pb	SIMS	Zircon	Claeson & Antal Lundin 2012b
46	Rhyolite	Tjåresvare	Arvidsjaur group	7377901	627101	26H5g	BS	1880	Magmatic	U-Pb	SIMS	Zircon	SGU unpublished
47	Rhyolite	Savvemoajvve	Arvidsjaur group	7401492	728024	27J0i	N	1880	Magmatic	U-Pb	SIMS	Zircon	SGU unpublished
48	Trachyte	St. Samonåive	Arvidsjaur group	7413440	708143	27J2e	N	1880	Magmatic	U-Pb	SIMS	Zircon	SGU unpublished
49	Rhyolite	Danielstugan	Arvidsjaur group	7338075	781845	25K7j	BS	1876±6	Magmatic	U-Pb	SIMS	Zircon	Kathol et al. 2008b
50	Rhyolite	Benbryteforsen	Arvidsjaur group	7318701	726699	25J3i	BS	1874±13	Magmatic	U-Pb	TIMS	Zircon	Kathol & Persson 2007b
51	Rhyolite	Sörhårås	Arvidsjaur group	7444982	657294	27I9e	BS	1872±9	Magmatic	U-Pb	SIMS	Zircon	Nysten et al. in press
52	Trachyte	Kallak	Arvidsjaur group	7414247	681408	27I2j	N	1870	Magmatic	U-Pb	SIMS	Zircon	SGU unpublished
53	Felsic volcanic rock	Kaddåive	Arvidsjaur group	7400390	693216	27J0b	N	1870	Magmatic	U-Pb	SIMS	Zircon	SGU unpublished
54	Rhyolite	Makkavare	Arvidsjaur group	7305649	634580	25H1j	BS	1869±6	Magmatic	U-Pb	SIMS	Zircon	Morris et al. 2015
55	Rhyolite	Tjappisvare	Arvidsjaur group	7440594	735518	27K8a	N	1868±6	Magmatic	U-Pb	SIMS	Zircon	Claeson & Antal Lundin 2012b
56	Doleritic rock	Aitik mine, Salmijärvi	Arvidsjaur group	7449156	759915	<Null>	N	1813±5	Magmatic	U-Pb	SIMS	Zircon	Sarlus et al. 2016
57	Uranium mineralisation	Pleutajokk	Arvidsjaur group	7352137	615246	26H0f	BS	1770-1710	not known	Pb-Pb	TIMS	Wölsendorfite et al.	Löfvendahl & Åberg 1982
58	Uranium mineralisation	Pleutajokk	Arvidsjaur group	7352137	615246	26H0f	BS	1738±20	not known	U-Pb	Not known	Uraninite	Hålenius et al. 1986
59	Uranium mineralisation	Pleutajokk	Arvidsjaur group	7352137	615246	26H0f	BS	1700	not known	U-Pb	TIMS	Wölsendorfite et al.	Löfvendahl & Åberg 1982

Table 3, continued.

Number	Lithology	Locality	Lithological unit	N (SR99)	E (SR99)	Map (RT90)	Tectonic subunit	Age (Ma)	Age Interpretation	Isotopic system	Method	Material	Reference
60	Migmatitic sandstone	Skierfajaure	Snavva–Sjöfallet group	7376878	626793	26H5g	BS	1890	Max depositional	U-Pb	SIMS	Zircon	SGU unpublished
61	Aplite	Munka	Snavva–Sjöfallet group	7385760	627746	26H7i	BS	1787-1742	Metamorphic	Re-Os	N-TIMS	Molybdenite	Stein 2006
62	Migmatitic sandstone	Skierfajaure	Snavva–Sjöfallet group	7376878	626793	26H5g	BS	1760	Metamorphic	U-Pb	SIMS	Zircon	SGU unpublished
63	Uranium mineralisation	Lulep Manak	Snavva–Sjöfallet group	7444920	654238	27I9d	BS	1720-1710	not known	Pb-Pb	TIMS	Wölsendorfite	Löfvendahl & Åberg 1982
64	Uranium mineralisation	Lulep Manak	Snavva–Sjöfallet group	7444920	654238	27I9d	BS	1690	not known	U-Pb	TIMS	Wölsendorfite	Löfvendahl & Åberg 1982
65	Granite	Kåtaberget	Perthite monzonite suite	7307228	746011	25K1b	BS	1901-1869	Metamorphic	Re-Os	N-TIMS	Molybdenite	Stein 2006
66	Granite	Björnberget	Perthite monzonite suite	7372883	795964	26L4c	N	1885±5	Magmatic	U-Pb	SIMS	Zircon	Bergman et al. 2016
67	Granite	Njuorokvaratj	Perthite monzonite suite	7337930	672696	25I7h	BS	1882±6	Magmatic	U-Pb	TIMS	Zircon	Kathol & Aaro 2006a
68	Quartz monzonite	Svartberget	Perthite monzonite suite	7372314	863931	26M4f	Ö	1881±7	Magmatic	U-Pb	TIMS	Zircon	Åkerman & Kero 2012c
69	Syenite	Hakkasfallet	Perthite monzonite suite	7431997	789571	27L6a	N	1881±8	Magmatic	U-Pb	SIMS	Zircon	Hellström et al. 2012a
70	Granite	Ritavare	Perthite monzonite suite	7418372	680995	27I3j	N	1880	Magmatic	U-Pb	SIMS	Zircon	SGU unpublished
71	Monzonite	Njuorramjauratj	Perthite monzonite suite	7421360	690793	27J4b	N	1880	Magmatic	U-Pb	SIMS	Zircon	SGU unpublished
72	Granite	Gissjalgielas	Perthite monzonite suite	7343825	637359	25I8a	BS	1880±7	Magmatic	U-Pb	TIMS	Zircon	Mellqvist & Aaro 2006a
73	Granite	Kattisberget	Perthite monzonite suite	7399810	837803	26M9a	N	1880-1850	Magmatic	U-Pb	TIMS	Zircon	Åkerman & Kero 2012b
74	Granite	Luvos	Perthite monzonite suite	7395713	673708	26I9h	BS	1878±5	Magmatic	U-Pb	SIMS	Zircon	Hellström et al. 2015
75	Granite	Mårdberget	Perthite monzonite suite	7405539	799646	27L0c	N	1878±7	Magmatic	U-Pb	SIMS	Zircon	Hellström et al. 2012c
76	Granite	Ljuolas	Perthite monzonite suite	7366179	648256	26I3c	BS	1877±5	Magmatic	U-Pb	SIMS	Zircon	Hellström et al. 2015
77	Monzodiorite	Romiovaara	Perthite monzonite suite	7438730	862406	27M7f	Ö	1877±7	Magmatic	U-Pb	SIMS	Zircon	Jonsson & Kero 2013b
78	Granite	Kaltisberget	Perthite monzonite suite	7405485	743795	27K0b	N	1876±5	Magmatic	U-Pb	SIMS	Zircon	Claeson & Antal Lundin 2012b
79	Granite	Dájdavárre	Perthite monzonite suite	7354680	670292	27I1g	BS	1876±5	Magmatic	U-Pb	SIMS	Zircon	Hellström et al. 2015

Table 3, continued.

Number	Lithology	Locality	Lithological unit	N (SR99)	E (SR99)	Map (RT90)	Tectonic subunit	Age (Ma)	Age Interpretation	Isotopic system	Method	Material	Reference
80	Granite	Juoksjokko	Perthite monzonite suite	7394421	688335	26J8a	N	1876±6	Magmatic	U-Pb	TIMS	Zircon	Skiöld et al. 1993
81	Granite	Strittjebäcken	Perthite monzonite suite	7304441	675191	25I0h	BS	1876±7	Magmatic	U-Pb	TIMS	Zircon	Kathol & Aaro 2006b
82	Monzonite	Kattilakoski	Perthite monzonite suite	7406611	889300	27N0a	Ö	1874±10	Magmatic	U-Pb	TIMS	Zircon	Jonsson & Kero 2013a
83	Granite	Nilivaara	Perthite monzonite suite	7417966	790924	27L3b	N	1874±5	Magmatic	U-Pb	SIMS	Zircon	Hellström et al. 2012c
84	Quartz monzonite	Rengärdorna	Perthite monzonite suite	7415690	853517	27M2d	Ö	1874±7	Magmatic	U-Pb	TIMS	Zircon	Jonsson & Kero 2013c
85	Granite	Långheden	Perthite monzonite suite	7449626	833368	27L9j	N	1872±4	Magmatic	U-Pb	TIMS	Zircon	Hellström et al. 2012b
86	Granite	Sundsnäs	Perthite monzonite suite	7339056	808062	25L7e	N	1870	Magmatic	U-Pb	Laser ICP-MS	Zircon	SGU unpublished
87	Granite	Guorbavare	Perthite monzonite suite	7352793	612922	26H0f	BS	1870±40	not known	U-Pb	SIMS	Zircon	SGU unpublished
88	Granite porphyry	Linavare	Perthite monzonite suite	7425183	737293	27K4a	N	1870±6	Magmatic	U-Pb	Laser ICP-MS	Zircon	Claeson & Antal Lundin 2012b
89	Quartz monzodiorite	Hirvaskoski	Perthite monzonite suite	7433237	890047	27N6b	Ö	1869±7	Magmatic	U-Pb	TIMS	Zircon	Jonsson & Kero 2013b
90	Granite	Reuna	Perthite monzonite suite	7342018	697995	25J8c	BS	1867±8	Magmatic	U-Pb	TIMS	Zircon	Kathol et al. 2006
91	Granite	Satter	Perthite monzonite suite	7437956	801867	27L7d	N	1866±12	Magmatic	U-Pb	SIMS	Zircon	Hellström et al. 2012a
92	Granite	Välbmabuolda	Perthite monzonite suite	7310211	638692	25I2a	BS	1866±33	Magmatic	U-Pb	TIMS	Zircon	Mellqvist & Aaro 2006b
93	Granite	Guorbavare	Perthite monzonite suite	7351922	614099	26H0f	BS	1864+20/19	Magmatic	U-Pb	TIMS	Zircon	Wilson et al. 1985
94	Granite	Lessuvaara	Perthite monzonite suite	7421003	794213	27L3b	N	1864±7	Magmatic	U-Pb	SIMS	Zircon	Hellström et al. 2012c
95	Dacitoid to andesitoid	Tjäkkaure	Late Svecofennian supracrusta rock	7404458	683199	27I0j	N	1770	Uncertain	U-Pb	SIMS	Zircon	SGU unpublished
96	Granite	Träsk-Alkus	Lina suite	7376770	865087	26M4f	Ö	1870±6	Uncertain	U-Pb	SIMS	Zircon	Åkerman & Kero 2012c
97	Granite	Allebuoda	Lina suite	7359244	620590	26H2g	BS	1870-1801	Metamorphic	Re-Os	N-TIMS	Molybdenite	Stein 2006
98	Granite	Stenselekojan	Lina suite	7313200	711991	25J2f	BS	1792±16	Magmatic	U-Pb	TIMS	Zircon	Kathol et al. 2006
99	Granite	Storliden	Lina suite	7303757	693803	25J0b	BS	1792±5	Magmatic	U-Pb	N-TIMS	Zircon	Skiöld et al. 1993
100	Granite	Slättkullen	Lina suite	7366630	707545	26j3e	BS	1790±5	Magmatic	U-Pb	SIMS	Zircon	Morris & Hellström 2016
101	Granite	Luppioberget	Lina suite	7381258	884983	26M5j	Ö	1783±11	Magmatic	U-Pb	SIMS	Zircon	Åkerman & Kero 2012a

Table 3, continued.

Number	Lithology	Locality	Lithological unit	N (SR99)	E (SR99)	Map (RT90)	Tectonic subunit	Age (Ma)	Age Interpretation	Isotopic system	Method	Material	Reference
102	Granite	Klinten	Lina suite	7330862	857639	25M5e	Ö	1783±3	Magmatic	U-Pb	TIMS	Multi mineral	Wikström & Persson 1997b
103	Aplite	Allebuouda	Lina suite	7359244	620590	26H2g	BS	1767±9	Magmatic	U-Pb	TIMS	Zircon	Öhlander & Billström 1989
104	Pegmatite	Råneå	Lina suite	7321726	831458	25L4j	N	1765±14	Magmatic	U-Pb	TIMS	Columbite-Tantalite	Romer & Wright 1992
105	Uranium mineralisation	Harrejokk	Lina suite	7360841	607986	26H2e	BS	1736±162	not known	U-Pb	Not known	Uraninite	Hålenius et al. 1986
106	Syenite	Boden	Edefors suite	7316067	807789	25L2e	N	1810	Magmatic	U-Pb	SIMS	Zircon	SGU unpublished
107	Granite	Spikberg	Edefors suite	7343378	755312	25K8d	BS	1803±10	Magmatic	U-Pb	TIMS	Zircon	Kathol & Persson 2008c
108	Quartz monzonite	Lillraudok	Edefors suite	7349445	609001	26H0e	BS	1803±5	Magmatic	U-Pb	SIMS	Zircon	Kathol & Hellström 2015
109	Gabbro	Notträsk	Edefors suite	7320675	811056	25L3e	N	1800	Magmatic	U-Pb	Laser ICP-MS	Zircon	SGU unpublished
110	Monzonite-quartz-monzonite	Tiurevaara	Edefors suite	7402757	772018	27K0h	N	1793±10	Magmatic	U-Pb	Laser ICP-MS	Zircon	Claeson & Antal Lundin 2012b
111	Quartz monzonite	Tvärträsket	Edefors suite	7378805	726008	26J5i	N	1790	Magmatic	U-Pb	SIMS	Zircon	SGU unpublished
112	Granite	Norra Kierkåive	Edefors suite	7403252	738664	27K0a	N	1780	Magmatic	U-Pb	SIMS	Zircon	SGU unpublished
113	Quartz monzonite	Jervas	Edefors suite	7403249	650222	27I0c	BS	1780	Magmatic	U-Pb	SIMS	Zircon	SGU unpublished
114	Gabbro	Ruoutevare	Edefors suite	7388439	715280	26J7f	N	1780	Uncertain	U-Pb	SIMS	Zircon	SGU unpublished
115	Diatexite (granodioritic)	Grundforshed	Metamorphic rocks	7366607	818116	26L3g	N	1880	Metamorphic	U-Pb	SIMS	Zircon	Bergström et al. in prep.-a
116	Lamprophyre	Storön, Kalix	Mesoproterozoic rocks	7312297	869628	25M2g	Ö	1141±14	Magmatic	Ar-Ar	Step-wise heating	Biotite	Kresten et al. 1997
117	Lamprophyre	Storön, Kalix	Mesoproterozoic rocks	7311023	870094	25M1g	Ö	1141±14	Magmatic	Ar-Ar	Step-wise heating	Biotite	Kresten et al. 1997
118	Lamprophyre	Kalix	Mesoproterozoic rocks	7317428	862712	25M3f	Ö	1141±14	Magmatic	Ar-Ar	Step-wise heating	Biotite	Kresten et al. 1997
119	Lamprophyre	Storön, Kalix	Mesoproterozoic rocks	7313338	869665	25M2g	Ö	1128±14	Magmatic	Ar-Ar	Step-wise heating	Biotite	Kresten et al. 1997
120	Syenite	Ruoddeeváre	Seve Nappe Complex	7439031	608674	27H8e	SNC	1761±9	Magmatic	U-Pb	TIMS	Zircon	Rehnström 2003
121	Syenite	Ruoddeeváre	Seve Nappe Complex	7439031	608674	27H8e	SNC	1744±10	not known	U-Pb	TIMS	Titanite	Rehnström 2003
122	Amphibolite	Råvvejaure	Seve Nappe Complex	7444103	587314	27H9a	SNC	465±1	Cooling	Ar-Ar	Step-wise heating	Hornblende	Dallmeyer & Stephens 1991
123	Amphibolite	Råvvejaure	Seve Nappe Complex	7442654	591232	27H8b	SNC	464±12	Cooling	Ar-Ar	Step-wise heating	Hornblende	Dallmeyer & Stephens 1991

Age errors are given at 2 sigma or 95% confidence interval. SGU unpublished ages are rounded to nearest ten and given without age error. Age and age interpretation for unpublished ages are preliminary. Many of the age determinations are only presented as numbers on bedrock geology maps without published metadata or analytical data, see reference list.
N = Norrbotten lithotectonic unit (Svecokarelian Orogen). **Ö** = Överkalix lithotectonic unit (Svecokarelian Orogen). **BS** = Bothnia-Skellefteå lithotectonic unit (Svecokarelian Orogen). **SNC** = Seve Nappe Complex (Caledonian orogen)

CORED BOREHOLES

Drill cores from 2 833 cored boreholes from the project area are stored at SGU in Malå (Fig. 15). There are also drill logs, measurement logs, lithogeochemical data and metadata linked to the drill cores. Approximately 44 000 metres from 322 drill cores in the project area were scanned using hyperspectral infrared core imaging during 2014–2015 by SGU (Fig. 15). Data can provide information about the mineralogy of the drill core as a complement to the physical drill cores stored in Malå. High-resolution optical and infrared (IR) pictures were taken. The drill core data can be accessed via SGU Map viewer Drill cores (www.sgu.se).

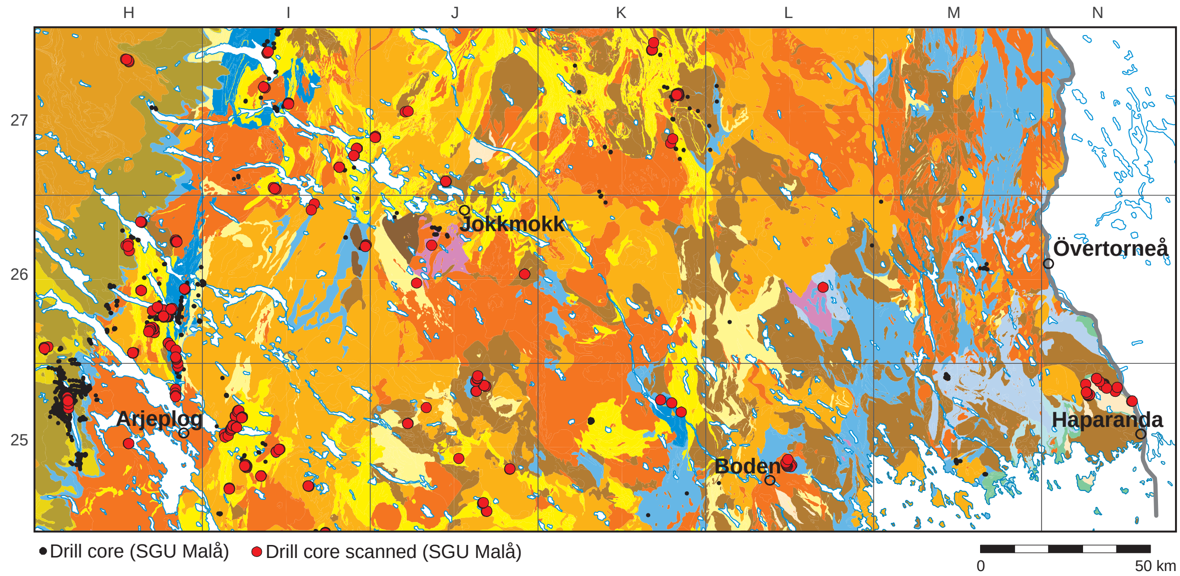

Figure 15. Location of cored boreholes with drill cores stored at SGU in Malå. 322 drill cores were scanned with hyperspectral infrared core imaging by SGU during 2014–2015. Geological units as in Figure 17b.

GEOPHYSICAL MODELLING

Particular geological structures and units have been selected as subjects for geophysical modelling in order to produce three-dimensional information on these structures and units respectively. Areas and profiles, where modelling has been carried out, are shown in Figure 16.

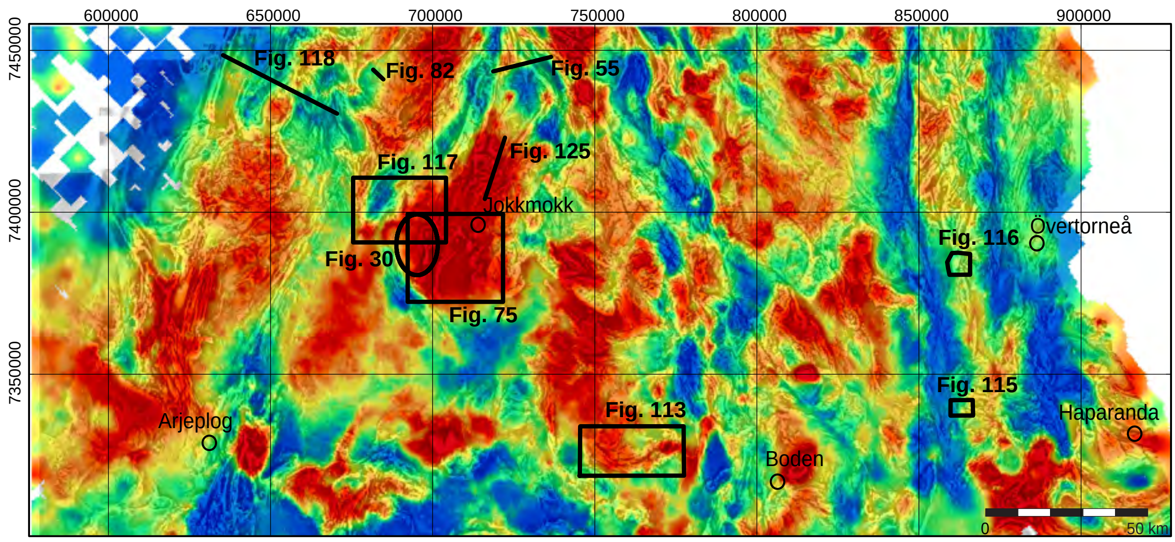

Figure 16. Location of areas and profiles where geophysical modelling has been carried out is shown with black polygons and lines. The background map is a combination of magnetic anomaly (grey scale) and gravity field (colour). Both the magnetic and the gravity fields are filtered to enhance shallow source anomalies. Grid is in SWEREF 99.

4. Regional tectonic framework

Stefan Bergman

The project area is located in the northwest of the Fennoscandian Shield (Fig. 1) and contains parts of several lithotectonic units. The Luleå–Jokkmokk zone (LJZ), which crosses the area, is the border between solely Proterozoic rocks to the southwest (Bothnia–Skellefteå lithotectonic unit), and an area in the northeast where Proterozoic rocks are present, together with exposed and concealed Archaean rocks: the Norrbotten and Överkalix lithotectonic units. The boundary between the latter units is the Pajala deformation belt (PDB, Fig. 1). In the west, the Precambrian crystalline bedrock is covered by Ediacaran to Cambrian sedimentary rocks, and overthrust by rocks belonging to the Caledonian orogen.

The Archaean rocks were formed during the 2.9–2.6 Ga Lopian orogeny. In the earliest Proterozoic, the Archaean crust was intruded by mafic magmas during rifting, and mafic volcanic rocks and sediments (Karelian) were deposited in the rifts and on the thinned older crust. The Svecokarelian orogeny (2.0–1.8 Ga) marks the shift to a convergent tectonic setting, during which volcanic and sedimentary rocks were formed and intruded by several generations of intrusive rocks. Several phases of regional deformation, including major folding and shearing, occurred mostly under low to intermediate pressure and variable temperature conditions.

5. Geological units

Benno Kathol, Ulf Bergström, Martiya Sadeghi, Ildikó Antal Lundin & Carl-Axel Triumf

INTRODUCTION

On the basis of the age and geological history of rock sequences, the bedrock in the project area of southern Norrbotten County can be divided and assigned to four lithotectonic units. These are the Svecokarelian orogen, the Ediacaran to Cambrian sedimentary cover sequence, the Caledonian orogen and a minor unit comprising Mesoproterozoic rocks.

The Svecokarelian orogen of the project area is subdivided into the Norrbotten, Bothnia–Skellefteå and Överkalix lithotectonic units (SGU 2017). These lithotectonic units are further divided into eight subareas (BS1–3, N4–6 and Ö7–8), corresponding to the eight stratigraphic columns in the stratigraphic scheme of the Svecokarelian orogen in the project area (Figs. 17a, b).

Most of the bedrock in northern Sweden and Finland was formed or reworked by Svecokarelian orogenic processes, which lasted from c. 1.96 to 1.75 Ga. Svecokarelian intrusive rocks, Svecofennian supracrustal rocks and pre-existing Karelian and Archaean rocks make up the major part of the Svecokarelian orogen in the project area and are the main subjects of this project. Given the aims of the project, less attention has been paid to the nappe sequences of the Caledonian orogen and the underlying Ediacaran to Cambrian sedimentary cover sequence.

The following description of the geological units in the project area is based mainly on descriptions of geological maps at a scale of 1:50 000, and secondarily on reports on maps at a scale of 1:250 000, compiled by SGU. Further references cited in this chapter are given in the text itself.

SVECOKARELIAN OROGEN

Archaean rocks >2.50 Ga

Within the project area, Archaean rocks occur in the Haparanda, Boden and Porjus map areas. The largest occurrences are situated in the easternmost part of the project area to the north and south of Haparanda. A sizeable massif between Haparanda and Kukkola was termed the Kukkola gneiss complex by Silvennoinen et al. (1987). In this complex, Archaean rocks crop out in an anticline with northwest–southeast-striking axial surfaces around Leipijärvi. This Kukkola gneiss complex is the northwesterly continuation of the Pudasjärvi complex (<http://gtkdata.gtk.fi/Kalliopera>), which forms the bedrock in large areas to the southeast in Finland. The Archaean rocks of the Kukkola gneiss complex comprise tonalite, trondhjemite (Fig. 18a), gabbro, granite and amphibolite; in the stratigraphic scheme (Fig. 17a) they are shown in column Ö8. The rocks are metamorphosed, recrystallised

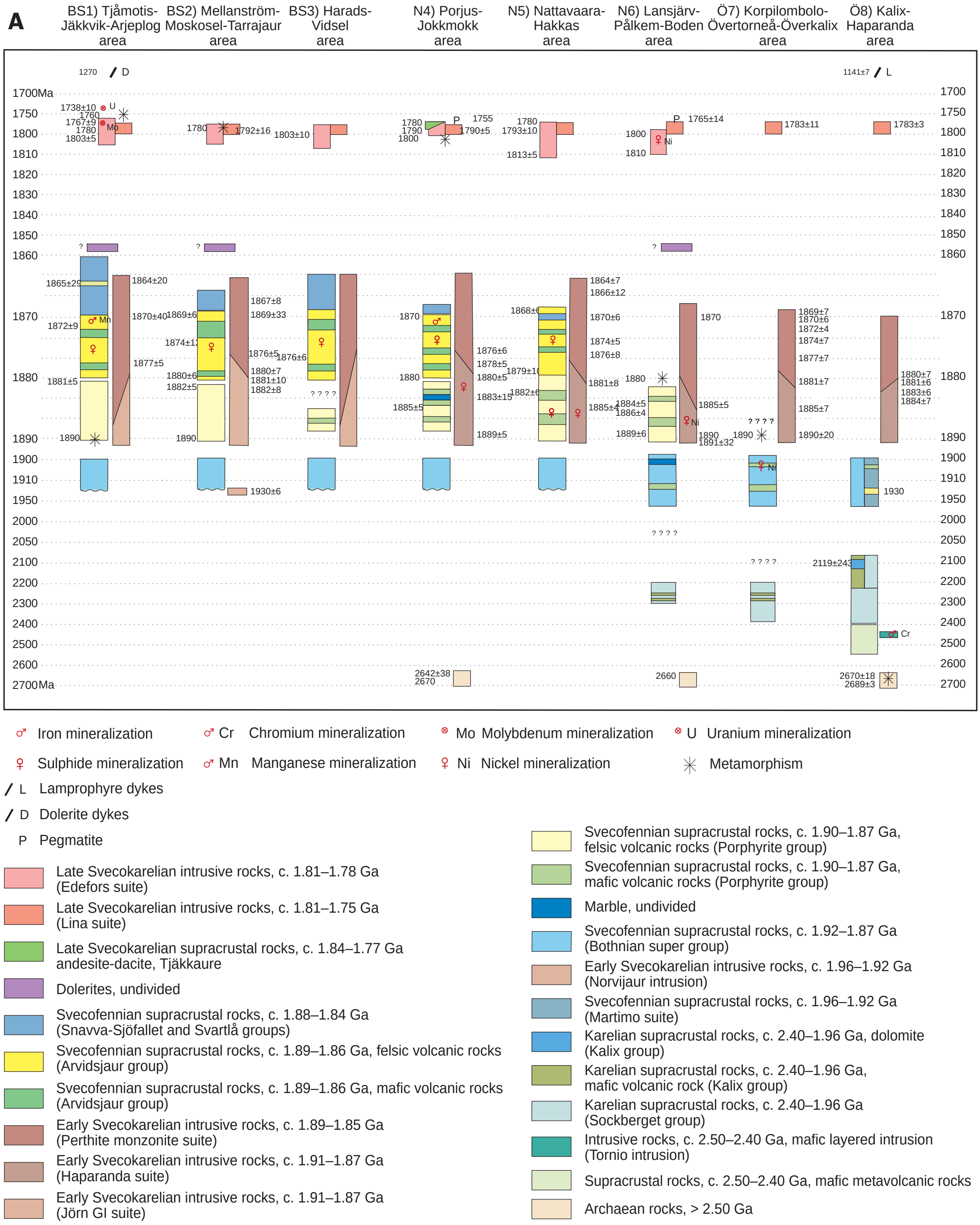

Figure 17. A. Stratigraphic scheme for subareas BS1–3, N4–6 and Ö7–8. For delineation of subareas BS1–3, N4–6 and Ö7–8, see Figure 17B.

and show gneissic structures with banding and veining (Fig. 18b). Some of them are interpreted as diatexites. U-Pb zircon dating of a metatonalite from the Kukkola gneiss complex yielded a crystallisation age of 2 689 ± 3 Ma (Bergström et al. 2015a). Bergström et al. (2015a) suggested that c. 2.67 Ga zircon rims and also a previously published age of 2 670 ± 18 Ma (Öhlander et al. 1987b) reflect metamorphic recrystallisation.

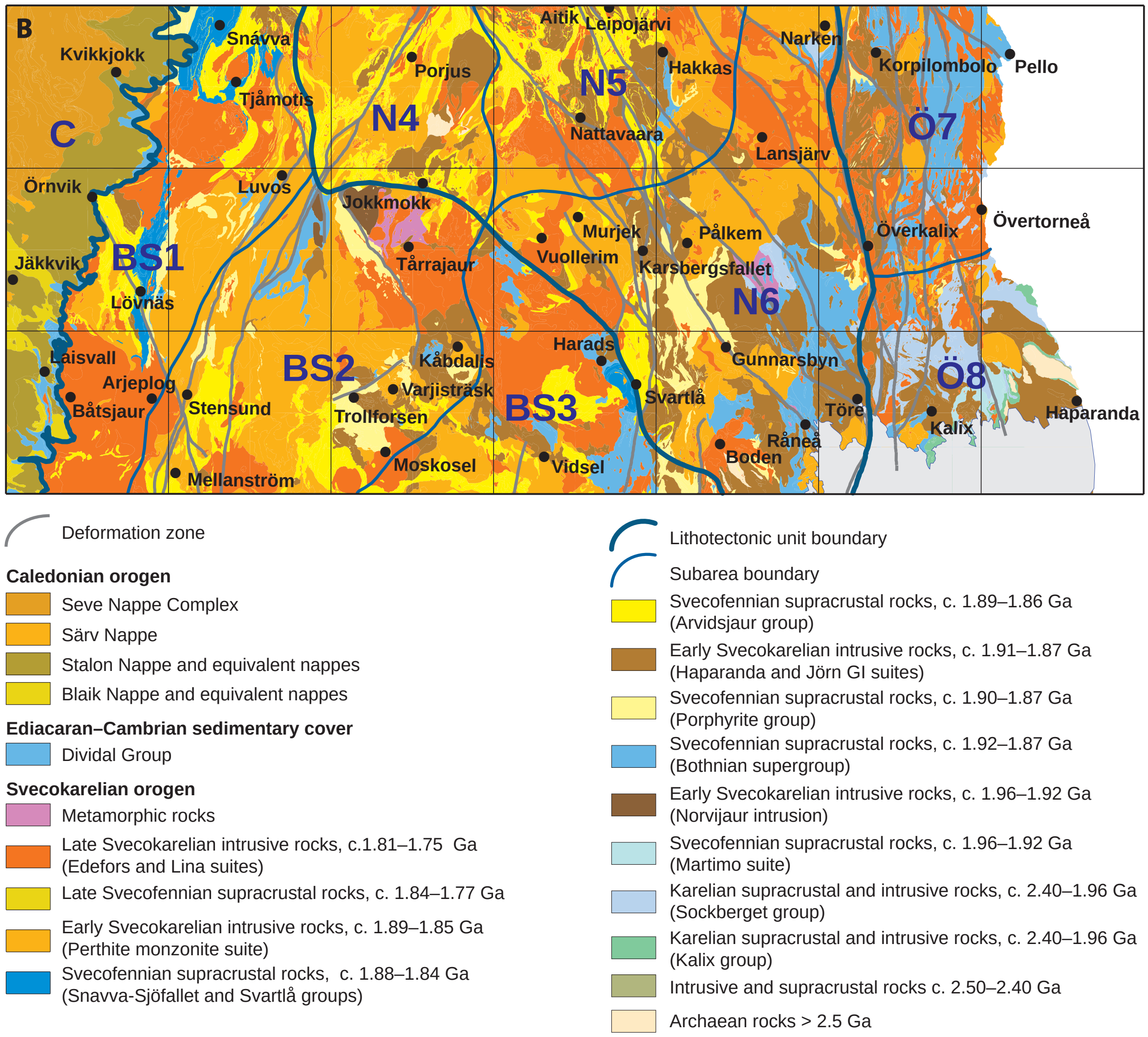

Figure 17. **B.** Simplified bedrock map of the project area, showing lithotectonic units C = Caledonian orogen and platformal sedimentary cover rocks, BS = Bothnia–Skellefteå, N = Norrbotten, Ö = Överkalix and subareas BS1–3, N4–6 and Ö7–8 corresponding to columns BS1–3, N4–6 and Ö7–8 in Figure 17A.

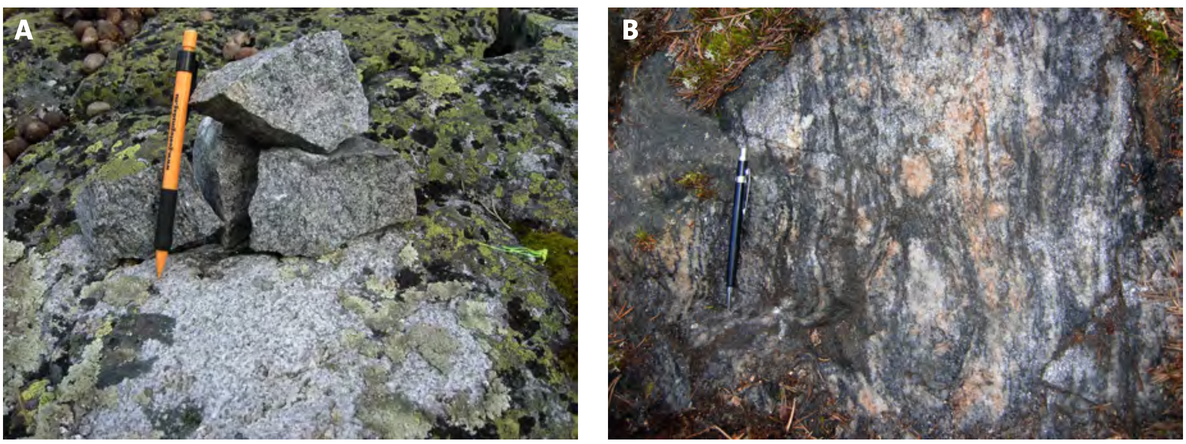

Figure 18. **A.** Trondhjemite from the Kukkola gneiss complex. Leipijärvi, about 20 km northwest of Haparanda (7344868/901072). **B.** Migmatitic metatonalite. Pitkäjärvi, about 16 km northwest of Haparanda (7344554/906492). Photos: Ulf Bergström.

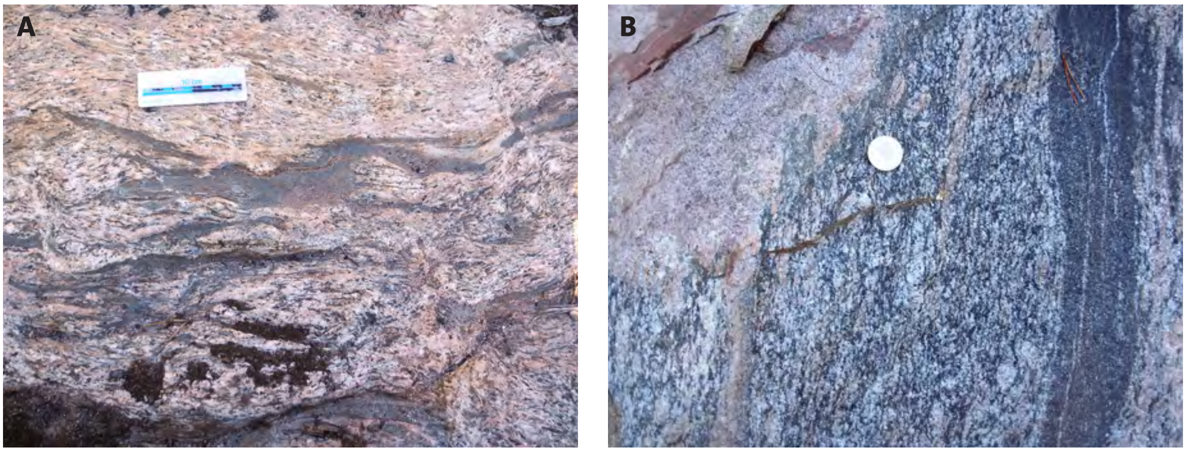

Figure 19. **A.** Archaean porphyritic granite with deformed xenoliths of metasedimentary rocks. Gruvberget, about 5.6 km southeast of Boden (7312361/809193). Photo: Martiya Sadhegi. **B.** Archaean porphyritic granitoid intruded by granite of the Lina suite. Lillberget, south of Unbyn, about 14 km south-southeast of Boden (7303260/809224). Photo: Benno Kathol.

Much of another larger massif of Archaean rocks in the Haparanda archipelago is covered by the Baltic Sea. The occurrence of this massif is not confirmed by field observations; it is instead interpreted from geophysical features, mainly magnetic anomalies as a westerly continuation of the Pudasjärvi complex in Finland.

There are also two minor massifs of Archaean rocks in the Haparanda area. North of lake Präntijärvi, outcropping Palaeoproterozoic rocks suggest the occurrence of an anticline. The central part of the anticline is not exposed, but a low-magnetic anomaly indicates that the central part consists of Archaean rocks. A geophysical model of this area is presented in Bergman et al. (2014). The minor massif south of Kattilasaari is also interpreted from the magnetic anomaly map without any support from field observations.

Three massifs or tectonic blocks of Archaean rocks are found southeast of Boden. They are elongated with a northwest–southeasterly strike and normally consist of porphyritic intrusive rocks whose composition ranges from granodiorite to monzodiorite (Debon & LeFort 1983. Two of these massifs were described for the first time by Mellqvist (1999). The third one is only confirmed by one outcrop at Lindvallsmyran in the Sunderbyn area (SGU, unpublished data). All three Archaean massifs show a higher degree of metamorphism and deformation than the surrounding Palaeoproterozoic rocks. The Archaean rocks to the southeast of Boden are shown in column N6 of the stratigraphic scheme (Fig. 17a).

The largest massif in the Boden area at Gruvberget and Markberget consists of porphyritic, strongly foliated and recrystallised granitoids, which occur as intrusions in a supracrustal sequence of sedimentary and volcaniclastic rocks (Fig. 19a). An Sm-Nd analysis from the porphyritic granitoid at Gruvberget shows strongly negative ε_{Nd}-values.

The second massif lies west of the village of Unbyn. The predominant rock type is a porphyritic granitoid (Fig. 19b) with minor amounts of tonalite-trondhjemite-granodiorite (TTG)-gneisses. The granitoid has been dated at Lillberget close to Unbyn (U-Pb on zircon) at 2 661 ± 3 Ma (Sadeghi & Hellström 2018b.) and a Sm-Nd analysis from this rock shows $\varepsilon_{Nd\ (T=1890\ Ma)}$-values of -12, which is comparable to the strongly negative ε_{Nd}-values obtained at Gruvberget.

In addition, Archaean rocks from the nearby Luleå area, just south of the project area, show strongly negative ε_{Nd}-values and ages ranging from 2.71 Ga to 2.65 Ga (Lundqvist et al. 1996b, Wikström et al. 1996a, Mellqvist et al. 1999b and references therein).

Archaean rocks occur also in one sizeable massif and three smaller ones between Jokkmokk and

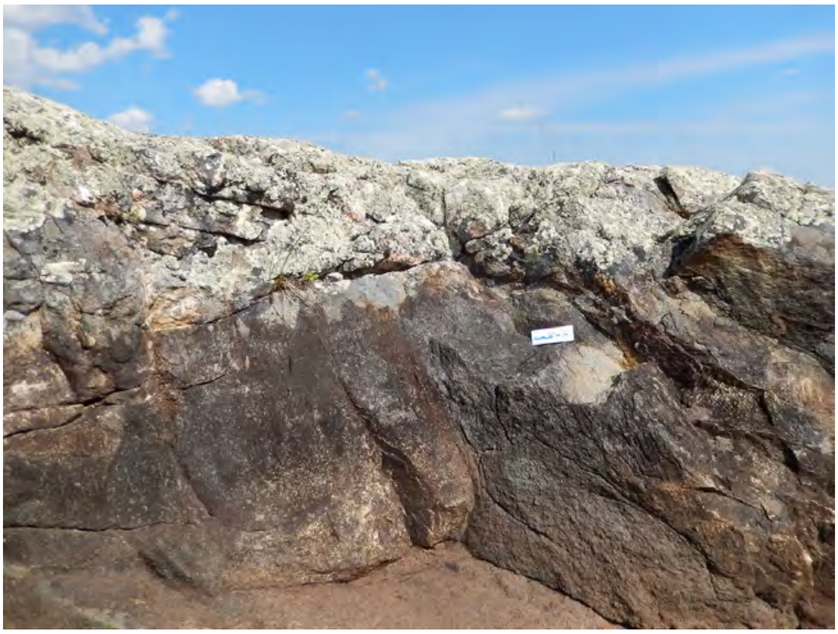

Figure 20. Contact between Archaean gneiss (bottom) and granite of the Lina suite (top). Stora Luleälven, about 21.5 km northeast of Jokkmokk (7412982/726292). Photo: George Morris.

Figure 21. Archaean coarsely porphyritic and strongly deformed quartz monzonite. Ánávárre, about 19 km north-northeast of Jokkmokk (7414586/717936). Photo: Benno Kathol.

Porjus. In some places, the massifs of Archaean rocks in this area are confined by deformation zones, but in others, the surrounding Palaeoproterozoic intrusive rocks show primary intrusive contacts with the Archaean bedrock (Fig. 20). The relationship between the larger Archaean massif and the surrounding Palaeoproterozoic rocks is inferred from a geophysical model along a north–northeast-striking profile (see chapter 6 *Structure and metamorphism*, p. 146 ff). The Archaean rocks can be divided into two rock types: a porphyritic granite to monzonite and an association of felsic gneisses containing mafic dykes of uncertain age.

The porphyritic granite to monzonite is strongly deformed, recrystallised and contains phenocrysts between 5 and 30 mm in size in a fine-grained to finely medium-grained groundmass (Fig. 21). The crystallisation age is 2 642 ± 38 Ma (Mellqvist 1999, Mellqvist et al. 1999a).

Figure 22. Association of Archaean granodioritic gneiss and reoriented basic dykes. Rimokojan, about 21 km north-northeast of Jokkmokk (7414758/722028). Photo: Benno Kathol.

Figure 23. **A.** Boudinaged basic dyke in granodioritic Archaean gneiss. Rimokojan, about 21 km north–northeast of Jokkmokk (7414837/721822). Photo: Benno Kathol. **B.** Contact between Archaean granodioritic gneiss (top) and basic dyke (bottom). The foliation in the gneiss and the contact form an acute angle. Rimokojan, about 21 km north-northeast of Jokkmokk (7414837/721822). Photo: Benno Kathol.

The association of felsic gneisses comprises grey to dark grey, equigranular, fine-grained strongly foliated gneisses and schists varying in composition from granitic to granodioritic in the west to granodioritic to tonalitic in the eastern parts of the larger massif (Fig. 22). These gneisses are best exposed along the northern and southern shore of Stora Luleälven, where they show a pronounced, steeply to vertically dipping foliation and a constant northeasterly strike. U-Pb zircon dating of a granodioritic gneiss from Rimokojan at Stora Luleälven has yielded an age of 2 671 ± 6 Ma (Kathol et al. in press).

Within these Archaean gneisses, 5 to 120 cm thick dykes of dark grey, equigranular, fine-grained and foliated basic rocks occur (Fig. 23a). These dykes are boudinaged (Fig. 23a) and almost totally reoriented into concordance with the pronounced foliation within the gneisses. A truncating relationship can still be observed in places, however (Fig. 23b). The age of these dykes is uncertain; because of the truncating contacts with the gneisses they must be younger than the foliation in the latter. However, there are intrusions of massive to weakly foliated, equigranular, medium-grained gabbros to diorites, assigned to the Palaeoproterozoic Haparanda suite within the gneiss–dyke association. This suggests that the dykes must have undergone reorientation and deformation before the emplacement of rocks of the Haparanda suite but after deformation of the Archaean rocks.

Two analyses of zircon rims of the sample from Rimokojan are concordant and give an age of 2 610 ± 5 Ma, which is interpreted to date a metamorphic event at c. 2.61 Ga (Kathol et al. in press). This event might be related either to formation of the strong foliation in the Archaean rocks or deformation and reorientation of the basic dykes, or both.

Intrusive and supracrustal rocks, c. 2.50–2.40 Ga

The Archaean Kukkola gneiss complex, as part of the Pudasjärvi complex, has been intruded by the Tornio intrusion (Söderholm & Inkinen 1982), in Sweden also called the Kukkola intrusion (Filén 2001). The Tornio intrusion, with an assumed age of 2.44 Ga, is assigned to the Peräpohja suite in Finland, which has been dated at 2 433 ± 4 Ma and 2 428 ± 35 Ma (Perttunen & Vaasjoki 2001). The Swedish part of the Tornio intrusion has previously been described by Claesson et al. (1982, 1983) and Lundmark (1984a). The first map of the Swedish part of the intrusion was presented by Claesson & Hålenius (1981).

The thickness of the Tornio intrusion varies between several metres and about 200 m. The intrusion comprises ultramafic rocks such as pyroxenite, peridotite, hornblendite, serpentinite and talc-carbonate rocks (Fig. 24), with layers of basic rocks such as norite, gabbro, amphibolite and anorthosite. The

Figure 24. Metaultramafic rock with secondary amphibole and carbonate. Revonsaari, about 10 km north of Haparanda (7341542/913381). Photo: Stefan Bergman.

rocks are metamorphosed and show serpentinisation and chlorite-talc-carbonate alteration to a varying degree; narrow bands of chromite and dissemination of chromium-bearing magnetite also occur.

According to Lundmark (1984a), pyroxenite and peridotite of the Tornio intrusion have intruded volcanic and metasedimentary rocks, which therefore predate the intrusion and must have been deposited under the Neoarchaean to Siderian.

The Tornio intrusion and the Archaean rocks of the Kukkola gneiss complex, or Pudasjärvi complex, form the basement of the Karelian supracrustal rocks.

Karelian supracrustal and intrusive rocks c. 2.40–1.96 Ga

The Karelian supracrustal and intrusive rocks are divided into the Kalix group and the Sockberget group. Both groups have similar ages of around 2.1 Ga, and are considered to be different facies types, emplaced in different depositional environments. They probably correspond to the Kivalo group (Perttunen et al. 1995) in the Peräpohja schist belt in Finland. Detrital zircons from six quartzite samples from different levels in the Kivalo group all have U-Pb zircon ages, suggesting an Archaean provenance of these supracrustal rocks (Perttunen & Vaasjoki 2001).

Kalix group

A unit of layered rocks, predominantly comprising eruptive greenstones was first described from Kalix parish as the Kalix group by Svenonius (1915). He also included minor occurrences of limestone, dolomite, slates (schists?) and sandstones in this group. The supracrustal rocks in the Kalix–Haparanda area have also been named Kalix series (Åhman 1960), Kalix greenstone and schist belt (Lager & Loberg 1990) and Kalix greenstone belt (Öhlander et al. 1992). Detailed sedimentological studies of the supracrustal rocks have been carried out by Lager & Loberg (1990) and Wanke & Melezhik (2005). These authors divide the supracrustal sequence into three main groups (see Bergman et al. 2014), and they interpret the sequence to represent deposition in a rift environment, evolving from a marine rift via a marine-influenced rifted continental margin to a shelf environment with deposition of carbonates. According to Martinsson & Billström (2006), the Kalix greenstones mainly consist of basaltic lavas and volcaniclastic rocks derived from a depleted mantle source. They show low to moderate TiO_2 content and a chemical composition resembling mid-ocean ridge basalts (MORB). However, the upper part of this sequence is extremely high in TiO_2 (5–6%). The MORB rocks are overlain by basalt of a transitional character and interlayered dolomites of the Vitgrundet formation (see below). Martinsson & Billström (2006) propose that the chemostratigraphy of the Kalix greenstones, including Sm-Nd isotope analyses, suggests variable magma sources and progressive changes during magma evolution in the final stage of a continental break-up.

Here, we use a further division of the Kalix group and follow the nomenclature of Åhman et al. (1990), Lundqvist et al. (1996a) and Lukkarinen & Lundqvist (2000), who summarised the mainly volcanic rocks under the name Karlsborg formation and separated the mainly carbonate part as the Vitgrundet formation.

The Karlsborg formation mainly consists of basic and intermediate metavolcanic rocks (basalt-andesite) (Fig. 25a), which are covered by the Baltic Sea across much of the Haparanda and Kalix archipelagos. On land, they are exposed in coastal areas at Storön, Karlsborg, Båtskärsnäs and Sangis. North of Haparanda, basalt-andesite (Fig. 25b) occurs around the Kukkola gneiss complex, either overlying the Archaean gneisses or rocks of the Tornio intrusion. North-northwest of Karungi, tholeiitic basalt to andesite overlies quartz arenite of the Sockberget group (Åkerman & Kero 2012d).

A subordinate body of gabbro surrounding the Archaean massif at Präntijärvi is interpreted to be an intrusion genetically related to the basalt-andesites of the Karlsborg formation. Minor layers of quartz arenite occur as thin intercalations in the western parts of the basalt-andesite at or close to the border to younger sedimentary rocks of the Bothnian supergroup.

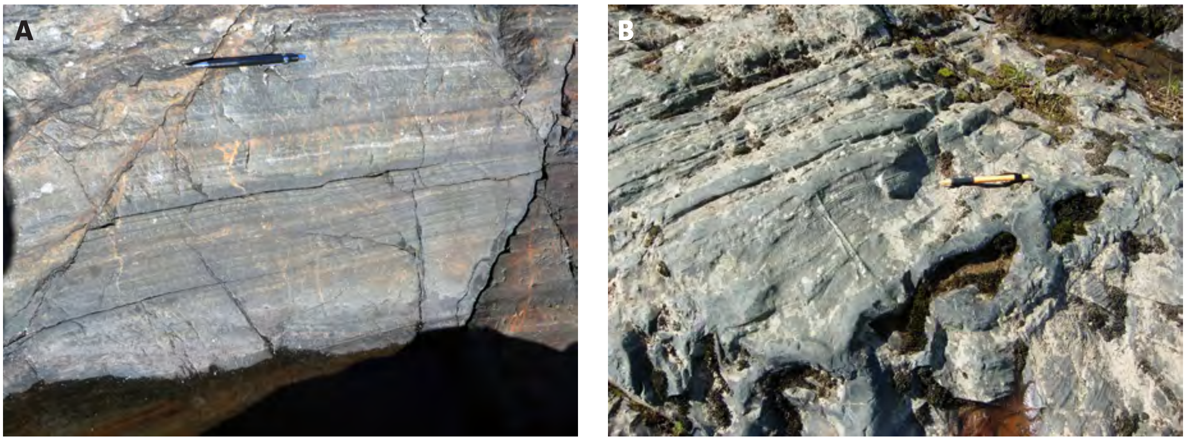

Figure 25. **A.** Banded volcaniclastic metabasaltic rock. Säivisnäs, about 20 km east of Kalix (7324239/890604). Photo: Stefan Bergman. **B.** Layered sequence of basalt and andesite of the Kalix group. Kukkola, about 14 km north-northwest of Haparanda (7345466/909680). Photo: Ulf Bergström.

Figure 26. Dolomite with stromatolite in quartz-rich metasandstone. Säivisnäs, about 21 km east of Kalix (7324574/891957). Photo: Stefan Bergman.

Rocks of the Vitgrundet formation overlie the Karlsborg formation and occur in several limited areas along the coast from Hastaskäret to Säivisnäs. They are mainly dolomites, found in the Kalix archipelago by Gejer (1931), with well-preserved primary structures such as stromatolites (Fig. 26). Southeast of Kalix, layers of quartz arenite are interlayered within the dolomites.

Dolomites of the Vitgrundet formation have been dated at c. 2.1 Ga using the lead isotope method (Öhlander et al. 1992). Variations in the carbon isotope composition throughout the carbonate sequence accord with the global evolution curve (carbon isotopic event) at c. 2.1 Ga (Melezhik & Fallick 2010).

Sockberget group

Karelian metasedimentary rocks are summarised under the name Sockberget group (Silvennoinen et al. 1987, Lundqvist et al. 1996a) and are assigned to the c. 2.2 Ga Jatulian quartzites (Wikström 1996). The Sockberget group is equivalent to the Kuusijärvi quartzite formation (Kuusijärvi *kvartsitformation*) of Sjöstrand et al. (1984).

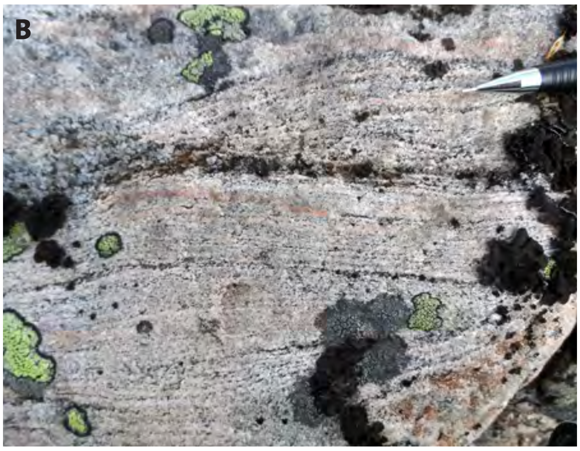

Figure 27. **A.** Folding in metasandstone with mica-rich layers. West of Präntijärvi, about 24 km east-northeast of Kalix. (7333712/894311). **B.** Metatexitic metasandstone. West of Präntijärvi, about 24 km east-northeast of Kalix. (7333712/894311). Photos: Stefan Bergman.

Most of the Sockberget group rocks occur in subarea 8 and in the southeast of subarea 7 (Fig. 17b), to the north and west of Övertorneå. Much of the bedrock is made up of metasandstone, meta-arenite, impure, greyish-white quartzite or meta-quartz arenite and metagreywacke. These rocks normally predominantly comprise quartz and feldspar, with a limited amount of mica-rich layers (Fig. 27a). An alternation of predominantly quartz-feldspar and mica-rich bands is interpreted to represent the original layering in the rocks, although locally the mica layers are considered to originate from flattened remnants of basic rocks. Massive quartzite beds occur and have thicknesses of up to several tens of metres. The rocks have been heavily recrystallised, so primary structures other than the inferred bedding have not been observed. In wide areas, the rocks of the Sockberget group contain minor amounts of fuchsite, resulting in greenish tints.

Fuchsite is a chromium-bearing variety of muscovite, and the anomalous chromium content of Sockberget group rocks is probably due to chromite minerals in heavy mineral fractions. Erosion and relatively short westward transport of chromite from 2.44 Ga, chromite-rich layered intrusions in Finland (Rasilainen et al. 2016) would explain the distribution of fuchsite in the southeast of the project area.

Calc-silicate bands as well as intercalations of basic lavas and volcaniclastic rocks are common. The rocks of the Sockberget group are migmatised to varying degrees (Fig. 27b) and interfused by granites and pegmatites. Veins of quartz and feldspar, irregular-shaped granite inclusions and cross-cutting granite dykes are common. The metagreywackes show gneissic and metatexitic structures, are garnet-bearing and contain intercalations of black shales and mica schists. Locally, cordierite, and in less altered parts of the greywackes, andalusite and staurolite, have been observed. Bands or lenses of mica-rich rocks occur locally as intercalations within the quartzites and are hard to distinguish from sedimentary rocks of the Bothnian supergroup. In general, the Sockberget group rocks show higher susceptibility values, higher potassium content and lower densities than the overlying rocks of the Bothnian supergroup. The Tornio intrusion and related or Archaean rocks constitute the basement of the Sockberget and Kalix groups in the Haparanda area; in all other areas a basement of the Karelian rocks is not exposed.

Rocks of the Sockberget group also occur in subarea 6 (Fig. 17b), southwest of Narken and around lakes Muggträsket and Talljärv, northeast of Gunnarsbyn. Additionally, minor occurrences are situated to the north of Tväredet and to the north of Morjärv.

The Karelian rocks of the Narken area are meta-arenite to metagreywacke, including pure quartzite and mica-bearing quartzite-like rocks (Hellström et al. 2012d, Jonsson & Kero 2013d). They normally

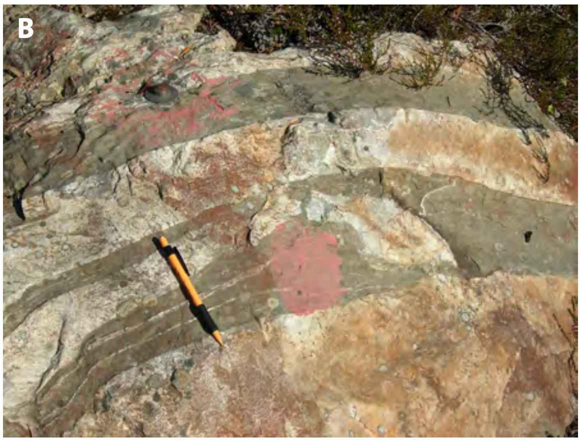

Figure 28. **A.**Quartz-rich metasandstone (quartzite) of the Sockberget group. Talljärv, about 28 km west-southwest of Överkalix (7369435/ 824979). Photo: Benno Kathol. **B.** Mafic sills in metasandstone of the Sockberget group. Talljärv, about 28 km west–southwest of Överkalix (7369435/ 824979). Photo: Ulf Bergström.

show a distinct alternation of quartz-feldspar and biotite-chlorite bands, which is interpreted as primary bedding. Porphyroblasts of potassium feldspar, muscovite and andalusite are locally common. Fuchsite occurs locally, lending a greenish tint to the meta-arenites. Intercalations of basic lavas and volcaniclastic rocks, as well as calc-silicate bands, occur in the west of the area. Certain parts of the metasedimentary rocks probably consist of volcaniclastic material.

The metasedimentary rocks in the Narken area are significantly better preserved than the younger Svecofennian sedimentary rocks of the Bothnian supergroup to the east of Kalixälven; migmatitisation is absent in the rocks at Narken.

The westernmost exposures of the Sockberget group are situated between Pålkem and Överkalix. In the area around lakes Muggträsket and Talljärv, quartz-rich metasandstones occur in the central part of a north–northwest-striking anticline (Bergström et al. 2015b). These rocks are overlain on both sides with a primary depositional contact by younger rocks of the Bothnian supergroup. The metasandstones of the Sockberget group are very fine-grained, light grey to white in colour (Fig. 28a), with preserved primary structures such as bedding and lamination. There are also 1–10 m thick intercalations of grey, mica-rich greywackes and dark grey lava horizons and sills of basaltic composition (Fig. 28b).

Intrusive, supracrustal and metamorphic rocks 1.96–1.75 Ga

Svecofennian supracrustal rocks, c. 1.96–1.92 Ga (Martimo suite)

The Martimo formation was originally defined in Finland by Perttunen (1985), who assigned the group to the informal, 2.05–1.95 Ga Lower Kaleva unit. A minimum age for the Martimo formation of 1880 Ma is given by intrusions of granitoids of the Haparanda suite (Perttunen 1985).

The Martimo formation is part of the Paakkola group (Perttunen et al. 1995, Perttunen & Vaasjoki 2001), which is divided into the sedimentary Martimo formation and the predominantly volcanic Väystäjä formation. The Martimo formation consists of turbiditic mica schists and phyllites with black schist intercalations. The volcanic rocks of the Väystäjä formation are pillowed tholeiitic basalts accompanied by minor tuffites and acid volcanic rocks. (Perttunen & Hanski 2003). Parts of the Paakkola group have subsequently been considered to be lithodemic in nature, and the northern part of the Martimo formation has been renamed the Martimo suite or Martimo Belt (Lahtinen et al. 2015b), whereas the southern part is called the Karunki formation in the Paakkola group.

Three minor occurrences of fine-grained sedimentary rocks, close to the border with Finland to the north and south of the Kukkola gneiss complex, are directly related to rocks of the Martimo suite in Finland and therefore assigned to this suite. In the area around Karlsborg and Sangis, a sequence of metamorphosed fine-grained rocks has previously been assigned to the Råneå group (Åhman et al. 1990, Wikström 1996, Bergman et al. 2014). In map areas 25M Kalix NO and SO, these rocks have been described as slates, schists and siltstones. In map area 25N Haparanda, these rocks have been mapped as fine-grained to finely medium-grained greywackes, fine-grained sandstones and subordinately as schists and phyllites (from the SGU database).

Volcanic intercalations are a characteristic component of this metasedimentary sequence (Wikström 1996). Mafic compositions predominate, but felsic volcanic rocks have been observed at a number of localities, for example in map area 25M Kalix NO (Wikström 1996). In map area 25N Haparanda NV, similar volcanic rocks have been found in the Risijärvi area. There, rhyolitic and dacitic intercalations occur within lower amphibolite facies siltstones and greywacke (Bergström et al. in preparation-b). A rhyolite from this area has yielded a U-Pb zircon age of c. 1.93 Ga (Bergström et al. in preparation-b). Based on this age, the metasedimentary sequence in the Karlsborg–Sangis area is assigned to the 1.96–1.92 Ga Martimo suite rather than to the c. 1.92–1.87 Ga Råneå group.

Early Svecokarelian intrusive rocks, c. 1.96–1.92 Ga (Norvijaur intrusion)

The Norvijaur intrusion mainly consists of metamorphosed granodiorite, granite and subordinate tonalite, the granites locally being considered intrusions or dykes in the granodiorite (Fig. 29). Multi-element and rare earth element (REE) diagrams indicate a close relationship between the granodiorite and the granite, and both rock types are interpreted as being more or less coeval. Minor pods of quartz monzonite to dioritoid occur and show contact relationships to the granodiorite, suggesting that these rocks also are coeval with the main intrusion. The granitoids are normally medium-grained, but fine-grained varieties occur widely and are interpreted as probable subvolcanic intrusions.

Figure 29. Grey granodiorite and light grey granite from the Norvijaur intrusion. Noarvejávrre, about 24 km west of Jokkmokk (7392060/690320). Photo: Lotta Olausson.

The metagranitoids of the Norvijaur intrusion have previously been dated (U-Pb on zircon) at 2 010 ± 40 Ma (TIMS, Skiöld & Larsson 1978) and 1 926 +13/-11 Ma (TIMS, Skiöld et al. 1993). Renewed dating using U-Pb SIMS techniques yielded an age of 1 930 ± 6 Ma (Hellström 2015). The ages obtained are similar to those obtained from the Knaften area south of the Skellefte District (Wasström 1993, 1996, 2005), from the central Bothnian Basin at Husum and Setjärn (Lundqvist et al. 1998), from the Barsele area (Eliasson et al. 2001) and from intrusions in the Robertsfors group (Skiöld & Rutland 2006). Two samples from the Norvijaur intrusion show slightly positive $\varepsilon_{Nd\ (T=1890\ Ma)}$ values, indicating that the melts of this intrusion do not have a major Archaean source rock component (Öhlander et al. 1993).

The rocks of the Norvijaur intrusion are more or less penetratively deformed and locally display a folding of the foliation. The rocks show low potassium (1.4–3.2%), uranium (0.7–3.5 ppm) and thorium content (4.4–11.0 ppm). Their density lies between 2 639 and 2 856 kg/m^3, with somewhat higher densities in the eastern part of the intrusion.

The Norvijaur intrusion gives rise to a heart-shaped high-magnetic anomaly (Fig. 30a). The susceptibility values measured on petrophysical samples range from 80 to 2 500 × 10^{-5} SI units, with a median value of 1 500 × 10^{-5} SI units. A three-dimensional susceptibility model was constructed using inverse modelling technique to illustrate the shape and the depth distribution of the intrusion. The cell size was set at 250 × 250 × 125 m and the model is restricted to susceptibility values of between 1 and 10 000 × 10^{-5} SI units.

The result of the modelling is shown in Figure 30b, where a susceptibility isosurface of 1 500 × 10^{-5} SI units was chosen to visualise the susceptibility distribution that would cause the observed magnetic field. The model shows a bowl-shaped body, with inward-dipping contacts, the western contact being clearly steeper. It also shows moderately dipping contacts in the east and more flat-lying contacts to the northeast. According to the model, the intrusion has a minimum depth of 4 km in its southern and middle section. However, it is difficult to obtain reliable indications about the contact relationships in the northern part of the intrusion due to the lack of anomalies.

Three massifs of granodiorite to tonalite surrounded by metasedimentary rocks of the Bothnian supergroup occur to the west of the Norvijaur intrusion. The two northern massifs show REE patterns similar to that of the Norvijaur intrusion and are therefore considered to be related to the latter (Hellström & Berggren in press).

Due to the age relationships of the Norvijaur intrusion and the surrounding supracrustal rocks, the Norvijaur intrusion and the two massifs to the west constitute a basement to the Svecofennian supracrustal rocks in the area. The granitoid of the Norvijaur intrusion has been weathered in situ and the weathering surface is overlain by immature arkosic metasandstones and conglomerates, passing upwards into metagreywackes with intercalations of tuffites and mafic metalavas (Skiöld et al. 1993). On top of that follow meta-argillites and at the top of the sequence a calcitic marble. Thus, there must have been a hiatus due to weathering and depositional contact. The sedimentary sequence is about 800 m thick (Markkula 1977, Skiöld et al. 1993) and is cut by the 1 876 ± 6 Ma Juoksjokko granite (Skiöld et al. 1993).

Claeson & Antal Lundin (in press-a) describe the contact between the Norvijaur intrusion and the volcanic rocks to the north of it as a primary depositional contact, but with a deformation zone that is tens of metres thick and only affects the granitoid. The authors interpret the rocks within the zone to be deformed granitoids and assume these rocks correspond to the arkose and quartzite layer described by Markkula (1977). Claeson & Antal Lundin (in press-a) still postulate the depositional character of the contact, but assign the overlying rocks as recrystallised and hydrothermally altered volcanic rocks, including volcaniclastic rocks of varying composition from rhyolitic to basaltic (Fig. 31). Högbom (1931) denominates the bedrock in this area as consisting of "leptites" with intercalations of mica schists, epiclastic rocks and agglomerates. Here we assign these rocks to the 1.90–1.87 Ga Porphyrite group.

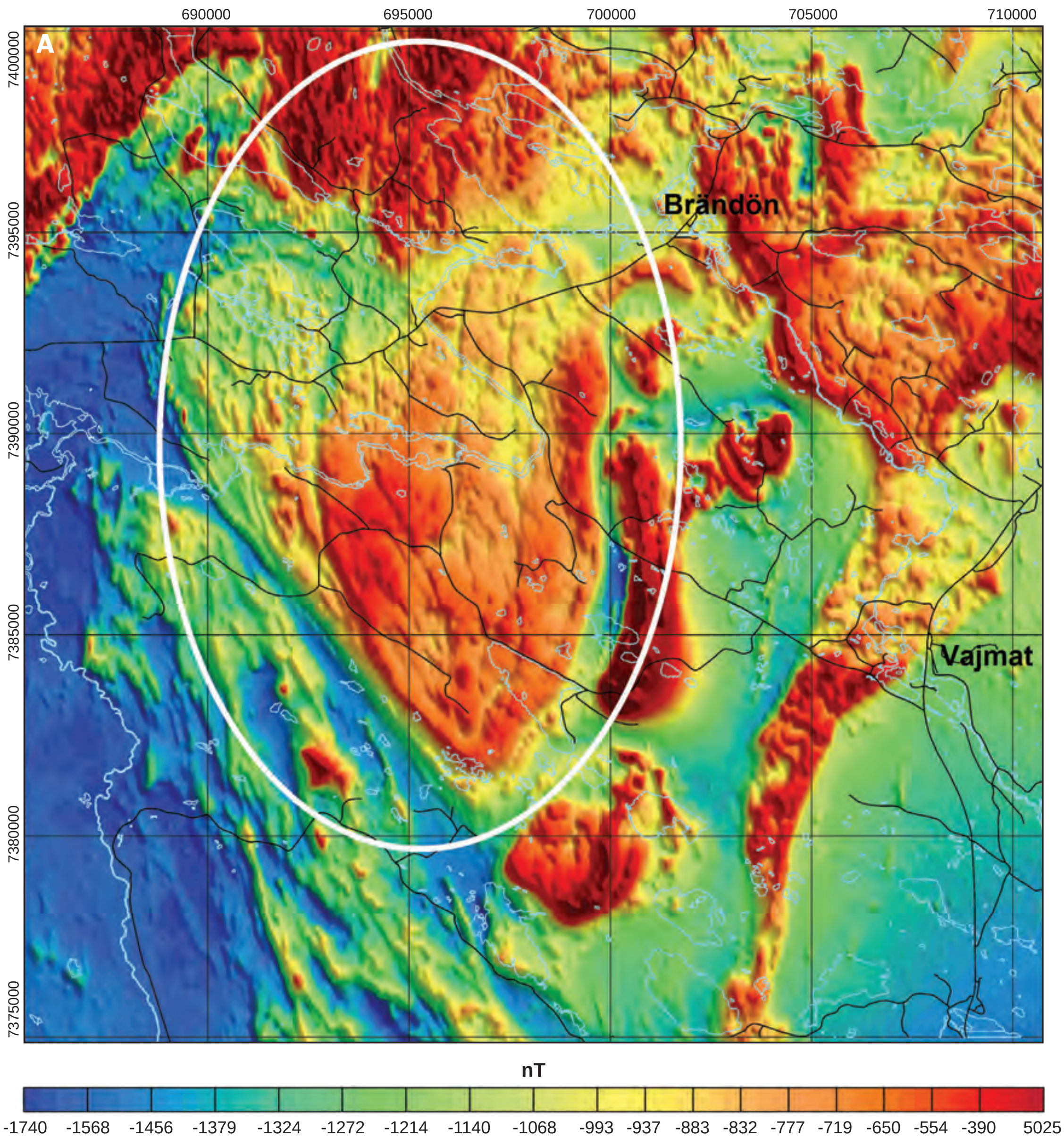

Figure 30. **A.** Magnetic anomaly map of the Noarvejávrre area. The heart-shaped Norvijaur intrusion is marked with a white ellipsoid. The location of the model area is shown in Figure 16.

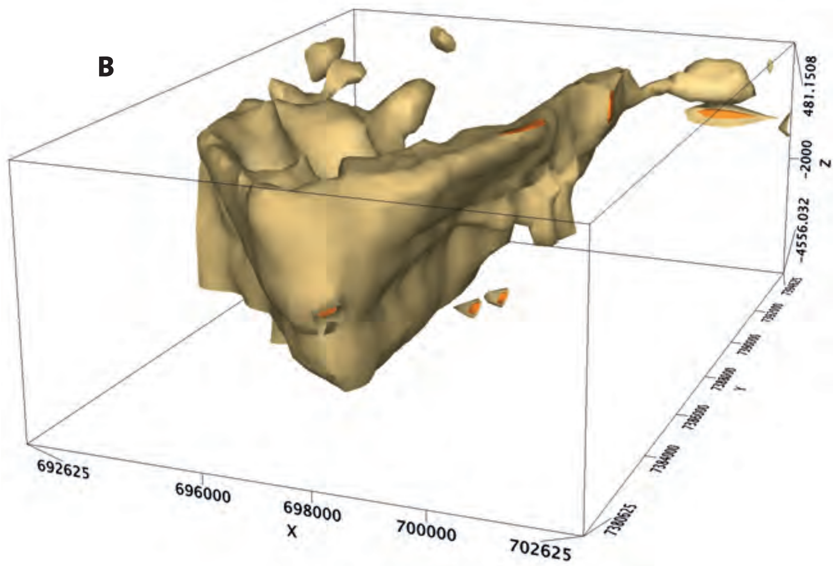

Figure 30. **B.** The three-dimensional susceptibility model presented as a susceptibility isosurface of 1500×10^{-5} SI units. View from the south-southeast.

Figure 31. Hydrothermally altered and strongly deformed basic volcanic rocks. Noarvejávrre, about 24 km west of Jokkmokk (7394185/689858). Photo: Benno Kathol.

Svecofennian supracrustal rocks, c. 1.92–1.87 Ga (Bothnian supergroup)

Svecofennian metasedimentary rocks, mainly greywackes in the Bothnian Basin (Hietanen 1975, Kumpulainen 2009), which were deposited as turbidites to the southwest of the Archaean basement, are connoted as the Svecofennian Härnö group on the Bedrock Map of Central Fennoscandia (Lundqvist et al. 1996a) and in the description accompanying the map (Kousa & Lundqvist 2000a).

In the Luleå area northeast of the Bothnian Basin, c. 2.1–1.9 Ga Kalevian-type phyllites, schists and greywackes, resting on the Archaean basement, are gathered under the name Råneå group on the Bedrock Map of Central Fennoscandia (Lundqvist et al. 1996a, Lukkarinen & Lundqvist 2000). Those authors considered the sedimentary rocks of the Råneå group to be transitional in age to the greywackes of the Svecofennian Härnö group in the Bothnian basin (Hietanen 1975). The boundary between the two groups is arbitrarily drawn on the Bedrock Map of Central Fennoscandia (Lundqvist et al. 1996a, Lukkarinen & Lundqvist 2000).

In southern Norrbotten County, metasedimentary rocks that are older than 1.87 Ga and are deposited in large sedimentary basins either constitute a northern extension of the Svecofennian Härnö group or have been assigned to the Råneå group (Silvennoinen et al. 1987, Lundqvist et al. 1996a).

The bedrock map of the Regional geological and geophysical maps of the Skellefte District and surrounding areas (Kathol et al. 2005) draws no distinction between similar lithologies, whether they are resting on an Archaean basement or on an unknown substratum. The transitional rocks of the Råneå group are therefore included in what was called the Bothnian supergroup by Kathol & Weihed (2005).

Metasedimentary rocks in the Överkalix lithotectonic unit, partly affected by deformation in the Pajala deformation belt (Luth et al. 2018b), were assigned to the Råneå group by Silvenoinen et al. (1987) and Lundqvist et al. (1996a). Lahtinen et al. (2015-a) collectively named hornblende-bearing metasedimentary rocks, metapelites and meta-arkose to orthoquartzite, which at least partly correspond to the Råneå group in the Pajala deformation belt, the Uusivirka Suite. Provenance studies by detrital zircon analyses yielded ages between 1.96 Ga and 1.91 Ga (Lahtinen et al. 2015-a), which results in a maximum depositional age of c. 1.91 Ga. This is younger than previously assumed by Silvenoinen et al. (1987) and Lundqvist et al. (1996a). Thus, we consider the Råneå group not to be of Kalevian type as Lukkarinen & Lundqvist (2000) state, but to be coeval with the Svecofennian metasedimentary rocks in the Bothnian Basin (cf. Kathol & Weihed 2005) and in sedimentary basins to the north. For this reason, we follow Kathol & Weihed (2005) and include the Råneå group in the Bothnian supergroup.

In the Bothnian Basin proper (Hietanen 1975), the sedimentary sequence of the Bothnian supergroup was intruded by Svecokarelian granitoid magmas at c. 1.95 Ga at Knaften (Wasström 1993, 1996, 2005), at 1.93 Ga at Husum and Seltjärn (Lundqvist et al. 1998) and in the timespan 1.92–1.87 Ga by magmas of the Jörn GI and Haparanda suites (Bergman et al. 2001, Kathol & Weihed 2005 and references therein). Detrital zircons found in low-grade greywackes of the Bothnian Basin range in age from 2.97 to 2.60 Ga and 2.12 to 1.88 Ga (Claesson et al. 1993). Thus, sedimentation in the Bothnian Basin proper started before 1.95 Ga and continued up to at least 1.87 Ga.

Rocks of the Bothnian supergroup occur in all three lithotectonic units (SGU 2017) in the project area, i.e. the Norrbotten and Överkalix lithotectonic units to the northeast, and within the Bothnia–Skellefteå lithotectonic unit southwest of the Luleå–Jokkmokk zone.

In most areas, the Bothnian supergroup has been intruded by early Svecokarelian rocks of the Haparanda, Jörn GI and Perthite monzonite suites as well as late Svecokarelian 1.81–1.75 Ga rocks of the Edefors and Lina suites. In the Narken area west of Korpilombolo, in the Tallberg area southeast of Pålkem, in several areas between Överkalix and Övertorneå and north and east of Morjärv, the Bothnian supergroup is interpreted to overly the Karelian Sockberget group. This stratigraphic relationship is demonstrated northwest of Muggträsket between Pålkem and Överkalix, where metagreywackes of the Bothnian supergroup contain rounded clasts of quartzite of the adjacent Sockberget group (Fig. 32).

The majority of metasedimentary rocks of the Bothnian supergroup northeast of the Luleå – Jokkmokk zone occur in a north–northeast-striking belt between Råneå in the south and the area between Korpilombolo and Pello in the north, in the following called the Råneå–Pello belt. In the Överkalix area, the belt shows an offset along the western margin of the Pajala deformation belt that divides it into a northern zone, mainly situated in the Överkalix lithotectonic unit, and a southern zone in the Norrbotten lithotectonic unit. Minor occurrences northeast of the Luleå–Jokkmokk zone, outside the above-mentioned belt, are situated south of Hakkas and north of Boden. Southwest of the Luleå–Jokkmokk zone, metasedimentary rocks of the Bothnian supergroup crop out in widely dispersed, fairly small areas.

The rocks in the northern zone of the Råneå–Pello belt in the Överkalix lithotectonic unit have normally been identified as metagreywackes, but in the far northeast of the zone, meta-arkoses and paragneisses have been mapped as the predominant rock types in the Bothnian supergroup. Both greywackes and arenites are present in the Narken area, and the sedimentary bedrock south of Hakkas has mainly been described as consisting of paragneisses. Bedding has been frequently observed in arkoses and greywackes in the northwest of the northern zone north of Korpilombolo and somewhat less frequently in the same rock types in the central part of the zone. Bedding is a common structure in greywackes in the Narken area to the west of Korpilombolo, and also occurs in the area south of Hakkas (Fig. 33a).

In the central part of the southern zone of the Råneå–Pello belt in the Norrbotten lithotectonic unit and in the archipelago south of Kalix, the Bothnian supergroup comprises mainly mudstones and slates with intercalations of volcaniclastic rocks, carbonate rocks, black shales, quartzites and phyllites. These rocks have been metamorphosed to varying degrees.

Figure 32. Rounded quartzite clast of the Sockberget group in metagreywackes of the Bothnian supergroup. Stor-Muggberget, about 26.5 km west of Överkalix (7377631/824454). Photo: Ulf Bergström.

Well-preserved rocks with primary structures have been observed in the west of the southern zone. Bedding and cross-bedding normally occur in greywackes, arenites and mudstones, but are also present in rocks identified as migmatitic mudstones around Råneå. Bedding also occurs in two areas northeast of Boden. Graded bedding has been reported in partly migmatised mudstones from some places east of Råneå (Fig. 33b). Well-preserved rocks with intercalations of mudstone and sandstone show syngenetic erosion structures with sand-filled channels in muddy layers (Fig. 33c).

In most cases, metasedimentary rocks of the Bothnian supergroup in the Bothnia–Skellefteå lithotectonic unit to the southwest of the Luleå–Jokkmokk zone are denominated as paragneisses, except for two areas, one southwest of Vuollerim and one southeast of Luvos. The rocks in the former area have been mapped as greywackes and sandstones, those in the latter as mudstones and greywackes.

In the Bothnia–Skellefteå lithotectonic unit, bedding has only been observed at a few places in better preserved greywackes and sandstones at Harads, southwest of Vuollerim, northwest of Trollforsen and south of Luvos. Other primary structures such as roundness of grains and degree of sorting have been observed in sandy layers southwest of Vuollerim and sorting in greywackes to the east of Kåbdalis.

Tectonic foliation and banding is the most ubiquitous structure in the metasedimentary rocks of the Bothnian supergroup. Gneissic structures are common in the centre and north of the northern zone of the Råneå–Pello belt in the Överkalix lithotectonic unit, in the area south of Hakkas in the Norrbotten lithotectonic unit, and in almost all occurrences of the Bothnian supergroup in the Bothnia–Skellefteå lithotectonic unit (Fig. 34).

Figure 33. **A.** Examples of primary structures in the Bothnian supergroup. A. Metagreywacke with primary bedding. Askasvaara, about 16 km south of Hakkas (7420913/789939). Photo: Fredrik Hellström.

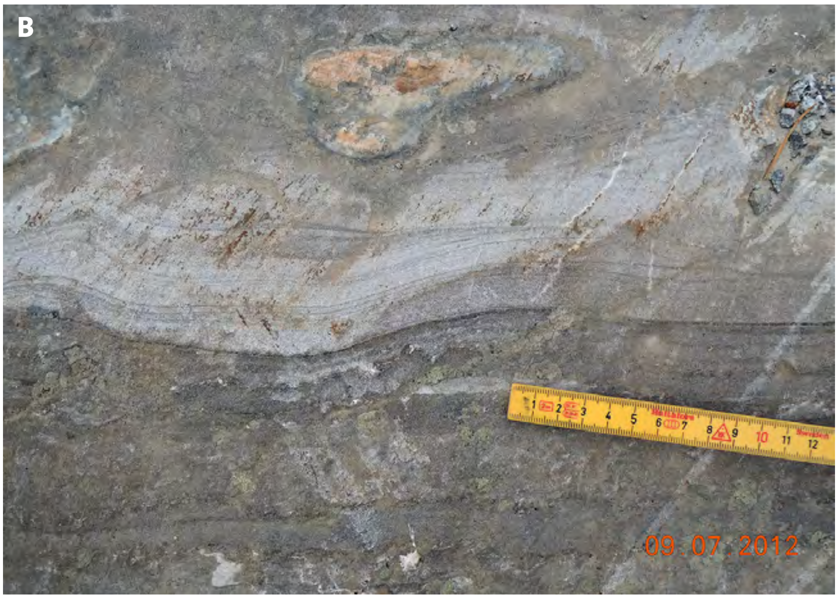

Figure 33. **B.** Well-preserved mudstone with thin beds of sandstone and normal grading. Note the skarn lenses towards the top of the photo. Rödberget, about 4.5 km east-northeast of Råneå (7324485/836425). Photo: Risto Kumpulainen.

Figure 33. **C.** Sand-filled erosional channel in mudstone layer, overlain by mudstone and sandstone layers. Hötäskkölen, about 7.8 km south of Råneå. Photo: Risto Kumpulainen.

Figure 34. Strongly deformed stromatic migmatite in the Bothnia-Skellefteå lithotectonic unit. Älvsborg, about 29 km east-northeast of Moskosel (7323765/729299). Photo: Benno Kathol.

Lineation is commonly developed in greywackes, paragneisses and migmatites of the Råneå–Pello belt, except for the arkoses in the northeast of the northern zone. In the occurrences of the Bothnian supergroup southwest of the Archaean boundary (Luleå–Jokkmokk zone), lineation is reported only from a sandstone southwest of Vuollerim, greywackes and quartzite at and east of Luvos, and from a sedimentary rock northeast of Varjisträsk.

Folding is common in almost all areas featuring rocks of the Bothnian supergroup, and it affects primary bedding (Fig. 35a) or secondary structures such as schistosity, gneissic structures or migmatitic veining. Fold structures are either regularly shaped or show refolding (Fig. 35b).

Partial melting has affected almost all rocks in the Norrbotten and Överkalix lithotectonic units and results in (Fig. 36a) the generation of metatexitic, stromatic and diatexitic migmatites. Schollen migmatites have been described from the area north of Boden, close to Tallberg southeast of Pålkem (Fig. 36b), and the area around Råneå in the southern zone of the Råneå–Pello belt.

Metatextic and stromatic structures (Fig. 34) have also been described in the Bothnia-Skellefteå lithotectonic unit, but are less common than in the Råneå–Pello belt.

Skarn lenses occur in migmatitic metagreywackes (Fig. 37a), in meta-arenites in the Narken area (Fig. 37b) and also in well-preserved greywackes and mudstones (Fig. 33b). Aluminosilicates are common in several types of the metasedimentary sequences and indicate protoliths with large amounts of phyllosilicates, such as mudstones and fine-grained layers of greywackes.

Cordierite occurs mainly in metagreywackes and paragneisses at several places in the northern zone, the north of the southern zone and southwest of Luvos (Fig. 38a). At Kvänberget southwest of Kåbdalis, abundant cordierite gives a patchy pattern on weathered surfaces of a paragneiss (Fig. 38b). Garnet has been frequently reported from the southern zone of the Råneå–Pello belt, from areas south of Hakkas, Korpilombolo and Luvos (Fig. 38a) and west of Kåbdalis. It occurs in sandstones, mudstones,

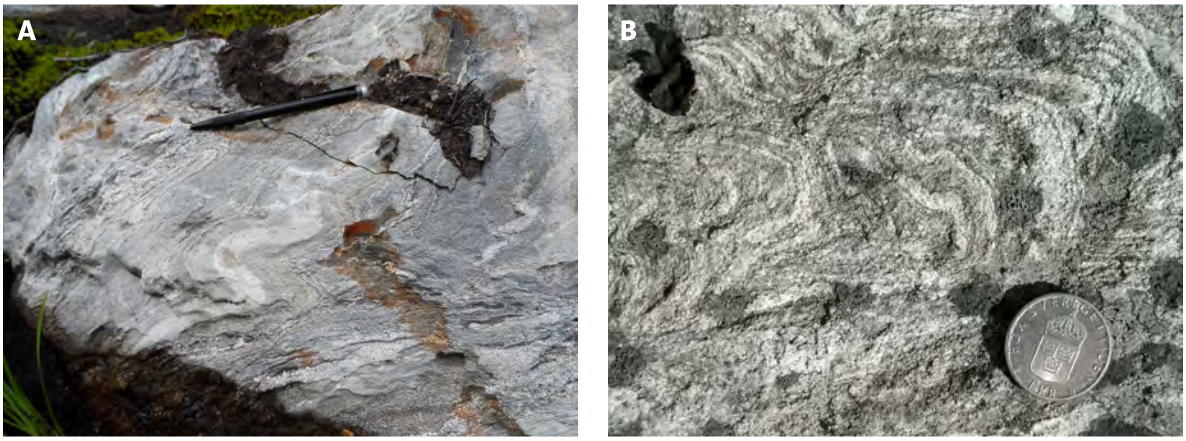

Figure 35. **A.** Metagreywacke and metasandstone showing primary bedding, foliation and veining, all deformed along flat-lying folds. Holmträsket, about 19 km northeast of Gunnarsbyn (7361988/817855). Photo: Stefan Bergman. **B.** Refolded folds in paragneiss. Kvänberget, about 8 km southwest of Kåbdalis (7341833/717901). Photo: Benno Kathol.

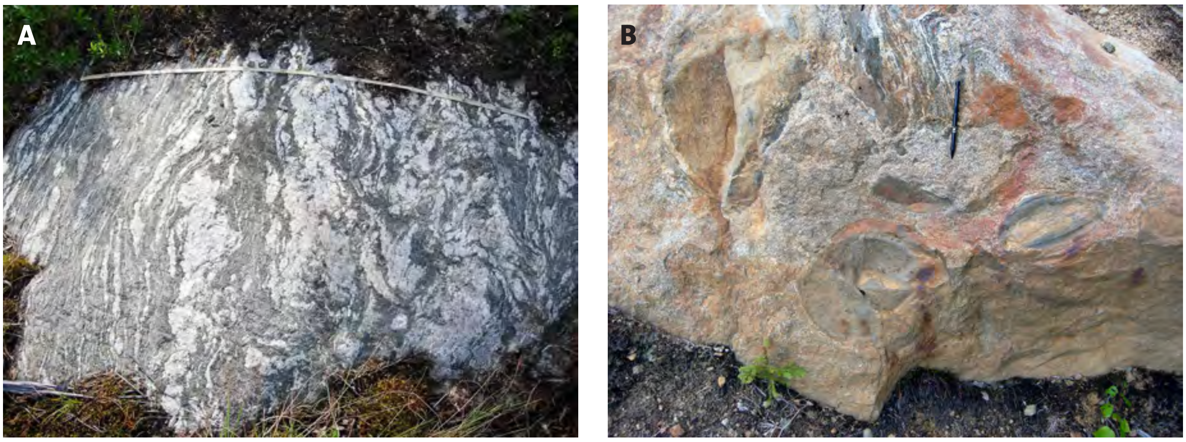

Figure 36. **A.** Migmatitic meta-argillitic gneiss showing veining and folding. Ketunkallio, about 25 km northwest of Övertorneå (7411296/873089). Photo: Vladislav Stejskal. **B.** Schollen diatexitic greywacke. Orrkölen, about 19.5 km east-southeast of Pålkem (7369758/812518). Photo: Ulf Bergström.

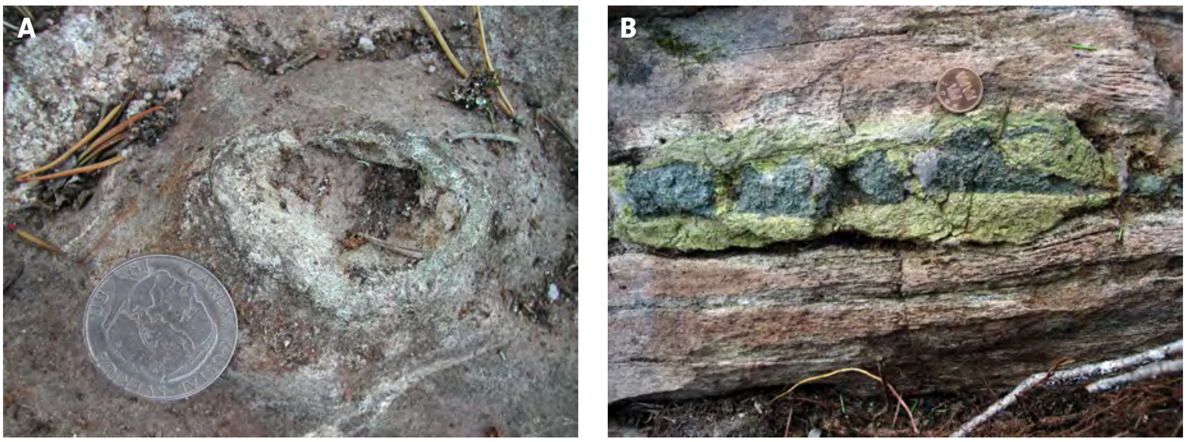

Figure 37. **A.** Skarn lens in paragneiss. Anders Persaberget, about 12 km north-northwest of Vidsel (7323692/748177). Photo: Benno Kathol. **B.** Skarn lens of dark green amphibole and light green epidote in meta-arenite. Lehmäjänkkä, about 20 km west of Korpilombolo (7435922/832715). Photo: Fredrik Hellström.

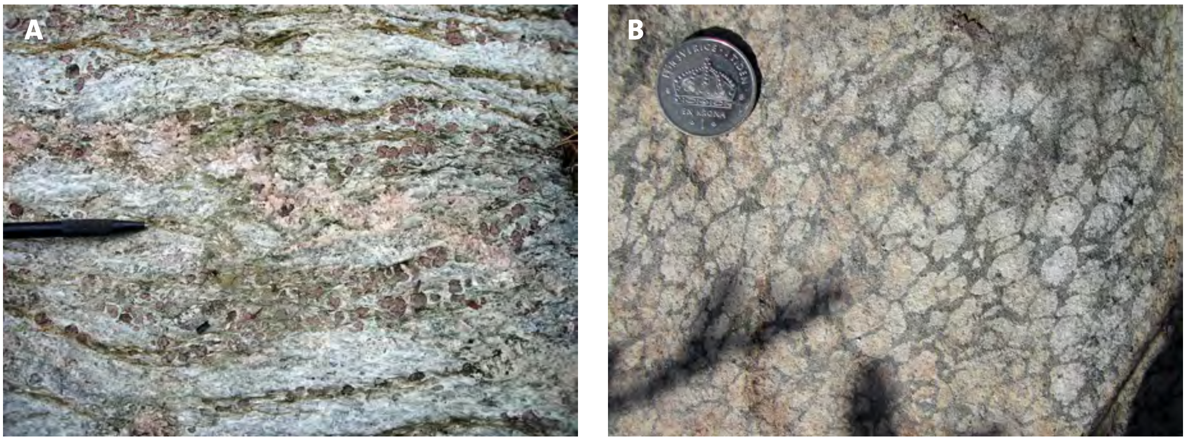

Figure 38. **A.** Garnet-, sillimanite- and cordierite-bearing paragneiss. Luspevárásj, about 4 km southwest of Luvos (7393986/668060). Photo: Fredrik Hellström. **B.** Cordierite patches in paragneiss. Kvänberget, about 8 km southwest of Kåbdalis (7341783/717902). Photo: Benno Kathol.

greywackes, paragneisses and migmatites; it is worth noting that garnet has not been found in the arkoses of the northern zone of the Råneå–Pello belt. Sillimanite occurs in the north of the northern zone, south of Korpilombolo and in the area southwest of Luvos (Fig. 38a). Andalusite has been reported from three places in migmatites between Boden and Råneå.

In the northern zone of the Råneå–Pello belt, amphibole is more or less common in greywackes, arkoses, arenites and paragneisses. Epidote has been observed in different rock types of the Bothnian supergroup in several scattered areas, mainly in the east and south of the project area. Epidote occurs together with amphibole in skarn lenses in the Narken area west of Korpilombolo (Fig. 37b). Beryl has been found in paragneiss and arkose east of Korpilombolo and in a gneiss northwest of Vidsel. Biotite is ubiquitous in all areas and rock types of the Bothnian supergroup, with the exception of the mudstones and greywackes in the centre of the southern zone. Scattered observations of graphite have been made south of Hakkas, in the centre of the northern zone, north of Boden and Råneå and southeast of Luvos.

Magnetite or pyrrhotite occurrences have been observed south of Hakkas, in the Narken area west of Korpilombolo, in the northern zone, north of Boden and southwest and southeast of Luvos. Pyrite and other sulphide minerals are described from the Narken and Korpilombolo area, the central part of the Råneå–Pello belt, the area north of Boden, northwest of Råneå, west of Kåbdalis and south and southeast of Luvos.

In several areas, for example east of Lövnäs and southwest of Vuollerim, the metasedimentary rocks of the Bothnian supergroup have been intruded by late Svecokarelian granitic magmas, which now form minor massifs of the Lina suite. These granites are more resistant to weathering and outcrop as smallish hills, whereas the metasedimentary rocks are found in small outcrops lower down the hills, and supposedly also occur in the non-exposed lowlands between the hills. This can lead to misinterpretation of the bedrock in areas where there is no difference in the magnetic properties between intrusive and metasedimentary rocks on the magnetic anomaly map.

Intercalations of basalt and andesite in the metasedimentary sequence occur to the north and west of Korpilombolo, in north–south-striking zones between Vidsel and Boden and to the north of Harads. In the last-mentioned area, bedding has been observed in several places, and the mafic volcanic rocks have been interpreted as volcaniclastic sequences in the paragneisses. One sizeable occurrence of strongly foliated dacite and rhyolite is situated north of Vidsel and has been assigned to the Bothnian supergroup (Kathol et al. 2012b).

Two marble occurrences, one northwest and one southwest of Råneå, are embedded in migmatised metagreywackes of the Bothnian supergroup.

Locally, the occurrences of metasedimentary rocks of the Bothnian supergroup are outlined by uniform low-magnetic or uniform banded patterns on the magnetic anomaly map. In the Råneå–Pello belt and in areas situated below the highest coastline, the relationship between magnetic anomalies and the occurrences of metasedimentary rocks is proven by high outcrop density and field observations.

Delineation of the Bothnian supergroup is more problematic in the west of the project area, i.e. in subareas 1 and 2, particularly south of Luvos, where the rocks of the Bothnian supergroup occur as megaxenoliths in intrusive rocks of the Perthite monzonite suite and both show very similar magnetic signatures. These megaxenoliths are proven only by a few field observations, but their existence is confirmed by gravity anomalies, and the outlines have been drawn following contrasts on the magnetic anomaly map.

Svecofennian supracrustal rocks c. 1.90–1.87 Ga (Porphyrite group)

Within the project area, Svecofennian volcanic rocks are divided into the Porphyrite and the Arvidsjaur groups. This is mainly due to different age intervals for the evolution of different volcanic arc systems and related deposition of the volcanic sequences of either group (see below). Thus, this division is less dependent or not dependent at all on major differences of internal structures.

Volcanic sequences, now assigned to the Porphyrite group by Offerberg (1967), Martinsson & Perdahl (1995) and Bergman et al. (2001), occur in the north of Norrbotten County. These rocks were formerly included in the Svionian Kiruna–Arvidsjaur series (*Kiruna–Arvidsjaurserien*) by Ödman (1957).

Offerberg (1967) classified porphyritic basalts and andesites with minor intercalations of felsic volcanic rocks in the Kiruna area under the name Porphyrite group (*Porfyritgruppen*) and distinguished this group from the younger Kiruna porphyries (*Kirunaporfyrerna*). He also stated there was no sharp dividing line (boundary) between the groups. The Porphyrite group probably represents the oldest Svecofennian volcanic rocks in that area (Offerberg 1967).

Martinsson & Perdahl (1995) followed this division of the Svecofennian volcanic rocks into a stratigraphically lower Porphyrite group and upper Kiruna porphyries based on geochemical properties and tectonic settings and extended it into all of northern Norrbotten County. The volcanic rocks of the Porphyrite group predominantly comprise andesites, showing arc-type signature with low titanium, zirconium and chromium content, but high alkali content, the latter probably reflecting high alkali contents in the crust. The calc-alkaline phase of the Porphyrite group represents early stages of Svecokarelian magmatism on an Archaean continental margin, with crustal reworking and magmatism and predominantly intermediate products. Lundqvist et al. (1996a) placed the Skellefte group together with the Porphyrite group, and the Arvidsjaur group together with the Kiruna porphyries in two different stratigraphic units.

During mapping of map areas 25J Moskosel in southern Norrbotten County, the existence of terrestrial subaerial volcanic rocks older than the 'classic' Arvidsjaur group rocks was indicated by field relationships and indirectly by radiometric dating of a granodiorite of the Jörn GI suite (Kathol & Persson 2007a). Radiometric dating of the volcanic rocks was therefore carried out. A U-Pb zircon age of 1 880 ± 6 Ma (Kathol et al. 2008a) was obtained from a coherent feldspar porphyritic rhyolite within a mainly volcaniclastic sequence at Trollforsen, northwest of Moskosel. This age suggests the existence of a shallow basin with volcanic-derived infill before the development of the Arvidsjaur volcanic arc. The volcaniclastic sequence of the Trollforsen–Abmoälven area is therefore considered to have been deposited in a back-arc environment and derived from a terrestrial volcanic arc that was active before the Arvidsjaur terrestrial arc (Kathol et al. 2008a). Consequently, these 'older' subaerial volcanic rocks have been distinguished from the rocks of the Arvidsjaur group in map area 25J Moskosel (Hartvig & Aaro 2012a, b; Kathol & Aaro 2012).

U-Pb zircon ages of volcanic rocks significantly older than 1.88 Ga have been obtained for a rhyolite from Skuppesavon (1 890 Ma; Hellström in preparation-a), a dacitic migmatitic gneiss from Snierraudden (1 890 Ma; Hellström in preparation-b), a rhyolite to trachyte from Lagmansgraven (1 890–1 880 Ma;

Claeson et al. in preparation) and a rhyolite from Junitjakatj (1880 Ma; Hellström in preparation-c) In addition, U-Pb zircon dating of a rhyolite from Stasskölhuvudet, southwest of Gunnarsbyn and a rhyolite to dacite from Grassmyberget, east of Boden yielded ages of 1886 ± 4 Ma and 1884 ± 5 Ma, respectively (Sadeghi & Hellström 2015).

The ages obtained confirm the existence of a magmatic arc older than the arc that formed the volcanic rocks of the Arvidsjaur group. This magmatic arc is situated somewhere between the Arvidsjaur magmatic arc and the magmatic systems that formed the Porphyrite group of Martinsson & Perdahl (1995) and Bergman et al. (2001), and the Kiruna porphyries to the north of the project area. We therefore divide the volcanic rocks of the project area into the 'classic' Arvidsjaur group and an older group, which here is correlated with, and included in, the Porphyrite group of Bergman et al. (2001). The latter is based on consistent ages for the deposition of the older Svecofennian volcanic rocks in northern Norrbotten County and the project area.

Volcanic sequences of the Porphyrite group occur in the project area, in both the Bothnia–Skellefteå and the Norrbotten lithotectonic units and to a limited extent also in the Överkalix lithotectonic unit. However, it should be noted that the Porphyrite group in the project area is bimodal and contains more felsic volcanic rocks than does the Porphyrite group within the map area for northern Norrbotten County (Bergman et al. 2001).

In most areas, felsic volcanic rocks (rhyolite and dacite to rhyolite) are the predominant rock type in the Porphyrite group. Mafic volcanic rocks predominate only in the area southwest of Överkalix and southwest of Boden; in the Överkalix lithotectonic unit only mafic rocks have been observed within the Porphyrite group. Trachytoid rocks occur northwest of Tjåmotis, forming the basement of the Snavva–Sjöfallet group. Between Luvos and Arjeplog, the felsic volcanic rocks of the Porphyrite group occur as elongated megaxenoliths, oriented parallel to the Karesuando–Arjeplog deformation zone (KADZ), within a major intrusion of the Perthite monzonite suite.

Sedimentary sequences with metamorphic sandstones, mudstones and greywackes of extension varying between one and ten kilometres occur to the northwest of Tjåmotis, south of Kåbdalis and in limited areas between Moskosel, Trollforsen and Kåbdalis. The greywacke sequence at Tjåmotis hosts two stratiform iron mineralisations west and northwest of Tjåmotis, respectively. West of Jokkmokk, a lens of marble is intercalated with basalts and andesites of the Porphyry group that rest on the Norvijaur intrusion.

Coherent textures occur locally in andesites and dacites. Subvolcanic intrusions mainly show rhyolitic and dacitic and subordinate andesitic compositions. Basaltic and andesitic lavas have been observed locally north of Moskosel, northwest of Gunnarsbyn and southwest of Boden. Rhyolitic lavas occur in the megaxenoliths of the Porphyrite group northeast of Arjeplog. Volcaniclastic varieties occur mostly in rhyolites, are less frequent in dacites and andesites and almost absent in basalts. A classification into coherent, subvolcanic and volcaniclastic rocks and lavas has not been applied in the Överkalix lithotectonic unit, possibly due to high metamorphic grade.

The predominant rock type in the occurrences around Korpilombolo is andesite. Scattered occurrences between Korpilombolo and Överkalix consist of amphibolite, paragneiss and greywacke. In the north of subarea 8, andesite is the predominant rock type, with subordinate amphibolite, ultramafic rock and sedimentary rock. The volcanic rocks southwest of Överkalix have bimodal compositions with andesite-basalt and rhyolite.

Dacite and rhyolite are somewhat more frequent than andesite and basalt in the Svartlå–Gunnarsbyn–Pålkem area, with subordinate occurrences of quartzite and ultramafic rock. South of Pålkem, the observed rocks vary in composition between dacite and andesite. On the geological map of the project area, these rocks are included in the dacite-rhyolite unit. Scattered minor occurrences between Hakkas and Lansjärv mainly consist of dacite. Southwest of Boden, felsic and mafic volcanic rocks with minor intercalations of greywacke occur on both sides of the Luleå–Jokkmokk zone.

The rocks of the Porphyrite group in the Moskosel–Trollforsen–Kåbdalis area are predominantly

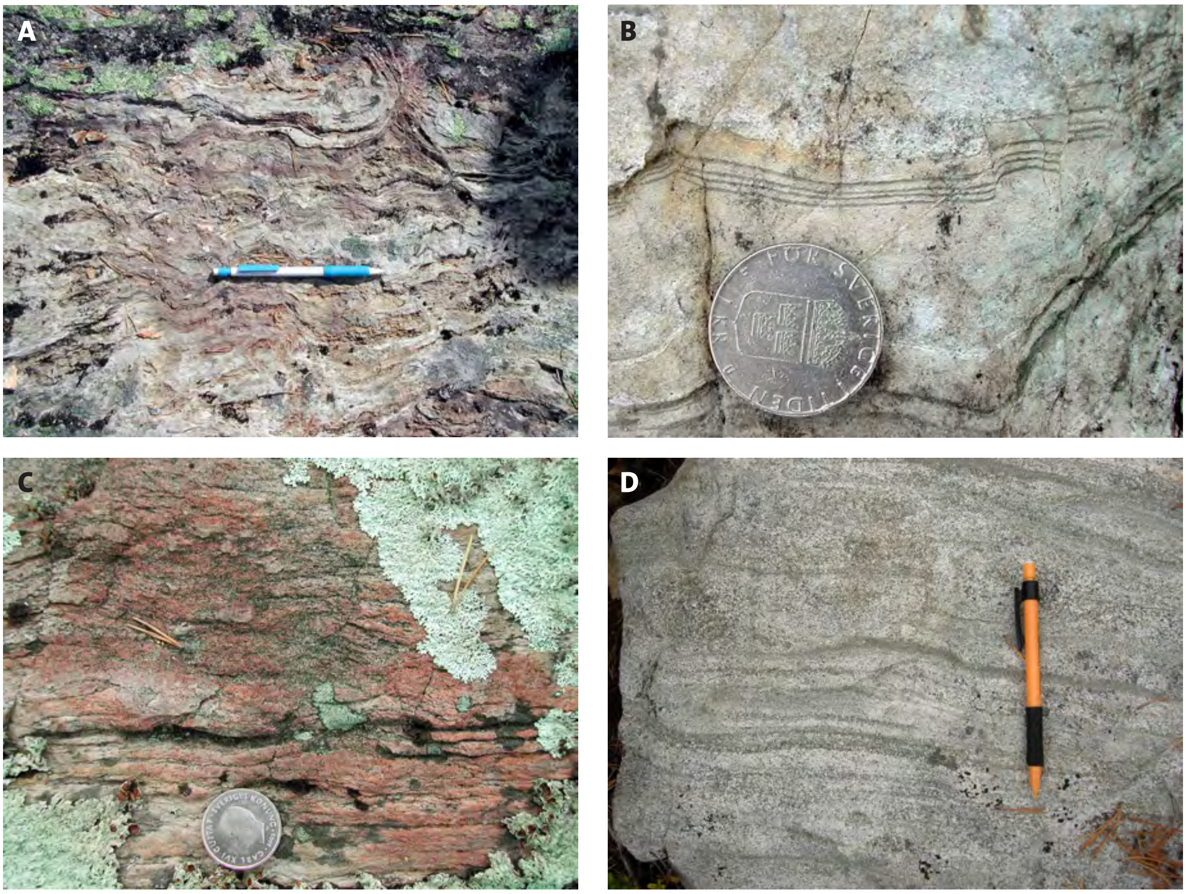

Figure 39. **A.** Syngenetic deformation (escape structures, load casts) in layered sandstone and siltstone. Bonadalen, about 7.5 km south of Kåbdalis (7338233/724349). Photo: Benno Kathol. **B.** Syngenetic folded and faulted layers and graded bedding in laminated volcanic sandstone. Base of a coarser sandstone layer just above the dark grey laminae. Trollforsen, about 19 km northwest of Moskosel (7329288/692630). Photo: Benno Kathol. **C.** Redeposited and foliated volcaniclastic rhyolite (fine-grained volcanic sandstone). Getsvinsmyran, about 11.5 km south-southeast of Kåbdalis (7334975/728819). Photo: Benno Kathol. **D.** Dacitic, plagioclase porphyritic volcanic sandstone interpreted as mass flow deposit. Grundträsk, about 17.5 km south-southeast of Pålkem (7361905/799900). Photo: Ulf Bergström.

rhyolites and dacites, with subordinate sandstone, siltstone, conglomerate, andesite and basalt. Some scattered occurrences of limestone have been observed between Moskosel and Trollforsen. Basalt, andesite and dacite are common to the west of Jokkmokk and Tårrajaur. Trachytic compositions with higher alkali content have been observed in both the felsic and mafic rocks. Between Tjåmotis and Kvikkjokk, greywacke, sandstone, breccia and limestone occur within the predominant rhyolite, andesite and basalt. Rhyolite and dacite are the most common rock types in the westernmost area, between Luvos and Arjeplog, followed by arenite and sandstone and basalt-andesite. Higher metamorphic grades are indicated by the occurrence of gneisses, amphibolites and paragneiss.

Bedding is the most common primary structure in both volcanic and sedimentary rocks of the Porphyrite group; graded bedding has been observed in sandstones at Moskosel and Varjisträsk and north of Gunnarsbyn. Convolute bedding is described from sandstone and siltstone in a volcaniclastic sequence at Abmoälven northwest of Moskosel. Escape structures such as load casts occur in layered sandstones south of Kåbdalis (Fig. 39a). The sedimentary sequence at Trollforsen consists of layered or laminated siltstones and fine-grained sandstones with minor intercalations of limestone. Graded bedding and cross-bedding are common in this sequence, and well-preserved syngenetic folding and faulting of small-scale lamination occurs (Fig. 39b). Primary lamination is also common in volcaniclastic rhyolites, dacites and andesites and fine-grained sandstones and siltstones within the Moskosel

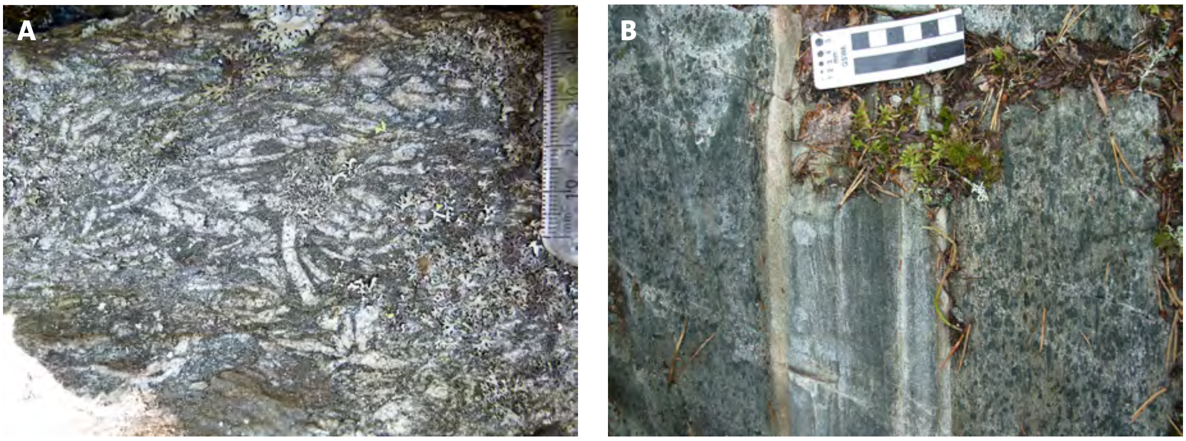

Figure 40. **A.** Plagioclase porphyritic andesite with lath-shaped phenocrysts. Parallel oriented phenocrysts are interpreted to be the result of flow banding in lava flows. Rörmyrhatten, about 16.5 km west of Boden (7314249/789527). Photo: Charlotta Brandt. **B.** Strongly foliated and partly mylonitic plagioclase and amphibole porphyritic andesite. Lill-Lobbtjärnen, about 18 km southwest of Boden (7303043/794546). Photo: Paul Evins.

–Trollforsen–Kåbdalis area, north of Lövnäs northwest of Gunnarsbyn and west of Boden. Cross-bedding has also been reported from volcaniclastic and sedimentary rocks close to Moskosel and Varjisträsk and south and southeast of Boden. Volcanic sandstones (Fig. 39c) and subordinate volcanic mudstones, siltstones and conglomerates are common in the Svartlå–Gunnarsbyn–Pålkem and Moskosel–Trollforsen–Kåbdalis areas, southwest of Boden and between Arjeplog and Luvos. Porphyritic textures occur locally. South of Pålkem, many of these volcanic sandstones have been interpreted as mass flow deposits (Fig. 39d).

Breccias have been found in both felsic and mafic volcanic rocks in the Moskosel–Trollforsen–Kåbdalis area, west of Boden and Gunnarsbyn and south of Överkalix. Primary structures such as graded bedding, cross-bedding, ripples, load casts and flute casts, convolute lamination and syngenetic folds have also been described from volcanic greywackes (Falk 1973) of the Abmorälven area, northwest of Moskosel.

Within the Bothnia–Skellefteå and the Norrbotten lithotectonic units, the volcanic rocks of the Porphyrite group show equigranular, inequigranular and porphyritic textures (Figs. 40a, b) and all varieties are found side by side. Feldspar, including potassium feldspar and plagioclase, is by far the most common phenocryst mineral. All types of phenocryst occur in all areas in the Norrbotten and Bothnia–Skellefteå lithotectonic units, with the exception of quartz phenocrysts, which are absent southwest of Boden. No phenocrysts have been described in the Överkalix lithotectonic unit, and the volcanic rocks are described as equigranular to inequigranular.

Locally, the volcaniclastic rocks of the Porphyrite group include volcanic breccias, showing fragments, which in many cases are elongated and oriented along the foliation (Fig. 41).

Pillow structures have been found northwest of Tjåmotis, northwest of Gunnarsbyn and west of Boden. Flow banding has been observed in andesites and basalts southwest of Boden, north of Moskosel and north of Luvos. Eutaxitic textures occur in rhyolites and subordinately in dacites north of Lövnäs between Moskosel and Trollforsen, north of Pålkem and southwest of Boden and Råneå. Lithophysae have mainly been reported from rhyolites and dacites in the area Moskosel–Trollforsen–Kåbdalis and from two occurrences west of Boden. Recrystallisation is common in the Porphyrite group. Spherulites have been observed in rhyolites in the Moskosel–Trollforsen–Kåbdalis area.

Generally, all rocks belonging to the Porphyrite group are foliated (Fig. 42) and in many cases also folded, and almost all rocks have been described as banded. In places, both volcanic and sedimentary rocks of the group have been described as gneissic. Lineation or mineral lineation is common but is rarer in the easternmost occurrences between Korpilombolo and Överkalix and absent west and north-

Figure 41. Strongly foliated, dacitic to andesitic volcanic breccia with elongated fragments of granodiorite, dacite, metabasite and quartz. Bratt-Gallaberget, about 12.5 km south-southwest of Pålkem (7367395/789200). Photo: Stefan Bergman.

Figure 42. Strongly foliated and banded amphibole porphyritic andesite. Storåholm, about 18.5 km southwest of Pålkem (7363645/784223). Photo: Benno Kathol.

west of Tjåmotis. Massive fabrics are virtually absent in the eastern part of the Porphyrite group (subareas 5–8) but relatively common in the west.

Veining is a common feature in all occurrences. Migmatitic structures are most common southwest of Boden, but also occur in other areas within the Överkalix lithotectonic unit and southwest of the Luleå–Jokkmokk zone.

Epidote is common in all rock types northwest of Gunnarsbyn, southwest of Boden, north of Lövnäs and in the Moskosel–Trollforsen–Kåbdalis area. Garnet has been observed in volcanic, sedimentary and calc-silicate rocks, but is restricted to the areas southwest of the Luleå–Jokkmokk zone. Sillimanite is reported from volcanic sandstones north of Lövnäs. Hematite and magnetite occur in rhyolite, dacite, andesite and volcanic sandstones and, with a few exceptions, are restricted to areas southwest of the Luleå–Jokkmokk zone. This also applies to chalcopyrite, unspecified sulphide minerals and

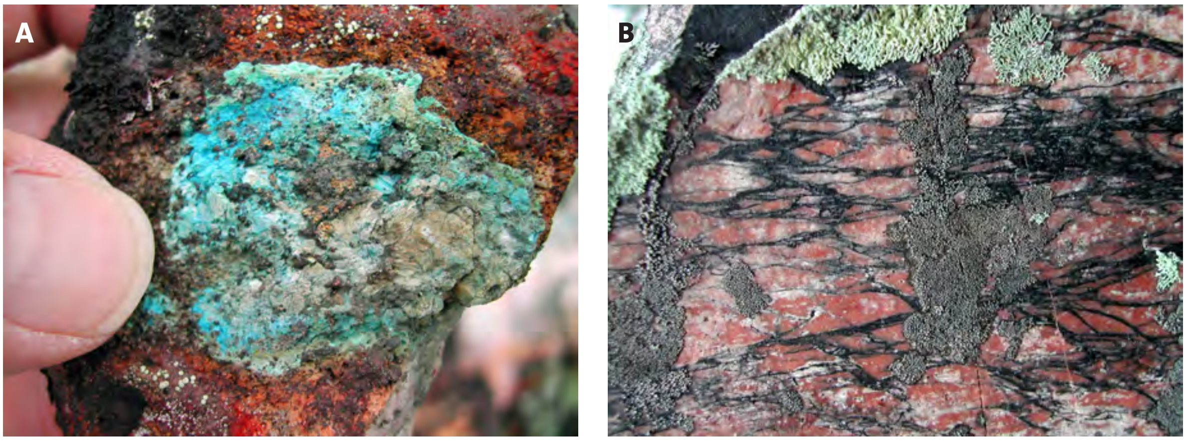

Figure 43. **A.** Malachite and other secondary copper minerals in carbonate rock and rhyolite. Nedre Ljusselet, about 9 km north of Moskosel (7322289/703815). Photo: Benno Kathol. **B.** Microcrystalline tourmalinite in rhyolite. Nedre Ljusselet, about 9 km north of Moskosel (7322289/703815). Photo: Benno Kathol.

pyrite, the latter occurring mostly in rhyolites and dacites. Malachite has been observed southwest of Boden, northwest of Moskosel (Fig. 43a) and southeast of Luvos. Microcrystalline tourmalinite occurs as an up to 40 cm wide dyke, fissure fillings and veins in rhyolite on the southern shore of the Piteälven river north of Moskosel (Fig. 43b), indicating hydrothermal alteration of the volcanic rocks.

Early Svecokarelian intrusive rocks, c. 1.91–1.87 Ga (Haparanda and Jörn GI suites)

In the project area and elsewhere in northern Sweden, 1.91–1.87 Ga calc-alkaline intrusive rocks are assigned either to the Jörn GI suite (Kathol & Weihed 2005) or the Haparanda suite (Bergman et al. 2001, Mellqvist et al. 2003). The former was formerly known as the Jörn suite after the Jörn Granitoid Complex (Wilson et al. 1987). The latter name stems from the original Haparanda series of Ödman et al. (1949) as described by Ödman (1957). This division is based on differences in magma derivation and emplacement in different tectonic environments (Mellqvist et al. 2003).

The boundary between calc-alkaline intrusive rocks of both suites is defined by isotope geochemical characteristics, among other criteria (Mellqvist 1999, Mellqvist et al. 1999b, Mellqvist et al. 2003). The rocks of the Jörn GI suite generally have positive $\varepsilon_{Nd\ (T=1.9)}$ values, suggesting magma derivation from juvenile sources. Calc-alkaline intrusive rocks of the Haparanda suite show negative $\varepsilon_{Nd\ (T=1.9)}$ values, indicating more mature sources for magma derivation and a closer relationship to an Archaean crust (Mellqvist 1999, Mellqvist et al. 2003).

The Jörn GI suite was formed in a juvenile island arc terrane that was subsequently accreted to the Archaean craton during the Svecokarelian orogeny, whereas the Haparanda suite was formed within or in marginal parts of the Archaean craton (Mellqvist et al. 2003). The transition zone between intrusive rocks with positive and negative $\varepsilon_{Nd\ (T=1.9)}$ values defines the Archaean–Proterozoic boundary, with the Haparanda suite occurring to the northeast, and the Jörn GI suite to the southwest of this boundary. Öhlander et al. (1993) named this boundary the Luleå–Jokkmokk zone. Results from Sm-Nd data, acquired during various SGU mapping projects over the past decade, confirm the previously outlined Archaean–Proterozoic boundary and in parts delineate the zone in greater detail.

Within the rocks of the Jörn GI and Haparanda suites in the project area, twelve radiometric age determinations, interpreted as crystallisation ages, have been published (Wikström & Persson 1997a, Mellqvist et al. 2003, Lundmark et al. 2005a, Kathol & Persson 2007a, Åkerman & Kero 2012b, c, Claeson & Antal Lundin 2012c, Hellström et al. 2012c, Jonsson & Kero 2013c, Bergman et al. 2015a, Nysten et al. 2018 and Sarlus et al. 2016). The analyses were carried out using the U-Pb method on zircons, either by SIMS or TIMS techniques. The ages obtained range from 1.89 to 1.88 Ga or from 1.91 to 1.87 Ga, taking error intervals into account.

Due to the similarities in structures, textures and mineral content, no distinction has been drawn in the following description between the Jörn GI suite and the Haparanda suite. Within the project area, both suites comprise rocks whose composition varies widely, from ultrabasic and gabbroid to dioritoid, tonalite and granodiorite to syenitoid and granite. These rocks occur in all subareas (see Fig. 17b), but are more frequent in the northeast of the project area. In the west, rocks of the Jörn GI and Haparanda suites occur only sparsely, and the early Svecokarelian intrusive rocks predominantly comprise alkali-calcic rocks of the Perthite monzonite suite (see below).

The most common rock type is tonalite to granodiorite, followed by granodiorite to granite, monzodiorite to granodiorite, gabbroid to dioritoid rocks and granite *sensu stricto*. Larger intrusions of granite have been observed west of Moskosel and east of Nattavaara, between Tarrajaur and Vuollerim and south of Råneå. Granites *sensu stricto* do not occur in the Överkalix lithotectonic unit east of the Pajala deformation belt. Minor occurrences of syenitoid to granite are situated southwest of Aitik, northwest of Vidsel, northeast of Råneå and between Kalix and Haparanda. South of Narken, small bodies of syenitoid rocks occur within the Pajala deformation belt. Pegmatites are common in most of the rocks of the Jörn GI and Haparanda suites, but occur more frequently in the north of the Överkalix lithotectonic unit and southwest of Boden. Gabbroid and dioritoid rocks occur as scattered minor intrusive bodies over the whole area, except subarea 1. They are almost always situated inside or in contact with larger felsic intrusions, indicating magmatic differentiation.

The rocks of the Jörn GI and Haparanda suites are generally medium-grained; a small proportion are fine-grained, and coarse-grained varieties occur subordinately. The majority of the felsic rocks are grey (Fig. 44a) or reddish grey in colour. Red, brownish red or greyish red and light grey to white varieties are less common (Fig. 44b). An example of the last-mentioned variety is the Jokkmokk granitoid (Lundmark et al. 2005a), which is exposed in a large massif northwest of Jokkmokk. The mafic and ultramafic rocks are mostly described as black, dark grey and subordinately dark green and green (Fig. 44c).

The rocks of the Jörn GI and Haparanda suites have been equally reported as equigranular and inequigranular, and both varieties occur in all areas side by side. Porphyritic varieties are less common but have also been found in all areas. Phenocrysts range from potassium feldspar and quartz to mafic minerals such as amphibole. The majority of the phenocryst material consists of unspecified feldspar, potassium feldspar and plagioclase. Almost all rocks are described as recrystallised or altered in the outcrop database.

Most of the rocks of the Jörn GI and Haparanda suites are foliated and in many places also gneissic. Massive varieties (Fig. 44a) are somewhat less common, but occur together with the deformed varieties due to heterogeneous deformation. Lineation and folds are also common structures. In some places, there is a gradient from almost undeformed to strongly foliated rock over a short distance within the same outcrop, due to a nearby deformation zone (Fig. 45a). More or less massive rocks have been found around Vidsel and west of Moskosel.

Many of the rocks of the Haparanda suite have been described as metamorphosed, and locally as migmatitic. Within the Jörn GI suite southwest of the Luleå–Jokkmokk zone, metamorphosed or migmatised rocks occur on the northeastern shore of lake Tjeggelvas, southeast of Örnvik (Fig. 45b), where they have been described as granitic to granodioritic gneisses (Tjeggelvas gneiss complex) of uncertain, possibly supracrustal origin by Berndtsson (1983) and Berndtsson et al. (1984). However, Silvennoinen et al. (1987) and Koistinen et al. (2001) included this complex in the early orogenic 1.91–1.88 Ga granitoid intrusive rocks. Here, the Tjeggelvas gneiss complex is included in the Jörn GI suite. Additionally, migmatised rocks have been found north and east of Tårrajaur and between Trollforsen and Kåbdalis. Veining is a common structure in both the Jörn GI and the Haparanda suites (Fig. 45c).

Figure 44. **A.** Medium-grained, massive granodiorite. Risurova, about 13 km north of Hakkas (7450062/787237). Photo: Fredrik Hellström.

Figure 44. **B.** Finely medium-grained, foliated, leucocratic granodiorite. Haraudden quarry, about 3.5 km northwest of Jokkmokk (7398413/711263). Photo: Benno Kathol.

Figure 44. **C.** Ultramafic rock with lenses and folded bands of differing composition. Storlandet at Gran-träsk, about 28 km southwest of Överkalix (7365409/829602). Photo: Stefan Bergman.

Figure 45. **A.** Varying degree of deformation in porphyroblastic tonalite close to a deformation zone. Subvertical foliation strikes southwest–northeast. Östra Labtjevare (Lábttjevárre), about 8.5 km west of Varjisträsk (7332665/696696). Benno Kathol.

Figure 45. **B.** Foliated, folded and weakly migmatised granodiorite. On the shore of lake Tjeggelvas northwest of Silbakjávrre, about 10 km east-southeast of Örnvik (7386457/620911). Photo. Stefan Persson.

Figure 45. **C.** Gneissic and veined granodiorite. Nordanå, about 14 km northwest of Vuollerim (7391882/744482). Photo: Per Nysten.

Figure 46. **A.** Metadioritoid with mafic magmatic enclaves, indicating magma mingling. The largest enclave is approximately 25 cm long. Quarry at Kurkijänkkä, about 5 km west-southwest of Haparanda (7329900/910975). Photo: Stefan Bergman. **B.** Elongated mafic enclave in strongly foliated quartz monzodiorite. The enclave contains feldspar grains stemming from the quartz monzodiorite, which indicates magma mingling. Gunnaberget, about 0.7 km north of Harads (7342654/769299). Photo: Benno Kathol.

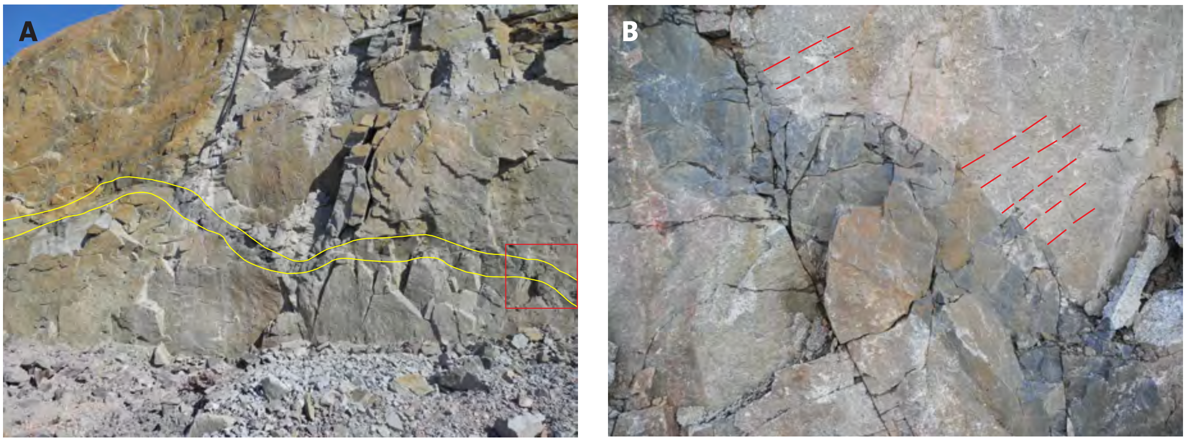

Figure 47. **A.** Dacitic dyke (marked in yellow) in foliated granodiorite. The dyke cross-cuts the foliation in the granodiorite and thus postdates regional metamorphism in the area. Norramark quarry, about 21.5 km southeast of Boden (7301804/821195). Photo: Martiya Sadeghi. **B.** Close-up of the contact between a dyke and host rock. Foliation in the host rock is marked with red lines. For location of this photo see red rectangle in Figure 47a. Photo: Benno Kathol.

Magma mingling structures are common in the areas north of Moskosel and around Vidsel, but have also been described from some scattered places elsewhere in the project area (Figs. 46a and b). Intrusion breccias occur between Korpilombolo and Överkalix.

Dykes are ubiquitous in all occurrences of the rocks of the Jörn GI and Haparanda suites. Most of the dykes consist of pegmatite, aplite and granite; other rock types are dolerite, amphibolites, and volcanic rocks of basaltic to rhyolitic composition. Most of the dyke intrusions are considered to be significantly younger than the host rocks. In several places they truncate the foliation in the host rock, thus postdating at least one phase of deformation and metamorphism (Figs. 47a, b). In other places, dykes are considered coeval with the main intrusion. Within the Jokkmokk granitoid northwest of Jokkmokk, swarms of mafic inclusions are interpreted as mafic dykes comagmatic with the granitoid magma (Fig. 48a). Southeast of Murjek, foliation in a quartz monzodiorite is cut by a discordant granitic dyke, associated with a nearby intrusion of the Perthite monzonite suite (Fig. 48b).

Enclaves, inclusions and xenoliths also occur frequently in the rocks of the Jörn GI and Haparanda suites. The most common rock types are diorite and gabbro, andesite, amphibolite, basic rock and pegmatite. Other common inclusions consist of tonalite, granodiorite, granite, quartz diorite, dacite, rhyolite, basalt and metamorphic rocks. Sedimentary and ultramafic rocks occur subordinately.

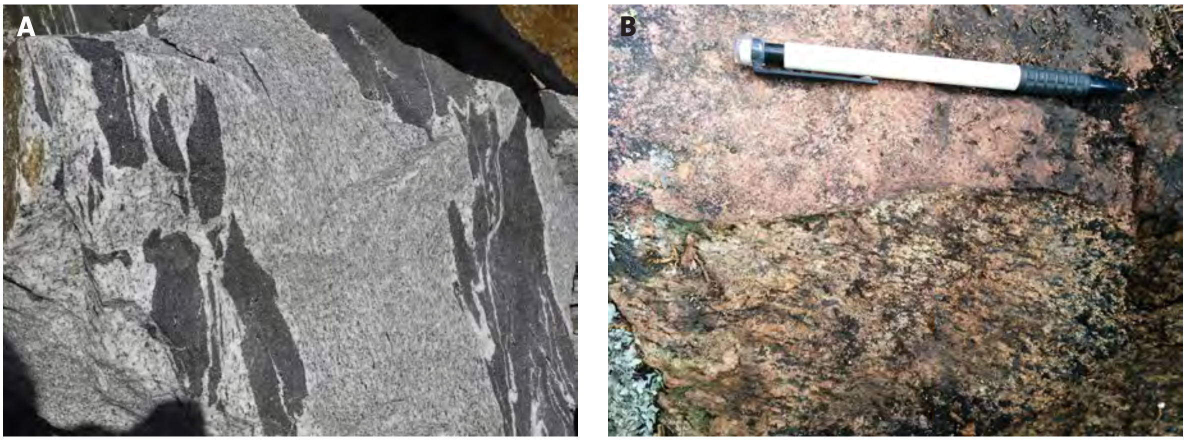

Figure 48. **A.** Comagmatic mafic inclusions, interpreted as intrusions (dykes) in leucocratic granodiorite. The elongated inclusions are approximately 20 cm wide. Haraudden quarry, about 3.5 km northwest of Jokkmokk (7398413/711263). Benno Kathol. **B.** Contact between granitic dyke, associated with the Perthite monzonite suite, and quartz monzodiorite. The dyke cuts the foliation in quartz monzodiorite. Pakkoforsen, about 18 km east-southeast of Murjek (7379521/778290). Photo: Stefan Bergman.

Amphibole occurs in all kind of rocks in the Jörn GI and the Haparanda suites. Epidote and chlorite occur less frequently, but are widespread like amphibole. However, they have not been reported from the southeast of the project area. Both occur in all rock types, but with most of the epidote in granodiorites. Fissure fillings of quartz have mainly been observed in the west and south of the project area. Magnetite has been described mainly from granites, granodiorites and pegmatites, and subordinately from gabbros in the entire project area, except for subarea number 8, west and northwest of Haparanda. Hematite occurs in granitoids southeast of Örnvik, north of Moskosel and east of Nattavaara. Pyrite and unspecified sulphide minerals occur in places in granite, granodiorite, gabbro and dolerite. Chalcopyrite occurs mainly in mafic intrusive rocks, and calc-silicates occur in several places.

Svecofennian supracrustal rocks, c. 1.89–1.86 Ga (Arvidsjaur group)

Within the project area, Svecofennian volcanic rocks have been divided into two groups, one older and one younger than 1.88 Ga. The older group has been correlated with and included in the Porphyrite group (see above). The younger one has been dated at Benbryteforsen (Kathol & Persson 2007b), Danielstugan (Kathol et al. 2008b), Tjappisvare (Claeson & Antal Lundin 2012c), Makkavare (Morris et al. 2015), Sörhårås (Nysten et al. in press) and at Kaddåive, Kallak, Rimpos, St. Samonåive and Savvemoajvve (SGU, unpublished) within the time interval 1.88–1.86 Ga (1.89–1.86 Ga when errors are taken into account). Thus, these volcanic rocks were formed in the same time interval as the rocks of the 'classic' Arvidsjaur group to the south of the project area (see below). Due to a direct spatial relationship with the Arvidsjaur group to the south, we therefore assign 1.89–1.86 Ga Svecofennian volcanic rocks of the project area to the Arvidsjaur group, as originally defined in the municipality of Arvidsjaur to the north of the Skellefte district.

In the latter area, Svecofennian subaerial or terrestrial felsic and mafic volcanic rocks that occur north of the Skellefte district (Kathol & Weihed 2005) have been described by Högbom (1937) and Kautsky (1957) under the name Arvidsjaur porphyries. Gavelin (1955) named liparitic, dacitic and andesitic volcanic rocks of the same area the Arvidsjaur series. The modern name Arvidsjaur group was used by Lundberg (1980), Weihed et al. (1992), Allen et al. (1996) and Kathol & Weihed (2005), among others.

Volcanic sequences, here assigned to the Arvidsjaur group, pass into the Kiirunavaara group (Martinsson 2004) directly to the north of the northern boundary of the project area. A possible correlation between the 1.88 –1.86 Ga volcanic rocks of southern Norrbotten County with the Kiirunavaara group (Martinsson 2004) to the north has been dismissed due to locally higher ages of the rocks to the north. The spatial relationship between the Arvidsjaur group in the project area on one side and the Kiirunavaara group, as well as the Porphyrite group, was not within the scope of this project, but will be left for further investigation, for example by mapping key areas by way of volcanological and geochemical investigations.

Within the project area, the Arvidsjaur group is restricted to the area west of a line between Boden and Hakkas. To the west of this line, rocks of the Arvidsjaur group occur together with the coeval igneous rocks of the Perthite monzonite suite. According to Kathol & Rapp (1996), Kathol & Persson (1997), Kathol & Triumf (2004) and Kathol & Weihed (2005), the Arvidsjaur group and the Perthite monzonite suite have been shown to be comagmatic in areas south of the project area. A comagmatic origin is also inferred in the project area, and the rocks of the Arvidsjaur group thus represent the supracrustal products of the 1.88–1.86 Ga magmatism.

South of the project area, the supracrustal rocks of the Arvidsjaur group, almost exclusively of volcanic origin, extend to the north from areas occupied by Skellefte group metavolcanic rocks, far into Norrbotten County. Rocks of this 'classic' Arvidsjaur group have yielded radiometric ages in the interval 1.88–1.86 Ga at Norr-Döttern (Löfvendahl & Åberg 1982), Bure and Gråberget-Skyberget (Skiöld et al. 1993), Brännbergsliden (Lundström & Persson 1999), Fagervik (Lundqvist et al. 2000) and Fågelberget (Kathol & Triumf 2004).

As indicated by these age determinations, the Arvidsjaur group is slightly younger, but with overlapping time intervals, than the 1.92–1.87 Ga old, subaqueous Skellefte group. This is also supported by field relationships in the transition zone between the two groups (Grip 1935, Bergström 1997, Thunehed 2000, Kathol & Triumf 2004). The Arvidsjaur group rocks were thus emplaced to the north and in the contact area on top of the metavolcanic rocks of the Skellefte group, which are considered to be the southern equivalent to the rocks of the Porphyrite group.

The volcanic rocks of the Arvidsjaur group are rhyolitic to basaltic; a characteristic feature is their exclusively subaerial nature and the general absence of interbeds of deep-water sedimentary rocks. Abundant subaerial eruptive and depositional processes and the relative scarcity of proximal volcanic facies of the felsic rocks of the Arvidsjaur group suggest they were emplaced by voluminous, explosive volcanic activity, probably related to continental calderas. The mafic rocks in the Arvidsjaur area seem predominantly comprise laterally extensive, coherent, coarsely plagioclase-porphyritic andesites with relatively few volcaniclastic interbeds. These rocks seem to have formed either as rather low viscous lavas, capable of flowing long distances or as subvolcanic intrusions (Kathol & Weihed 2005).

Volcaniclastic varieties are by far the most commonly observed rock types within the volcanic sequences of the Arvidsjaur group in the project area. Coherent textures have been reported, mainly from rhyolites and dacites and subordinately from andesites and basalts. Subvolcanic intrusions occur in almost all areas with Arvidsjaur group rocks, but there are remarkably frequent observations of subvolcanic intrusions in a northwest-striking belt from Jokkmokk to Tjåmotis. Lavas are almost absent north of the Luleå–Jokkmokk zone. South of this zone, major occurrences of amygdaloid andesitic and subordinate rhyolitic lavas have been found east of Stensund. Southwest of Vidsel, dacitic to rhyolitic lavas predominate.

Volcanic breccias and conglomerates of rhyolitic to andesitic composition occur in the south between Svartlå and the area south and southwest of Trollforsen (Fig. 49). Volcanic sandstones are common in the same area, but have also been described in the western and northern occurrences of the Arvidsjaur group. Some rare volcanic breccias have been described from the Porjus area.

Two sizeable occurrences of spectacular conglomerates have been encountered south of Lake Jeäddnjájávrrie west of Trollforsen. The northern one consists of polymict, poorly sorted volcanic conglomerates and breccias with clasts, up to 20 cm in diameter, of porphyritic felsic volcanic rocks and subordinate fine-grained granite and medium-grained sandstone. The southern occurrence shows a clearly epiclastic,

Figure 49. Volcanic breccia with clasts of feldspar porphyritic rhyolite (dark grey) and compressed pumice fragments (darker green at the coin) in an epidotised matrix. Ráhkkurvárrie, about 21 km west of Moskosel (7313437/682122). Photo: Benno Kathol.

carbonate-cemented, clast-supported, layered and poorly sorted conglomerate which occurs intercalated with a carbonatic sandstone (Fig. 50).

In the Bure area, south of the project area, red polymict conglomerates and reddish arkosic and tuffitic sandstones were named the Loito formation by Perdahl & Einarsson (1994). The latter constitutes the uppermost unit in a supracrustal sequence that was correlated with the Vargfors group. Rocks of the Loito formation occur within the Karesuando–Arjeplog deformation zone (KADZ), and extend into the project area south of Mellanström. Here, it is represented by a polymict conglomerate, consisting of one to ten-centimetre-sized clasts of felsic volcanic rocks and subordinate laminated reddish sandstone in a very fine-grained to fine-grained matrix.

Finer-grained sedimentary rocks, belonging to the Arvidsjaur group, occur as intercalations within the volcanic rocks of the group in several areas. Sandstone, quartzite, arkose and greywacke occur west of Lövnäs, west of Porjus and northwest of Nattavaara. Sandstones occur north and west of Vidsel and several minor occurrences of sandstone have been found around Moskosel.

Bedding and lamination are common in the rocks of the Arvidsjaur group (Fig. 51a), except for the northeasternmost area north of Nattavaara. Massive beds are reported from volcanic sandstones and sedimentary rocks. Fragment-bearing rocks occur in all areas but are somewhat more frequent between Luvos and Jokkmokk, north and west of Moskosel and north of Harads. Hydrothermal alteration has mostly been reported from dacites and rhyolites in the area between Jokkmokk, Tjåmotis and Porjus.

Equigranular, inequigranular and porphyritic rocks in the Arvidsjaur group occur side by side in all areas, but most of the volcanic rocks have been described as porphyritic. Amphibole phenocrysts occur

Figure 50. Carbonate-cemented conglomerate with clasts mainly consisting of volcanic rocks. The conglomerate is interlayered with carbonate sandstone. Vietjiekvárrie, south of Lake Jeäddnjajávrrie, about 16.5 km west of Trollforsen (7332155/676686). Photo: Benno Kathol.

in dacite, andesite and basalt in the southern and western areas and between Jokkmokk and Luvos. Feldspar phenocrysts are ubiquitous in porphyritic rhyolites to andesites. Quartz and potassium feldspar phenocrysts are most common in rhyolites and dacites (Fig. 51b). Rhyolites with quartz, potassium feldspar and unspecified feldspar phenocrysts occur northeast and southwest of Moskosel and east of Harads. Plagioclase phenocrysts occur mainly in andesites and dacites (Fig. 51c), but subordinately also in basalts and rhyolites. Plagioclase and amphibole phenocrysts occur in andesites and dacites and subordinately in basalt northwest of Lövnäs and east of Stensund. Quartz- feldspar porphyritic rhyolites and dacites occur almost everywhere. Rare crystal tuffs have been observed within the occurrences around Moskosel.

Lithophysae are common features in many rhyolites in the southern areas between Arjeplog and Svartlå. Locally, they consist of a nucleus of quartz surrounded by feldspar (Fig. 52a). In other places, they are filled by quartz only (Fig. 52b). Spherulites have been observed in the south of the map area. They occur frequently in the Rakkur area south of Trollforsen in glassy, flow-banded rhyolites or reomorphic ignimbrites (Fig. 52c). In this area, there are also very well-preserved ignimbrites and ash flow tuffs with obsidian flows up to several tens of centimetres thick (Fig. 52d). Within these well-preserved volcanic rocks, lithophysae and spherulites have grown over planar structures, which are therefore interpreted to be primary structures, either bedding or compaction surfaces.

Eutaxitic textures (fiamme), in many cases indicating bedding in ignimbrites (Fig. 53a), have been found in the Bothnia–Skellefteå lithotectonic unit and east of Harads, but these textures have not or have only rarely been reported from the northern and northeastern parts of the group. Lithophysae

Figure 51. **A.** Bedding in volcaniclastic rhyolite. East of Gárddevárre, about 10 km west-southwest of Porjus (7431616/700249). Photo: Per Nysten.

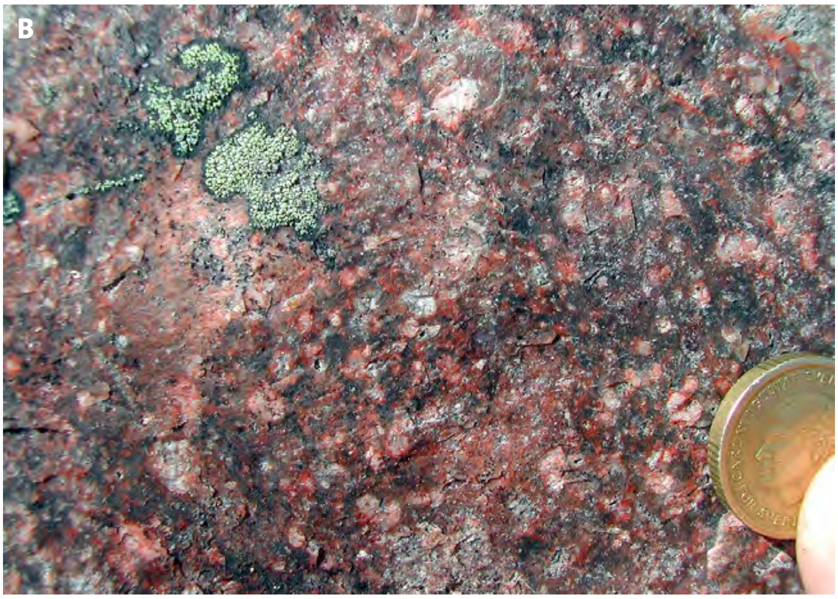

Figure 51. **B.** Quartz-feldspar porphyritic rhyolite. Suddiesvárrie, about 16 km west of Moskosel (7313194/686939). Photo: Benno Kathol.

Figure 51. **C.** Plagioclase porphyritic and amygdaloidal coherent andesite. The randomly oriented tabular plagioclase phenocrysts illustrate the isotropic nature of the andesite. Storklinten, about 4.5 km northeast of Svartlå (7336630/783815). Photo: Benno Kathol.

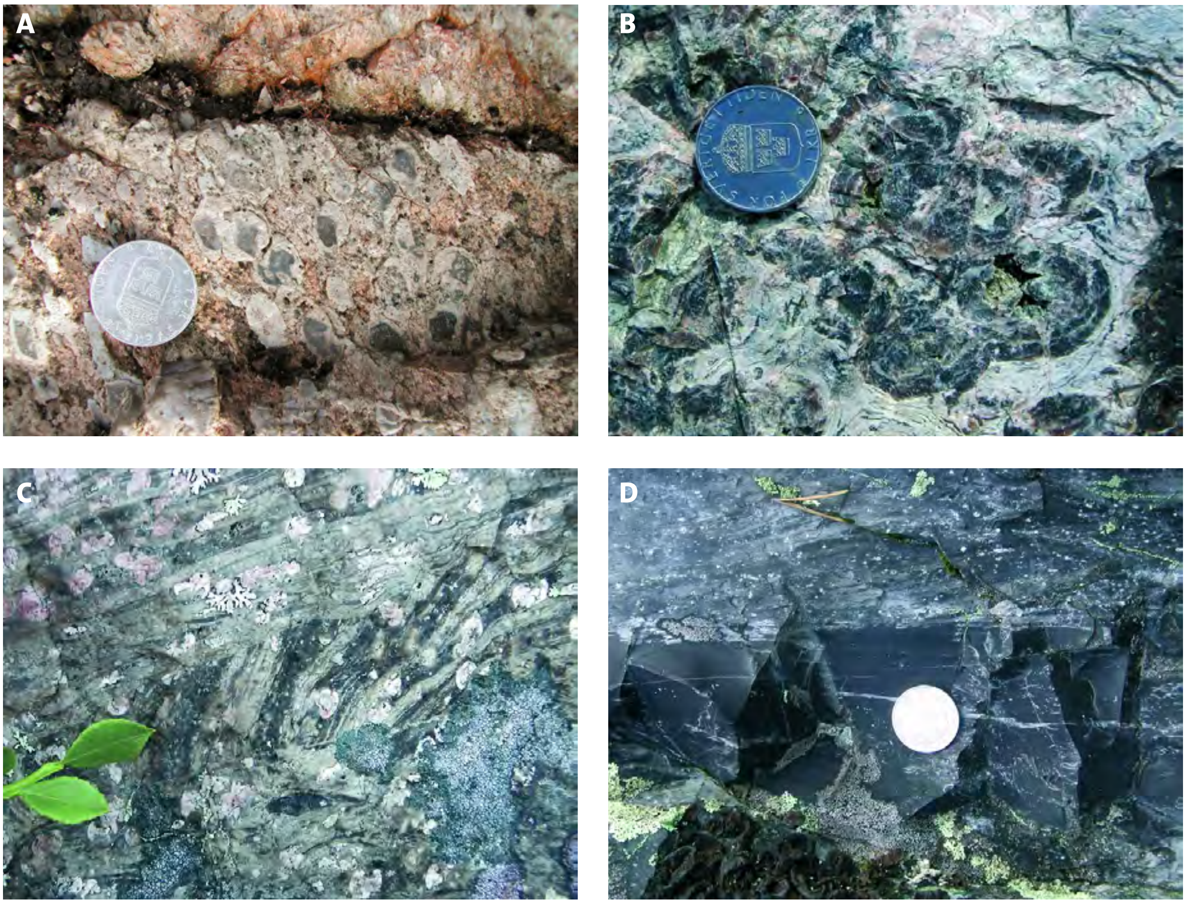

Figure 52. **A.** Quartz-feldspar-filled lithophysae in well-preserved volcaniclastic rhyolite. Svarttjärnsberget, about 21 km southwest of Vidsel (7301610/733673). Photo: Benno Kathol. **B.** Quartz-filled lithophysae in rhyolite. Local boulder southwest of Lake Ráhkkur, about 22.5 km west of Moskosel (7310520/680690). Photo: Benno Kathol. **C.** Flow-banded and apparent cross-bedded rhyolite with spherulites, growing over the flow banding. Ráhkkurvárrie, about 21 km west of Moskosel (7313480/682110). Photo: Benno Kathol. **D.** Obsidian flow in volcaniclastic rhyolite. "Glasberget" southwest of Lake Ráhkkur, about 23 km west of Moskosel (7310185/680278). Photo: Benno Kathol.

and spherulites are formed by the devitrification of volcanic glass and, in combination with eutaxitic textures, confirm the subaerial nature of the volcanic rocks of the Arvidsjaur group.

Flow banding and igneous flow structures occur in the west and south, and locally show apparent cross-bedding i.e. flow-banded layers that discordantly cut other flow-banded units (Fig. 52c). Another type of flow structures has been observed in a rhyolitic volcanic breccia east of Harads. Here, the matrix of the breccias shows flow banding, and the whole rock is interpreted to be either a reomorphic ignimbrite or an intrusion breccia within a subvolcanic intrusion (Fig. 53b).

Foliation or unspecified banding has been observed in almost all rocks of the Arvidsjaur group. Lineation and mineral lineation are also common but more frequent in the Jokkmokk–Luvos–Porjus area. Massive rocks commonly occur side by side with foliated rocks in the south and west of the Arvidsjaur group and in the Jokkmokk area, but otherwise foliation is sparsely developed. No massive varieties have been observed around Porjus and northwest of Nattavaara. The felsic volcanic rocks are more fractured than the mafic varieties.

Recrystallisation is a common feature but occurs even more frequently in all volcanic rock types in the area between Tjåmotis, Luvos and Porjus (Fig. 54a). Epidote is ubiquitous in all rocks of the Arvidsjaur group. It occurs as an alteration mineral, fissure fillings, aggregates or skarn layers in both volcanic and sedimentary rocks (Fig. 54b). Chlorite has a similar appearance but is less common. Garnet

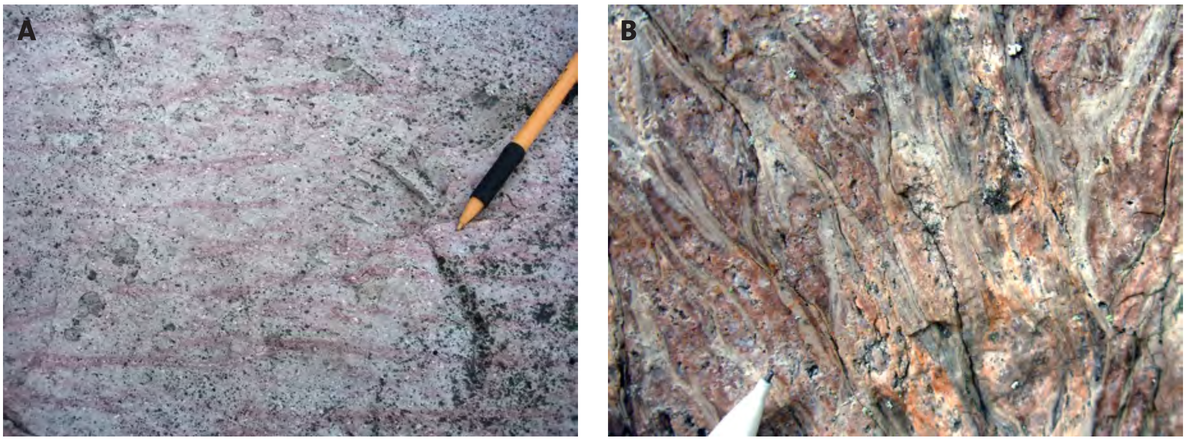

Figure 53. **A.** Eutaxitic texture in volcaniclastic rhyolite. Nedra Odjursberget, about 17 km northeast of Harads (7354329/780611). Photo: Ulf Bergström. **B.** Volcanic breccia with flow-banded matrix. The rock is interpreted to be either a reomorphic ignimbrite or an intrusion breccia within a subvolcanic intrusion. Gåvoberget, 8.5 km northeast of Harads (7346257/776495). Photo: Stefan Persson.

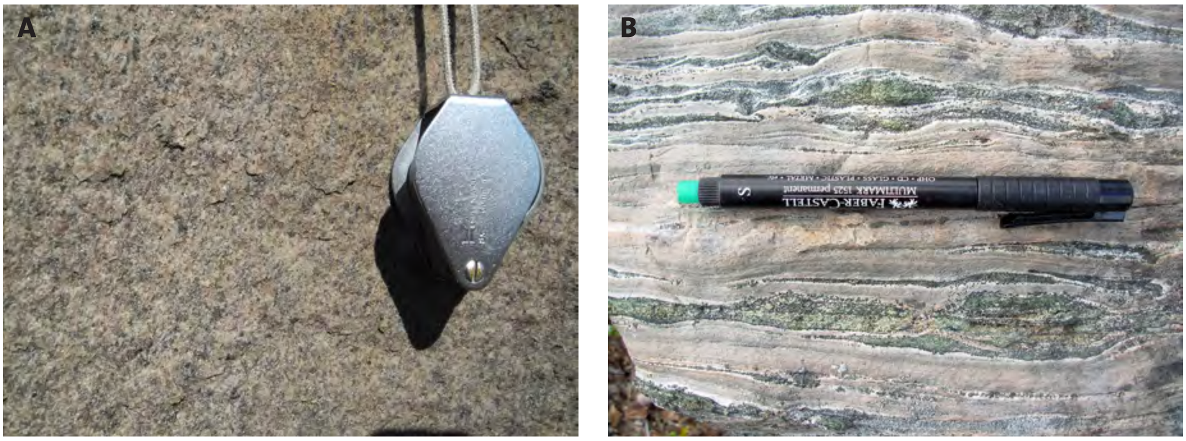

Figure 54. **A.** Strongly recrystallised rhyolite interpreted to be of volcaniclastic origin. Road cutting at Báktevárásj, about 13 km south of Porjus (7421553/712456). Photo: Benno Kathol. **B.** Skarn layers with epidote and chlorite in very thinly bedded (Ingram 1954) volcanic sandstone. Local boulder east of Brännspiken, 19.5 km southwest of Harads (7328472/755712). Photo: Benno Kathol.

occurs locally in all areas of the Arvidsjaur group rocks. Calcite occurs locally as amygdales in andesites and as fissure fillings in felsic volcanic rocks, and fluorite has been observed in rhyolites north of Tjåmotis, southeast of Porjus and southwest of Lövnäs.

Hematite has been found mainly in the northern occurrences of the Arvidsjaur group rocks. In the south-central part at Moskosel, magnetite occurs ubiquitously in all types of volcanic rocks, but has been sparsely observed in sedimentary rocks. In addition to molybdenum mineralisations, molybdenite has been reported from a few places north of Luvos. Pyrite and, less frequently, chalcopyrite occur mainly in rhyolites, dacites and andesites and subordinately in basalts in all occurrences of the Arvidsjaur group rocks. This also applies to unspecified sulphide minerals.

In several areas, the outcrop density is low or non-existent, and previous geological maps are based on only few observations that do not normally represent the bedrock of the entire unexposed area. Weathering-resistant rock types are thus overrepresented in existing outcrops. In these cases, geophysical modelling was used to compile the geological map.

In the north of Muddus National Park, northeast of Porjus, there is an increased gravity and magnetic total field intensity. Much of the area is covered by bogs, so outcrops are sparse or lacking. On existing geological maps, the area is shown to predominantly comprise rhyolite to dacite, along with

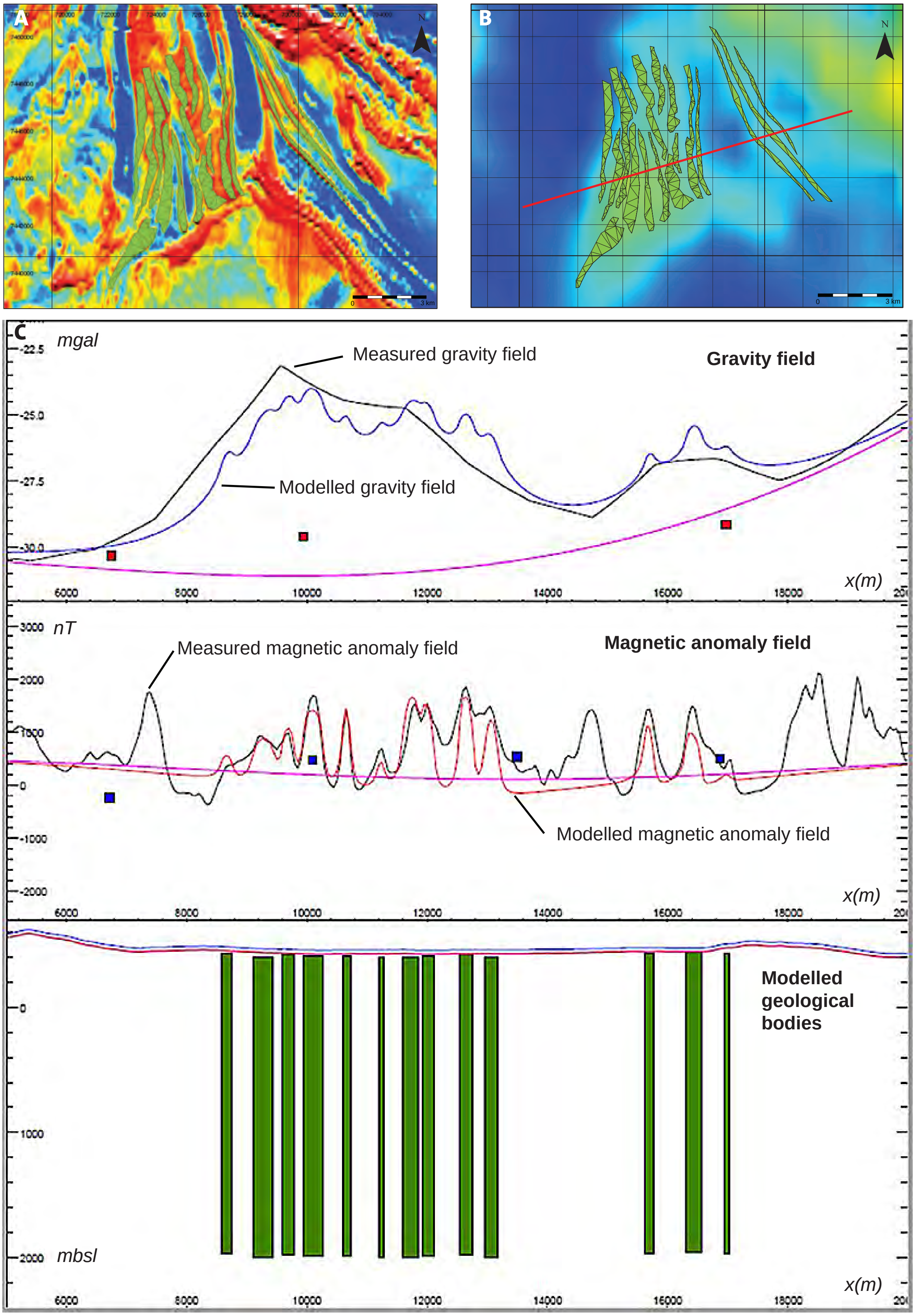

Figure 55. **A.** Filtered magnetic total field with modelled profile and source bodies. Red colours: high magnetic anomalies, blue colours: low magnetic anomalies. The location of the model area is shown in figure 16. **B.** Filtered gravity field with location of the modelled profile (red line) and the source bodies (green fields). Yellow and green colours: mass excess, bluish colours: mass deficiency. **C.** Modelling result of the gravity and magnetic field presented as a profile.

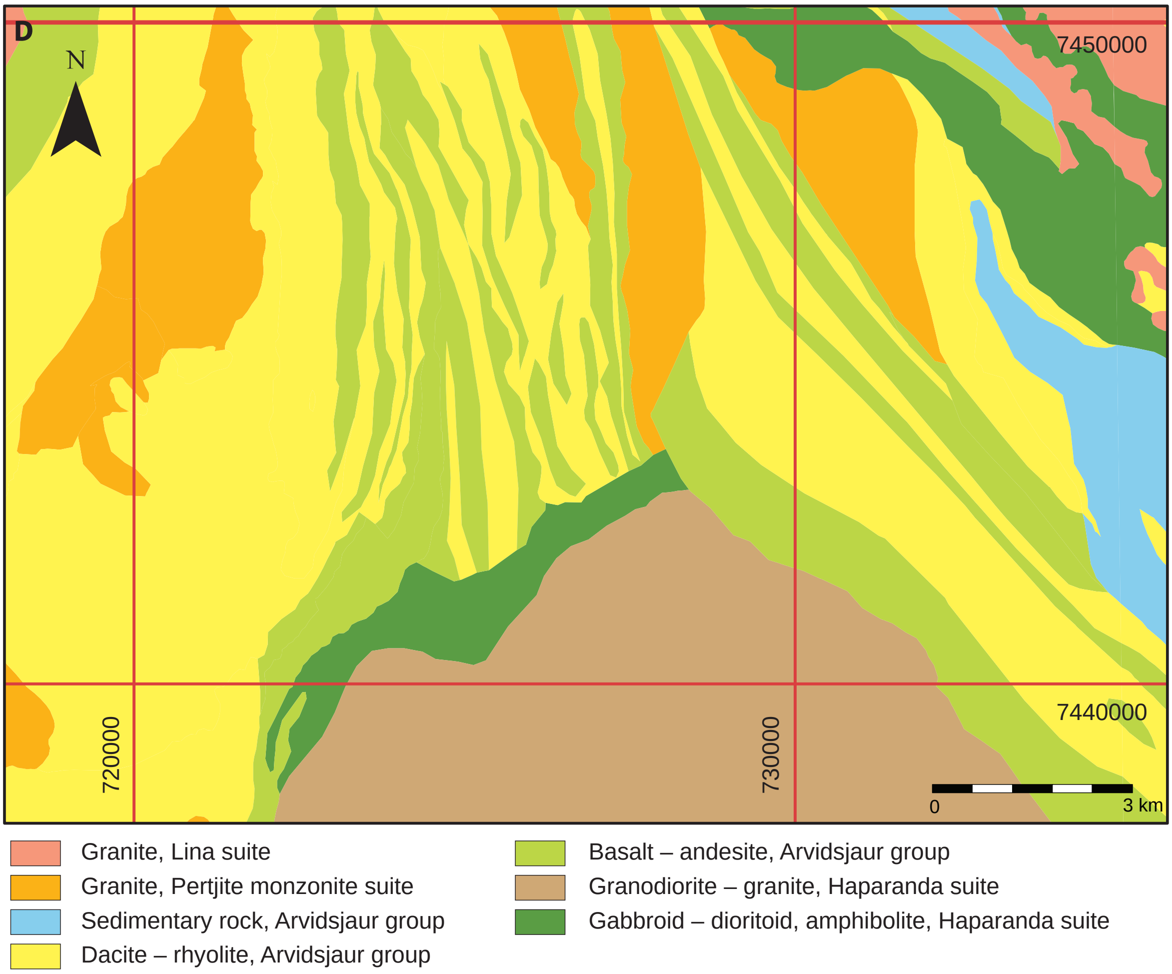

Figure 55. **D.** Revised geological map over the modelling area.

granite (Silvennoinen et al. 1987). There are few observations of andesites and basalts in the area, and modelling has been carried out along two profiles over the anomaly with the hypothesis that the source of the anomalies consists of highly magnetised rocks of mafic composition (Figs. 55a–d). In practice, modelling was carried out by tracing the assumed source to the magnetic bodies and giving them vertical dips with a depth extension down to approximately 2 km. The density was set at 2 850 kg/m^3, which accords with the density of the basalt-andesite and trachybasalt group of rocks in the Arvidsjaur Group (see Table 4). The magnetic susceptibility used in the modelling varied between 2 000 and 13 000 × 10^{-5} SI units. This interval represents the upper part of the field of the standard deviation for the basalt-andesite and trachybasalt group.

The modelling was kept simplistic. The aim was to investigate whether the source bodies of presumed andesitic composition could explain the anomaly complex qualitatively, rather than to achieve a perfect fit. Hence, concordance between the measured and modelled fields is only approximate. The result suggests that mafic rocks need to occur in the bedrock to explain the source of the anomaly in the area. The modelling has resulted in a change in the geological map, with the introduction of andesite in several rock units at the expense of rhyolite to dacite and granite.

Svecofennian supracrustal rocks, c. 1.88–1.84 Ga (Snavva–Sjöfallet and Svartlå groups)

Ödman (1957) described a north–south-striking, approximately 160 km long belt of sedimentary rocks between Lake Kakirjaure (Gágirjávri) in the north and Lake Hornavan in the south as *Snavva–Sjöfalls-serien* (the Snavva–Sjöfallet series). North of Lake Kakirjaure, the Snavva–Sjöfallet series is covered by the Ediacaran–Cambrian sedimentary cover and by thrust units of the Caledonian orogen. Thus, the northern extension and the true length of the belt are unknown. The thickness of the northern part of this sedimentary unit was estimated at approximately 10 km by Ödman (1957), while Kumpulainen (2003) estimated the total thickness to be only 6 km.

From Lake Saggatsjön (Saggat) and southwards to Lake Hornavan, the sedimentary rocks of the Snavva–Sjöfallet series show higher metamorphic grade, with growth of sillimanite in the arenitic layers and cordierite and garnet in the mica schists (Ödman 1957). The "Sjöfallet quartzites" (arenites) and Snavva metasedimentary rocks were distinguished on the basis of gradual facies variation from terrestric or shallow environments for the former, and subaqueous deeper basins for the Snavva rocks (Ödman 1957).

Zachrisson & Witschard (1995a, b) also distinguished between rocks of the Sjöfallet facies, which are mainly found at the base of the group resting on volcanic rocks of the Kirunavaara group, and rocks of the Snavva facies. The former consist of conglomerates, mudstones and feldspathic sandstones with well-preserved sedimentary structures indicating a continental to shallow water depositional environment. Monotonous grey feldspathic quartzite, meta-arkose and white quartzite represent the Snavva facies, with deposition in a deep-water environment. The sedimentary sequence of the Snavva facies overlies the rocks of the Sjöfallet facies with interfingering relationships.

Contrary to these facies models, Kumpulainen (2003) claimed that the red and fine-grained Sjöfallet facies occurs in the upper part of the group. The sedimentary features studied by Kumpulainen (2003) favour a more high-energy shallow marine depositional environment for most of the lower (Snavva) part of the successions of the Snavva–Sjöfallet group. A probable depositional environment for the upper (Sjöfallet) part of the group is stated as an estuary. Around and to the south of Snavva, primary structures are obliterated due to a higher grade of metamorphism, and these rocks could equally have been of turbiditic greywacke origin unrelated to the Snavva–Sjöfallet rocks.

In its northern part, the Snavva–Sjöfallet group shows low magnetisation and a uniform magnetic pattern, which in the vicinity of Lake Sitojaure (Sijddojávrre), just outside the project area, abruptly changes to high-magnetic, more irregular patterns on the magnetic anomaly map. However, it is unclear whether this magnetic gradient represents the above-mentioned transition in depositional facies types or a transition in metamorphic grade.

In the project area, the Snavva–Sjöfallet group comprises a succession of sandstones, arkoses and greywackes with minor intercalations of quartzite and mainly matrix-supported conglomerates, with clasts consisting of porphyritic volcanic rocks, granite and vein quartz. In areas where the bedrock shows a higher metamorphic grade, the sedimentary rocks are altered to paragneisses and migmatites and, to a small extent, to schists.

South of Tjåmotis, this sedimentary succession is intruded by late Svecokarelian (1.80–1.77 Ga) granites, quartz monzonites, diorites and gabbros of the multiple Hárrevárddo intrusion (Claeson & Antal Lundin in press-b), which divides the Snavva–Sjöfallet group into a northern and a southern part, here called the Tjåmotis and Lövnäs areas, respectively. Sparse xenoliths of the Snavva–Sjöfallet group within the intrusion mainly consist of quartzite, arkose or arenite. The Hárrevárddo intrusion also provides a minimum age of c. 1.8 Ga for deposition, deformation and metamorphism of the sedimentary succession.

The metamorphic grade in the Snavva–Sjöfallet group increases from low-grade at Stora Sjöfallet and within the Tjåmotis area, southwards to high-grade, migmatised rocks, with sillimanite, cordierite and garnet in the north of the Lövnäs area. In the low-grade area, the sedimentary sequence mainly

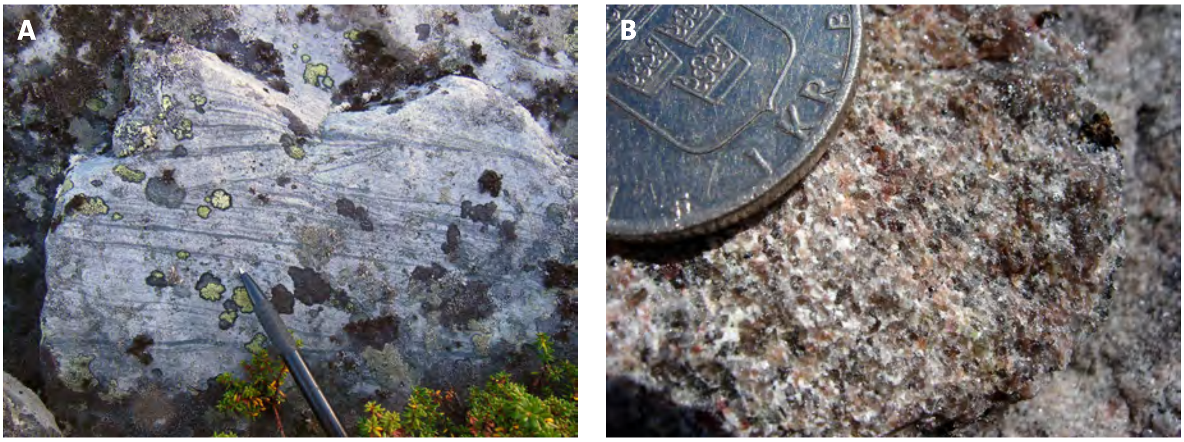

Figure 56. **A.** Cross-bedding in sandstone, enhanced by horizons of heavy minerals. Roahtek, about 15 km west-northwest of Tjåmotis (7431223/641592). Photo: Stefan Persson. **B.** Arkose with recognisable grains. Sarvvátj, about 23 km north-northeast of Lövnäs (7383820/633402). Carl-Henrik Pettersson.

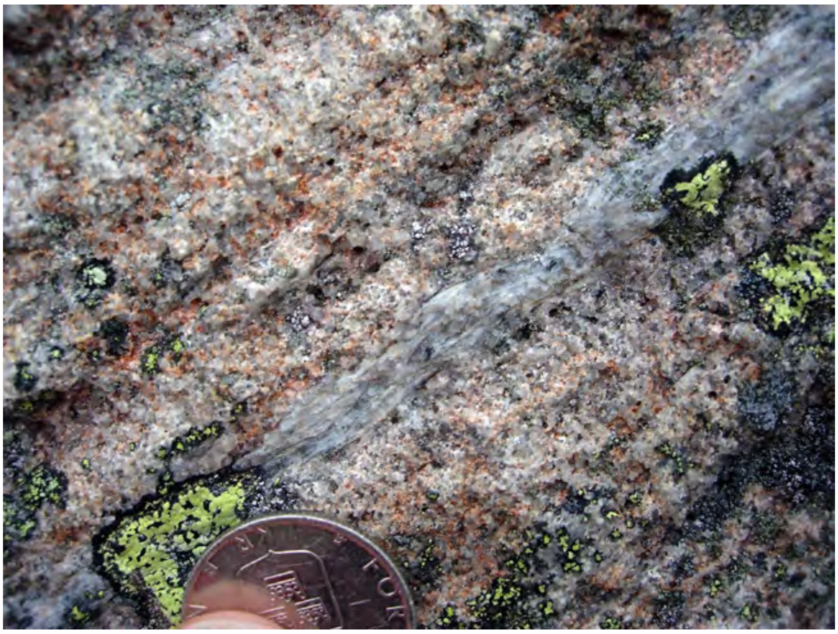

Figure 57. Fibrous sillimanite in recrystallised arkose. Dábmuk, about 20 km north-northeast of Lövnäs (7380796/632206). Photo: Carl-Henrik Pettersson.

consists of sandstones showing very well-preserved primary structures such as bedding and cross-bedding (Fig. 56a). Locally, the original grain size and grain shapes can also be observed (Fig. 56b). Recrystallisation and growth of metamorphic minerals are common in the high-grade northern part of the Lövnäs area (Fig. 57). Different degrees of migmatisation are expressed as granitic veins in sandstone, arkoses or quartzites, as well as stromatic (Fig. 58a), nebulitic and diatexitic structures (Fig. 58b). South of Lövnäs, the Snavva–Sjöfallet group and underlying volcanic rocks are truncated by a north–northwest-striking deformation zone. The part of the Snavva–Sjöfallet group that occurs south of this zone shows low metamorphic grade. The predominant rock types are sandstones, arkoses and conglomerates with preserved primary structures. Further south, paragneisses and quartzites indicate a somewhat higher metamorphic grade.

Typical features of the higher grade rocks of the Snavva–Sjöfallet group are strong variations from well-preserved rocks to diatexites o a scale of several tens of metres. South of Tjåmotis, quartzite with bedding and cross-bedding passes via andalusite- and sillimanite-bearing layers into diatexite with sillimanite.

Figure 58. **A.** Stromatic migmatite. Svierdek, about 22 km north-northeast of Lövnäs (7381896/635396). Carl-Henrik Pettersson. **B.** Diatexitic migmatite. Dábmuk, about 20 km north-northeast of Lövnäs (7380920/632803). Carl-Henrik Pettersson.

At Njavve between Kvikkjokk and Tjåmotis, a polymict conglomerate contains rounded and angular clasts of phenocryst-bearing felsic volcanic rocks, sandstone, quartzite, vein quartz, light granitoids and subordinate mafic intrusive rocks. The conglomerate has been recrystallised and foliated to varying degrees, with elongated clasts oriented along the foliation. Migmatisation varies perpendicular to bedding on a scale of a few metres. It is debated whether this selective migmatisation in both examples is due to differences in composition in different beds or the influence of fluids migrating along bedding or foliation surfaces.

North of Lövnäs, there are some elongated and foliation-parallel intercalations of fine-grained, foliated amphibolites of basaltic composition in the mainly sedimentary sequence of the Snavva–Sjöfallet group. The protoliths of these intercalations are interpreted to be coherent rocks, either dykes or sills.

Bedding has been observed in sandstones, arkoses, greywackes and quartzites in the Lövnäs area and the south of the Tjåmotis area. In the north of that area, bedding has only been observed in a few places. Cross-bedding occurs locally in both areas (Fig. 56a). Up to one metre thick massive beds have been recorded from arkoses south of Lövnäs. Although most of the sedimentary rocks of the Snavva–Sjöfallet group have been altered or recrystallised, primary textures such as different degrees of sorting and roundness of grains have been observed in sandstones, arenites and greywackes, but locally also in the paleosome of migmatitic rocks.

Sillimanite is the commonest metamorphic mineral, and has been observed in almost all sedimentary rocks of the Snavva–Sjöfallet group (Fig. 57). Andalusite occurs in sandstone, quartzite, greywacke and paragneiss of the Tjåmotis area south of Tjåmotis, but is somewhat rarer north of there. Cordierite has been found mainly in paragneisses and migmatites west of Tjåmotis and north of Lövnäs. Garnet is found in sandstones, quartzites, arkoses and greywackes, in both the Tjåmotis and the Lövnäs area. Epidote is reported from the entire belt within the project area. There seems to be a rough zonation of metamorphic minerals in the Lövnäs area, with cordierite more common in the northwest and garnet in the southeast.

Hematite and, to a somewhat lesser extent, magnetite are common oxide minerals in the north and centre of the Lövnäs area. Several distinct magnetic anomalies occur in the Lövnäs area, mainly north of Lövnäs. These are caused by thin layers of banded iron ore (magnetite) associated with limestone and skarn (Fig. 59). Stratiform iron mineralisations north-northwest of Tjåmotis (Nysten et al. 2014), at the boundary between the Snavva–Sjöfallet group and the underlying Arvidsjaur group, can be assigned either to the former or the latter group. Here we include them in the Snavva–Sjöfallet group. It should be noted that sulphide minerals have not been observed in the whole Snavva–Sjöfallet group, except one observation of molybdenite at the Munka prospect.

Figure 59. Magnetite and skarn bands in fine-grained sandstone. Guonek, about 4 km northeast of Lövnäs (7363546/630893). Photo: Erik Nordfeldt.

Figure 60. Recrystallised volcaniclastic rhyolite, sandstone or arkose? Håhpális, about 4.7 km southeast of Lövnäs (7358630/631131). Photo: Benno Kathol.

Metamorphic rocks of sedimentary origin on both sides of Lake Tjaktjajávrre, north of Tjåmotis, have been described as Snavva sediments, and were interpreted to be older than overlying volcanic series (Ödman 1947). This stratigraphic relationship was later revised by Carlon (1984), Zachrisson & Witschard (1995a, b), Kumpulainen (2003) and Nysten et al. (2014), who state that the sequence is overturned and the Snavva–Sjöfallet group stratigraphically overlies the volcanic units.

In the Tjåmotis area, the transition from volcanic rocks to the overlying Snavva–Sjöfallet group is gradational with redeposited volcaniclastic material, chemical sedimentary rocks, carbonate rocks and mafic volcanic rocks (Carlon 1984). Within the Lövnäs area, the rocks of the Snavva–Sjöfallet group and the underlying mainly felsic volcanic rocks of the Porphyrite group are strongly recrystallised and may have originated as volcaniclastic or epiclastic sediments (Fig. 60). This makes it difficult to draw conclusions about the nature of the contact between the groups. According to Kumpulainen et al. (2003), the Snavva–Sjöfallet group was deposited conformably on the volcanic substratum, i.e. the contact is a disconformity.

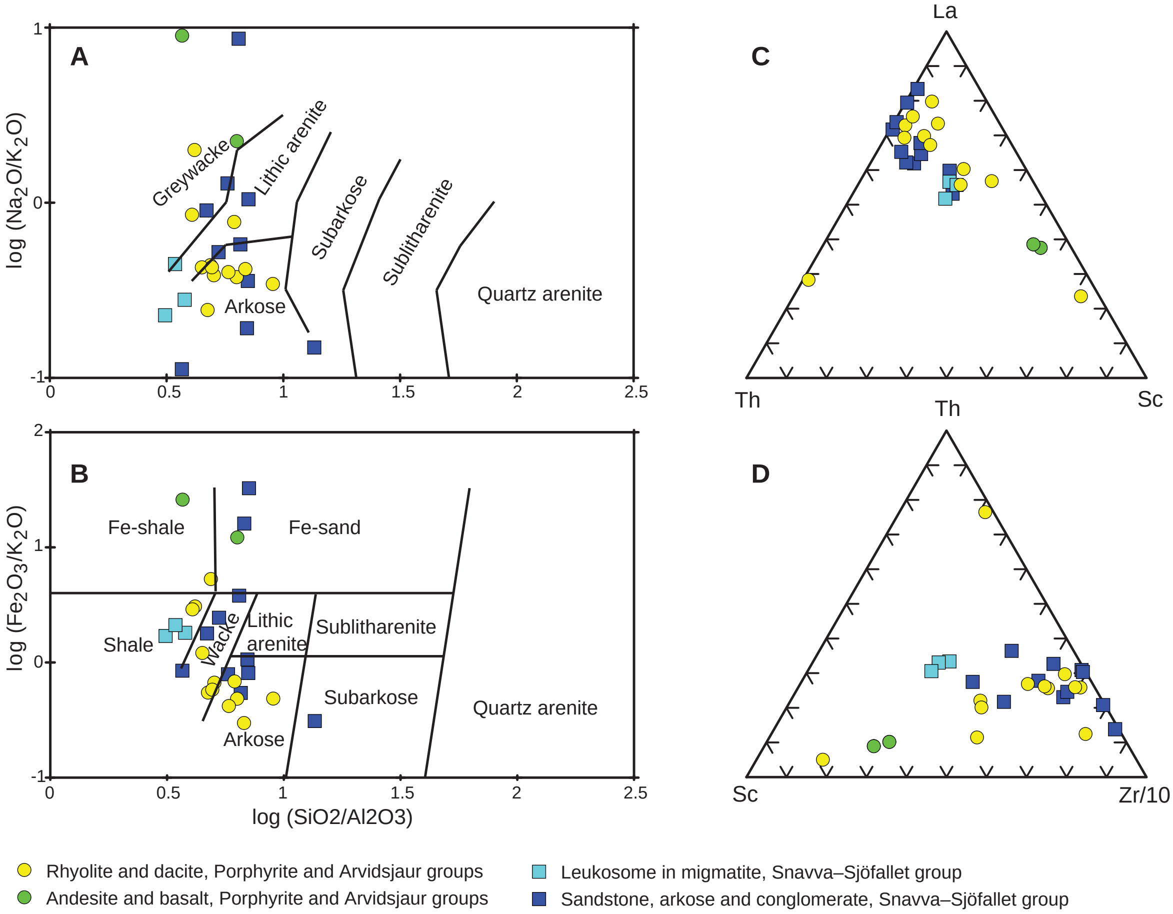

Figure 61. Diagrams showing geochemical analyses from the Snavva–Sjöfallet group and the Porphyrite and Arvidsjaur groups. **A.** Classification diagram for sedimentary rocks according to Pettijohn et al. (1972). **B.** Classification diagram for sedimentary rocks according to Herron (1988). **C** and **D.** Ternary diagrams according to Bhatia & Crook (1986).

Geochemical discrimination diagrams by Pettijohn et al. (1972), Bhatia & Crook (1986) and Herron (1988) show no significant differences between sandstones, arkoses and conglomerates of the Snavva–Sjöfallet group and volcaniclastic rocks and volcanic sandstones from the underlying Porphyrite and Arvidsjaur groups (Figs. 61a–d). This might indicate that the clastic sediments of the Snavva–Sjöfallet group are derived from the volcanic rocks of the Porphyrite and Arvidsjaur groups. Provenance studies on zircon would be necessary to prove this assumption.

A conglomerate with a rounded clast of a sillimanite-bearing, quartz-rich sedimentary rock (sillimanite quartzite) has been observed in the north of the Ábbmo peninsula north-northeast of Lövnäs (Fig. 62). The occurrence of sillimanite seems to be confined to the clast material, which indicates that the clasts are derived from a previously metamorphosed sedimentary rock. Whether this rock belongs to the Snavva–Sjöfallet group, the Bothnian supergroup or some other unit, at least two phases of metamorphism with intervening uplift and erosion are recorded by this relationship.

Svecofennian, c. 1.88 Ga old or younger, well-preserved supracrustal rocks west of Svartlå are named the Svartlå group, or previously the Svartlå series (Svartlåserien; Grip 1946). The name Svartlå group was mentioned on the Geological map of pre-Quaternary rocks in Northern Fennoscandia (Silvenoinen et al. 1987) and was retained on the Bedrock map of Central Fennoscandia (Lundqvist et al. 1996a) and by Lindström et al. (2000). Silvenoinen et al. (1987) and Lundqvist et al. (1996a) placed the Svartlå group together with the Snavva–Sjöfallet group and the Loito formation of the Bure group in what

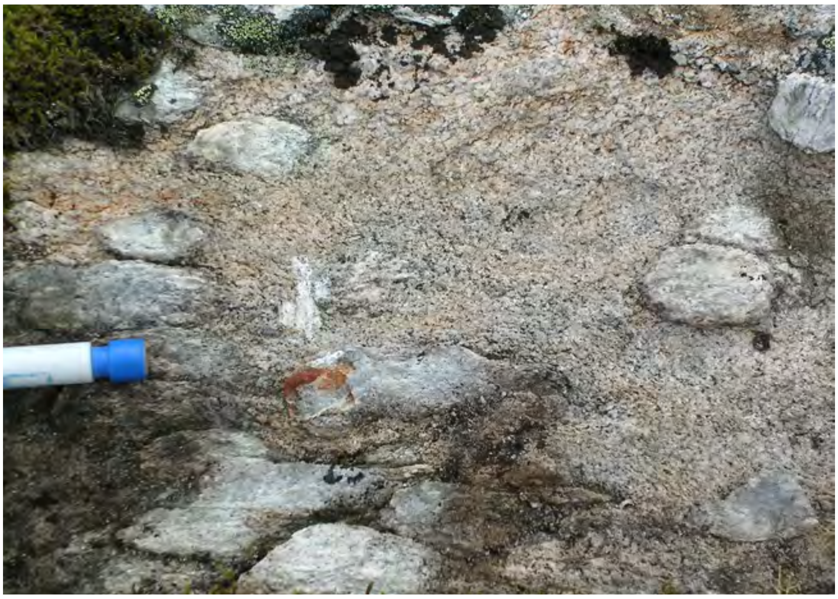

Figure 62. Conglomerate with rounded clasts of a sillimanite-bearing, quartz-rich sedimentary rock. Ábbmo peninsula, about 14 km north-northeast of Lövnäs (7375070/630551). Photo: Daniel Larsson.

these authors call the Upper Svecofennian assemblages. In this project, the Svartlå group is correlated with the Snavva–Sjöfallet group further to the west.

The rocks of the Svartlå group occur in a north–south elongated bowl-shaped structure on top of metasedimentary rocks of the Bothnian supergroup. In the east, the Svartlå group locally overlies ignimbritic rhyolites of the Arvidsjaur group (Kathol et al. 2012b). The Svartlå group is divided into two units consisting of sandstones and arkoses with grain sizes from medium sand to very coarse sand, and greywackes and argillites ranging in grain size from silt to medium sand. Massive beds of sandstone up to 2 m thick occur locally in the former unit, and andalusite porphyroblasts are common in the finer-grained layers of the latter unit (Fig. 63a). The two units are interlayered with each other, but in general the greywacke and argillite unit forms the bottom and top of the bowl-shaped structure and the sandstones and arkoses occur in the central parts. Intercalations of mafic volcanic rocks, locally showing pillow structures and subordinate felsic laminated tuffs (Fig. 63b) and volcanic breccias (Fig. 63c) occur within the sedimentary sequences. Almost without exception, the greywackes display structures such as graded bedding and load casts, which are typical of turbidites (Fig. 63d).

Most of the sedimentary rocks of the Svartlå group show acid to intermediate compositions, and Kathol et al. (2012b) assume that the clastic material was derived from volcanic rocks, probably those of the Arvidsjaur group in the east. However, a significant proportion of coarse quartz and feldspar grains in the sandstones and arkoses indicate that the Svartlå group was also derived from coarser-grained intrusive rocks and migmatitic rocks of the Bothnian supergroup.

In earlier literature, the Svartlå group was considered to rest with an unconformity on the metasedimentary rocks of the Bothnian supergroup. This interpretation was probably based on the well-preserved character of the rocks of the Svartlå group in contrast to the strongly deformed and migmatised rocks in the Bothnian supergroup. Recent mapping by SGU suggests that the Svartlå group overlies the volcanic rocks of the Arvidsjaur group with a disconformity, but that both groups rest with a major unconformity on the rocks of the Bothnian supergroup.

Deposition in a subaqueous environment is confirmed by the turbiditic character of the sedimentary units, which requires a water depth of at least 300 m, and the existence of pillow lavas. This contrasts with the gradual transition from the ignimbritic volcanic rocks in the east, which indicate subaerial conditions during deposition.

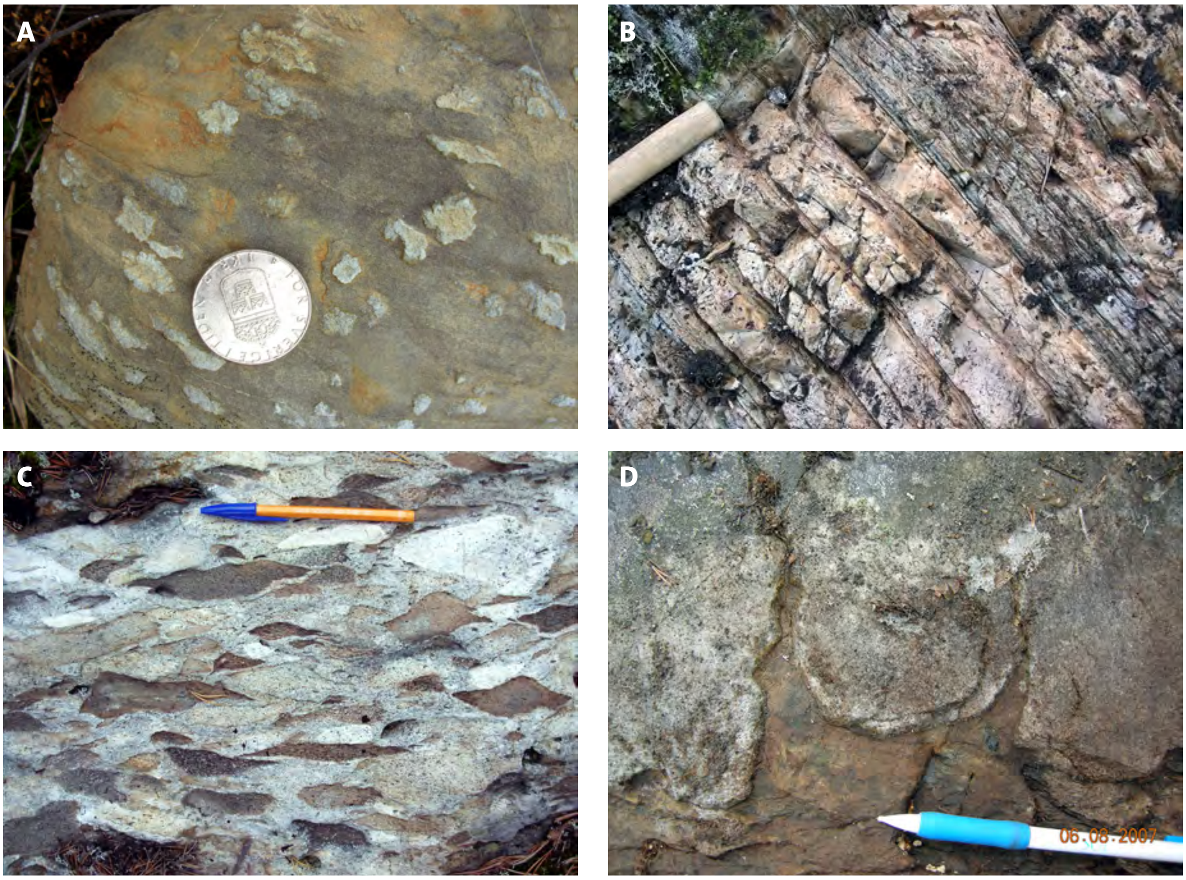

Figure 63. **A.** Turbiditic greywacke with andalusite porphyroblasts. Kängesberget, about 5.5 km south of Svartlå (7329250/778821). Photo: Benno Kathol. **B.** Thin-bedded rhyolitic tuff. Kängesberget, about 5 km south of Svartlå (7329890/780465). Photo: Risto Kumpulainen. **C.** Breccia with elongated dacitic and andesitic fragments oriented parallel to the foliation. Groundmass consists of rhyolitic volcanic sandstone with arkosic composition. Local boulder at Flakaberget, about 3 km south-southwest of Svartlå (7332242 778172). Photo: Benno Kathol. **D.** Load casts in turbiditic sandstone. Flakaberget, about 2.7 km south-southwest of Svartlå (7332380/778630). Photo: Risto Kumpulainen.

Early Svecokarelian intrusive rocks, c. 1.89–1.85 Ga (Perthite monzonite suite)

Early Svecokarelian alkali-calcic intrusive rocks, mainly granites and syenitoids and subordinate diorites and gabbros, occur throughout Norrbotten County and the north of Västerbotten County. These rocks are named the Perthite monzonite suite. Towards the southwest, the suite is confined along a northwest–southeast-striking line between Skellefteå and Sorsele, which is more or less parallel with the main structures in the Skellefte district. This line is also (sub-) parallel with the Luleå–Jokkmokk zone further to the northeast. This contrasts with the early Svecokarelian calc-alkaline Jörn GI suite, which does not show such a distinct boundary towards the south or southwest. Within the Perthite monzonite suite, no distinction is drawn between juvenile or Archaean crust-influenced magma generation, as with the Jörn GI and Haparanda suites (see above).

Rocks of what is now called the Perthite monzonite suite have been described from the Kiruna area and Masugnsbyn as quartz syenites to granites and were called Perthite-granites by Geijer (1931). Similar rocks in map area 29L Lainio have been called Perthite monzonites (Witschard 1970). The bedrock in much of map area 28J Fjällåsen consists of monzonites and quartz monzonites and was named the Perthite Granite series by Witschard (1975). Later, Witschard (1984) introduced the name Perthite monzonite suite for the rocks occurring in a broad belt parallel to the Caledonides.

Within the rocks of the Perthite monzonite suite in the project area, radiometric age determinations, interpreted as crystallisation ages, have been published by Skiöld et al. (1993), Wikström et al. (1996b),

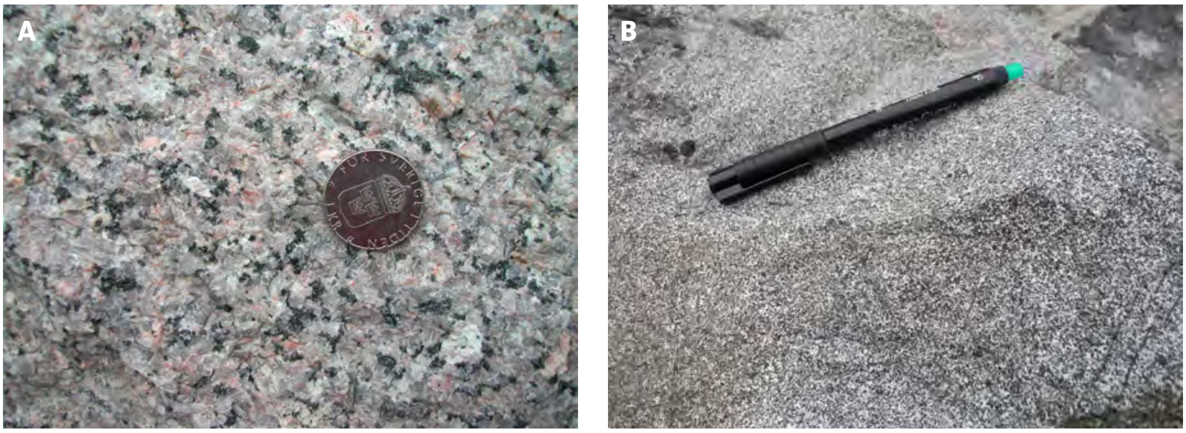

Figure 64. **A.** Medium- to coarse-grained, massive granite. Road cutting, about 800 m west of Varjisträsk (7332239/704343). Photo: Benno Kathol. **B.** Finely medium-grained, massive, equigranular and subophitic gabbro. Road cutting at Padjerim, about 10 km west-northwest of Vuollerim (7382410/740426). Photo: Per Nysten.

Kathol & Aaro (2006a, b), Mellqvist & Aaro (2006a, b), Åkerman & Kero (2012c), Claeson & Antal Lundin (2012c), Hellström et al. (2012a, b, c), Kathol et al. (2012b), Jonsson & Kero (2013a, b, c) and Hellström et al. (2015). The analyses were carried out using the U-Pb method on zircons, using either the SIMS or TIMS technique. The ages obtained range from 1.88 to 1.86 Ga or, if error intervals are taken into account, from 1.89 to 1.85 Ga.

Recent U-Pb zircon dating of a quartz monzonite from the area north of Sjávnjaluokta in the Sjaunjaätno massif (Witschard 1975) yielded a crystallisation age of 1878 ± 4 Ma (Kathol & Hellström in press). The latter authors propose the area north of Sjávnjaluokta within the Sjaunjaätno massif as the lectotype area (see Kumpulainen 2017) for the Perthite monzonite suite in Norrbotten and northern Västerbotten counties.

South of the project area, the rocks of the Perthite monzonite suite have been proved to be coeval and comagmatic with the volcanic rocks of the Arvidsjaur group (see page 41, Arvidsjaur group). Within the project area, the Perthite monzonite suite shows a close spatial relationship with the Arvidsjaur group rocks, but locally also with the Porphyrite group. This highlights the need for further investigation and evaluation of the relationship between the Arvidsjaur and the Porphyrite groups. A close relationship with the volcanic rocks of the Arvidsjaur group implies that magma generation and intrusion are related to a continental arc, with the Arvidsjaur group rocks as the supracrustal (extrusive) products.

In the Överkalix lithotectonic unit and the eastern part of the Norrbotten lithotectonic unit, rocks of the Perthite monzonite unit occur as isolated massifs with no or very little spatial relationship to Svecofennian volcanic rocks. This might indicate that the present ground surface represents a deeper erosional level in these lithotectonic units.

Hellström et al. (2015) show that the Vuolvojaur granite, which makes up much of the Perthite monzonite suite in the west of the project area, has an upper crustal trace element geochemical signature. The authors suggest that the granite formed at a convergent margin above a subduction zone dipping to the present north. This concept is here applied to the Perthite monzonite suite in the whole project area. In contrast, an intra-plate emplacement of the rocks of the Perthite monzonite suite has been suggested by Billström et al. (2010).

Virtually all of the bedrock of the Perthite monzonite suite within the project area consists of granite *sensu stricto* (Fig. 64a). Syenitoid to granite is the predominant rock type in the northern part of the Överkalix lithotectonic unit (subarea 7 and the north of subarea 8). Rocks of syenitoid to granitic composition also occur south of Örnvik, between Moskosel, Luvos, Porjus and Jokkmokk, south of Hakkas and around Narken. Granodiorite to granite occurs as a larger massif south of Råneå, minor occurrences of rocks of tonalitic to granodioritic composition have been reported from the area around

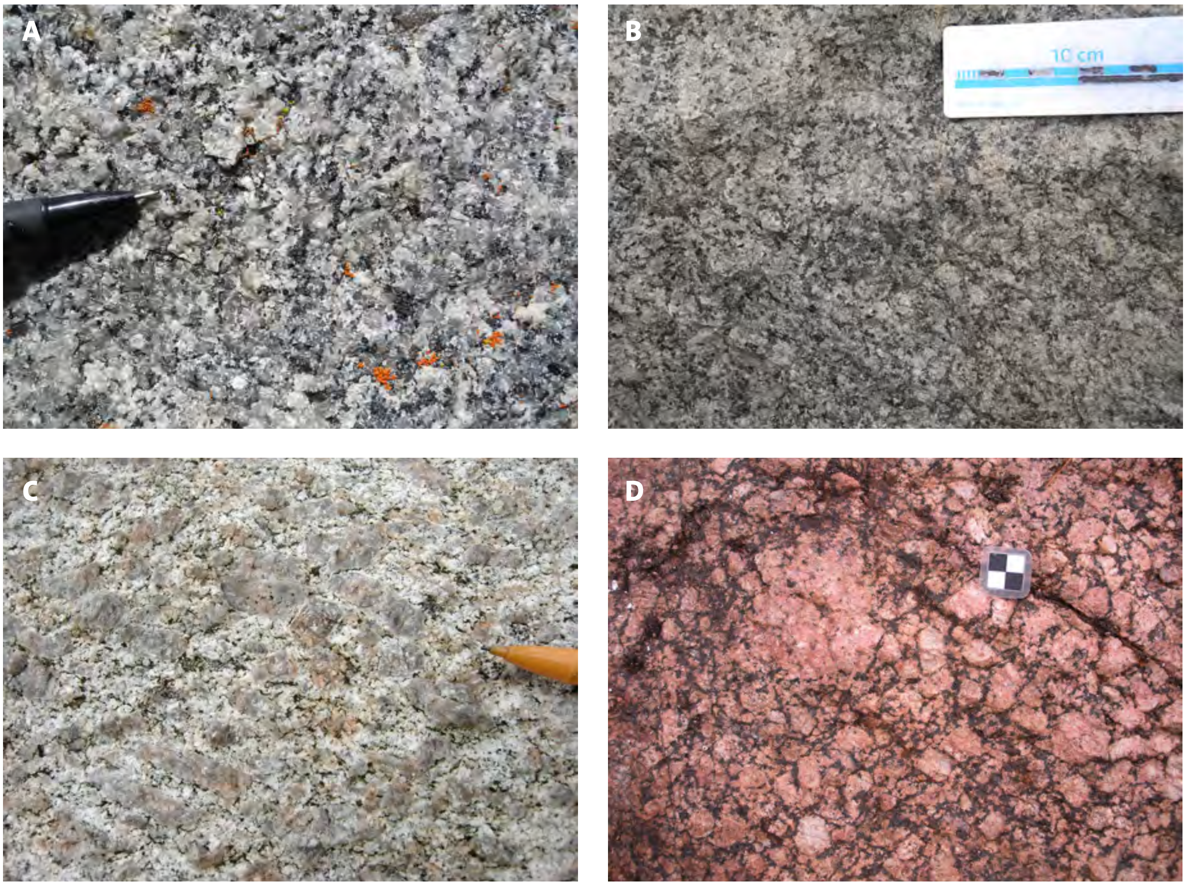

Figure 65. **A.** Medium-grained, relict coarse-grained, inequigranular, foliated and lineated granodiorite to granite. Rock fall at Davvevárre, about 7 km southeast of Kvikkjokk (7423171/623189). Photo: Benno Kathol. **B.** Medium- to coarse-grained, massive, inequigranular to porphyritic syenitoid rock. Road cutting at lake Hundsjön, about 15 km north of Boden (7331448/809738). Photo: Martiya Sadeghi. **C.** Microcline porphyritic, coarsely medium-grained, massive granite. Parallel orientation of phenocrysts is interpreted to represent magmatic flow banding (magma flow). Haisukangas, about 25 km northeast of Kalix (7344420/889353). Photo: Ulf Bergström. **D.** Potassium feldspar porphyritic monzonite with amphibole-rich groundmass. Note that granitic aggregates (to the left of the scale) contain conspicuously fewer mafic minerals and more quartz crystals than the monzonite. Njuorramjávrásj, about 34 km northwest of Jokkmokk (7421360/690793). Photo: Dick Claeson.

Moskosel, Trollforsen and Varjisträsk, as well as between Hakkas and Lansjärv. A large massif of monzodiorite to granodiorite with a north–south extension of about 40 km is situated west of Boden. Minor occurrences of monzodiorite to granodiorite occur mainly in the centre of the map area between Arjeplog and Porjus. Gabbroid to dioritoid rocks are present in almost all of the Perthite monzonite suite occurrences east of the Karesuando–Arjeplog deformation zone (Fig. 64b). They are mostly located inside or in contact with felsic intrusive rocks of the Perthite monzonite suite. A minor isolated occurrence constitutes a megaxenolith in late Svecokarelian (1.80–1.77 Ga) intrusive rocks west of Arjeplog. In addition, three massifs occur in the sedimentary sequence of the Svartlå group southeast of Harads. One of them occurs in contact with basalt and andesite of the Svartlå group, which might indicate a genetic relationship (generation from subvolcanic magma chambers) between the rock types.

An elongate occurrence of mafic rock in the archipelago south of Töre has been interpreted as dolerite; the mafic rock strikes roughly north–south, parallel to the general structural trend in the Pajala deformation belt. Ultramafic intrusive rocks have been found as 1–2 kilometre-sized bodies within sedimentary rocks of the Sockberget and Bothnian groups southeast of Överkalix. Most of the gabbroid to dioritoids are either inequigranular (Figs. 65a, b) or porphyritic (Figs. 65c, d), but equigranular varieties also occur. All three varieties are present side by side in most occurrences of the Perthite monzonite suite.

Most of the rocks of the Perthite monzonite suite have a medium-grained groundmass with subordinate finely medium-grained and somewhat less coarsely medium-grained varieties. Fine-grained groundmass also occurs, but rocks with coarse-grained groundmass are subordinate. Phenocrysts are generally <20 mm in size; rocks with phenocrysts >20 mm occur subordinately. This applies to feldspar phenocrysts; amphibole and quartz phenocrysts are normally smaller than 10 mm. Feldspar, especially potassium feldspar, is the most common phenocryst mineral. Quartz phenocrysts occur subordinately, and amphibole phenocrysts are rare.

Locally, the porphyritic texture is hard to recognise on both fresh and smoothly weathered surfaces (Figs. 66a, b). In many cases recrystallisation obscures the original porphyritic texture of the rock (Fig. 66c).

The mafic intrusions of the Perthite monzonite suite are similar to those of the Jörn GI and Haparanda suites, in terms both of their macroscopic character and their geochemical composition (including trace element spectra), and they are therefore difficult to distinguish from each other. Many mafic intrusions have been assigned to the Perthite monzonite suite merely because of their spatial relationship with felsic rocks of this suite. In places, magma mingling and magma mixing structures support this classification.

Hybrid rocks evolving from magma mixing between granitic to syenitoid and gabbroid to dioritoid phases have been observed in several places. Quartz monzodioritic to monzonitic hybrid rocks southwest of Karsbergfallet show rapakivi texture and hornblende-mantled quartz grains (ocelli), indicating magma mixing (Figs. 67a, b). In addition, the presence of mafic magmatic enclaves in the felsic rocks indicates magma mingling. Rapakivi textures have also been observed east of Varisträsk, west of Boden and at a few places between Hakkas and Korpilombolo. Numerous inclusions of coarsely feldspar-porphyritic granite have been observed in a gabbroid to dioritoid intrusion around Njuöniesvárrie southwest of Trollforsen. Up to 3 cm large feldspar phenocrysts have migrated from the granitic inclusions into the mafic magma, indicating magma mingling between felsic and mafic phases. The occurrence of ocelli indicates that magma mixing has also taken place in this area (Fig. 67c). Mafic magmatic enclaves have also been observed in places east of Arjeplog and Gunnarsbyn, west of Jokkmokk and Boden, south of Hakkas, Karsbergsfallet and Pålkem and around Narken.

Foliated, gneissic and banded varieties occur side by side with massive rocks in many areas of the Perthite monzonite suite. In several cases, elongate feldspar phenocrysts show a preferred orientation, but it is not obvious whether this is an igneous flow structure or the result of overprinting solid-state deformation (Fig. 68a). Distinct linear structures occur (Fig. 68b, c) in many areas in the Bothnia–Skellefteå and the Norrbotten lithotectonic unit, but are subordinate to tectonic foliation. Within the Överkalix lithotectonic unit, lineation has mainly been reported from the areas southeast of Överkalix and southwest of Övertorneå.

Recrystallisation of the Perthite monzonite suite rocks is common and most intensive on both sides of the Karesuando–Arjeplog deformation zone and in the north of the Norrbotten lithotectonic unit, coinciding with areas with most frequent observations of linear structures. Migmatisation occurs at several places in the southeast of the Norrbotten lithotectonic unit around Boden. Veining as a type of migmatisation is a common feature east of Lövnäs, between Arjeplog and Moskosel, and between Boden and Gunnarsbyn. Hydrothermal alteration has been reported from granites in the area between Tjåmotis and Jokkmokk.

In the project area, large continuous areas with consistently deformed bedrock of the Perthite monzonite suite occur, as well as areas of predominantly undeformed and massive bedrock. To the west of Trollforsen, undeformed massive granites form extensive, smooth outcrops exposing almost fracture-free bedrock surfaces extending over several hundred square metres (Fig. 69).

Dykes occur almost everywhere in the rocks of the Perthite monzonite suite. Most of them consist of pegmatite, followed by less common granite and aplite. Dolerite dykes and dykes of gabbro to diorite and quartz diorite are subordinate, except for the area between the Ligga and Harsprånget power stations between Jokkmokk and Porjus, where dolerite dykes up to several metres thick are exposed.

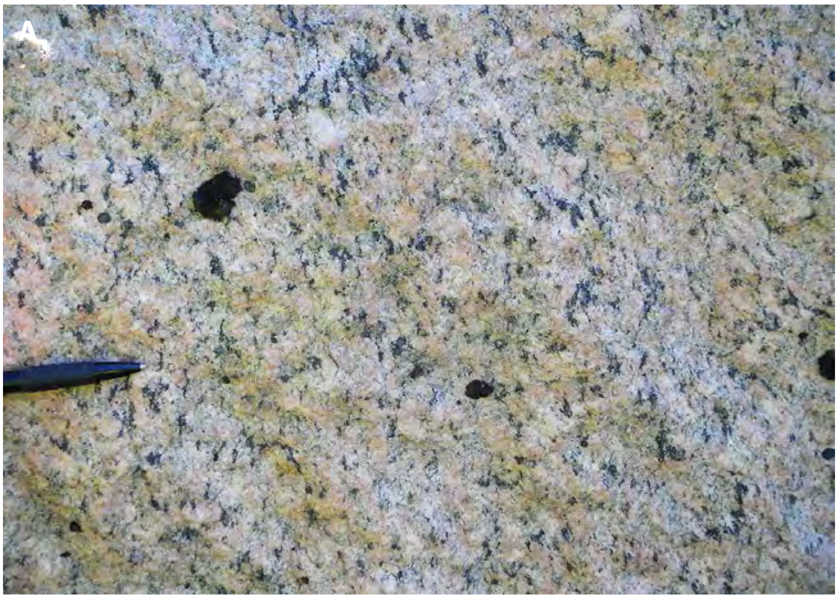

Figure 66. **A.** Recrystallised, relict medium-grained, feldspar porphyritic, foliated granite. Road cutting at road E 45 south of Harsprånget, about 10 km south of Porjus (7424763/711152). Photo: Benno Kathol.

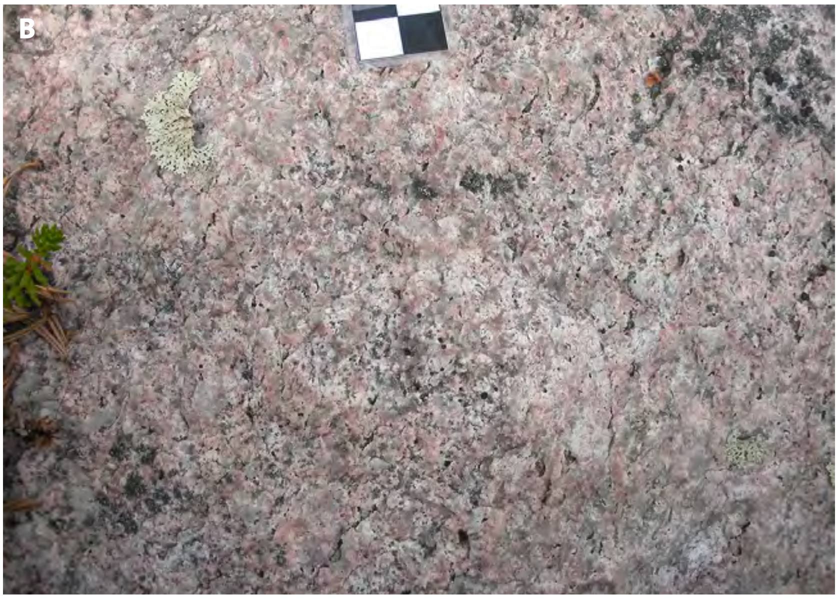

Figure 66. **B.** Weathered surface of recrystallised, medium- to coarse-grained, porphyritic and foliated granite. Juovvavárre, about 16 km east-northeast of Luvos (7401116/685625). Photo: Dick Claeson.

Figure 66 **C.** Recrystallised, relict porphyritic (?), medium-grained, foliated and lineated granite. Access road to the Randi power station, about 17.5 km northwest of Jokkmokk (7406304/699959). Photo: Benno Kathol.

Figure 67. **A.** Monzonitic, hybrid, porphyritic rock with rapakivi texture and hornblende-mantled quartz grains (ocelli). Randaträskberget, about 6 km southwest of Karsbergsfallet (7372075/776544). Photo: Stefan Bergman.

Figure 67. **B.** Quartz monzodioritic hybrid rock with abundant hornblende-mantled quartz grains (ocelli). Randaträskberget, about 6.7 km southwest of Karsbergsfallet (7371472/776477). Photo: Stefan Bergman.

Figure 67. **C.** Magma mingling and mixing between mafic and felsic magmas and migrating feldspar-phenocrysts. Njuöniesvárrie, about 29 km west-northwest of Moskosel (7322404/675033). Photo: Benno Kathol.

Figure 68. **A.** Alkali feldspar-porphyritic granite with medium-grained groundmass. Parallel orientation of the phenocrysts may be the result of igneous flow banding or solid-state deformation. Southern Brändön, about 22 km south of Råneå (7301789/ 836301). Photo: Martiya Sadeghi.

Figure 68. **B.** Distinct linear structure in recrystallised, relict porphyritic granite. The surface shown is parallel to the lineation. Road cutting between Mellan-Stubba and Sör-Stubba, about 14 km north-east of Porjus (7445020/719070). Photo: Benno Kathol.

Figure 68. **C.** Strongly developed linear structure in recrystallised, fine-grained, relict medium-grained, porphyritic granite. Close to Stora Luleälven at Bergmyran, about 26 km south-southeast of Porjus (7413325/724891). Photo: Benno Kathol.

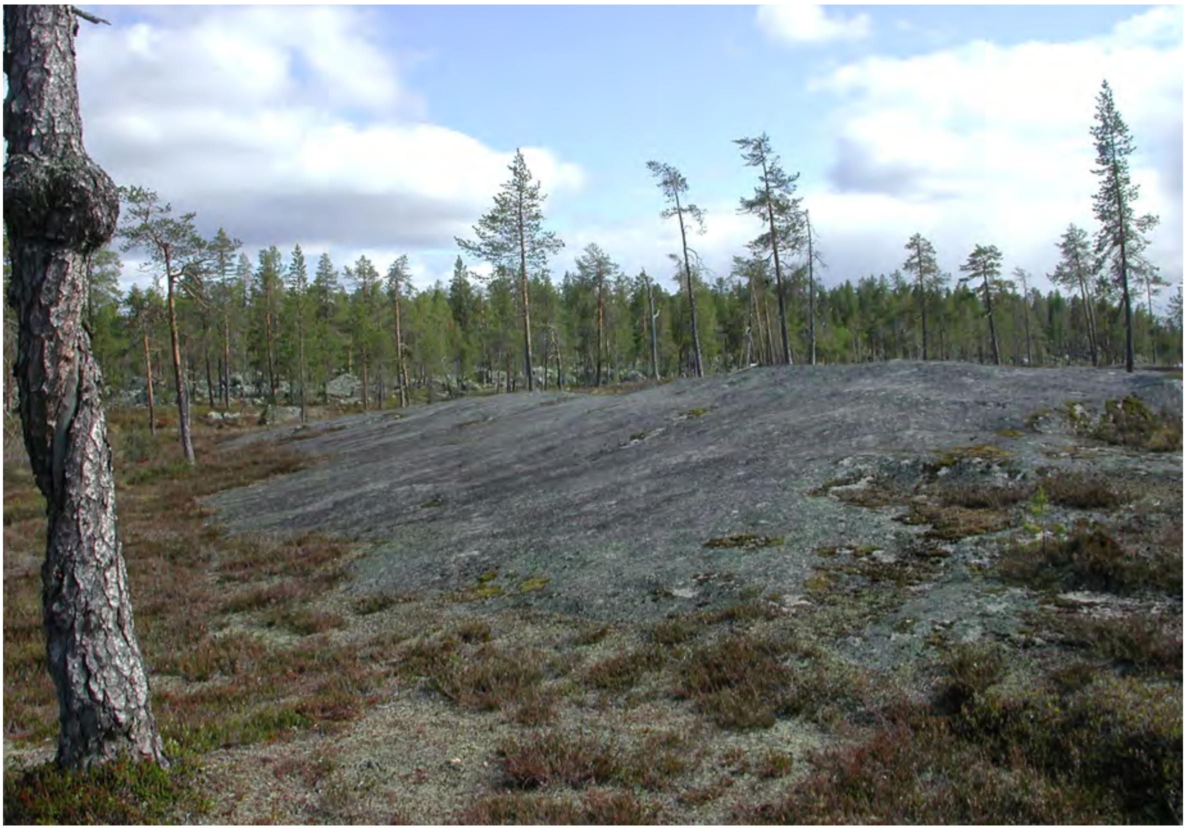

Figure 69. Large outcrops of almost fracture-free massive granite. Fracture-free surfaces of 20 × 20 m are not unusual. Bavlavuöbmie, south of Jäkna, about 28 km northwest of Moskosel (7330566/680982). Photo: Benno Kathol.

The dykes show approximately north–south orientation and occur in granites of the Perthite monzonite suite (Fig. 70a).Subordinate dykes of volcanic rocks also occur, and are most commonly of andesitic and rhyolitic composition. In several cases, the dykes (particularly pegmatite and granite) are considered to be coeval with, or slightly younger than the host rocks. In other places, the dykes cut the foliation in the Perthite monzonite suite host rock and are thus younger than the host rock and the formation of the foliation (Fig. 70b). However, for most observations no information on the age of the dykes is available.

Inclusions and xenoliths occur frequently in the Perthite monzonite suite. They mostly comprise intrusive rocks. About a quarter of them consist of volcanic rocks, but sedimentary rocks are rare. Among the intrusive rocks, felsic varieties are somewhat more common than mafic ones. Volcanic inclusions and xenoliths mostly consist of andesite and rhyolite.

The granites and syenitoids of the Perthite monzonite suite are characterised by strongly perthitic feldspars and, locally, the occurrence of pyroxene, mainly clinopyroxene and rare orthopyroxene (Ödman 1957, Witschard 1984). Amphibole is a common constituent in mafic rocks, and also in granites and subordinately in syenitoids and granitoids. Fluorite has been observed mainly in granites and subordinately in syenitoid rocks in the west of the project area.

Magnetite has been found in many places in the Perthite monzonite suite to the west of the Pajala deformation belt, but is rare within and east of the belt. Hematite has been observed locally in the major occurrences of the Perthite monzonite suite in the west between Arjeplog, Porjus and Moskosel, southeast of Hakkas, northwest of Boden and at Narken. Magnetite and hematite both occur mainly in granites, and less frequently in granitoids and syenitoids. Magnetite has also been found in pegmatites. Sulphide minerals, including pyrite and chalcopyrite, have been observed in roughly the same areas

Figure 70. **A.** Dolerite dykes in granite of the Perthite monzonite suite. Drained riverbed of River Stora Luleälven below the Harsprånget power dam at "Utsikten", about 8.5 km south of Porjus (7425979/710965). Photo: Benno Kathol.

Figure 70. **B.** Zoned dyke of light quartz diorite in coarsely porphyritic quartz monzonite (Degerberget granite) of the Perthite monzonite suite. The dyke cuts the foliation, indicated by red lines, in the quartz monzonite. Southern Brändön, about 22 km south of Råneå (7301789/836301). Photo: Benno Kathol.

as magnetite, but less frequently than the latter. They occur mainly in felsic rocks and somewhat less in mafic varieties. Within the Överkalix lithotectonic unit, pyrite and chalcopyrite have only been found in a gabbroid to dioritoid intrusion east of Korpilombolo. Fissure fillings of quartz and quartz dykes and veins occur frequently in the Skellefteå–Bothnia and Norrbotten lithotectonic units, but are only rarely observed in the Överkalix lithotectonic unit.

Late Svecokarelian supracrustal rocks, c. 1.84–1.77 Ga

Grey to dark grey basaltic andesite to andesite at Tjäkkaure northeast of Luvos show banding and lineation, the latter defined by the orientation of fragments. Banding and lineation are both interpreted as primary magmatic structures. The volcanic rocks at Tjäkkaure are better preserved than the surrounding volcanic rocks of the Arvidsjaur group (Claeson & Antal Lundin in press-b). U-Pb zircon dating of these rocks yielded a crystallisation age of c. 1770 Ma (SGU unpublished). Claeson & Antal Lundin (in press-b) interpret the volcanic rocks at Tjäkkaure to be related to the bimodal Hárrevárddo

Figure 71. Subvolcanic porphyritic granite to quartz monzonite. Bergnäs, about 42 km southwest of Arjeplog (7301763/598365). Photo: Benno Kathol.

intrusion to the west, rather than to the late Svecokarelian volcanic rocks at Dobblon (Skiöld 1988) to the south of the project area.

South of Båtsjaur, intrusive rocks of granitic-quartz monzonitic or rhyolitic-latitic composition occur. Locally, they display distinct porphyritic textures (Fig. 71). The rocks are massive and are interpreted to be subvolcanic intrusions (Kathol et al. 2014). Trace elements indicate that the porphyritic rocks can be correlated with the late Svecokarelian granites, which cover vast areas to the west of the Caledonian front in map area 25H Arjeplog. Distinct boundaries between the subvolcanic rocks and the late Svecokarelian granites have not been observed, but these rock types seem to pass gradationally into each other. This implies shallow level late Svecokarelian magmatism and that extrusive phases might exist that could be correlated with the volcanic rocks of the Gippervare formation in the Dobblon area approximately 35 km further to the south (Einarsson 1979, Skiöld 1988). However, a comparison of the geochemical character of the rock types does not support a correlation.

Late Svecokarelian intrusive rocks, c. 1.81–1.75 Ga (Edefors and Lina suites)

Within the project area, late Svecokarelian intrusive rocks are represented by the Lina and the Edefors suites. Rocks of the Edefors suite occur in four major massifs and a number of minor massifs to the west and southwest of the Nautanen deformation zone. To the northeast of the latter, the late Svecokarelian intrusive rocks are exclusively assigned to the Lina suite. To the west and southwest of the Nautanen deformation zone, rocks of the Lina suite also form some larger and a number of minor massifs, but to a somewhat lesser extent than the Edefors suite. There are only a few places where rocks of the Lina and the Edefors suites occur in contact which each other, but age relationships have not been observed. Normally the rocks of both suites occur as isolated massifs within older, early Svecokarelian intrusive or Svecofennian supracrustal rocks.

Holmqvist (1906) described a red, medium-grained, biotite-granite from the area around the railway bridge over Linaälven, approximately 26 km northwest of Gällivare, and called it Lina granite. Geijer (1931) expanded the use of this name to include all geologically and petrographically similar granites in the Kiruna–Gällivare–Pajala area. Ödman (1957) and Magnusson (1962) assigned migmatite granites as Lina granites and a series of non-migmatite-related granites, syenites and gabbros, e.g. the Edefors granite and the Boden syenite, to the "late Karelian intrusive rocks". Ödman (1957) further expanded the use of the name Lina granite to the whole of Norrbotten County.

The Edefors suite has been described from the Luleå–Edefors (Harads) area by Öhlander & Skiöld (1994). According to those authors, the rocks of the Edefors suite range from alkali-rich and distinctly metaluminous syenites to granites, which were formed in an extensional environment with a small input of older crustal material. Crystallisation from dry magmas is indicated by the scarcity of pegmatites and aplites (Öhlander & Skiöld 1994), whereas the granites of the Lina suite are usually associated with pegmatites. In some areas these pegmatites form larger massifs within the granites (Öhlander & Skiöld 1994). This statement can be confirmed in the project area, where the majority of pegmatites occur within the Lina suite, compared with distinctly less frequent pegmatites in the Edefors suite.

The field characteristics and petrophysical properties of the Edefors suite are very similar to those of the early Svecokarelian Perthite monzonite suite (Bergman et al. 2001). Indeed, Ödman (1957) had earlier included the Jokkmokk granite and the Degerberg granite in the "late Karelian intrusive rocks". However, based on U-Pb zircon dating, these rocks were later assigned to the early Svecokarelian Haparanda and Perthite monzonite suite, respectively, (Lundmark et al. 2005a, Wikström et al. 1996b).

The rocks of the Lina suite are considered to be the result of remobilisation of continental crust with a small amount of juvenile input (Öhlander et al. 1987a, Öhlander & Skiöld 1994). Mellqvist et al. (1999b) studied crustal reactivation and assimilation processes in rocks of different ages relative to juvenile accretion at an Archaean cratonic margin. According to these authors and Öhlander et al. (1999), 1.8 Ga granites of the Lina suite south of the Luleå–Jokkmokk zone show strongly negative $\varepsilon_{Nd\ (T=1.8)}$ values, although they occur together with juvenile early Svecokarelian intrusive rocks of the Jörn GI suite with positive $\varepsilon_{Nd\ (T=1.9)}$ values (see above). In these areas, the Archaean crust was interpreted to have been overthrust by c. 1.9 Ga juvenile early Svecokarelian rocks, and 1.8 Ga late Svecokarelian granitic magmas transported a negative $\varepsilon_{Nd\ (T=1.8)}$ signature from the Archaean crust and intruded the now allochthonous juvenile upper part of the crust, forming 1.8 Ga granites with negative $\varepsilon_{Nd\ (T=1.8)}$ values. The existence of juvenile units, overthrust onto the Archaean crust at depth (Öhlander et al. (1999) is in accordance with the south–southwest-dipping reflectors indicated from the reflection seismic work by the BABEL Working Group (1990).

To the south of the project area, late Svecokarelian intrusive rocks, related to the Lina suite have been described as Härnö and Skellefte granites (Kousa & Lundqvist 2000a) or the Skellefte–Härnö suite (Kathol & Weihed 2005). The Edefors suite has age and compositional characteristics in common with parts of the Transcandinavian Igneous Belt (Gorbatschev & Bogdanova 1993) in southern and central Sweden. Here, we use the names Lina suite and Edefors suite for the late Svecokarelian intrusive rocks of the project area.

Within in the project area, radiometric age determinations of rocks of the Edefors and Lina suites have been published by Romer & Wright (1992), Skiöld et al. (1993), Wikström & Persson (1997b), Kathol & Persson (2008c), Åkerman & Kero (2012a), Claeson & Antal Lundin (2012c), Kathol et al. (2012b), Kathol & Hellström (2015) and Morris & Hellström (2016). The analyses were carried out using the U-Pb method on zircon, using either the SIMS or TIMS technique. The ages obtained were interpreted as crystallisation ages and range from 1.80 to 1.77 Ga or from 1.81 to 1.75 Ga, taking error intervals into account.

Granite is by far the most commonly observed rock type in the Lina suite (Fig. 72a), one-third of which consists of pegmatitic varieties (Fig. 72b). Granodiorite and syenitoid are rare. Within the Pajala deformation belt, rocks of the Lina suite occur as minor, foliated bodies. Outside this belt they are undeformed or only slightly deformed.

Most occurrences of the Edefors suite consist of granite *sensu stricto* (Fig. 73a) and intrusive rocks of syenitoid to granitic composition (Fig. 73b). Occurrences where the syenitoid predominates are situated west of Arjeplog and around Boden (Boden syenite). Some of the major massifs of the Edefors suite are described as multiple intrusions, such as the Hárrevárddo intrusion south of Tjåmotis (Claeson & Antal

Figure 72. **A.** Medium-grained, equigranular, massive granite of the Lina suite. Road cutting at road E 45 close to Stenträsk, about 23 km northwest of Kåbdalis (7372075/734427). Photo: Benno Kathol. **B.** Transition from fine-grained granite and aplite (left) to coarse-grained, pegmatite with graphic granite texture (right) of the Lina suite. Pirkkolavaara, about 34 km north of Övertorneå (7424080/886613). Photo: Erik Jonsson.

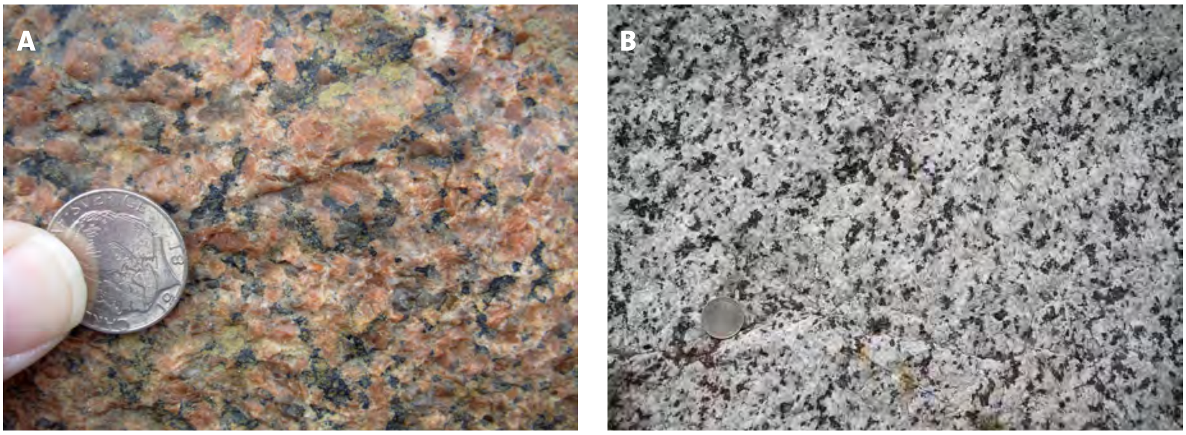

Figure 73. **A.** Medium-grained to coarse-grained, inequigranular, massive granite of the Edefors suite. Kallkällberget, about 14 km west of Harads (7343378/755312). Photo: Benno Kathol. **B.** Medium- to coarse-grained, weakly porphyritic, massive quartz monzonite of the Edefors suite. Small quarry above Lillraudok, about 30 km northwest of Arjeplog (7349445/609001). Photo: Benno Kathol.

Lundin in press-b) and the syenitoid to granite intrusion south of Nattavaara (Claeson & Antal Lundin 2012c). Minor intrusions of monzodioritic to granodioritic composition occur southeast of Jokkmokk and within the Hárrevárddo intrusion (Claeson & Antal Lundin in press-b) south of Tjåmotis.

Major mafic massifs with locally layered gabbros within the Edefors suite are the Ruoutevare gabbro southwest of Jokkmokk (Claeson & Antal Lundin in press-a) and the Notträsk gabbro northeast of Boden (Fig. 74a), the latter described by Arvanitidis (1982), Widenfalk et al. (1985), Filén (1987) and Sadeghi et al. (in press). Layered gabbro also occurs in the Hárrevárddo intrusion. A small layered gabbro intrusion with ultramafic parts has been encountered at the southern shore of Lake Hornavan northwest of Arjeplog (Fig. 74b, c; Kathol et al. 2010). Other intrusions from 1 to 15 km in size of gabbroid to dioritoid composition occur west of Nattavaara and at the northeastern margin of the Bothnia–Skellefteå lithotectonic unit along a line from Tjåmotis, through Luvos, Tårrajaur, Kåbdalis and Harads, to south of Boden. Two small bodies of ultramafic intrusive rocks have been observed west-southwest of Vuollerim and one southwest of Jokkmokk. Gabbroid to dioritoid and ultramafic intrusions occur both inside and in contact with the felsic massifs, and as isolated bodies within older rocks.

The gabbroid rocks, including the Ruoutevare gabbro, and the mafic granulites southwest of Jokkmokk cause the most prominent positive gravity anomaly in the project area. (Fig. 75a). Petrophysical

Figure 74. **A.** Medium- to coarse-grained, ophitic olivine gabbro of the Edefors suite. Notträsk, about 5.6 km northeast of Boden (7320701/810043). Photo: Paul Evins.

Figure 74. **B.** Medium- to coarse-grained, inequigranular, layered gabbro of the Edefors suite. Close to Tjålmåk on the southern shore of Lake Hornavan, about 35 km northwest of Arjeplog (7354249/606851). Photo: Benno Kathol.

Figure 74. **C.** Orbicular weathering of ultramafic rock within gabbro of the Edefors suite. The outcrop can only be seen at low water level in Lake Hornavan. Close to Tjålmåk on the southern shore of Lake Hornavan, about 36 km northwest of Arjeplog (7354403/606451). Photo: Benno Kathol.

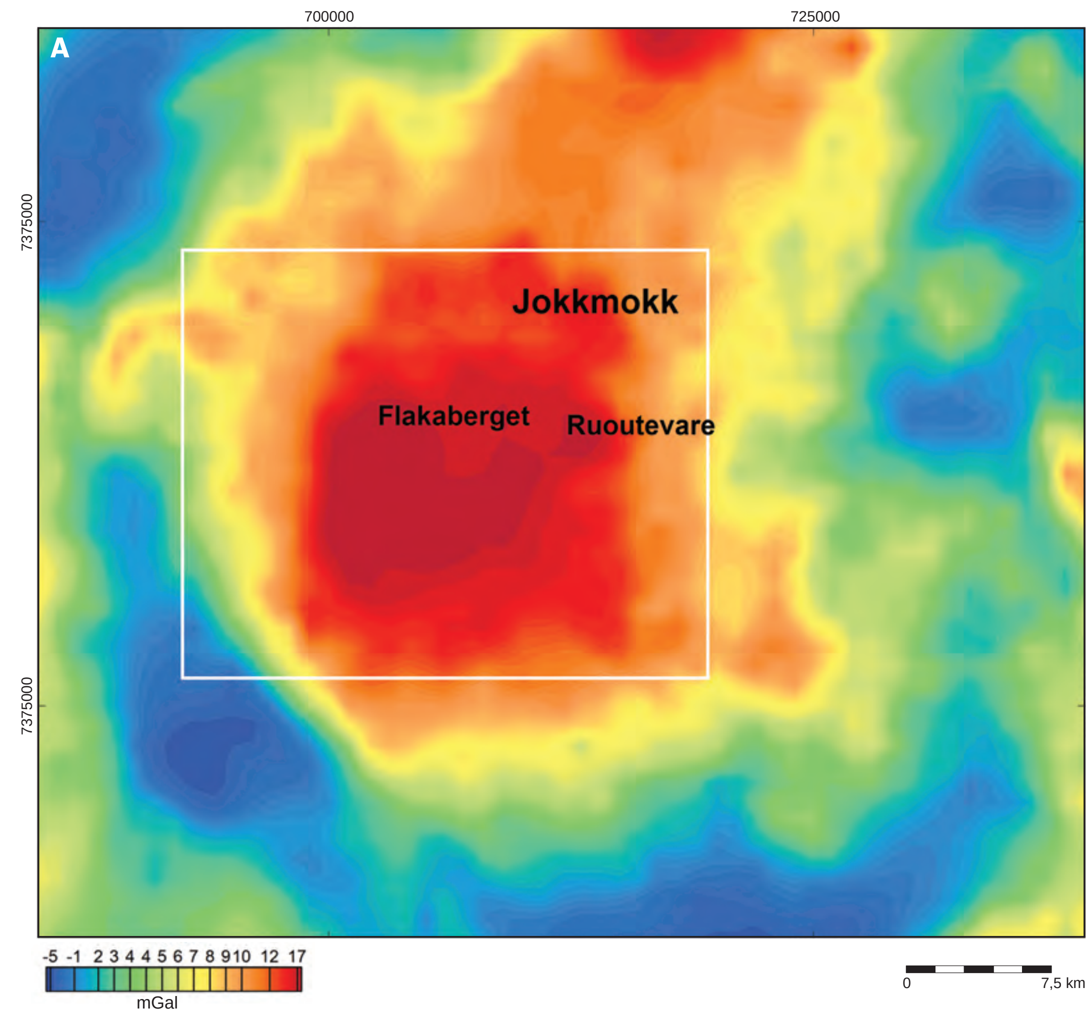

Figure 75. **A.** Bouguer anomaly map of the most prominent positive gravity anomaly in the project area. The white rectangle shows the position of the model in the horizontal plane. The location of the model area is shown in Figure 16.

sampling has been carried out in the gabbroid rocks and the mafic granulites at different times. The gabbroids have a density range between 2 763 and 3 290 kg/m^3, with a median density of 2 930 kg/m^3, whereas the granulites range between 2 736 and 3 000 kg/m^3, with a median density of 2 801 kg/m^3. The obvious reason for granulite facies metamorphism and partial melting was the heat input from the very large quantities of basic magma at 1 000 to 1 250 °C, which later crystallised to form gabbroid rocks and ultramafic cumulates. A 3D inversion model has been constructed with a cell size of 500 × 500 × 250 m (X ,Y, Z), its main purpose being to obtain information about the spatial distribution of the gabbroids relative to the mafic granulites. In the inversion a constraint has been applied to force the source body densities into the interval between 2 600 and 3 350 kg/m^3. The model has been cut to an area where observations of gabbroid rocks were made in outcrops. The area is shown as a white rectangle in Figure 75a. Since the gabbroid rocks have the highest densities, an isosurface corresponding to a density of 2900 kg/m^3 has been chosen to delineate the shape of the gabbroids in the area.

The volumes with the highest densities (above 2 900 kg/m^3) are assumed to represent the distribution of the gabbroids. The model indicates that the depth extent of the gabbroids is at least 9 km and that their volume exceeds 200 km^3 (Fig. 75b). The largest body obtained from the model is located in the middle of the area and clearly dips to the east.

A prominent gravity anomaly is observed adjacent to the Tjaktjajaure dam (Fig. 75c), and quartz monzonite is observed in the numerous outcrops located in the area of the gravity maximum. Modelling

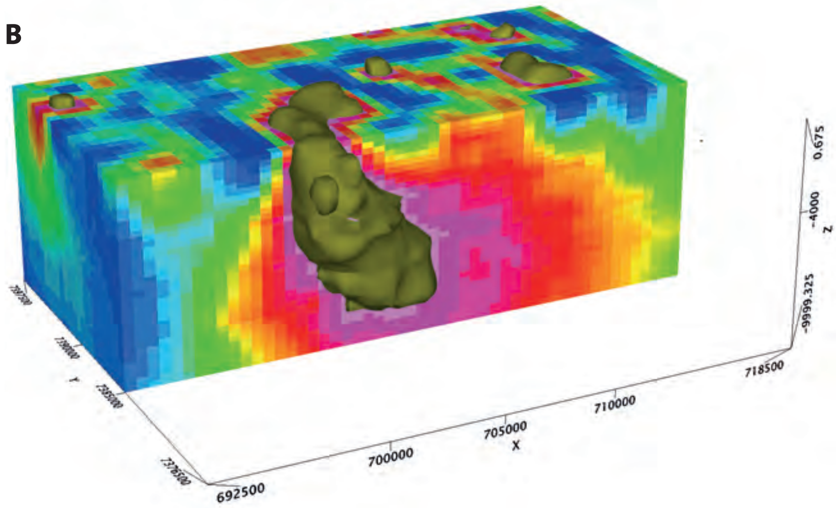

Figure 75. **B.** The 3D density model of the study area. The isosurface corresponds to density values of 2 900 kg/m³ and is assumed to delineate gabbroids. The isosurface is shown in brown.

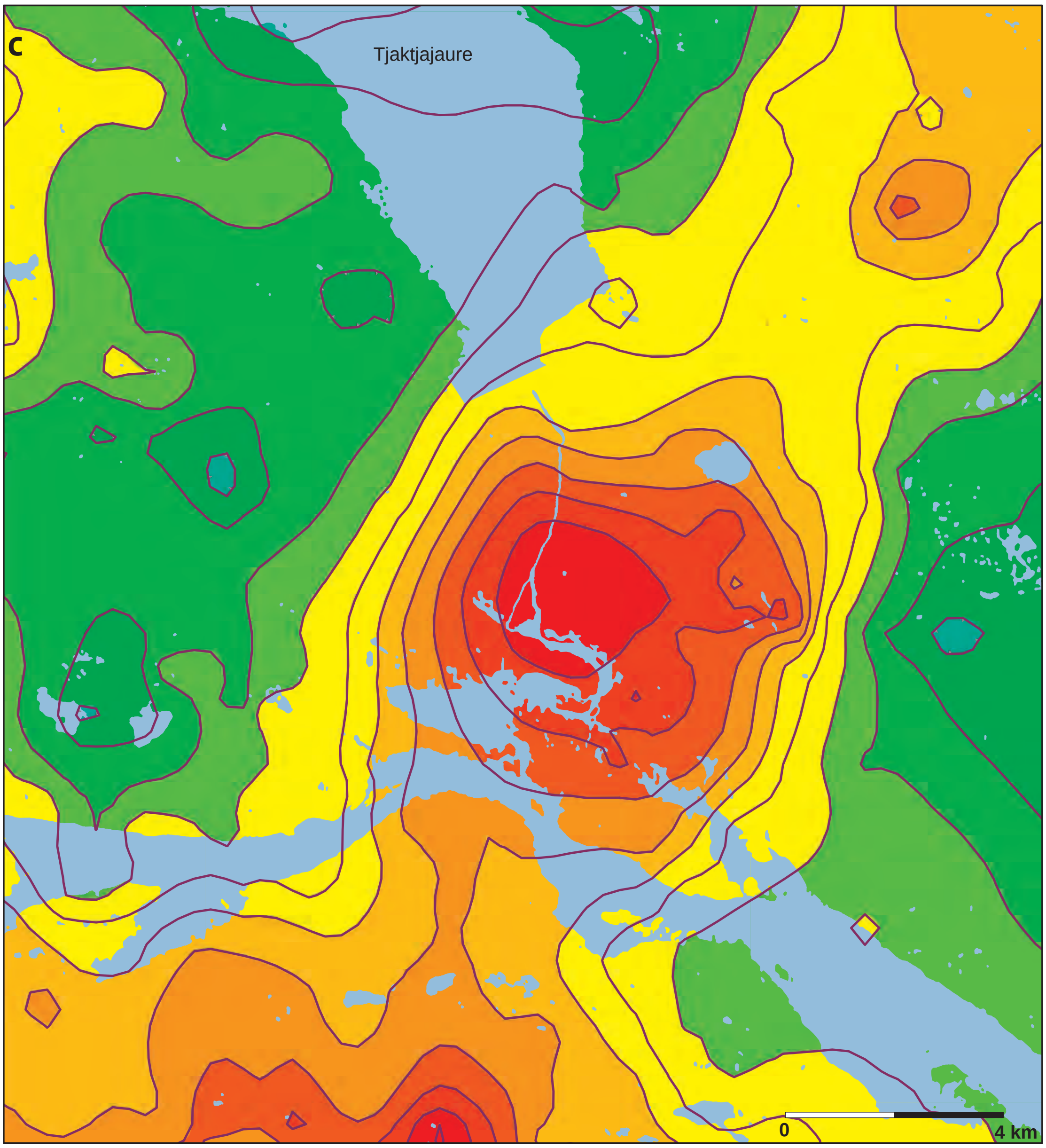

Figure 75. **C.** Gravity anomaly adjacent to the Tjaktjajaure dam. The figure shows a filtered gravity field of the area. Reddish colours represent gravity high and green colours gravity low.

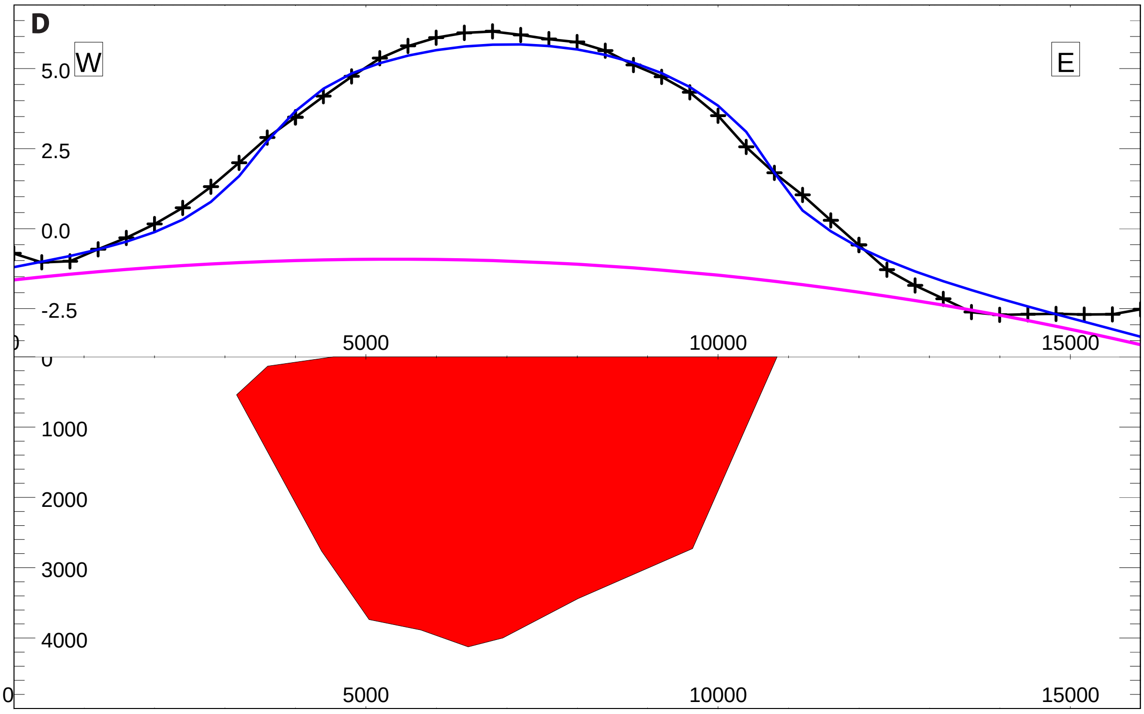

Figure 75. **D.** Modelled profile over the anomaly at Tjaktjajaure. Modelled geological body (below) and corresponding geophysical response (above).

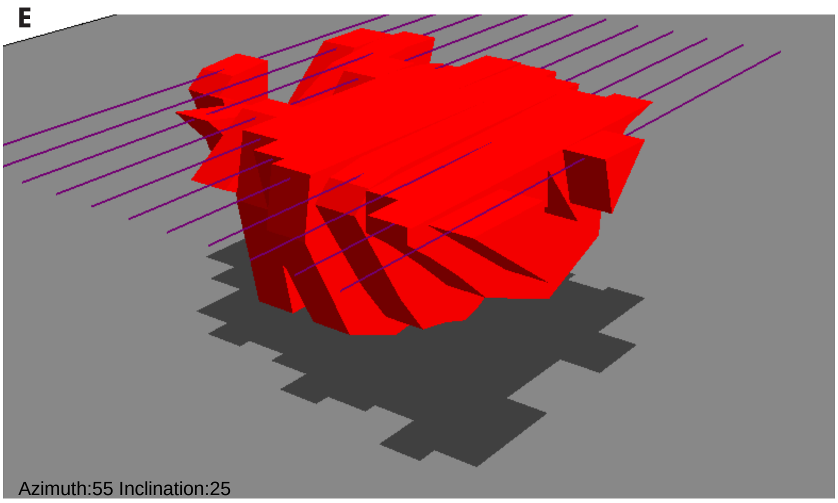

Figure 75. **E.** Three-dimensional model of the source body. View from northeast.

of the gravity field was carried out to evaluate whether the density of the quartz monzonite was sufficiently high to explain the gravity anomaly, or if the intrusion should be expected to contain also mafic components.

In the modelling of the gravity field (Fig. 75d), the surrounding density was set to 2 630 kg/m^3. The observed gravity field could be explained by a bowl-shaped source body with a density of 2 710 kg/m^3 which is equal to the average density of samples from the quartz monzonite in the outcrops. This density is slightly higher than the average for the entire syenitoid-granite group as presented in Table 4, but well within the limits of the standard deviation.

The obtained modelling indicates that the quartz monzonite intrusion itself is the probable source to the entire local gravity maximum (Fig. 75e). The maximum vertical extension of the intrusion is modelled to approximately 4 km.

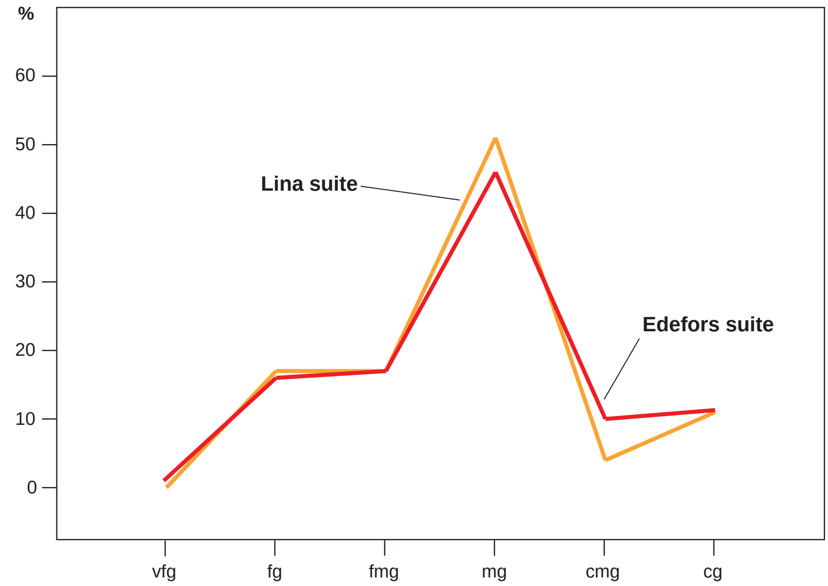

Figure 76. Simple diagram of grain-size distributions of the Lina and Edefors suites. Grain sizes stem from field observations. Grain sizes: vfg: very fine-grained; fg: fine-grained; fmg: finely medium-grained; cmg: coarsely medium-grained; cg: coarse grained.

Figure 77. Finely to coarsely porphyritic granite, in which the alignment of feldspar phenocrysts is interpreted to be a magmatic flow structure. Southwestern slope of Vitberget, about 18 km north-west of Vidsel (7325700/739879). Photo: Benno Kathol.

Most rocks of the Edefors and Lina suites are medium-grained; fine-grained and coarse-grained varieties are subordinate. A simple grain-size distribution diagram based on grain-size observations in the field for both suites displays a very similar pattern (Fig. 76).

The majority of the rocks of the Edefors and Lina suites have been described as equigranular or inequigranular and a minor proportion as porphyritic (Lina suite 10% and Edefors suite 35%). Phenocryst sizes of 2–10 mm are most frequent in the Lina suite, whereas they are 5–20 mm in the Edefors suite. Coarsely porphyritic varieties are subordinate in the Edefors suite and rare in the Lina suite.

Most of the phenocrysts in both suites consist of feldspar and particularly potassium feldspar (Fig. 77). Quartz phenocrysts are subordinate in the Lina suite and rare in the Edefors suite. Quartz phenocrysts in the Lina suite are commonest in the granite massif around Lansjärv. Amphibole phenocrysts are rare in both suites.

Recrystallisation is common in the granites of the Lina suite east of Lansjärv and south of Överkalix. Otherwise, recrystallisation is typical of small, kilometre-sized intrusions along the Nautanen defor-

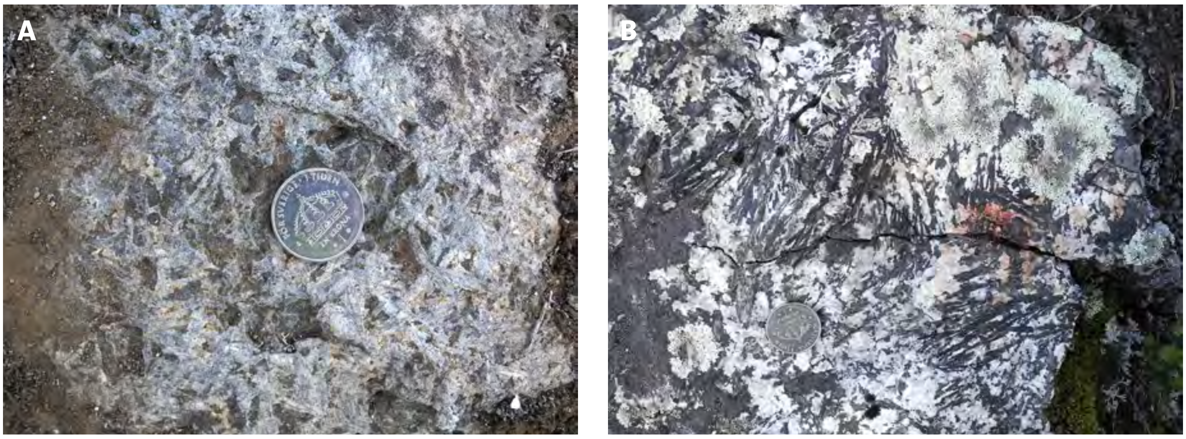

Figure 78. **A.** Spinifex texture in coarse-grained, massive ultramafic rock. Övre Görjeå, about 12 km southwest of Vuollerim (7371600/740845). Photo: Benno Kathol. **B.** Hornblende garben (radiating hornblende crystals) in gabbro pegmatite. Övre Görjeå, about 12 km southwest of Vuollerim (7371600/740845). Photo: Benno Kathol.

mation zone, north of Jokkmokk and around Lövnäs. Pegmatitic and subordinate aplitic textures, in many places with graphic granite textures, occur almost everywhere in the Lina suite.

Within the Edefors suite, recrystallisation has most frequently been reported from gabbroid to dioritoid intrusions southwest of Jokkmokk. Recrystallisation also occurs, albeit somewhat less frequently, in the north of the syenitoid to granite massif southwest of Arjeplog, in the southeast of the Hárrevárddo intrusion and in syenitoid to granitic rocks southeast of Nattavaara. Recrystallisation is rare or has not been observed in the larger massifs between Vidsel and Vuollerim, west of Mellanström, and around Boden.

Hydrothermal alteration has been observed at several places between Tjåmotis and Luvos. Rapakivi textures are commonplace north of Luvos, southeast of Jokkmokk and Nattavaara and between Kåbdalis and Harads. Spinifex textures and hornblende garben (radiating hornblende crystals) occur in ultramafic rocks and related gabbro pegmatites (Figs. 78a, b).

Granular weathering is common in the least deformed south–central area between the Karesuando–Arjeplog and the Nautanen deformation zones. In this area the rocks are not recrystallised, and granular weathering is probably favoured by simple straight-grain boundaries within these rocks.

Most of the observed rocks of the Lina suite are massive; about one-third of observations describe the rocks as deformed. Among these rocks, foliation is the most common feature, and linear structures are subordinate. Most of the deformed rocks of the Lina suite occur northeast of the Nautanen deformation zone. In the area southwest of this zone deformed rocks are less common and have been found mainly in the west and north. In most cases, massive and deformed rocks occur side by side; a sizeable area solely comprising massive rocks is situated south of Tårrajaur (between Jokkmokk and Kåbdalis). Igneous flow structures have been reported from the granite massif southeast of Lansjärv.

Most of the observed rocks of the Edefors suite are massive; about one-third of observations describe the rocks as weakly deformed. Among the latter, foliation is the most common feature and linear structures are subordinate. Foliated rocks are concentrated south of Tjåmotis and north of Luvos, south of Jokkmokk, southeast of Nattavaara and north of Harads. In contrast to the Lina suite, several sizeable rock volumes made up solely of massive rocks occur within the Hárrevárddo intrusion, the syenite to granite massif west of Arjeplog, southwest of Nattavaara and in the large massif of the Edefors suite in the south-central part of the project area. Frequent igneous flow structures have been found in quartz monzonite, monzonite and monzodiorite of the Hárrevárddo intrusion, in granite, quartz monzonite and monzonite southeast of Jokkmokk, and in granite in the massif east of Mellanström.

Figure 79. Granite with charnockitic mineral composition. The presence of orthopyroxene has been confirmed in thin section. Orrmyrberget, about 17.5 km west-northwest of Harads (7347750/752533). Photo: Benno Kathol.

Magnetite is common in granites and pegmatites in almost all occurrences of the Lina suite in the project area. Hematite and goethite occur in granite and pegmatite, but are much more scattered than magnetite. Pyrite is the most commonly observed sulphide mineral, but occurs in only a few places. Rare observations of chalcopyrite, pyrrhotite and molybdenite have also been made. Fluorite has been observed in minor occurrences of granite and pegmatite east and west of Lövnäs and northwest and northeast of Tjåmotis. Garnet occurs in granite and pegmatite at scattered places in the project area. Tourmaline occurs in pegmatite northeast of Nattavaara and south of Råneå.

Amphibole is a common constituent of both felsic and mafic rock types in the Edefors suite. Pyroxene is more concentrated to gabbroid rocks south of Jokkmokk. Olivine has been observed occasionally in gabbroid rocks northwest of Boden and south of Jokkmokk. Epidote is scarce or absent; more frequent observations have been made south and east of Jokkmokk and northwest of Luvos. Magnetite has been observed mainly in felsic intrusive rocks in all of the major massifs of the Edefors suite. Hematite observations are confined to the granite massif south of Tjåmotis and east of Mellanström. Sparse observations of sulphide minerals such as pyrite, and to a lesser extent chalcopyrite, pyrrhotite and molybdenite, have been made in most occurrences of the Edefors suite, but they seem to be absent from the major granite massifs between Kåbdalis and Harads and east of Mellanström. A number of observations of fluorite have been made in granite southeast of Tjåmotis. Charnockitic mineral compositions have been observed in massive granites at a few places south of Vuollerim (Fig. 79).

Dykes of varying composition occur almost everywhere in the rocks of the Lina suite. Most of them consist of pegmatite and subordinate granite. Mafic dykes have been observed in the Lövnäs area, northeast of Moskosel and north and south of Överkalix. In the Edefors suite, different types of dykes occur mainly in granite and syenitoid in the major massifs. Somewhat fewer observations of dykes have been made in the syenitoid to granitic massif southwest of Arjeplog. Almost 90% of the dykes in bedrock of the Edefors suite have been described as pegmatite, granite and aplite. Dykes of gabbroid to dioritoid and syenitoid composition are rare, as are dykes of volcanic rocks and dolerites. Most inclusions in the Lina suite consist of felsic intrusive rocks, mainly granite, granodiorite and tonalite. Equal amounts of mafic intrusive rocks and sedimentary rocks have been reported, and together they constitute the same amount as the felsic intrusive rocks. Volcanic rocks are subordinate.

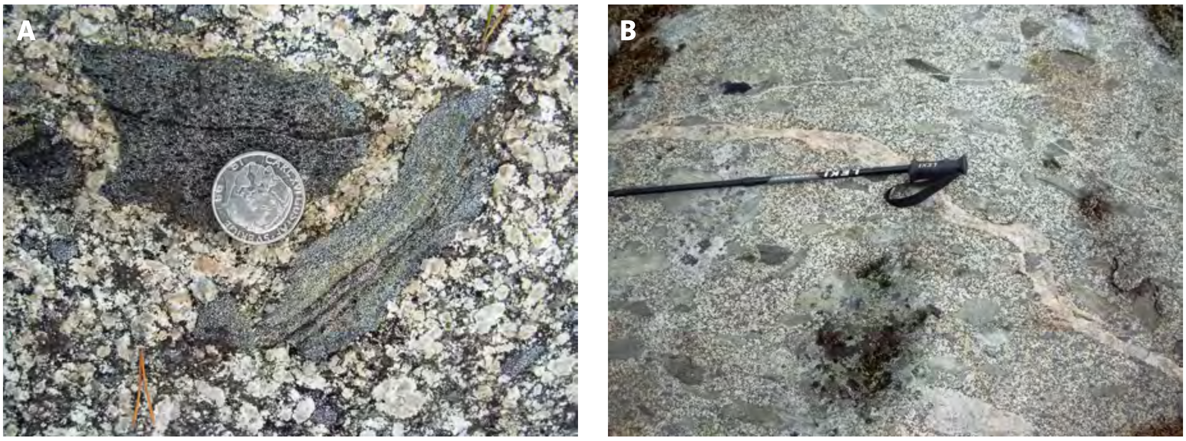

Figure 80. **A.** Xenolith of amphibole-porphyritic mafic volcanic rock (to the upper left of the coin) and paragneiss (to the right of the coin) in finely porphyritic granite. Inre Rengärdberget, about 28 km southwest of Boden (7303572/781829). **B.** Abundant xenoliths of paragneiss and amphibole-porphyritic mafic volcanic rock in finely porphyritic granite. Inre Rengärdberget, about 28 km southwest of Boden (7303572/781829). Photos: Benno Kathol.

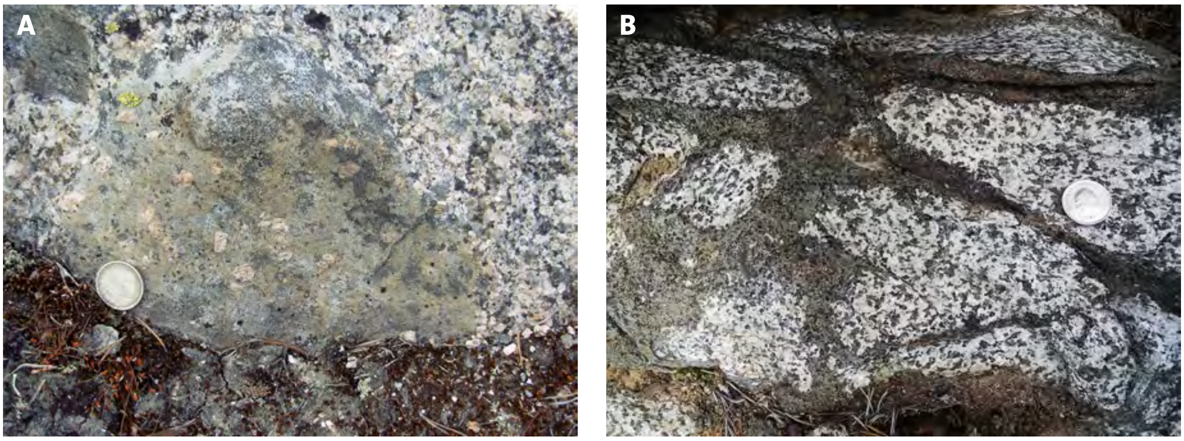

Figure 81. **A.** Magma mingling structure with fine-grained enclave with scattered feldspar crystals, emanated from the surrounding finely porphyritic granite. Vålberget, about 21 km southeast of Kåbdalis (7336003/743660). **B.** Intrusion breccia with fragments of quartz monzonite in a gabbroid to ultramafic, intrusive matrix. Lissjmávárre, about 13.5 km southwest of Vuollerim (7370162/740243). Photos: Benno Kathol.

Magma mingling in the Lina suite has only been described from two places: one at the southern shore of Lake Hornavan between Arjeplog and Jäkkvik with enclaves of diorite in granite, and one south of Övertorneå with tonalite enclaves in pegmatite granite.

Inclusions have been observed most frequently in the major occurrences of the Edefors suite. These are situated in the northeastern part of the Bothnia–Skellefteå lithotectonic unit and around Boden in the Norrbotten tectonic unit. Inclusions are sparser in the massifs south of Nattavaara, southwest of Arjeplog and east of Mellanström. Inclusions occurring in the rocks of the Edefors suite consist mainly of volcanic rocks, followed by granite, gabbro and diorite and sedimentary rocks. Among the volcanic rocks, rhyolite predominates, with somewhat fewer observations of dacite and andesite. Basalt is subordinate. The sedimentary inclusions consist mainly of metasandstone and subordinately of paragneiss and metagreywacke (Fig. 80a). Locally, xenoliths make up significant volumes of the bedrock (Fig. 80b).

Magma mingling has only been observed at a few places in the two larger granite massifs of the Edefors suite between Vidsel and Vuollerim in the least deformed south-central part of the project area

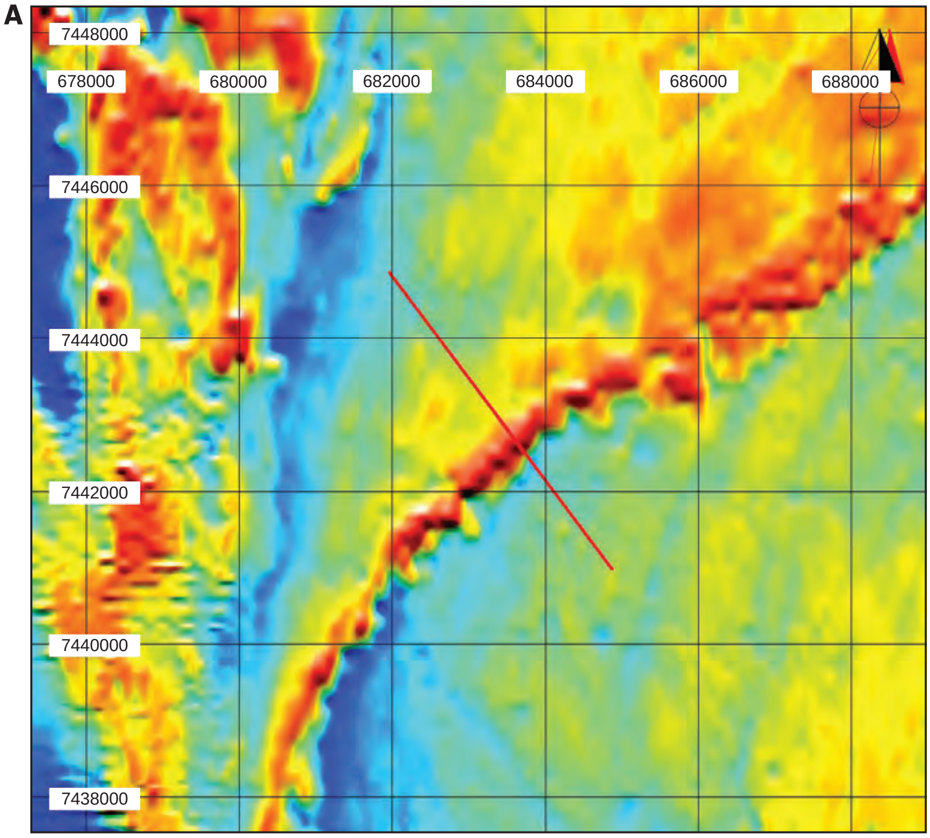

Figure 82. **A.** Magnetic anomaly map of a part of the Nabrenjarka dolerite. The profile for modelling is indicated by a red line. The location of the model area is shown in Figure 16.

(Fig. 81a). An intrusion breccia has also been found in the south-central part, southeast of Vuollerim, where intrusion of mafic to ultramafic magma has brecciated a quartz monzonite (Fig. 81b).

The Nabrenjarka dolerite occurs as a system of dyke intrusions mainly to the north of the project area. The largest body is a flat-lying, bowl-shaped intrusion. The dolerite intruded several rock types, including the late Svecokarelian, 1.80 to 1.77 Ga Lina suite, which means that the dolerite must be younger than this. Minor dykes of the Nabrenjarka dolerite system are overlain with a major unconformity by Ediacaran to Cambrian sedimentary cover rocks to the north of the project area.

Witschard (1975) and Witschard & Zachrisson (1995) described the dolerite as the Nabrenjarka gabbro diabase, occurring as a somewhat circular and continuous dyke more than 70 km long, with a maximum width of more than 1 km. The contact has a general dip towards a central part, situated in the middle of map area 28I Stora Sjöfallet SO, to the north of the project area. The average gabbro of the dyke is medium- to coarse-grained, massive and very dark. The thicker parts of the dyke have a gabbroid texture, whereas thinner parts and minor dykes are fine-grained and show ophitic to porphyritic textures.

Within the project area, the Nabrenjarka dolerite has been observed in one outcrop northwest of Porjus. Here, the rock is a greenish-black, massive, medium- to coarse-grained gabbro. It is subophitic and contains disseminated magnetite and pyrite (Nysten et al. 2015). Otherwise, the Nabrenjarka dolerite could not be verified by outcrop observations, but due to high magnetite content, the dyke can clearly be traced in the magnetic anomaly map (Fig. 82a). According to geophysical modelling (Fig. 82b), the southernmost part of the main Nabrenjarka dolerite dyke dips moderately to the northwest.

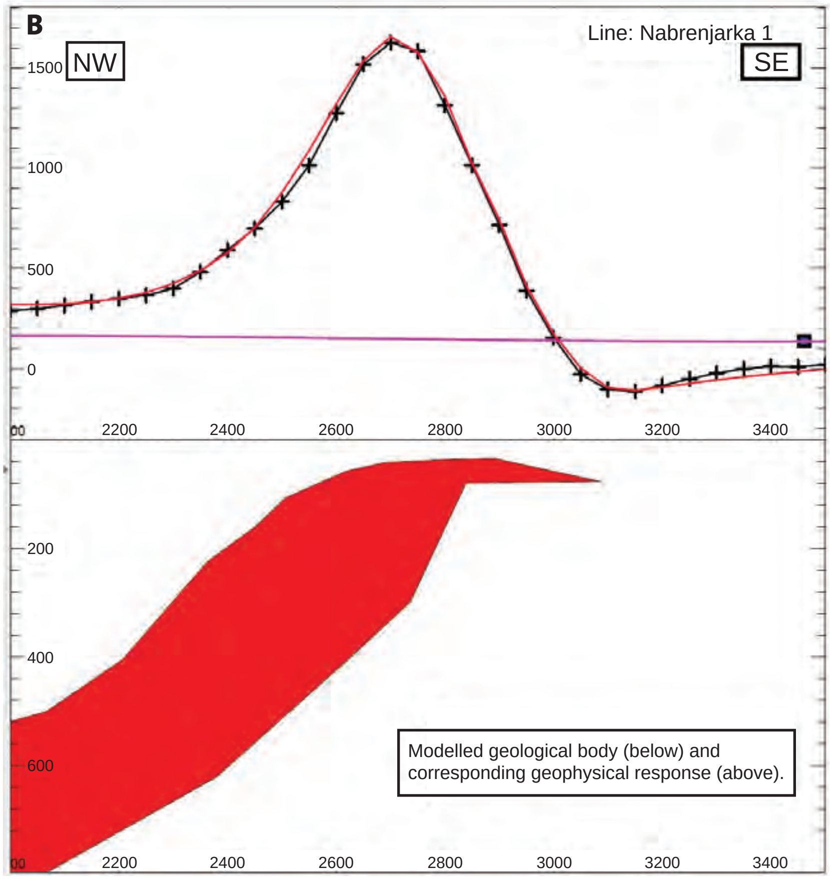

Figure 82. **B.** Geophysical model of the Nabrenjarka dolerite.

Metamorphic rocks

Two large massifs of mafic granulite and a minor body of felsic granulite occur in the area south of Jokkmokk (Claeson & Antal Lundin in press-a). The felsic granulite occurs in the central part of the western mafic granulite massif. The definition of mafic granulite by Coutinho et al. (2007) has not been verified by observations of orthopyroxene in a hand specimen or thin section. The term granulite is here based on partial melting of the basic and intermediate volcanic rocks of the area and the generation of migmatites. These rocks could also be called basic to intermediate migmatites formed under low-P granulite facies metamorphic conditions (Claeson & Antal Lundin press-a). More information on the metamorphic conditions of these rocks is given in chapter 6 *Structure and metamorphism*.

The mafic granulites show schollen migmatite structures with rafts of basic volcanic rocks floating in leucosome (Fig. 83a), as well as metatexitic varieties (Fig. 83b). The protoliths to these rocks are interpreted as basalts, andesites and dacites, and the granulite facies metamorphism is considered to have been caused by heat from the intrusion of large amounts of basic magma forming the late Svecokarelian gabbros and diorites within the same area.

The basaltic parts normally show no melting and no leucocratic veins, and these parts float like rafts in a leucosome which results from melting of andesites and dacites in the volcanic sequence (Claeson & Antal Lundin press-a).

The mafic granulites show low susceptibility values, commonly below 100×10^{-5} SI units, in contrast to the highly magnetic gabbroid rocks. The mafic granulites and the gabbroid rocks together have high densities between 2736 and 3290 kg/m^3. These rocks cause an intense gravity high in the area southwest of Jokkmokk. A three-dimensional gravity model of the mafic granulites and the basic intrusions of the area is given in Claeson & Antal Lundin (in press-a). Despite their high density, the mafic

Figure 83. **A.** Partial melting of folded and fragment-bearing andesite. Sör-Råvåive, about 16 km southwest of Jokkmokk (7386704/ 701956). **B.** Folding in metatexitic andesite to basalt. Northwest of Vajmatberget, about 19 km southwest of Jokkmokk (7384280/703513). Photos: Dick Claeson.

Figure 84. Diatexitic migmatite of granodioritic composition and melanosome of greywacke. Orrkölen, about 19.5 km southeast of Pålkem (7369758/ 812518). Photo: Ulf Bergström.

granulites were classified as metasedimentary rocks on previous maps (Nylund & Nisca 1981, *Jokkmokksprojektet* 1981). However, it cannot be ruled out that the bedrock in the area that has undergone granulite facies metamorphism partly consisted of sedimentary rocks, and if so, probably derived from basic and intermediate rocks rather than acidic ones.

At Njallatjåhkkå, approximately 24 km south of Tjåmotis, a diatexitic migmatite granite occurs as a minor body, about one kilometre in diameter, and as dykes in deformed dacites and rhyolites of the Arvidsjaur group and in sedimentary rocks of the Snavva–Sjöfallet group (Claeson & Antal Lundin in press-b). The migmatite granite is fine-grained to coarse-grained and varies from massive to distinctly banded and foliated. It is assumed that the migmatite granite is a result of partial melting of the volcanic rocks of the area at c. 1.78 Ga, caused by the Hárrevárddo intrusion (Claeson & Antal Lundin in press-b).

The bedrock around Tallberg and Långsel southeast of Pålkem consists of grey, finely medium-grained to medium-grained massive or weakly foliated diatexitic migmatite with granodioritic leucosome (Fig. 84). These rocks have previously been assigned to the Haparanda suite (Koistinen et al. 2001, Bergman et al. 2012). This migmatite massif is surrounded by metasedimentary rocks of the Bothnian supergroup and the Sockberget group. Rafts of variable metasedimentary rocks of the Bothnian supergroup up to a size of one kilometre also occur inside this massif. On the magnetic anomaly map, the migmatite and the surrounding metasedimentary rocks show a uniform low-magnetic pattern typical of areas with metasedimentary rocks. Felsic intrusive rocks of the Haparanda suite normally show significantly higher magnetic anomalies. The granodioritic composition of these migmatites (diatexites) is probably similar to the composition of the greywacke protoliths. Numerous dark grey, fine-grained inclusions are now interpreted as "infertile" restites.

A U-Pb zircon dating of a granodioritic diatexitic migmatite southeast of Pålkem (see Fig. 84) has yielded an age of c. 1 880 Ma (Bergström et al. in preparation-a), which marks the timing of the peak metamorphism in the east-central part of the project area. The age is similar to the metamorphic age obtained in the Boden area (Sadeghi & Hellström 2018), in contrast to younger ages close to 1.8 Ga from the Jokkmokk area and further west (Lundmark et al. 2005b, Hellström in preparaion-b), and from areas to the east (Bergman et al. 2006, Lahtinen et al. 2015a).

The occurrence of these high-grade rocks in the lower grade metasedimentary environment is thought to be a result of complex metamorphic conditions in the metasedimentary rocks, with steep metamorphic gradients between areas with lower amphibolite facies and higher metamorphic facies.

Some minor bodies of diatexitic migmatite with sedimentary rocks as protoliths occur on both sides of the Råneälven river, northwest of Råneå in rocks of the Bothnian supergroup.

MESOPROTEROZOIC ROCKS

Mesoproterozoic to Neoproterozoic sandstone, siltstone and claystone of the Muhos formation occur on the seabed of the Bothnian Bay (Lundqvist et al. 1996a, Kousa & Lundqvist 2000b, Winterhalter 2000). These rocks probably extend into the project area in the Kalix archipelago south of Kalix.

There are three dolerite dykes in the west of the project area. Two of them, occurring southwest of Arjeplog, have their main extension south of the map area, where they have been described by Eliasson et al. (2003a, b). These authors correlated the dykes with those in the Storuman area even further to the south. They stated that the chemical and mineralogical composition of the dolerites infers correlation with the c. 1 250 Ma Central Scandinavian Dolerite Group (CSDG), as described by Gorbatschev et al. (1979) and Greiling (1992).

The dolerite dyke southwest of Lövnäs has not been observed in outcrop. It is inferred from nearby observations of minor dolerite dykes within the granite, and its shape and extent is interpreted from geophysical data. It is hypothetically correlated with the Mesoproterozoic dolerite dykes southwest of Arjeplog.

Alkaline ultramafic lamprophyres and subordinately associated carbonatite dykes form north–south-trending dyke swarms in the Kalix area and the Kalix archipelago. The dykes of these areas show great similarities to petrographically related rocks from the alkaline Alnö complex (Kresten et al. 1981). The dykes are normally 1–5 cm thick, but in some places reach a thickness of up to one metre (Åhman et al. 1990). Of the dykes observed by Åhman et al. (1990), some 30% are rich in mica (Alnöite type), 50% picrite-porphyritic and 20% carbonatitic. Further descriptions of these kimberlitic dykes have been given by Larsson (1943) and Åhman (1950, 1967).

EDIACARAN–CAMBRIAN SEDIMENTARY COVER

Along the Caledonian erosional front and below the overthrust Caledonian bedrock, a thin autochthonous succession of tectonically almost undisturbed sedimentary cover rocks rests unconformably on the Palaeoproterozoic rocks of the Svecokarelian orogen. In northern Scandinavia this Ediacaran to Cambrian succession is named the Dividal Group (Pettersen 1878, Føyn 1985). Thelander (1982) divides the Dividal Group into a lower part, mainly consisting of sandstone and siltstone, called the Torneträsk Formation, and an upper overlying part called the Alum Shale Formation. The sedimentary cover was also described by Kulling (1982).

Figure 85. **A.** Well-sorted arenite with well-rounded grains. Grain sizes range from coarse to very coarse sand. Weathered surface. Árdnasjávrre, about 20 km west-northwest of Lövnäs (7365951/607731). **B.** Well-sorted, layered quartz arenite with well-rounded grains. Layering is indicated by intercalations of fine-grained, dark material. Grain sizes range from medium to coarse sand. Cut surface. Såvvovárre, about 4.3 km east-southeast of Laisvall (7334843/601894). Photos: Benno Kathol.

In the area of Lake Laisan at Laisvall, this sedimentary succession has been divided into the Laisvall formation, the Siltstone formation and the Alum Shale Formation (Lilljequist 1973). A Greywacke formation was also included into the autochthonous sedimentary cover. However, these greywackes are now assigned to the Blaik Nappe Complex of the Lower Allochthon (Thelander 2009a, Greiling et al. 2018). Willdén (1980) revised this stratigraphy and added a basal conglomerate and arkose unit: the Ackerselet formation. This formation is overlain mainly by arenites and quartz arenites of the Såvvovare formation, which, together with the Ackerselet formation, corresponds to the Laisvall formation of Lilljequist (1973). The Såvvovare formation is overlain by the Grammajukku formation, consisting of mudstones, siltstones and grey to dark brown sandstones. These rocks are in turn overlain by black mudstones and shales, rich in organic matter (alum shales), of the Alum Shale Formation (cf. Gee 1972, Bergström & Gee 1985). According to Andersson et al. (1985), the Alum Shale Formation ranges in age from Middle to Late Cambrian.

Within the project area, the sedimentary cover sequence is exposed along the Caledonian front between the Vindelälven river in the south and Lake Tjaktjajávrre west of Snávvá in the north. The sequence has been mapped most intensively from south of Laisvall to the area northeast of Örnvik. In this area, it consists mainly of arenite and quartz arenite (Fig. 85a, b), and subordinate conglomerate, siltstone and shale. The Alum Shale Formation is confined to the Laisvall area, where alum shales occur in large volumes.

The Ediacaran to Cambrian sedimentary cover sequence is truncated at different levels by the floor thrust of the overlying nappe pile. In the far southwest of the project area, the sedimentary cover sequence is missing or eroded, and the allochthonous rocks of the Caledonian orogen rest directly on the Palaeoproterozoic rocks of the Svecokarelian orogen. More detailed information about the Ediacaran to Cambrian sedimentary cover sequence in the project area can be found in Lilljequist (1973), Willdén (1980) and Thelander (2009b).

CALEDONIAN OROGEN

The Caledonian orogen in Scandinavia is made up of a sequence of westerly-derived nappes, thrust onto the Palaeoproterozoic rocks of the Svecokarelian orogen and its autochthonous Ediacaran to Lower Palaeozoic sedimentary cover (Fig. 86). The nappes have traditionally been grouped into the Lower, Middle, Upper and Uppermost Allochthons (Kulling 1972, 1982; Gee & Zachrisson 1979; Gee et al.

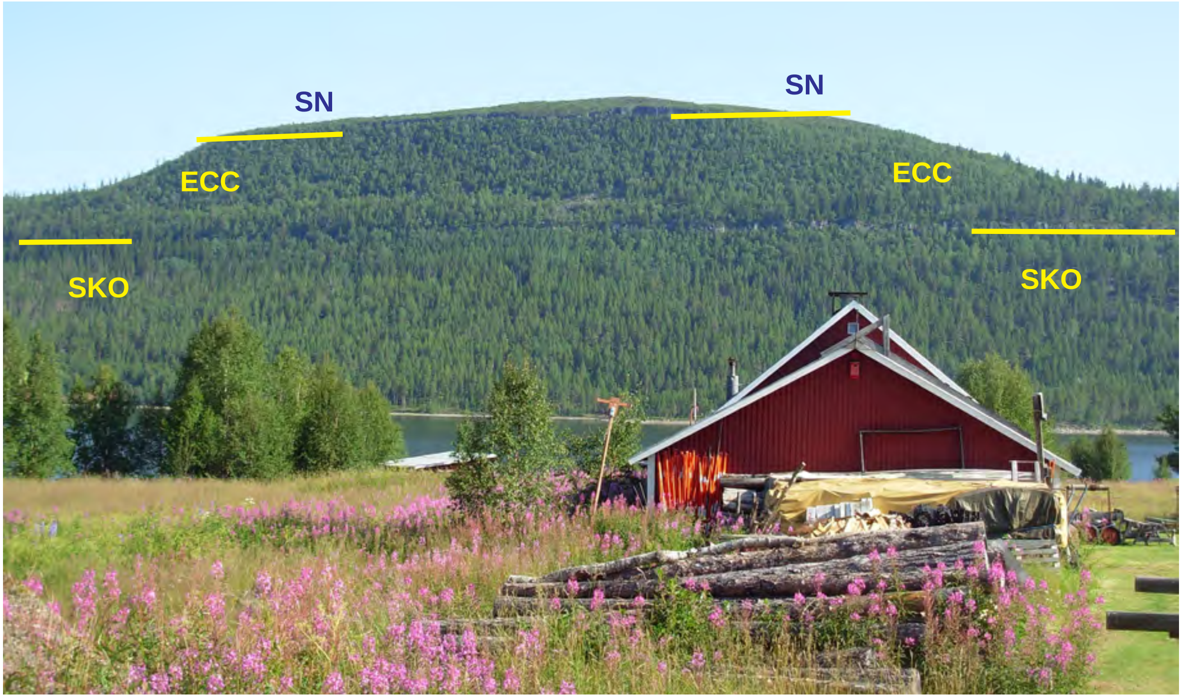

Figure 86. Laisvikberget, demonstrating three major geological units in the project area. SKO: Svecokarelian orogen; ECC: Ediacaran to Cambrian sedimentary cover (Dividal Group); SN: Stalon Nappe. View from Södra Laisvik towards the north-northeast. Södra Laisvik, about 31 km northwest of Arjeplog. Photo: Benno Kathol.

1985). In general, the lower and easternmost emplaced tectonostratigraphic units (Blaik Nappe and equivalents, Stalon Nappe and equivalents) originate from areas situated at the Neoproterozoic to Early Palaeozoic margin of Baltica, whereas the higher units are derived from the Baltica–Iapetus transition zone (Seve Nappe Complex and lowermost Köli Nappes) or from marine, island arc environments (higher Köli Nappes). These are now situated in the central and western parts of the orogenic belt.

According to Greiling et al. (1998), the Lower Allochthon of the above-mentioned classic division, including the Blaik Nappe and equivalent nappes, has undergone exclusively Scandian (Middle to Late Silurian) deformation and metamorphism. The Middle Allochthon with the Stalon Nappe and equivalent nappes, the Särv Nappe and the Seve Nappe Complex of the Upper Allochthon show traces of Finnmarkian (Early Ordovician) events. The tectonostratigraphic sequences from the Lower Allochthon to the Seve Nappes are interpreted as parts of the imbricated and shortened margin of Baltica. The Köli Nappes of the Upper Allochthon represent exotic or outboard terranes, whereas the Rödingsfjället Nappe Complex of the Uppermost Allochthon was derived from the continent of Laurentia. The Köli Nappes and the Rödingsfjället Nappes were amalgamated with the Baltoscandian platform during the collision of the Baltica and Laurentia continents.

The establishment of the Lower Allochthon post-dates the emplacement of the Middle and Upper Allochthon. Imbrication and formation of duplex structures within the Lower Allochthon led to deformation of the Middle and Upper Allochthons and of the boundary between the Seve and Köli nappes. A final emplacement of the whole nappe pile into its present position on the Baltoscandian platform occurred during the Silurian and Early Devonian (Greiling & Zachrisson 1999 and Greiling et al. 1999). Final uplift and formation of the present mountain range in Scandinavia are related to the opening of the Atlantic Ocean during the Tertiary, c. 65 Ma ago (Greiling & Zachrisson 1999).

The Caledonian bedrock of the project area comprises units of the Blaik, Stalon, Särv nappes and the Seve Nappe Complex. More detailed information about the Caledonian orogen in the project area can be found in Lilljequist (1973), Thelander (2009b) and Greiling et al. (2018).

Figure 87. Part of the Gautojaure duplex at Lake Gautojaure. View from the road between Hällbacken and Gautosjö to the south-west. Thrust surfaces are indicated by yellow arrows. Viejenäs, about 20 km northwest of Laisvall. Photo: Benno Kathol.

Blaik Nappe and equivalent nappes

The Blaik Nappe and equivalent nappes represent the easternmost and lowermost tectonostratigraphic unit in the Caledonian orogen in the project area. It is made up of structural slices and horses, consisting of sedimentary sequences and minor occurrences of basement-derived crystalline rocks.

The structural slices form a system of imbricate fans, which, in places where the roof thrust (basal thrust of the Stalon Nappe) is preserved, can be designated duplexes. Major duplexes are the Björnide duplex south of Jäkkvik and the Gautojaure duplex, which partly extends into the project area north of Laisvall (Fig. 87). Further to the south, the eastern parts of the Hemfjäll–Råvojaure duplex occur in the southwestern corner of the project area.

Basement-derived crystalline rocks of mainly syenitoid to granitic composition occur at the base of some horses in the Björnide duplex and as an isolated slice underneath the Stalon Nappe between Jäkkvik and Lövnäs. The sedimentary sequence of the Blaik Nappe is divided into the Risbäck Group, the Sjoutälven Group with the Gärdsjö Formation (Asklund & Thorslund 1935, Gee et al. 1978), and the Tåsjön Group with the Fjällbränna and Norråker formations (Gee et al. 1974). The Risbäck Group (Kulling 1972, Kumpulainen 1982, Zachrisson 1997) varies in thickness from a couple of metres to several hundred metres. Basal polymictic conglomerates are overlain by arkose and subordinate conglomeratic arkose, which, in the older literature, were called "sparagmites". At the top of the group, dolomite and breccia constitute the Kalvberget Formation, which is the uppermost part of the Risbäck Group.

Conglomerate and arkose of the Risbäck Group form parts of the Gautojaure and Hemfjäll duplexes. Further to the north, greywacke, quartz arenite and quartzite of the Risbäck Group occur only in minor slices between the autochthonous sedimentary cover sequence and the Stalon Nappe. Within the Gautojaure and Ravovare duplexes, conglomerate and arkose of the Risbäck Group are overlain by quartzite, greywacke (Fig. 88a) and mudstone of the Gärdsjön Formation of the Sjoutälven Group. Outside the duplex structures, rocks of the Gärdsjön Formation directly overlie the sedimentary cover sequence and are overthrust by the Stalon Nappe.

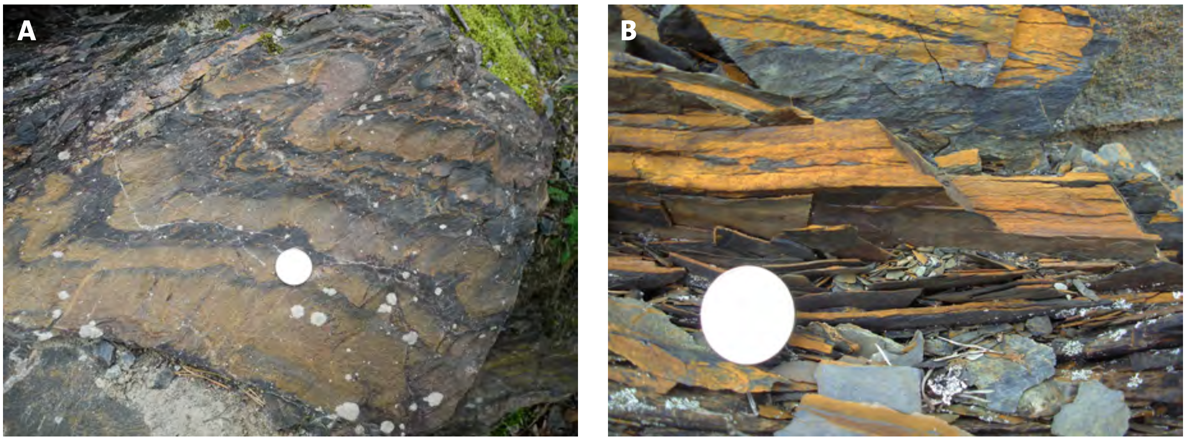

Figure 88. **A.** Folded greywacke of the Gärdsjö formation, showing graded bedding from arenitic (light brown) to muddy (dark grey) layers. North of Märkforsen, about 18.5 km northwest of Laisvall (7348108/583264). **B.** Typical carbonate weathering on fracture surfaces in greywacke of the Norråker formation. Harrselet, about 4 km north-northwest of Jäkkvik (7368119/586304). Photos: Benno Kathol.

Within the Björnide and the Hemfjäll–Råvojaure duplexes and southwest of Båtsjaur, the Gärdsjön Formation is followed upwards by the Fjällbränna Formation. This formation comprises black mudstone and alum shale of Middle to Late Cambrian age and it corresponds to the Alum Shale Formation in the Ediacaran to Cambrian sedimentary cover sequence.

The uppermost stratigraphic unit of the Blaik Nappe in the map area is the Norråker Formation, which occupies the western part of the Blaik Nappe culmination north of Jäkkvik. The contact between rocks of the Gärdsjö Formation and the Norråker Formation in this culmination is interpreted as a depositional contact, in which the alum shale of the Fjällbränna Formation has been eroded on a foreland bulge before deposition of the greywackes of the Norråker Formation. Most of the Norråker Formation is made up of turbiditic units of fine-grained, 10 cm-scale layered, typically carbonate-bearing greywacke and shale (Fig. 88b). This greywacke-shale succession ranges in age from the Lower to the Middle Ordovician.

Stalon Nappe and equivalent nappes

Within the project area, the Stalon Nappe and equivalent nappes (Stalon Nappe according to Kulling 1942, 1955) occurs as a 10–45 km broad belt at the eastern margin of the Caledonian orogen. In the south of this belt, approximately south of Örnvik, the Stalon Nappe has been overthrust onto different units of the Blaik Nappe and equivalent nappes. In the north, the Stalon Nappe mainly rests on the Ediacaran to Cambrian sedimentary cover sequence.

The Stalon Nappe and equivalent nappes comprise basement-derived crystalline rocks displaying varying degrees of deformation, derived from the Svecokarelian basement and Neoproterozoic sedimentary cover rocks, mainly arkosic arenite, originating from the Neoproterozoic margin of Baltica. The lithological units occur within different tectonic slices, separated by shear zones (Fig. 89).

Major volumes of crystalline, basement-derived rocks occur north of Kvikkjokk and south of Laisvall. The former consist of granite, syenitoid rocks and subordinate granodiorite. These rocks are possibly a southern continuation of the mainly crystalline Akkajaure Nappe Complex (Björklund 1985, 1989) to the northwest of the project area. The other major occurrence of crystalline rocks is situated south of Laisvall and consists of cataclastic syenite and granite, and subordinate gabbro (Lilljequist 1973). A foliated meta-quartz syenite from a small basement slice east of Harrvik, about 60 km south of the project area, has yielded a U-Pb zircon age of 1 766 +15/-12 Ma (Greiling et al. 2002).

Figure 89. Shear zones on the northeastern slopes of Rijmotjåhkkå (Rijmobákte). View from Rimobäcken towards the southwest. Shear zones are indicated by yellow lines. Rimobäcken, about 6 km southeast of Jäkkvik. Photo: Benno Kathol.

Figure 90. Phyllonitic meta-arkose of the Stalon Nappe, showing typical deformation style with shear bands indicating top-to-the-east kinematics, view to the north. Riebnesströmmen, about 24 km west-northwest of Lövnäs (7366263/603911). Photo: Benno Kathol.

In the centre of the metasedimentary sequence of the Stalon Nappe, which is mapped in more detail, phyllonitic meta-arkose and arkosic meta-arenite are the most common rock types in some places (Fig. 90). Phyllite, gneiss, mica schist and slate are also common, whereas quartz arenite, quartzite and greywacke are subordinate.

The rocks of the Stalon Nappe have been described by Lilljequist (1973) in the Laisvall area and by Greiling & Kumpulainen (1989) in the Kvikkjokk area. In addition, information about the Stalon Nappe in the north of the project area can be found in Thelander (2009b), and in the southwest and far southwest of the project area in Greiling et al. (2018).

Särv Nappe

The Särv Nappe Complex (Särv nappes) was originally defined and described by Strömberg (1955, 1961) and Kumpulainen (1980) in Jämtland County in the centre of the Caledonian orogen in Scandinavia. The typical feature of the Särv Nappe Complex is that the protoliths of the metasedimentary rocks have been intruded by dolerite, in contrast to the otherwise similar metasedimentary rocks of the Stalon Nappe. The dolerites intruded at 620–570 Ma (Claesson & Roddick 1983); their genesis is related to the initial opening of the Iapetus Ocean (Kumpulainen & Nystuen 1985). In the project map area, mica schist and meta-arkose with dolerite dykes make up the mountain Pieljekaise south of Jäkkvik; further occurrences of the Särv Nappe Complex are situated north of Jäkkvik and west of Örnvik.

Seve Nappe Complex

Rocks of the Seve Nappe Complex occur in the northwest of the project area and have not been investigated in this context. A description of these units is given in Thelander (2009a, b). Only a brief summary is given here.

The Seve Nappe Complex is thrust over the Stalon Nappe and other equivalent nappes or the Särv Nappe (Greiling et al. 2018). It comprises separate nappe units. From the bottom, they consist of Palaeoproterozoic gabbroid to dioritoid, anorthositic and ultrabasic or ultramafic rocks, derived from the Svecokarelian orogen. These rocks are overlain by nappe units emanating from the Neoproterozoic Baltica–Iapetus transition zone. From below, they start with a unit of mainly amphibolites, overlain by nappes consisting of gneiss, mica schist, quartzite, calcareous schist, calc-silicate rock, limestone and sandstone. The uppermost unit of the Seve Nappe Complex in the project area comprises a sequence of arkosic arenites, quartzites and siltstones that have been intruded by dolerite dykes at 620–604 Ma (Thelander 2009a, b).

LITHOGEOCHEMISTRY IN THE SVECOKARELIAN OROGEN

The Geological Survey of Sweden (SGU) collected and analysed 1951 geochemical samples from the project area under the regular bedrock mapping programme and during geological investigations in the Barents Project. The whole rock geochemistry package was selected for lithogeochemistry analyses for the Barents Project at ALS Scandinavia AB Lab. This package combines whole-rock analyses by lithium metaborate/tetraborate fusion, acid digestion and ICP-AES analysis plus carbon and sulphur by combustion furnace to quantify the major elements in a sample. Lithogeochemical analyses were mostly carried out by ACME Lab (Vancouver- Canada) and ALS Scandinavia AB (Luleå, Sweden). At the ACME Lab, the samples were analysed for major, minor and trace elements using ICP-optical emission spectrometry following dilute nitric acid digestion. Trace elements, including the full rare earth element suite, are derived from three digestions followed by either ICP-AES or ICP-MS. A lithium borate fusion was applied for the resistive elements, four-acid digestion for the base metals and aqua regia digestion for volatile gold-related trace elements.

Lithogeochemistry is a powerful tool for identifying, classifying and discriminating rock units, as shown by a number of previous studies in northern Sweden (e.g. Perdahl & Frietsch 1993, Ahl et al. 2001, Bergman et al. 2001, Lundh et al. 2014). Several major rock units have been identified in the project area. The aim of the lithochemical study is to identify and classify the bedrock based on geochemical composition of rocks, and secondly to use the lithochemistry to discriminate between rocks of different units as suites and groups and give some clues on tectonic interpretation of these units.

The samples, forming the basis for all lithogeochemical data in the project area, have been classified in terms of rock type and stratigraphy from field observations. Radiometric age determination (Table 3) and the bedrock map prepared for the project area in southern Norrbotten were used to verify the geological properties of the rocks. Only analyses of well-defined samples are included in the data sets. Ambiguous samples, such as rocks with possible alteration patterns, unclear or absent geological coding, coordinate uncertainties and technical flaws, have been removed from the sample sets.

Archaean rocks >2.50 Ga

In Sweden, Archaean Rocks outcrop only in Norrbotten County and are composed of ca. 3.5–2.5 Ga gneissic and migmatitic rocks of varying composition. The southernmost outcrops occur in scattered massifs between Luleå and Piteå, near Boden and north of Jokkmokk, along the northwest-trending Luleå–Jokkmokk zone, which coincides with the change from positive $\varepsilon_{Nd\,(T)}$ to negative $\varepsilon_{Nd\,(T)}$ when moving from southwest to northeast. However, Archaean rocks are thought to underlie the Palaeoproterozoic rocks north of the Luleå–Jokkmokk Zone. The largest exposure of Archaean rocks is found north of Kiruna, north of the project area. Rock classification of Archaean rocks is severely hampered by the wide variety of rock composition and strong metamorphic overprint found in these rocks. A few samples may be recognised as classic TTG (tonalite-trondhjemite-granodiorite) gneisses (Fig. 91a), with a high sodium content, and a calcic to calc alkaline trend (Fig. 91b). Another recognisable unit consists of porphyritic intrusive rocks, which normally show quartz monzonitic to granitic composition (Fig. 91a). In the TTG gneiss subset, a few samples show trondhjemite composition with a characteristic positive Eu anomaly and a depletion of heavy rare earth elements (HREE; Fig. 91e). Previous studies (Ahl et al. 2001) showed higher Al_2O_3 content and lower K_2O and Rb content in the Archaean rocks compared with younger, Palaeoproterozoic rock units in their northern area, which roughly corresponds to Norrbotten County.

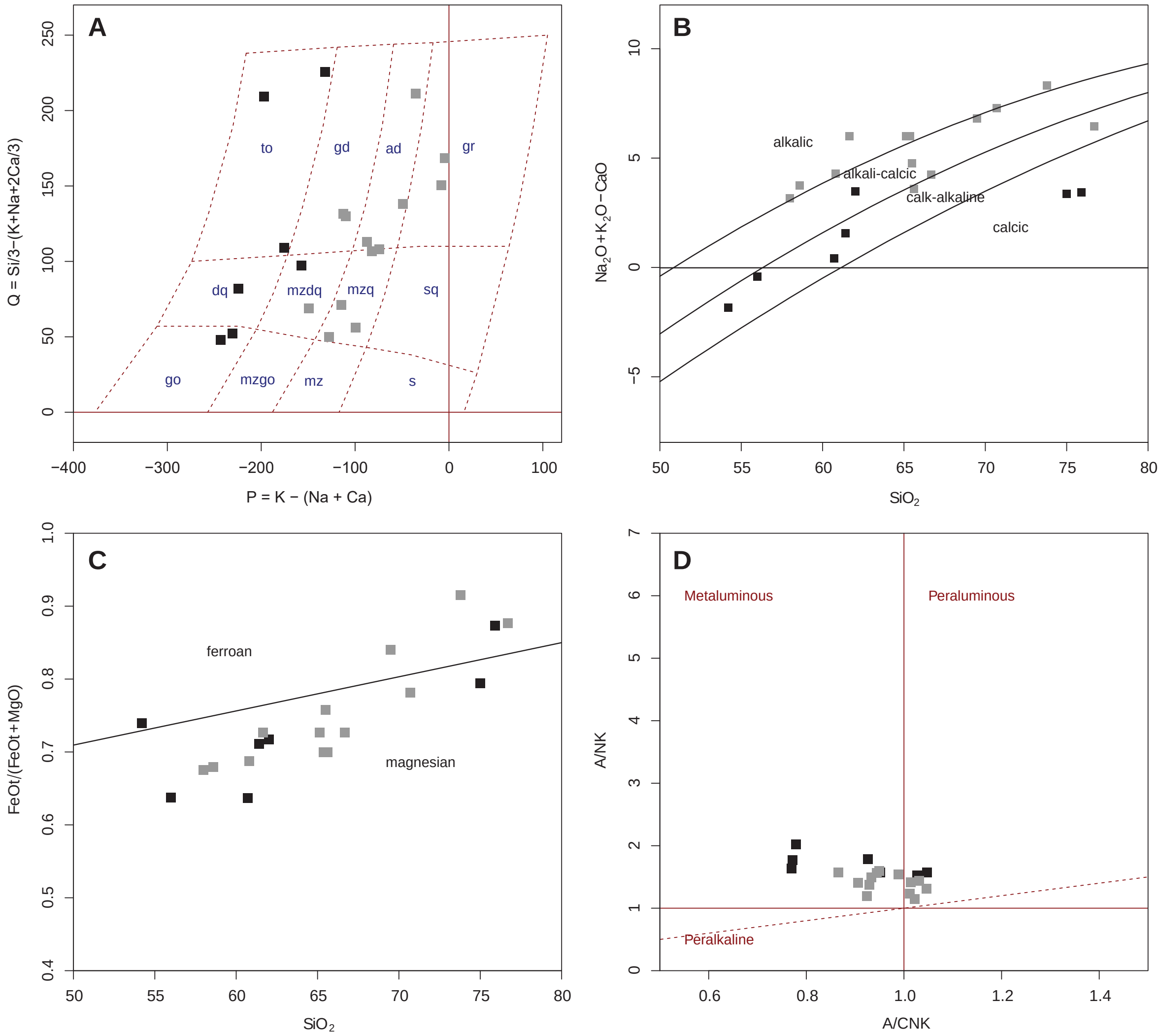

Figure 91. Lithogeochemical features of Archaean rocks. **A.** P-Q diagram of Debon & Lefort (1983) to=tonalite, gd=granodiorite, ad=adamellite, gr=granite, dq=quartz diorite, mzdq=quartz monzodiorite, mzq=quartz monzonite, sq=quartz syenite, go=gabbro, mzgo=monzo gabbro, mz=monzonite, s=syenite. **B.** Modified Alkali Index (MALI) diagram of Frost et al. (2001). **C.** Fe number (Fe/Mg) diagram of Frost et al. (2001). **D.** Classification diagram of Shand (1943).

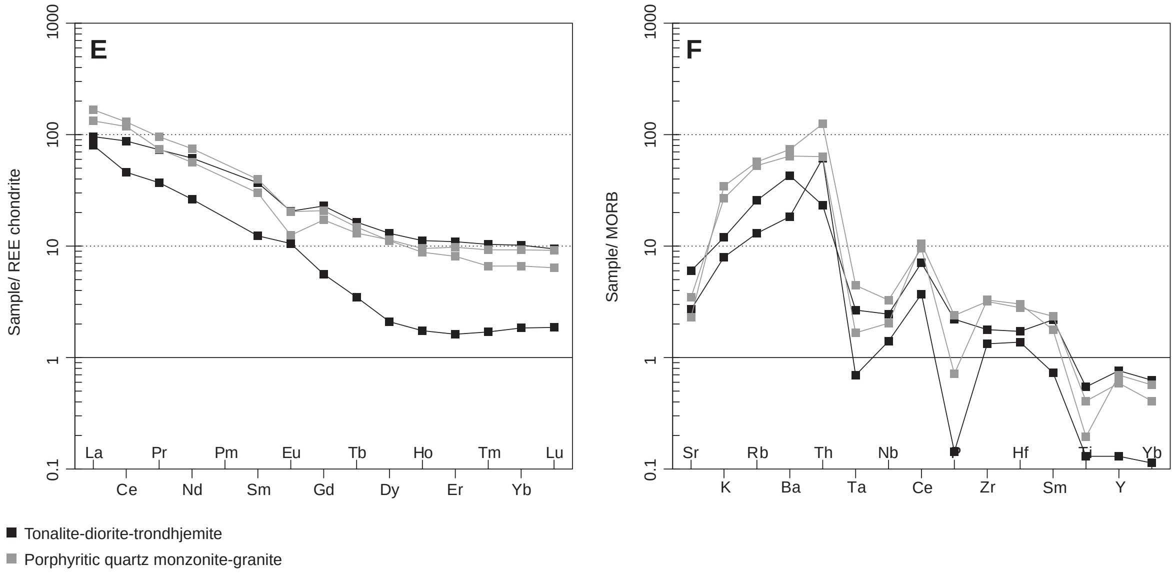

Figure 91. **E.** REE plot normalised to chondrite (Boynton 1984). Curves are arithmetic means for tonalite-granodiorite and trondhjemite samples (black squares) and porphyritic quartz monzonites and granites (grey squares). **F.** Spider diagram normalised to MORB (Pearce1983).

Karelian supracrustal and intrusive rocks c. 2.40–1.96 Ga

Kalix group

Most metavolcanic rocks in the Kalix group (the Karlsborg formation) are basaltic in composition, with some trachybasaltic members (Fig. 92a). A number of samples are K-enriched due to alteration (Fig. 92b), and a nomenclature diagram (Fig. 92c) based on trace elements also suggests that Kalix group rocks are basalts.

The samples of the Kalix group can be divided into two types, in which some samples of one type are enriched in elements such as alkalis, Zr, Nb and Ti, and have a more alkaline character; they are alkali basalts. The other type comprises subalkaline basalts. In a rare earth elements (REE) plot (Fig. 92e), both types show almost identical curves, but with an elevated level for alkali basalts. In a spider plot normalised to mid-ocean ridge basalts (MORB), alkali basalts show a general enrichment, mainly in the compatible elements, while subalkaline basalts have a Ta-Nb trough (Fig. 92f).

Tectonic interpretation of the lithogeochemical character of the Kalix group was discussed in the section *Karelian supracrustal and intrusive rocks c. 2.40–1.96 Ga* in the beginning of chapter 5 *Geological units*; the lithogeochemical data reflect the evolution of a rift zone, in which the most evolved, Ti-rich alkali basalts were formed in the most evolved stage.

The 2.5–2.0 Ga chronological interval also includes poorly exposed volcanic and sedimentary rocks, including the ultramafic rocks of the Tornio intrusion surrounding the Archaean Kukkola gneiss complex, and basaltic rocks forming lava flows and sills in the Jatulian metasandstones of the Sockberget group. Three samples from mafic volcanic rocks in these units are included in the Kalix group diagrams (Figs. 92a–f). These rocks are similar to the subalkaline basalts in the Karlsborg formation, with low K content and a Ta-Nb trough.

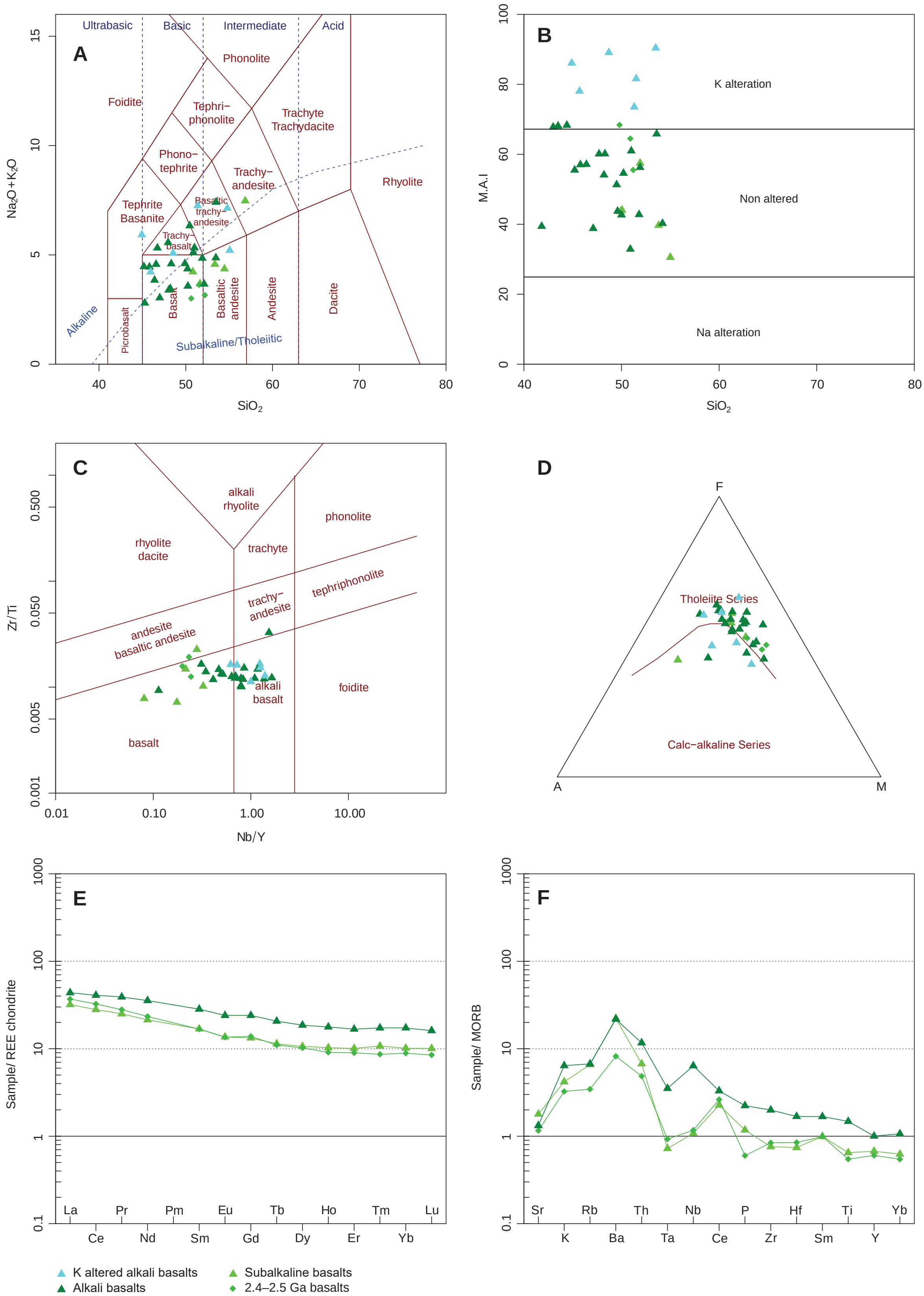

Figure 92. Lithogeochemical features of the Kalix group. **A.** Total alkali-silica (TAS) diagram after Le Bas et al. (1986). **B.** Alteration diagram of Ishikawa et al. (1976). MAI is 100(K_2O+MgO)/*K_2O+MgO+(2*Na_2O). Non-altered rocks generally MAI=25-65. **C.** Trace element classification diagram of Pearce (1996). **D.** A-F-M diagram of Jensen (1976) showing the tholeiitic character of the Kalix group. **E.** REE plot normalised to chondrite (Boynton 1984). Kalix samples are presented by statistical means for the alkaline and subalkaline subgroups. **F.** Spider diagram normalised to MORB (Pearce1983), samples as above.

Intrusive, supracrustal and metamorphic rocks, c. 1.96–1.75 Ga

Early Svecokarelian intrusive rocks, c. 1.96–1.92 Ga (Norvijaur intrusion)

A small number of samples have been collected from the Norvijaur intrusion, located southwest of Jokkmokk. Four of them are included in the Haparanda and Jörn GI suites diagrams (Figs. 94a–f). The Norvijaur intrusion has a granodioritic-tonalitic composition with some granitic parts and has been dated at c. 1.93 Ga (Hellström 2015). Igneous rocks of similar age and composition to the Norvijaur granodiorite are rare in the Svecokarelian orogen. The Knaften intrusion, dated at c. 1.95 (Waström 1996) is possibly related. The few granodiorite-tonalite samples of the Norvijaur intrusion follow a very clear calk-alkaline trend and return K_2O/Na_2O ratios of about 0.5. A spider plot of trace elements normalised to MORB shows fairly smooth depletion of Sr, P and Ti and a Ta-Nb-trough. Characteristic chondrite-normalised REEs show no Eu anomaly and a depletion of the HREEs (Fig. 94e).

Svecofennian supracrustal rocks, c. 1.90–1.87 Ga (Porphyrite group)

As discussed above (Ch. 5), the Porphyrite group is not easily defined compositionally, and a large variety of rocks occur within the 1.90–1.86 Ga chronological interval. In this study, the Porphyrite group sample set has been split into two halves: one from the eastern volcanic belts shown in columns N5 and N6 in Figure 17a, the other representing the western volcanic belts (columns BS1–BS3, N4 in Fig. 17a). In the eastern belts, volcanic rocks of dacitic-andesitic composition predominate, with relatively minor intercalations of basalt-andesites and rhyolites, whereas rhyolitic composition predominates in the western belts. (Fig. 93a). This main element terminology is verified by the trace element content (Fig. 93c). Some samples from the eastern belts show mild sodic alteration patterns (Fig. 93b), while Kalteration is mainly found in the western belts. The Porphyrite group samples plot mainly in the alkali-calcic field of the MALI diagram (Fig. 93d). The lithogeochemical composition of the Porphyrite group is very similar to that of the Haparanda suite (see below).

The rare earth elements (REE) diagram shows rather flat, mild concave upward patterns with a negative Eu anomaly for the most fractionated, rhyolitic samples (Fig. 93e). A spider diagram normalised to MORB (Pearce 1983) shows subduction-related patterns with enrichment of compatible elements, Ta-Nb trough and negative spikes for Sr, P and Ti for the most fractionated rhyolite samples. REEs from both belts show similar patterns in the spider diagram, but the deeper Eu anomaly in the rhyolites from the western volcanic belts is a notable deviation from that observation.

Early Svecokarelian intrusive rocks, c. 1.91–1.87 Ga (Haparanda and Jörn GI suites)

Early Svecokarelian intrusive rocks of the Haparanda and Jörn GI suites are widespread in the north and east of Norrbotten County (Witschard 1984). The suites are defined by a continuous compositional trend from gabbro to granite with quartz monzodiorites and granodiorites predominating (Fig. 94a). Rocks of more tonalitic composition occur, but these outliers may be caused by a mild sodic alteration. These rocks generally show a calk-alkaline to alkali-calcic trend (Bergman et al. 2001) (Fig. 94b). The Haparanda and Jörn GI suites are magnesian (Fig. 94c), and show a meta-aluminous character grading into peraluminous for the most fractionated granitic parts (Fig.94d). No substantial compositional difference can be seen between the two suites.

The REE diagram by Boynton (1984) shows a mild concave upward pattern for the whole compositional range, and a negative Eu anomaly for the granitic parts (Fig. 94e). Spider diagrams of trace elements normalised to MORB (Pearce 1983) show the typical pattern of subduction-related processes with enrichment of the compatible elements, the Ta-Nb trough and negative anomalies of Sr, P and Ti in the felsic compositional range (Fig. 94f). Low concentrations of Y, Rb and Nb and higher concentrations of Sr were noted as a particularly common feature of the Haparanda and Jörn G1 suites by Ahl et al. (2001).

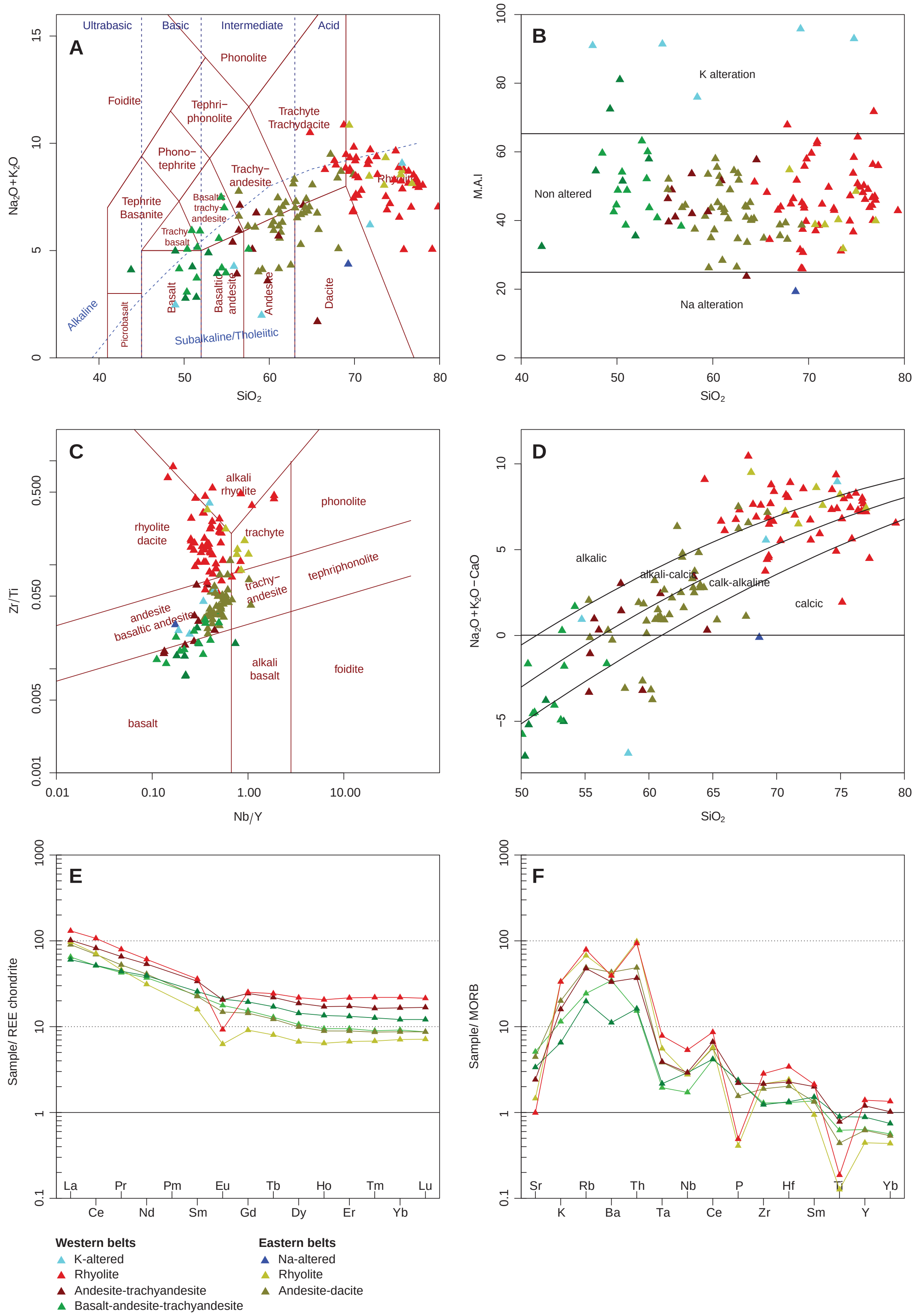

Figure 93. Lithogeochemical features of the Porphyrite group. **A.** Total alkali-silica (TAS) diagram after Le Bas et al. (1986). **B.** Alteration diagram of Ishikawa et al. (1976). MAI is 100(K_2O+MgO)/*K_2O+MgO+(2*Na_2O). Non-altered rocks generally MAI=25-65. **C.** Trace element classification diagram of Pearce (1996). **D.** MALI diagram of Frost et al. (2001). **E.** REE plot normalised to chondrite (Boynton 1984). Porphyrite group samples are presented by statistical means for the basalt-andesite, dacite-andesite and rhyolite subgroups. **F.** Spider diagram normalised to MORB (Pearce1983), samples as above.

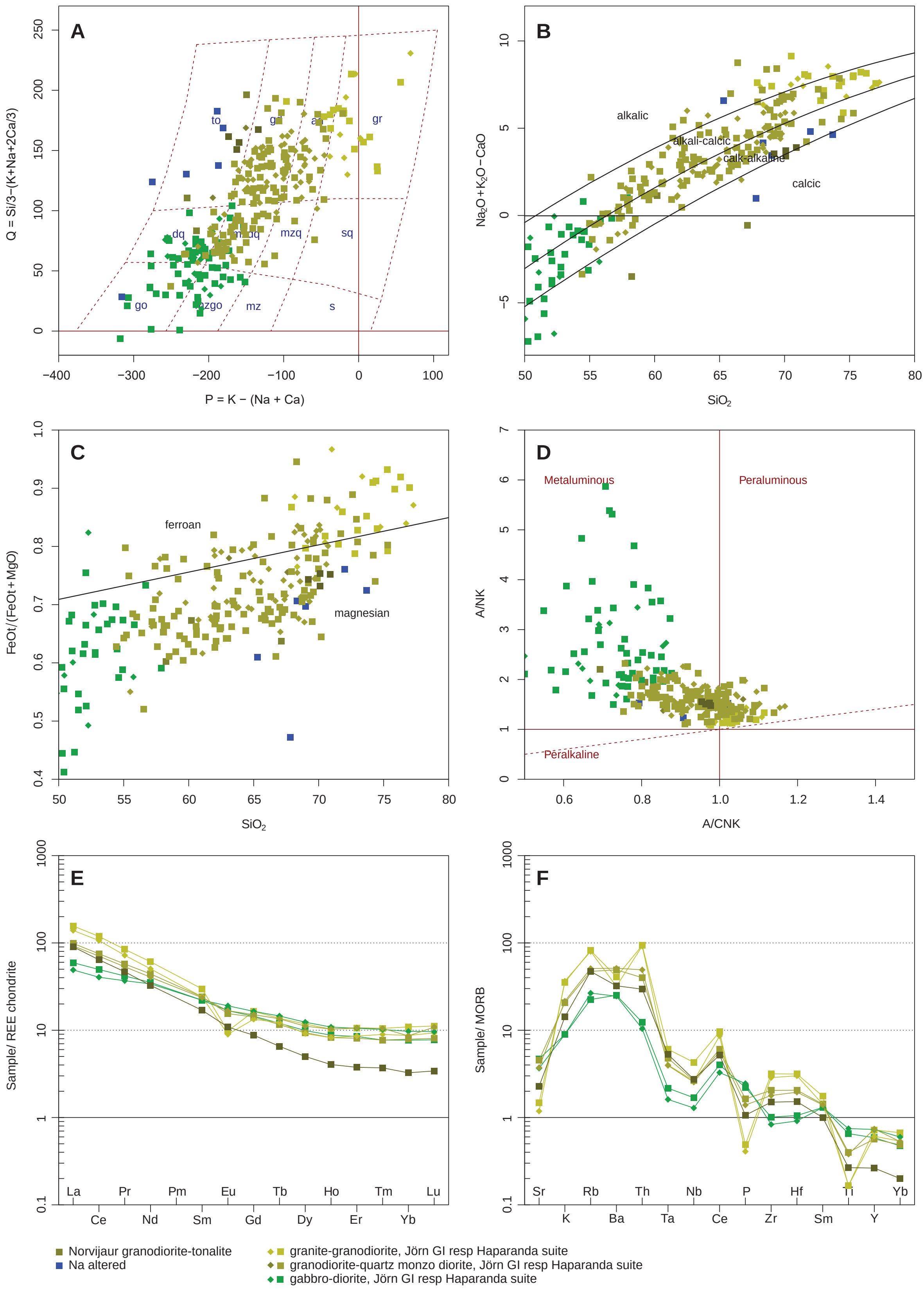

Figure 94. Lithogeochemical features of the Haparanda and Jörn G1 suites. **A.** P-Q diagram of Debon & Lefort (1983) to=tonalite, gd=granodiorite, ad=adamellite, gr=granite, dq=quartz diorite, mzdq=quartz monzodiorite, mzq=quartz monzonite, sq=quartz syenite, go=gabbro, mzgo=monzo gabbro, mz=monzonite, s=syenite. **B.** Modified Alkali Index (MALI) diagram of Frost et al. (2001). **C.** Fe number (Fe/Mg) diagram of Frost et al. (2001). **D.** Classification diagram of Shand (1943); **E.** REE plot normalised to chondrite (Boynton 1984). Haparanda and Jörn G1 samples are presented by statistical means for the gabbro-diorite, granodiorite-quartz monzodiorite, granite-granodiorite and sodic subgroups. **F.** Spider diagram normalised to MORB (Pearce 1983), samples as above.

Svecofennian supracrustal rocks, c. 1.89–1.86 Ga (Arvidsjaur group)

The Arvidsjaur group includes considerably more examples of volcanic rocks of varying lithogeochemical composition in the continuous trend from basalt through intermediate andesite/dacite to high-silica rhyolite (see TAS diagram, Fig. 95a), compared with the Porphyrite group. Otherwise the two groups share many features.

A small proportion of the Arvidsjaur group samples plot in the trachyte/trachydacite field of the TAS diagram (Fig. 95a). This feature may partly be an effect of K and Na-alteration found in the Arvidsjaur group (Fig.95b), but since alteration seems to be confined to rocks of rhyolitic composition, it is more likely that these K-enriched intermediate rocks have a primary magmatic signature. Similar K enrichment also exists in the Perthite monzonite suite suite (see below). Perdahl & Frietsch (1993) identified an Arjeplog subprovince in the west of the project area, where bimodal, high K-Zr volcanic rocks predominate. The patterns are not visible in a classification diagram based on trace elements (Fig. 95c). The Arvidsjaur group samples are alkali-calcic in a MALI diagram (Fig. 95d), albeit with a huge spread, possibly due to K and Na-alteration but also reflecting the existence of trachytes.

The REE plot (Fig. 95e) shows negative Eu anomalies for all compositions from basalt to rhyolite, and the MORB-normalised spider diagram (Pearce 1983) shows the typical Ta-Nb trough (Fig. 95f).

Early Svecokarelian intrusive rocks, c. 1.89–1.85 Ga (Perthite monzonite suite)

Like the Haparanda and Jörn GI suites, the Perthite monzonite suite shows a compositional trend from gabbro to granite, but granitic compositions clearly predominate (Fig. 96a). In general, the rocks of the Perthite monzonite suite show a potassium-enriched, alkali-calcic to shoshonitic trend (Fig. 96b). In the intermediate compositional interval, there is a fairly distinct group of quartz monzonites, with elevated K_2O (Fig. 96a, b), similar to that observed in the Arvidsjaur Group (see above). The rocks of the Perthite monzonite suite are generally ferroan (Fig. 6c) and show a combined metaluminous-peraluminous signature (Fig. 96d). The rocks of fractionated granitic composition plot close to the peralkaline field.

REE diagrams reveal negative Eu anomalies (Fig. 96e), and a trace element spider diagram, normalised to MORB (Pearce 1983), shows a Ta-Nb trough and negative P and Ti anomalies (Fig. 96f), particularly for the granitic components. In comparison with the Haparanda and Jörn GI suites, the curves are flatter in chondrite-normalised diagrams, with deeper Eu anomalies, and the spider diagram based on trace element content shows deeper P and Ti troughs, which suggests more advanced fractional crystallisation. However, the Haparanda, Jörn GI and Perthite monzonite suites show a similar element distribution.

Late Svecokarelian intrusive rocks, c. 1.81–1.78 Ga (Edefors suite)

The rocks of the Edefors suite range in composition from gabbro-diorite via syenite and quartz syenite to quartz monzonite and granite (Fig. 97a). The gabbroid rocks of the Edefors suite have a calc-alkaline to tholeiite affinity, whereas the more felsic varieties have a high potassic, alkaline affinity (Fig. 97b). The suite displays a ferroan (Fig. 97c) and metaluminous to peraluminous character (Fig. 97d).

For the REE distribution in the Edefors suite (Fig. 97e), quartz syenitic to quartz monzonitic rocks from the intermediate compositional range display concave upward patterns with no Eu anomaly, apart from a smaller subset with a mild positive Eu-anomaly (Fig. 97e). Granites have negative Eu-anomalies (Fig. 97e). Spider diagrams normalised to MORB show marked positive anomalies of Ce and Hf-Zr, the negative Ta-Nb trough as well as negative anomalies of P and Ti (Fig. 97f).

Late Svecokarelian intrusive rocks, c. 1.81–1.75 Ga (Lina suite)

The rocks of the Lina suite are massive or locally foliated, equigranular, light reddish or pink, usually granites *sensu stricto* with a eutectic minimum melt composition (Ödman 1957) and a fairly restricted range of granitic compositions (Fig. 98a). They show a high potassic, calc-alkaline to shoshonitic affinity (Fig. 98b). The granites of the Lina suite show a somewhat lower Fe number (Fig. 98c) than those

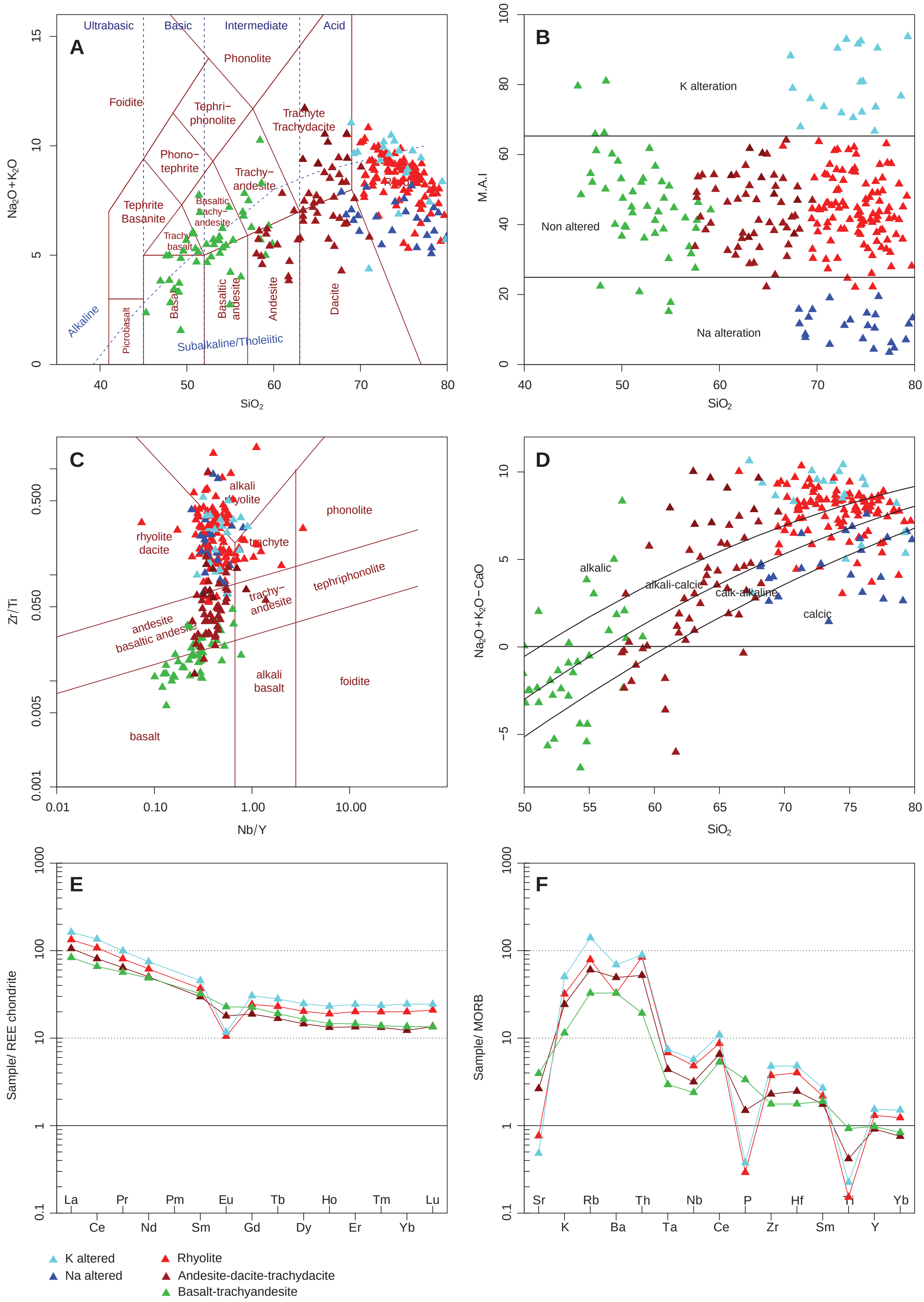

Figure 95. Lithogeochemical features of the Arvidsjaur group. **A.** Total alkali-silica (TAS) diagram after Le Bas et al. (1986). **B.** Alteration diagram of Ishikawa et al. (1976). MAI is 100(K_2O+MgO)/*K_2O+MgO+(2*Na_2O); Non-altered rocks generally MAI=25-65. **C.** Trace element classification diagram of Pearce (1996). **D.** Modified Alkali Index (MALI) diagram of Frost et al. (2001). **E.** REE plot normalised to chondrite (Boynton 1984). Arvidsjaur group samples are presented by statistical means for the basalt-andesite, dacite-quartz trachyte and rhyolite subgroups. **F.** Spider diagram normalised to MORB (Pearce1983), samples as above.

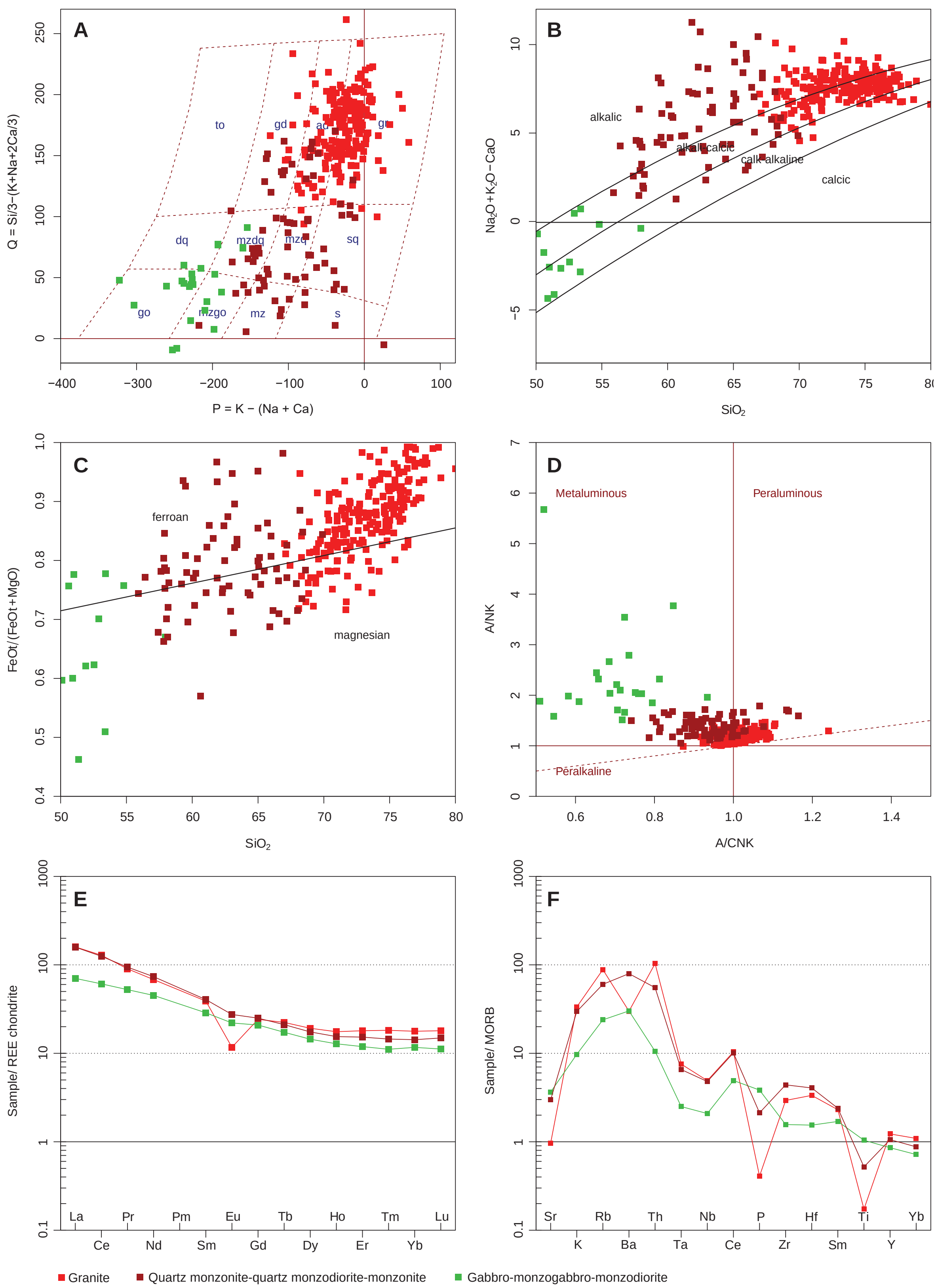

Figure 96. Lithogeochemical features of the Perthite monzonite suite. **A.** P-Q diagram of Debon & Lefort (1983) to=tonalite, gd=granodiorite, ad=adamellite, gr=granite, dq=quartz diorite, mzdq=quartz monzodiorite, mzq=quartz monzonite, sq=quartz syenite, go=gabbro, mzgo=monzo gabbro, mz=monzonite, s=syenite. **B.** Modified Alkali Index (MALI) diagram of Frost et al. (2001). **C.** Fe number (Fe/Mg) diagram of Frost et al. (2001). **D.** Classification diagram of Shand (1943). **E.** REE plot normalised to chondrite (Boynton 1984). Perthite monzonite suite samples are presented by statistical means for the gabbro-diorite, granodiorite-quartz monzodiorite-quartz monzonite and granite subgroups. **F.** Spider diagram normalised to MORB (Pearce 1983), samples as above.

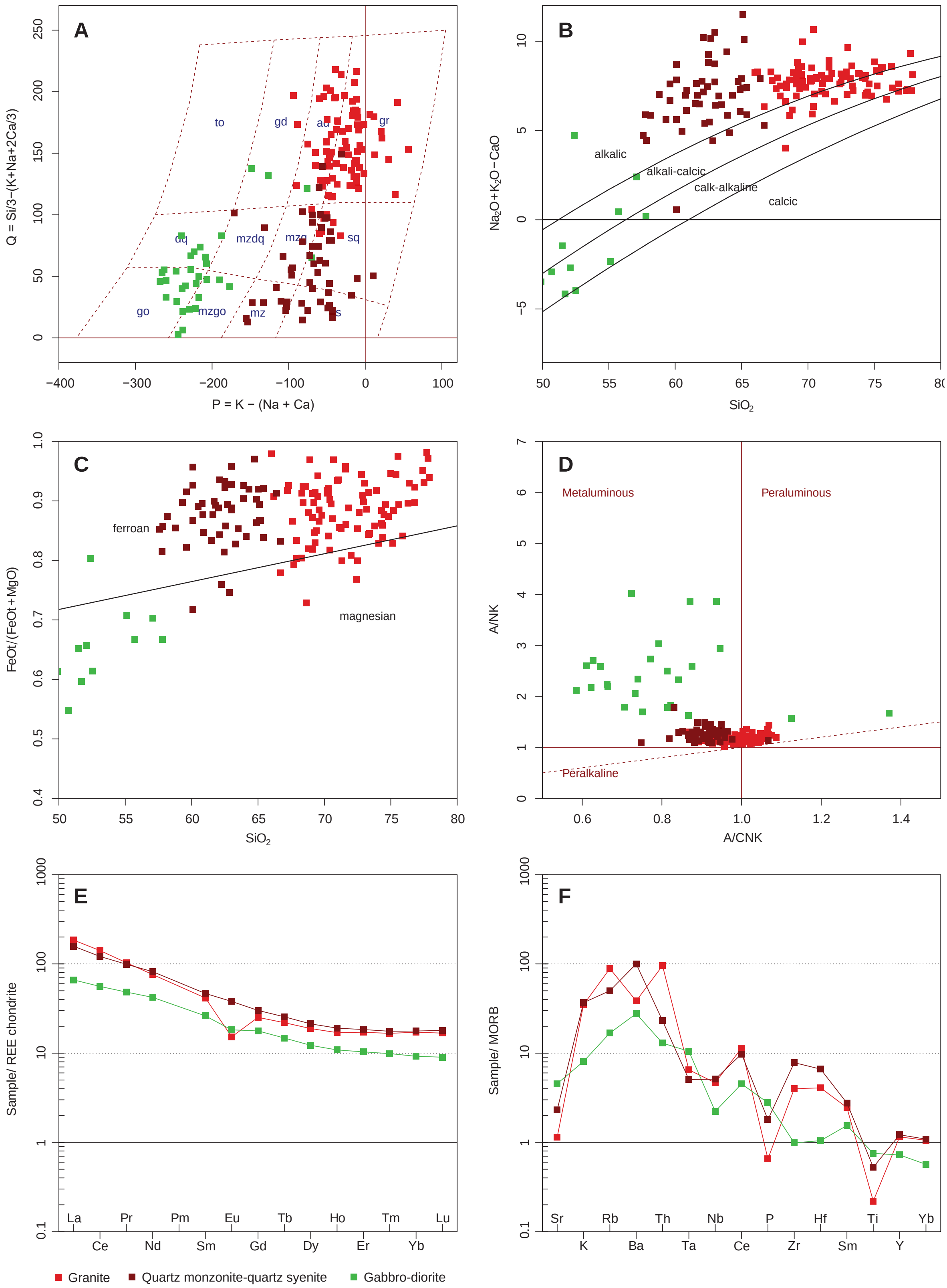

Figure 97. Lithogeochemical features of the Edefors suite. **A.** P-Q diagram of Debon & Lefort (1983) to=tonalite, gd=granodiorite, ad=adamellite, gr=granite, dq=quartz diorite, mzdq=quartz monzodiorite, mzq=quartz monzonite, sq=quartz syenite, go=gabbro, mzgo=monzo gabbro, mz=monzonite, s=syenite. **B.** Modified Alkali Index (MALI) diagram of Frost et al. (2001). **C.** Fe number (Fe/Mg) diagram of Frost et al. (2001). **D.** Classification diagram of Shand (1943). **E.** REE plot normalised to chondrite (Boynton 1984). Edefors samples are presented by statistical means for the gabbro-diorite, quartz monzonite-quartz syenite and granite subgroups, including smaller subgroups with K-enriched monzonites-syenites with positive Eu anomaly and granodiorites-granites. **F.** Spider diagram normalised to MORB (Pearce 1983), samples as above.

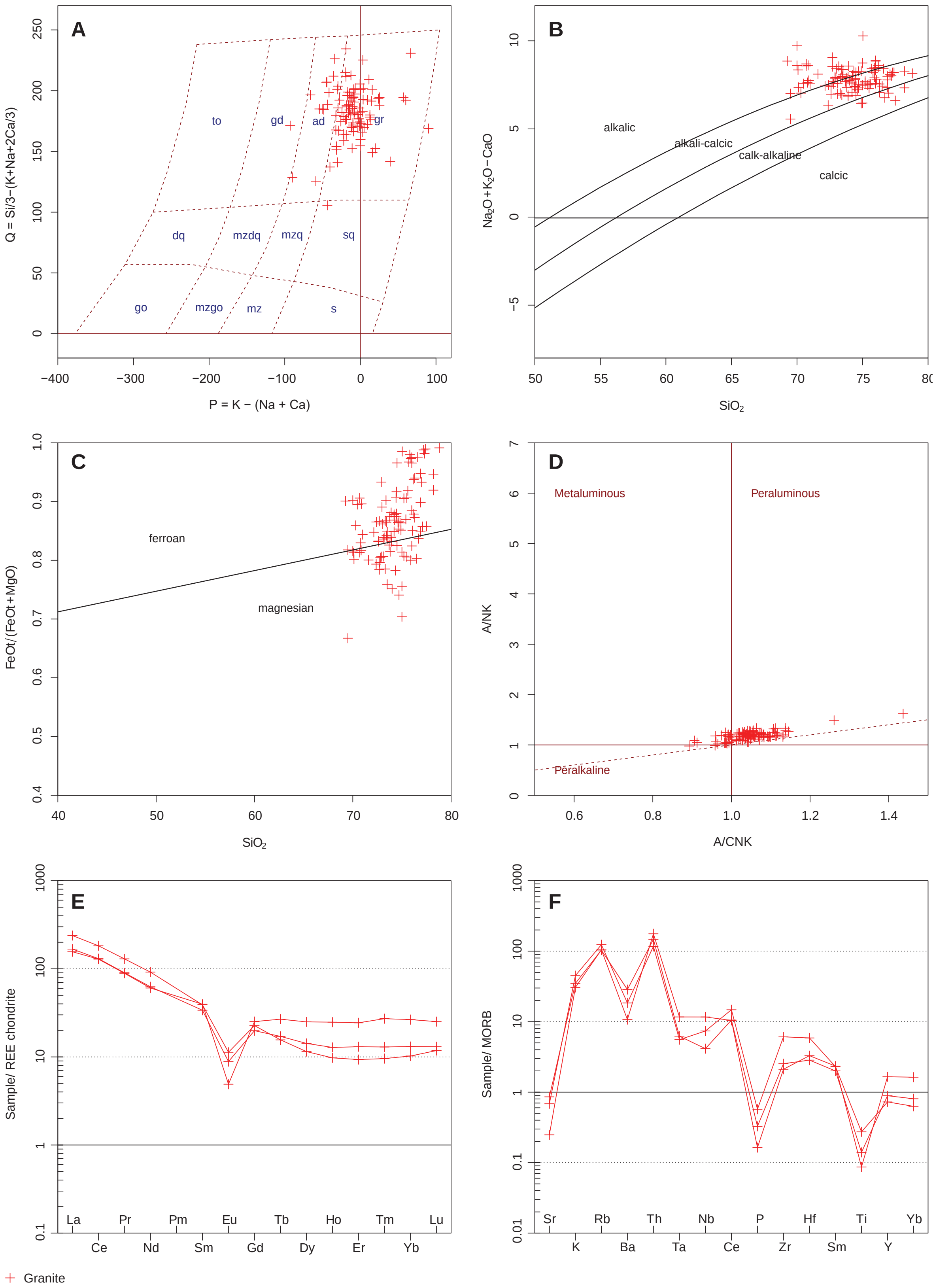

Figure 98. Lithogeochemical features of the Lina suite. **A.** P-Q diagram of Debon & Lefort (1983) to=tonalite, gd=granodiorite, ad=adamellite, gr=granite, dq=quartz diorite, mzdq=quartz monzodiorite, mzq=quartz monzonite, sq=quartz syenite, go=gabbro, mzgo=monzo gabbro, mz=monzonite, s=syenite. **B.** MALI diagram of Frost et al. (2001). **C.** Fe number diagram of Frost et al. (2001). **D.** Classification diagram of Shand (1943). **E.** REE plot normalised to chondrite (Boynton 1984). Lina samples are presented by statistical means for the granite, including curves for the samples with the lowest SiO_2 and highest SiO_2 in the dataset. **F.** Spider diagram normalised to MORB (Pearce1983), samples as above.

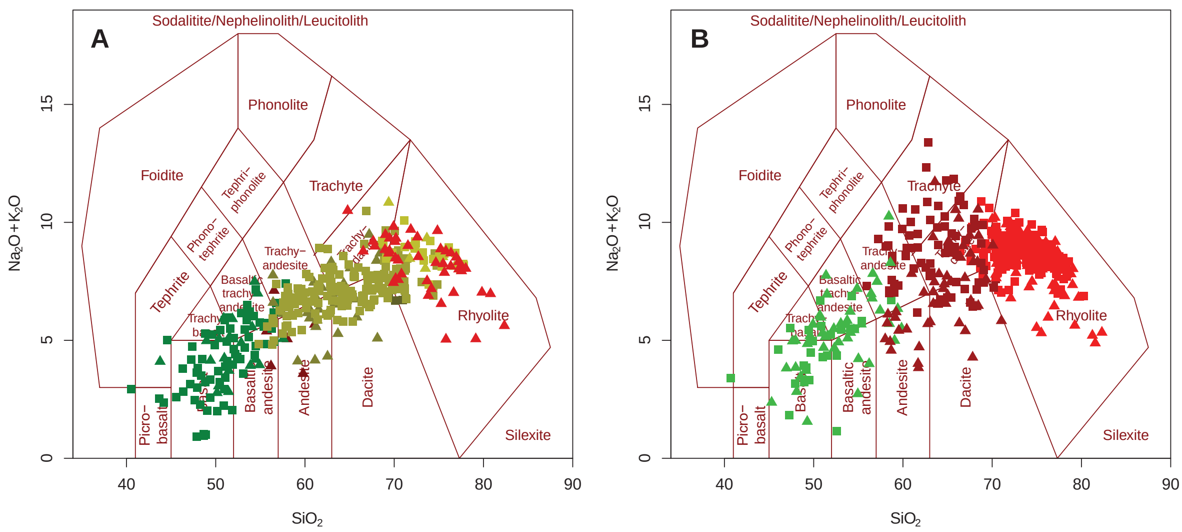

Figure 99. Comparison between the volcanic and intrusive components in the Arvidsjaur arc complex. **A.** Samples from the Porphyrite group and the Haparanda and Jörn GI suites in the total alkali-silica (TAS) diagram of Middlemost (1985). **B.** Samples from the Arvidsjaur group and the Perthite monzonite suite in the total alkali-silica (TAS) diagram of Middlemost (1985). Symbols as in Figures 93–96.

of the Edefors suite, and they are mainly peraluminous (Fig. 98d). The granites are thought to have been formed during melting and remobilisation of continental crust, including pelitic and semipelitic sedimentary rocks with a small input of juvenile material (Öhlander & Skiöld 1994). Pegmatite and aplite veins are common, and the Lina suite is mildly enriched in elements such as Li, Rb, Cs, U and Th. REE diagrams, normalised to chondrite, show a negative gradient from the LREEs to MREEs, with negative Eu anomalies and concave upward patterns from MREE to HREE (Fig. 98e). Spider diagrams normalised to MORB (Fig. 98f) show very strong negative anomalies of Sr, P and Ti, and a more moderate negative Ba anomaly.

Tectonic interpretation

There is a very easily identified link between the Porphyrite group and the Haparanda and Jörn GI suites. In Figure 99a, both units are plotted in a Middlemost (1985) TAS diagram. There is a virtually 100% overlap and a stable, linear trend without many outliers, with quartz monzodioritic compositions predominating (dacite-andesite in the Porphyrite group). The most felsic components are predominantly rhyolites from the western volcanic belts. The Porphyrite group and the Haparanda and Jörn GI suites are combined into one magmatic event. The Haparanda and Jörn GI suites form the subvolcanic supply to the Porphyrite group volcanism in a magmatic arc that was roughly coeval with the subaqueous Skellefte volcanic arc south of the project area. A similar relationship can be noted for the samples of the Arvidsjaur group and the Perthite monzonite suite, which are plotted in Figure 99b. The overall trend is curved, with a K-enriched trachytic/monzonitic component and rhyolites/granites predominating. This combined magmatic unit of the Arvidsjaur group and the Perthite monzonite suite forms the Arvidsjaur terrestric arc. The composition of this combined unit suggests an increased maturity and a thicker crust. Age data strongly verify this twofold evolution of the Arvidsjaur terrestric arc complex and an earlier magmatic arc. Apart from the predominance of rhyolitic compositions in the Arvidsjaur group and the Perthite monzonite suite, the main difference between the two arc systems are the potassic, trachytic compositions found in the Arvidsjaur group and quartz monzonite to monzonite in the Perthite monzonite suite, which do not have a counterpart in the Porphyrite group or the Haparanda and Jörn GI suites.

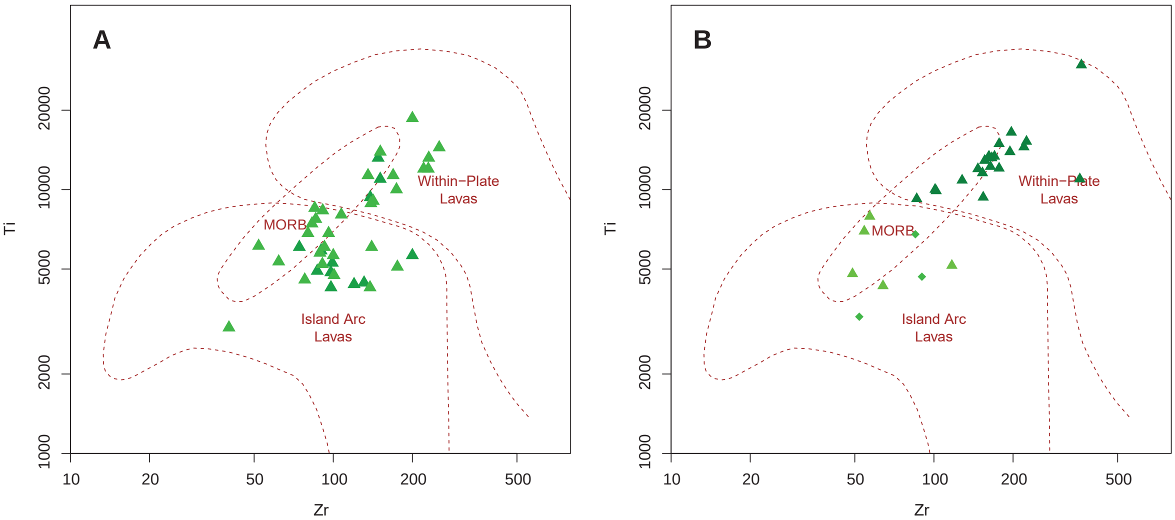

Figure 100. Zr-Ti diagram of Pearce (1982). **A.** Basaltic rocks from the Arvidsjaur and Porphyrite groups show a scattered distribution of samples in both within-plate and arc fields, reflecting the appearance of different subgroups in both groups. **B.** Samples from the Kalix group, gathering around the MORB field. Symbols as in Figures 92, 93 and 95.

Apart from the lithochemical differences mentioned above, the Porphyrite and the Arvidsjaur groups are in many ways quite similar, and it is not easy to distinguish them tectonically. Bergman et al. (2001) point out that the Porphyry group, which might correspond to the Arvidsjaur group in the project area, generally has a tendency towards high titanium and zirconium, which can be used as a tool for distinguishing the Arvidsjaur group from the Porphyrite group. Our data show that it is not an easy task to separate these groups based on this ratio, as there is significant overlap in Ti and Zr concentrations at given compositions. In Figure 100a, we show that discrimination between basaltic rocks from the Arvidsjaur and Porphyrite groups is not easily achieved, and the data sets return ambiguous results from the tectonic interpretation. Both groups include samples that form subsets plotting in both fields of the diagram. The samples from the Kalix Group plot scattered within and around the MORB field in the same diagram (Fig. 100b). It is interesting that the subalkaline basalts and the older 2.5 Ga basalts plot distinctly in the volcanic arc field and the alkali basalts in the MORB field, reflecting the new input of primitive magma. A possible scenario is a rift environment for these rocks, in which increasing alkalinity in the basalts is related to the evolution of the rift. The subalkaline basalts are related to the initial stages and more distal positions relative to the main rift stage.

In Figure 101, another diagram (Meschede 1986) is used to distinguish basaltic rocks tectonically. The basalts of the Porphyrite and Arvidsjaur groups plot mainly in the volcanic arc fields (Fig. 101a) The alkali basalts of the Kalix group are mainly in the MORB field (Fig. 101b), but show a trend towards the arc field. The subalkaline basalts of the Kalix group and the older 2.5 Ga basalts definitely have an arc signature.

The Edefors and Lina suites are almost contemporary, having formed in a late phase of the Svecokarelian deformation and metamorphism. The Edefors suite mainly comprises granites, with syenitoid and gabbroic rocks and characteristics similar to A-type granites, i.e. high concentrations of Na_2O+K_2O, Zr, Nb, Y and a high Fe/Mg ratio (Fig. 97c). The rocks of the Lina suite have a restricted granitic composition, and a predominantly peraluminous trend (Fig. 98d). The Lina suite suggests more affinity to S-type granites. There is a clear overlap between the granites of the Lina suite and those of the Edefors suite, both with an unclear I-S-A-granite signature in diagrams of all kinds (Figs. 97a–f, 98a–f). This probably reflects the complicated, mixed source of crustal melts in this region; including the Archaean basement, magmatic arc components and unevenly distributed metasedimentary rocks.

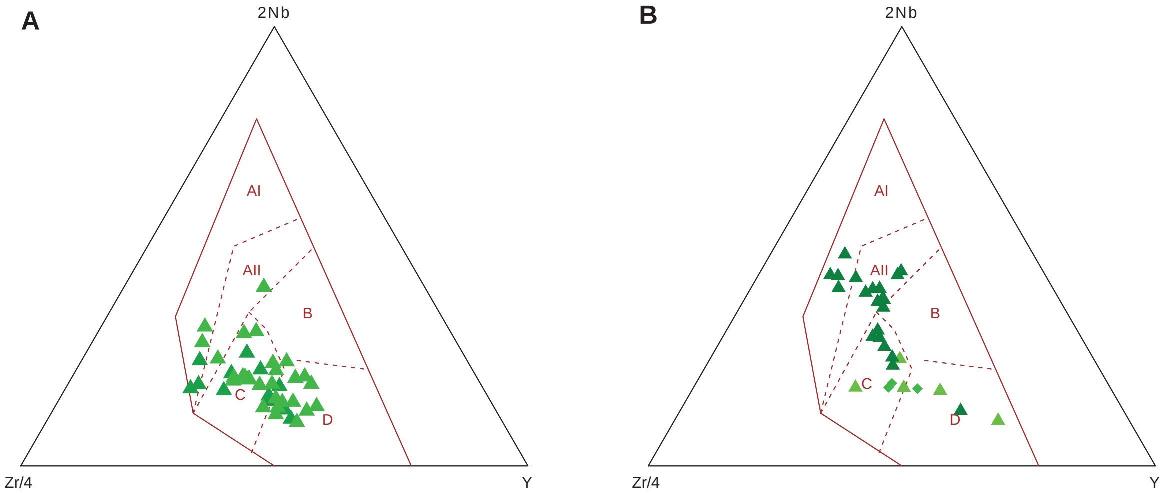

Figure 101. Tectonic interpretation of basalts according to Meschede (1986). AI-AII: Within-Plate Alkaline Basalts, AII-C: Within-Plate Tholeiites, B: P-type Mid-Ocean Ridge Basalts, D: N-type Mid-Ocean Ridge Basalts, C-D: Volcanic Arc Basalts. **A.** Samples from the Porphyrite and Arvidsjaur groups. Most samples are in the C field for Arc Basalts. **B.** Samples from the Kalix group. Alkali basalts from the Kalix group are mainly in the within-plate fields, while subalkaline basalts are in the arc basalt fields. Symbols as in Figs. 92, 93 and 95.

PETROPHYSICAL AND GAMMA RADIATION (GAMMA RAY) DATA IN THE SVECOKARELIAN OROGEN

A general description of the spatial distribution and character of petrophysical and gamma radiation data is given in chapter 3 *Base data* (Figs. 10 and 11).

All existing petrophysical and gamma radiation data in the area were compiled using GIS tools. In order to produce quality-controlled statistics on these data for the different rock units, a thorough examination was made of the measuring points and samples stored in the databases at SGU. Samples and measuring points with severe uncertainties as to geographical position, rock classification, source (boulder or outcrop) etc. have been rejected. The remaining samples and measuring points were attributed to the various rock units existing in the map area of southern Norrbotten County and have been investigated statistically for their content of potassium, uranium and thorium, density, magnetic susceptibility and Königsberg factor (denoted Q). The results of the statistical compilation are presented in Table 4.

Table 4. Statistics on petrophysical and gamma radiation (gamma ray) properties of the different rock units of the project area in southern Norrbotten.

To illustrate the petrophysical (magnetic susceptibility and density) and gamma radiation (potassium and thorium) properties of different rock units, the data have been grouped into the following four major groups: Palaeoproterozoic and Archaean metaintrusive rocks, Palaeoproterozoic and Archaean metavolcanic and volcanic rocks, Palaeoproterozoic intrusive rocks and Palaeoproterozoic metasedimentary and sedimentary rocks. Mean values with standard deviations have been plotted for magnetic susceptibility v. density (Figs. 102–105) and for potassium v. thorium (Figs. 106–109).

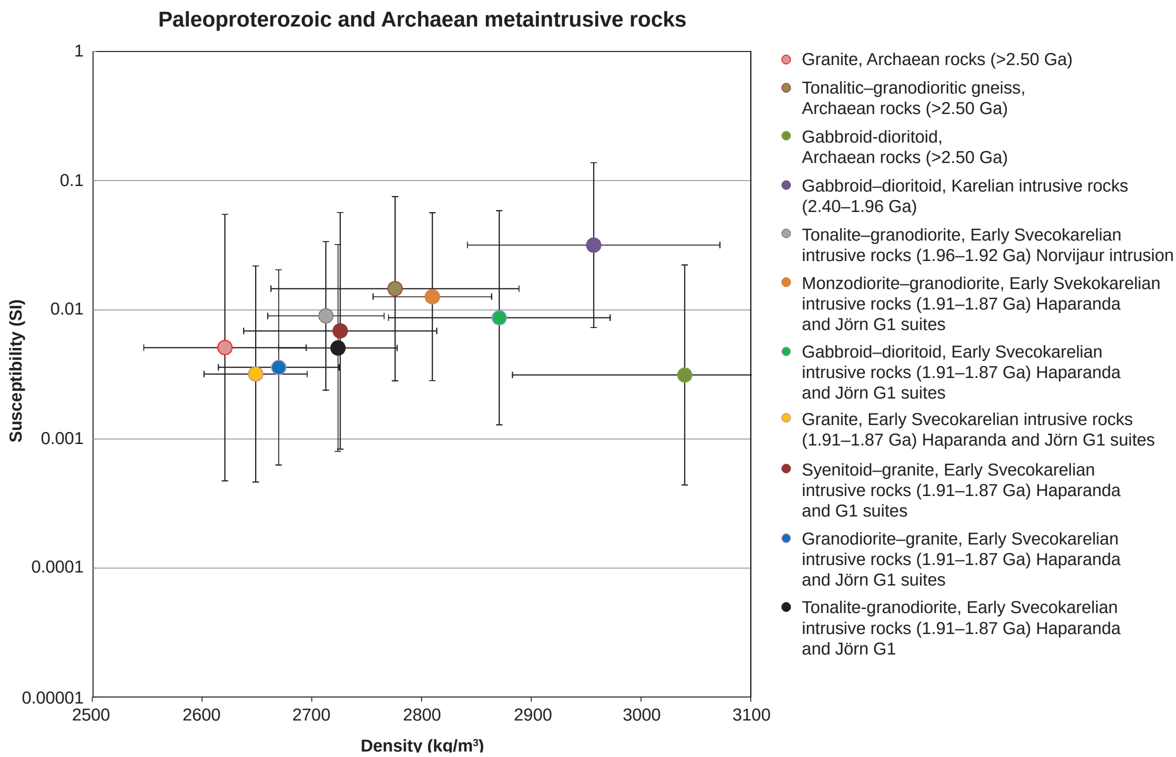

Figure 102. Magnetic susceptibility v. density for Palaeoproterozoic and Archaean metaintrusive rocks.

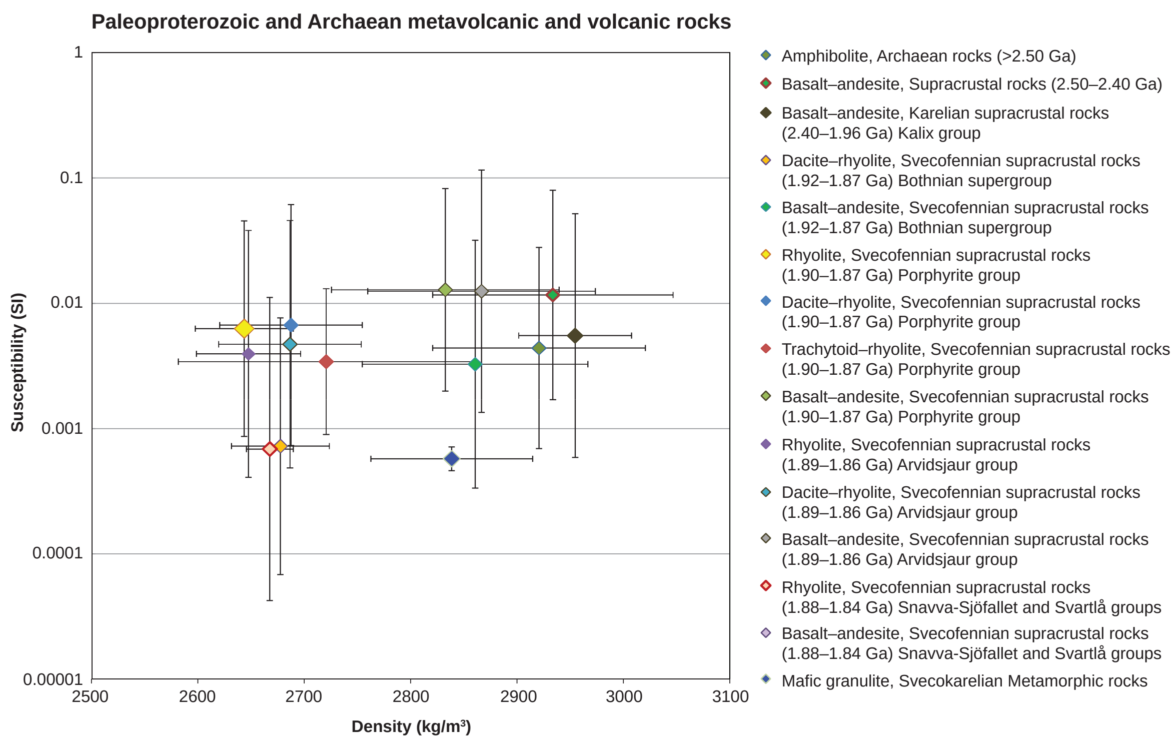

Figure 103. Magnetic susceptibility v. density for Palaeoproterozoic and Archaean metavolcanic and volcanic rocks.

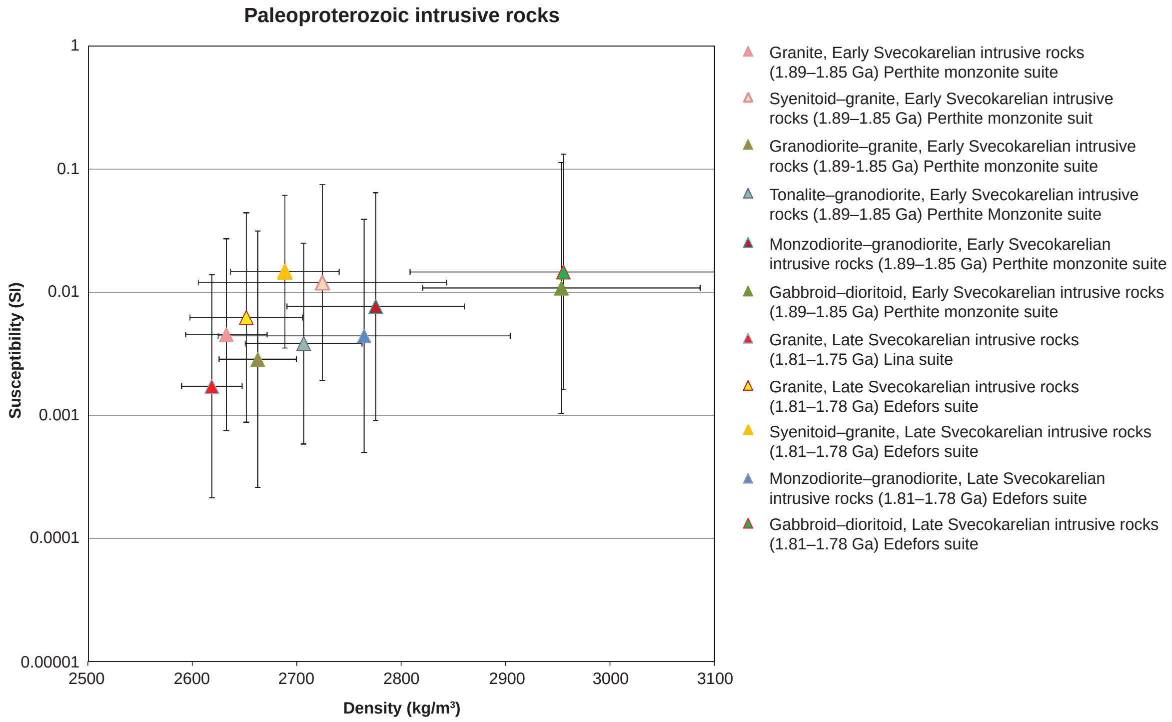

Figure 104. Magnetic susceptibility v. density for Palaeoproterozoic intrusive rocks.

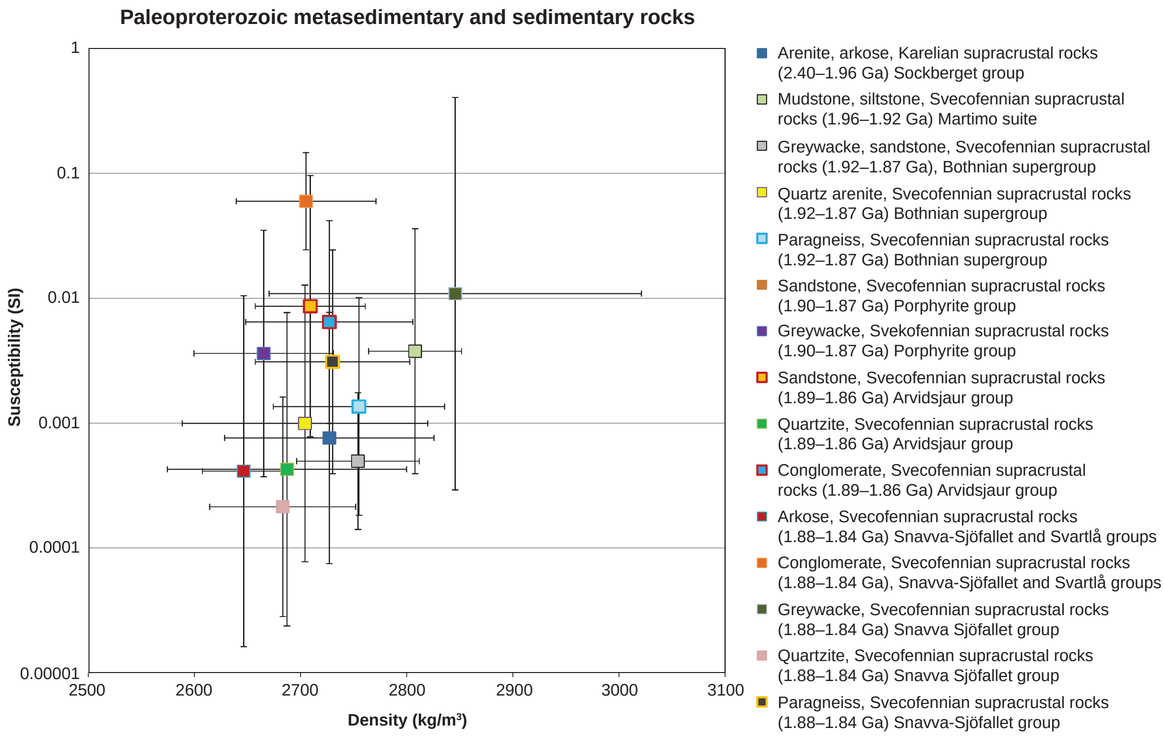

Figure 105. Magnetic susceptibility v. density for Palaeoproterozoic metasedimentary and sedimentary rocks.

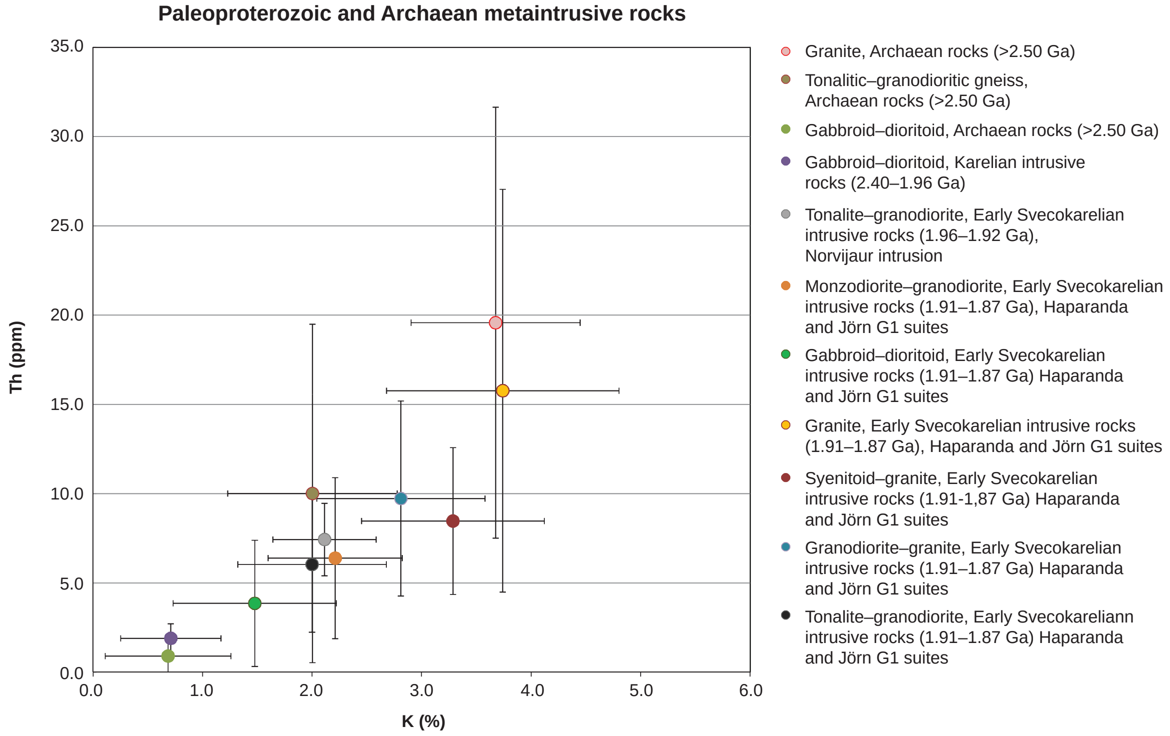

Figure 106. Thorium v. potassium for Palaeoproterozoic and Archaean metaintrusive rocks.

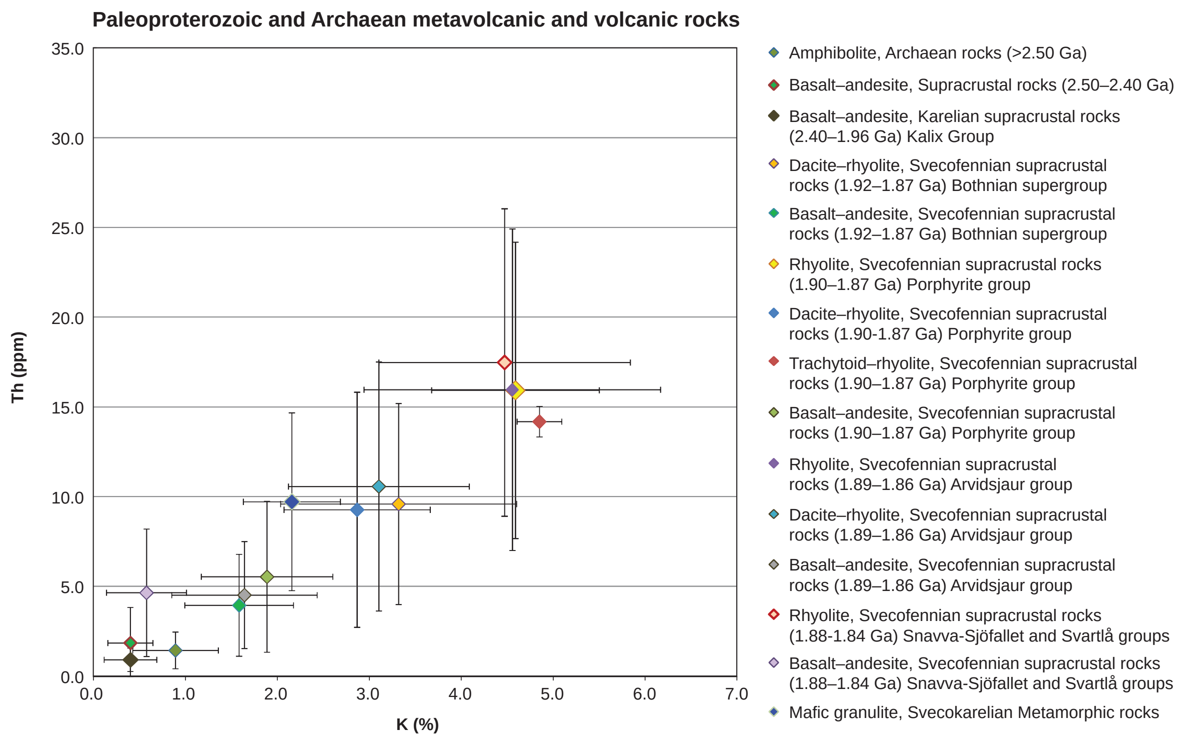

Figure 107. Thorium v. potassium for Palaeoproterozoic and Archaean metavolcanic and volcanic rocks.

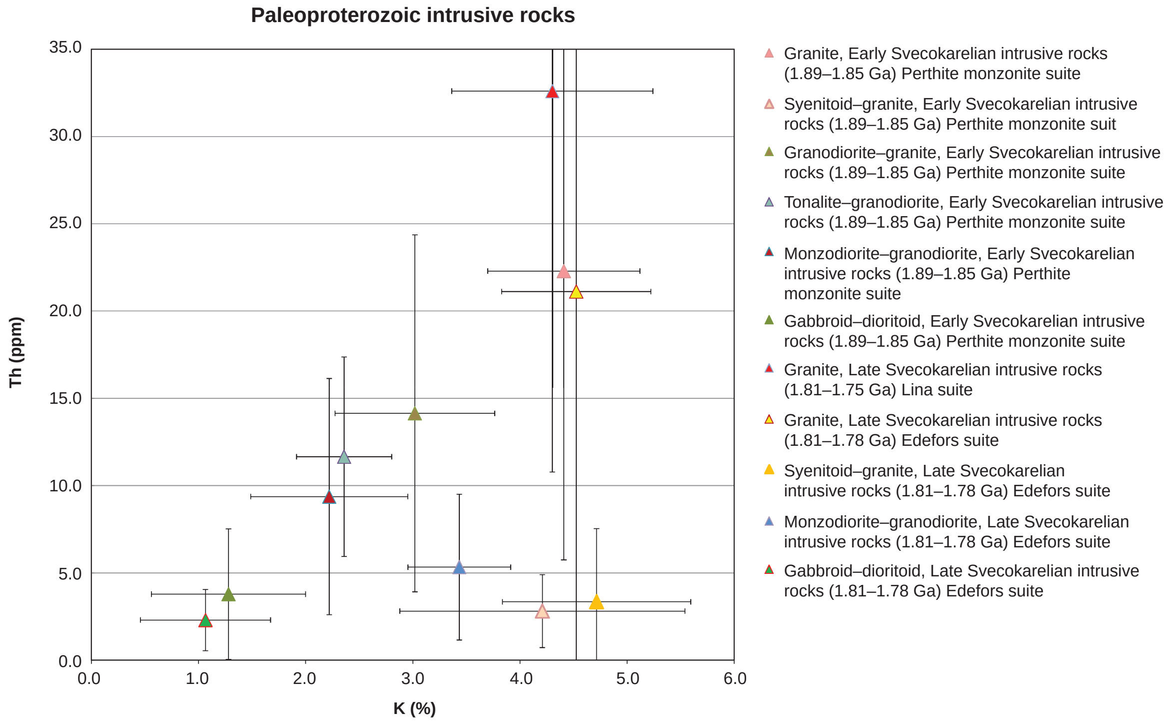

Figure 108. Thorium v. potassium for Palaeoproterozoic intrusive rocks.

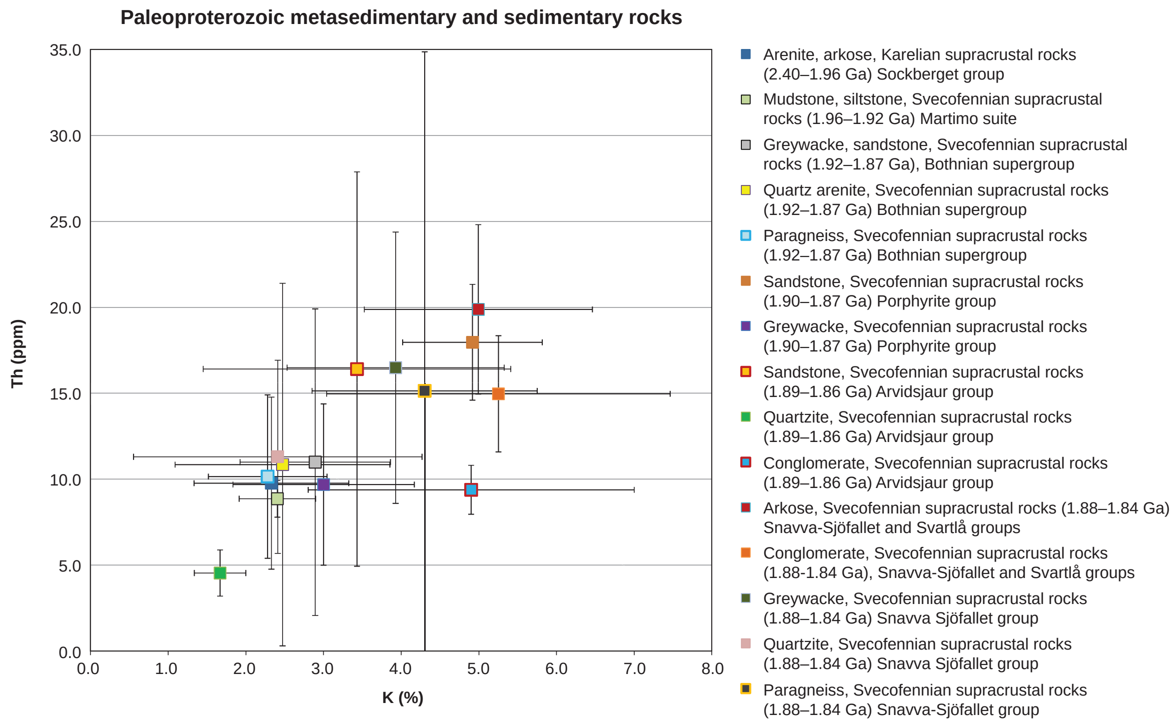

Figure 109. Thorium v. potassium for Palaeoproterozoic metasedimentary and sedimentary rocks.

Table 4. Statistics on petrophysical and gamma radiation (gamma ray) properties of the different rock units of the project area in southern Norrbotten County.

Geological unit	**Rock type**	**No. of samples**	**K (%)** mean/median	**K (%)** std. dev.	**(K%)** min/max	**U** (ppm) mean/median	**U** (ppm) std. dev.	**U** (ppm) min/max	**Th** (ppm) mean/median	**Th** (ppm) std. dev.	**Th** (ppm) min/max	**No. of samples**	**Density** mean (kg/m³)	**Density** std. dev. (kg/m³)	**Magnetic susceptibility** log mean (SI)	**Magnetic susceptibility** std. dev. [decades]	**No. of samples**	**Q value** median	**Q value** min/max
Svecokarelian Metamorphic rocks	Diatexitic migmatite	14	2.4/2.5	0.3	1.5/2.7	2.3/2.2	1.1	0.6/3.9	9.8/8.8	3.5	1.4/14.9	1	2722	NA.			1	0.3	
Svecokarelian Metamorphic rocks	Mafic granulit	16	2.2/2.2	0.5	1.4/3.1	2.9/2.5	2.0	0.8/9.5	9.7/10.2	5.0	2.9/18.4	15	2838	76	0.00057	0.095	9	0.2	0.04/0.43
Late Svecokarelian intrusive rocks (1.81–1.75 Ga) Lina suite	Pegmatite	391	3.9/3.9	1.2	0.3/7.8	26.3/14.0	62.7	0.2/972	33.4/25.4	28.7	1.0/191.0	594	2618	29	0.00172	0.907	484	0.27	0/77
Late Svecokarelian intrusive rocks (1.81–1.75 Ga) Lina suite	Granite*	1002	4.3/4.4	0.9	0/8.5	10.3/5.8	16.4	0/339.8	32.6/27.8	21.8	0.1/266.8	594	2618	29	0.00172	0.907	484	0.27	0/77
Late Svecokarelian intrusive rocks (1.81–1.75 Ga) Lina suite	Granodiorite-granite											36	2707	55	0.00592	0.926	28	0.28	0.05/1.7
Late Svecokarelian intrusive rocks (1.81–1.78 Ga) Edefors suite	Granite	922	4.5/4.6	0.7	0.6/6.7	5.5/3	8.8	0/138	21.1/12.4	22.1	0.2/142	602	2651	54	0.00625	0.851	536	0.31	0.03/48
Late Svecokarelian intrusive rocks (1.81–1.78 Ga) Edefors suite	Syenitoid-granite	145	4.7/4.8	0.9	2.1/7.5	3.4/1.8	4.2	0.1/26.8	3.4/1.8	4.2	0.1/26.8	111	2688	52	0.01473	0.620	102	0.41	0.02/11
Late Svecokarelian intrusive rocks (1.81–1.78 Ga) Edefors suite	Monzodiorite-granodiorite	52	3.4/3.4	0.5	2.4/4.8	2.7/2.2	1.8	0.2/8.4	5.3/3.6	4.2	1.2/15.7	17	2764	140	0.00443	0.948	10	0.27	0.15/0.84
Late Svecokarelian intrusive rocks (1.81–1.78 Ga) Edefors suite	Gabbroid-dioritoid	98	1.1/1	0.6	0/2.4	0.9/0.7	0.7	0/2.7	2.3/2	1.8	0/8.6	302	2955	147	0.01465	0.958	298	0.61	0.02/27
Late Svecokarelian intrusive rocks (1.81–1.78 Ga) Edefors suite	Ultrabasic intrusive rock											13	3243	133	0.02279	0.922	13	1.7	0.31/6.8
Late Svecokarelian intrusive rocks (1.81–1.78 Ga) Edefors suite	Dolerite	5	1.1/0.8	0.8	0.5/2.5	1.4/0.8	1.1	0.3/2.7	2.7/1.7	2.1	1/6	7	2922	44	0.00964	0.664	7	1.3	0.36/3
Late Svecokarelian supracrustal rocks (1.84–1.77 Ga)	Dacite-rhyolite	10	2/2	0.7	0.4/3.1	4.1/3.5	1.4	2.6/6.3	7.8/7.7	1.0	6.1/9.8	2	3100	260	0.38764	0.091	2	1.8	0.09/3.5

Table 4, continued.

Geological unit	**Rock type**	**No. of samples**	**K (%)** mean/ median	**K (%)** std. dev.	**(K%)** min/ max	**U** (ppm) mean/ median	**U** (ppm) std. dev.	**U** (ppm) min/ max	**Th** (ppm) mean/ median	**Th** (ppm) std. dev.	**Th** (ppm) min/ max	**No. of samples**	**Density** mean (kg/m^3)	**Density** std. dev. (kg/m^3)	**Magnetic susceptibility** log mean (SI)	**Magnetic susceptibility** std. dev. [decades]	**No. of samples**	**Q value** median	**Q value** min/ max
Late Svecokarelian supracrustal rocks (1.84–1.77 Ga)	Basalt-andesite											1	2867	NA.	NA.	NA.	1	6.7	NA.
Early Svecokarelian intrusive rocks (1.89–1.85 Ga) Perthite monzonite suite	Granite	2469	4.4/4.4	0.7	1/8.1	5.5/3.8	6.7	0/101.1	22.3/19	16.5	0.3/ 354.6	1298	2632	39	0.00453	0.779	1106	0.22	0.02/ 45
Early Svecokarelian intrusive rocks (1.89–1.85 Ga) Perthite monzonite suite	Syenitoid-granite	120	4.2/4.2	1.3	0/ 7.6	2.8/2.3	2.1	0.6/ 10.5	2.8/2.3	2.1	0.6/ 10.5	82	2724	119	0.01200	0.796	71	0.2	0.04/ 13
Early Svecokarelian intrusive rocks (1.89–1.85 Ga) Perthite monzonite suite	Granodiorite-granite	151	3/3.1	0.7	1/4.6	3.9/2.8	3.0	0.6/ 16.5	14.1/ 11.3	10.2	2.3/73.1	8	2662	37	0.00286	1.042	4	0.21	0.17/ 0.43
Early Svecokarelian intrusive rocks (1.89–1.85 Ga) Perthite monzonite suite	Tonalite-granodiorite	37	2.4/2.4	0.4	1.6/ 3.3	3.6/3.3	1.9	0.9/8.4	11.7/ 10.4	5.7	4.8/ 27.8	83	2706	56	0.00384	0.816	65	9.2	0.03/ 17
Early Svecokarelian intrusive rocks (1.89–1.85 Ga) Perthite monzonite suite	Monzodiorite-granodiorite	57	2.2/2.1	0.7	0.7/4	3.6/2.7	2.5	0.1/12.3	9.4/7.4	6.8	1.5/ 29.3	10	2775	85	0.00768	0.925	7	0.25	0.05/ 1.9
Early Svecokarelian intrusive rocks (1.89–1.85 Ga) Perthite monzonite suite	Gabbroid-dioritoid	99	1.3/1.2	0.7	0.2/ 3.3	1.4/1	1.5	0/8.8	3.8/2.7	3.7	0/20.1	376	2953	133	0.01086	1.019	357	0.34	0.03/ 31
Early Svecokarelian intrusive rocks (1.89–1.85 Ga) Perthite monzonite suite	Dolerite	8	1.7/1.4	0.6	1.2/ 2.4	1.3/1.2	0.6	0.4/2.3	3.7/3.8	0.6	2.5/4.6	84	2933	56	0.00930	0.845	81	0.33	0.03/ 5.1
Early Svecokarelian intrusive rocks (1.89–1.85 Ga) Perthite monzonite suite	Ultrabasic intrusive rock											3	3159	116	0.04192	1.301	3	0.68	0.24/ 0.9

Table 4, continued.

Geological unit	Rock type	No. of samples	K (%) mean/median	K (%) std. dev.	(K%) min/max	U (ppm) mean/median	U (ppm) std. dev.	U (ppm) min/max	Th (ppm) mean/median	Th (ppm) std. dev.	Th (ppm) min/max	No. of samples	Density mean (kg/m³)	Density std. dev. (kg/m³)	Magnetic susceptibility log mean (SI)	Magnetic susceptibility std. dev. [decades]	No. of samples	Q value median	Q value min/max
Svecofennian supracrustal rocks (1.88–1.84 Ga) Snavva–Sjöfallet and Svartlå groups	Skarn, calc silicate rock											4	3009	281	0.00123	0.615	4	0.26	0.03/0.59
Svecofennian supracrustal rocks (1.88–1.84 Ga) Snavva–Sjöfallet and Svartlå groups	Sandstone											124	2703	77	0.00036	0.667	120	25	0.07/423
Svecofennian supracrustal rocks (1.88–1.84 Ga) Snavva–Sjöfallet and Svartlå groups	Arkose	26	5.0/4.9	1.5	2.1/5.9	2.6/1.1	2.6	0.1/8.1	19.9/19.8	4.9	10.4/35.3	5	2646	39	0.00041	1.406	3	27	0.18/99
Svecofennian supracrustal rocks (1.88–1.84 Ga) Snavva–Sjöfallet and Svartlå groups	Conglomerate	18	5.3/4.5	2.2	3.1/9.1	3.4/3.7	1.5	0.8/6.4	15/14.3	3.4	8/22	4	2705	66	0.05970	0.389	4	0.3	0.15/11
Svecofennian supracrustal rocks (1.88–1.84 Ga) Snavva–Sjöfallet and Svartlå groups	Greywacke	163	3.9/4.1	1.4	0.7/7.3	3.0/2.7	1.6	0.2/7.1	16.5/16.7	7.9	1.5/52.8	9	2846	176	0.01084	1.572	6	0.68	0.1/132
Svecofennian supracrustal rocks (1.88–1.84 Ga) Snavva–Sjöfallet and Svartlå groups	Quartzite	21	2.4/1.8	1.9	0/7.2	1.9/1.6	1.2	0/4.7	11.3/10.4	5.6	2.8/22	18	2683	69	0.00021	0.879	14	2.7	0.2/46
Svecofennian supracrustal rocks (1.88–1.84 Ga) Snavva–Sjöfallet and Svartlå groups	Paragneiss	24	4.3/4.3	1.4	1.2/7.3	3/3	10.0	1.2/50.8	15.1/15.1	19.7	2.8/85.5	10	2730	73	0.00309	0.896	9	0.88	0.04/22
Svecofennian supracrustal rocks (1.88–1.84 Ga) Snavva–Sjöfallet and Svartlå groups	Rhyolite	31	4.5/4	1.4	1.3/7.4	6/4.9	4.7	2.3/26.1	17.5/17.2	8.6	5.8/44.8	6	2667	22	0.00068	1.210	5	10	0.25/68
Svecofennian supracrustal rocks (1.88–1.84 Ga) Snavva–Sjöfallet and Svartlå groups	Basalt-andesite	4	0.6/0.6	0.4	0.2/1	2.2/0.9	3.2	0.1/7	4.7/3.2	3.5	2.3/9.9	14	2908	119	0.00409	1.047	13	0.25	0.03/104

Table 4, continued.

Geological unit	**Rock type**	**No. of samples**	**K (%)** mean/ median	**K (%)** std. dev.	**(K%)** min/ max	**U** (ppm) mean/ median	**U** (ppm) std. dev.	**U** (ppm) min/ max	**Th** (ppm) mean/ median	**Th** (ppm) std. dev.	**Th** (ppm) min/ max	**No. of samples**	**Density** mean (kg/m³)	**Density** std. dev. (kg/m³)	**Magnetic susceptibility** log mean (SI)	**Magnetic susceptibility** std. dev. [decades]	**No. of samples**	**Q value** median	**Q value** min/ max
Svecofennian supracrustal rocks (1.89–1.86 Ga) Arvidsjaur group	Rhyolite	662	4.6/4.3	1.6	0.2/ 10.4	4.3/3.9	2.8	0/26.2	16/14.4	9.0	0.3/75.1	224	2647	49	0.00394	0.986	183	0.24	0.03/ 232
Svecofennian supracrustal rocks (1.89–1.86 Ga) Arvidsjaur group	Dacite-rhyolite	279	3.1/3.1	1.0	0.9/ 7.7	4/3.6	2.2	0.1/20.1	10.6/ 9.2	6.9	0.9/ 64.0	603	2686	67	0.00470	0.988	565	0.37	0.03/ 150
Svecofennian supracrustal rocks (1.89–1.86 Ga) Arvidsjaur group	Trachytoid-rhyolite											5	2724	103	0.04007	0.825	5	0.2	0.08/ 2.4
Svecofennian supracrustal rocks (1.89–1.86 Ga) Arvidsjaur group	Basalt-andesite, trachy-basalt	315	1.7/1.7	0.8	0.1/4	2/1.7	1.3	0/9	4.6/4	3.0	0/15.3	528	2866	107	0.01245	0.967	488	0.35	0.03/ 217
Svecofennian supracrustal rocks (1.89–1.86 Ga) Arvidsjaur group	Sandstone	27	3.4/3.1	2.0	0.3/ 10.8	4.4/3.7	4.0	1.8/22.6	16.4/ 15.2	11.5	3.9/61	10	2709	52	0.00861	1.047	8	0.47	0.06/ 1.8
Svecofennian supracrustal rocks (1.89–1.86 Ga) Arvidsjaur group	Quartzite	9	1.7/1.6	0.3	1.2/5	0.4/0.5	0.3	0/0.8	4.5/4.5	1.3	3/16.5	18	2687	113	0.00042	1.256	11	1.1	0.15/ 83
Svecofennian supracrustal rocks (1.89–1.86 Ga) Arvidsjaur group	Greywacke											2	2735	52	0.00260	1.440	2	0.1	0.09/ 0.12
Svecofennian supracrustal rocks (1.89–1.86 Ga) Arvidsjaur group	Argillite, siltstone etc.											46	2770	111	0.00350	1.041	45	0.4	0.07/ 367
Svecofennian supracrustal rocks (1.89–1.86 Ga) Arvidsjaur group	Gneiss, paragneiss											11	2732	75	0.01092	0.995	10	0.71	0.04/ 31
Svecofennian supracrustal rocks (1.89–1.86 Ga) Arvidsjaur group	Conglomerate	10	4.9/4.8	2.1	2.0/ 8.3	2.5/2.3	0.9	1.5/3.8	9.4/9.5	1.4	7.4/11.3	12	2727	79	0.00643	0.812	12	1.5	0.1/ 127
Early Svecokarelian intrusive rocks (1.91–1.87 Ga) Haparanda and Jörn GI suites	Granite	448	3.7/3.8	1.1	0.8/ 6.5	4.4/3.1	4.5	0/32.9	15.8/ 13.5	11.3	0.7/69.3	391	2648	47	0.00319	0.837	334	0.25	0.04/ 28

Table 4, continued.

Geological unit	Rock type	No. of samples	K (%) mean/ median	K (%) std. dev.	(K%) min/ max	U (ppm) mean/ median	U (ppm) std. dev.	U (ppm) min/ max	Th (ppm) mean/ median	Th (ppm) std. dev.	Th (ppm) min/ max	No. of samples	Density mean (kg/m^3)	Density std. dev. (kg/m^3)	Magnetic susceptibility log mean (SI)	Magnetic susceptibility std. dev. [decades]	No. of samples	Q value median	Q value min/ max
Early Svecokarelian intrusive rocks (1.91–1.87 Ga) Haparanda and Jörn GI suites	Syenitoid-granite	34	3.3/3.2	0.8	1.7/ 5.1	2.3/2.4	1.1	0.6/5.3	8.5/8.6	4.1	1/2.9	38	2725	88	0.00689	0.916	34	0.19	0.03/ 32
Early Svecokarelian intrusive rocks (1.91–1.87 Ga) Haparanda and Jörn GI suites	Granodiorite-granite	695	2.8/2.8	0.8	1/ 8.7	3.2/2.9	2.1	0/21.4	9.7/8.9	5.5	0.4/ 76.2	29	2669	55	0.00359	0.756	15	0.27	0.06/ 15
Early Svecokarelian intrusive rocks (1.91–1.87 Ga) Haparanda and Jörn GI suites	Tonalite-granodiorite	324	2/2	0.7	0.1/ 6.1	2.2/1.9	1.6	0/11	6/5.4	3.8	0/24.1	394	2723	54	0.00508	0.801	296	0.23	0.02/ 35
Early Svecokarelian intrusive rocks (1.91–1.87 Ga) Haparanda and Jörn GI suites	Monzodiorite-granodiorite	180	2.2/2.2	0.6	0.3/ 3.7	1.8/1.7	1.3	0/7.5	6.4/5.8	4.5	0.1/34.7	25	2809	54	0.01267	0.650	24	0.68	0.06/ 9.1
Early Svecokarelian intrusive rocks (1.91–1.87 Ga) Haparanda and Jörn GI suites	Gabbroid-dioritoid	222	1.5/1.4	0.7	0.1/ 3.6	1.2/0.9	2.1	0/29	3.9/3	3.5	0/20.2	925	2870	101	0.00871	0.829	893	0.53	0.01/ 302
Early Svecokarelian intrusive rocks (1.91–1.87 Ga) Haparanda and Jörn GI suites	Dolerite	16	1.2/1	0.6	0.4/ 2.5	0.9/0.7	0.6	0.3/1.9	2.1/1.5	1.5	0.8/5.8								
Early Svecokarelian intrusive rocks (1.91–1.87 Ga) Haparanda and Jörn GI suites	Ultrabasic intrusive rock											22	3034	193	0.02017	0.845	21	1.3	0.35/ 6.1
Svecofennian supracrustal rocks (1.90–1.87 Ga) Porphyrite group	Sandstone	32	4.9/4.8	0.9	3.7/ 6.7	12.7/ 4.4	45.8	1.7/ 263.5	18/17.1	3.4	13.4/ 29.1	30	2665	66	0.00360	0.987	24	0.21	0.09/ 32
Svecofennian supracrustal rocks (1.90–1.87 Ga) Porphyrite group	Greywacke	12	3/2.6	1.2	1.8/ 5.4	3.6/3.5	1	2.4/6.2	9.7/9.1	4.7	3.7/19.6	30	2665	66	0.00360	0.987	24	0.21	0.09/ 32
Svecofennian supracrustal rocks (1.90–1.87 Ga) Porphyrite group	Rhyolite	142	4.6/4.4	0.9	2.7/ 7.9	3.9/3.1	3.0	0.6/18	15.9/ 14.7	8.3	2.9/53.1		2643	46	0.00626	0.860	36	0.34	0.07/ 27

Table 4, continued.

Geological unit	**Rock type**	**No. of samples**	**K (%)** mean/ median	**K (%)** std. dev.	**(K%)** min/ max	**U** (ppm) mean/ median	**U** (ppm) std. dev.	**U** (ppm) min/ max	**Th** (ppm) mean/ median	**Th** (ppm) std. dev.	**Th** (ppm) min/ max	**No. of samples**	**Density** mean (kg/m³)	**Density** std. dev. (kg/m³)	**Magnetic susceptibility** log mean (SI)	**Magnetic susceptibility** std. dev. [decades]	**No. of samples**	**Q value** median	**Q value** min/ max
Svecofennian supracrustal rocks (1.90–1.87 Ga) Porphyrite group	Dacite-rhyolite	120	2.9/2.9	0.8	1.2/ 5.3	2.9/2.5	1.8	0.3/12.6	9.3/7.5	6.5	1.4/33.2	107	2687	67	0.00668	0.962	94	0.27	0.02/ 22
Svecofennian supracrustal rocks (1.90–1.87 Ga) Porphyrite group	Basalt-andesit	107	1.9/1.9	0.7	0.3/ 3.3	2/1.7	1.4	0/9.3	5.5/4.3	4.2	0.2/4.9	76	2832	107	0.01279	0.809	71	0.28	0.04/ 1313
Svecofennian supracrustal rocks (1.90–1.87 Ga) Porphyrite group	Trachytoid-rhyolite	6	4.9/4.8	0.2	4.6/ 5.2	4.1/4.5	1.0	2.8/5.2	14.2/ 14.1	0.8	13.3/ 15.2	4	2720	139	0.00341	0.582	3	0.14	0.04/ 0.34
Svecofennian supracrustal rocks (1.92–1.87 Ga) Bothnian supergroup	Greywacke, sandstone	72	2.9/2.7	1.0	1.2/ 6.6	2.7/2.3	1.4	1/8.5	11/9.3	8.9	4.8/ 70.3	67	2754	58	0.00049	0.548	53	0.18	0.04/ 329
Svecofennian supracrustal rocks (1.92–1.87 Ga) Bothnian supergroup	Paragneiss	33	2.3/2.3	0.8	0.7/ 3.8	2.4/2.2	1.1	0.8/6.6	10.2/ 11.7	4.8	2.2/25.1	100	2755	81	0.00135	0.872	60	0.26	0.03/ 9.3
Svecofennian supracrustal rocks (1.92–1.87 Ga) Bothnian supergroup	Quartz arenite	24	2.5/2	1.4	1.0/ 4.9	2.2/1.4	2.6	0.1/12.3	10.9/7	10.5	1.6/53.4	14	2704	116	0.00099	1.109	12	0.31	0.08/ 1.1
Svecofennian supracrustal rocks (1.92–1.87 Ga) Bothnian supergroup	Marble	5	0.2/0.3	0.1	0.1/ 0.3	0.5/0.5	0.4	0/1	0.5/0.7	0.3	0/0.8	1	2597	NA.	NA.	NA.	0	NA.	NA.
Svecofennian supracrustal rocks (1.92–1.87 Ga) Bothnian supergroup	Mudstone											40	2842	209	0.00064	0.278	40	0.11	0.03/ 2.1
Svecofennian supracrustal rocks (1.92–1.87 Ga) Bothnian supergroup	Dacite-rhyolite	17	3.3/3.1	1.3	1.1/ 5.4	3.2/2.7	1.3	1.7/5.6	9.6/7.5	5.6	3.7/17.6	10	2677	46	0.00072	1.025	10	0.73	0.07/ 27
Svecofennian supracrustal rocks (1.92–1.87 Ga) Bothnian supergroup	Basalt-andesite	17	1.6/0.6	0.6	0.5/ 2.3	2.2/1.4	1.4	0.8/4.6	4/2.8	2.8	0.4/8.4	29	2860	106	0.00326	0.989	28	0.29	0.06/ 12

Table 4, continued.

Geological unit	Rock type	No. of samples	K (%) mean/median	K (%) std. dev.	(K%) min/max	U (ppm) mean/median	U (ppm) std. dev.	U (ppm) min/max	Th (ppm) mean/median	Th (ppm) std. dev.	Th (ppm) min/max	No. of samples	Density mean (kg/m³)	Density std. dev. (kg/m³)	Magnetic susceptibility log mean (SI)	Magnetic susceptibility std. dev. [decades]	No. of samples	Q value median	Q value min/max
Early Svecokarelian intrusive rocks (1.96–1.92 Ga) Norvijaur intrusion	Granodiorite-granite											3	2693	53	0.00276	1.047	3	0.28	0.15/0.45
Early Svecokarelian intrusive rocks (1.96–1.92 Ga) Norvijaur intrusion	Tonalite-granodiorite	16	2.1/2	0.5	1.4/3.2	2/1.8	0.8	0.7/3.5	7.4/7.2	2.0	4.4/11	47	2712	53	0.00900	0.575	46	0.16	0.02/3.3
Early Svecokarelian intrusive rocks (1.96–1.92 Ga) Norvijaur intrusion	Gabbroid-dioritoid											4	2915	54	0.00066	0.081	4	0.13	0.06/0.34
Svecofennian supracrustal rocks (1.96–1.92 Ga) Martimo suite	Mudstone	22	2.4/2.4	0.5	1.3/3.1	1.9/1.9	0.4	0.9/2.6	8.9/8.7	1.1	7.1/11.3	41	2808	44	0.00375	0.981	40	0.19	0.03/112
Svecofennian supracrustal rocks (1.96–1.92 Ga) Martimo suite	Dacite											1	2710	NA.	NA.	NA.	NA.	NA.	NA.
Karelian supracrustal rocks (2.40–1.96 Ga) Sockberget group	Quartzite (quartz arenite?)	24	1.4/1.4	0.8	0.1/3.0	0.8/0.7	0.9	0/4	4.6/4.3	2.4	1.8/11.5	190	2727	99	0.00076	1.008	180	0.34	0.01/40
Karelian supracrustal rocks (2.40–1.96 Ga) Sockberget group	Arenite, arkose	48	2.3/2.5	1.0	0.6/4.3	1.3/1.1	1.1	0/3.9	9.8/8.5	5	2.3/25.8	190	2727	99	0.00076	1.008	180	0.34	0.01/40
Karelian supracrustal rocks (2.40–1.96 Ga) Kalix group	Limestone-dolomite	3	0.7/0.7	0.2	0.6/0.9	0.1/0.1	0.2	0.6/0.9	0.9/0.8	0.4	0.6/0.9	1	2924	NA.	NA.	NA.	1	2.4	NA.
Karelian supracrustal rocks (2.40–1.96 Ga) Kalix group	Quartz-arenite	6	2.5/2.6	0.3	2.0/2.9	1.9/1.6	0.8	2/2.9	9.3/8.8	1.2	2/2.9	1	2737	NA.	NA.	NA.	1	0.22	NA.
Karelian supracrustal rocks (2.40–1.96 Ga) Kalix group	Basalt-andesite	12	0.4/0.4	0.3	0.1/0.6	0.3/0.2	0.3	0.1/0.9	0.9/0.8	0.7	0.1/2.1	13	2954	53	0.00551	0.973	11	0.23	0.06/10
Karelian intrusive rocks (2.40–1.96 Ga) Kalix group	Gabbroid-dioritoid	12	0.7/0.5	0.5	0.3/1.6	0.2/0	0.2	0/0.6	1.9/1.9	0.8	0.6/3.1	12	2956	115	0.03179	0.638	11	0.36	0.06/0.85

Table 4, continued.

Geological unit	**Rock type**	**No. of samples**	**K (%)** mean/ median	**K (%)** std. dev.	**(K%)** min/ max	**U** (ppm) mean/ median	**U** (ppm) std. dev.	**U** (ppm) min/ max	**Th** (ppm) mean/ median	**Th** (ppm) std. dev.	**Th** (ppm) min/ max	**No. of samples**	**Density** mean (kg/m³)	**Density** std. dev. (kg/m³)	**Magnetic susceptibility** log mean (SI)	**Magnetic susceptibility** std. dev. [decades]	**No. of samples**	**Q value** median	**Q value** min/ max
Karelian intrusive rocks (2.40–1.96 Ga) Kalix group	Amphibolite	16	0.9/0.5	1.1	0/ 2.9	0.1/0	0.3	0/2.9	2.4/1	3.2	0/2.9								
Supracrustal rocks (2.50–2.40 Ga)	Basalt-andesite	9	0.4/0.3	0.2	0.1/ 0.8	0/0	0.0	0.1/0.8	1.9/0.8	2.0	0.1/0.8	3	2933	113	0.01164	0.835	3	6	0.24/ 9.4
Archean rocks (>2.50 Ga)	Granite	20	3.7/3.4	0.8	2.8/ 4.9	2.2/1.6	2.2	0/7.2	19.6/ 19.6	12.1	2.0/ 42.8	3	2620	74	0.00512	1.032	3	0.56	0.22/ 0.64
Archean rocks (>2.50 Ga)	Tonalitic-grano-dioritic gneiss	51	2/1.8	0.8	0.8/ 3.6	0.9/ 0.4	1.1	0/5.9	10/6.8	9.5	0.1/38.8	28	2775	113	0.01463	0.713	28	0.28	0.07/ 0.92
Archean rocks (>2.50 Ga)	Granitic gneiss											9	2661	40	0.00851	0.566	7	0.14	0.09/ 0.15
Archean rocks (>2.50 Ga)	Gabbroid-dioritoid	6	0.7/0.7	0.6	0/1.5	0.4/ 0.3	0.4	0/0.9	0.9/0.8	0.9	0/2.2	4	3039	157	0.00314	0.852	4	0.25	0.16/ 6.4
Archean rocks (>2.50 Ga)	Amphibolite	10	0.9/0.8	0.5	0.3/ 1.8	0.2/0.1	0.3	0/0.9	1.4/1.4	1.0	0.3/2.8	8	2920	100	0.00438	0.803	7	0.31	0.04/ 3.4
Archean rocks (>2.50 Ga)	Tonalitic-grano-dioritic gneiss											13	2702	42	0.00303	0.989	11	0.51	0.1/3.8

* Granites and pegmatites in the Lina suite are shown as separate rock types due to their different gamma ray properties

6. Structure and metamorphism

Stefan Bergman, Ildikó Antal Lundin, Carl-Axel Triumf & Dick Claeson

INTRODUCTION

The bedrock in the area has experienced several events of deformation and metamorphism during Neoarchaean to Palaeoproterozoic times. These regional events were followed by multiple phases of more local brittle deformation during a wide time span from the Statherian to late to postglacial times in the Quaternary. General structural information can be found in the descriptions accompanying the SGU 1:50 000 bedrock maps and in other publications (Ödman 1957, Witschard 1984), but detailed studies and regional structural analyses are still lacking. For the adjacent areas, however, regional structural frameworks have been provided by more recent studies, i.e. in northern Norrbotten County (Bergman et al. 2001, Grigull et al. 2018, Luth et al. 2018a, b), the Skellefte district to the south (Kathol & Weihed 2005, Skyttä et al. 2012), Finnish Lapland to the east (Ward et al. 1989, Hölttä et al. 2007, Lahtinen et al. 2015b) and in northern Norway (Bergh et al. 2010, Angvik 2014, Henderson et al. 2015).

DUCTILE STRUCTURES

Structural trends and fabric orientations

During reconnaissance work before the acquisition of airborne geophysical data, Ödman (1957) recognised locally preserved, older fabrics with an easterly trend overprinted by younger, regionally distributed fabrics with a northerly trend. Witschard (1984) also considered that the general structural pattern, with 'blocks' enveloped by long, narrow belts, was established as long ago as during rifting of the Archaean basement, when rift valleys were successively infilled by sediment and volcanic material. These structures were subsequently modified during the Svecokarelian orogeny into a mosaic of somewhat rounded nuclei enveloped by heterogeneous 'mobile zones'.

The structural trends from generalised form lines of tectonic foliation and magnetic connections are shown in Figure 110, together with the major deformation zones. These are the Karesuando–Arjeplog deformation zone (KADZ), Nautanen deformation zone (NDZ), Pajala deformation belt (PDB), Vidsel–Röjnoret shear system (VRSS) and Karsbergsfallet deformation zone (KDZ), and are described in more detail in the section *Ductile shear zones*. The general form line pattern shows a predominance of northeast trends in the western part and north-northwest to north in the eastern part. In the easternmost and westernmost parts of the project area in particular, the form lines resemble patterns of tectonic foliation associated with major ductile shear zones (PDB and KADZ, respectively, Fig. 110). Adjacent to other deformation zones, form lines often curve into near parallelism with the zone. Away

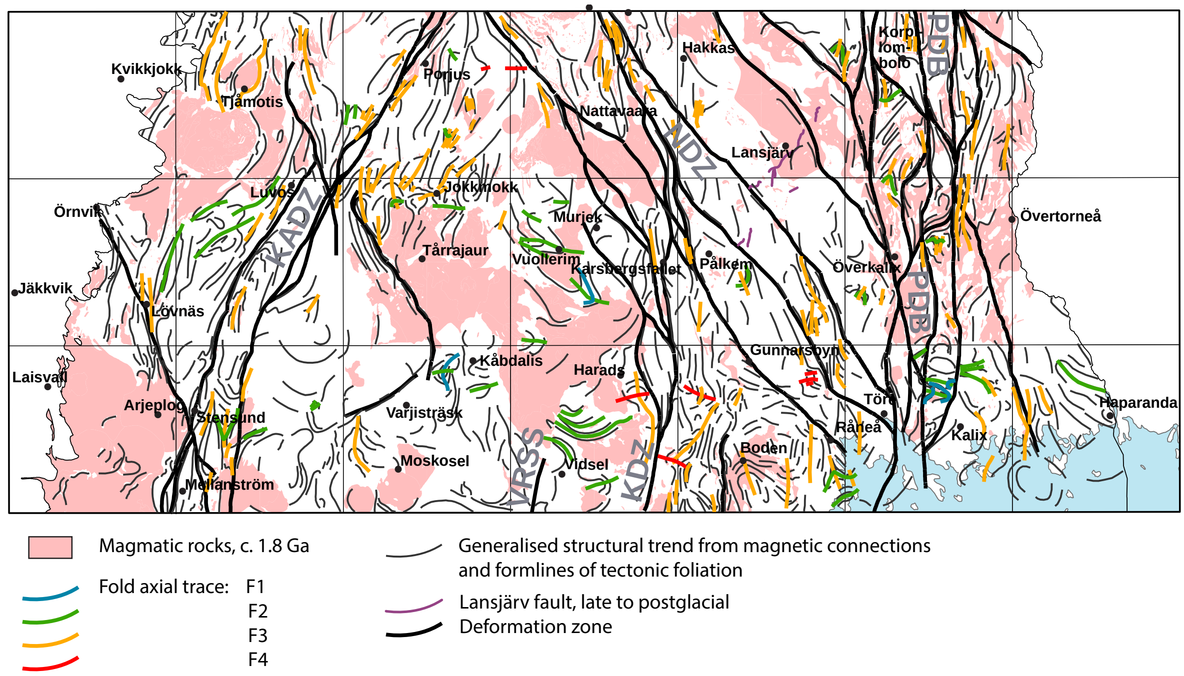

Figure 110. Generalised structural trends displayed by form lines of tectonic foliation as well as magnetic connections that are interpreted to represent tectonic foliation and the main ductile shear zones. Fold axial traces are indicated with thick lines whose colour denotes their relative age. KADZ = Karesuando–Arjeplog deformation zone, NDZ = Nautanen deformation zone, PDB = Pajala deformation belt, VRSS = Vidsel–Röjnoret shear system, KDZ = Karsbergsfallet deformation zone.

from the deformation zones the form lines display major fold structures, sigmoidal shapes, ellipsoidal shapes or irregular patterns. In general, these patterns are more likely to record earlier parts of the structural evolution that are obscured in other places by younger deformation zones.

Apart from the general form line pattern, smaller domains can be defined where the structural pattern is more homogeneous. Figure 111 shows the boundaries of six domains, together with locations of structural measurements. When defining the location of domain boundaries, the major shear zones were important, and a compromise between the number of domains and structural homogeneity was made. Stereograms showing fabric orientations for each domain are presented in Figure 111. A total of 13 920 structural measurements from 11 324 field localities are plotted on the stereograms. Different generations of fabrics are not distinguished; the diagrams illustrate the main trends and amount of variation in each domain.

In the Arjeplog–Tjåmotis domain, there is a fairly homogeneous north-northeast form line trend, parallel to the deformation zone in the east, and several tight to isoclinals fold closures are present. The stereogram shows that most foliations have steep dips, with a slight predominance towards the east. Together with moderately dipping foliations, they display a girdle on the contoured stereogram with a π-axis close to the maximum concentration of lineations and fold axes, which plunge gently to moderately towards the southwest. Folds in the north of this domain are addressed in a later section.

In the narrow Karesuando–Arjeplog deformation zone domain, the form lines show tight folds between the two main branches of the zone. The fold limbs are more or less parallel to the zones. Foliations are tightly concentrated to a north–northeast strike with a predominant steep dip to the east. There are possibly two maximum concentrations of lineations, one steep and one moderately plunging, both with a south–southwest trend. Fold axes show a similar pattern.

The Jokkmokk domain displays north–northeast-trending form lines in the north, similar to the Arjeplog–Tjåmotis domain, and more variable patterns further south. Like the domains to the west, the foliations tend to dip steeply and predominantly towards the east. The contoured poles to foliation

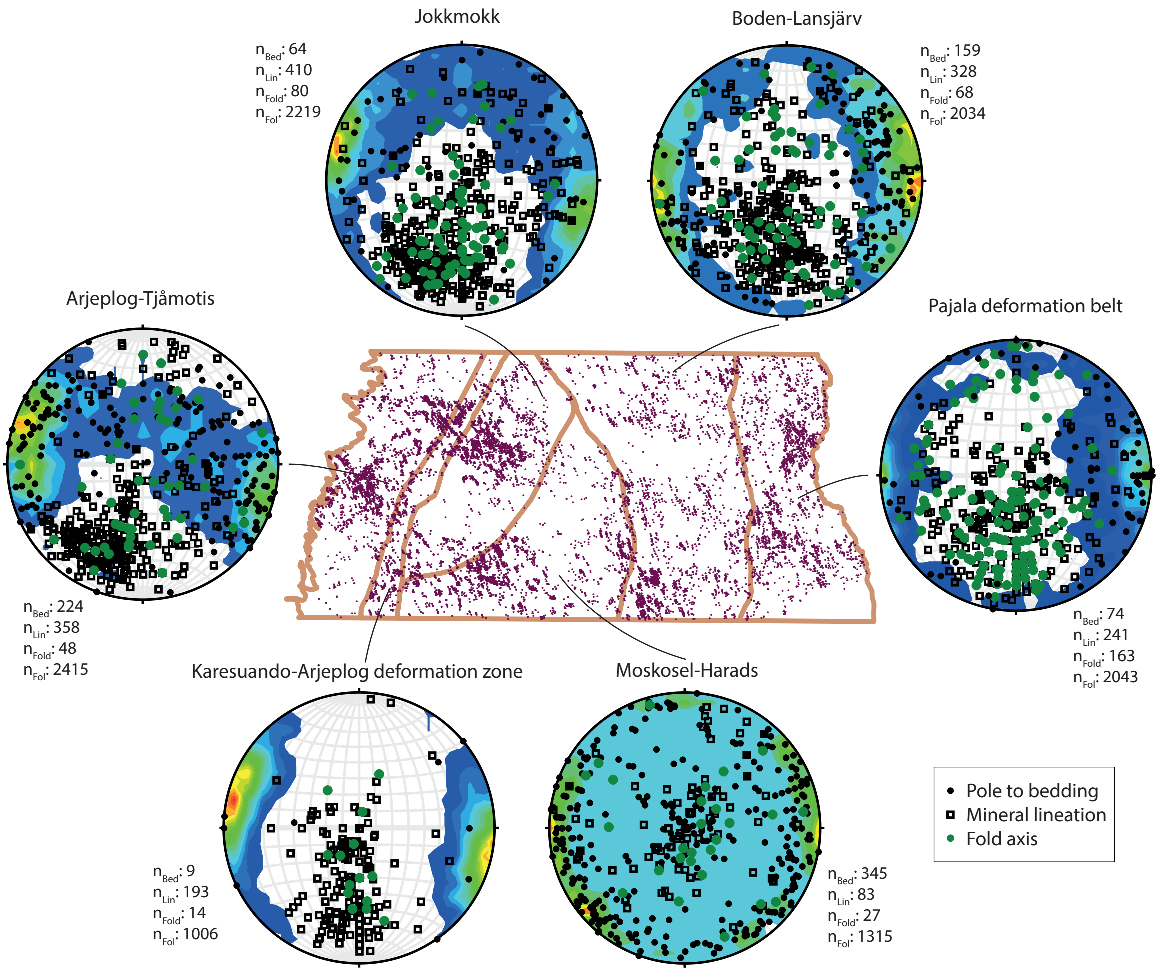

Figure 111. Equal area stereographic plots (lower hemisphere) of field measurements of planar and linear structures from the structural domains. The contours represent poles to foliation. The structural domains and locations of the structural measurements are shown on the map. The number of measurements are indicated by the following abbreviations: Bed = bedding, Lin = mineral lineation, Fold = fold axis, Fol = foliation.

apparently show a girdle with a steep to moderately south–southwest-plunging π-axis. The lineations and fold axes show a broad distribution from steep to roughly southwest plunges.

Distribution of foliation orientations in the Moskosel–Harads domain is highly heterogeneous, which is at least partly due to a complex deformation history. The preserved early folds in this domain are addressed in the section *Major fold structures*. The stereogram shows concentrations of steep and gently plunging fold axes, but very few moderate plunges.

In the Boden–Lansjärv domain, foliations generally strike north to north-northwest in the northern and central part, whereas the southern part is characterised by variable strikes. The contoured poles to foliation show a steeply west-dipping maximum, in contrast to the structural domains in the west, where easterly dips predominate. Lineations and fold axes generally plunge moderately to the south, but there is a large scatter in the orientations. A penetrative, steep northeast-striking foliation, was reported by Talbot et al. (1989) and Talbot (2001). This foliation is axial planar to kilometre-scale upright folds and is associated with subvertical lineation.

The easternmost domain, which includes the Pajala deformation belt, is characterised by a network of deformation zones, in which foliations mostly strike to the north, and lenses between the zones, with variable patterns and foliation orientations. Lineations and fold axes have a wide variety of orientations, but most plunges are between southwest and southeast.

Major fold structures

In a regional study of southern Norrbotten County and areas to the south, Grip (1946) found two major fold orientations: an older one with a west–northwest orientation (*Skelleftefältsveckningen*) and a younger one oriented approximately north–south (*karelska veckningen*), predominating to the north. This general pattern of Grip (1946) is still valid, although much more detail has been revealed by recent bedrock mapping and geophysical campaigns.

The patterns of structural trends reveal a large number of folds with wavelengths up to several tens of kilometres. Axial traces of folded structural trends are outlined in Figure 110. Where curved axial traces indicate refolded folds, the younger fold axial trace is also outlined. Based on these overprinting patterns, four generations of folds are distinguished with different colours. The earliest folds (F_1 and F_2) are mainly preserved in the south-central part of the project area, where only minor younger overprinting occurred. They are also found in lenses between deformation zones within the PDB. Folds with axial trace orientations that are close to the orientation of adjacent ductile shear zones have provisionally been assigned to the third folding phase (F_3), and F_4-folds have locally been identified where D_3 structures are folded. It must be emphasised that folds have been assigned to different generations purely using orientation and overprinting relationships, and the folds need not necessarily be coeval in different parts of the area.

F_1 and F_2 folds

The earliest folds are preserved in the south-central part of the project area. The F_1 fold axial traces have a wide variation in orientations due to later folding. Near Moskosel, a cleavage that cross-cuts bedding is interpreted as S_1 (Fig. 112a). To the northeast, a foliation assigned to S_1 is folded by F_2 folds (Fig. 112b). Axial traces of F_2 folds have fairly consistent east to east-northeast orientations in the Kåbdalis–Vidsel area, and orientations close to west-northwest further north.

Southwest of Harads, the magnetic anomaly pattern shows that F_2 fold axial traces undulate between west-northwest and east-northeast, probably due to a later folding event. The magnetic banding is intersected

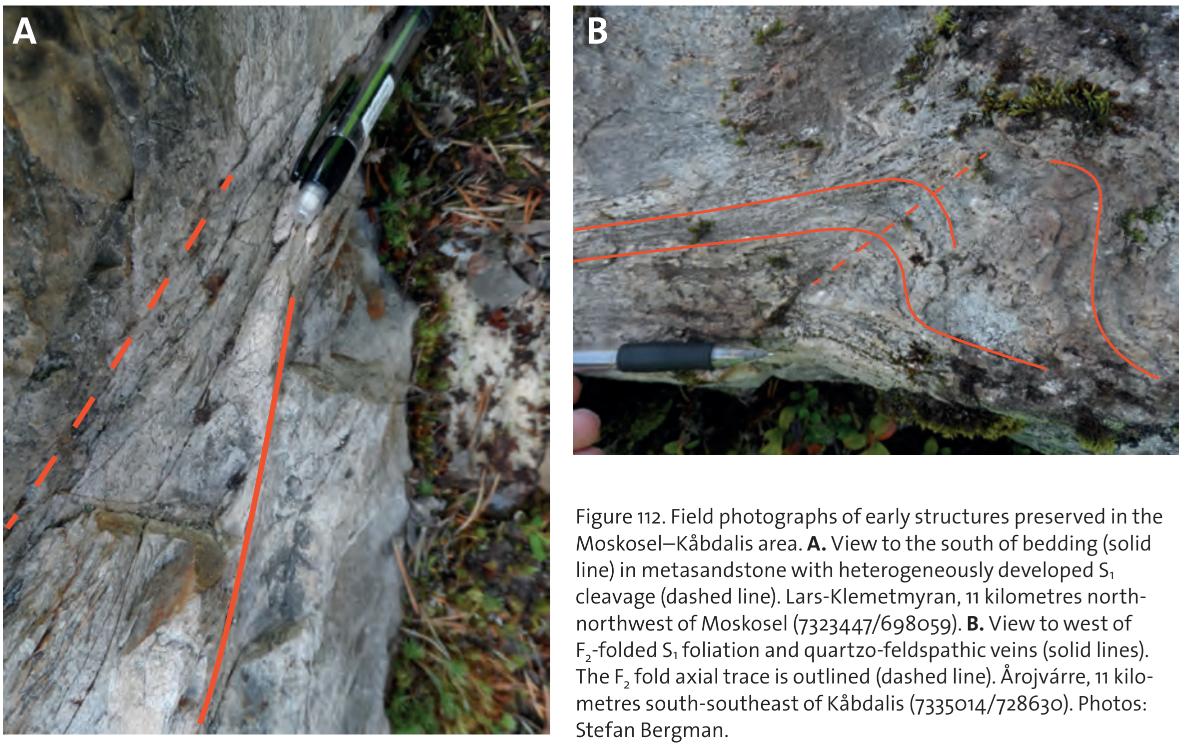

Figure 112. Field photographs of early structures preserved in the Moskosel–Kåbdalis area. **A.** View to the south of bedding (solid line) in metasandstone with heterogeneously developed S_1 cleavage (dashed line). Lars-Klemetmyran, 11 kilometres north-northwest of Moskosel (7323447/698059). **B.** View to west of F_2-folded S_1 foliation and quartzo-feldspathic veins (solid lines). The F_2 fold axial trace is outlined (dashed line). Årojvárre, 11 kilometres south-southeast of Kåbdalis (7335014/728630). Photos: Stefan Bergman.

by several deformation zones. A 3D susceptibility model (Fig. 113) was constructed from airborne measurements of the magnetic field of an area of 480 km^2 to constrain the geometry of the early folds. The model shows that the major F_2 folds have gently plunging fold axes and steeply northward-dipping axial planes.

Measured orientations of bedding in the metavolcanic and metasedimentary rocks are plotted in Figure 114. The π-axis has a nearly horizontal plunge to the west, which is consistent with the 3D model in Figure 113.

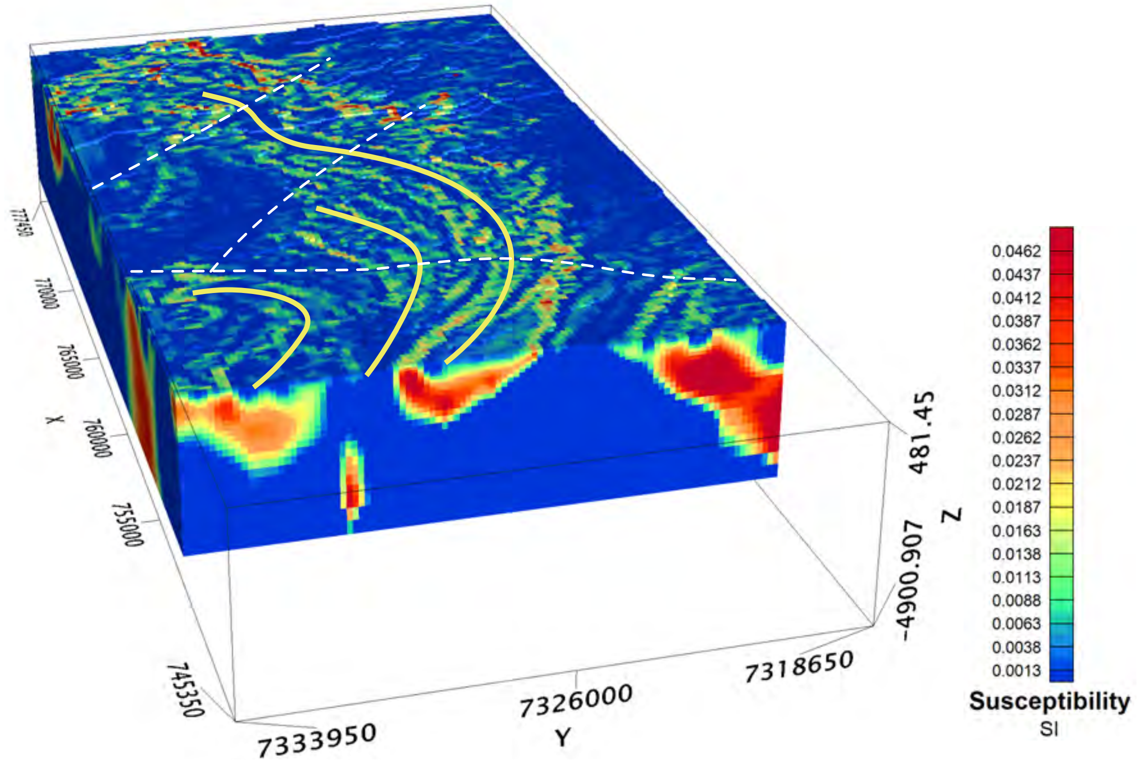

Figure 113. 3D susceptibility model from airborne measurements of the magnetic anomaly field southwest of Harads. The cell size was set to 150 metres in the horizontal directions and 75 metres in the vertical direction. The area of the model is 32 x 15 kilometres. Yellow lines are axial surface traces of F_2 folds and broken white lines are deformation zones. View looking down to the east-southeast. The location of the model is shown in Figure 16.

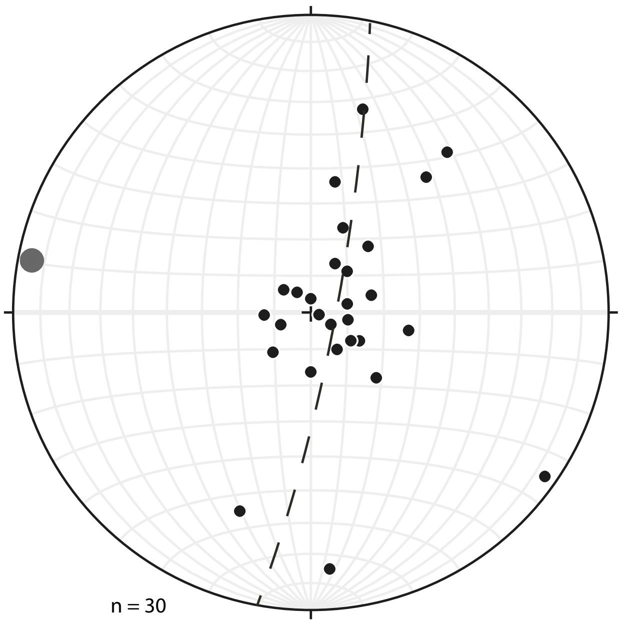

Figure 114. Equal area stereographic plots (lower hemisphere) of poles to bedding in the metavolcanic and metasedimentary rocks in the area southwest of Harads. The broken line is the best fit great circle, and the grey dot is the π-axis. The latter and the fold axis in the 3D model (Figure 113) have similar orientations.

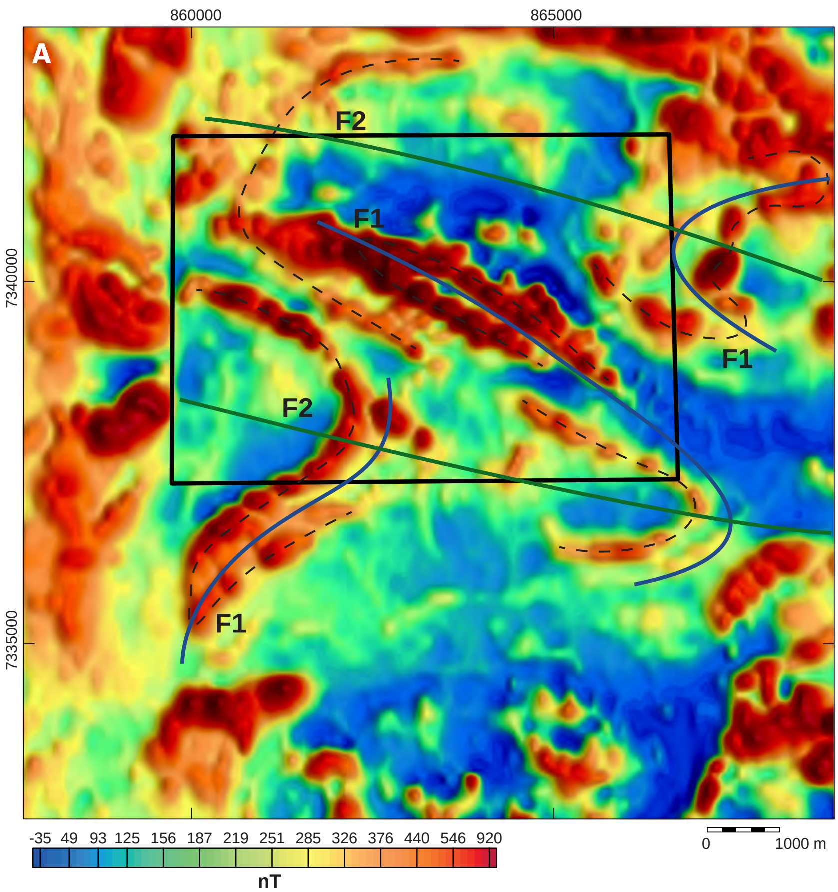

Figure 115. **A.** Fold interference pattern northwest of Kalix interpreted from magnetic anomaly data. Broken black lines are magnetic maxima representing different lithologies within a metasandstone unit, mafic bands within that unit and contacts with felsic meta-intrusive rocks. Blue lines are interpreted F_1 fold axial traces and green lines F_2 axial traces.

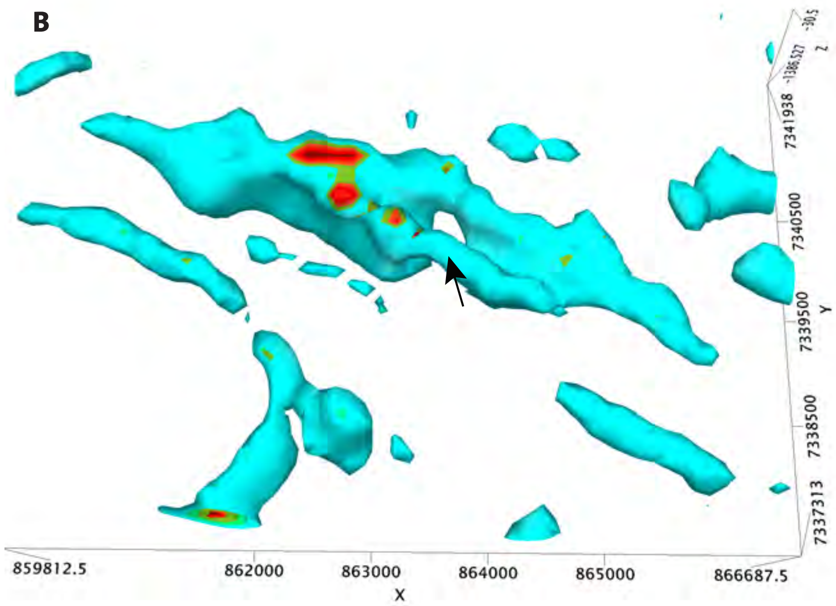

Figure 115. **B.** Susceptibility model of the gently plunging, isoclinal F_1 synform (black arrow) in the central part of A, presented as a susceptibility isosurface of 0.03 SI. View looking down towards the northwest. The cell size was set at 125 metres in the horizontal directions and 75 metres in the vertical direction. The location of the model is shown with the black square in Figure 115a, and in Figure 16.

Fold interference patterns in which isoclinals folds are refolded by folds with approximately east–west axial traces occur in an 8 km wide low-strain lens between two north–south-striking deformation zones in the PDB at Stor-Lappträsket, 15 km northwest of Kalix, in the far southeast of the project area, (Fig. 115a). Based on the similar orientations and geometric relations, these folds are correlated

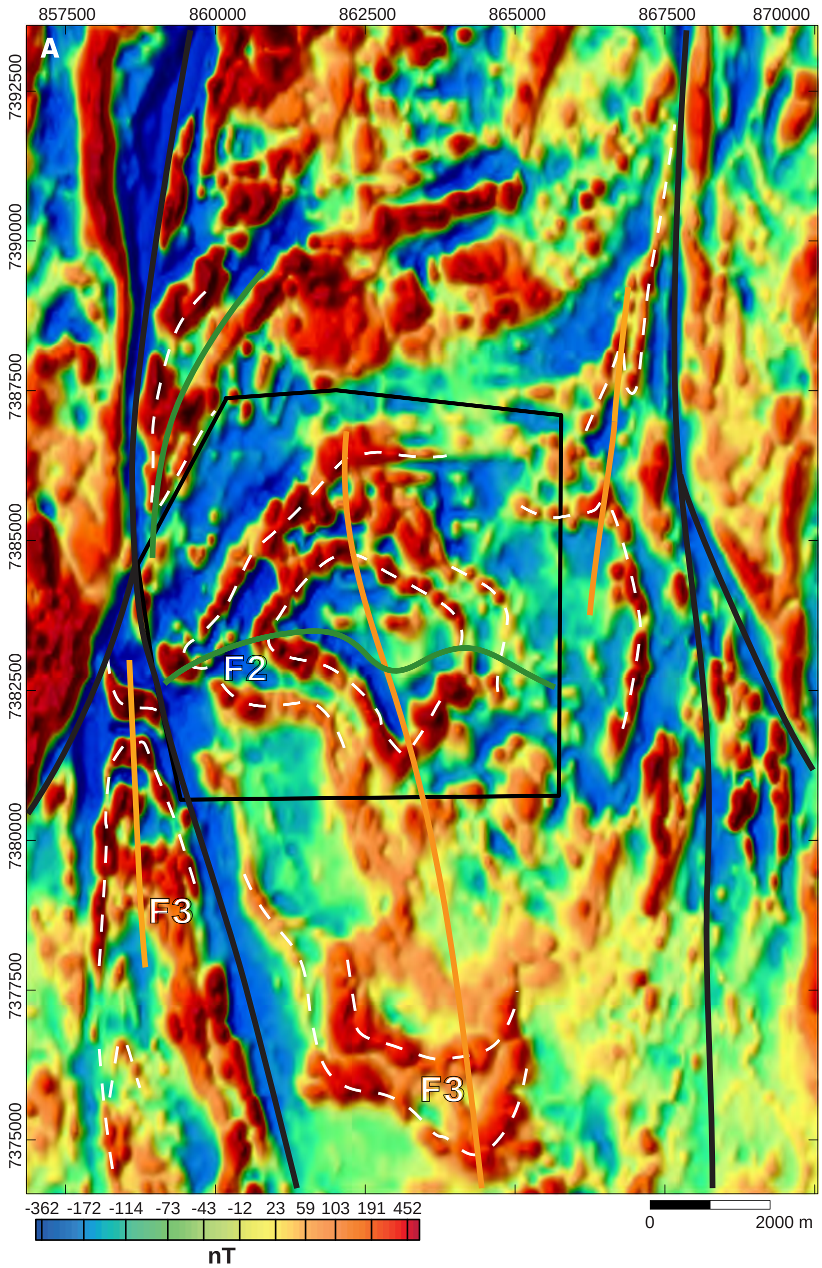

Figure 116. **A.** Fold interference pattern east-northeast of Överkalix interpreted from magnetic anomaly data. The magnetic field is filtered to enhance the shallow source anomalies. Broken white lines are magnetic connections; green and orange lines are fold axial traces of F_2 and F_3, respectively, and black lines are deformation zones.

with F_1 and F_2 above. In order to analyse the geometry of the F_1 fold, a high-resolution 3D susceptibility model was created using inversion technique. The model is presented as susceptibility isosurfaces corresponding to 0.03 SI. The model clearly shows that the F_1 fold is a gently plunging, isoclinal synform with a steep axial plane (Fig. 115b).

Other overprinting relationships are preserved at Miekojärvi to the north in the same belt, 13 km east-northeast of Överkalix. Here, fold interference patterns have resulted from approximately east–west and north–south-oriented fold axial traces (Figs. 116a, b). The favoured interpretation is that the north–south folding is the youngest. A 3D susceptibility model shows that the magnetic bands in the central closed structure dip steeply in the southwest, whereas elsewhere in the structure they dip inwards. The oldest fold here is correlated with F_2 above, and the younger F_3 folds are virtually parallel with the Pajala deformation belt. The F_2 fold axial plane dips steeply to the south, and both F_2 and F_3 appear to have gently plunging fold axes.

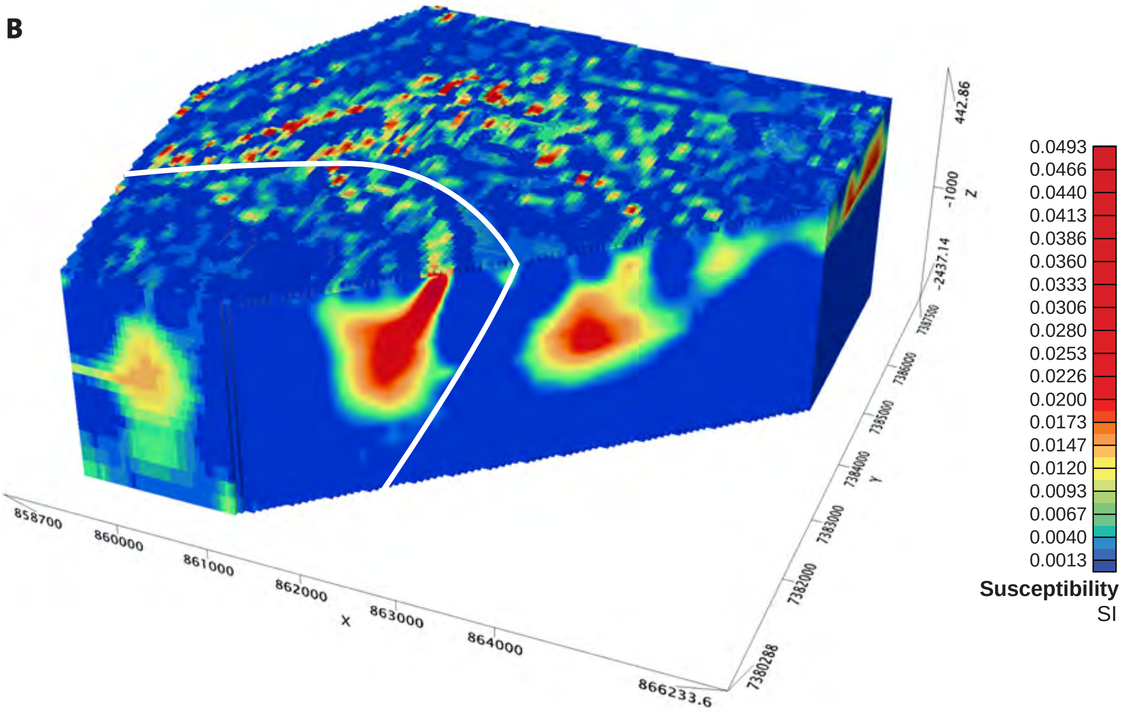

Figure 116. **B.** View from southeast of 3D susceptibility model from airborne measurements of the magnetic anomaly field. The cell size was set at 50 metres in the horizontal directions and 25 metres in the vertical direction. The white line shows an interpretation of the axial trace of the F_2 fold. The location of the model is shown with the black polygon in Figure 116a and in Figure 16.

F_3 folds; northwest to northeast folds associated with major ductile shear zones

The interpretation of fold axial plane traces from form lines of tectonic foliation (Fig. 110) shows that most of them are subparallel to a nearby ductile shear zone, e.g. those near the Nautanen deformation zone. In the area to the north, Bergman et al. (2001) suggested that some of the large fold structures located near regional deformation zones may have formed earlier, but assumed their present shapes when the zones were active. This also applies to folds in the area between Kalix and Haparanda, where there are a number of folds that are clearly indicated by the map pattern where Archaean or Karelian rocks are exposed in anticlines and Svecofennian rocks are preserved in synclines. These folds have northwest–southeast axial planes far from the Pajala deformation belt, but they are closer in orientation to the belt nearer to it.

A good example of folds spatially associated with deformation zones is found west of Jokkmokk, where one of the limbs in a folded package of felsic and mafic metavolcanic rocks is parallel to splays of the KADZ. The hinge is located at the intersection between the KADZ and a north–northwest-oriented deformation zone. A 3D model was constructed to investigate the geometry of the fold (Figs. 117a, b). The synforms plunge moderately to the north-northeast and have steep axial planes. The antiform in between also has a steep axial plane, but the orientation of the fold axis is less clear in this part of the model.

The northeast folds between Jäkkvik and Luvos possibly belong to an older generation because they appear to rotate close to the KADZ, but in general the relative ages of the folds with north to northeast-oriented fold axial traces west of the KADZ are uncertain.

In the Tjåmotis area, metasandstone of the Snavva–Sjöfallet group stratigraphically overlies felsic metavolcanic rocks, but the east-dipping succession there is inverted (Carlon 1984, Nysten et al. 2014). The presence of a complex overturned easterly-dipping synclinorium was suggested by Carlon (1984), who presented a structural evolution as follows. The first deformation phase is represented by isoclinal

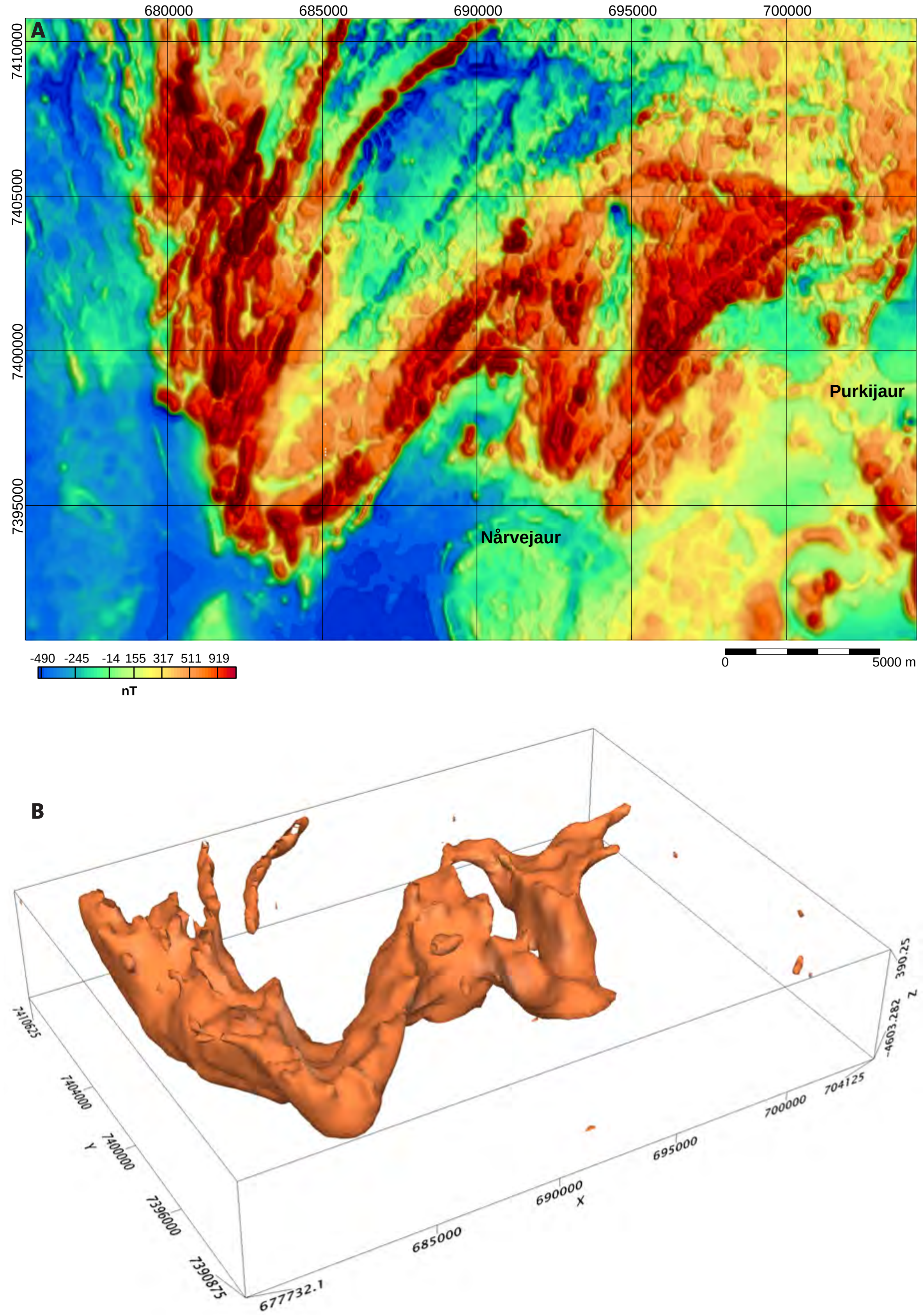

Figure 117. **A.** Major F_3 folds shown in the total magnetic field of the area west of Jokkmokk. **B.** Susceptibility model of gently north-plunging F_3 folds, presented as a susceptibility isosurface of 0.05 SI. View looking down towards the northeast. The cell size was set at 250 metres in the horizontal directions and 125 metres in the vertical direction. The location of the model is shown in Figure 16.

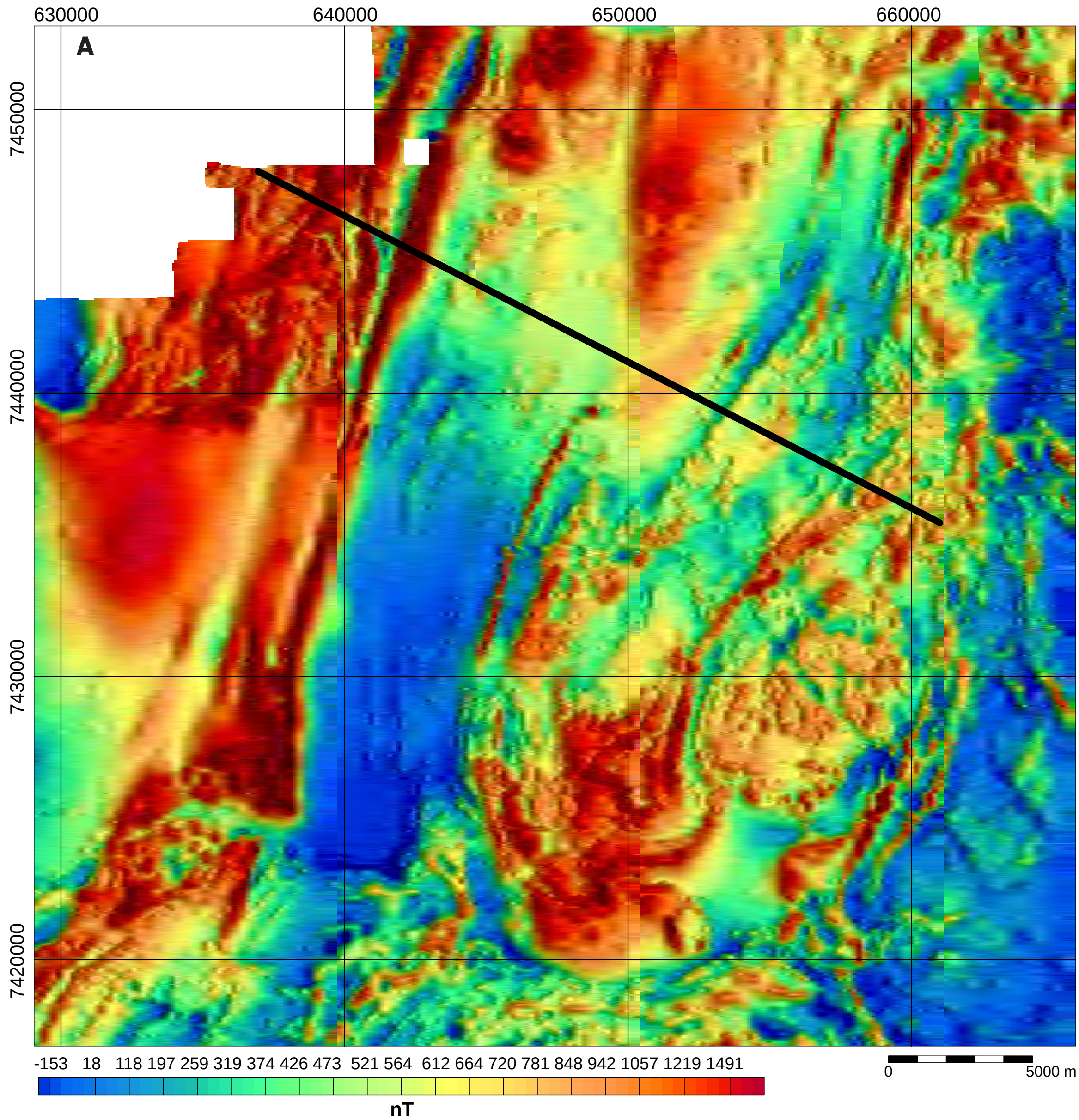

Figure 118. **A.** Magnetic anomaly map of the Tjåmotis area. The black line shows the position of the modelled profile in Figure 118b. The profile length is approximately 28 kilometres.

F_1 folds of bedding, with gently plunging axes and steeply east-dipping axial planes. This deformation was accompanied by porphyroblast growth and partial melting. The early axial planes were folded around northeast to southwest-trending F_2 fold axes. Gentle dips in some areas may be related to open F_3 folds caused by younger intrusive bodies.

A geophysical model (Figs. 118a, b) was constructed, using both the magnetic field and the gravity field, together with results from determination of petrophysical properties of numerous rock samples from the area. Samples of the sedimentary rocks of the Snavva–Sjöfallet group show that high relative remanent magnetisations occur; Q-values above 50 are common. Since the orientation of the remanence vector is unknown in much of the area, modelling of the magnetic field was not forced to good matching along the entire profile. Moreover, in the northwest of the profile, where volcanic rocks predominate, only a few magnetic anomalies were selected for modelling, merely to give a general indication of the dip. The overall fit between the measured and modelled data in gravity is considered sufficiently good

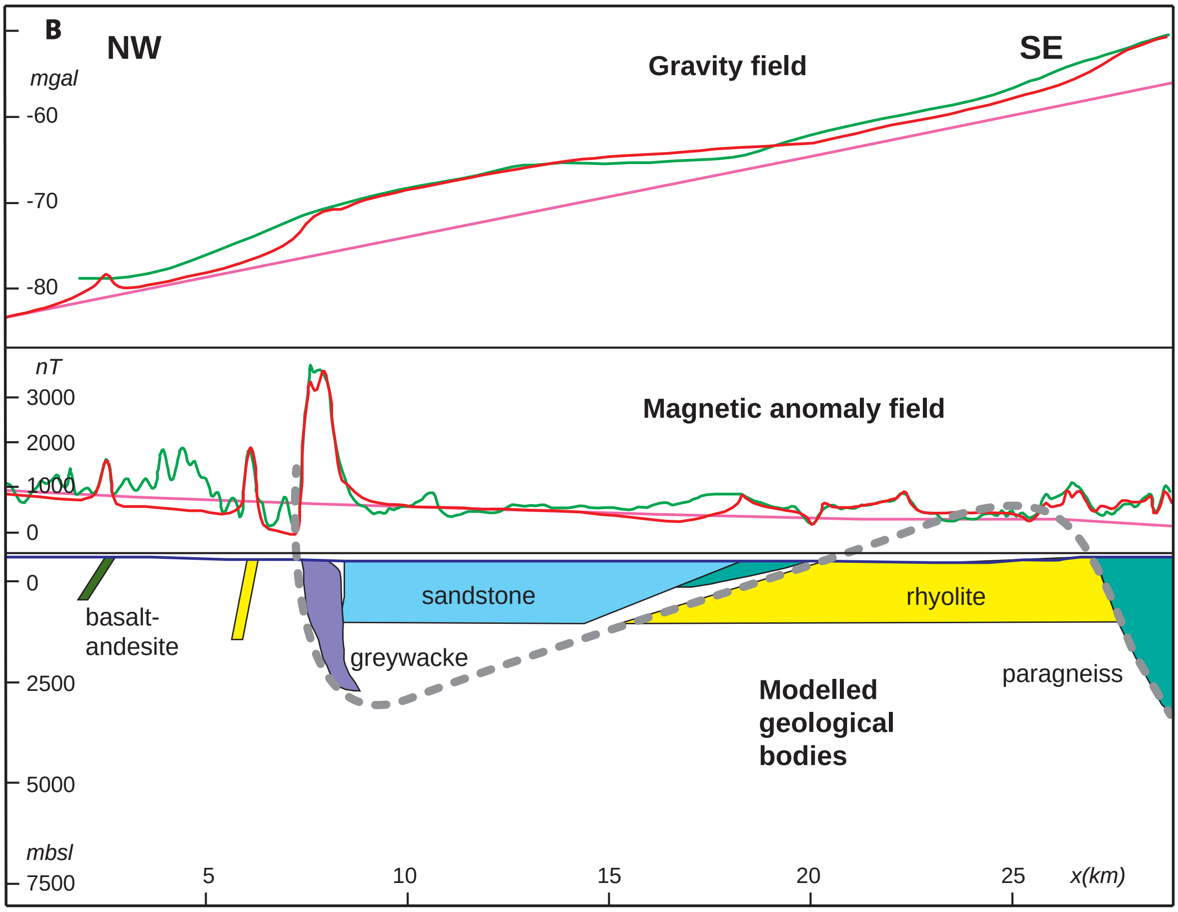

Figure 118. **B.** Geophysical 2D model across the supracrustal rocks north of Tjåmotis. The gravity field is at the top (green curve is measured data, red curve is the response from modelling, purple line is the regional field), and the magnetic field is in the middle (green curve is measured data, red curve the responsefrom modelling, purple line is the regional field). An interpretation of the geometry of the F_3-folded contact (broken grey line) between metavolcanic rocks and metasedimentary rocks in the Snavva–Sjöfallet group is included. The location of the profile is shown with the black line in Figure 118a and in Figure 16.

to support the idea that the sedimentary rocks are located in a local synform with a maximum depth of less than 3 km. The model shows that the southeastern contact of the main body of the Snavva–Sjöfallet group dips gently to moderately to the northwest, in contrast to the observed southeastward-dipping, inverted bedding at the surface (Carlon 1984, Nysten et al. 2014). These exposed southeast-dipping beds must reflect some local structural feature, e.g. the short limb of a northwest-vergent asymmetric fold. The geophysical model also shows that the northwestern contact of the Snavva–Sjöfallet group dips steeply to the southeast. Thus, the Snavva–Sjöfallet group occupies a major F_3 syncline, with a gently plunging fold axis and a steeply northwest-dipping axial plane. The fold axes undulate from gently south-southwest to gently north-northeast plunges. This is reflected in some closed, elliptical structures that are evident on magnetic field maps.

In the area southeast of Harads, the Svartlå group, with well-preserved supracrustal rocks, occupies an open syncline, which, together with the underlying metavolcanic rocks of the Arvidsjaur group, overlies metatexitic paragneiss exposed to the north and south (Figs. 119a, b). The eastern margin of the syncline is mainly controlled by a regional, west-dipping shear zone. Grip (1946) suggested that the contact between the Svartlå group and the underlying Arvidsjaur volcanic rocks is discordant, but Kathol et al. (2012b) found it to be merely a disconformity. Instead, they recognised an unconformity below the Arvidsjaur group.

Figure 119. **A.** Metasandstone in the Svartlå group with a well-preserved clastic texture. Flakaberget, 13 kilometres southeast of Harads (7332383/777973). **B.** Metatexitic paragneiss below the unconformity. Granberget, 26 kilometres west-southwest of Boden (7312986/780352). Photos: Stefan Bergman.

In the paragneiss south of the Svartlå group there is a system of south-plunging folds with approximately north–south-striking axial planes with moderate to steep dips to the east (Kathol & Jönberger 2012b). In this area there are about 5 syncline–anticline pairs across the 7 km wide supracrustal belt, which is in marked contrast to the single syncline in the younger Svartlå Group to the north (Kathol & Jönberger 2012a). These different folding patterns were the basis for postulating an angular unconformity below the Arvidsjaur group (Kathol et al. 2012b). The age of this surface is constrained by the c. 1.88 Ga age of migmatitisation recorded in paragneiss (Sadeghi & Hellström 2018a., Bergström et al. in preparation-a) and the depositional age of 1 876 ± 6 Ma of the overlying metavolcanic rock (Kathol et al. 2008b). Another possibility for the nature of the paragneiss–Arvidsjaur group contact is that a detachment zone is present there. This would be consistent with an extensional core-complex model (Skyttä et al. 2012) designed for the Skellefte district to the south.

Both the map outline of the Svartlå group and its individual rock units define an elliptical geometry, with the youngest rocks in the centre. It is suggested that this is the result of two folding events, post-dating the tight folding of the paragneiss, an older one with an approximately north–south-striking axial plane, and a younger one with the axial plane lying east–west.

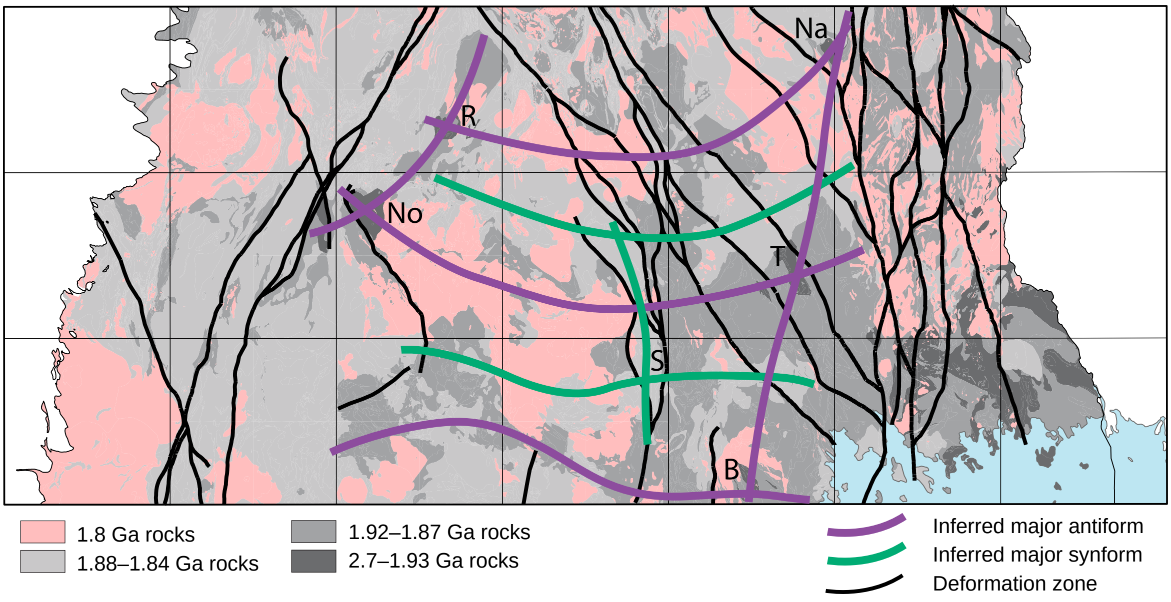

Figure 120. Regional antiforms and synforms interpreted from the distribution on the ground surface of lithological units of differing age. Note the presence of older rocks where two antiforms cross. The metasedimentary rocks at Svartlå occupy a high stratigraphic position and are located where two synforms cross. B = Boden, Na = Narken, No = Norvijaur, R = Rimokojan, S = Svartlå, T = Tallberg.

F_4 folds

The axial traces of the youngest Svecokarelian folds are oriented approximately east–west. They can be identified where shear-zone parallel D_3 folds are folded, such as in the Svartlå area, referred to above, and also further to the south and east (Fig. 110). The Muddus structure between Porjus and Nattavaara has some fold-like bends of magnetic bands in the central and eastern part, which it is suggested are F_4 folds. The similar orientation of many of the F_2 and F_4 axial traces creates uncertainty in some cases about the generation to which a certain fold belongs.

There is a general, albeit vague, pattern in the distribution of ages of lithological units on the ground surface in the region between the KADZ and the PDB. Units with ages in the interval 1.88–1.84 Ga (Perthite monzonite suite, Arvidsjaur group and related units) define two east–west-oriented, wavy linear belts (Fig. 120). These are interpreted as open F_4 (or possibly F_2) synforms. An east–west-oriented antiform connecting two pre-1.92 Ga units is outlined in the belt between these synforms. Similarly, antiforms exposing pre-1.92 Ga units can be outlined to the north and south. Most of the 1.8 Ga intrusive suites are located at these antiforms. The alignment in a north–south direction of the older rocks at Boden, Tallberg and Narken may not be a coincidence, but the result of F_3-F_4 fold interference, as suggested for the geometry of the Svartlå group above. It also follows from this interpretation that the distribution of the older rocks to the northwest, at Norvijaur and Rimokojan, is due to the interference of F_3 and F_4 antiforms. The wavelength of the major F_4 folds is in the order of 50 km (Fig. 120), which suggests they have a large interlimb angle, i.e. they are gentle folds. There is no indication in the available data that major ductile deformation zones have been affected by F_4 folding, indicating that shearing outlasted all folding.

Ductile shear zones

This section describes the major ductile shear zones or belts. They commonly have an early ductile history and were later partly reactivated in the brittle regime. New structural observations are also presented from the west of the Luleå–Jokkmokk zone (Archaean–Proterozoic palaeoboundary), where the presence of a thrust belt has been suggested (Mellqvist et al. 1999a).

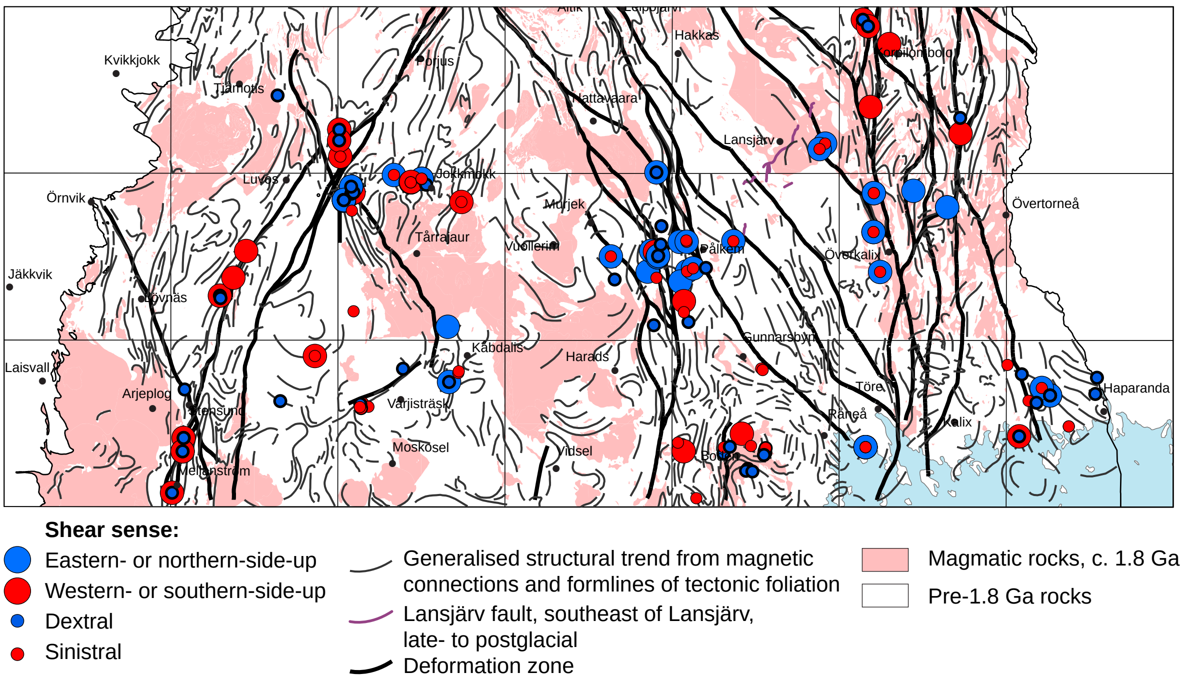

Figure 121. Structural map with kinematic information from high-strain rocks. Note the systematic western-side-up movement along the KADZ, predominantly northeastern-side-up along the NDZ and kinematic partitioning along the PDB.

Karesuando–Arjeplog deformation zone

The Karesuando–Arjeplog deformation zone (KADZ, Bergman et al. 2001), one of the largest deformation zones in Sweden, is an approximately 400 km long belt of steeply dipping, ductile shear zones. Its location is mostly inferred from geophysical data, but observations of high-strain rocks have been made at several locations along strike. Individual zones either anastomose and enclose lenses with a lower degree of deformation, or occur as sub-parallel zones. In the project area, the KADZ has a general northeast to north-northeast strike. The width is up to 5 km in the north, including intervening low-strain zones. In the south there are two parallel shear zones 10 km apart.

Foliations within the KADZ strike north-northeast and dip steeply. Lineations have variable plunges towards the south or south-southwest (Fig. 111). All the kinematic information recorded from the KADZ shows western-side-up movement (e.g. Hellström & Berggren in press), in most cases associated with a dextral strike-slip component (Fig. 121, Figs. 122a–d). This accords well with the results of Bergman et al. (2001) from the north of the zone, although recent detailed studies have shown a more complex evolution (Luth et al. 2014). In the Loito shear zone, a segment of the KADZ located some 25 km southwest of the project area, Bergman Weihed (2001) reported both western-side-up and eastern-side-up kinematics.

Nautanen deformation zone

The Nautanen deformation zone (Witschard 1996) is one of several regional ductile deformation zones with a northwesterly strike in the central part of the project area, which together form an approximately 45 km wide belt, named the Bothnian–Senja shear (or fault) zone (Henkel 1987, 1991). The Nautanen deformation zone is a belt of steeply dipping, ductile shear zones with a length of more than 150 km. The location has largely been inferred from geophysical data, and observations of high-strain rocks have been made mainly in the southeast. In the southeast, it merges with some splays of the Pajala deformation belt. Talbot et al. (1989) suggested that the PDB initiated before the shear zones

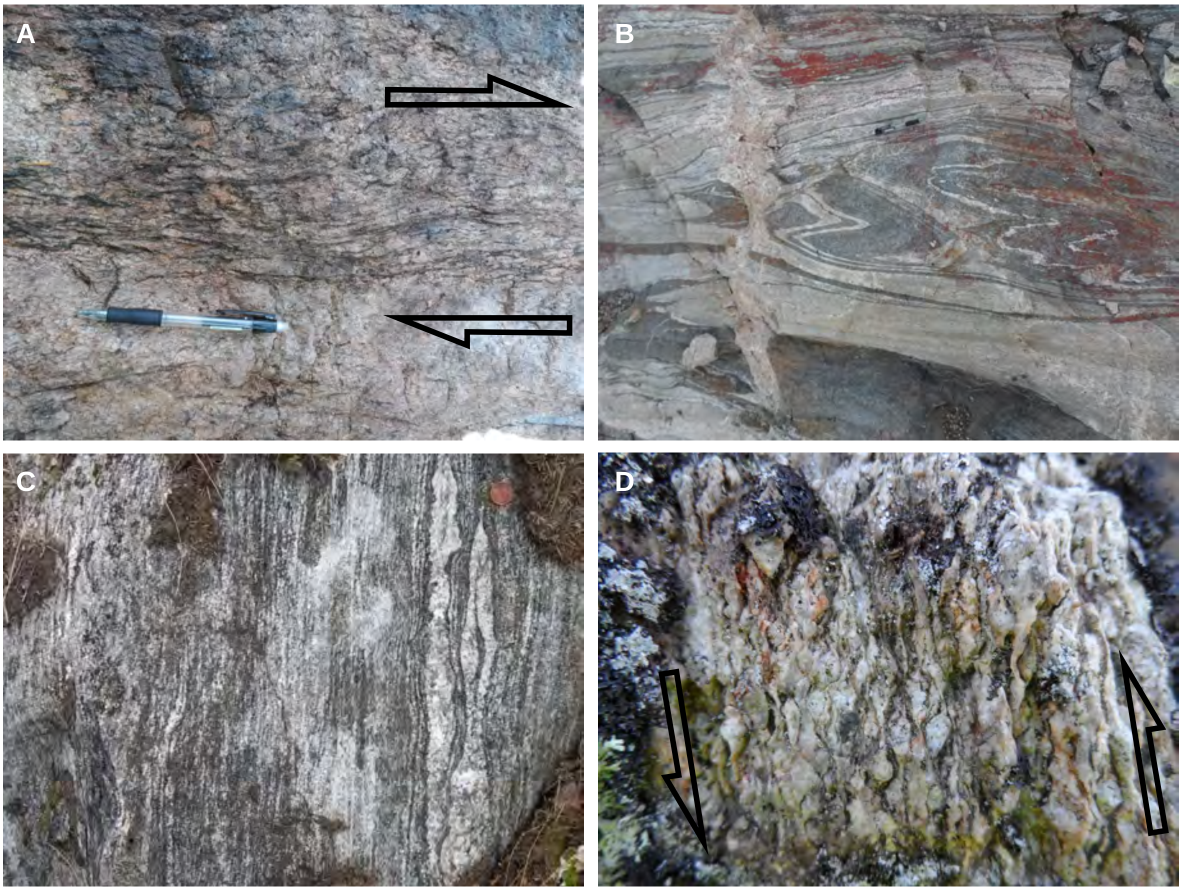

Figure 122. **A.** Mylonitic augen gneiss and leucogranite within the KADZ. S-c fabric shows dextral movement with a western-side-up component. The pencil points to the southwest on the slightly south-dipping top surface of the outcrop. Parkijaur, 30 kilometres northwest of Jokkmokk (7409588/685749). **B.** Tectonic lens within the PDB with preserved older, tight folds in highly attenuated, isoclinally folded layers of quartzo-feldspathic gneiss and amphibolite, cross-cut by late stage pegmatite. View to the west on top surface. Etu-Aapua, 18 kilometres east of Korpilombolo (7439520/870580). **C.** Early deformation within the PDB. Isoclinally folded and strongly stretched quartzo-feldspathic veins in paragneiss. The preserved magmatic texture in some of the veins suggests that deformation occurred while the rock was still partially molten. View to the north on steep surface. The coin is 19 mm in diameter. Vittakero, 16 kilometres northwest of Övertorneå (7395910/870848). **D.** Mylonite from the PDB with sigma porphyroclasts and s-c fabric indicating east-side-up movement. View to the north on steep surface. Vännäsberget, 8 kilometres northwest of Överkalix (7384271/845970). Photos: Stefan Bergman.

with a northwesterly strike. In the central part there is a north-trending splay, the Karsbergsfallet deformation zone, described below.

The mineral stretching lineation along the Nautanen deformation zone has an orientation close to the dip direction of the mylonitic foliation. A sinistral sense of shear (Talbot et al. 1989) and oblique sinistral and eastern-side-up movement (Bergström et al. 2015b) have been reported from several shear zones with northwesterly strike along the south of the zone (Fig. 121). North of the project area, the southwest side has moved upwards relative to the northeast side (Bergman et al. 2001, Lynch et al. 2018a). It is an open question whether the contrasting kinematics between the northern and southern parts reflect multiple deformation events or lateral variations during the same event.

Pajala deformation belt

The Pajala deformation belt (PDB, Fig. 110) is about 40 km wide and consists of steeply dipping, anastomosing ductile shear zones enclosing tectonic lenses with a lower degree of deformation, in which parts of the earlier structural history are preserved (Figs. 116a, b, Fig. 122b). Some shear zones define lithological breaks and separate segments with different metamorphic grades. In the belt as a whole, lineations plunge either steeply or gently to moderately to the south. The PDB is a conspicuous structural feature with a northerly trend on magnetic and gravity maps. In Sweden it can be followed for about 300 km, and including the continuation in Finland and Norway, it is at least 500 km long. It has been described and named in regional studies by various authors (Berthelsen & Marker 1986, Henkel 1991, Kärki et al. 1993, Olesen & Sandstad 1993, Wikström 1995, Wikström et al. 1996b, Bergman et al. 2001, Patison et al. 2006, Henderson et al. 2015, Luth et al. 2018b, Grigull et al. 2018). The nomenclature used in Luth et al. (2018b) is followed here.

Field observations have shown rocks that were highly strained in ductile to brittle conditions. The local presence of magmatic texture in quartzo-feldspathic veins in highly-strained gneiss (Fig. 122c) shows that the PDB was active even during the peak of metamorphism. A large component of flattening is indicated by local observations of strongly horizontally and vertically stretched layers. The flattening was preceded by isoclinal folding. Sinistral and western-side-up kinematics have been recorded in amphibolite facies mylonites, but shear sense indicators are generally not obvious. The most commonly observed mylonite type, which formed in the ductile to brittle-ductile regime under retrograde conditions, shows better developed sigma porphyroclasts, s-c fabric and other kinematic indicators (Fig. 122d). The PDB in the project area is kinematically partitioned into a northern segment with western-side-up movement with a dextral component, and a southern segment, in which eastern-side-up movement with a sinistral component predominates (Fig. 121).

Regional sinistral sense of shear can be deduced from aeromagnetic maps (Wikström et al. 1996b). Berthelsen & Marker (1986) suggested that an older phase of dextral movement preceded the sinistral phase. In the south, field observations of dextral shear sense in migmatites and dominant sinistral shear sense in lower amphibolite facies support this structural development in general (Wikström 1995, Wikström et al. 1996b). Sinistral strike-slip combined with eastern-side-up movement was also reported, which is supported by the new results presented in Figure 121. North of the project area, recent structural mapping and 3D modelling (Luth et al. 2018b) have revealed a wedge shaped geometry for the PDB, with steeply east-dipping shear zones along its western margin and steeply west-dipping shear zones in the east. The internal structure of the wedge consists of multiple, elongate, ellipsoidal domes.

Structure at the Archaean–Proterozoic boundary in the Jokkmokk area

In a study of the Archaean–Proterozoic boundary in the Jokkmokk area, Mellqvist et al. (1999a) drew attention to zones of gently southwest-dipping strong foliation that were interpreted as thrusts with transport to the north. They were observed at a few field localities and elsewhere interpreted from magnetic anomaly data as a set of undulating zones. Recent field studies including kinematic analysis could not unequivocally confirm the thrust interpretation. Stretching lineations and fold axes generally have gentle plunges to the south-southwest, whereas foliations are predominantly steeply east-dipping (Fig. 123). The stretching lineation is commonly well-developed, irrespective of the orientation of the foliation. Banding and foliation are isoclinally folded (Fig. 124a). The relatively high metamorphic grade limits the amount of available kinematic indicators, but some asymmetric structures could be used to deduce the local sense of shear. Three of the five localities where shear sense could be determined show thrusting towards the northeast (Fig. 124b), whereas the opposite, normal movement to the southwest, was recorded at two localities. It is unclear whether this is due to multiple deformation events, different positions within major folds (sheath folds?), for example, or other structures formed during a single event.

The magnetic and gravity anomalies caused by the Archaean gneiss unit north-northeast of Vajkijaur, and an adjacent Proterozoic metagabbro, have been modelled using the forward technique (Fig. 125a, b). The model parameters are shown in Table 5. The model shows that the Archaean gneiss unit is a south-dipping block and the contact with the metagabbro dips to the north in the upper kilometre and to

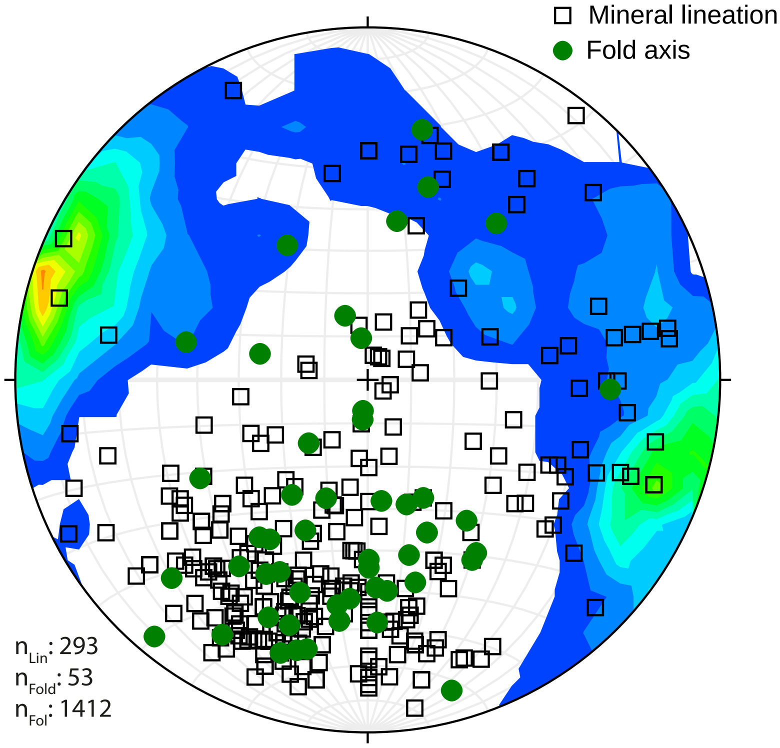

Figure 123. Orientations of structural data from the Jokkmokk area. Equal area stereographic plots (lower hemisphere) of lineations and fold axes. Contours of poles to foliation are shown in blue to red colours. The number of measurements are indicated by the following abbreviations: Lin =mineral lineation, Fold = fold axis, Fol = foliation.

Figure 124. Structural features at the Archaean–Proterozoic palaeoboundary in the Jokkmokk area. **A.** Isoclinally folded amphibolite bands in gneissic granitoid. View to the north on inclined surface. Sasskam, 6 kilometres northwest of Jokkmokk (7397465/707465). **B.** Winged feldspar aggregate resembling delta porphyroclast indicating top-to-northeast thrusting. View to the southeast on steep surface. Linaberget, 10 kilometres east-southeast of Jokkmokk (7391663/722571). Photos: Stefan Bergman.

the south further down in the crust. It is also obvious that the bulk composition of the Archaean rocks is mafic, in contrast to the more felsic compositions observed at the surface (Kathol et al. 2015). Field observations have shown that the gneiss unit is partly bounded by deformation zones and partly by intrusive contacts (Kathol et al. 2015). If the contacts shown in Figures 125a, b are tectonic, one of several possibilities is that the north-dipping contact is a reverse fault, and the south-dipping one is a thrust that reaches the surface some 3 km north of the boundary of the two units. An interpretation involving a south-dipping thrust is in line with the model of Mellqvist et al. (1999a), referred to above.

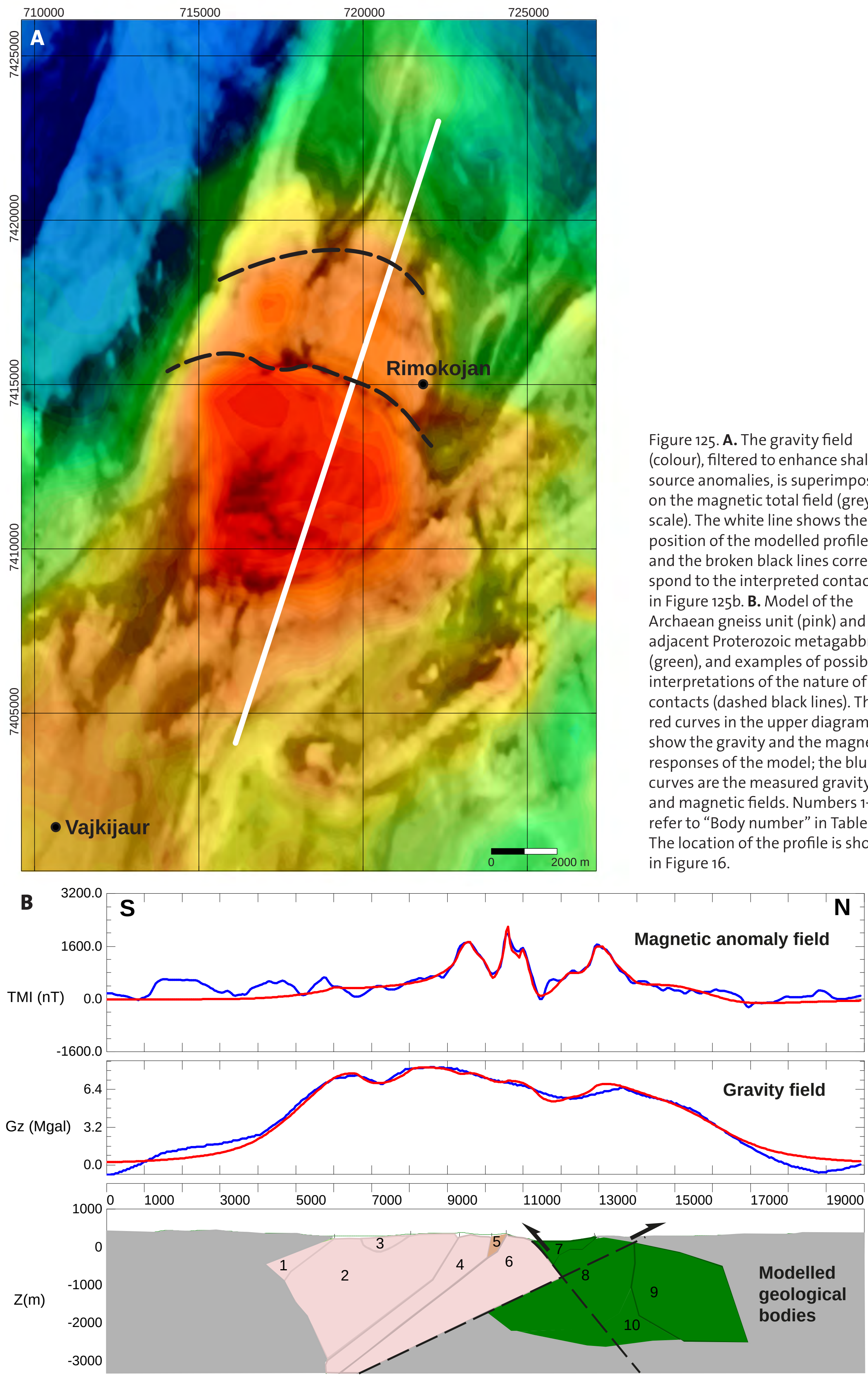

Figure 125. **A.** The gravity field (colour), filtered to enhance shallow source anomalies, is superimposed on the magnetic total field (greyscale). The white line shows the position of the modelled profile and the broken black lines correspond to the interpreted contacts in Figure 125b. **B.** Model of the Archaean gneiss unit (pink) and adjacent Proterozoic metagabbro (green), and examples of possible interpretations of the nature of the contacts (dashed black lines). The red curves in the upper diagrams show the gravity and the magnetic responses of the model; the blue curves are the measured gravity and magnetic fields. Numbers 1–10 refer to "Body number" in Table 5. The location of the profile is shown in Figure 16.

Table 5. Model parameters used in Figures 125a, b.

Body number	Density (kg/m^3)	Magnetic susceptibility (SI)	Remanent magnetisation (A/m)
1	2 800	0.0001	0.09
2	2 800	0.01	0.5
3	2 650	0.01	
4	2 800	0.06	0.35
5	2 750	0.015	
6	2 790	0.07	
7	2 640	0.001	
8	2 800	0.07	0.5
9	2 800	0.05	0.8
10	2 620	0.001	
Background	2 670	0.00001	

Other shear zones

A northwest-striking shear zone along the southwestern margin of the Norvijaur intrusion, west-southwest of Jokkmokk, dips steeply towards the northeast. In the north of the zone it rotates towards a northerly orientation, and kinematic indicators show eastern-side-up movement. Highly-strained supracrustal rocks enveloping the northwestern part of the Norvijaur intrusion dip northwest and show southeastern-side-up movement. The large amount of rotation of the high-strain zone and the systematic "pluton-side-up" kinematics suggest the zone is folded with a northwest-striking axial plane.

The Karsbergsfallet deformation zone (KDZ, Fig. 110) consists of an anastomosing network of high-strain zones and intervening low-strain lenses. It has a north–south orientation, a length of at least 150 km and a width of up to 10 km or more. In the north it is joined with the Nautanen deformation zone; in the south it terminates some tens of kilometres south of the project area. It is poorly exposed, but in the vicinity of Karsbergsfallet in the Råneälven river (Figs. 126a, b) there are outcrops offering evidence of both ductile and brittle-ductile shearing. The deformation is associated with strong retrogression and formation of chlorite. S-c fabrics and other kinematic indicators show eastern-side-up movement, in some places with a dextral strike-slip component (Fig. 126c). The KDZ was active at 1.8 Ga or later, since it partly affects granite of that age (Fig. 126d, Kathol et al. 2012b).

West of Vidsel is the northern end of the north–south-oriented and approximately 120 km long Vidsel–Röjnoret shear system (VRSS, Fig. 110). Eastern-side-up kinematics have been observed in the south, outside the project area (Bergman Weihed 2001).

An approximately 25 km long shear zone near Varjisträsk has an unusual east–northeast orientation. A few observations of sinistral movement have been made near Labtjevare (Fig. 126d). In the general area around this shear zone, east of the KADZ, a number of minor shear zones with significant sinistral or dextral components have been observed. The poles to these shear zones plot in different quadrants in the stereogram of Figure 127, which indicates approximately west-northwest extension or moderately south-plunging shortening. An analysis of shear zones in the Haparanda area gave a similar result (Bergman et al. 2014). Analysis of minor shear zones that postdate isoclinal folding, at a locality 9 km east-northeast of Boden, showed northwest–southeast shortening (Sadeghi et al. in press). However, a system of deformation zones in the Boden area affecting the Lina granite indicates north–south shortening (Kathol et al. 2011).

Figure 126. **A.** Small shear zone with east-side-up movement in the Karsbergsfallet deformation zone. View to the north on steep surface. Karsbergsfallet, 14 kilometres west-southwest of Pålkem (7375900/781478). **B.** Brittle-ductile mylonite with reverse sense of movement along pronounced stretching lineation. View to the southwest on inclined outcrop surface. Fallheden, 14 kilometres west-southwest of Pålkem (7376288/781653). **C.** Shear bands indicating dextral shearing of c. 1.8 Ga granite in the northern part of the KDZ, close to the junction with the NDZ. Peinisvaara, 24 kilometres southeast of Nattavaara (7401317/780812). **D.** Top view of mylonitic granodiorite with sigma porphyroclasts and shear bands showing sinistral movement sense. Östra Labtjevare, 20 kilometres north-northwest of Moskosel (7331031/693899). Photos: Stefan Bergman.

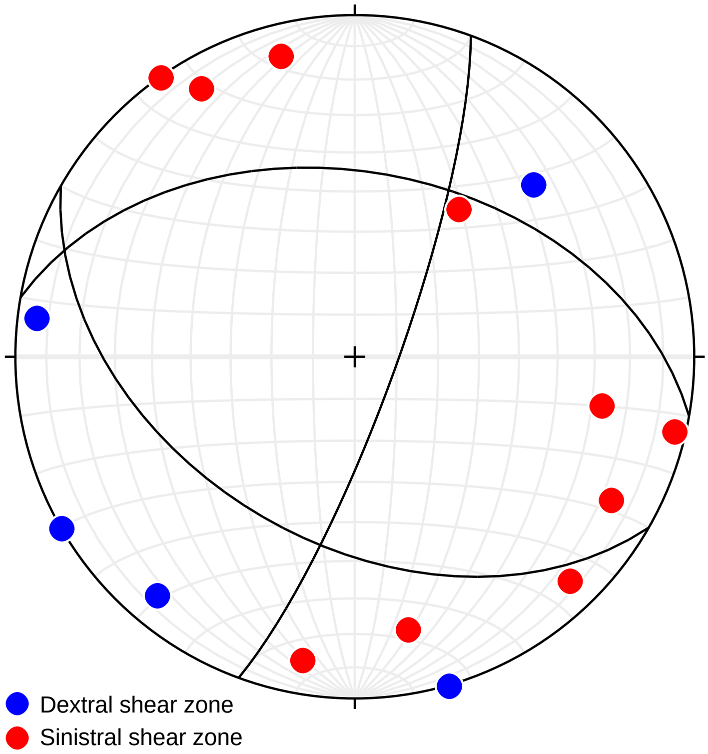

Figure 127. Stereogram (Schmidt projection, lower hemisphere) of poles to boundaries of ductile strike-slip shear zones in the area east of the KADZ and south of Jokkmokk. Dextral (blue) and sinistral (red) shear zones separate into quadrants indicating approximately west-northwest extension or moderately south-plunging shortening (190/45).

Evidence of separate deformation events and their age constraints

Archaean deformation

Archaean granitoid gneiss at Rimokojan has a pronounced northeast–southwest-oriented foliation that is cross-cut at a small angle by mafic dykes (Kathol et al. 2015). The dykes themselves are foliated and boudinaged: structures that were formed during a second deformation phase. This polydeformed unit of gneiss and mafic dykes was later intruded by magmas of the Haparanda suite, and all these rocks were subsequently deformed during a third deformation phase (Kathol et al. 2015). The first deformation phase, predating the mafic dykes, is most likely of Neoarchaean age, whereas the second one could be either Neoarchaean or Orosirian in age.

Archaean migmatitic gneisses in the Kukkola complex are exposed in an antiformal structure with a northwesterly axial surface trace. Since the Palaeoproterozoic cover rocks are also folded, the folding is inferred to have taken place during the Svecokarelian orogeny. Mesoscopic folds with axial surfaces parallel to the major antiform are accompanied locally by weak, axial surface foliation. However, there is a significant contrast in metamorphic grade and degree of deformation between the Archaean gneisses and the younger, Palaeoproterozoic rocks. The gneissosity is also cut by less deformed dykes, probably related to the Haparanda suite (Bergman et al. 2014). These observations suggest that the Archaean gneisses in the core of the antiform were affected by Archaean deformation and metamorphism, and only the folding of these gneisses occurred during the Svecokarelian orogeny. The Archaean metamorphism is reflected in zircon rims with a U-Pb age of 2.67 Ga (Bergström et al. 2015a).

The gneissic foliation in the Archaean rocks in the Boden area is generally cut by mafic dykes (Mellqvist et al. 1999b), which might indicate that the foliation formed in the Archaean. The gneissic foliation strikes west–northwest, the same orientation as the elongate gneiss bodies themselves, and also the same orientation as the foliation in the surrounding Proterozoic rocks. This indicates a substantial Proterozoic structural overprint. Archaean structures cut by intrusive rocks of the Haparanda suite have been found locally further south in the Luleå area (Wikström & Söderman 2000).

Early Svecokarelian deformation (c. 1.88 Ga)

Evidence of early Svecokarelian deformation from the areas to the north and south mainly include observed relationships between deformed and undeformed rocks, in some cases combined with radiometric dates (e.g., Skiöld & Öhlander 1989, Lundström et al. 1999, Bergman et al. 2001, Kathol & Weihed 2005). In the project area, supracrustal xenoliths with strong foliation or quartzo-feldspathic veins in less deformed intrusive rocks of the Haparanda and Jörn GI suites have been observed (Bergström et al. 2015b, Kathol et al. 2012b, Figs. 128a, b), implying deformation and metamorphism before or during the intrusion of these suites. West of Pålkem, dykes of weakly foliated granite (Perthite monzonite suite) cross-cut a strong penetrative fabric in Haparanda suite metaquartz monzodiorite (Bergman et al. 2016). A similar observation is reported about 20 km southeast of Boden (Sadeghi et al. in press). In general, there is a potential for finding evidence of early Svecokarelian deformation in areas where plutonic rocks of the Perthite monzonite suite are isotropic or only weakly foliated. Areas of this kind, which largely escaped subsequent ductile deformation, are common in the central part of the project area.

From Aitik, north of Nattavaara and just outside the project area, Wanhainen et al. (2005) report at least four episodes of metamorphism and magmatism, with one of the main metamorphic peaks in the time interval 1.89–1.87 Ga. Structures that can be constrained in time by radiometric ages are present in a few areas. In the Jokkmokk area, the first deformation produced a bedding-parallel foliation in the Norvijaur formation (Markkula 1977). The foliation was later folded around flat to moderately south–southwest-plunging fold axes with steep north–northeast-trending axial planes during east–west shortening (Lundmark et al. 2005a). The Jokkmokk granitoid and Haparanda suite intrusive rocks intruded the folded Norvijaur formation but also show similar structures indicating east–west shortening (Lundmark et al. 2005a). A likely interpretation is that this deformation was contemporaneous with the magmatism at c. 1.88 Ga.

Another example of early Svecokarelian deformation with age constraints is in the Kalix area, where a swarm of mafic and felsic dykes intruded during movements in the Pajala deformation belt at c. 1.88 Ga (Wikström 1995, Wikström et al. 1996b). The age of this dyke swarm also provides a minimum age for deformation and migmatisation, because the dykes clearly cross-cut the orogenic deformation structures and migmatised sedimentary gneisses (Wikström et al. 1996b). The structures in this area generally strike east–west. Due to their orientation and relative age, they are correlated with the D_1 or D_2 structures (see

Figure 128. Field evidence for deformation and metamorphism prior to intrusion of the Haparanda and Jörn GI suites.
A. Quartzo-feldspathic veins in supracrustal rock truncated by metagranodiorite (Haparanda suite). Västerberget, 35 kilometres southeast of Pålkem (7354983/822092). Photo: Stefan Bergman. **B.** Strongly foliated xenoliths of paragneiss within less deformed metatonalite (Jörn GI suite). Risliden, 34 kilometres southwest of Harads (7323214/740877, reproduced from Kathol et al. 2012b). Photo: Benno Kathol.

above) preserved in the PDB. A correlation with the early structures further west also appears reasonable.

Two recent U-Pb zircon age determinations on diatexitic migmatite from southeast of Pålkem and southeast of Boden both yielded ages of c. 1.88 Ga (Bergström et al. in preparation-a, Sadeghi & Hellström 2018a). These results can be used to constrain the age of a possible unconformity between paragneiss and overlying more weakly metamorphosed supracrustal rocks of the Arvidsjaur and Svartlå groups, mentioned in a previous section. Together with the evidence presented above, the 1.88 Ga migmatite ages suggest that an early Svecokarelian structural and metamorphic history is present, if not predominant, in much of the project area. Available data suggest that substantial magmatism, deformation and metamorphism all occurred close to 1.88 Ga.

Molybdenite from aplite to pegmatite phases in coarse-grained granite 8 km southwest of Vidsel was dated using the Re-Os method (Stein 2006). The age 1 875 ± 6 Ma was interpreted as development of metamorphic leucosomatic pockets. However, mapping in the area by SGU in 2006 showed that the granite is only very weakly recrystallised and foliated, which seems incompatible with metamorphic temperatures high enough to produce partial melts.

Late Svecokarelian deformation (c. 1.8 Ga)

Field evidence of late Svecokarelian deformation is ubiquitous within and adjacent to major deformation zones, where rocks of the Perthite monzonite suite or younger are affected. The youngest ductile deformation in the Nautanen deformation zone impacted and consequently post-dated the formation of granite in the 1.8 Ga Lina suite. Similar observations were made by Sadeghi et al. (in press) near a northwest-oriented major shear zone in the Boden area. Along the KADZ there is a very wide belt where rocks of the Perthite monzonite suite have a gneissic foliation, e.g. the Porjus granite.

In some areas, radiometric dating provides tighter constraints on the ages of these younger events. Ductile deformation and partial melting occurred in the KADZ at c. 1.78 Ga (Hellström & Berggren in press), and migmatisation also occurred in the Kalix area at that time (Wikström & Persson 1997b). One of the main metamorphic peaks at Aitik, north of Nattavaara, occurred in the time interval 1.81–1.77 Ga (Wanhainen et al. 2005). A U-Pb titanite age of c. 1.81 Ga from a metagranodiorite probably reflects the peak of the youngest high-T metamorphic event in the Jokkmokk area (Lundmark et al. 2005a). The steep gneissic fabric strikes north-northeast and there is a pronounced southwest-plunging lineation. In addition to the metamorphic peak, this titanite age probably also corresponds to the deformation phase D_3. From the same intrusive body, it was suggested that Re-Os molybdenite ages of c. 1.75 Ga were the products of a high-T metamorphic event that formed pegmatite (Lundmark et al. 2005b). However, it is unclear whether any regional fabric was produced during this event or whether it only included the introduction of external melt or fluid. For the same reason a range of molybdenite ages presented by Stein (2006) from an area 90 km west of Jokkmokk are not discussed here.

The shallowly south-dipping deformation zones that have been interpreted as thrusts (Mellqvist et al. 1999a, Lundmark et al. 2005a), referred to in a previous section, were formed after the emplacement of the Jokkmokk granitoid, i.e. after 1.88 Ga. Mellqvist et al. (1999a) and Öhlander et al. (1999) gave a time interval of 1.9–1.8 Ga for movement on the thrusts, while Lundmark et al. (2005a) suggested they were active at c. 1.8 Ga as reactivation of the Archaean–Proterozoic palaeoboundary.

The presence of both (pre-)1.88 Ga migmatites and c. 1.78 Ga migmatites in different segments in the south of the Pajala deformation belt also suggests considerable movements after 1.78 Ga (Wikström & Persson 1997b). In the north, variably deformed leucosome indicates that movement in the belt was associated with migmatisation, which occurred within the time interval 1.82–1.78 Ga (Bergman et al. 2006).

Penetrative ductile deformation probably ended close to c. 1.78 Ga. Although located in the KADZ, the c. 1.77 Ga volcanic rocks at Tjäkkaure only show very weak metamorphic effects (Claeson & Antal Lundin in press-b, see also the section *Metamorphism*), indicating that penetrative ductile deformation had ceased at that time in this area.

Figure 129. **A.** Steeply dipping, northwest-striking brittle deformation zone. Gidákvárásj, 25 kilometres northeast of Tjåmotis (7448017/669074). Photo: Carl-Axel Triumf. **B.** Steeply dipping, northeast-striking fracture zone in pegmatitic granite. Washed outcrops downstream of Letsi power station, 22 kilometres west of Murjek (7386005/739260). The width of the image is approximately 1 metre. Photo: Per Nysten. **C.** Brecciated granitic rock with tourmaline in the matrix, 17 km southwest of Boden (7309425/790178). Photo: Charlotta Brandt.

BRITTLE DEFORMATION ZONES

Brittle deformation zones are rarely exposed, and breccia and other brittle fault rocks have only been locally observed (Figs. 129a–c). The larger zones have mainly been interpreted from geophysical and elevation data.

There are 644 measurements of fractures and brittle deformation zones in the field observation database. These outcrop scale structures are mostly steeply dipping and have weakly developed preferred orientations in west–northwest and north–northwest to northeast directions (Figs. 130a, b). In contrast, the map scale deformation zones in the whole project area have predominantly northwest to north–northwest and north–south orientations (Fig. 130c).

The geographical distribution is far from even, e.g. northwest, northeast and north–south orientations are typical in the Jokkmokk–Tjåmotis region (Claeson & Antal Lundin in press-a, b), whereas northeast orientations are less common further east. In an interpretation of aeromagnetic and elevation data in the east of the project area, Henkel (1987) distinguished three distinct systems of lineaments: steeply dipping northwest and north-striking, and gently dipping north–northeast-striking. Weakly developed east–west and northeast lineaments were also identified. A characteristic feature is the presence of lineaments, mostly interpreted as brittle deformation zones, parallel to and concentrated along major ductile shear zones, suggesting that ductile structures have been reactivated under brittle conditions.

At Lansjärv there is a set of faults that were active during or shortly after the latest glaciation (Lagerbäck 1979, Lagerbäck & Witschard 1983). They are oriented northeast to north-northeast, dip to the southeast and show reverse sense of movement.

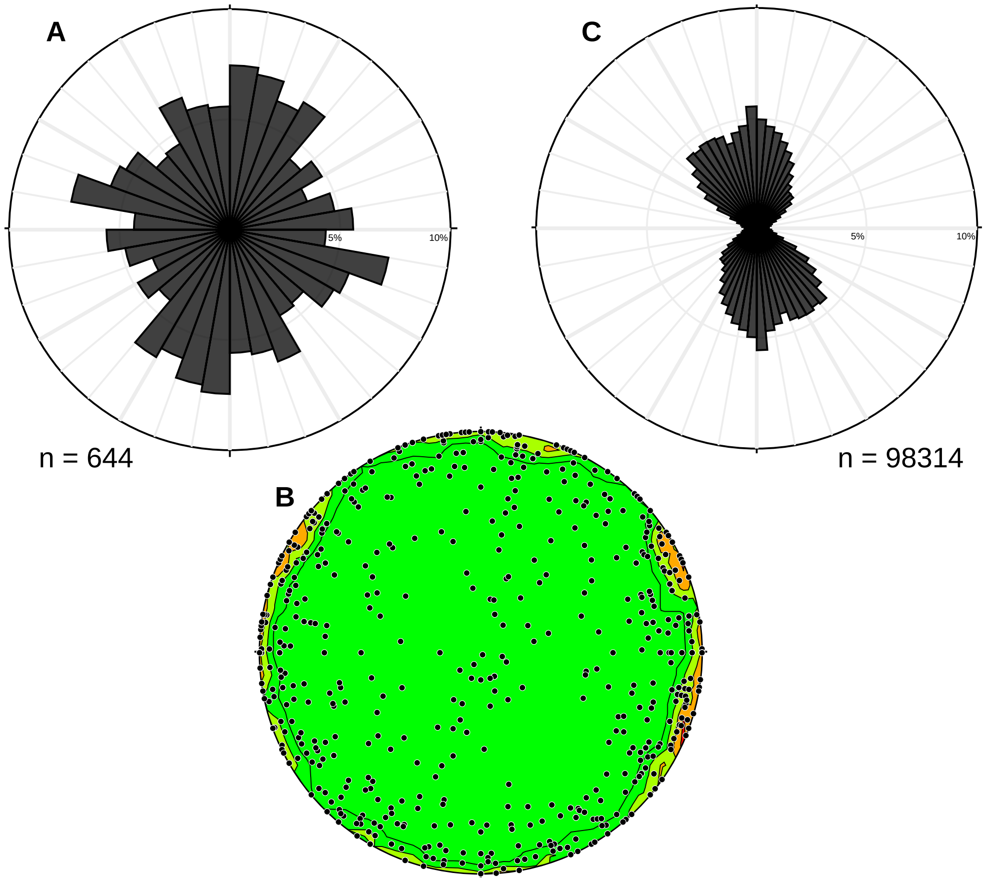

Figure 130. **A.** Rose diagram with orientation distribution of 644 fractures and brittle deformation zones measured in the field. There are weak maxima in the west-northwest and north-northwest to northeast. **B.** Poles and contours on an equal area stereogram (lower hemisphere) using the same measurements as in Figure 130a. **C.** Orientation distribution of deformation zones mapped and interpreted at a scale of 1:50 000 to 1:250 000. Lines were extracted from the map database and the orientation of 98 314 individual line segments was plotted on the diagram. Most deformation zones have northwest to north-northwest and north orientations.

METAMORPHISM

Input data, terminology, and constraints

Metamorphism and facies concepts in this section are based on definitions found in several textbooks, e.g. Kerrick 1991, Spear 1993, Yardley 1993, Bucher & Frey 1994, Fettes & Desmons 2007, Pirajno 2009. A conceptual framework for how metamorphism relates to the type of tectonic-setting envisaged for southern Norrbotten County may be studied in, e.g., Collins 2002, Hyndman et al. 2005.

The metamorphic information in this section and on the metamorphic map (Fig. 131) is based on the following: 1) classification into five groups: a) Non-metamorphic, sub-greenschist facies to greenschist facies; b) Greenschist facies; c) Epidote-amphibolite facies to middle amphibolite facies; d) Upper amphibolite facies, migmatitic; e) Granulite facies, garnet amphibolite facies, partly migmatitic. 2) Key metamorphic minerals. 3) Textures and structures. 4) The metamorphic facies or grade according to available data. Most of this data are available from detailed map descriptions and the maps themselves, data stored in various bedrock databases at SGU, exploration reports and other published literature from the project area.

For the most part, rocks predominantly consisting of quartz and feldspar do not record mineral parageneses to characterise the metamorphic overprinting present in the project area. Since much of the bedrock in the project area consists of rocks of quartzofeldspathic composition, most of the useful information on metamorphic facies or grade is derived from mafic and pelitic rocks, as well as the

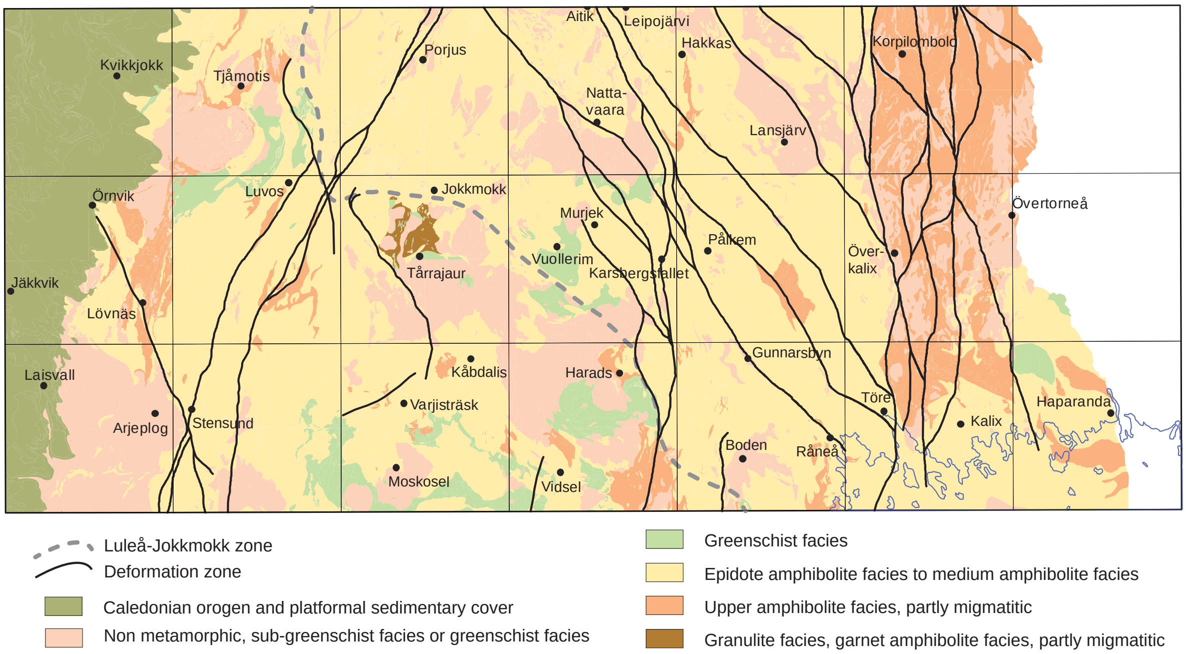

Figure 131. Regional variation in metamorphic overprinting in southern Norrbotten County and major deformation zones.

onset of partial melting in all types of rock. To some degree, this provides the necessary support for the regional metamorphism of southern Norrbotten County. In some areas, e.g. most of map area 27K Nattavaara, the bedrock is mostly covered with Quaternary deposits and lakes, thus hampering detailed metamorphic interpretation. There is also a difference between areas mapped at a scale of 1:50 000 and those at 1:250 000 in terms of detail and density of observations.

Few thermobarometric studies have been performed in the project area, but some just outside the area are reported below. There are no studies revealing details of overprinting by different phases of Archaean, Svecokarelian, and possibly Sveconorwegian metamorphic events. There are few age determinations focusing on dating of metamorphic events, for example metamorphic rims and overgrowths on zircon, since geochronological work has concentrated on determining magmatic crystallisation ages. Detailed studies addressing relationships between metamorphism and deformation are lacking.

Regional metamorphic variation

The metamorphic map is an attempt to show the variation and distribution of the Svecokarelian metamorphic overprinting present in the bedrock in the project area (Fig. 131). The Archaean and Palaeoproterozoic rocks have undergone several episodes of metamorphism and deformation, in which metamorphic conditions vary from subgreenschist facies to granulite facies. High T – low to medium P regional metamorphism characterise large areas of southern Norrbotten County. The late Svecokarelian supracrustal c. 1.77 Ga volcanic rocks, c. 1.84–1.77 Ga Lina suite and Edefors suite rocks mostly show no metamorphic overprinting, except for greenschist to epidote-amphibolite facies at contacts and within deformation zones. These observations suggest that no major regional metamorphic event affected the project area after c. 1.77 Ga. Geochronological studies of metamorphism are rare in the project area. Well-preserved primary structures in the supracrustal rocks, independent of age, occur in all parts of the project area. However, the preservation of primary structures also depends on factors such as the degree of deformation, access to metamorphic fluids, and compositions of the rocks, and is therefore not an indication of metamorphic conditions.

Överkalix lithotectonic unit

In the Överkalix lithotectonic unit, Archaean and Svecokarelian rocks mostly display high-grade, upper amphibolite facies metamorphic conditions, with formation of diatexite (Fig. 131). Only the southern parts have been subjected to epidote-amphibolite facies to middle amphibolite facies metamorphism. There is a great contrast in the degree of metamorphism between the Archaean and the Palaeoproterozoic bedrock in the south. The Archaean bedrock was metamorphosed during Archaean time under amphibolite facies metamorphic conditions, and migmatites are common (Bergman et al. 2014). In the southeast and south, the Proterozoic bedrock is well-preserved with primary structures, and the metamorphic grade varies from upper greenschist facies to lower amphibolite facies. There is also a gradient with increasing grade among the Palaeoproterozoic rocks from the east to the Pajala deformation belt in the west (Åkerman & Kero 2012e). The presence of andalusite in metasedimentary rocks west of the Kalixälven river and the lack of andalusite and presence of sillimanite to the east also show that a metamorphic discontinuity exists along the Pajala deformation belt (Fig. 131, Jonsson & Kero 2013d). The prevalence of sillimanite, cordierite, and garnet in migmatitic sedimentary gneisses in the northeast, shows that the bedrock was metamorphosed under upper amphibolite facies conditions (Jonsson & Kero 2013d).

Norrbotten lithotectonic unit

Upper amphibolite facies rocks and migmatites are found throughout the Norrbotten lithotectonic unit, but the rocks most commonly reflect metamorphic conditions of epidote-amphibolite facies to middle amphibolite facies (Fig. 131). The Archaean rocks have been metamorphosed during at least two metamorphic events (Kathol et al. 2015). Large areas with diatexitic migmatite occur 25 km northeast of Boden (Sadeghi et al. in press) and 25 km southeast of Pålkem (Bergström et al. 2015), indicating upper amphibolite facies conditions.

Bothnia-Skellefteå lithotectonic unit

In the Bothnia–Skellefteå lithotectonic unit, the highest grade rocks are granulites south of Jokkmokk. Upper amphibolite facies rocks and migmatites are present throughout the area, but the bedrock most commonly displays epidote-amphibolite facies to middle amphibolite facies conditions (Fig. 131). Apparently lower-grade metamorphic rocks occur in the far west, e.g. in the north of the Snavva–Sjöfallet group. Those rocks lack a close spatial relationship with the c. 1.80 Ga magmatism in the area (Nysten et al. 2014, 2015, Claeson & Antal Lundin in press-b). The metasedimentary rocks close to the latter intrusions show high-grade metamorphic overprinting and often severe deformation. Svecofennian supracrustal rocks of the Arvidsjaur group in the south predominantly reflect greenschist facies metamorphic conditions.

Distribution of key metamorphic minerals

The distribution of some key metamorphic minerals found in the project area is presented below. Metamorphic minerals such as epidote, micas, chlorite, amphibole, and feldspars are not plotted in Fig. 132, but all information has been used to compile the metamorphic map.

Garnet is present in all metamorphic rocks throughout the project area (Fig. 132). However, the widespread occurrence of garnet has not been interpreted as relating to high-pressure metamorphism, due to the total lack of other minerals that are stable under high-pressure metamorphic conditions e.g. kyanite, chloritoid, talc and omphacite.

Andalusite occurs in metasedimentary rocks in the northwestern, south-central, and southeastern parts, and sporadically in the northeast, i.e. in all lithotectonic units of the Svecokarelian orogen in the project area (Fig. 132). Sillimanite is virtually confined to the area west of the Karesuando–Arjeplog

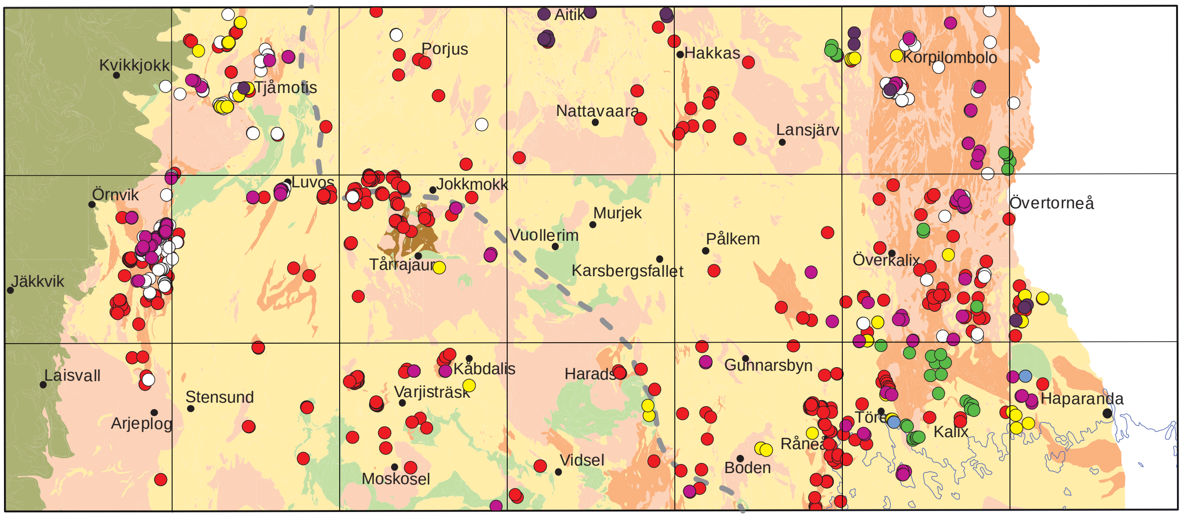

Staurolite Fuchsite Andalusite Garnet Scapolite Cordierite Sillimanite

Figure 132. Occurrence of some key metamorphic minerals in southern Norrbotten County. For legend for the background map see Figure 131.

deformation zone and within the Pajala deformation belt. It is mostly found in metasedimentary rocks, but is also reported from rhyolitoid volcanic rocks of the Arvidsjaur group.

Cordierite occurs throughout the area and is essentially found in metasedimentary rocks, whereas staurolite is only observed in the Bothnian supergroup and the Martimo suite in the south of the Överkalix lithotectonic unit.

The limited areal and sporadic occurrence of the above aluminium-rich key metamorphic minerals is related to the occurrence of rocks of suitable composition, as well as the metamorphic conditions needed for the formation of the particular mineral. Additionally, partial melting of a metamorphic rock during prograde metamorphism, forming migmatite, may consume the above minerals or alter their proportions, but they may also form as retrograde minerals after peak metamorphism.

Fuchsite or chrome mica is a Cr-bearing variety of the mineral muscovite. It is only observed in the east of the project area, mostly in the Överkalix lithotectonic unit, where it mainly occurs in amphibolite to upper amphibolite facies, partially migmatised rocks. Since fuchsite is most commonly observed in greenschist facies assemblages, the fuchsite in the amphibolite facies rocks in the Överkalix lithotectonic unit is interpreted to have formed after peak metamorphic conditions as a retrograde mineral.

Pressure–temperature determinations

Thermobarometric studies of metasedimentary rocks in the Narken area, 27M Korpilombolo NV, indicated regional metamorphic temperatures of about 300–500 °C at pressures between 0.5 and 4.7 kbar (Carlsson 1993).

Thermobarometric determinations in northern Norrbotten County resulted in two groups, 2–4 kbar at 510–570 °C and 6–7.5 kbar at 615–805 °C, but it was unclear whether these were different events or the same one (Bergman et al. 2001).

In the Nautanen deformation zone at Nautanen just north of the project area, a recent thermobarometric study of supracrustal rocks shows average pressures below 4 kbar and a temperature range of approximately 475 °C to just below 700 °C (Tollefsen 2014). The highest temperatures were recorded close to a granite intrusion and an increase of temperature towards the later intrusive rocks was interpreted as a possible regional or prograde contact metamorphism that might not be related to the Nautanen deformation zone.

The bedrock in the Skellefte and Arvidsjaur districts, south of the project area, show mostly greenschist facies metamorphism and possibly even lower metamorphic conditions based on thermobarometric studies (Nicolson 1993, Kathol & Weihed 2005). Most other rocks adjacent to the project area, apart from the youngest intrusive rocks, have been affected by medium- to high-grade metamorphism, possibly upper amphibolite facies conditions at mostly low-pressures, as indicated by thermobarometry (Kathol & Weihed 2005).

Hydrothermal metamorphism

Significant hydrothermal alterations are evident in many volcanic rocks in the project area. This is essential knowledge, since ore mineralisation is often spatially related to hydrothermal alteration (e.g. Gifkins et al. 2005). The protolith of the deposits and the host rocks are frequently severely altered, and metasomatism forms rocks that show no resemblance to the original protoliths (e.g. Gifkins et al. 2005). Few of the alterations relating to hydrothermal activity have been studied in southern Norrbotten County, despite their potential use in mineral exploration.

Various metasomatic alterations of feldspar, particularly sericitisation and albitisation, are also present in most rocks, and are usually linked to hydrothermal activity in and around deformation zones (Claeson & Antal Lundin 2012c). Hydrothermally formed epidote is commonly found in the volcanic rocks of all generations, and alteration is sometimes pervasive, but usually occurs as fracture filling.

The hydrothermally altered felsic volcanic rocks of the Arvidsjaur group occurring in the southeast of map area 27K Nattavaara, exhibit very low potassium content (0.2–0.4%), which suggests albitisation of the feldspars. At Namai (7410746/693008), 25 km northwest of Jokkmokk, the altered felsic volcanic rocks of the Arvidsjaur group show a potassium content of 0.9%, whereas the unaltered felsic volcanic rock shows a potassium content of 5.5% (Claeson & Antal Lundin in press-c). In some cases, the volcanic rock is almost completely white and has been depleted in potassium. At other locations, alteration resulted in strong red colouration of the volcanic rock. Hydrothermal alteration has been observed in a rhyolite of the Arvidsjaur group north-northwest of Hájkak (7420844/710390) 13 km south of Porjus, where enrichment of sodium and almost complete depletion of potassium is recorded (Kathol et al. 2015).

At Latanjarka (7424356/657974), 3 km southeast of Tjåmotis, strong hydrothermal alteration is observed in a sequence of dacitoid and andesitoid rocks of the Arvidsjaur group. Skarn consisting of pink feldspar, magnetite, emerald green epidote, green amphibole, and manganese oxides psilomelane-hausmannite occurs, the manganese oxides appearing as powder on surfaces and sometimes as solid crystals (Claeson & Antal Lundin 2015).

Felsic volcanic rocks of the Arvidsjaur group in the area west of Svanisträsket (7346197/778250), 10 km northeast of Harads, have been hydrothermally altered, leading to the formation of sericite- and dumortierite-bearing quartzite (Kathol et al. 2012b).

Hydrothermally formed tourmalinite such as dykes, apophyses, and fracture fillings in rhyolite of the Porphyrite group occur south of Nedre Ljusselet (7322336/703679), 10 km north of Moskosel, and north of Suddesvare (7313256/686749), 15 km west of Moskosel (Kathol et al. 2012a).

Scapolite is present as a secondary mineral formed during hydrothermal alteration of mostly volcanic rocks of the Arvidsjaur group in map area 27K Nattavaara. According to Frietsch et al. (1997), this suggests the presence of a high-chlorine fluid, and alteration is strongest close to deformation zones (Claeson & Antal Lundin 2012c). Scapolite usually forms porphyroblasts, but locally also occurs as veinlets and euhedral crystals in vugs. There are observations reported from thin sections of gabbros where scapolite completely replaces plagioclase (27K Nattavaara). Scapolite is sporadically observed in Svecofennian basalt to andesite and sedimentary rocks of the Bothnian supergroup in map area Korpilombolo NV, and in sedimentary rocks of the Sockberget group in map area Karungi SV (Fig. 132).

The Aitik deposit, just north of map area 27K Nattavaara, has been affected by several metamorphic

Figure 133. Drill core from Svikkomaa (7425104/761261). A. Half-metre-wide quartz-filled zone with vugs where quartz crystals have grown. Photo: Dick Claeson.

Figure 134. Red pigmented, extensively altered quartz monzodiorite, brecciated and with quartz-filled fractures. Drill core from Svikkomaa. Photo: Dick Claeson.

Figure 135. Zone where the rock is brecciated with traversing quartz-filled fractures and extensive red to pink pigmentation. Drill core from Svikkomaa. Photo: Dick Claeson.

events, some related to regional metamorphism, others to magmatic activity with associated hydrothermal alterations (Wanhainen et al. 2005).

A combined geophysical and geological investigation of relatively small but numerous circular, low-magnetic anomalies visible in the airborne magnetic data in the Nattavaara map area, showed pervasive alterations and pipe-like structures resembling those found in porphyry-epithermal breccia-pipe systems or similar geometries (Claeson et al. 2012). The alteration zones consist of quartz-filled fractures and pervasive green to red staining (Figs. 133–136).

Minerals from the epidote group and chlorite indicate moderate temperatures and low pressure

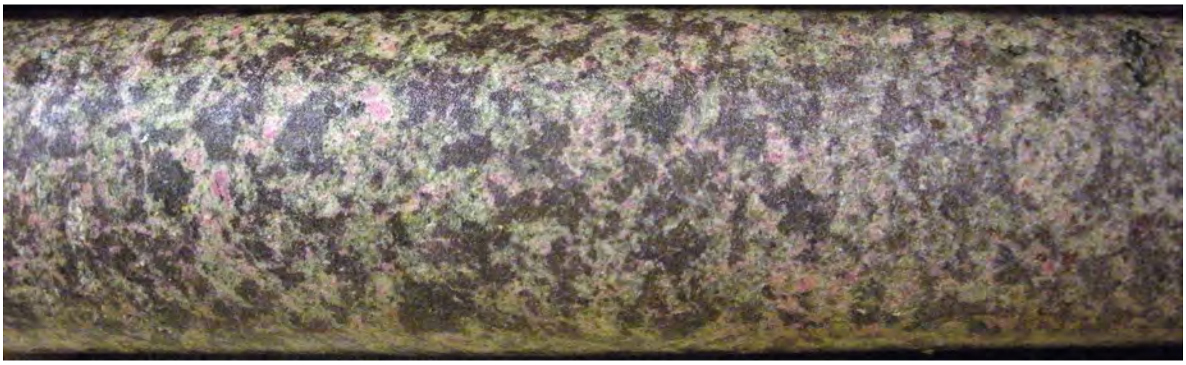

Figure 136. Green and red pigmented, significantly altered quartz monzodiorite. Drill core from Svikkomaa. Photo: Dick Claeson.

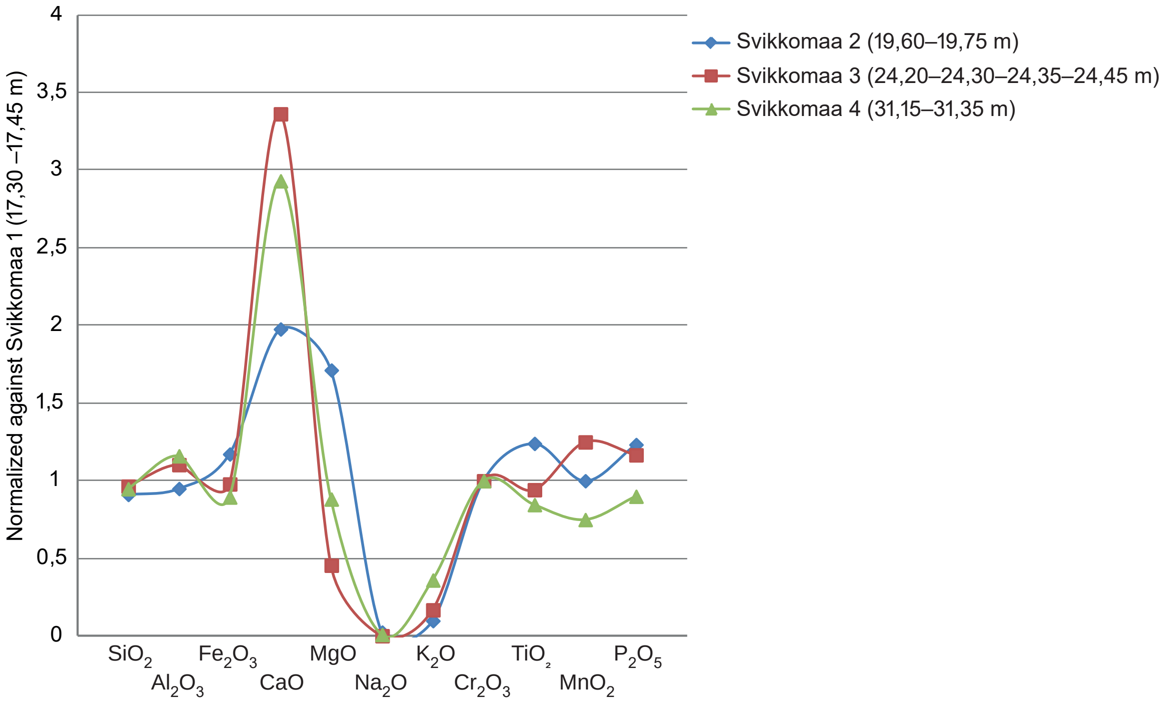

Figure 137. Plot of severely altered rock samples from the drill core at Svikkomaa, normalised against a rock sample of well-preserved monzodiorite from the same drill core.

during alteration. The large number of open spaces in the quartz-rich zones, with the presence of vuggy quartz, indicates alteration at relatively shallow depth, suggesting conditions resembling an epithermal environment (e.g. Thompson & Thompson 1996, Gifkins et al. 2005, Pirajno 2009). The conditions may also be likened to those in root-zones of breccia-pipes (e.g. Pirajno 2009), as well as root-zones of some porphyry systems (e.g. Seedorff et al. 2008). Hydrothermal activity is usually caused by high concentrations of aqueous fluids or vapours and carbon dioxide originating from acid magmatic systems, at shallow crustal depth (e.g. Pirajno 2009). The compositions of epidote-zoisite in the drill core from Svikkomaa resemble compositions reported from metamorphic environments in greenschist to amphibolite facies conditions (Grapes & Hoskin 2004).

The geochemical analyses show a significant reduction of sodium and potassium and strong enrichment of calcium in the altered quartz monzodiorite-monzodiorite compared with the relatively unaltered monzodiorite (Fig. 137). Whether it is the green or the red pigmentation that predominates in the alteration, the different pigmentations reflect similar metasomatism (cf. Fettes & Desmons 2007 for definition). The pattern in Figure 137 reflects the chemical compositions of the newly formed chlorite and the epidote group minerals (Deer et al. 1992). The REE diagram displays similar patterns for the altered and the unaltered rocks, but generally lower concentrations for the altered quartz monzodiorite-monzodiorite (Claeson et al. 2012).

There are a variety of pipe-like formations where it is considered that hydrothermal activity is one of the factors giving rise to deposits containing ores of various kinds (e.g. Pollard et al. 1991, Pirajno 2009). The samples analysed in this work lack mineralised parts. However, the indications that the fluids contained dissolved sulphur render the pipe-like formations potential targets for future studies, since metals are easily dissolved and transported in hydrothermal solutions containing sulphur (e.g. Seward 1973, Zezin et al. 2007, Wilkinson et al. 2009). These results should also be used for exploration of the region, i.e. hydrothermal systems generated from the c. 1 790 to 1 800 Ma granite to monzodiorite magmas may localise and concentrate metals in older overlying volcanic successions and form ore deposits (Claeson et al. 2012).

In the c. 1.80 Ga granite belonging to the Edefors suite 3.5 km northeast of Tjåmotis, an anomalous area is present where hydrothermal alteration of the granite has formed unakite (Fig. 138). The plagioclase is mostly altered to epidote and chlorite is also present, along with signs of episyenitisation (Fig. 139).

Figure 138. Hydrothermally altered granite in which plagioclase has been replaced by epidote and the rock is altered to a unakite (7428689/657713). Photo: Carl-Axel Triumf.

Figure 139. Close-up of unakite (7428689/657713). Photo: Anders Gustafsson.

Detailed observations relating to metamorphism

Karelian supracrustal and intrusive rocks, c. 2.40–1.96 Ga

The carbonate rocks in the Karelian Kalix Greenstone Belt of the Kalix group record greenschist facies and epidote-amphibolite facies metamorphism within a 600 m thick succession of volcanic, volcaniclastic and siliciclastic rocks (Melezhik & Fallick 2010).

Svecofennian supracrustal rocks, c. 1.92–1.87 Ga (Bothnian supergroup)

Cordierite, sillimanite, garnet, and gahnite (green spinel) occurs in grey, banded paragneiss of the Bothnian supergroup in map area 26I Luvos (Hellström & Berggren 2014). The coexistence of gahnite, garnet, sillimanite and cordierite is diagnostic of high-grade conditions (e.g. Nichols et al. 1992). Although the gahnite only occurs in the zinc-mineralised parts of Luspevaratj, it suggests upper amphibolite facies, and just to the northeast possibly epidote-amphibolite facies conditions. The paragneiss at the Luspevaratj deposit (7395441/668533), 3 km southwest of Luvos, shows fibrous sillimanite and altered cordierite (Fig. 140), as well as gahnite with needles of quartz (Fig. 141). Garnet, sillimanite and cordierite are found just south of Luspevaratj (Fig. 142).

Well-preserved metasedimentary rocks, sandstone and arkose, of the Bothnian supergroup in the west of map area 26K Murjek show bedding; sorting and roundness of grains are discernible. This indicates low-grade metamorphism, possibly greenschist facies. The greywacke of the Bothnian supergroup in the same area shows different degrees of metamorphic overprinting, at some localities greenschist facies metamorphism, whereas migmatitic veining is evident in other places, suggesting amphibolite facies conditions. To some extent this probably depends on rock composition, whereby rocks with less mica or other hydrous minerals are less prone to readily alter and may therefore lack veins. However, the most strongly altered metasedimentary rocks are those close to the younger intrusive rocks of the Edefors suite, where granite, quartz monzonite, gabbroid, and ultramafic rocks interact. In some outcrops the greywacke of the Bothnian supergroup form xenoliths in intrusion breccia (Figs. 143, 144).

The prevalence of sillimanite, cordierite, and garnet in the migmatitic sedimentary gneisses of the Bothnian supergroup in the centre and east of map area 27M Korpilombolo, shows that rocks have

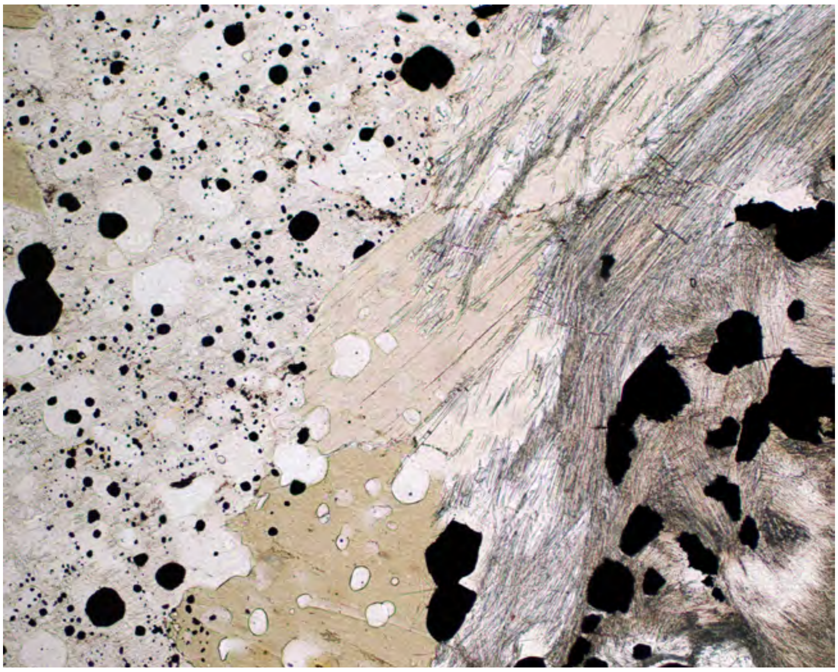

Figure 140. Paragneiss from Luspevaratj showing fibrous sillimanite to the right, altered cordierite with rounded opaque inclusions to the left, and biotite in the centre. Polarised light with parallel nicol; the long side of the image is approximately 1.4 mm (7395441/668533). Photomicrograph: Fredrik Hellström.

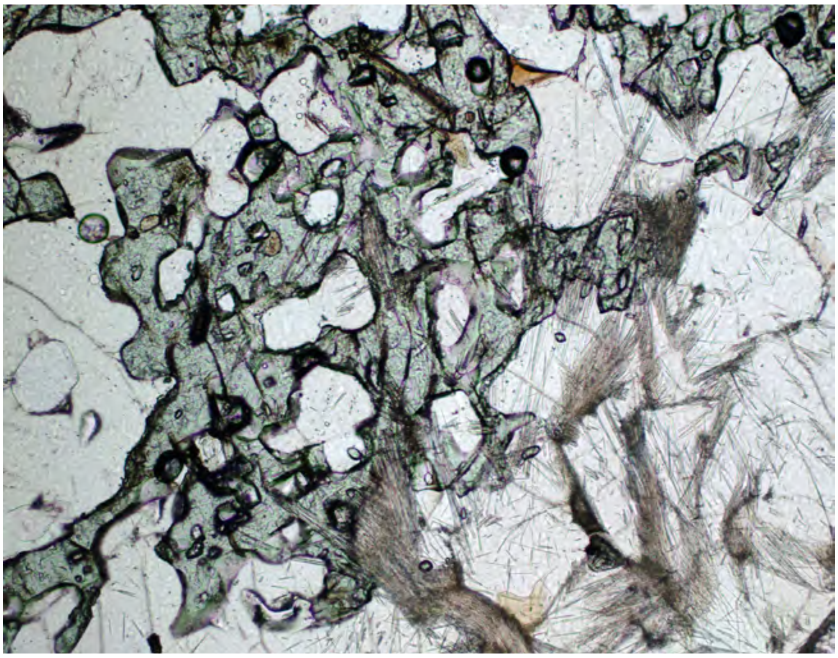

Figure 141. Green spinel in paragneiss from Luspevaratj with quartz. Needles of fibrous sillimanite seen to the right. Polarised light with parallel nicol; the long side of the image is approximately 1.4 mm (7395441/668533). Photomicrograph: Fredrik Hellström.

Figure 142. Garnet-, sillimanite- and cordierite-bearing paragneiss south of Luspevaratj (7393986/668060). Photo: Fredrik Hellström.

Figure 143. Magmatically deformed Edefors quartz monzonite in an intrusive breccia with xenoliths of greywacke. Note the lighter appearance of the former when in contact with xenoliths (7370128/740100). Photo: Benno Kathol.

Figure 144. Close-up of incipient brecciation of the greywacke by the Edefors quartz monzonite (7370128/740100). Photo: Benno Kathol.

been metamorphosed under upper amphibolite facies conditions (Jonsson & Kero 2013d). Other observations indicating high-grade conditions include coronas of plagioclase around corroded garnet and spinel in cordierite in garnet-rich migmatite (Jonsson & Kero 2013d). A possible interpretation of the spinel-cordierite association is that it represents the effects of a contact metamorphic thermal influence by intrusive rocks. Corundum has also been found in silica-poor biotite-muscovite-feldspar-sillimanite gneiss of unknown origin at Isovaara (Jonsson & Kero 2013d). The corundum occurs mostly as subhedral porphyroblasts that have overgrown the foliation, and it is therefore likely that corundum formed during a relatively late stage of the tectonothermal evolution.

Preserved bedding is common in the metasedimentary rocks of the Bothnian supergroup in the southeast of the project area where the metamorphic grade is lowest. Porphyroblasts of cordierite or muscovite occur locally, and quartz veins are common. The rocks are estimated to have been metamorphosed under lower amphibolite facies conditions. To the west, metamorphic overprinting is more severe and estimated to be middle amphibolite facies, with local occurrence of garnet and abundant quartz-feldspar veins (Bergström et al. 2015).

In the Bothnian supergroup in the south of map area 25M Kalix NV, the presence of staurolite and andalusite indicates lower amphibolite facies metamorphism of metasedimentary rocks (Fig. 145). In the northwest, the metasedimentary rocks are often veined; cordierite occurs frequently and occasional presence of garnet is reported (Wikström 1995). Further to the east in map area 25N Haparanda, key indicator minerals are cordierite and andalusite. The degree of metamorphism increases to the northwest and is accompanied by incipient anatexis of mica-rich rocks (Fig. 146).

Figure 145. Staurolite and andalusite in the Bothnian supergroup, indicating lower amphibolite facies, southern part of map area 25M Kalix NV (7328084/851525). Photo: Stefan Bergman.

Figure 146. Foliated metasiltstone with 5–10 mm large porphyroblasts of andalusite, southwestern part of map area 25N Haparanda NV (7328271/891933). Photo: Stefan Bergman.

Figure 147. Hornblende blastesis in basalt from the Porphyrite group. Metamorphic grade varies from epidote-amphibolite to amphibolite facies (7363380/784280). Photo: Ulf Bergström.

Svecofennian supracrustal rocks, c. 1.90–1.87 Ga (Porphyrite group)

Volcanic rocks in parts of map area 26K Murjek belong to the Porphyrite group. Hornblende blastesis in basalt from this area illustrates epidote-amphibolite to amphibolite facies metamorphism (Fig. 147).

Early Svecokarelian intrusive rocks, c. 1.91–1.87 Ga (Haparanda and Jörn GI suites)

The Haparanda and Jörn GI suites have undergone one or more metamorphic events. Garnet is observed in map area 25K Harads in granodiorite to tonalite (Kathol et al. 2012b). High-grade metamorphism is also apparent in gneissic granodiorite to tonalite of the Haparanda suite east of Roavoajvve, some 20 km northeast of Jokkmokk (Kathol et al. 2015). The Haparanda suite rocks in map areas 27K Nattavaara and 27L Lansjärv have been metamorphosed in places at high temperature and moderate pressure to form gneisses with granitic and pegmatitic veinlets, veins, and sizeable areas of anatectic granite (Claeson & Antal Lundin 2012c, Hellström et al. 2012d). The western part of map area 25M Kalix NV consists of relatively well-preserved granodiorite, while in the east granodiorite shows migmatisation (Wikström 1995).

Early Svecokarelian metamorphic rocks

Significant areas of metamorphic rocks such as diatexite and metatexite migmatites occur 25 km northeast of Boden (Sadeghi et al. in press), and diatexite migmatitic rocks 25 km southeast of Pålkem (Bergström et al. 2015). The protolith of the former is probably the surrounding metagreywacke of the Bothnian supergroup, whereas the protolith of the latter is a metagreywacke from the same unit or from the Sockberget group. The estimated degree of metamorphism is middle amphibolite facies at the latter location (Bergström et al. 2015). Age determinations show ages of around 1.88 Ga for the formation of migmatites (Sadeghi & Hellström 2018a, Bergström et al. in preparation-a).

Svecofennian supracrustal rocks, c. 1.89–1.86 Ga (Arvidsjaur group)

Well-preserved rocks of the Arvidsjaur group showing low-grade metamorphism are common in the south-central part of the project area. This applies particularly to rocks west of the Karsbergsfallet deformation zone in the Harads area (Kathol et al. 2012a, b).

The metamorphic overprinting of the Arvidsjaur group rocks in map area 25I Stensund NV and NO reached approximately lower amphibolite facies, but is locally higher and in places seems to have reached upper amphibolite facies conditions (e.g. Kathol & Aaro 2006a, b, Mellqvist & Aaro 2006a, b). In comparison, metamorphism of the bedrock in map areas 25I Stensund SV and SO, as well as in other parts of the Skellefte and Arvidsjaur areas mostly varies between greenschist and lower amphibolite facies. The metamorphic grade generally increases towards the northern map areas. Further to the north, in map areas 27J Porjus NV and NO, signs of migmatisation have also been observed in rhyolite of the Arvidsjaur group at Porjusberget (Nysten et al. 2015). Along the road between Vuollerim and Jokkmokk, map area 26K Murjek, a banded and foliated rhyolite occurs that displays lower amphibolite facies conditions.

At Tjerkisberget (7376949/731144) 26 km southeast of Jokkmokk, cordierite and sillimanite occur in mica-rich metasedimentary rocks of the Arvidsjaur group that are possibly volcaniclastic in origin. Porphyroblasts of cordierite with inclusions of biotite and quartz show poikiloblastic and porphyroblastic textures (Figs. 148a, b). The mostly anhedral to subhedral cordierite grains are xenoblastic, which along with the numerous inclusions, indicates low-grade metamorphism (e.g. Deer et al. 1997). The inclusions define an internal foliation parallel to the longitudinal axes of the poikiloblasts. This foliation is discordant to the matrix foliation defined by biotite draped around the poikiloblast (Figs. 148a, b). This suggests that deformation continued after the poikiloblast growth. The cordierite crystals grew during prograde metamorphism; their larger size and rigidity compared to the matrix

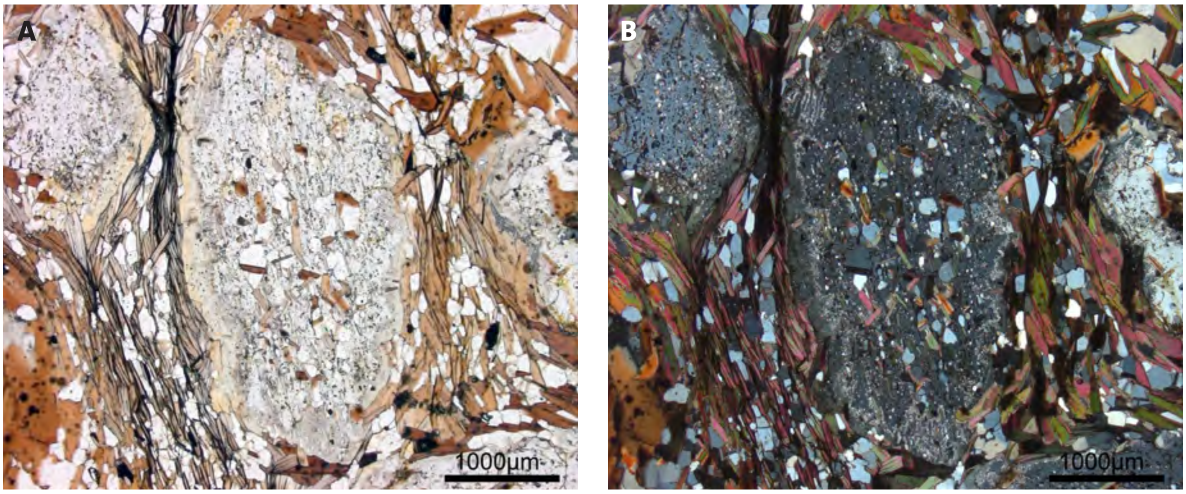

Figure 148. Alteration in fractures and at the edges of cordierite crystals with formation of yellowish pinite. **A.** Plane polarised light. **B.** Crossed nicols (7376949/731144). Photomicrograph: Dick Claeson.

forced deformation to be partitioned into the finer-grained and softer matrix (e.g. Vernon 1998). The common alteration of cordierite to yellowish pinite is also seen in fractures and along grain boundaries (Figs. 148a, b).

Svecofennian supracrustal rocks, c. 1.88–1.84 Ga (Snavva–Sjöfallet and Svartlå groups)

North of Tjåmotis, the metamorphic grade increases from north to south in the metasedimentary rocks of the Snavva–Sjöfallet group east and south of the syenitoid-granite intrusion north of Tjåmotis, as well as on the western flank of the intrusion, where the transition from sedimentary rocks to Arvidsjaur volcanic rocks occurs (Nysten et al. 2014). Sillimanite-rich gneisses (locally cordierite-bearing) in particular are present in the higher grade rocks. Sillimanite and manganese-bearing andalusite (viridine) are present just south of Tjåmotis village near the Latanjarka wollastonite deposit (Fig. 149). The wollastonite clearly shows that contact metamorphism has been caused by the younger granitic intrusion, and the latter also produced sillimanite-bearing diatexitic rocks displaying a granitic texture (Nysten et al. 2015). Highly variable behaviour of different lithologies during metamorphism can be observed here, from sandstone with preserved primary sedimentary structures via aluminium silicate-bearing metasedimentary rocks to diatexite within tens of metres (Fig. 149). Garnet and sillimanite ± andalusite together with anatectic melt, along with an absence of cordierite in most rocks of the Snavva–Sjöfallet group, point to a pressure above 3 kbar for the rocks in map area 27I Tjåmotis SV (Claeson & Antal Lundin 2015). Partial melting under water-saturated conditions starts in metapelitic rocks at 650–700 °C (Bucher & Frey 1994). Since most of the rocks encountered show lower amounts of mica minerals than ordinary metapelite, formation of anatectic melts indicates that temperatures were higher than 650–700 °C. Grossular garnet, piemontite and epidote are common skarn minerals in marble associated with the Ultevis manganese mineralisation, north and south of the Seitevare dam at the Tjatjisvare and Rakten localities, respectively.

The Snavva–Sjöfallet group is composed of sandstone, arkose, greywacke and claystone, including conglomerate. In different areas these rocks are to varying degrees altered into paragneiss, slate, and mica schist (Fig. 150). The metamorphic grade throughout the Snavva–Sjöfallet group generally increases towards the south (Kathol et al. 2011, 2012c). In map areas 26H Jäkkvik NO and SO, low-grade rocks and migmatitic rocks occur in the Snavva–Sjöfallet group, where the migmatites are characterised in many places by the occurrence of sillimanite, garnet and cordierite. Migmatisation is common

Figure 149. Metasedimentary rock belonging to the Snavva–Sjöfallet group carrying up to 25 x 8 mm large Mn-andalusite (viridine) crystals oriented in bands. Adjacent to these, sillimanite-bearing bands occur in the same kind of rock (7425333/657912). Photo: Per Nysten.

Figure 150. Conglomerate with clasts of a sillimanite-bearing, quartz-rich metasedimentary rock, northern Apmohalvön (7375070/630551). Photo: Daniel Larsson.

in map area 26H Jäkkvik NO, except in areas approximately 25 km southeast of Örnvik, at Vuotsas (7377800/634300) and in the area between lakes Tapmuk (7380802/632420) and Pällajaure (7379000/629800). The degree of anatexis and migmatisation varies from weak with granitic veins in sandstone or quartzite to stromatite (Fig. 151), nebulite and diatexite (Kathol et al. 2011).

High-grade metasedimentary rocks possibly belonging to the Snavva–Sjöfallet group contain sillimanite southeast of Parinåive, 11 km northwest of Porjus (Nysten et al. 2015). Recrystallisation and growth of blasts are other expressions of metamorphism.

Well-preserved rocks showing low-grade metamorphism are usually found in map area 25K Harads, in particular the Svartlå group west of the Karsbergsfallet deformation zone (Kathol et al. 2012b). Andalusite occurs in greywacke and argillite in the Svartlå group.

Figure 151. Stromatite migmatite, southeast of Hapakjauratj (7381896/635396). Photo: Carl-Henrik Pettersson.

Early Svecokarelian intrusive rocks, c. 1.89–1.85 Ga (Perthite monzonite suite)

The Perthite monzonite suite rocks of map areas 27K Nattavaara, 27J Porjus and 27L Lansjärv show metamorphic overprinting in amphibolite facies (Claeson & Antal Lundin 2012c, Hellström et al. 2012d, Claeson & Antal Lundin in press-c). Formation of granitic and pegmatitic veinlets, veins, and larger parts of anatectic granite is evident in some gneissic varieties. The northwest of map area 26K Murjek predominantly comprises recrystallised and foliated red metagranite. High-grade rocks such as a gneissic, porphyroblastic granite are found in the northwest of map area 25I Stensund e.g. at Gassabårktjärn (7338200/639200), 12 km northeast of Arjeplog (Mellqvist & Aaro 2006a). The relict porphyritic granites of the Perthite monzonite suite often show sugary grain due to recrystallisation (e.g. Nysten et al. 2015).

Well-preserved intrusive rocks of the Perthite monzonite suite showing low-grade metamorphism are present in map areas 25K Harads (Kathol et al. 2012b) and in 25J Moskosel (Kathol et al. 2012a).

Late Svecokarelian supracrustal rocks, c. 1.84–1.77 Ga

The youngest late Svecokarelian supracrustal rocks, c. 1.77 Ga volcanic sequences in map area 27I Tjåmotis SO at Tjäkkaure (7404458/683199), 30 km west-northwest of Jokkmokk, are well-preserved. They are significantly better preserved than the surrounding amphibolite facies volcanic rocks of the Arvidsjaur group, with only minor growth of sub-grains of quartz. Minor undulose extinction is seen under the microscope, with aggregates of amphibole, all indicative of low-grade metamorphic recrystallisation (Claeson & Antal Lundin in press-b). In places, they are hydrothermally altered, and epidote occurs in the rock and as fracture fillings. Magnetite occurs as aggregates, often with amphibole.

Late Svecokarelian metamorphic rocks

Rocks formed under granulite facies conditions are found only in parts of map area 26J Jokkmokk NV and NO (Claeson & Antal Lundin in press-a). The mafic granulite definition used in Coutinho et al. (2007) is not verified by petrographic work or observation of orthopyroxene, but the mafic granulite is inferred from partial melting of basic and intermediate rocks. Future, more detailed studies may

Figure 152. Schollen migmatite in a former volcanic sequence. The protolith is basaltic to andesitic in composition. Light-coloured veins of granodiorite-tonalite-trondhjemite compositions (7386061/703460). Photo: Dick Claeson.

conclude that most of the rocks in the area should be renamed basic to intermediate migmatite, formed under granulite facies conditions. The mafic granulites of map area 26J Jokkmokk in the area south of Jokkmokk show schollen migmatite with rafts of basalt and restite 'floating' in the neosome (Claeson & Antal Lundin in press-a, Fig. 152). The protolith is interpreted to have been mostly volcanic rocks of andesitic, basaltic and to a lesser extent dacitic in composition. The anatectic minimum melts are granodioritic, tonalitic and trondhjemitic in composition and not granitic. This is in line with experimental data showing the melts generated from basic and intermediate rocks undergoing dehydration melting (e.g. Beard & Lofgren 1991). Facies boundaries depend on temperature and lithostatic pressure as well as P_{H_2O}. Decreasing P_{H_2O} lowers the transition to the higher-grade facies (e.g. Spear 1993). Experimental data suggest amphibolite to granulite transition at 800–850 °C with $P_{H_2O} = P_{total}$. But natural parageneses show lower temperatures for the transition at 700–750 °C, evidencing the importance of access to H_2O during metamorphism (e.g. Spear 1993). As pointed out in Bucher & Frey (1994), mafic migmatites, amphibolites, and mafic granulites may occur next to each other at the same temperature (e.g. 750 °C, P = 6 kbar), the only variance being the composition of the fluid phase present in the different rocks at the time of metamorphism. Garnet is present in the mafic granulites but is not interpreted as related to high-pressure metamorphism within the area with mafic granulite (Figs. 153a, b), since no mineral assemblages in the gabbros or the granulites indicate crystallisation of the gabbros or metamorphism at elevated pressures. The obvious reason for granulite facies metamorphism and partial melting is the heat input from the very large amounts of basic magmas at 1 000 to 1 250 °C, which later crystallised to form gabbroid rocks and ultramafic cumulates at c. 1.80 Ga.

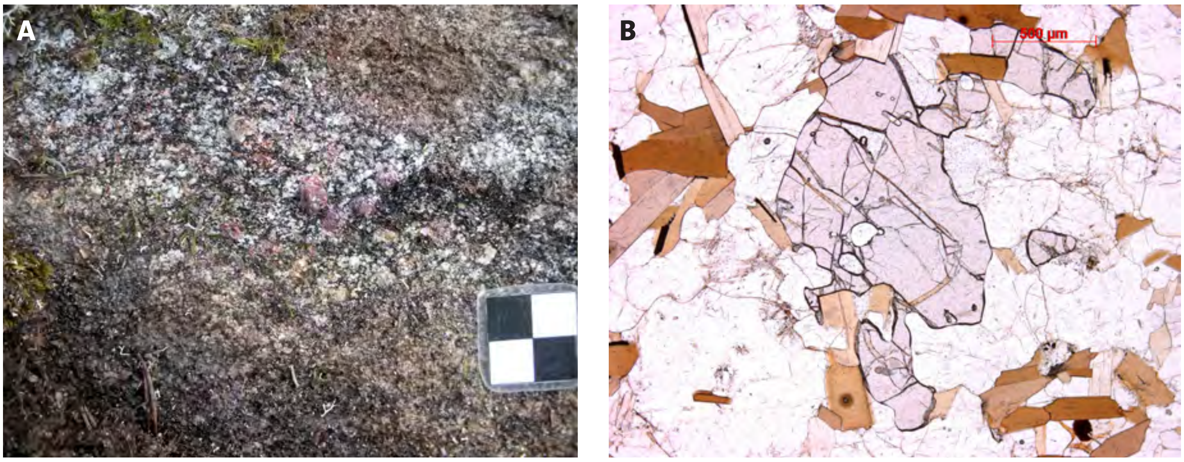

Figure 153. **A.** Veined garnet amphibolite with 1–10 mm large garnet crystals (1–5%) from the mafic granulite area in 26J Jokkmokk NV (7386612/702587). **B.** Garnet amphibolite of andesitic origin showing garnet, plagioclase, biotite and quartz. Same rock as in A. Photo and micrograph: Dick Claeson.

Summary

The metamorphic overprinting of the rocks in the project area is heterogeneous, and at present not enough studies have been performed to compile a reliable, detailed metamorphic map. However, this compilation shows that several regional metamorphic events have taken place. Major magmatic activity has altered rocks into migmatites, which to the naked eye bear no resemblance to their protoliths. After c. 1.77 Ga no major regional metamorphic event above greenschist facies has overprinted the project area. Strongly variable behaviour during metamorphism of different lithologies with varying contents of hydrous minerals can be observed. This is partly due to contact metamorphism related to intrusive events of different ages. Few alterations associated with hydrothermal activity have been studied in the project area, despite their possible use in mineral exploration.

7. Mineral resources

Dick Claeson & Per Nysten

MINING HISTORY

The project area is situated between the copper- and iron-rich Northern Norrbotten ore province and the polymetallic Skellefte district. The two most important ore deposits in the area are Laisvall at the Caledonian front in the far west and Laver in the south. Lead and zinc were mined at Laisvall in the late 20th century; copper was the main commodity at Laver. It is also worth noting that the large active Aitik mine is just north of the project area. Boliden has recently extended its Aitik mining operations further south into the project area (Boliden 2017). Other metals of importance occurring in sub-economic amounts in the project area are nickel, molybdenum, platinum-group elements (PGE), gold, chromium, titanium, manganese, uranium, thorium, and locally rare earth elements (REE). Extensive exploration programmes, including geophysical and geochemical investigations coupled with bedrock mapping and drilling, have been utilised to investigate these deposits further. The story behind the discovery of manganese mineralisation at Ultevis is interesting: it began with boulders found near Murjek in 1935. In 1943 they were traced back to their origin from outcrops at Stuor Njåskes, more than 120 km away.

Industrial minerals such as wollastonite, aluminium silicates, carbonate rocks, and feldspar have been explored in southern Norrbotten County, and have to some extent been mined as well. More detailed information on the conditions and history of exploration is given under the description of each deposit.

CLASSIFICATION OF DEPOSITS

In the following description, mineral deposits have been classified according to the style of mineralisation and their relation to the host rocks, although the genetic implications are always open to discussion (Fig. 154). We have adhered to the genetic interpretation in earlier work, if this is not obviously incorrect in light of current knowledge. Metallic deposits are divided into the following categories: igneous types including gabbroic to ultramafic layered intrusions and porphyry copper types; stratiform–stratabound ores including base metals and iron oxides; sulphide deposits hosted by supracrustal rocks; epigenetic base metal deposits together with hydrothermal veins; other metal deposits. Within this last-mentioned group, a subdivision is presented according to the main commodity present. The classification of industrial mineral deposits is mainly based on commodity. Additionally, one deposit of dimension stone is described, as well as some major quarries for aggregate rock.

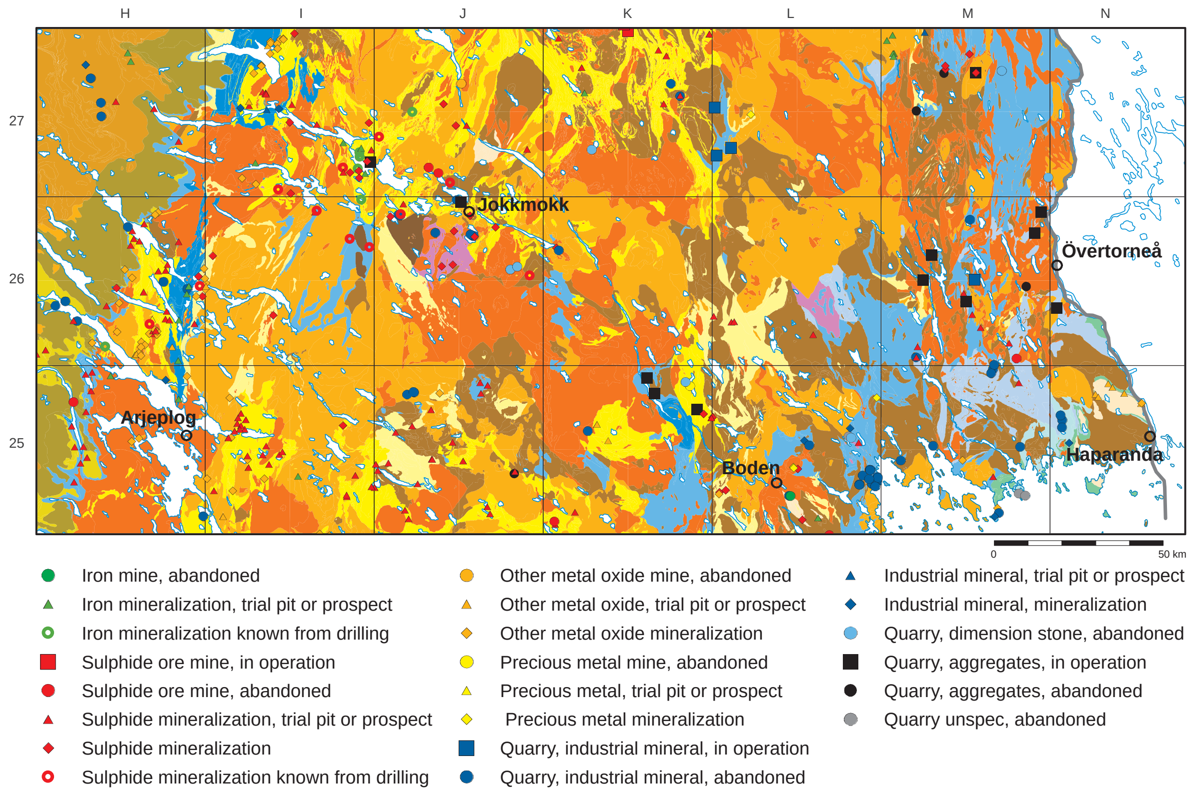

Figure 154. Distribution of the principal types of metallic and non-metallic mineral deposits in southern Norrbotten County. The deposits are presented on a simplified bedrock geological map. Geological units as in Figure 17b.

ORE DEPOSITS RELATED TO MAGMATIC ACTIVITY

Gabbroic copper-nickel(-PGE) ore deposits of Notträsk type occur close to Boden, at Fiskelträsk (26L Pålkem) and Saivovaara (27K Nattavaara). Layered, mafic to partly ultramafic PGE and gold-containing intrusions are found at Kukkola (25N Haparanda) and Ruoutevare (26J Jokkmokk), the former also bearing chromium (Filén 2001). Deposits hosted by felsic rocks of copper-(gold, molybdenum) porphyry type occur at Vaikijaur (26J Porjus), Laver (25K Harads), Jårbojoki (27K Nattavaara) and Aitik (28K Gällivare–27K Nattavaara). The main part of the large open cut mine at Aitik is situated north of the project area, but the mineralised zone extends into map sheet 27K Nattavaara.

Gabbroic copper-nickel (platinum, palladium, gold) deposits

Notträsk type nickel-iron-copper-gold-(PGE) (25L Boden)

The deposit at Notträsk is situated 7 km northeast of Boden. The nickel-sulphide mineralisation has been known since the early 19th century, and in 1908 a nickel-bearing vein was found when a well was bored. Further prospecting by Boliden and SGU in the 1940s and 1970s was unsuccessful. In 1975 an outcrop of massive nickel-bearing pyrrhotite-rich gabbro was found during road construction. Gränges International drilled four holes in 1977, and geophysical measurements located electrical conductors in the south of the area. In 1978–80 LKAB Exploration made further geophysical measurements and took biogeochemical samples. Arvanitidis (1982) published a detailed investigation of the Notträsk intrusion. Further drilling took place that year, along with additional geophysical measurements. During 1988–1989 Swedish Geological AB (SGAB) drilled five holes in a profile of the inner parts of the intrusion to investigate PGE-bearing rocks and make a stratigraphy of the cumulate rocks (Filén et al. 1989). Only sub-economic levels of PGE and gold were reported; notable grades of platinum and palladium were found in only two of the sections drilled in 1988–89 in the central part of the intrusion. Anomalous PGE values were found in the anorthositic olivine gabbro associated with disseminated sulphides. Content of platinum, palladium and gold are reported as Pt 0.1–1.1 ppm, Pd 0.08–0.3 ppm, Au 0.01–0.17 ppm, but reproducibility of the values was not good. This was attributed to nugget effects. Despite several efforts by a number of companies to locate economically viable deposits of nickel, copper, PGE or gold, none has yet been successful. Prospecting continued in 2016. The PGE and gold mineralisation has also been described using geochemical and mineralogical data (Hassan 2008).

The Notträsk intrusion is funnel-shaped with a zoned arrangement of the interior. It consists of marginal border rocks, a ferrogabbroic rock series, a troctolitic-anorthositic series and a gabbroic rock series. The zones show modal layers, in cases repeated in a rhythmic way. The pluton intrudes paragneisses and is surrounded by pyroxene hornfels and a dioritic-granodioritic rock association. The marginal border group around the southern contact displays different sulphide mineralisation types. Petrologically, the mineralisations may be classified into those hosted in igneous rocks and those hosted by pyrrhotite-graphite schists. Physically, they occur as disseminations and massive mineralisations. The dissemination type is associated with quartz-biotite-bearing gabbronorite. Calcite and chlorite form late-stage veinlets cutting both sulphides and silicates, where the sulphides show fairly sharp contacts with silicates. The latter also appear to have been replaced by sulphides. Fragments of massive sulphide and pyrrhotite-graphite schist are readily found in disseminated ore. The massive mineralisation type consists of polycrystalline pyrrhotite grading into disseminated types, and also into breccia-type mineralisation closely related to fault and shear-zones. These zones may have been important for the extension of the associated alteration. Pyrrhotite constitutes 89% of total sulphides and occurs in all types of mineralisation at Notträsk. Pentlandite constitutes 5% of total sulphides occurring as two different types. Pentlandite-A occurs as large granular patches that can form narrow veins within pyrrhotite and between pyrrhotite grains, while pentlandite-B is found in pyrrhotite as thin lamellae. Alteration of pentlandite-A resulted in the formation of violarite. Chalcopyrite constitutes approximately 6% of all sulphides forming simple intergrowths with granular pentlandite, irregular masses with pyrrhotite, and is observed between pyrrhotite grains. It also occurs as isolated grains in silicates, fracture fillings, and as early segregation droplets. Additional minerals are mackinawite, gersdorffite, cobaltite and cubanite. Pyrite is secondary after pyrrhotite, and magnetite with ilmenite exsolution lamellae has been noted. Widenfalk et al. (1985) made a multidisciplinary investigation of Notträsk, comparing the vertical zoning of the intrusion to similar massifs in Alaska. The Sudbury ores in Canada were also compared, and it was suggested that the ores are not *in situ* cumulates but deep differentiates intruded later than the main intrusion. This conclusion, termed "diapiric re-emplacement" by Widenfalk et al. (1985) was not substantiated by field observations. Drilling by Filén et al. (1989) supported the suggested geometric form and petrogenesis advocated by Arvanitidis (1982).

Kukasjärvi (26M Överkalix)

North and northwest of the Stora Pahtavaara copper deposit, the mining company Boliden carried out a drilling campaign with 15 boreholes in the late 1970s and early 1980s, on a prospect named Kukasjärvi, consisting of a nickel-copper mineralised ultramafic sill. This deposit is calculated to contain 2.6 Mt (million tonnes) at 0.4% Ni and 0.4% Cu, but the nickel content as sulphide is too low to be of economic interest (Åkerman & Kero 2012e). Another prospect was investigated by diamond drilling by Boliden during this period: at Furuberget (26M Överkalix), where chalcopyrite and pentlandite occur in a differentiated mafic sill. This deposit is calculated to contain 50 thousand tonnes at 0.3% Ni and 0.16% Cu (Åkerman & Kero 2012e).

Gunnarsdjupträsk gabbro (25L Boden)

The Gunnarsdjupträsk gabbro is a layered basic intrusion, which was investigated in the 1980s for PGE and nickel. No significant amounts were found, however (Filén 1990). 3D modelling of the intrusion was made by Antal Lundin et al. (2013). As of 2016 Boliden had an exploration permit for copper in the area.

Fiskelträsk (26L Pålkem)

At Fiskelträsk Boliden localised a nickel-copper mineralised gabbro using boulders, bedrock mapping, geophysical measurements, and drilling of 11 boreholes with a total length of 1 600 m in the 1970s. An estimate of 3 Mt at 0.24% Ni, 0.23% Cu, and 0.02% Co was made. As of 2016 Nordic Resources AB had an exploration permit for nickel-copper.

Saivovaara (27K Nattavaara NV)

A copper mineralisation with 0.2% Cu was found in a gabbroid rock at Saivovaara. The mineralisation has a high susceptibility (22 800 × 10^{-5} SI units) and very strong remanent magnetisation (132 A/m). In a small area northeast of Saivovaara a strong magnetic field is present that turns the compass needle when passing. The magnetic field is so powerful that it is not possible to measure the anomaly using a standard proton magnetometer (max 120 000 nT detection limit). The anomaly where the measurement cannot be performed is approximately 20–30 m wide. The cause of the anomaly is probably a rock with high magnetite content. A profile of a nearby magnetic anomaly shows high total field values up to 60 000 nT. Model calculation of the profile shows that susceptibility of 30 000 × 10^{-5} SI units corresponding to 10% magnetite is needed to explain this anomaly. If the anomaly could be caused by a rock that has a strong remanent magnetisation, susceptibility would be completely subordinate to remanence (Claeson & Antal Lundin 2012c).

Ruoutevare (26J Jokkmokk NO)

A 1 to 3 m wide ultramafic and ultrabasic cumulate is found within the gabbro intrusion at Ruoutevare, probably a layer but only found at one location (Claeson & Antal Lundin in press-a). The cumulate rock consists of large oikocrysts of clinopyroxene, olivine, amphibole, disseminated chalcopyrite, pyrite, pyrrhotite, and magnetite (Claeson & Antal Lundin 2013). Lithogeochemical analysis shows anomalous PGE and gold content (42 ppb Pt, 49 ppb Pd, 26 ppb Au), i.e. 10 times higher than average values in the gabbro (Claeson & Antal Lundin 2013). A modal analysis of a thin section yielded 59% clinopyroxene, 15% olivine, 17% amphibole and 9% opaque minerals (Fig. 155). Petrophysical data on the ultramafic and ultrabasic cumulate: density = 3 186 kg/m^3, susceptibility = 14 939 × 10^{-5} SI units, remanence 8.3 A/m.

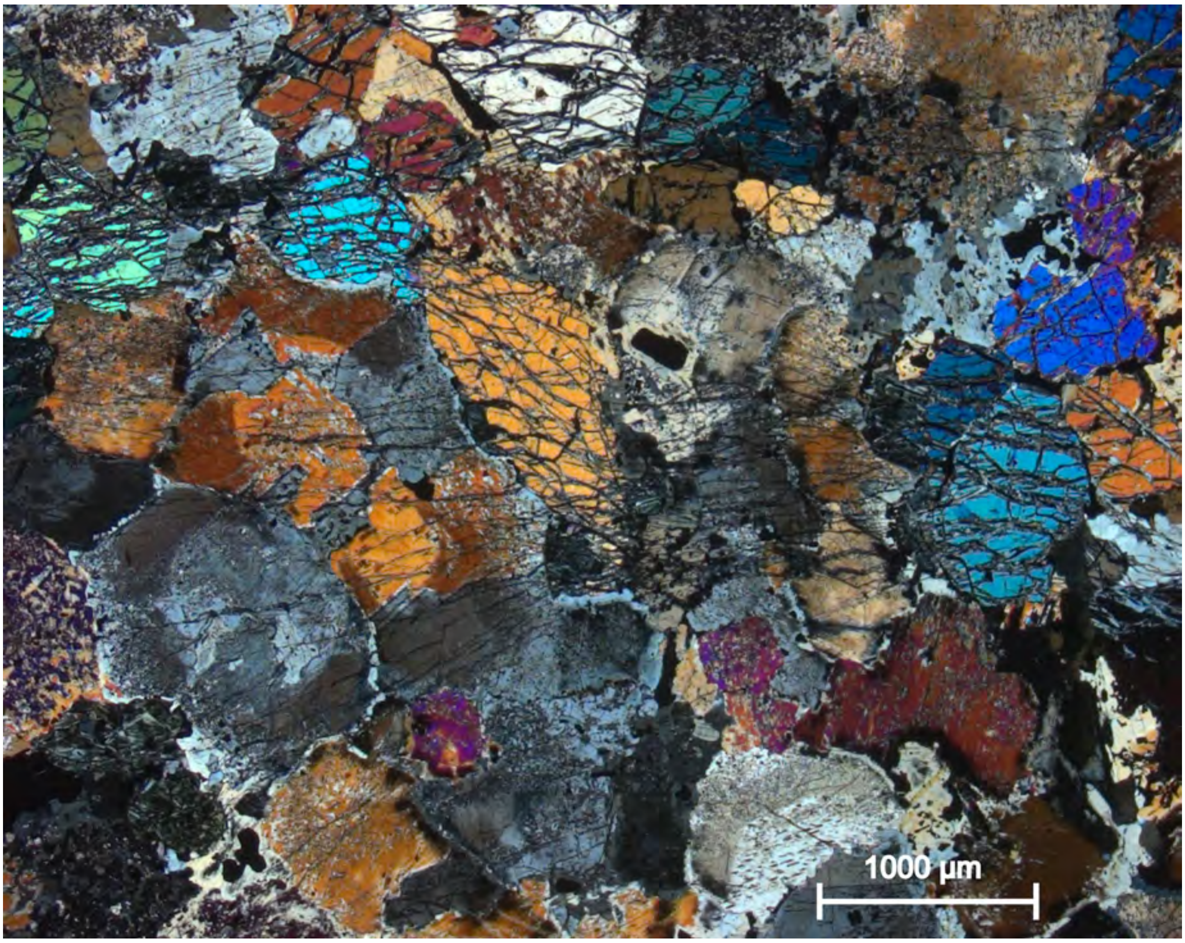

Figure 155. Several centimetre large oikocrysts of clinopyroxene and chadacrysts of olivine, and amphibole, disseminated chalcopyrite, pyrite, pyrrhotite and magnetite in a PGE-Au-anomalous mineralised ultramafic and ultrabasic cumulate rock (7388439/715280). Photomicrograph: Dick Claeson.

Kukkola chromium (platinum, palladium, gold) type deposits

Kukkola layered intrusion (25N Haparanda NV)

Prospecting for chromium was carried out in 1981–82 at the Tornio layered intrusion (Söderholm & Inkinen 1982) in the east of Norrbotten County. The eastern part of the intrusion is located in Finland and has been investigated by the company Outokumpu Oy. Bedrock mapping and boulder tracing, together with geophysical measurements and diamond drilling were all used to characterise the intrusion. The Tornio–Kukkola layered intrusion intrudes 2.7 Ga Archaean gneisses (Bergström et al. 2015) and overlying supracrustal rocks, and has been correlated with nearby intrusions in Finland that are 2.4 Ga old. The intrusion consists of mafic to ultramafic layers; several chromite-bearing horizons occur in the latter. These consist of disseminated and locally also massive chromitites with individual layers up to 13 cm thick. Mineralogical studies show that chromium-bearing magnetite predominates in the disseminated type, and chromite is present in the massive type. Preliminary investigation of precious metals showed elevated content of both PGE and gold in several parts of the gabbro (Filén 1990). In metaperidotite, 3.6 ppm Au was reported from a 2.7 m long drill core section with chromite-rich dissemination. Additionally, 0.64 ppm Pt and 1.1 ppm Pd was present in a 0.1 m long drill core section of metapyroxenite. Further PGE-anomalous environments consist of serpentine- and amphibole-rich ultramafic rocks.

Porphyry type deposits

Aitik

Aitik is considered a porphyry copper deposit. At present, most of the mine is situated just outside of the project area, but the mineralisation extends into map sheet 27K Nattavaara, as well as the planned expansion of the Salmijärvi open pit mine by Boliden (2016), and it is therefore presented here. The first indications of the ore deposit were boulders with chalcopyrite found in the early 1930s. The mineralisation was discovered a few years later. Exploitation of the deposit did not become economically viable until the 1960s. This was because it is a low-grade copper-gold-silver mineralisation. The mine started operating in 1968, and now has an annual production of 35 Mt ore. The ore deposit consists mainly of strongly altered and metamorphosed volcanic and volcaniclastic rocks of varying composition, chalcopyrite and pyrite being the ore minerals of main importance. The ore deposit is currently excavated in a 3 km long and 450 m deep open pit mine. Expansion plans will extend the mine's lifespan to at least 2030 and double its ore production capacity (Boliden 2016). An earlier description of Aitik was given in Bergman et al. (2001); only more recent data and ideas are presented here. The volcanic rocks of the ore zone and the subvolcanic quartz monzodiorite intrusion situated in the structural footwall are probably more or less coeval, indicated by an age of 1 887 ± 8 Ma for the subvolcanic quartz monzodiorite (Wanhainen et al. 2006) and 1 882 ± 6 Ma for an andesitoid agglomerate volcanic rock at Sammakkovaara, some 23 km southeast of Aitik (Claeson & Antal Lundin 2012c). The recovery of gold has always been an issue at Aitik, with typically less than 50% Au recovered. Several gold mineralogy studies have been performed to help increase the recovery (e.g. Sammelin (Kontturi) et al. 2011, and references therein). Although the gold recovery is unchanged with depth in the mine, due to a more common association involving native gold and silicate minerals that are not caught with the copper flotation in use, it has been suggested that the overall gold grade increases with depth (Sammelin (Kontturi) et al. 2011). A protracted period of magmatic, hydrothermal and metamorphic activity in the Aitik area is evident through Re-Os dating of molybdenite and U-Pb dating of titanite (Wanhainen et al. 2005). At Ahmavaara about 7 km west of Aitik, there is a sizeable area with well-preserved feldspar porphyritic monzonite to monzodiorite. Small amounts of syenitic rocks are present and show gradual transitions to monzonite (Claeson & Antal Lundin 2012c). A monzogabbro showing mingling and mixing structures with the other rocks at Ahmavaara is interpreted as coeval with them. Well-exposed outcrops of these rock associations are found at the Aitik mine tailings pond just north of map area 27K Nattavaara. U-Pb zircon age determination of a monzonite to syenite from the site at the Aitik mine tailings pond indicates a formation age of about 1 806 ± 7 Ma (Claeson & Antal Lundin 2012c). This shows that these massive rocks are not related to the Perthite-monzonite suite (e.g. Witschard 1996) but to a 1.8 Ga bimodal magmatic event. These facts should be used in future work to explain the protracted period of activity in the Aitik ore zone. Other occurrences of this bimodal magmatism could be used for future exploration in the whole area when looking for multiple remobilisation of ore elements or minerals by heat and hydrothermal input relating to younger magmatism. From a genetic point of view, the Aitik ore may be classified as a large-volume, low-grade porphyry-style copper-gold-silver ore. Mineral reserves and resources estimates (Boliden Annual Report 2015) in thousand tonnes are: proven reserves 850 000, probable 377 000 at 0.23% Cu; mineral resources measured 252 000 Cu 0.15%, Au 0.09 ppm, Ag 0.8 ppm, Mo 18 ppm; indicated 1 313 000 Cu 0.16%, Au 0.09 ppm, Ag 0.8 ppm, Mo 23 ppm; inferred 281 000 Cu 0.14%, Au 0.09 ppm, Ag 0.6 ppm, Mo 20 ppm.

Jårbojoki (27K Nattavaara NO)

Two deposits at Jårbojoki, located about 13 km southeast of the Aitik deposit, were discovered in 1949 and magnetic, electromagnetic (slingram) and IP (induced polarisation) ground geophysical measurements were carried out in 1965 (Carlson 1982). The weak slingram anomalies were diamond drilled

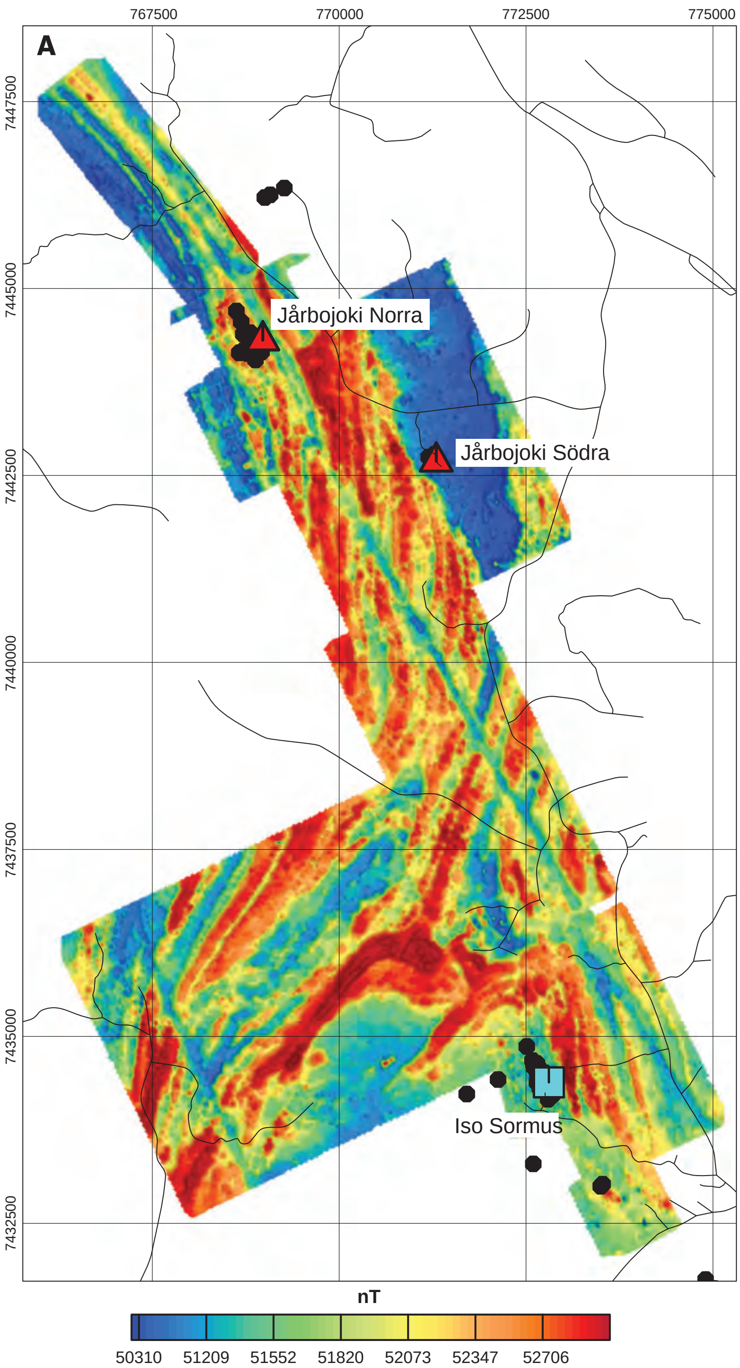

Figure 156. Ground geophysical measurements of the Jårbojoki–Iso Sormus area. The measurements were made with a line distance of 80 m and point distance of 20 m. **A.** Magnetic total field. Round symbols show the location of the drill holes. Red triangles show the locations of the Jårbojoki Norra and Jårbojoki Södra sulphide mineralisations; the blue square shows the location of the olivine-serpentine deposit at Iso Sormus.

during 1969–71 down to about 200 m, in total 17 boreholes (Figs. 156a, b). The Jårbojoki Norra and Jårbojoki Södra deposits are situated approximately 2.5 km apart and the host rocks are different (Figs. 156a, b). The Jårbojoki Norra mineralisation is in altered metasedimentary and volcanogenic rocks; sericitic alteration is relatively common (Carlson 1982). Pyrite and chalcopyrite occur repeatedly in sections of the boreholes adjacent to the area showing slingram anomalies. Drilling intersected two zones of copper and gold mineralisation extending over 700 m in the strike direction. Significant ore zones and significant chalcopyrite-bearing sections are identified in individual boreholes. Borehole 69701 shows 1.75% Cu through 8.5 m of the drill core; borehole 69705 has an extensive copper mineralisation intersected of about 100 m length (Carlson 1982). A number of anomalous gold assays exist at Jårbo-

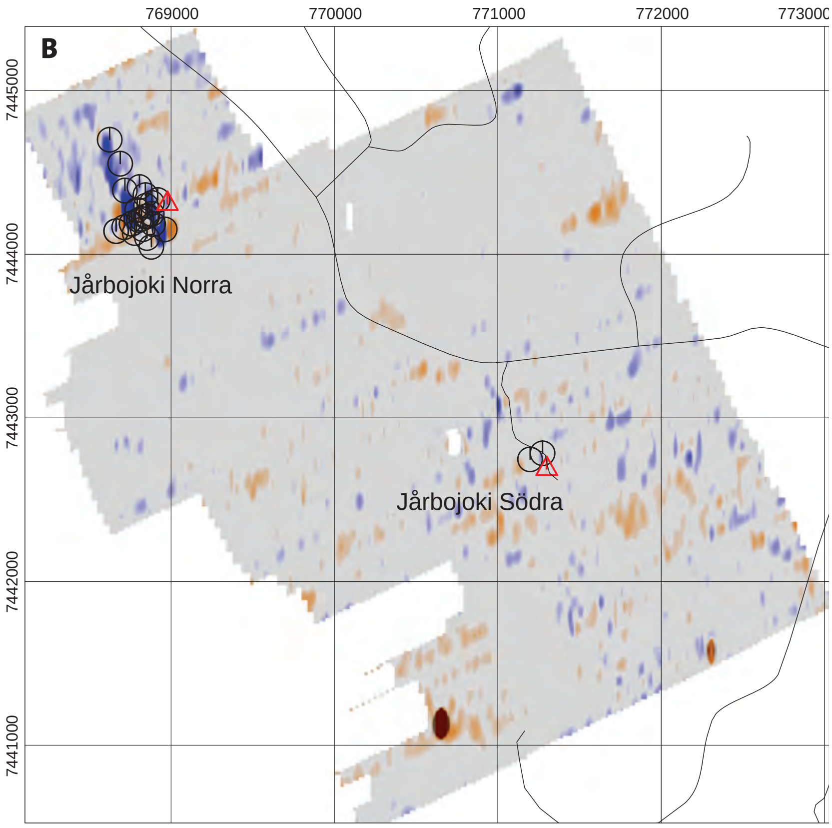

Figure 156. **B.** Electromagnetic (slingram imaginary component) ground measurements of Jårbojoki Norra and Jårbojoki Södra. Drill hole locations are marked with black circles. Red triangles show the location of sulphide mineralisations.

joki Norra at levels of 0.4 to 1.9 g/t Au. Borehole 70701 shows 1.9 g/t Au in a 3.2 m section. The Jårbojoki Södra mineralisation is situated in a dioritoid at depth, with chalcopyrite dissemination in the host rock as well as in quartz veins (Carlson 1982). A few drill cores obtained in 1969 show weak grades of up to about 0.25% Cu, which led to prospecting focused on Jårbojoki Norra. In recent mapping by SGU, the bedrock at Jårbojoki Norra was designated as belonging to plagioclase phenocryst-bearing basic and intermediate volcanic rocks, and the Jårbojoki Södra mostly as intermediate volcanic rocks and a c. 1.80 Ga feldspar porphyritic granite to monzonite (Claeson & Antal Lundin 2012a).

Vaikijaur copper-gold-(molybdenum) (26J Porjus SV)

The Vaikijaur deposit is situated 15 km northwest of Jokkmokk. It was originally discovered as a result of an extensive exploration campaign by SGU in the late 1960s. During 1979–80 geophysical measurements, geological mapping and quaternary geological investigations were carried out, together with boulder tracing. Drilling commenced in 1981 and continued in 1982–83. An ore microscopy investigation was also made to characterise the distribution of copper and gold. No ore resource estimate has been made.

The Vaikijaur deposit occurs well within the "Jokkmokk granitoid". The rock is a pale grey to off-white, fine- to medium-grained, equigranular to inequigranular, foliated and lineated granite to granodiorite with occasional usually grey to off-white 5–20 mm large phenocrysts of potassium feldspar. In some places a blue tint is seen in quartz. There are plenty of fissure and fracture fillings of quartz (Fig. 157). These are interpreted to be late magmatic in most cases, and cut each other at places, indicating multiple generations. It has been suggested that these are of importance in the continued exploration of the intrusion (Claeson & Antal Lundin in press-c). Lithogeochemical, petrophysical and gamma radiation measurements carried out on the rocks of the intrusion and ocular assessments

Figure 157. Quartz-filled fractures in Jokkmokk granitoid (7404691/708937). Photo: Ildikó Antal Lundin.

show that the Jokkmokk granitoid is of albite granite affinity (Claeson & Antal Lundin in press-c). Albite granites have often been described as the result of post-magmatic, metasomatic transformations in earlier studies, but have recently often proved to be igneous (Černý 1991a, b, Barboni & Bussy 2013). The mineralised part of the Jokkmokk granitoid shows clear zonation, with a foliated and weathered central zone containing disseminated pyrite, molybdenite and minor chalcopyrite. This part is clearly seen from the induced polarisation measurements (Fig. 158). Several types of alteration are present. A grey-green compact rock with sericitised feldspar and chloritised biotite is found together with iron sulphides and abundant epidote. Thin veins of compact sulphides are common. In addition, the biotite is brownish in the altered granite due to oxidised iron in the mineral. Another type of alteration appears as weathered zones carrying quartz, sulphides and epidote, with the primary feldspars totally decomposed. Secondary feldspar occurs locally.

The richest copper (gold) mineralisation is found in the outer part of the central zone. A zone of disseminated magnetite occurs close by. It mostly occurs just outside the copper-bearing zone and has been used as a marker horizon. Outwards from the central pyrite-rich zone, heterogeneous migmatitic granite follows that is partly silicified and contains skarn minerals with traces of chalcopyrite, molybdenite, and scheelite. Outside this zone the granite becomes homogeneous and more like "normal" Jokkmokk-type granite. According to Lundmark (1984b), the alteration zones and the mineralised fractures of the copper-gold-molybdenum mineralisation at Vaikijaur were formed due to hydrothermal solutions penetrating permeable zones in the granite as the result of tectonic pressure caused by a mafic intrusion. The Vaikijaur mineralisation was dated by Lundmark et al. (2005b) using Re-Os on molybdenite, resulting in 1 889 ± 10 Ma and 1 868 ± 6 Ma ages. The Jokkmokk granitoid was earlier dated at 1 883 ± 15 Ma using multi-fraction zircon (U-Pb TIMS Lundmark et al. 2005a). In contrast to the Norrbotten County iron oxide-copper-gold ores, which typically show strongly saline solutions, results from fluid inclusions and isotope studies (O, H) from Vaikijaur show solutions that are instead low to medium saline, water- and CO_2-rich (Lundmark et al. 2006). The isotopic studies (O, H) show a mix of magmatic and seawater signatures. Lundmark et al. (2005b) described Vaikijaur as a porphyry copper-gold-molybdenum mineralisation. The above observations are interpreted by Claeson & Antal Lundin

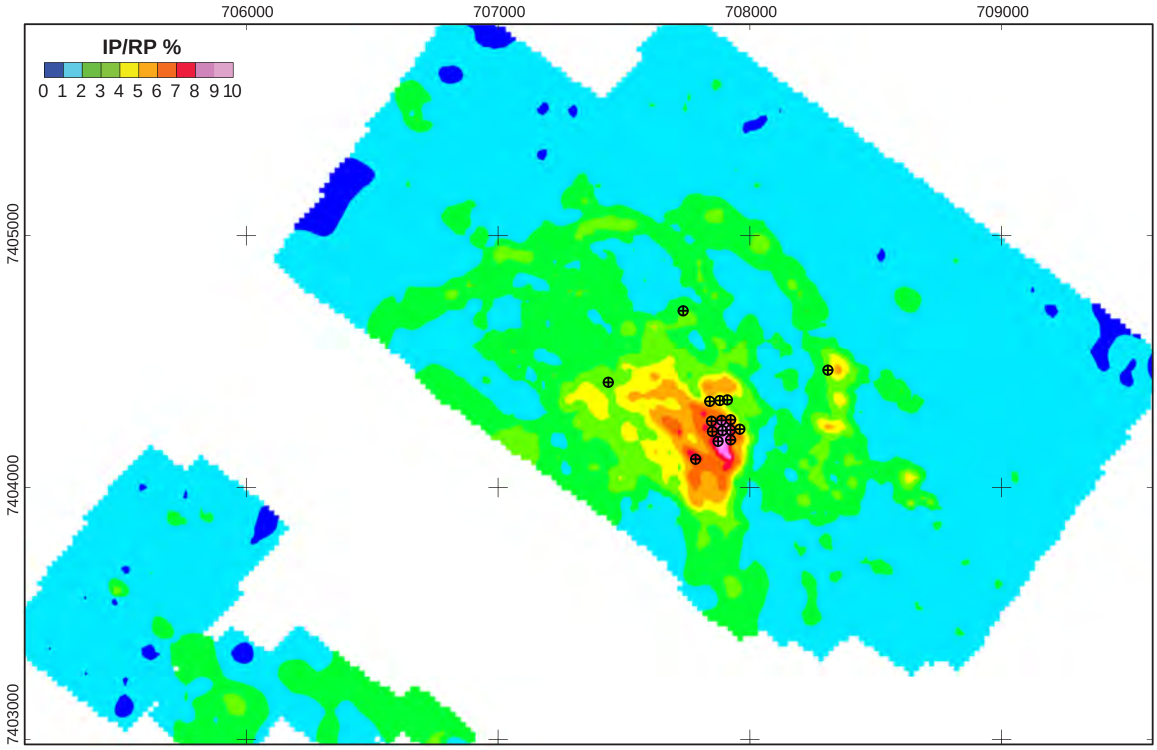

Figure 158. Induced polarisation at Vaikijaur. Black symbols (circles) show the location of the drill holes on IP anomalies.

(in press-c) as evidence that ore genesis was syngenetic or epigenetic and syngenetic, i.e. diplogenetic (cf. Lovering 1963).

Ground geophysical measurements were taken in the early 1980s. The magnetic field, electromagnetic field (slingram) and induced polarisation (IP) were measured over an area of 4 km^2. The measurements were made with a line distance of 40 to 80 m and a point distance of 10 to 20 m. Most of the boreholes were drilled in the anomalies caused by the mineralisation (Fig. 158).

Laver (25K Harads SV)

The Laver copper deposit is situated 15 km southwest of Vidsel. It was found by Boliden in 1930 using geoelectrical methods in association with copper-mineralised boulders. A total of 1.5 Mt of ore containing 1.51% Cu, 0.2 ppm Au and 36 ppm Ag was mined between 1934 and 1946. Old mining maps of Laver are available in PDF format at www.sgu.se. According to Ödman (1943), the ore occurs mainly at the contact between rhyolite (liparite by Ödman) and overlying banded tuff belonging to the Arvidsjaur volcanic suite. This contact strikes northwest–southeast and dips 70° to the southwest. The ore occurred as 1) breccia ore in rhyolite; 2) vein ore at the contact between rhyolite and tuff; and 3) ore-bearing fault zones cutting both type 1 and type 2 ores. Chalcopyrite and pyrrhotite are the main ore minerals in the old mine; minor quantities of sphalerite and galena occur in veins 1–2 m long. A local occurrence of native silver was found at the 130-m level in an east–west-striking fault. The mineralisation mainly comprises sulphides in disseminations and veins. The main minerals of the present-day Laver deposit are chalcopyrite, pyrrhotite, pyrite, molybdenite, magnetite and sphalerite. From a genetic point of view, the ores may be classified as a large-volume, low-grade porphyry-style copper-gold-molybdenum mineralisation (Aitik-type). Ore mineral resources estimates (Boliden 2015) in thousand tonnes are: measured 1100 Cu 0.20%, Au 0.11 ppm, Ag 4.4 ppm, Mo 18 ppm; indicated 512400 Cu 0.22%, Au 0.13 ppm, Ag 3.1 ppm, Mo 36 ppm; inferred 550600 Cu 0.21%, Au 0.10 ppm, Ag 3.1 ppm, Mo 33 ppm. The Laver area has been is a designated site of national interest since 2014.

STRATIFORM-STRATABOUND ORE DEPOSITS (BASE METALS AND IRON)

Iron ores

A north–south to north-northeast–south-southwest-trending zone of iron mineralisations, hosted by supracrustal rocks, is found in the areas covered by map sheets 27J Porjus NV, SV, 27I Tjåmotis SO and 26I Luvos NO. The deposits at Kallak, Parkijaure, Akkihaure, and Åkosjegge are relatively well investigated and thus considered to be ore deposits, whereas Pakko, Maivesvare, and Tjårovaratj are regarded as potential ore targets (Johansson 1980). Both the Kallak and the Åkosjegge deposits are interpreted to occur in association with volcanic host rocks, the latter in gneissic skarn rocks, however, suggesting metasedimentary rock components as well.

Kallak and Parkijaure (27I Tjåmotis SO)

A sizeable area with iron mineralisation at Kallak–Björkholmen–Parkijaure has been known since the 1940s when SGU discovered the first outcrops, and extensive work, e.g. core drilling, was carried out (Eriksson BRAP83801). Ground geophysical surveys using magnetometry and gravity measurements were performed in 1947 (Kallak North) and 1968–1970; ore estimates were presented in 1980. A combined estimate of iron ore for Kallak– Björkholmen–Parkijaure was approximately 149 Mt using gravity data and about 123 Mt using magnetic data, without correction for a possible 30% hematite in both Kallak occurrences, resulting in approximately 161 Mt (Johansson 1980). Exploration has recently been supplemented with core drilling in the north and south (2010–14). Jokkmokk Iron Mines AB-Beowolf Mining plc. have completed drilling and other investigations, and in November 2014 estimated that the "Kallak deposit", i.e. resources in the area Kallak North and South together, contain more than 150 Mt of ore with 26.2 to 27.5% Fe, and that Kallak North is open to the north and at depth (<http://beowulfmining.com/projects/sweden/kallak>). Trenches and blasted test pits excavated by Jokkmokk Iron Mines AB in the iron mineralisation at Kallak were visited during SGU field work in 2014 (Fig. 159). The acid volcanic rock found in the pits and trenches is a garnet-bearing quartz trachyte with empty or rusty amygdules. The highly magnetite-rich bedrock at Kallak shows foliation and lineation, contains fragments of both felsic and mafic volcanic rocks; banding with the surrounding acid volcanic rock is obvious (Figs. 160, 161). Limited amounts of skarn consisting of amphibole, garnet, epidote, pink to orange calcite, and greenish apatite were found in both the quartz trachyte and the iron mineralisation. A sample of the iron ore shows 34.1% SiO_2, 1.24% Al_2O_3, 62.3% Fe_2O_3, 1.67% CaO, 2.26% MgO, 0.23% Na_2O, 0.27% K_2O, 0.05% TiO_2, 0.33% MnO, and 0.09% P_2O_5. Low concentrations of V 19 ppm, S 0.09%, Cu 2.3 ppm, Th 1.12 ppm, Nb 1.9 ppm, and Zr 19 ppm do not indicate a close connection to Kiruna-type apatite iron ore. A thin section of the iron mineralisation shows a fine laminated pattern defined by lamina of opaque minerals and quartz trachyte (Fig. 162). The quartz trachyte (Fig. 163) sampled at the trench for lithogeochemical analysis shows 63.1% SiO_2, 13.7% Al_2O_3, 7.47% Fe_2O_3, 2.33% CaO, 2.46% MgO, 2.79% Na_2O, and 6.55% K_2O. In addition, a high content of barium at 2 350 ppm was reported, possibly indicating that a volcanic-hydrothermal process was active. The iron ore and the quartz trachyte have similar REE patterns, but the mineralisation shows significantly lower levels of REE (Fig. 164). The multi-element spider diagram shows similar trends for the two samples, but the iron mineralisation has significantly lower levels than the quartz trachyte (Fig. 165).

Age determination of the quartz trachyte shows there to be a heterogeneous set of zircon, the oldest being Archaean c. 2 700 Ma, and that the likely age of the volcanic rock is c. 1873 Ma (SGU unpublished U-Pb SIMS data). The interpretation of the results from the above investigations is that the iron ore was deposited in a volcanogenic environment, rather than in a sedimentary environment with a previously proposed relationship to quartz banded iron ores, (e.g. Frietsch 1963, Frietsch 1997).The quartz banding that Frietsch (1963, 1997) mentions, was not observed during recent mapping by SGU (Claeson & Antal Lundin in press-b), either in outcrops or in available recently drilled cores. Nor are quartz

Figure 159. Excavation trench and test pits at Kallak (7414247/681408). Photo: Dick Claeson.

Figure 160. Outcrop of iron mineralisation at Kallak with bands of quartz trachyte (7414247/681408). Photo: Dick Claeson.

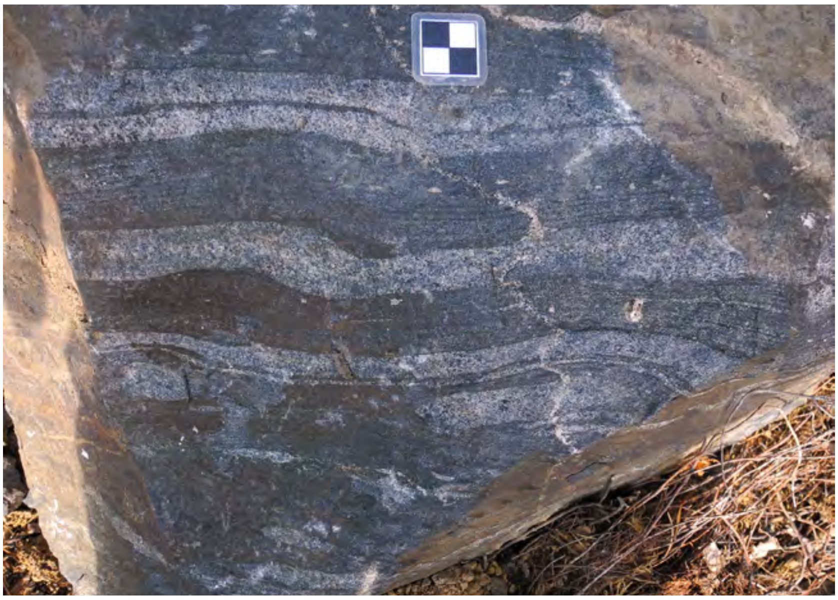

Figure 161. Close-up of banding on a millimetre and centimetre scale at Kallak, made up of magnetite-rich and quartz trachyte bands (7414247/681408). Photo: Dick Claeson.

Figure 162. A fine laminated appearance is defined by the distribution of the opaque minerals at Kallak, plane-polarised light. Photomicrograph: Dick Claeson.

Figure 163. Close-up of the sampled quartz trachyte from the excavation trench at Kallak (7414247/681408). Photo: Dick Claeson.

bands ever mentioned in the drill logs from the 1940s and 50s, although there is plentiful banding related to the appearance of the ore or the volcanic rocks (Eriksson BRAP83801). Martinsson et al. (2016) write that Kallak consists of a Banded Iron Formation, but nothing in the data presented here or our interpretation of the ore genesis even suggests that the ore remotely resembles a banded iron formation (BIF) or that there is any occurrence of chert. Ödman (1957) stated: "Nothing can be said with certainty about the origin of the ore material. The ore environment is volcanic – the leptite in the area is interpreted to be tuffitic rocks – and it seems likely that iron was precipitated from the volcanic thermal water". Frietsch (1997) states "In the intermediate-felsic volcanic rocks of the c. 1.9 Ga Porphyry Group in the region west and northwest of Jokkmokk and southwest of Malmberget, there are quartz banded iron ores of volcanogenic origin". The felsic components of bands and laminae found within the iron ore, clearly visible in thin section (Fig. 162) consist of quartz trachyte and not of quartz-rich sedimentary layers or chert. This feature is also observed in parts of the rock surface exposed by the exploration trenches (Fig. 160, 161). These observations suggest that the ore genesis should be interpreted as syngenetic or diplogenetic (cf. Lovering 1963, Claeson & Antal Lundin in press-b).

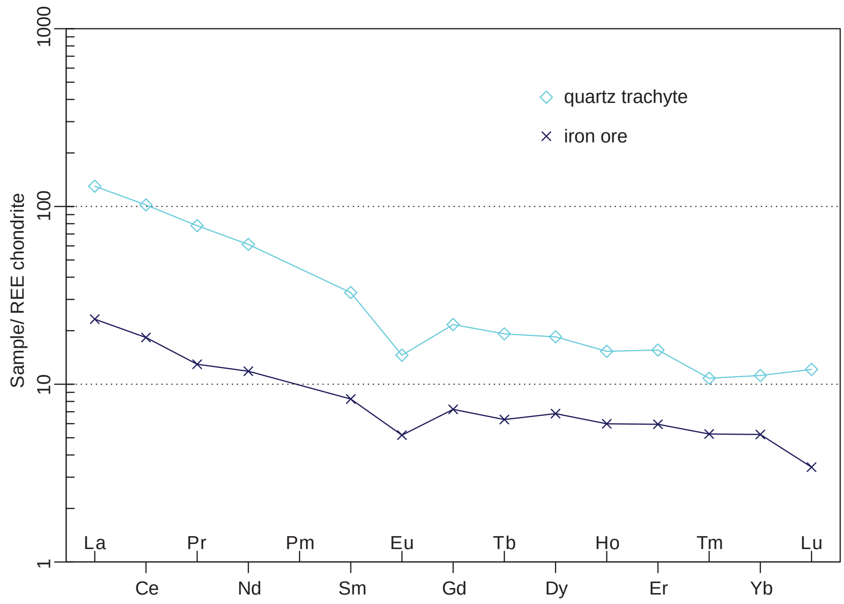

Figure 164. REE diagram with data from lithogeochemical analyses of the quartz trachyte host rock and the iron ore at Kallak. Normalising values for chondrite from Boynton (1984).

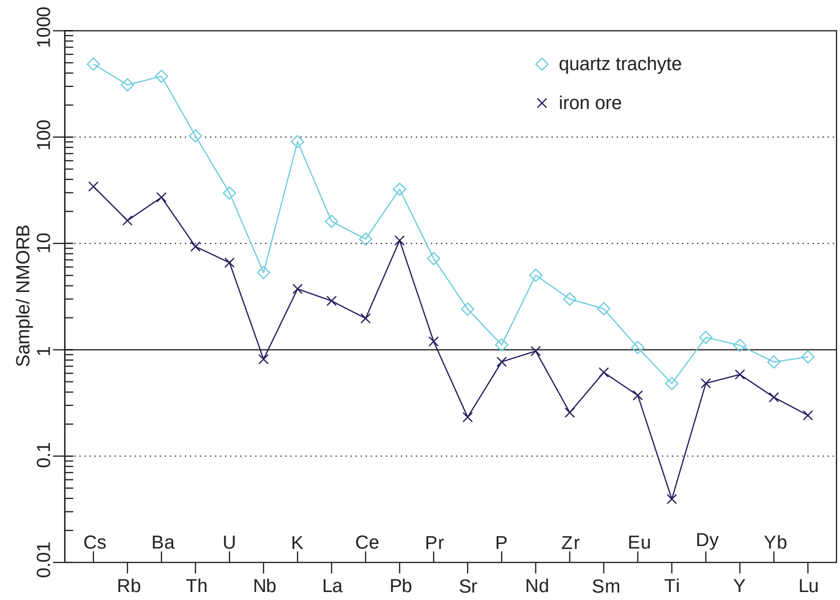

Figure 165. Multi-element diagram with data from lithogeochemical analyses of the quartz trachyte host rock and the iron ore at Kallak. Normalising values for N-MORB from Sun & McDonough (1989).

Magnetic susceptibility measured with a hand-held meter on outcrop and trench varies, for quartz trachyte: 0.0007 to 0.01, and from 0.046 to 0.12 SI units. Susceptibility for magnetite mineralisation and ore parts varies from 0.34–0.99 SI units and >1 (overflow for the instrument) (Table 6). Comprehensive ground measurements of the magnetic field, electromagnetic field (slingram) and dense gravity measurements of the mineralisation are from previous exploration campaigns. The measurement distance between points varies between 10–20 metres and 40–80 metres, the line spacing between 20 and 80 metres, but up to 150 m from the mineralisation. The area investigated is 18 km long and approximately 5 km wide; the measurements were made between 1968 and 1970 (Fig. 166a, b). The Kallak area has been a designated site of national interest since 2013.

Table 6. Petrophysical properties from Kallak North. Ore samples from outcrop and exploration pit, and samples of quartz trachyte with abundant magnetite from exploration pit. Coordinates in Sweref 99.

No.	N (SR 99)	E (SR 99)	Sample	Density (kg/m^3)	Magnetic susceptibility (SI)	Remanent magnetisation (A/m)
1	7414071	681318	Ore, outcrop	3 832	5.5	40.3
2	7414247	681408	Ore, exploration pit	3 975	3.8	70
3	7414246	681408	Ore, exploration pit	3 725	1.3	63
4	7414071	681318	Quartz trachyte with abundant magnetite, exploration pit	3 233	0.53	7
5	7413879	681284	Quartz trachyte with abundant magnetite, exploration pit	3 287	1.5	99.4

Åkosjegge (27J Porjus NV, SV)

Airborne geophysical measurements were carried out in Norrbotten County as part of the iron inventory programme between 1963 and 1973, and new discoveries were made, including the "Jokkmokk" ores and Åkosjegge (Frietsch 1997). Ground geophysical surveys using magnetometry and gravity measurements were performed during 1969–1970 (Johansson 1980). Two drill cores (SGU borehole Nos. 72601, 72602) were drilled in 1972, and geophysical borehole logging involving the use of a borehole magnetometer was conducted. The borehole logs show an iron mineralisation with parts of skarn; the rocks are classified as grey to green skarn-bearing gneiss. The closest outcrops (600 m and 800 m from the ore body) are hydrothermally altered and veined amphibole- and magnetite-rich basaltoid to andesitoid volcanic rocks (Claeson & Antal Lundin in press-c). A very small percentage of the two approximately 200 m deep boreholes were classified as magnetite iron ore, with a reported iron content of 10–24%, and it is unclear whether they encountered the mineralisation indicated by the geophysical data (Fig. 167a, b). A calculation of the iron ore deposit potential based on geophysical data suggests an approximate tonnage of 75 Mt (Johansson 1980). Frietsch (1997) states that the ore zone is about 1.5 km long and 500 m wide, with an iron content of about 30% Fe.

Akkihaure (26I Luvos NO)

The magnetite mineralisation causing the positive magnetic anomaly at Akkihaure is mainly located below lake Akkihaure, and no outcrops have been discovered (southernmost yellow symbol in Fig. 166a, b). Geophysical surveys by SGU using magnetometry and gravity measurements in the 1960s located the magnetite mineralisation at Akkihaure (Frietsch 1997). One cored borehole (SGU borehole No. 72704) was drilled in 1972. The ore-bearing zone strikes north–south and forms a steeply dipping, isoclinal fold that is open to the north. A magnetic profile measurement was made to determine the width and dip of the magnetic body. The highest value in the profile was measured at 77100 nT. At a nearby location, the proton magnetometer could not record a value, probably because the magnetic field was stronger than its upper detection level (Hellström & Berggren 2014). According to the borehole log, the magnetic body is located in amphibole-biotite-feldspar gneiss, but a recent report describes the rock as a strongly altered dacite (Hellström & Berggren 2014). The ore-bearing area is about 650 m long and 50–60 m wide, the largest mineralised zone being up to 30 m wide and situated in the western limb of the fold. Calculations based on data from gravity and magnetic measurements indicate a tonnage of 12 to 13 Mt of iron ore (Johansson 1980). A lithogeochemical analysis of a small portion of the core from the iron mineralisation shows: 48.4% Fe, 0.01% P, 0.01% Ti, <0.01% Mn and 13 ppm V (section 178.35 to 178.62 m, Hellström & Berggren 2014).

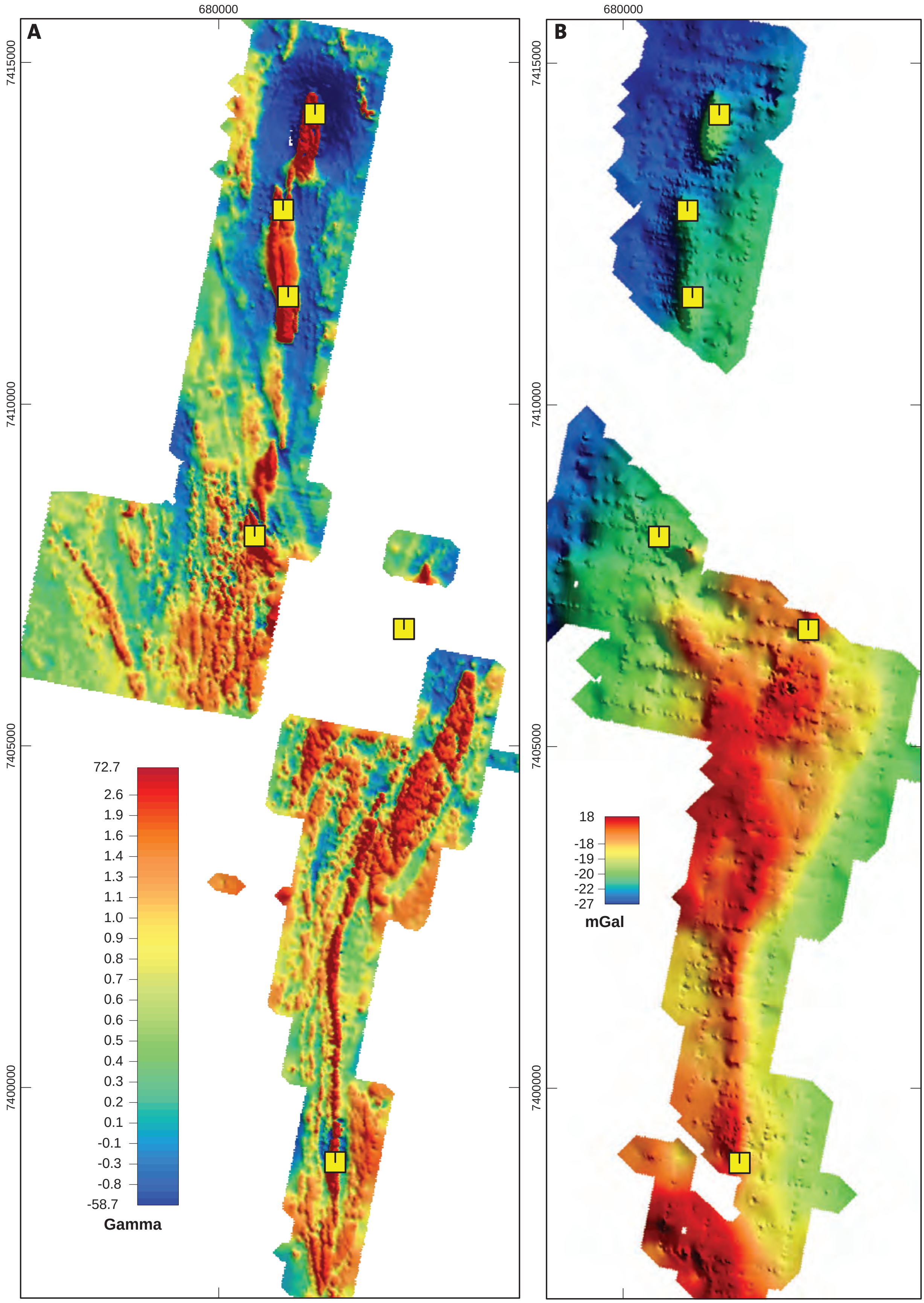

Figure 166. Geophysical anomaly maps of the Kallak area based on ground measurements. The iron oxide mineralisations (ore) are shown as yellow squares. **A.** Magnetic anomaly map, vertical component. **B.** Terrain-corrected Bouguer anomaly map.

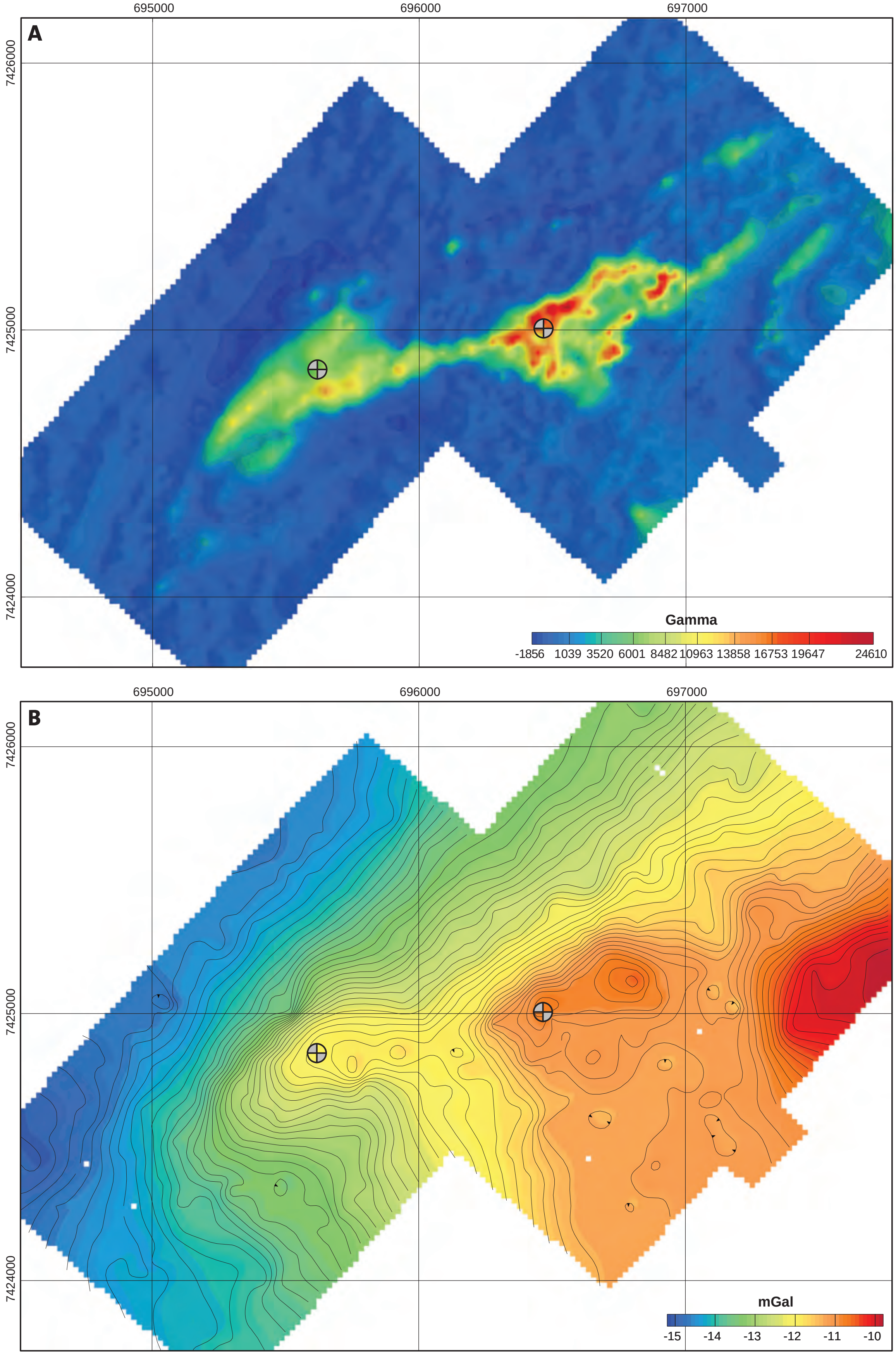

Figure 167. Geophysical anomaly maps of the Åkosjegge area based on ground measurements. The circles show the location of the drill holes. **A.** Magnetic anomaly map, vertical component. **B.** Gravity anomaly map.

Kaddevaara (27K Nattavaara NV)

Magnetic and gravimetric ground measurements were performed in 1971. This was followed by diamond drilling to about 190 m in 1972 (borehole 72001), in which an iron ore mineralisation was located at Kaddevaara. Geochemical analysis shows 26 m of iron-mineralised rock in the core, with average values of 42.3% Fe, 0.19% P, and 1.39% S, with minor amounts of copper. The recent mapping by SGU suggests that the mineralisation is situated in a larger intrusion of microgabbroid rock (Claeson & Antal Lundin 2012b).

Narken area (27M Korpilombolo NV)

Several small iron mineralisations occur in the Narken area 15 km northwest of Korpilombolo. These may be characterised as breccia-infill in metasedimentary rocks. They contain iron sulphide to varying degrees (Jonsson & Kero 2013d). These mineralisations were discovered in 1946 during regional geological mapping of Norrbotten County by SGU. This area was re-mapped in 1970, and the deposits have been described by Frietsch (1972) and Jonsson & Kero (2013d). According to Frietsch (1972), the mineralisations are of late origin, formed by the action of metasomatic solutions in a tectonic zone, except for at Myllyniemi (27M 8a) and Kartovaara (27M 9a), where the sulphides (mainly pyrite) are locally abundant. The latter two locations also show significantly greater proportions of magnetite. At the edge of the newly excavated area at the Vattuvaara mineralisation, single, small patches of blue secondary copper minerals, possibly along with chalcocite, are observed in the metamorphosed sedimentary rock next to the iron oxide mineralisation. Many properties of the mineralisation suggest an affiliation with iron oxide-copper-gold deposits (Jonsson 2008).

Vattuvaara (breccia-type) (27M Korpilombolo NV)

The Vattuvaara mineralisation, which is the largest deposit in the Narken area, is situated 1.5 km southeast of Narken village. It is well exposed in outcrops and in a stripped and excavated area 35 × 20 m in size. The mineralisation comprises a spectacular breccia, in which a matrix of iron oxides, epidote, chlorite, including accessory amounts of sulphides and apatite, display plentiful fragments of banded, metasedimentary rocks (Jonsson & Kero 2013d). The iron oxides predominantly comprise hematite, which is mainly formed by martitisation (oxidation of initially formed magnetite). Sulphides are very much subordinate at the Vattuvaara mineralisation (Jonsson & Kero 2013d). The mineralisation appears to have been formed in conjunction with brittle deformation and extensive hydrothermal alteration (Frietsch 1972, Jonsson 2008). A survey using a gamma-ray spectrometer revealed anomalously high radioactivity, and a geochemical analysis shows elevated concentrations of uranium and thorium, particularly Th content, reported at 71 ppm.

Kartovaara (27M Korpilombolo NV)

A small excavation in a hematite-magnetite-pyrite-bearing skarn occurs on the northwestern side of Kartovaara hill, 4.5 km northeast of Narken. It consists of iron oxides in a fine-grained matrix of epidote and biotite. In addition, pyrite occurs as mm-sized euhedral crystals in the iron oxide-skarn matrix. Accessory minerals are quartz, chlorite, apatite and allanite. The mineralisation is surrounded by albite-rich alteration rocks. A lithogeochemical analysis reveals anomalous contents of REE (total 1350 ppm), with cerium contributing to 50% of this amount. This is most probably due to the allanite content (Jonsson 2008, Bergman & Hellström in preparation). The mineralisations at Kartovaara and Myllyniemi show locally abundant amounts of sulphides, mainly pyrite, and both show significantly greater proportions of magnetite than at Vattuvaara (Jonsson & Kero 2013d).

Skarn iron ore and manganese-oxide-skarn ore deposits (Ultevis)

Iron-dominant skarn ore occurs at Rappen (26H Jäkkvik) and manganese-dominant skarn ore is found in a 20 km long mineralised zone stretching from map sheet 27I Tjåmotis into 28I Stora Sjöfallet. BIF-type iron mineralisation is also found locally here.

Rappen (26H Jäkkvik)

The Rappen prospect is situated east of lake Rappen and was investigated by Stora Kopparbergets Bergslag AB in the 1960s. The company drilled 17 boreholes to investigate the iron ore. Geological mapping was performed in 1978–82 and in 1990 geophysical measurements were carried out in profiles across the contact between volcanic rocks and granite. In 1991 and 1992 Nämnden för statens gruvegendom contracted the company Swedish Geological AB (SGAB) to perform a survey using magnetometry, gravimetry, slingram and IP. Lastly, four short boreholes were drilled at Tjuoiva in a mineralisation consisting of hematite breccia, with chalcopyrite and cobaltian pyrite in one of the drill cores (Ljung 1992). The Rappen iron ore area can be followed from 8 km north-northwest of Arjeplog approximately 40 km northwards. From south to north the following deposits are known: Sakka, Skomern, Rebak, Rappen, and Hejka. The iron ore, together with limestone and skarn, occupies the upper part of a sedimentary sequence consisting of gneisses, mostly feldspar quartzite and mica schist. Volcanic rocks with mafic intercalations occur east of the sedimentary gneisses.

The skarn iron ore consists of magnetite-rich bands alternating with skarn layers. Small amounts of hematite are also present, and the predominant skarn minerals are garnet, tremolite-actinolite and epidote; pyroxene and biotite occur locally. The ore is mostly less than 10 m wide; the average grade is 27% Fe, 0.4-0.7% Mn, and 0.03-0.06% P.

Ultevis manganese-iron-(arsenic-barium-tungsten-fluorine) (27I Tjåmotis NV)

The first indication of a manganese mineralisation was found as a manganese-bearing boulder at Vuotnajaure (map sheet 26K Murjek) some 120 km to the east-southeast of the outcrops at Ultevis. A prolonged boulder tracing campaign was undertaken in 1941–42, and additional boulders were found in the region. Several unsuccessful attempts were made (including drilling) to locate the outcrop. Finally, in late 1943, the first outcrops were found at Stuor Njåskes (map sheet 28I Stora Sjöfallet SV). Prospecting efforts, geophysical investigation and geological mapping, then intensified and continued until late 1946.

The following mineralisation types have been encountered: 1) sedimentary manganese-iron deposits; 2) epigenetic manganese-iron mineralisation; 3) pegmatitic veins with manganese minerals; and 4) disseminations with molybdenum-bearing scheelite.

In the central and westernmost parts of map area 27I Tjåmotis NV, there is a transition from felsic volcanic rocks belonging to the Arvidsjaur group in the east, to sedimentary rocks of the Snavva–Sjöfallet group in the west (Fig. 168). A marble horizon occurs in the latter rocks, close to the contact with feldspar-phyric rhyolite. This marble is the host rock for syngenetic manganese mineralisations occurring intermittently over more than 20 km. This manganese-bearing zone can be followed from Lastak and Tjatjisvare south of Tjaktjajaure via Rakten and Sörhårås into the Ultevis area (28I Stora Sjöfallet SV and SO). High concentrations of tungsten, molybdenum, arsenic, and uranium are also found locally. The oxide minerals bixbyite, braunite, hollandite and hematite, which occur together with piemontite- and garnet-skarn, constitute the ores (Fig. 169–171). Locally, fluorite, barite, svabite (Ca-arsenate) and Ba-feldspar (hyalophane) are also present. Manganese-bearing green andalusite and manganese-bearing pink muscovite are found in aggregates up to 10 cm, within the metasedimentary rocks (sandstone, arkose, and conglomerate), close to the marble horizon. Epigenetic pegmatite-hosted manganese mineralisations are also found in the rhyolite (Ödman 1957).

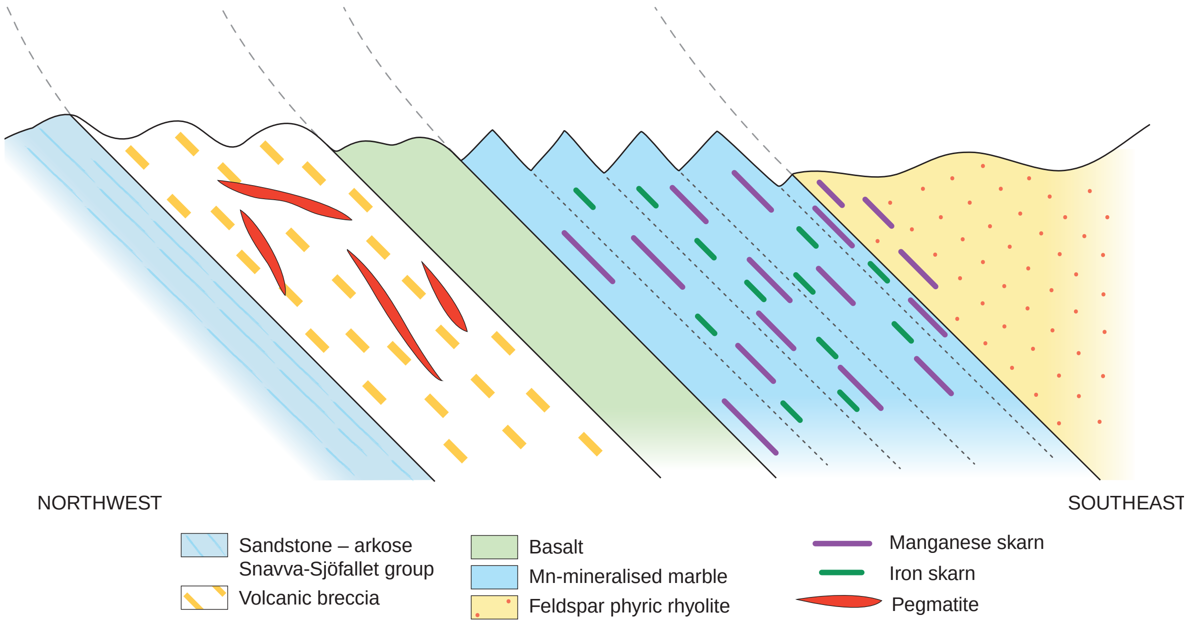

Figure 168. Profile at the Rakten locality. The manganese skarn mineralisation occurring at the contact zone between felsic volcanic rocks of the Arvidsjaur group, and overlying metasedimentary rocks of the Snavva–Sjöfallet group are shown. The stratigraphic sequence is overturned. Illustration: Per Nysten and Tone Gellerstedt.

It is suggested that the mineralisation may represent exhalation from one or several hydrothermal vents at the top of the volcanic sequence of rocks. The manganese-iron-barium-arsenic mineralisation appears to be a time-stratigraphic marker, an exhalation that formed in shallow water under oxidising conditions in an unstable tectonic environment, marked by vertical fault movements (Carlon 1984).

Porjusvare (27J Porjus NO)

The manganese mineralisation at Porjusvare is described by Geijer (1918) and commented on by Ödman (1947). This deposit consists of spessartine garnet, rhodonite and minor amounts of manganese oxides surrounded by a coarse-grained microcline-rich quartz monzonite to syenite, pegmatite and rhyolite. The rhyolite partly forms a banded, fine-grained rock and occurs partly as quartz-phyric foliated, more coarse-grained rock, possibly part of a subvolcanic intrusion. This rock is intruded by pegmatites. Ödman (1947) reported hausmannite occurring in the ore, but a newly made polished section shows braunite and hematite but no hausmannite. Along cleavage planes in microcline, small inclusions of other manganese oxides (pyrolusite?) occur. Rhodonite in the rock is very pale pink and difficult to distinguish from feldspar. The garnet is yellowish orange to brown and forms coarse skarn pods intergrown with manganese oxides. Wine-red piemontite has been observed in small amounts. Magnetite is locally present in the rhyolite as a few mm-sized porphyroblasts. Genetically, the suggestion made by Ödman (1947) that this mineralisation is related to the rhyolite accords with our observations, although pegmatites and granite-like rocks of possibly subvolcanic origin are also present.

Figure 169. Hollandite as fibrous to coarse radial masses (7446274/657919). Photo: Per Nysten.


Figure 170. Bixbyite as aggregates and euhedral crystals (7446274/657919). Photo: Per Nysten.

Figure 171. Piemontite-quartz skarn (7444777/656154). Photo: Per Nysten.

Stratiform (stratabound) sulphide deposits

Laisvall type (25H Arjeplog)

Sandstone-hosted, disseminated, lead-zinc mineralisation occurs in Neoproterozoic, possibly Ediacaran, to Lower Cambrian metasedimentary rocks along the eastern front of the Scandinavian Caledonides. The largest and best known of these deposits is Laisvall (Lilljequist 1973, Willdén 2004). Two similar, unexploited prospects, Maiva and Niepsurt are known in the vicinity of Laisvall.

The Laisvall lead-zinc deposit is situated 5 km north of Laisvall village at lake Storlaisan, 45 km west of Arjeplog. An exploration campaign by Boliden found Pb-mineralised boulders close to Laisvall, and the boulder train was followed to lake Storlaisan. A systematic drilling campaign started in 1939, and the mineralisation was intersected the same year. Development of the mine began in 1941 and small-scale production started in 1943. By 1985 production had increased to 1.45 Mt ore a year. Original ore reserves were estimated at 80 Mt, with 4% combined lead and zinc. A total of 65 Mt at 4.6% Pb, 0.6% Zn and some Ag was extracted between 1943 and 2001. Old mining maps of Laisvall are available in PDF format at www.sgu.se.

The host rock of the Laisvall deposit forms part of an extensive autochtonous platformal sequence that was overthrust by the nappes of the Caledonian orogen. The basement consists of granite and syenite, on which glacio-fluvial sandstones of the Ackerselet formation are deposited. Above follows the ore-bearing Såvvovare formation, consisting of shale and quartzitic sandstones. Three units are distinguished: the lower, middle, and upper sandstone, in which ore grade mineralisation is confined to the lower and upper units. The Såvvovare formation is overlain by shale and siltstone in the Grammajukku formation, and further upwards by the Alum Shale Formation. The deposit is sheet-shaped and elongated northeast–southwest. It comprises varying lead and zinc content in thin sandstone layers. The ore minerals occur as less than 1 cm large spots in massive sandstone. These spots are mostly randomly distributed, but may be concentrated along bedding planes. The principal minerals were deposited in the order calcite, barite, fluorite, sphalerite and galena. The minerals infill pore spaces in the sandstone.

Genetic models proposed through the years are: 1) hydrothermal or basin-brine model; or 2) groundwater or meteoric water model. Investigations performed to explain the genesis of the deposit include: 1) the spatial relationship of the ore; 2) the illite crystallinity of the shales; 3) fluid inclusions; 4) hydrocarbons; 5) isotopic composition of calcite carbon and oxygen; 6) sulphur isotopes of sulphides and sulphate; 7) Pb isotopes of galena; 8) Sr isotopes of barite and phosphorite; and 9) N and C isotopes of organic matter in shales. Recent work by Saintilan et al. (2016 and additional references therein) presents data on the conditions and timing of ore formation leading to Laisvall-type deposits, suggesting a Mississippi Valley-type deposit formed at 467 ± 5 Ma (Saintilan et al. 2015).

SULPHIDE DEPOSITS HOSTED BY SUPRACRUSTAL ROCKS

Base metal sulphides in the form of a copper-zinc mineralisation occur within high-grade paragneisses in the Luspevaratj deposit in map area 26I Luvos. In map area 25I Stensund, the Lulepotten copper deposit is hosted by basaltic to andesitic lavas. Both these sulphide deposits are found in the major Karesuando–Arjeplog deformation zone.

Small base metal deposits are also found at several places in the area covered by map sheet 25J Moskosel. These can be separated into 1) zinc-lead-(silver-copper) associated with iron sulphides, mainly in metasedimentary rocks; and 2) copper-zinc-lead-silver coexisting mainly with pyrite, as fracture-fillings within felsic sub-aerial metavolcanic rocks. In addition, locally weak sulphide disseminations occur associated with copper and gold partly in hydrothermally altered zones, and as fracture-fillings with quartz and tourmaline (Gustafsson 2009).

Luspevaratj (26I Luvos NO)

The Luspevaratj deposit is situated 45 km west of Jokkmokk. The area has been investigated by geological mapping and boulder tracing. Ground geophysical measurements were carried out 1972, and a geochemical survey was made in 1972–73. Additional magnetic and electromagnetic (VLF) measurements were performed during recent mapping (Antal Lundin et al. 2012a). The mineralisation has also been investigated by diamond drilling, which showed that the content of sulphide minerals decreases with depth. The mineralisation is a copper-zinc sulphide deposit in a supracrustal unit some 1.5 km wide and 20 km long, coinciding with the Karesuando–Arjeplog deformation zone (Antal Lundin et al. 2012a, Persson 1975). The mineralisation occurs in a series of lenticular schists and paragneiss layers that are rich in mica, cordierite, garnet, gahnite, with minor sillimanite (Antal Lundin et al. 2012a, b, Persson 1975). Disseminated sulphides occur in quartz-rich gneisses in zones with a maximum width of 12 m, parallel with the schistosity of the rock. Sulphides consist of pyrrhotite, pyrite, sphalerite, chalcopyrite, arsenopyrite, galena and minor molybdenite. Sphalerite in particular is found in close association with gahnite, and to some extent in garnet and cordierite-bearing zones. Silver content up to 80 ppm has been noted in association with the sulphides.

Lulepotten (25I Stensund NV)

Most of the ore prospects found in the area covered by map sheet 25I Stensund occur in parts affected by the Karesuando–Arjeplog deformation zone. The geology and mineralisation of the Radnejaure area, where Lulepotten is included, has been described by Padget (1966, 1971).

The Lulepotten copper deposit is situated 14 km east of Arjeplog; interest in this area was sparked by the discovery of several copper-mineralised boulders at lake Lulepotten. An electromagnetic (slingram) investigation gave a weak but distinct anomaly, and in February 1960 a borehole intersected a significant copper mineralisation. Subsequent drilling has shown that the mineralisation occurs as disseminations in steeply inclined zones approximately conformable with the schistosity and in contact with granitic rocks found west of the deposit. Various copper minerals occur in conjunction with basaltic–andesitic lavas and a strong positive gravimetric anomaly at the lake Gublijaure. Disseminated copper minerals in lavas occur as bornite and chalcocite, whereas somewhat richer associations of chalcopyrite-bornite-quartz are found in weakness zones. The sulphide minerals occur in narrow bands, as impregnations or in chunks, usually in quartz-filled fractures. The mineral paragenesis also includes magnetite and some fluorite. Chlorite, scapolite, garnet and epidote are products of hydrothermal alteration (Padget 1971). The mineralisation is younger than the granite. The deposit has a width of 20–25 m for a distance of 1.15 km and was drilled down to a depth of 500 m (Mellqvist & Aaro 2006a).

The estimated resource for the Lulepotten ore prospect is: 5.13 Mt with 0.73% Cu, 0.26 ppm Au and 7.48 ppm Ag with a cut-off of 0.4% Cu. A cut-off of 1% Cu resulted in 1.40 Mt ore with 1.57% Cu (Padget 1971, Sandahl 1973). There are several additional occurrences of Cu mineralisations along the Karesuando–Arjeplog deformation zone. To the north of Lulepotten these comprise Sadenåive, Soggovare, Lilla Sågberget, Smaltjärn, Kvarnbäcken, Ballek Västra and Norra and Rebraur Västra; to the south they are Jonastjärn 1 and 2, Geråive, Lövlund and Virka (Padget 1971, Sandahl 1973, Mellqvist & Aaro 2006a, b). Ballek Norra in particular is similar to the Lulepotten deposit (Sandahl et al. 1981). Uranium and copper occur in an albite-chlorite-quartz rock at the contact between orthogneiss and felsic metavolcanic rocks at Västra Rebraur.

Tjärrovare (25J Moskosel)

The Tjärrovare prospect (zinc, lead, copper, silver) has been the subject of extensive investigation, and in 1968 boulders containing zinc and lead were found in the Tjärrovare area at the locality named “Blyberget”, whose name derives from the lead-rich rocks. Prospecting (e.g. boulder tracing, drilling) was reported during 1979–86. Ore minerals occur as 1) silver-bearing galena and tetrahedrite, sphalerite, chalcopyrite and pyrite at Blyberget; and 2) chalcopyrite, sphalerite and pyrite at Tjärrovare (Einarsson & Stenberg 1985, Kathol et al. 2012a). The former occurs with calcium-magnesium minerals and the latter with sericitic alterations. The host rock for both types is a gneissic metapelitic rock occurring as schlieren in meta-arenitic gneiss. The richest parts are found adjacent to a contact between metapelite and what has been called "pseudo-quartzite" (Gustafsson 2009). The metal-rich parts are interpreted as having been formed along a stratigraphic palaeo-surface consisting of pelitic sediments in an intracontinental basin. The average metal content of 109 mineralised boulders is: 0.95% Cu, 0.98% Pb, 1.26% Zn, and 194 ppm Ag (Kathol et al. 2012a). The results of the drilling are less encouraging; the best core sections do show much higher content of metals than the averaged boulders but only for a couple of metres, whereas the best boulders have even higher concentrations (Kathol et al. 2012a). Three additional boreholes were drilled at Tjärrovare in 1990 to investigate whether the deposit could continue towards the southwest, where one core showed 0.3 ppm Au and 403 ppm Ag for a 3-metre section (Ljung & Einarsson 1990). In 1985 a similar mineralisation was found at Kvänberget, three km south of Tjärrovare. The deposit is weakly auriferous at 0.3–0.4 ppm (Kathol et al. 2012a).

Additional zinc, lead, copper and silver prospects within the area covered by map 25J Moskosel are known from Kaskatjåkkå and Varjisträsk, copper-zinc-iron prospects north of Malmesjaure, and copper prospects occur at Trollforsarna, Njuktavare-Stor-Tjärget and Benbrytefors (Kathol et al. 2012a).

Kiuri and Pallemvaratj (27I Tjåmotis NV, NO)

The Kiuri area is situated 5 km northwest of Tjåmotis. A follow-up programme of bog geochemical work by SGU from the late 1970s to early 1980 led to the discovery of anomalously silver-rich boulders in 1983, up to 2000 ppm Ag. In the summer of that year trenching, mapping, and sampling were undertaken together with ground geophysical investigation. Drilling began in late 1983. Notably, Linnaeus visited this area in the 18th century, and his silver-lead vein occurring high up at Kiuri hill was rediscovered by LKAB.

The geology at Kiuri is complex. The host rocks consist of interbedded subaerial rhyolite with volcanogenic arkoses and pelitic rocks. In biotite-rich zones Ag-bearing galena and fluorite occur in association with amazonite and pyroxene. Silver-rich veins are also found locally.

A similar geological setting is also found at Pallemvaratj, 4 km east-northeast of Tjåmotis. Here galena-sphalerite-chalcopyrite-pyrite occurs with fluorite in red quartzo-feldspathic and biotite-bearing gneisses of unknown origin, possibly volcaniclastic arkoses. Interbedded with these are iron-leached sulphide and fluorite-bearing gneisses with white sugary quartz (Carlon 1984).

Iekelvare with Pälkasbäcken and Malmtjärn (27I Tjåmotis SO)

The following three mineralisations are very close to each other geographically, but occur in very different rocks, some of which are of supracrustal origin. They are not described separately, since they are probably not present in mineable quantities, They do serve to demonstrate the potential of this area, however.

The Cu-Au mineralisation at Iekelvare occurs in a dioritic rock; the predominant ore minerals are chalcopyrite, pyrite and sphalerite, with minor impregnations consisting of galena, complex sulphosalts, arsenopyrite, and pure gold (Lundmark 1983a, b, Martyn 1984, Lundmark & Hålenius 1984, Einarsson 1985). The richly mineralised sections are not seen in outcrop, only in drill cores.

Geophysical and geological studies were performed at Pälkasbäcken in the 1980s (e.g. Lundmark 1983a, b, Martyn 1984, Einarsson 1985). A number of mineralised boulders and outcrops containing mainly chalcopyrite and pyrite were found in granitoids and supracrustal rocks.

Additional drilling and geochemical analyses in the Iekelvare–Pälkasbäcken area in 2004–2005 resulted in no further work.

The name Malmtjärn does not exist on the topographic map, but the name is that of the lake located in the area between Iekelvare and Pälkasjaure (Einarsson 1985). Besides proven mineralisation of pyrite, chalcopyrite and molybdenite in outcrop, there are several interesting boulders in the vicinity containing copper and tungsten, which have not yet been found in outcrop (Einarsson 1985). During a field visit at Malmtjärn dacitoid to andesitoid and granitoid to monzodiorite were identified, all of them hydrothermally altered and recrystallised, with disseminated sulphide minerals such as pyrrhotite and pyrite (Claeson & Antal Lundin in press-b).

Tjäula (27I Tjåmotis SO)

This mineralisation occurs in strongly altered dacite to andesite, partly as biotite-rich gneisses. According to a classification based on lithogeochemical analysis, andesite to trachyandesite with a latitic affinity is the predominant rock type. The mineralisation consists of disseminated cobaltian pyrite, chalcopyrite, pyrrhotite and magnetite, which is seen in the analysis of a chalcopyrite-bearing sample as >1% Cu, 726 ppm Co, 117 ppm Mo, 562 ppm Zn, 96 ppb Au, and 25 ppm Se. Minor amounts of molybdenite, sphalerite and trace of electrum are also reported from Tjäula (Carlon 1984). This prospect was also investigated by diamond drilling in 1984–85, when 10 boreholes with a total length of about 800 m were drilled and geophysical ground surveys conducted to try to determine the distribution of the mineralisation and quantify its content (Fig. 172a, b). However, no mining has taken place to date (e.g. Rösholt 1985b, Larsson 1993). The mineralisation dips shallowly to the east, has an estimated width of 3–5 m and a length exceeding 700 m (Larsson 1993).

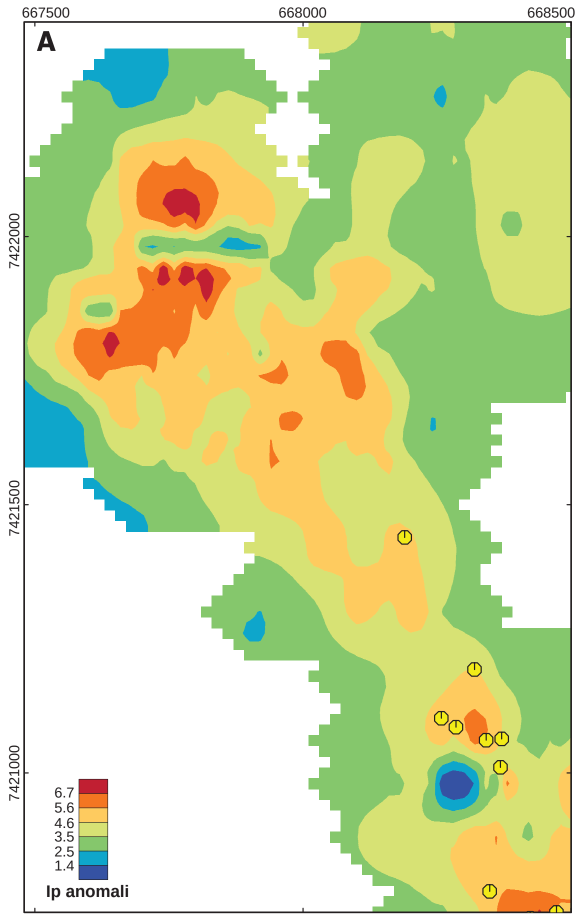

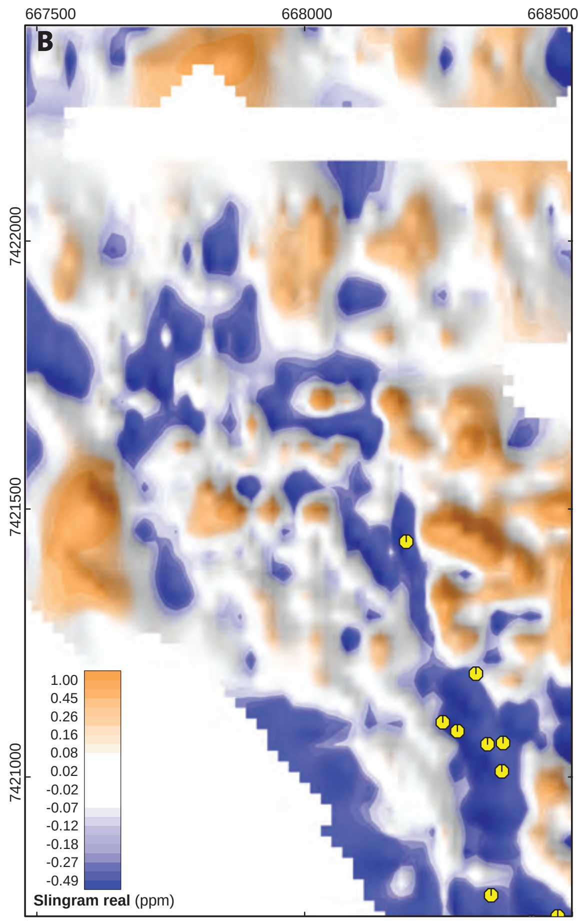

Figure 172. Geophysical anomaly maps based on ground geophysical measurements at Tjäula. Locations of drill holes are shown with yellow symbols. **A.** Induced polarisation (IP). **B.** Slingram, real component.

Björkholmen, Tjäkkaure, Parkijaure, Tallberget (27I Tjåmotis SO, 27J Porjus SV)

A mineralisation with bornite, chalcopyrite, pyrite, and malachite occurs in a number of outcrops along a linear belt in map area 27I Tjåmotis SO, e.g. Björkholmen, Tjäkkaure, and Parkijaure (Antal Lundin et al. 2011). This has been interpreted as a possible indication of regional conditions for copper and gold in the area's volcanic deposits (Rösholt 1985a). Tallberget in map area 27J Porjus SV is seen in the continuation of this linear occurrence and displays similar ore minerals. Geophysical measurements, core drilling and lithogeochemical analyses have been conducted at Tallberget (Rösholt 1985a, Claeson & Antal Lundin in press-c). A mineralised outcrop at Tallberget consists of hydrothermally altered, grey andesite to dacite with mafic fragments in the volcanic rocks. Chalcopyrite, malachite, bornite, and covellin are present, and epidote occurs as impregnation and fracture fillings (Claeson & Antal Lundin in press-c). The dacitoid to andesitoid rocks in the surrounding area are porphyritic, with feldspar phenocrysts whose amounts vary between 0 and 10%. They normally show foliation and lineation, with biotite in the matrix and sometimes amphibole. Susceptibility is usually relatively high, from 3 600 to 11 700 × 10^{-5} SI units.

Kårvo (27I Tjåmotis SO)

A previously unknown mineralisation 1 km north-northeast of Kårvo was found during a geophysical anomaly follow-up in 2011. It contains the minerals hematite, pyrite, sphalerite, molybdenite, chalcopyrite and bornite in hydrothermally altered dacite, trachyte, and trachyandesite (Antal Lundin et al. 2012a). A lithogeochemical analysis of a trachyandesite to trachyte shows 1% Zn and 565 ppm Cu, with elevated content of silver, bismuth, cadmium, mercury, indium, molybdenum, lead, antimony and tellurium. The position of the mineralisation coincides with a positive magnetic anomaly. The dacite shows high susceptibility: between 3 430 and 7 200 × 10^{-5} SI units. The dacite is hydrothermally transformed and light coloured adjacent to the mineralisation where susceptibility is lower: between 2 100 and 2 680 × 10^{-5} SI units. Susceptibility of the mineralised part is even lower: between 15 and 310 × 10^{-5} SI units. The measured profile across the positive magnetic anomaly shows no large minima at the level of the mineralisation, but about 30 m from the mineralised outcrops, the field strength is reduced by over 2 000 nT (Antal Lundin et al. 2012a). This is therefore considered an interesting target for further exploration.

Kanivare (26J Jokkmokk NV)

During field work in 2012 SGU found an apatite-bearing iron sulphide mineralisation 1 km southeast of Kanivare. It shows an anomalous uranium content (160 ppm U, Antal Lundin et al. 2012b). The country rock consists of metamorphically banded basaltic to andesitic rocks, locally rusty and hydrothermally altered. The mineralised part consists of pyrrhotite, pyrite, chalcopyrite, sphalerite, bornite and covellite. A lithogeochemical analysis shows 662 ppm Ni, 1115 ppm Cu, 10.8% S and elevated content of bismuth, lead, rhenium, selenium, tellurium and uranium. The content of REE_{tot} including yttrium is 635 ppm. Concentrations of gold and palladium are low. Calculation of the apatite content from 5.77% P_2O_5 yields approximately 14 wt% apatite. A thin section of a mineralised sample shows almost exclusively pyrrhotite as an ore mineral (Fig. 173) and mostly clinopyroxene as a silicate mineral (Fig. 174). The extensive occurrence of pyrrhotite is also seen in polished samples as well as in the observed outcrops. The mineralisation was investigated in 2013 using geophysical methods, and the locations of the measurements are shown in Figures 175a–c. Four electromagnetic ground VLF profiles were measured over the mineralised and hydrothermally altered rocks. Gamma radiation was measured using a hand-held gamma-ray spectrometer. The resistivity models obtained after inversion of the four VLF profiles are shown in Figure 176. The results of the VLF measurements show an area with very low resistivity that has a width of 20–30 m and a length exceeding 200 m. Depth penetration falls with a decrease in resistivity and an increase in frequency, which means that the mineralisation could be followed to a depth of just over 30 m. Measurement using multi-frequency EM methods, for

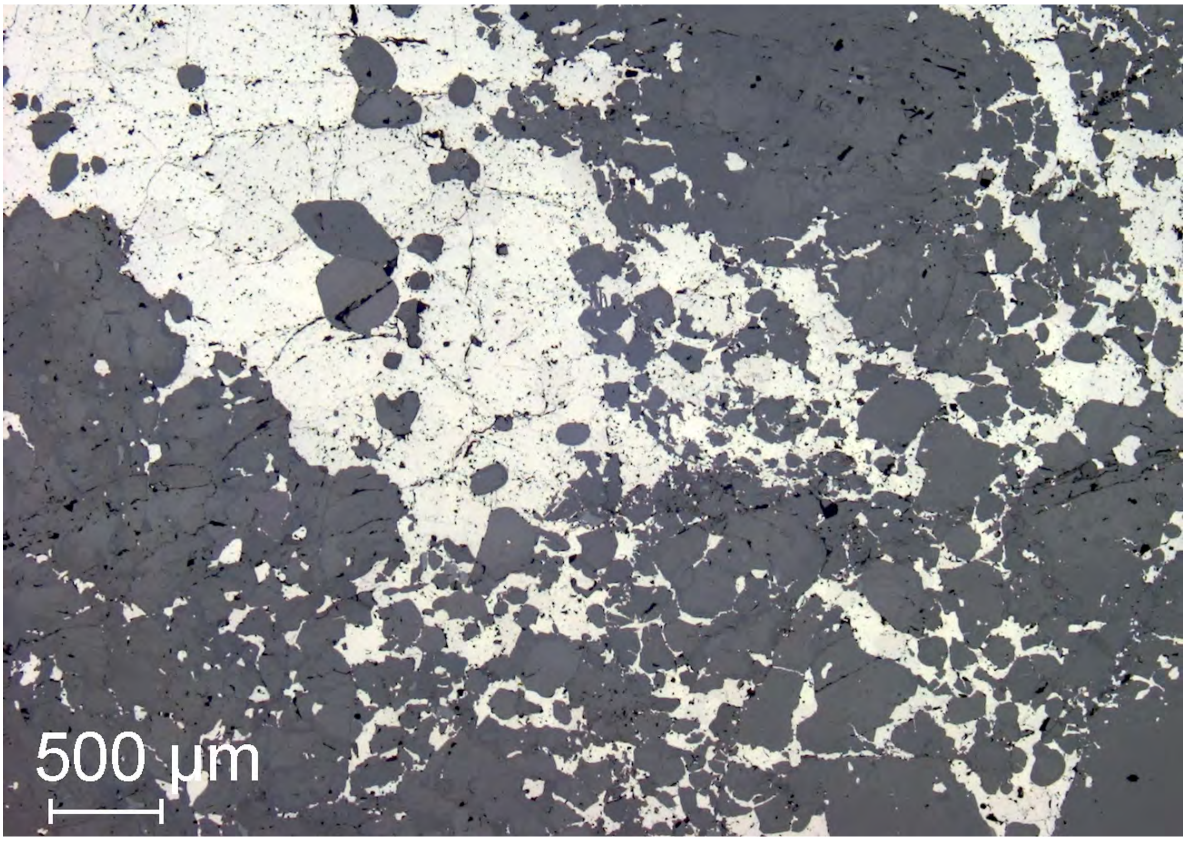

Figure 173. Pyrrhotite (bright) and silicate minerals (grey) in a thin section from the iron-sulphide mineralisation at Kanivare, reflected light (7397813/694183). Photomicrograph: Dick Claeson.

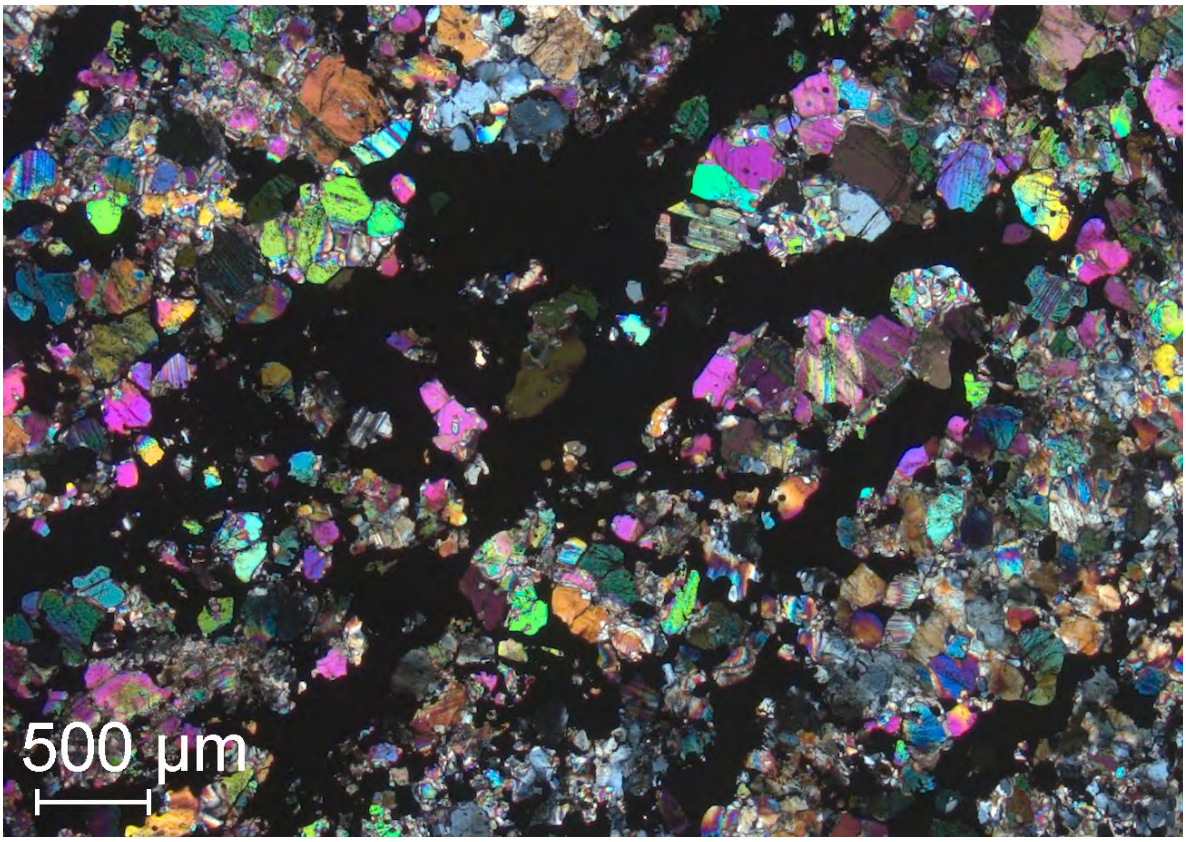

Figure 174. Clinopyroxene and pyrrhotite in a thin section from the iron-sulphide mineralisation at Kanivare, plane-polarised light, crossed nicols (7397813/694183). Photomicrograph: Dick Claeson.

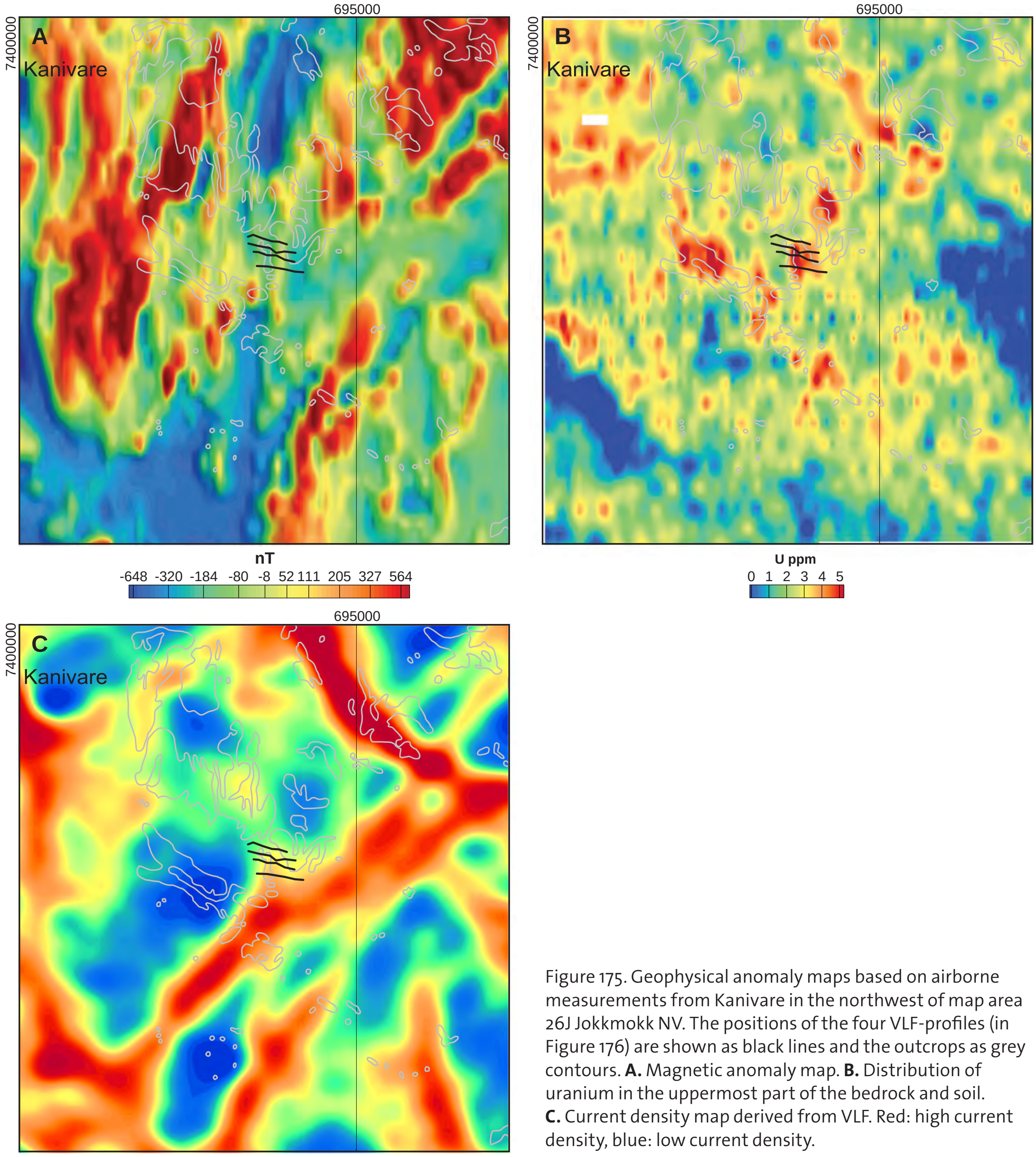

Figure 175. Geophysical anomaly maps based on airborne measurements from Kanivare in the northwest of map area 26J Jokkmokk NV. The positions of the four VLF-profiles (in Figure 176) are shown as black lines and the outcrops as grey contours. **A.** Magnetic anomaly map. **B.** Distribution of uranium in the uppermost part of the bedrock and soil. **C.** Current density map derived from VLF. Red: high current density, blue: low current density.

example, would give a much higher resolution at depth. The four sections have been measured with 60 m line spacing, and cover approximately 240 m of the mineralisation in the longitudinal direction (north–south). The mineralisation coincides with a north–south-trending deformation zone (the same zone as at Lullekietjeforsen (Figs. 175a–c, (Claeson & Antal Lundin in press-c), and the anomalies relating to the deformation zone can also be seen in the resistivity models as low-resistivity areas. The north–south-trending deformation zone is crossed by a northeast-trending deformation zone just south of the mineralisation (Figs. 175a–c). The mineralised rocks also show high uranium concentrations: between 140 and 422 ppm U measured on outcrops. The elevated uranium content can also be seen in the airborne measured data. Another interesting geophysical aspect is the high remanence: 48 and 226 A/m, and high Q-value: 15 and 119 of the mineralised samples, whereas the surrounding rocks lack remanence. But neither the genesis of the mineralisation, nor its potential, is clear.

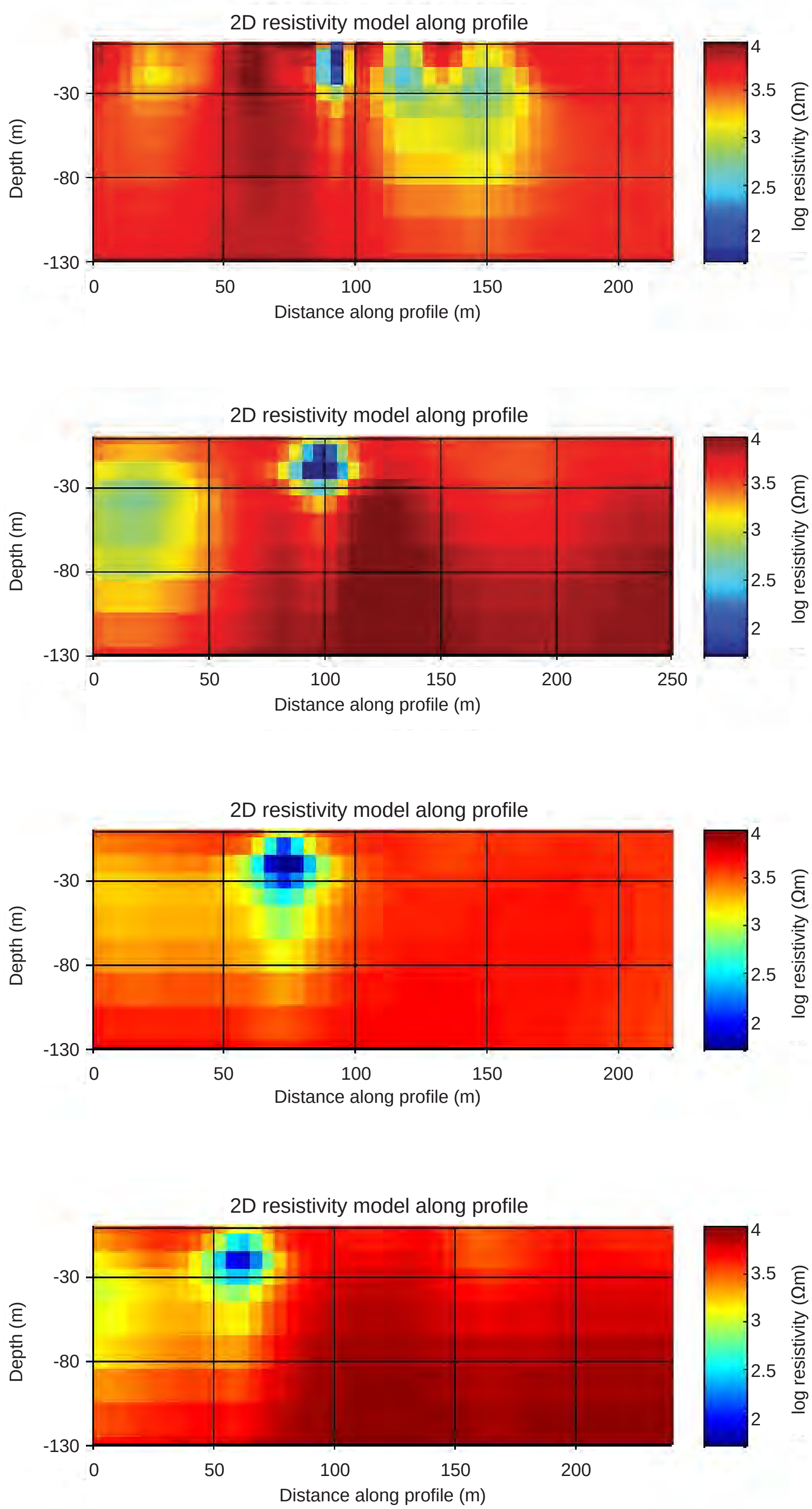

Figure 176. Resistivity models derived from VLF data. The profiles are arranged from north to south, where the first image corresponds to the northernmost profile in Figures 175a–c. The mineralisation indicated shows very low resistivity (dark blue).

Figure 177. Mineralised (Zn, Cu) banded volcanic rocks west of Norvijaur (7394185/689858). Photo: Lotta Olausson.

Norvijaur (26J Jokkmokk NV)

Banded, metamorphosed basic to intermediate volcanic rocks, with disseminated sphalerite and chalcopyrite present in the mafic parts in some outcrops, occur in the Norvijaur area (Fig. 177, Claeson & Antal Lundin in press-a). LKAB drilled one borehole in 1986, but reported only pyrrhotite, pyrite and a few crystals of chalcopyrite, in addition to graphite formed from reduced carbonate, in dark grey, tuffitic schist with numerous thin segments of skarn throughout the core (Johansson & Gustafsson 1986).

Tjerkisberget (26J Jokkmokk NO)

Earlier core drilling approximately 1.5 km northwest of Tjerkisberget revealed the presence of a sulphide mineralisation. It consists of disseminated pyrite and pyrrhotite, along with minor amounts of sphalerite, chalcopyrite and galena, according to drilling logs. Based on recent mapping of the area by SGU, the rocks found in outcrops consist mostly of andesite, dacite and basalt. There are also volcaniclastic rocks and mica-rich metasedimentary rocks, which sometimes contain cordierite and sillimanite (Claeson & Antal Lundin 2015). Sulphide minerals are also locally present (Claeson & Antal Lundin 2015). Hydrothermal alteration is common in dykes of grey granite in the area. Ground measurements of the magnetic, gravity and electromagnetic (HLEM) field were made along three profiles in 2004 by Suomen Malmi Oy on behalf of BHP Billiton over a narrow magnetic and electromagnetic anomaly beneath Tjerkisberget. The electromagnetic and magnetic anomalies coincide, and from the borehole logs it is clear that pyrrhotite is the cause of the magnetic anomaly (susceptibility up to $2\,500 \times 10^{-5}$ SI units), while the electromagnetic anomaly is caused by the presence of sulphides, including pyrrhotite (Fig. 178).

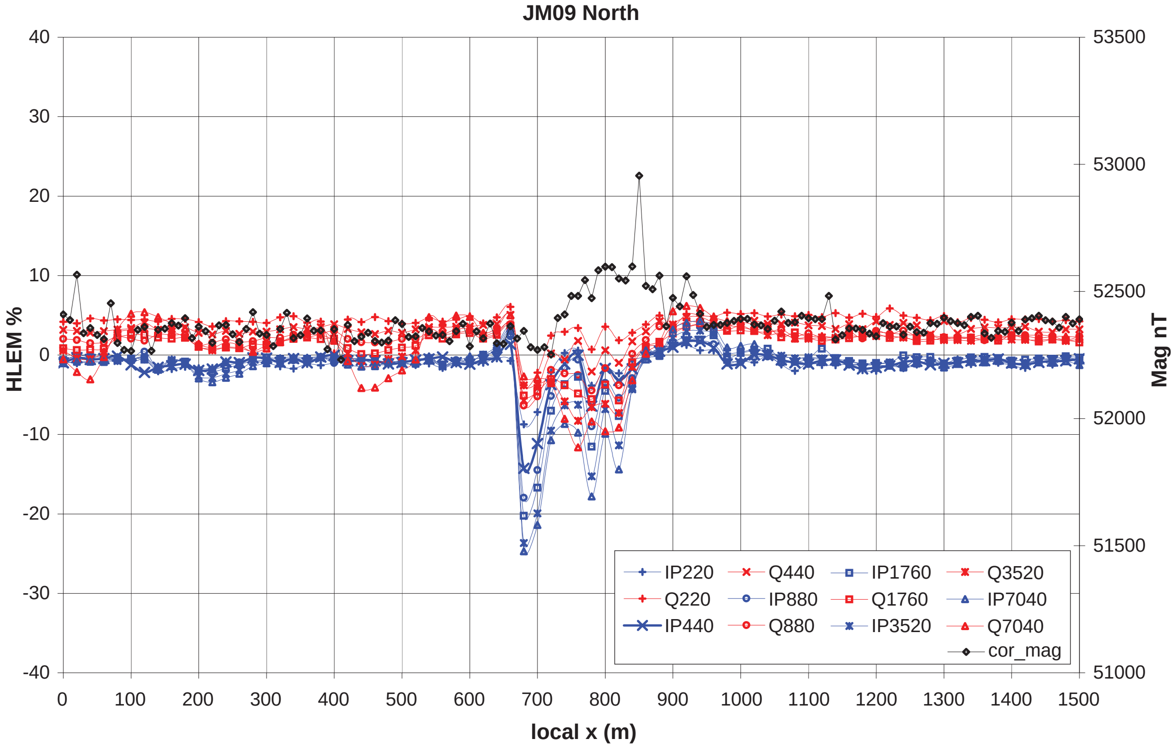

Figure 178. One of the ground electromagnetic measurements (EM) of the drilled anomaly in the Tjerkisberget area. A black line shows the magnetic field. The red and blue lines show real (IP) and imaginary (Q) component from the horizontal loop multifrequency EM measurements. The measurements were made by Suomen Malmi Oy (Lahti 2004). The magnetic and EM anomalies coincide well except for the first EM anomaly, which has a low magnetic signature.

Mineralisations in mafic granulite (26J Jokkmokk NV, NO)

A number of rusty outcrops are present in an area of mafic granulite to garnet amphibolite; three were sampled for lithogeochemical analysis by SGU. These were found to contain sulphide minerals with interesting levels of various elements, as described below. The mafic granulite rocks, locally diatexite with schollen migmatitic structures, are interpreted to constitute mainly metamorphosed trachybasalt to basaltic trachyandesite (Claeson & Antal Lundin in press-a). Earlier workers mapping the area suggested that the rocks were of sedimentary origin (Claeson & Antal Lundin in press-a).

Väst-Kieratj (7389972/709278): A sulphide mineralisation was found by SGU in 2012 west of Väst-Kieratj in a mafic granulite. A lithogeochemical analysis shows approximately 0.3% Cu, 0.5% Pb, 0.8% Zn, 5% S and elevated content of bismuth, indium, rhenium, antimony, selenium, tellurium and trace of gold, platinum and palladium (Antal Lundin et al. 2012b).

Nilsatjärn (7380003/708975): At a road cutting south of Nilsatjärn mafic granulite rocks are mineralised, containing 0.2% Cu and elevated content of bismuth, lead, rhenium, selenium, tellurium and thallium (Antal Lundin et al. 2012b).

Tebrikkullen (7379504/705666): At Tebrikkullen, about 5 km northwest of Tårrajaur, a mineralised mafic granulite of andesitoid to basaltoid composition shows 50.1% SiO_2, 19.7% Fe_2O_3, 1% S, and slightly elevated levels of 28 ppb Pt and 8 ppb Pd (Claeson & Antal Lundin 2013).

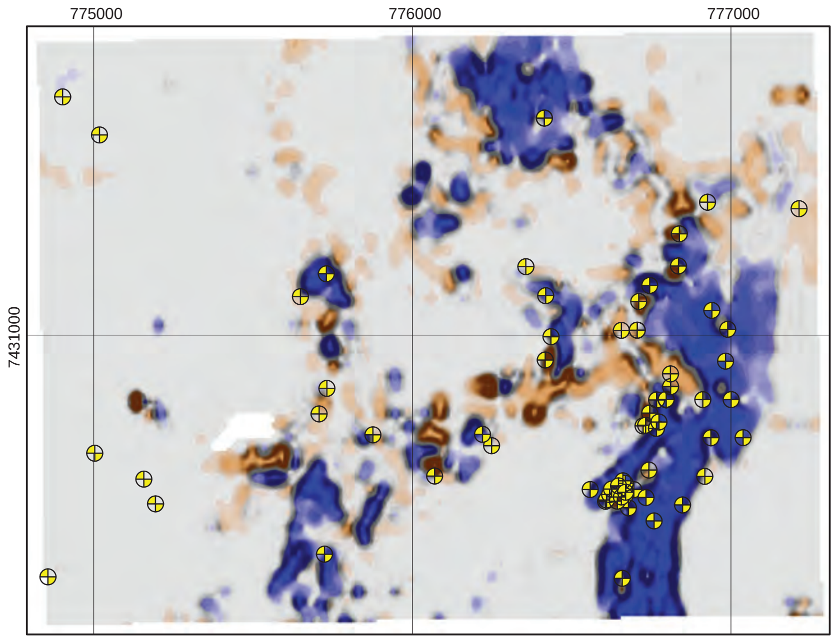

Figure 179. Electromagnetic (slingram) anomaly map at Puolalaki, imaginary component based on ground measurements. Shades of blue indicate high conductivity. The yellow symbols show the location of the drill holes.

Puolalaki (27K Nattavaara)

An occurrence of gold-copper-tungsten-arsenic mineralisation at Puolalaki attracted great interest during 1985–1991, when ground geophysical measurements, more than 2100 m of core drilling, along with lithogeochemical analyses and extensive moraine sampling were completed (Fig. 179, Hansson & Filèn 1991). The richest parts were found in acid intrusive rocks with considerable amounts of arsenopyrite, and 16–53 ppm Au was recorded in outcrop, boulder, and drill core (Hansson & Filèn 1991). Reported sulphides are pyrrhotite, arsenopyrite, chalcopyrite, pyrite, sphalerite and galena, with fewer occurrences of molybdenite. The presence of scheelite is also worthy of note. The base metals are found in metasedimentary rocks with intercalated tuffogenic rocks (Hansson & Filèn 1991).

Såkevare (26I Luvos)

Two separate zinc-lead-(silver) mineralisations in migmatised paragneisses were found via geophysical measurements, followed by diamond drilling between 2003 and 2007 by BHP-Intrepid, both called Såkevare (Fig. 180). The drill logs report graphite-bearing paragneisses with predominantly sphalerite and minor galena (Fig. 181).

Sluppojaure (26I Luvos)

Boulders and outcrops of sulphide-mineralised amphibolite occur about 9 km north-northeast of Skuppesavon and north-northeast of Sluppojaure. At two outcrops the mineralisation consists of pyrite, pyrrhotite, arsenopyrite and chalcopyrite, with traces of molybdenite. An older lithogeochemical analysis of a sulphide-rich part shows 1.5% Cu, 40 ppm Ag, and 0.2 ppm Au. At an outcrop approximately 130 m south-southeast of the old location, a 4 m wide garnet- and amphibole-skarn rock contains pods and disseminations of chalcopyrite and pyrrhotite. A sample for lithogeochemical analysis showed anomalous content of copper, zinc, arsenic, silver and gold (Antal Lundin et al. 2012b)

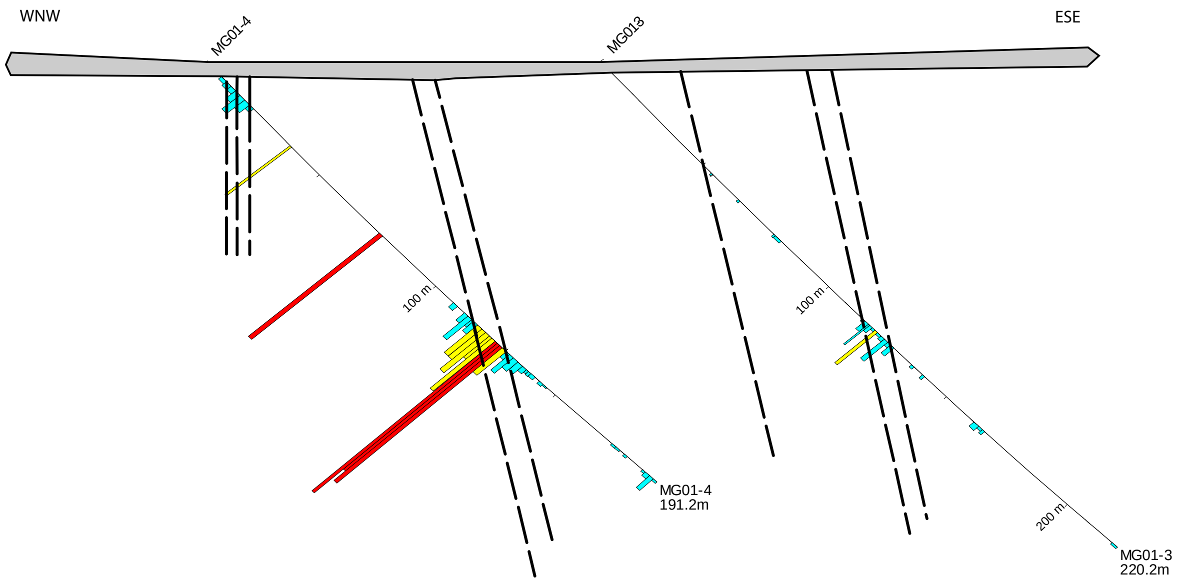

Figure 180. Zn-Pb-Ag anomalies from cored boreholes at Såkevare, peak levels in the image are at 1.65% Zn, 0.64% Pb, and 5.5 ppm Ag. Image from BHP-Intrepid.

Figure 181. Altered wacke to mudstone with pyrite, sphalerite and galena in veinlets and fractures in drill core from Såkevare. Photo: BHP-Intrepid.

Stora Pahtavaara (26M Överkalix)

Copper ore consisting of chalcopyrite and bornite associated with diopside and secondary copper minerals at the contact between metagreywacke, meta-arenite and amphibolite was mined during historical times. Today, two water-filled 10 m large holes surrounded by large dumps are visible at the mine. Locally, the dumps are rich in copper minerals and a chemical analysis of a random sample revealed >1% Cu, 9 ppm Ag and 248 ppb Au.

EPIGENETIC BASE METAL DEPOSITS AND GOLD-SILVER VEINS

Deposits displaying clear cross-cutting relationships with their host rocks, particularly of the vein type, are assigned an epigenetic origin below. Polyphase mineralisation is also recognised at some localities, e.g. Kiuri, where mobilisation has resulted in silver-rich veins occurring in association with hydrothermally altered rhyolitic host rocks.

Svanisträsk (25K Harads)

Auriferous sulphide mineralisations occur at Svanisträsk. They consist of pyrite, chalcopyrite and minor molybdenite in quartz-rich zones, and veins in a hydrothermally altered rock, with transitions to porphyritic red granite. This mineralisation has been known since the 1950s; chemical analyses from outcrops taken at that time showed a gold content of 0.6 to 0.4 ppm. Additional sampling and analyses made by SGAB in 1982 resulted in 0.1–0.2 ppm Au and 20–45 ppm Ag. These samples display a remarkably high bismuth content of 60 to 200 ppm (Carlson et al. 1983).

Korpilovaara (27M Korpilombolo)

On the western side of Korpilovaara, 2.4 km east of Korpilombolo, a small pegmatoid dyke of hydrothermal origin with visible amounts of bornite and malachite was noted by SGU during bedrock mapping in 2008. This dyke is hosted by metagreywacke and amphibolite, and strikes 119/74, which is parallel with the gneissosity of the migmatitic metagreywacke. Another outcrop with malachite was reported by SGU from the northern slope of Holmanpalo 8.5 km to the northeast (Jonsson & Kero 2013d). Copper-mineralised boulders were also found in the area.

Haapamaa/Korpilovaara (27M Korpilombolo)

In a small outcrop on the eastern side of the road between Övertorneå and Pajala, 3 km east of Korpilombolo, a quartz vein containing visible amounts of bornite, chalcopyrite, malachite and magnetite was found in 1997 by P. Lantto from Aapua. Lithogeochemical analysis performed on samples from this vein showed 5.4 ppm Au. The quartz vein was investigated in more detail during bedrock mapping by SGU in the area. It is 0.5 m wide, hosted by a metatexitic greywacke and strikes 80/85. Microscopy work and microprobe analysis revealed the presence of native gold and several palladium-tellurium-bismuth minerals in small amounts (Jonsson 2010).

Måskosgårsså (27J Porjus SO)

Veins of argentiferous galena are known from the Måskosgårsså canjon in Muddus national park (Eriksson 1979).

Ligga east (27J Porjus SO)

Local drusy, milky quartz veins occur on the banks of the Stora Luleälven river, 1 km east of Ligga farm. The veins are sparsely mineralised with chalcosite and malachite (Per Nysten, personal communication).

OTHER METAL DEPOSITS

Uranium

Elevated uranium and thorium content is known from several geological environments in the project area. Of these, the epigenetic vein deposits of Pleutajokk and Skuppesavon (26H Jäkkvik, 26I Luvos) are the most prominent. At Lulep Manak (27I Tjåmotis), a uranium-rich pegmatite forms the host rock, and at Tåresåive (27J Porjus) uranium and thorium occurs in association with REE and molybdenum in pegmatite granite. Anomalous uranium content is also recorded from a pyrrhotite-rich mineralisation in basic to intermediate volcanic rocks at Kanivare (26J Jokkmokk).

Pleutajokk-type

Pleutajokk (26H Jäkkvik SO)

Uranium-bearing boulders were discovered in 1969 by SGU prospecting personnel, who found uraniferous minerals in boulders along the Pleutajokk river. These boulders were observed due to the presence of yellow secondary uranium minerals without the aid of a scintillometer. An intensive exploration programme by SGU, including geochemical, geophysical, and geological methods began in 1970. By the end of 1976 they had discovered seven uranium deposits and uranium showings, named A to G (Gustafsson & Minell 1977). Exploration rights were transferred to LKAB in 1976, and diamond drilling of the prospects was intensified. LKAB continued exploration with drilling of the A deposit and more detailed investigation of the B ore zone between 1976 and 1981. Historical estimates of the Pleutajokk B ore zone resources were made by Robertson (Jonasson 1980) using geostatistical methods. Details of those investigations have been summarised by Phillips (2005), and a mineral resource estimate as of July 2005 is given at 1 479 tonnes U inferred and 551 tonnes U indicated.

Pleutajokk consists of several uranium concentrations within an area of 15 km^2, of which only the southwestern part has been investigated in detail. The mineralisation occurs as millimetre to centimetre-scale veinlets of sub-parallel quartz veins arranged en echelon in two intersecting zones forming a stockwork. Euhedral uraninite, mainly occurring at the quartz vein wall-rock interface, constitutes the ore. Small amounts of disseminated uraninite are also found in the wall rock immediately adjacent to the veins. Uranophane and kasolite are seen as yellow coatings on weathered surfaces. The wall rock is metasomatically altered up to 10 m on each side with Na-enrichment and K- and Si-depletion (Wilson & Åkerblom 1982). The alteration and mineralisation pattern appears similar to that found at Skuppesavon (see below). The country rock consists of metarhyolite of ignimbritic character and the mineralisation has a spatial association with intrusions of dolerite. In general, extensive uranium mineralisation was emplaced in the vicinity of the dolerites (Öhlander 1986). Like the rhyolites, the granites and the pegmatites are both anomalously rich in uranium and thorium (Öhlander 1986). The apparent age of the uranium deposits in the area is around 1.75 Ga, and they are thus younger than all rocks they appear in (Hålenius et al. 1986). The ore-bearing area is delimited to the east and west by younger granites and to the north by more intermediate volcanic rocks.

Uranium –Titanium

Skuppesavon (26I Luvos SV)

Several uranium mineralisations occur in a succession of recrystallised, albitised acid volcanic rocks at Skuppesavon near the Piteälven river (Antal Lundin et al. 2012a and references therein). The Skuppesavon deposit is an epigenetic uranium mineralisation occurring mainly as disseminations associated with Na- and Ca-metasomatism. The host rocks are largely rhyolitic with intercalations of dacitic and trachytic compositions. They are pink to grey, weakly to moderately foliated, partly containing tuff-like structures. Concordant skarn bands and andalusite-bearing horizons are also found (Smellie 1982, Laurikko 1983a, b). The uranium deposit was discovered in 1979 during ground radiometric follow-up of airborne radiometric anomalies. The uranium mineralisation occurs as stratabound disseminations associated with fractures striking north–northeast and dipping steeply to the west in metavolcanic rocks. Radioactive minerals, mainly uraninite and some uranium titanate, occur both in fractures and as impregnation in the host rock (Antal Lundin et al. 2012a). Uranium precipitation occurred where the mafic minerals e.g. pyroxene, amphibole, epidote, garnet and magnetite were most abundant (Hålenius et al. 1984). The initial investigation was carried out in 1980–81, and diamond drilling was performed in 1981–83, followed by geochemical sampling and IP-measurements during 1984–85. Drilling at the Skuppesavon south mineralisation has revealed a 400 m long mineralisation with an average cross-sectional area of 150 × 20 m and an average uranium content of 704 ppm. A calculation shows that the mineral deposit contains 688 tonnes of uranium (Laurikko 1983a, b). Preliminary results of U-Pb dating of zircon from the acid volcanic rock at Skuppesavon suggest a magmatic crystallisation age of c. 1.89 Ga (Antal Lundin et al. 2012a). Continental Precious Minerals Inc. had a permit for exploration of yttrium at Skuppesavon between 2005 and 2014, and drilled another two cored boreholes and conducted 29 ICP-MS analyses. None of the analyses indicated high content of yttrium or REE, but some showed anomalously high uranium content, up to 0.25% U_3O_8.

Lulep Manak (27I Tjåmotis NV)

This prospect was investigated by diamond drilling in 1974–75. Metasedimentary rocks belonging to the Snavva–Sjöfallet group, intruded by dolerite and pegmatite, are the host rocks for the uranium mineralisation at Lulep Manak. The dolerite is sub-concordant to the bedding in the surrounding quartzite. Lenses and pods of a grey biotite-pegmatite locally rich in uraninite occur immediately to the west of this dolerite. Activities more than 3 mR have been recorded at pegmatite outcrops and in drill cores (Sundbergh 1979). An ore reserve of 20 tonnes uranium at 800 ppm is estimated for the southern part of the area investigated.

Kvarnån (25K Harads NV)

The uranium mineralisation at Kvarnån was discovered by SGU 1971 during a follow-up of an air-borne radiometric anomaly. This prospect was investigated further by percussion drilling during 1971–73. Diamond drilling began in 1978 and ended in 1983, when 107 boreholes had been drilled. The mineralisation consists of disseminated uraninite, which occurs in a meta-arenite enclosed by intermediate metavolcanic rocks. These rocks and the mineralisation strike northeast–southwest with a dip of 35° to the northwest. The uraninite occurs in biotite-rich veins or in aggregates of hornblende + epidote. Preliminary tonnage was estimated at 1.94 Mt uranium ore at 731 ppm U, and a mineral resource as of July 2005 was estimated at 184 tonnes uranium inferred and 1238 tonnes uranium indicated (Phillips 2005). The smaller prospect Brännspiken occurs about 5 km southwest of Kvarnån, with a uranium content of up to 1700 ppm U (Kullman 1984, Svensson et al. 1981).

Molybdenum

Molybdenum occurs in two host minerals in the investigated area. The most widespread and important of these is molybdenite, found as disseminations and veinlets in aplite, pegmatite and granite (Allebuoda, Munka, Tåresåive). The other mode of occurrence is as a solid solution in scheelite-powellite in piemontite skarn, exemplified by Sörhårås in the Ultevis area.

Allebuoda (26H Jäkkvik)

Several types of investigation have been carried out in the Allebuoda area, including geological mapping (1:5 000), boulder tracing, diamond drilling, excavation and trenching, geochemical surveys, geophysical measurements and Quaternary geological investigations. The first mineralised boulders were found in 1968, east of Allebuoda hill. Additionally, LKAB Prospektering AB mined a small quantity of molybdenite in an open pit to obtain material for beneficiation properties.

The Allebuoda molybdenum and tungsten occurrences are located in the Rappen district (Walser & Einarsson 1982, Öhlander 1986). The area consists of metamorphosed supracrustal rocks that were intruded by granite. To the north and west these rocks are overthrust by nappes of the Caledonian orogen. The supracrustal rocks have been folded along north–south-trending axes, and the central part of a large anticline is characterised by highly metamorphosed veined gneisses (Walser & Einarsson 1982). The upper part of the metasedimentary sequence includes limestones, skarn bands and banded iron formations. These sedimentary rocks grade into predominantly acid volcanic rocks, partly tuffitic in nature. Two generations of granite intrude the supracrustal sequence and the younger forms a heterogeneous group of intrusions. The molybdenum mineralisations are associated with the younger generation of granite.

Three types of molybdenum mineralisations occur in the Rappen district: 1) disseminations or intensive mineralisations in aplites related to the younger granites; 2) molybdenite in quartz-veined granite; and 3) veins and disseminations of molybdenite in altered acid volcanic rocks.

The largest deposits, Munka and Allebuoda, are of type 1. The granites associated with the deposits form geophysically well-defined diapiric structures interpreted to be cupolas of underlying batholiths (Öhlander & Nisca 1985). Three mineralisations containing molybdenite are known in the Allebuoda area, the largest of which, the Allebuoda Stora (Björntjärn), is bound to a 10 m wide and 250 m long aplitic dyke dipping 45° to the northwest. An ore reserve of 418 150 tonnes containing 0.26% Mo was given for Allebuoda Stora (Hill 1981). The main molybdenum enrichment is confined to an aplitic apophyse intruding the supracrustal rocks. This aplite is irregularly richly mineralised, and molybdenite occurs interstitially, often in coarse aggregates. Fluorite is common, and pyrite dissemination is also present. Molybdenum-bearing quartz-veins are related to the aplite and form small zones of enrichment. Pegmatites are present in small amounts. It is suggested that the aplite and molybdenite enrichments at Allebuoda have been derived by magmatic differentiation from the granite. Several small scheelite deposits are also known in the Allebuoda area, and results from geochemical investigations indicate that further molybdenum mineralisations remain undiscovered (Öhlander 1986).

Munka (26H Jäkkvik)

The Munka prospect is situated east of lake Tjeggelvas, 11 km northeast of Stenudden. Based on a geochemical anomaly, a search for boulders was made in 1971, with several molybdenum-mineralised boulders being found 4 km east-northeast of Munkajaure. Additional boulders were found in 1972–73. Due to a lack of outcrops, magnetic surveys were conducted and diamond drilling was performed by SGU in 1972–77 and by LKAB in 1977–88. About 1.5 Mt of ore with 0.10–0.15% Mo is estimated to be present at Munka (e.g. Hübner & Einarsson 1980). The mineralisation occurs at the contact zone between granite and gneissic sedimentary rocks. In this zone the rocks are intruded by numerous granite, pegmatite and aplite dykes, with Mo only occurring in the aplite dykes. Their width can be up to 9 m. Large amounts of fluorite are also present in associated aplitic red granite. Boulders bearing zinc, copper, lead and silver are also found in the area.

Druggegruvan (26J Porjus SV)

The Druggegruvan mine, also known as Klubbudden, Vuottjåive or Maddaåive, is situated some 15 km northwest of Jokkmokk, and consists of a blasted shaft, 5 × 10 m, heaps of gangue, and parts of a runway out on the tailings. Molybdenite is present as flaky aggregates, lumps, and veins in pegmatite and in quartz-rich fracture fillings and zones, in which large amounts of pyrite are also present, along with chalcopyrite, pyrrhotite and magnetite (Claeson & Antal Lundin in press-c). Open fractures with abundant pyrite are also seen. The bedrock consists mostly of fine-grained to coarse-grained granite and pegmatite, with graphic granite texture in places, but foliated granite is also found surrounding the mineralisation and xenoliths of a basic rock. The mineralisation was discovered by locals before 1930. Some of the ore was processed in the 1940s and refined into 20 tonnes of molybdenum ore, yielding an average grade of 0.48% Mo. Early data from a test pit indicated refined ore at 1.65% Mo, and estimated the average grade of the deposit to be 0.13% Mo (Högbom 1931, Ödman 1942, 1957).

Pokehällan (26K Murjek NV)

Close to the Letsi hydroelectric power plant, 28 km southeast of Jokkmokk, a molybdenum prospect occurs in pegmatitic to aplitic granite belonging to the Lina suite (Högbom 1931).

Pakkosavoi (27J Porjus SO)

North of the Ligga hydroelectric power plant, sulphide mineralisations occur in hydrothermally altered foliated granite belonging to the Perthite monzonite suite. These alteration zones are up to one metre wide, and mainly consist of fine-grained muscovite and quartz. Sulphides present consist of pyrite, sphalerite, galena, chalcopyrite and molybdenite. The molybdenum content is about 0.1% (Kathol et al. 2015). Elevated radiation levels, with anomalous uranium and especially thorium content occur locally, along with a body of pure quartz, at least partly in a north–south-oriented fracture zone (Gustafsson 1979).

Kåtaberget (25K Harads SV)

The Kåtaberget molybdenum prospect was found during a mineral campaign in 1971, but was investigated more thoroughly by SGU between 1978 and 1980. An area of 800 m^2 was stripped, and geophysical measurements were also performed. The mineralisation consists of an uneven dissemination of molybdenite in a leucogranite. Traces of fluorite and chalcopyrite are present. Assessment of average molybdenum content in an area covering 17 000 m^2 was estimated to be less than 0.05%. In an area of 3 300 m^2 the molybdenum content was estimated at 0.1–0.15%. These results were considered to discourage further investigation (Sjöstrand 1981).

Tungsten-tin

Kuossavare (25J Moskosel)

At Kuossavare, scheelite and minor fluorite was found both in boulders and outcrop in 1968. This mineralisation consists of three thin, garnet-bearing horizons in a felsic metavolcanic rock with interlayered metasedimentary rocks. Analysis results show a content of up to 0.1% W. Scheelite is also known from Allebuoda, and molybdenum-bearing scheelite and tungsten-bearing powellite are known to be associated with a piemontite-quartz skarn at Ultevis.

Sågudden (27I Tjåmotis)

The Sågudden deposit is situated between Tjåmotis and Årrenjarka, where supracrustal rocks are intruded by fluorite-bearing aplites and dolerites. Diamond drilling has revealed a skarn zone at the contact between aplite and felsic metavolcanic rocks. This skarn consists of pyroxene, tourmaline, biotite, fluorite and quartz, and traces of pyrite, chalcopyrite, molybdenite, scheelite and cassiterite occur together with ilmenite and rutile. A 12 m long drill-core section contains an average of 0.18% Sn.

Rare earth elements (REE)

Tåresåive (27J Porjus SV)

Molybdenite occurs in hydrothermally altered granite, rhyolite, and pegmatite at Tåresåive. The granite is c. 1.88 Ga (SGU unpublished), but the analysed zircon was significantly metamict and the result more uncertain than normal. The granite makes up a major part of map area 27J Porjus SV, and is clearly visible on both the gravity and magnetic anomaly maps (Figs. 5, 8, Claeson & Antal Lundin in press-c). The mineralisation appears to be related to cracks and fissures, but molybdenite is also disseminated in the host rocks. This is the only place where this type of mineralisation has been observed in map area 27J Porjus SV. The mineralisation is a *mineraljaktsfynd* ("mineral hunt discovery") (Krister Mattsson, 79293), but only reported as containing molybdenite and emitting gamma radiation. A few fractures with a width of 10–30 cm and lengths of more than one metre containing compact molybdenite are seen in the outcrops (Fig. 182). A lithogeochemical analysis of a mineralised sample from Tåresåive indicated at least 15% Mo, and showed very high levels of rare earth elements. The combined REE show a minimum of 94 900 ppm (9.5%) REE_{tot}. If yttrium is included in the REE, the content increases to >100 600 ppm (Claeson & Antal Lundin in press-c). The mineralisation is extremely enriched compared with the surrounding granite (Fig. 183). The petrogenesis of the deposit is discussed at length in Claeson & Antal Lundin (in press-c), where late stage magmatic fluids and vapours are preferred as the cause, rather than magmatic fractionation alone. Metamict allanite-(Ce) is a feasible host for the rare earth elements. The small amounts of carbon (0.2%) and phosphorus

Figure 182. Fracture zone with compact molybdenite in hydrothermally altered granite, rhyolite and pegmatite (7421196/709317). Photo: Ildikó Antal Lundin.

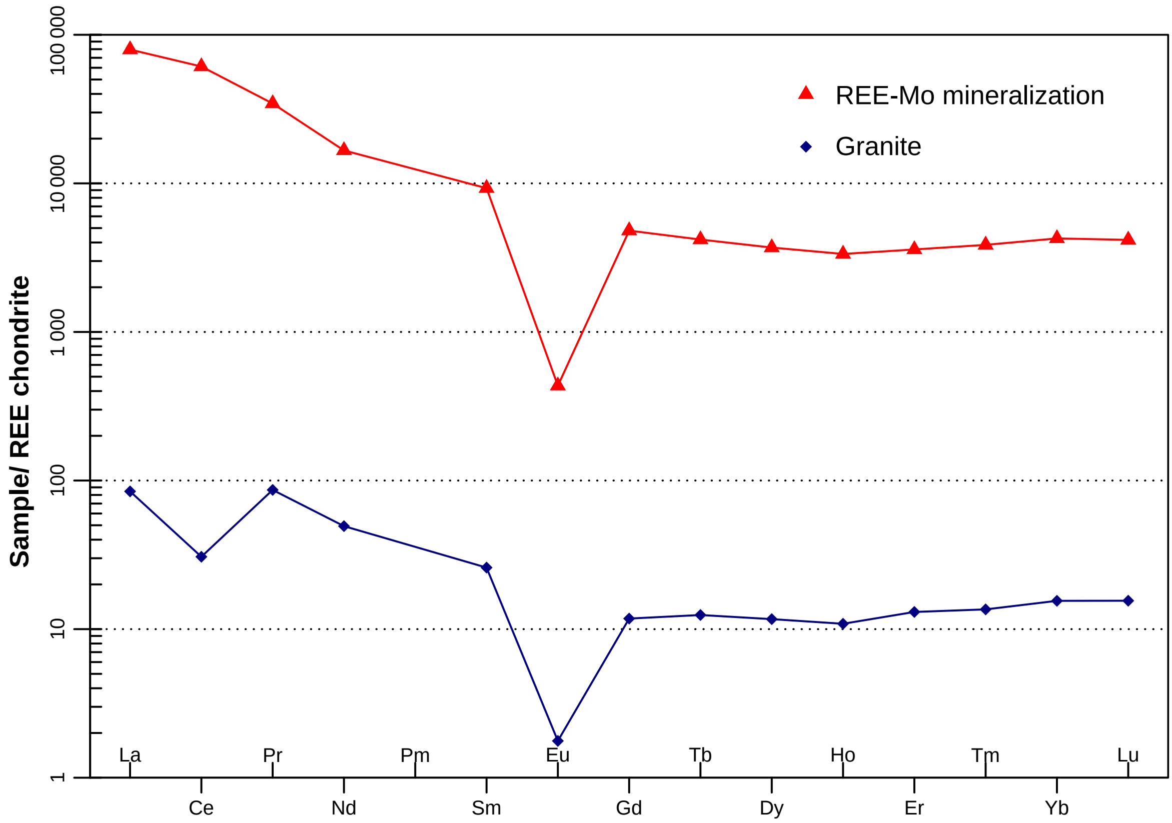

Figure 183. REE diagram with data from lithogeochemical analyses of granite and the REE-Mo mineralisation at Tåresåive. Normalising values for chondrite from Boynton (1984).

(0.7%) exclude both carbonate and phosphate minerals as major REE hosts. The potential of the mineralisation is unknown. The sample analysed displays elevated levels of 1490 ppm U, 2430 ppm Th, 396 ppm Nb, 36 ppm Ta, 37 ppm Se, 115 ppm Be, 380 ppm Pb, and 178 ppm W. Similar mineralised occurrences of uranium, thorium and rare earth elements are reported from Bokan Mountain, Alaska, for example (Philpotts et al. 1998, Dostal et al. 2011). However, the mineralisation is related to a complex peralkaline granitic intrusion with completely different compositions than the granite of Tåresåive, and molybdenite is not a major mineral. REE-, niobium- and molybdenum-rich quartz syenite and pegmatites are reported from the Kin prospect, British Colombia, Canada (Caudle et al. 2014), but none of them is a direct analogue of the mineralisation at Tåresåive, since they have a much higher proportion of niobium relative to molybdenum.

INDUSTRIAL MINERAL DEPOSITS

Granitic pegmatites, general characteristics

Granitic pegmatites may be divided into four main classes according to their degree of chemical fractionation: abyssal, muscovite, rare element and miarolitic (Černý 1991a, b). The rare element and miarolitic classes can be subdivided into lithium-cesium-tantalum (LCT) and niobium-yttrium-fluorine (NYF) types due to their chemical constituents. A moderately fractionated north–south-trending dyke swarm of pegmatites displaying LCT chemistry occurs south of Råneå. Two major pegmatite deposits belonging to the NYF-type occur south of Jokkmokk. At Reunavare 25J Moskosel NV, three separate pegmatite bodies occur in medium-grained, reddish-grey, undeformed early Svecokarelian granite (Kathol et al. 2012a).

Pegmatitic deposits intermediate between LCT and NYF occur at Kåivåive 25I Stensund SV, with beryllium, niobium-tantalum and REE minerals. Mineralogically less evolved "ceramic" types of pegmatite have been quarried at Isakberget on map sheet 26M Överkalix, for example.

The Råneå area

Quartz and feldspar were quarried in the first half of the 20th century in the coastal area between Råneå and Sundom. The pegmatite dykes strike north to north-northwest, have steep dips and intrude quartz diorite to granodiorite and migmatitic gneisses. Less than 10 000 tonnes of combined quartz + feldspar was mined at the largest quarry, Sörhällan. A common feature of several of these pegmatite dykes is the presence of tourmaline and locally also rose quartz. At Sörhällan, beryl, monazite, thorite and a strongly radioactive, black unidentified mineral occur. Columbite has also been noted at several localities. U-Pb dating of columbite from Råneå resulted in an age of 1 765 ± 14 Ma (Romer & Smeds 1994). Radioactive minerals also occur at Högträskkölen (e.g. wölsendorfite). Tourmaline-bearing pegmatites have been observed at Jerivaara (27M Korpilombolo NV) and at Niilivaara (27L Lansjärv NV).

The Jokkmokk area

Two large pegmatite bodies occur at Ruoutevare and at Flakaberget, 26J Jokkmokk NO and NV, respectively. Both pegmatites are situated entirely within large gabbroic intrusions (Claeson & Antal Lundin in press-a). The pegmatites and the Reunavare dykes are classified as NYF-pegmatites and most probably have very similar petrogenetic histories.

The pegmatite at Ruoutevare is a predominantly flat-lying but irregular body that has been mined in several quarries, mainly for production of quartz (9 286 tonnes at a market value of SEK 151 449) and feldspar (3 489 tonnes at a market value of SEK 48 978) during the years 1927–1944 (Sundius 1952). A list of the mining relics at Ruoutevare has been published by Norrbotten County Administrative Board (Senften 2008).

Characteristic features of the pegmatite at Ruoutevare are the local occurrence of very large biotite crystals, up to one metre in size, and euhedral magnetite crystals as 5 to 10 cm large rhomb-dodecahedrons, as well as metre-sized feldspar and quartz crystals (Fig. 184, Claeson & Antal Lundin in press-a). A suite of niobium-tantalum (REE-U-Th)-oxides, and REE-phosphates also occurs (Dagbo & Martinsson 1981). The scandium silicate thortveitite and beryl have also been noted at Ruoutevare. The pegmatite exhibits varying radiation characteristics; the uranium concentration is low in certain areas, between 1.2 and 4.6 ppm, and high in other parts, between 22 and 61 ppm.

The volatile-enriched granitic parent magma intruded the crystallised gabbroic host rocks while those rocks were cooling. The formation of large biotite, quartz and feldspar crystals found in these deposits may be explained by rapid crystal growth promoted by the presence of volatiles (e.g. water, fluorine) acting as fluxes and suppressing nucleation rates (e.g. Webber et al. 1999, London 2005, Nabelek et al. 2010). Small crystals, less than 5 mm, are not seen in the pegmatite at contacts with the

Figure 184. Pegmatite with metre-sized crystals of biotite and feldspar in a quarry at Ruoutevare (7388619/715070). Photo: Dick Claeson.

gabbro, except in dykes about ten centimetres wide (Fig. 185). The gigantic crystals inside the quarries are found only a few metres from the contacts with the gabbro. No proper zoning in the form of a central zone of differing composition has been observed. A more comprehensive description of contacts and contact phenomena is given in Claeson & Antal Lundin (in press-a). The position within the gabbroic intrusion indicates that the volatile-saturated granitic magma was able to stay hydrous and volatile-rich during cooling and crystallisation. Very few aplite dykes or ordinary granite bodies are recorded, and there are few signs of brittle behaviour of the gabbro at contacts or xenoliths of the gabbro in the pegmatite (Claeson & Antal Lundin in press-a). Field observations clearly show that the pegmatite lacks rapid cooling phenomena at contacts (Fig. 185), except in very narrow dykes. Both the pegmatite at Ruoutevare and Flakaberget are interpreted by Claeson & Antal Lundin (in press-a) to be more or less coeval with the gabbros they intruded and possibly related to locally occurring potassium feldspar porphyritic monzonite to granite rocks. Age determination of the pegmatite using both allanite and fergusonite (Y,REE)NbO_4 yielded an age of c. 1 795 Ma (Welin & Blomqvist 1964, Welin 1979).

Similar REE-uranium-thorium-bearing pegmatites are also known from Flakaberget and Reunavare. Quartz was the main commodity at Flakaberget (31 767 tonnes at a market value of SEK 477 000) and to a lesser degree feldspar (1 216 tonnes at a market value of SEK 21 000), during 1934–1944 (Sundius 1952). Both deposits show anomalous uranium and thorium content, where the mineral polycrase-(Y) is reported from Flakaberget (Chukanov 2013). At Flakaberget the uranium content varies between 69 and 453, and Th content from 75 to 430 ppm (Claeson & Antal Lundin in press-a). At Reunavare a gamma spectrometer measurement of a 2 m large biotite-rich aggregate shows 472 ppm U and 1 143 ppm Th. The yttrium silicate thalenite and the niobium-yttrium oxide fergusonite have also been documented here.

Vitvattnet (25M Kalix)

Vitvattnet is a deposit situated 23 km north of Kalix. It constitutes the core of an elongated 21 m long and approximately 3 m wide pegmatite in gneissic granite. It is surrounded by a 1–4 m wide zone of graphic pegmatite. The orientation of the gneissosity in the granite and the concordant pegmatite is 155/85. Chemical analysis of the quartz shows a low content of impurities (Shaikh et al. 1986).

Figure 185. Contact between pegmatite and gabbroid lacking chilled margin in a quarry at Ruoutevare (7388619/715070). Photo: Dick Claeson.

Graphite

Graphite-bearing, metasedimentary rocks occur at Huvudköllandet, 15 km northeast of Boden, and at Tväråkölen 11 km northwest of Råneå. Graphite was quarried at the former deposit in the early 20th century for use as a lubricant for cart wheels. At Tväråkölen, the mineralised graphite-bearing schist zone seems to be 1–2 m wide and surrounded by gneiss of sedimentary origin. Both deposits are regarded as uneconomic due to inferior quality and small volumes.

Raitajärvi (26M Överkalix)

Based on the results from electromagnetic (slingram) measurements, the Raitajärvi graphite prospect was investigated by SGU from the 1970s to the 1990s by diamond drilling, trenching and blasting (Åkerman & Kero 2012e). The graphite is locally of good quality, but areas with pyrrhotite do occur. The lenses of graphite are separated by metagreywacke. In 2013 Talga drilled 28 boreholes, totalling 3 666 m, resulting in an estimate of 4.3 Mt at 7.1% Cg (Talga 2016). Raitajärvi is a designated site of national and European interest.

Carbonate rocks

Carbonate rocks occur both as crystalline limestone and dolomite (calcite and dolomite marble) at several localities in the project area.

Prästholm (25L Boden)

A 100 m thick calcite marble layer occurs at Prästholm, 10 km north-northwest of Råneå, in a series of gneisses, where the Paulin and the Lundin quarries occur (Shaikh et al. 1989). A total of 45 000 tonnes was quarried at Paulin during 1948–55, for use as agricultural lime. The quality is uneven due to silicate inclusions. Marble was quarried at Lundin between 1965 and 1967. It was locally crack-free, homogeneous and of good quality.

Norvijaur (26J Jokkmokk NV)

In a volcanic sequence with volcaniclastic rocks, about 30 km west of Jokkmokk, a more than 5 km long horizon of metamorphosed carbonate rock occurs. It is interpreted as a biochemically precipitated rock associated with volcanic activity. Skarn minerals locally occur, but the marble is mostly fairly pure calcite; dolomitic compositions are rare (Fig. 186, Claeson & Antal Lundin in press-a). Basaltic to andesitic dykes are present in the marble. A detailed geological investigation was carried out by Högbom (1931). Three magnetic profiles were measured by LKAB in 1985 to locate the deposit. Petrophysical measurement gives a density of 2702 kg/m^3, susceptibility of -1×10^{-5} SI units, K = 0.1%, U = 0.6 ppm, and Th = 0.7 ppm (Claeson & Antal Lundin in press-a). The marble horizon is widest at Juoksjokko and south of Pelnijaure. The westernmost part at Juoksjokko was investigated in detail by diamond drilling in 1941, 1947, 1953 and 1965. At Juoksjokko, the marble is medium-grained, white to yellowish or bluish grey and banded. It is estimated that at least 100 000 tonnes of carbonate can be extracted for every metre of quarrying. A number of quarries have been in operation, and considerable quantities of marble blocks and crushed rock are left at these. The eastern part of the marble horizon (Pelnijaure marble deposit) is 160 m wide and at least 100 m deep. A test quarry was established by AB Nordmarmor in 1966–67, at which 170 000 tonnes of carbonate was extractable for every metre of quarrying, and it was estimated that 3 Mt of marble could be extracted down to a depth of 20 m (Müllern 1967). The estimated tonnage for the entire deposit is 2 to 7.5 Mt (Högbom 1931, 1981).

Figure 186. Quarry in recrystallised limestone at Norvijaur. Variation in purity and grain size, with bands of impurities and skarn that are more resistant to weathering (7394560/692620). Photo: Lotta Olausson.

Haraudden (26J Jokkmokk NV)

A small marble deposit of similar type as Norvijaur occurs at Haraudden, 6 km northwest of Jokkmokk, and has been quarried to a very limited extent (Claeson & Antal Lundin 2013). This deposit is estimated to contain some 30 000 tonnes of carbonate rock, but most of it occurs beneath the Luleälven river (Högbom 1931). The rock is medium-grained, white to yellowish or bluish grey and somewhat contaminated with pyroxene. An analysed sample shows 92.85% $CaCO_3$ and 0.50% $MgCO_3$.

Kalix archipelago (25M Kalix)

In the Kalix archipelago area, dolomite occurs mostly in association with sandstone, and to a lesser degree, with pyroclastic rocks and schist. Quarrying and burning of dolomite took place at Hastaskäret in the 19th century. Small-scale operations also took place at Lilla Trutskäret near Axelsvik and at Vitgrundet. Dolomite from a deposit situated at the southeastern cape of Säivisnäs was milled in the early 20th century. A relatively fracture-free dolomite found in the northeastern part of Lutskäret may possibly be used as dimension stone (marble tiles). The dolomite found at these deposits is mostly white to yellowish, locally grey, laminated and fine-grained (Shaikh et al. 1989). It is mostly pure, but at Hastaskäret it contains impurities in the form of phyllosilicates and amphibole.

Olivine-serpentine

Olivine altered to serpentine has been quarried at Iso Sormus and Purnu–Puolalaki map sheet 27K Nattavaara by LKAB since 1984 for use as an additive in pellets. This was a strategic innovation for the use of basic magnesium oxide pellets from LKAB instead of the Canadian acid pellets in use at the time, saving energy and improving the steel produced (LKAB 2016).

Fluorite

Fluorite is locally present as disseminations in granite belonging to the Lina suite, felsic metavolcanic rocks of the Arvidsjaur group, metasedimentary rocks of the Snavva–Sjöfallet group and sandstone associated with the Laisvall-type of mineralisation. According to current information, fluorite does not occur anywhere in economic concentrations.

Wollastonite

Several wollastonite prospects are known from the Tjåmotis area (27I Tjåmotis NV) under the names Lantanjarkka, Akatjvare, Vareluokta, Luokanjarka, Skalka, and Kårnanjunnje.

Lantanjarkka

Wollastonite was found on a small peninsula 1–2 km south of the village of Tjåmotis in the summer of 1980. Diamond drilling took place in 1982, and wollastonite was located in an easterly and a westerly zone, about 1 km apart from each other, where both zones strike towards the northeast. Wollastonite occurs, together with marble and skarn, at the contact between felsic metavolcanic rocks and metasedimentary rocks belonging to the Snavva–Sjöfallet group. The wollastonite is regarded to be the result of contact metamorphism caused by adjacent granitic intrusions (Holmqvist et al. 1983). Agglomeratic horizons are present at the top of the volcanic sequence. Outcrops are rare in this area and prospecting has primarily been in the form of trenching and diamond drilling. Mineralogical investigation shows that wollastonite occurs both free from calcite and as a part of the marble. Additional minerals in the skarn are microcline, quartz and grossular to andradite garnet. The wollastonite also contains minor manganese and magnesium in solid solution. The trenches have been filled in, but reference material can be studied adjacent to them. Locally, the wollastonite is very coarse, with up to 10 cm large crystals

Figure 187. Coarse-grained wollastonite from Lantanjarkka (7425505/656896). Photo: Per Nysten.

and crystal sections (Fig. 187). Diamond drilling in the eastern zone showed promising local wollastonite concentrations, but due to interveining rocks, the overall amount was not satisfactory. Lantanjarkka (also known as Latanjarka) has been a designated site of national interest since 1997.

Akatjvare

The Akatjvare wollastonite prospect, situated on the southern shore of Lake Tjåmotisjaure, was investigated in the 1980s by Jokkmokk Mineral and LKAB prospektering. Here the wollastonite content is estimated at 20–25%, with local concentrations of up to 40%. Based on drilling results, the amount is calculated to be at least 3 Mt. However, the location south of the lake is unfavourable, due to a lack of roads.

Andalusite

Sören (25M Kalix)

Northwest of the village of Sören close to Töre, andalusite-bearing mica schist occurs on the shores of Törefjärden. This area is 2.2 km long and 0.6–0.8 km wide, striking north-northwest–south-southeast, and is surrounded by granitoids belonging to the Haparanda suite (Shaikh et al. 1986). The mica schist is andalusite-bearing within an area of 600 × 200 m, and predominantly comprises biotite, with porphyroblasts of staurolite, garnet and cordierite. The outcrops show that andalusite occurs in zones of varying concentration. Individual crystals vary considerably in size, the predominant crystal size being 0.5–1 cm wide and 2–3 cm long (with a maximum of 3 × 10 cm). XRD analyses show that the average content is approximately 6 wt% andalusite and the amount of quartz (minor biotite and opaques) inclusions varies considerably (10–50 vol%).

Sillimanite

Sillimanite occurs locally in metasedimentary gneisses at several localities in map areas 27I Tjåmotis NV and NO, e.g. on the northern slope of Tjärko. A few, 1 m wide sillimanite-bearing zones were found at Hölandsberget (25M Kalix) (Shaikh et al. 1986).

Diatomite

An exhausted diatomite locality occurs at Kasker, map sheet 25H Arjeplog, 300 m south of Lake Makaure (Shaikh et al. 1986). This deposit was exploited by Boliden in the late 1930s and early 1940s.

At Ripats, map sheet 27K Nattavaara, an approximately 800 m^2 large area of 10 to 60 cm thick diatomite occurs beneath the peat; an analysis shows it to be purer than that of Kasker (Shaikh et al. 1986).

DIMENSION STONE

Dumortierite-bearing quartzite was found in boulders in 1979 close to Svaniträsket, map sheet 25K Harads NO (Shaikh et al. 1986). Trenching was performed by SGU in the early 1990s, revealing quartzite in an outcrop in a 1 m wide zone that could be followed for 30 m. Five cored boreholes with a total length of 143 m were drilled in 1992. This rock consists of blue dumortierite, an aluminium boro-silicate $Al_7BO_3(SiO_4)_3O_3$, which lends an intense blue colouration to the rock. The intended purpose was to use it as a dimension stone. No production has begun. Additional minerals are quartz, andalusite and small amounts of muscovite. The dumortierite quartzite is regarded as an alteration of a felsic metavolcanic rock by boron-bearing hydrothermal solutions, with enrichment of silicon, aluminium and boron. Since gold-anomalous rocks (2–5 ppm Au) are known from this region, a test for gold was also performed on the blue-coloured rock. However, the gold concentration proved to be below the detection limit of 0.01 ppm Au for all 10 tested boulders.

Banded and folded meta-arkose to quartzite with green fuchsite occurs at Paskavaara and Aapuaberget on map sheet 27M Korpilombolo, where this rock has been quarried as a dimension stone (Jonsson & Kero 2013d).

BEDROCK DEPOSITS FOR CONSTRUCTION AGGREGATES

On the northern shore of the Piteälven river, close to Benbryteforsen (25J Moskosel SO), there is an abandoned quarry named Moran, where rhyolite was quarried for aggregate (Kathol et al. 2012a).

Northeast of Grundsand (25K Harads), a black, fine-grained altered mafic rock is quarried for the production of aggregate (Kathol et al. 2012b). About 400 m north-northeast of Danielstugan (25K Harads), a strongly deformed ignimbritic rhyolite is used for the same purpose. Just below the viewpoint at Gunnaberget (25K Harads) near Harads, is an abandoned quarry in a fine- to medium-grained diorite to gabbro.

North of Jokkmokk close to Haraudden (26J Jokkmokk), a quarry has been opened in pale grey, fine medium-grained, inequigranular, foliated granite to granodiorite of Jokkmokk granitoid, with occasional pale grey, 5–20 mm large potassium feldspar phenocrysts (Claeson & Antal Lundin 2013).

Along the road between Vuollerim and Messaure at Brännlandet (26K Murjek), a red, foliated, fine- to medium-grained granite, probably belonging to the Perthite monzonite suite of rocks, was quarried in 2015.

A 20 × 30 m quarry has been opened close to the main road between Vuollerim and Jokkmokk at Pårrevare (26K Murjek), in a suite of syenitic to quartz monzonitic rocks. The syenite is pale grey to olive green, and the quartz monzonite is pink. Both rocks are porphyritic, with up to 2 cm large potassium feldspar megacrysts.

According to information from Norrbotten County Administrative Board, a quarry has been opened close to Letsi hydroelectric power plant at Suoksåive (26K Murjek NV). Since the area where the quarry is located was not visited during the recent SGU bedrock mapping programme, the character of the quarried rocks is presently unknown. Pegmatite, granite and gabbro are common in this part of the region.

The quarries at Flakaberget, Kivilaki and Lammivaara (all 26M Överkalix) are all located in red, heterogeneous pegmatite-granite (Åkerman & Kero 2012e). At Stor-Lappberget (26M Överkalix), a

Figure 188. Banded, possibly layered, acid (dacite) to intermediate volcanic rocks, with subordinate more acid and more basic bands, quarry at Parkijaure (7410072/684244). Photo: Dick Claeson.

similar rock with inclusions of quartz monzonite has been quarried, and red monzogranite is quarried at Tuorevaara (26N Karungi). Slättåsen quarry (26M Överkalix) has been established in heterogenous bedrock with rocks such as quartzite, amphibolite, and granite occurring. Koiravaara (26M Överkalix) is a combined moraine and bedrock quarry in which pegmatite-granite is visible on the floor.

Approximately 20 km west of Jokkmokk, a quarry (200 × 200 m, maximum height 25 m) is in operation at Parkijaure (27I Tjåmotis), in pale grey dacitic to intermediate metavolcanic rocks (Claeson & Antal Lundin in press-b). The volcanic rocks are banded, hydrothermally altered and partly veined (Fig. 188). Pegmatite occurs as dykes and veins. Fractures partly filled with epidote, hematite and chlorite are visible on the walls of the quarry.

South of Lansjärv (27L Lansjärv), a grey porphyritic granitoid with mafic enclaves is quarried by Svevia AB (Hellström et al. 2012d). This rock is cut by aplite-pegmatite dykes. Along the road between Hakkas and Ullatti, northwest of Satter (27L Lansjärv), a porphyritic reddish-grey granite was quarried in 2006.

A gabbro has been quarried by Swerock AB on the northern slopes of Romiovaara (27M Korpilombolo), 10 km east of Korpilombolo, since 2014. It has been used for road construction and windmill foundations in the area. The gabbro is locally cut by thin pegmatite dykes; alteration zones consisting of quartz, fluorite and biotite occur in association with those dykes. These zones are locally mineralised with pyrite and chalcopyrite. Chemical analysis of samples from the zones have revealed up to 1.1% Cu and 2.6 ppm Au (Bergman et al. 2015b). A medium-grained, foliated tonalite has been quarried 1 km east of Korpilombolo (27M Korpilombolo). The quarry, which is 70 × 60 m with a bench height of 20 m, is now disused.

8. Tectonic evolution of southern Norrbotten County

Stefan Bergman

The Archaean rocks were formed, but also deformed and metamorphosed in the Neoarchaean. The age of zircon rims in the Kukkola gneiss complex suggests metamorphism at 2.67 Ga (Bergström et al. 2015a). The ages of metamorphism in the other complexes remain to be determined. Although Archaean fabrics can be clearly identified in some areas based on cross-cutting relationships, the Archaean structural grain is generally close to parallel to that in the surrounding Proterozoic rocks, which suggests significant Proterozoic structural overprint.

In the earliest Proterozoic, a continental rifting event started with the intrusion of ultramafic–mafic rocks c. 2.44 Ga ago. The deposition of the Karelian supracrustal rocks and intrusions of mafic dykes and sills up to c. 2 Ga ago reflect deposition in a rifting-related tectonic setting. The stratigraphical record of the well-preserved rocks of the Kalix group demonstrates a change from a marine-influenced rifted margin to a rimmed carbonate shelf along a passive continental margin (Lager & Loberg 1990, Wanke & Melezhik 2005).

The general tectonic setting during the following Svecokarelian orogeny was probably an active continental margin, as first suggested by Hietanen (1975) for southwestern Finland. The oldest Proterozoic magmatic arc-related intrusive rocks near Jokkmokk are c. 1.93 Ga (Hellström 2015), and mark the fact that the Svecokarelian orogeny had started in the project area at that time. In some tectonic models the Norrbotten lithotectonic unit had been separated from the Överkalix lithotectonic unit in the east, and the precursor of the Pajala deformation belt (PDB) had an early history as a rifted continental margin, a convergent plate margin, and finally a collision zone at c. 1.92 Ga (e.g. Nironen 1997, Lahtinen et al. 2005, 2009, 2015a). Lahtinen et al. (2015a) favoured this model, but other possible interpretations of the significance of the PDB were given, including an intracontinental rift or strike-slip zone. Magmatism continued at c. 1.89 Ga, producing the Jörn GI and Haparanda suites and related volcanic units. The earliest dated Proterozoic deformation and metamorphism, recorded particularly in migmatitic rocks (Wikström et al. 1996b, Sadeghi & Hellström 2018a, Bergström et al. in preparation-a), occurred at c. 1.88 Ga, shortly before the deposition of the Arvidsjaur group and emplacement of the Perthite monzonite suite. The foliation in the rocks affected by the 1.88 Ga event has orientations between northwest and north, and the interpretation preferred here is that the D_1 folds west of the PDB are related to the 1.88 Ga event. From the Martimo belt in Finnish Lapland, just to the east of Övertorneå, Lahtinen et al. (2015b) report that the development of a north–south-trending S_1 fabric related to thin-skinned deformation, including east-directed thrusts and recumbent F_1 folds, was followed by north–south shortening producing east-west regional F_2 folds and a steeply dipping S_2 fabric.

These deformations, which relate to the Lapland-Savo orogeny, were completed by 1.89 Ga (Lahtinen et al. 2015b). The D_1 and D_2 structures preserved in tectonic lenses in the Överkalix lithotectonic unit appear to correlate well with those in the Martimo belt, although further studies are needed to verify this. Alternatively, they correlate with the D_1 and D_2 structures west of the PDB, which must have formed after 1.89 Ga, i.e. later than the early structures in the Martimo belt. The axial plane traces to major folds that formed during D_2 strike between west and northwest, and indicate a north to northeast bulk shortening direction. These folds are comparable to the earliest folds east of the KADZ in the north of Norrbotten County (Grigull et al. 2018, Luth et al. 2018b, Lynch et al. 2018b), and correlation with D_3 structures in the Martimo belt (Lahtinen et al. 2015b) is also possible. The clastic rocks of the Snavva–Sjöfallet group were deposited along an active continental margin; the lower part in a shallow marine environment. The upper part was probably formed in an estuary (Kumpulainen 2003). The timing of the deposition in relation to D_2 is unclear. The strong deformation in the Jokkmokk area occurred either during D_2 or D_3.

During the late stage (c. 1.8 Ga ago) of the Svecokarelian orogeny, the pre-existing rocks were reworked and two suites of new magmas were emplaced. Regional deformation was inhomogeneous and largely confined to deformation zones or belts (e.g. the KADZ and the PDB). The kinematic data collected in these and other zones show predominantly steep movement directions with western-side-up kinematics in the west and eastern-side-up kinematics in the east. In the PDB to the north of the project area, east–west shortening with, e.g., dextral shear along northeast-oriented shear zones was followed by north-northwest–south-southeast shortening (Luth et al. 2018b). As described earlier, the PDB in the project area is kinematically partitioned, with dextral and western-side-up movement in the Korpilombolo area, whereas eastern-side-up movement with a sinistral component predominates to the south. Analogously with the results of Luth et al. (2018b), the movement in the north and south may not have been synchronous, and the southern part represents the youngest stage of movement. The bulk shortening directions recorded by Luth et al. (2018b) are compatible not only with the kinematics in the PDB, but also with the orientations of the north–south F_3 folds and the east–west F_4 folds, respectively. Although 1.8 Ga intrusive rocks are distributed throughout the area, high-grade, low to intermediate pressure metamorphism was mainly confined to the west and east. Although there is evidence for deformation after 1.78 Ga (e.g. Wikström & Persson 1997b), the general lack of fabrics in the youngest rocks shows that the deformation was highly localised.

9. Key issues for future work

Stefan Bergman & Benno Kathol

This synthesis of the bedrock geology in southern Norrbotten County has identified several issues in need of further study. To improve our understanding of the geological evolution, within and between the various lithotectonic units, six issues are listed below:

- Characterisation of the Arvidsjaur and Porphyrite groups in terms of compositional variations, depositional settings and ages needs to be improved. The relationships to the Kiirunavaara group in the north also need to be established. Structural work is needed to determine whether the lower boundary of the Arvidsjaur group represents an unconformity, a deformation zone or both.
- The character and ages of metamorphism and their distribution is poorly known and should be studied.
- Did the Pajala deformation belt start as a suture (Lahtinen et al. 2015a) or has it always been an intracontinental deformation belt? More detailed characterisation of the lithological units, their geochemistry and geochrolology, and structural studies, including seismic surveys, are needed.
- Is there a thrust belt along the Luleå–Jokkmokk zone, as suggested by, e.g., Öhlander et al. (1993)? Detailed studies of the geometry, kinematics and timing of deformation along the zone are needed.
- Is the whole area north of the Luleå–Jokkmokk zone underlain by Archaean crust, as suggested by available Nd isotope data, and is there continuity of the greenstone cover sequence from northern Norrbotten County towards the southern boundary? Are there potentially mineralised greenstones at mineable depth?
- The nature and evolution of the brittle structures is an important topic for future study.

Acknowledgements

We would like to thank Carl-Henric Wahlgren (SGU) for reviewing the entire manuscript, providing valuable comments and proposing corrections. George Morris (SGU) is thanked for comments on and corrections to the lithogeochemical analyses sections. Magnus Ripa (SGU) checked and improved the translation of the *Introduction* into Swedish. Stefan Luth (SGU) gave valuable comments to early versions of the sections *Ductile structures* and *Brittle deformation zones*. Language control of the entire manuscript was done by Maxwell Arding. Tone Gellerstedt is thanked for many valuable comments during the editing work.

References

Ahl, M., Bergman, S., Bergström, U., Eliasson, T., Ripa, M. & Weihed, P., 2001: Geochemical classification of the plutonic rocks in central and northern Sweden. *Rapporter och meddelanden 106*, Sveriges geologiska undersökning, 82 pp.

Åhman. E., 1950: Ett fynd av frisk olivin i kimberlit från Kalix skärgård i Norrbotten. *Geologiska Föreningens i Stockholm Förhandlingar 72*, 207–211.

Åhman, E., 1960: The Kalix area. *In* G. Kautsky, P. Quensel, E. Åhman, R. Frietsch & P. Geijer (eds.): *International Geological Congress 1960. Guide to excursions Nos. A 32 & C 26*. Sveriges geologiska undersökning, 23–26.

Åhman, E., 1967: Västra Gräddmanhällan, Kalix skärgård, Norrbotten. *Geologiska Föreningens i Stockholm Förhandlingar 89*, 50–61.

Åhman, E., Wikström, A. & Henkel, H., 1990: Berggrundskartan 25M Kalix SO, skala 1:50 000. *Sveriges geologiska undersökning Ai 45*.

Åkerman, C. & Kero, L., 2012a: Bedrock map 26M Överkalix NO and 26N Karungi NV, scale: 1:50 000. *Sveriges geologiska undersökning K 396*.

Åkerman, C. & Kero, L., 2012b: Bedrock map 26M Överkalix NV, scale: 1:50 000. *Sveriges geologiska undersökning K 395*.

Åkerman, C. & Kero, L., 2012c: Bedrock map 26M Överkalix SO, scale: 1:50 000. S*veriges geologiska undersökning K 398*.

Åkerman, C. & Kero, L., 2012d: Bedrock map 26N Karungi SV, scale: 1:50 000. *Sveriges geologiska undersökning K 399.*

Åkerman, C. & Kero, L., 2012e: Beskrivning till berggrundskartorna 26M Överkalix NV, NO, SV, SO och 26N Karungi NV, SV. *Sveriges geologiska undersökning K 395–399*, 1–25.

Allen, R. L., Weihed, P. & Svenson, S.-Å., 1996: Setting of Zn-Cu-Au-Ag Massive Sulfide Deposits in the Evolution and Facies Architecture of a 1.9 Ga Marine Volcanic Arc, Skellefte District, Sweden. *Economic Geology 91*, 1022–1053.

Andersson, A., Dahlman, B., Gee, D.G. & Snäll, S., 1985: The Scandinavian alum shales. *Sveriges geologiska undersökning Ca 56*, 50 pp.

Angvik, T.L., 2014: *Structural development and metallogenesis of Paleoproterozoic volcano-sedimentary rocks of the Rombak Tectonic Window*. PhD thesis, University of Tromsø, The Arctic University of Norway, 248 pp.

Antal Lundin, I., Claeson, D. & Hellström, F., 2011: Sydvästra Norrbotten, berg. *In* S. Lundqvist (ed.): Sammanfattning av pågående verksamhet 2010. Berggrundsgeologisk undersökning. *SGU-rapport 2011:6*, Sveriges geologiska undersökning, 86–105.

Antal Lundin, I., Claeson, D., Hellström, F. & Berggren, L., 2012a: Berggrundsgeologisk undersökning, sydvästra Norrbotten. Sammanfattning av pågående verksamhet 2011. *SGU-rapport 2012:3*, Sveriges geologiska undersökning, 34 pp.

Antal Lundin, I., Claeson, D., Hellström, F. & Berggren, L., 2012b: Berggrundsgeologisk undersökning, sydvästra Norrbotten. Sammanfattning av pågående verksamhet 2012. *SGU-rapport 2012:21*, Sveriges geologiska undersökning, 44 pp.

Antal Lundin, I., Sadeghi, M. & Bastani, M., 2013: 3D-modell av Gunnarsträskgabbron. *SGU-rapport 2013:16*, Sveriges geologiska undersökning, 19 pp.

Arvanitidis, N., 1982: The geochemistry and petrogenesis of the Notträsk mafic intrusion, northern Sweden. Doctoral thesis. *Meddelanden från Stockholms Universitets Geologiska Institution 253*, 179 pp.

Asklund, B. & Thorslund, P., 1935: Fjällkedjerandens bergbyggnad i norra Jämtland och Ångermanland. *Sveriges geologiska undersökning C 382*, 1–110.

BABEL Working Group, 1990: Evidence for early Proterozoic plate tectonics from seismic reflection profiles in the Baltic shield. *Nature 348*, 34–38.

Barboni, M. & Bussy, F., 2013: Petrogenesis of magmatic albite granites associated to cogenetic A-type granites: Na-rich residual melt extraction from a partially crystallized A-type granite mush. *Lithos 177*, 328–351.

Beard, J.S. & Lofgren, G.E., 1991: Dehydration melting and water-saturated melting of basaltic and andesitic greenstones and amphibolites at 1, 3, and 6.9 kb. *Journal of Petrology 32,* 365–402.

Bergh, S.G., Kullerud, K., Armitage, P.E.B., Zwaan, K.B., Corfu, F., Ravna, E.J.K. & Myhre, P.I., 2010: Neoarchaean to Svecofennian tectono-magmatic evolution of the West Troms Basement Complex, North Norway. *Norwegian Journal of Geology 90*, 21–48.

Bergman Weihed, J., 2001: Palaeoproterozoic deformation zones in the Skellefte and Arvidsjaur areas, northern Sweden. *In* P. Weihed (ed.): Economic Geology Research 1. *Sveriges geologiska undersökning C 833,* 4668.

Bergman, S., Kübler, L. & Martinsson, O., 2001: Description of regional geological and geophysical maps of northern Norrbotten County (east of the Caledonian orogen). *Sveriges geologiska undersökning Ba 56,* 110 pp.

Bergman, S., Billström, K., Persson, P.-O., Skiöld, T & Evins, P., 2006: U-Pb age evidence for repeated Palaeoproterozoic metamorphism and deformation near the Pajala shear zone in the northern Fennoscandian shield. *GFF 128*, 7–20.

Bergman, S., & Stephens, M.B., Anderson, J., Kathol, B. & Bergman T., 2012: Bedrock map of Sweden, scale 1:1 million. *Sveriges geologiska undersökning K 423*.

Bergman, S., Bergström, U., Bastani, M., Jönberger, J., Juhojuntti, N. & Johansson, P., 2014: Regionalkartering i kartområdet 25N Haparanda, tidigare arbeten och resultat från fältarbetet 2013. *SGU-rapport 2014:07,* Sveriges geologiska undersökning, 29 pp.

Bergman, S., Hellström, F. & Bergström, U., 2015a: U-Pb zircon age of a metaquartz monzonite in the type area of the Haparanda suite. *SGU-rapport 2015:02*, Sveriges geologiska undersökning, 13 pp.

Bergman, S., Hellström, F., Bergström, U., Persson, L. & Sadeghi, M., 2016: U-Pb zircon age of a metagranite at Björnberget in the Pålkem area, northern Sweden. *SGU-rapport 2016:12,* Sveriges geologiska undersökning, 14 pp.

Bergman, T., Hellström, F. & Ripa, M., 2015b: Verksamhetsrapport 2014 Norrbottens malm och mineral. *SGU-rapport 2015:08*, Sveriges geologiska undersökning, 20 pp.

Bergström, J. & Gee, D.G., 1985: The Cambrian in Scandinavia. *In* D.G. Gee & B.A. Sturt (eds.): *The Caledonide Orogen – Scandinavia and Related Areas*. John Wiley & Sons, Chichester, 247–271.

Bergström, U., 1997: Marginal basin magmatism in an ancient volcanic arc: Petrology of the Palaeoproterozoic Malå-group basalts, Skellefte District, northern Sweden. *GFF 119*, 151–157.

Bergström, U., Bergman, S. & Hellström, F., 2015a: The Kukkola gneiss – protolith age of an Archean metatonalite, northern Sweden. *SGU-rapport 2015:07,* Sveriges geologiska undersökning, 12 pp.

Bergström, U., Bergman, S., Sadeghi, M., Persson, L. & Jönberger, J., 2015b. Regionalkartering i kartområdet 26L Pålkem, tidigare arbeten och resultat från fältarbetet 2014. *Sveriges geologiska undersökning SGU-rapport 2015:06*, 28 pp.

Berndtsson, A., 1983: Beskrivning till berggrundskartorna 26H Jäkkvik NO, 26I Luvos NV/NO och 26I Luvos SV/SO. *Sveriges Geologiska AB PRAP 83059*, 15 pp.

Berndtsson, A., Einarsson, Ö., Lundholm, I. & Quezada, R., 1984: Geologiska uppföljningsarbeten 1983. Jäkkvik/Luvos. *Sveriges Geologiska AB PRAP 84119*, 15 pp.

Berthelsen, A. & Marker, M., 1986. 1.9-1.8 Ga old strike-slip megashears in the Baltic Shield, and their plate tectonic implications. *Tectonophysics, 128*, 163–181.

Bhatia, M.R. & Crook, K.A.W., 1986: Trace element characteristics of graywackes and tectonic setting discrimination of sedimentary basins. *Contributions to Mineralogy and Petrology 92*, 181–193.

Billström, K., Eilu, P., Martinsson, O., Niiranen, T., Broman, C., Weihed, P., Wanhainen, C. & Ojala, J., 2010: lOGG and related mineral deposits of the northern Fennoscandian shield. *In* T.M. Porter (ed.): *Hydrothermal iron oxide copper-gold and related deposits: a global perspective, v. 4 – advances in the understanding of IOCG deposits*. PGC Publishing, Adelaide, 381–414.

Björklund, L., 1985: The Middle and Lower Allochthons in the Akkajaure – Tysfjord area, northern Scandinavian Caledonides. *In* D.G. Gee & B.A. Sturt (eds.): *The Caledonian Orogen – Scandinavia and related areas*. John Wiley & Sons Ltd, 515–528.

Björklund, L., 1989: Geology of the Akkajaure–Tysfjord–Lofoten traverse, N. Scandinavian Caledonides. *Geologiska institutionen, Chalmers tekniska högskola och Göteborgs universitet, doctoral thesis, publ A 59*, 214 pp.

Boliden 2017: Welcome to Boliden Aitik. Aitik folder in english, 8 pp. Accessed from <https://www.boliden.com/globalassets/investor-relations/reports-and-presentations/capital-markets-day/2012/cmd/12-welcome-to-boliden-aitik.pdf > 14 November 2017.

Boliden Annual Report 2015, 124 pp.

Boynton, W.V., 1984: Cosmochemistry of the Rare Earth Elements: Meteorite studies. *In* P. Henderson (ed.): *Rare earth element geochemistry. Elsevier Science B.V.*, 63–114.

Bucher, K. & Frey, M., 1994: *Petrogenesis of metamorphic rocks*. 6th Edition complete revision of Winkler's textbook. Springer-Verlag, 318 pp.

Cardozo, N. & Allmendinger, R.W., 2013: Spherical projections with OSXStereonet: *Computers & Geosciences 51*, 193–205.

Carlon, C.J., 1984: The BP-LKAB-Jokkmokk mineral joint venture Tjåmotis, Jokkmokk, Swedish Lappland. Comments, Notes and Recommendations (June–September 1984). *LKAB Report No Bsg 84-372*.

Carlson, L., 1982: Jårbojoki – Sammanfattning av 1965–1971 års prospekteringsarbeten och förslag till fortsatta undersökningar. *Sveriges geologiska undersökning BRAP 82048*, 41 pp.

Carlson, L., Fjellström, M., Lundqvist, A. & Niva, B., 1983: Guld i Älvsbynområdet. Resultat av 1982-års prospektering med sammanfattning och rekommendationer av prospekteringssituationen. *Sveriges Geologiska AB PRAP 83025*, 23 pp.

Carlsson, R., 1993: *Estimates of metamorphic conditions at Vattuvaara, northern Sweden*. Master thesis, Uppsala University, Institutionen för Geovetenskaper, Sweden, 38 pp.

Caudle, D.J, Groat, L.A., Cempirek, J. & Millonig, L.J., 2014: REE, Nb, Mo-bearing pegmatites from the Kin Property, near Revelstoke, BC. *2014 GSA Annual Meeting in Vancouver, British Columbia Paper No. 312-3.*

Černý, P., 1991a: Rare-element granitic pegmatites. Part 1: Anatomy and internal evolution of pegmatite deposits. *Geoscience Canada, 18*, 49–67.

Černý, P., 1991b: Rare-element granitic pegmatites. Part 2: Regional to global environments and petrogenesis. *Geoscience Canada, 18*, 68–81.

Chukanov, N.V., 2013: *Infrared spectra of mineral species: Extended library.* Springer, 295.

Claeson, D. & Antal Lundin, I., 2012a: Bedrock map 27K Nattavaara NO, scale 1:50 000. *Sveriges geologiska undersökning K 384*.

Claeson, D. & Antal Lundin, I., 2012b: Bedrock map 27K Nattavaara NV, scale 1:50 000. *Sveriges geologiska undersökning K 383*.

Claeson, D. & Antal Lundin, I., 2012c: Beskrivning till berggrundskartorna 27K Nattavaara NV, NO, SV & SO. *Sveriges geologiska undersökning K 383–386*, 22 pp.

Claeson, D. & Antal Lundin, I., 2013: Berggrundsgeologisk undersökning, sydvästra Norrbotten. Sammanfattning av pågående verksamhet 2013. *SGU-rapport 2013:18*, Sveriges geologiska undersökning, 27 pp.

Claeson, D. & Antal Lundin, I., 2015: Berggrundsgeologisk undersökning, sydvästra Norrbotten. Sammanfattning av pågående verksamhet 2014. *SGU-rapport 2015:03*, Sveriges geologiska undersökning, 32 pp.

Claeson, D. & Antal Lundin, I., in press-a: Beskrivning till berggrundskartorna 26J Jokkmokk NV, NO. Sveriges geologiska undersökning.

Claeson, D. & Antal Lundin, I., in press-b: Beskrivning till berggrundskartorna 27I Tjåmotis SV, SO. Sveriges geologiska undersökning.

Claeson, D. & Antal Lundin, I., in press-c: Beskrivning till berggrundskartan 27J Porjus SV. Sveriges geologiska undersökning.

Claeson, D., Antal Lundin, I., Persson, L., Jönberger, J. & Aaro, S., 2012: Undersökning av cirkulära magnetiska anomalier i Nattavaaraområdet. *SGU-rapport 2012:19*, Sveriges geologiska undersökning, 57 pp.

Claesson, L.-Å. & Hålenius, U., 1981: Kromprospektering 1981. *Sveriges geologiska undersökning BRAP 81085,* 15 pp.

Claesson, L.-Å., Filén, B. & Ekström, M., 1982: Delrapport över krommineraliseringen vid Kukkola. *Sveriges geologiska undersökning BRAP 82100*, 18 pp.

Claesson, L.-Å., Ullberg, A., Magnusson, J., Wiberg, B. & Ekström, M., 1983: Prospekteringsrapport, 1981–1982, Kukkola. *Sveriges Geologiska AB PRAP 83042*, 21 pp.

Claesson, S. & Roddick, J.C., 1983: ^{40}Ar-^{39}Ar data on the age and metamorphism of the Ottfjället dolerites, Särv Nappe, Swedish Caledonides. *Lithos 16*, 61–73.

Claesson, S., Huhma, H., Kinny, P.D. & Williams, I.A., 1993: Svecofennian detrital zircon ages – implications for the Precambrian evolution of the Baltic Shield. *Precambrian Research 64*, 109–130.

Collins, W.J., 2002: Hot orogens, tectonic switching, and creation of continental crust. *Geology 30*, 535–538.

Coutinho, J., Kräutner, H., Sassi, F., Schmid, R. & Sen, S., 2007: Amphibolite and Granulite. *In* D. Fettes & J. Desmons (eds.): *Metamorphic rocks: a classification and glossary of terms. Recommendations of the International Union of Geological Sciences Subcommission on the Systematics of Metamorphic Rocks*. Cambridge University Press, 51–57.

Dagbo, E. & Martinsson, O., 1981: Ruoutevarepegmatiten Jokkmokk en mineralogisk-geologisk undersökning. Examensarbete, Högskolan i Luleå 1981:081E, 61 pp.

Dallmeyer, R.D. & Stephens, M.B., 1991: Chronology of eclogite retrogression within the Seve Nappe Complex, Råvvejaure, Sweden: Evidence from 40Ar/39Ar mineral ages. *Geologische Rundschau 80*, 729–743.

Debon, F. & Le Fort, P., 1983: A chemical-mineralogical classification of common plutonic rocks and associations. *Transactions of Royal Society of Edinburgh, Earth Sciences 73*, 135–149.

Deer, W.A., Howie, R.A. & Zussman, J., 1992: An introduction to the rock-forming minerals, 2nd edition. *Pearson Education Ltd. Harlow,* 696 pp.

Deer, W.A., Howie, R.A. & Zussman, M.A., 1997: Rock-forming minerals: 1B – Sisilicates and Ring Silicates (second edition). *Geological Society of London,* 629 pp.

DePaolo, D.J., 1988: *Neodymium isotope geochemistry: an introduction*. Springer Verlag, 187 pp.

Dostal, J., Kontak, D.J., Hanley, J. & Owen, V., 2011: Geological Investigation of Rare Earth Element and Uranium Deposits of the Bokan Mountain Complex, Prince of Wales Island, Southeastern Alaska: Final Technical Report in Fulfillment of the Requirement under U.S. Geological Survey Grant G09PA00039, 122 pp.

Eliasson, T., Greiling, R.O., Sträng, T. & Triumf, C.-A., 2001: Bedrock map 23H Stensele, scale 1:50 000. *Sveriges geologiska undersökning Ai 126–129.*

Eliasson, T., Greiling, R.O. & Triumf, C.-A., 2003a: Bedrock map 24H Sorsele NO, scale 1:50 000. *Sveriges geologiska undersökning Ai 189.*

Eliasson, T., Greiling, R.O. & Triumf, C.-A., 2003b: Bedrock map 24H Sorsele NV, scale 1:50 000. *Sveriges geologiska undersökning Ai 187.*

Einarsson, Ö., 1979: Den prekambriska berggrunden i Dobblonområdet Västerbottens län. *Sveriges geologiska undersökning C 748*, 1–123.

Einarsson, Ö., 1985: Iekelvare, Prospekteringsarbeten utförda under 1984. *Sveriges Geologiska AB PRAP 85035*, 19 pp.

Einarsson, Ö. & Stenberg, L., 1985: Tjärrovare. Rapport över utförda prospekteringsarbeten 1985-08-01–1985-10-31. *Sveriges Geologiska AB, PRAP 86002.*

Eriksson, P., 1979: Tertialrapport. LKAB Prospektering. *Sveriges geologiska undersökning MINK 96056*, 4 pp.

Eriksson, T., year unknown: Järnmalmen vid Björkholmen i Jokkmokk socken. *Sveriges geologiska undersökning BRAP 83801*, 32 pp.

Falk, L., 1973: Vulkaniska gråvackor och vulkaniter i Arvidsjaurfältet. *Sveriges geologiska undersökning BRAP 00170*, 1–117.

Fettes, D. & Desmons, J., (eds.) 2007: *Metamorphic Rocks: A Classification and Glossary of Terms. Recommendations of the International Union of Geological Sciences Subcommission on the Systematics of Metamorphic Rocks.* Cambridge University Press, 244 pp.

Filén, B., 1987: PGE-prospektering 1986, Etapp II. *Sveriges Geologiska AB PRAP 87003,* 28 pp.

Filén, B., 1990: PGE-exploration in Sweden 1985–1990. *Sveriges Geologiska AB PRAP* 90026, 25 pp.

Filen, B., 2001: Swedish layered intrusions anomalous in PGE-Au. *In* P. Weihed (ed.): Economic geology research 1, 1999–2000. *Sveriges geologiska undersökning C 833*, 33–45.

Filén, B., Ekström, M. & Lundmark, L.-G., 1989: Notträsk 1989 Diamantborrning. *Sveriges Geologiska AB PRAP 89025*, 78 pp.

Føyn, S., 1985: The late Precambrian in northern Scandinavia. *In* D.G. Gee & B.A. Sturt (eds.): *The Caledonide Orogen – Scandinavia and Related Areas*, 233–246. John Wiley & Sons Ltd., Chichester.

Frietsch, R., 1963: Järnmalmsförekomster inom Norrbottens län. *Sveriges geologiska undersökning MINK 96240*, 35 pp.

Frietsch, R., 1997: The iron ore inventory programme 1963–1972 in Norrbotten county. *Rapporter och meddelanden 92*, Sveriges geologiska undersökning, 77 pp.

Frietsch, R., 1972: A late-metasomatic iron mineralization in the Narken area and its occurrence as glacial boulders at Kihlanki, both in northern Sweden. *Sveriges geologiska undersökning C 672*, 1–44.

Frietsch, R., Tuisku, P., Martinsson, O. & Perdahl, J.A., 1997: Early Proterozoic Cu-(Au) and Fe ore deposits associated with regional Na-Cl metasomatism in northern Fennoscandia. *Ore Geology Reviews 12,* 1–34.

Frost, B. R., Barnes, C. G., Collins, W. J., Arculus, R. J., Ellis, D. J. & Frost, C. D., 2001: A geochemical classification for granitic rocks. *Journal of Petrology 42,* 2033–2048.

Gavelin, S., 1955: Urbergsområdet inom Västerbottens län. *In* S. Gavelin & O. Kulling: Beskrivning till berggrundskarta över Västerbottens län. *Sveriges geologiska undersökning Ca 37*, 9–99.

Gee, D.G., 1972: The regional geological context of the Tåsjön uranium project, Caledonian Front, central Sweden. *Sveriges geologiska undersökning C 671*, 1–36.

Gee, D.G. & Zachrisson, E., 1979: The Caledonides in Sweden. *Sveriges geologiska undersökning C 769,* 1–48.

Gee, D.G., Karis, L., Kumpulainen, R. & Thelander, T., 1974: A summary of Caledonian front stratigraphy, northern Jämtland, southern Västerbotten, central Swedish Caledonides. *Geologiska Föreningens i Stockholm Förhandlingar 96*, 389–397.

Gee, D.G., Kumpulainen, R. & Thelander, T., 1978: The Tåsjön Décollement, central Swedish Caledonides. *Sveriges geologiska undersökning C 742*, 1–35.

Gee, D.G., Kumpulainen, R., Roberts, D., Stephens, M.B., Thon, A. & Zachrisson, E., 1985: Scandinavian Caledonides. Tectonostratigraphic Map. 1:2 mill. *Sveriges geologiska undersökning Ba 35*.

Geijer, P., 1918: En manganförekomst vid Porjus. *Sveriges geologiska undersökning C 287*, 1–18.

Geijer, P., 1931: Berggrunden inom malmtrakten Kiruna-Gällivare-Pajala. *Sveriges geologiska undersökning C 366*, 1–225.

Gifkins, C., Herrmann, W. & Large, R., 2005: *Altered volcanic rocks: A guide to description and interpretation.* Centre for Ore Deposit Research, University of Tasmania, 275 pp.

Gorbatschev, R. & Bogdanova, S., 1993: Frontiers in the Baltic Shield. *Precambrian Research 64*, 3–21.

Gorbatschev, R., Solyom, Z. & Johansson, I., 1979: The Central Scandinavian Dolerite Group in Jämtland, central Sweden. *Geologiska Föreningens i Stockholm Förhandlingar 101*, 177–190.

Grapes, R.H. & Hoskin, P.W.O., 2004: Epidote group minerals in low–medium pressure metamorphic terranes. *Reviews in Mineralogy & Geochemistry 56,* 301–345.

Greiling, R.O., 1992: Geochemical Analyses from the Central Scandinavian Dolerite Group in Västerbotten. Unpublished PM, *Sveriges geologiska undersökning BRAP 92011*, 8 pp.

Greiling, R.O. & Kumpulainen, R., 1989: The Middle Allochthon of the Scandinavian Caledonides at Kvikkjokk, northern Sweden: Sedimentology and Tectonics. *In* R.A. Gayer (ed.): *The Caledonide Geology of Scandinavia*, 79–89. Graham and Trotman.

Greiling, R.O. & Zachrisson, E., 1999: Berggrundskartan 23G Dikanäs NV och SV, 1:50 000. *Sveriges geologiska undersökning Ai 122–123.*

Greiling, R.O., Garfunkel, Z. & Zachrisson, E., 1998: The orogenic wedge in the central Scandinavian Caledonides: Scandian structural evolution and possible influence on the foreland basin. *GFF 120*, 181–190.

Greiling, R.O., Zachrisson, E., Thelander, T. & Sträng, T., 1999: Berggrundskartan 23G Dikanäs NO, SO, 1:50 000. *Sveriges geologiska undersökning Ai 124–125.*

Greiling, R.O., Stephens, M.B. & Persson, P.-O., 2002: Crystalline basement rocks in the Lower and Middle Allochthons, Västerbotten, Sweden: Palaeoproterozoic U-Pb zircon ages from the north-central Swedish Caledonides. *In* S. Bergman (ed.): Radiometric dating results 5. *Sveriges geologiska undersökning C 834*, 31–42.

Greiling, R.O., Kathol, B. & Kumpulainen, R., 2018: Nappe units along the Caledonian margin in central Scandinavia (Grong-Olden to Nasafjället): definition, distinction criteria and tectonic evolution. *GFF 140*, 66–89.

Grigull, S., Berggren, R., Jönberger, J., Jönsson, C., Hellström, F.A. & Luth, S., 2018: Folding observed in Palaeoproterozoic supracrustal rocks, northern Sweden. *In* S. Bergman (ed.): Geology of the Northern Norrbotten ore province, northern Sweden. *Rapporter och Meddelanden 141*, Sveriges geologiska undersökning, 205–257.

Grip, E., 1935: Die Arvidsjaurporphyre. Eine archäische Effusivgesteinsreihe im nördlichen Schweden. *Bulletin of the Geological Insitution of Upsala 25*, 135–220.

Grip, E., 1946: Arvidsjaurfältet och dess förhållande till omgivande berggrund. *Sveriges geologiska undersökning C 474*, 1–31.

Gustafsson, B., 1979: Pakkosavoi. Sveriges geologiska undersökning, Mineraljaktsprotokoll 79952, 1 p.

Gustafsson, B., 2009: Naturresurser inom kartområdet 25J Moskosel. *Sveriges geologiska undersökning MINK 0743*, 10 pp.

Gustafsson, B. & Minell, H., 1977: Case history of discovery and exploration of Pleutajokk uranium deposit, northern Sweden. Prospecting in areas of glaciated terrain, papers presented at a symposium organized by the Institution of Mining and Metallurgy, with the cooperation of the Geological Survey of Finland, Helsinki, 15–17 August 1977, 72–79.

Hålenius, U., Smellie, J.A.T. & Wilson, M.R., 1984: Uranium genesis within the Arjeplog–Arvidsjaur–Sorsele uranium province, northern Sweden. *Sveriges Geologiska AB IRAP 84056*, 45 pp.

Hålenius, U., Smellie, J.A.T. & Wilson, M.R., 1986: Uranium genesis within the Arjeplog–Arvidsjaur–Sorsele uranium province, northern Sweden. *In* H. Fuchs (ed.): Vein type uranium deposits, *IAEA-TECDOC-361,* IAEA, Vienna, 21–42.

Hansson & Filèn 1991: Slutrapport guld i Puolalaki. *Sveriges Geologiska AB PRAP 91028*, 241 pp.

Hartvig, F. & Aaro, S., 2012a: Bedrock map 25J Moskosel NV, scale 1:50 000. *Sveriges geologiska undersökning K 402.*

Hartvig, F. & Aaro, S., 2012b: Bedrock map 25J Moskosel NO, scale 1:50 000. *Sveriges geologiska undersökning K 403.*

Hassan, M., 2008: Platinum group elements and gold in the differentiated Notträsk gabbro, northern Sweden. *Master's Thesis 2008:38*. Department of chemical engineering and geosciences, Division of Ore Geology, Luleå University of Technology, 22 pp.

Hellström, F., 2015: SIMS geochronology of a 1.93 Ga basement metagranitoid at Norvijaur west of Jokkmokk, northern Sweden, *SGU-rapport 2015:01*, Sveriges geologiska undersökning, 18 pp.

Hellström, F. & Berggren, R., 2014: Berggrundsgeologisk undersökning sydvästra Norrbotten, 26I Luvos. *SGU-rapport 2014:01*, Sveriges geologiska undersökning, 14 pp.

Hellström, F.A. & Berggren, R., in press: Beskrivning till berggrundskartorna 26I Luvos SV, NV & NO. Sveriges geologiska undersökning.

Hellström, F., Carlsäter Ekdahl, M. & Kero, L., 2012a: Bedrock map 27L Lansjärv NV, scale 1:50 000. *Sveriges geologiska undersökning K 387.*

Hellström, F., Carlsäter Ekdahl, M. & Kero, L., 2012b: Bedrock map 27L Lansjärv NO, scale 1:50 000. *Sveriges geologiska undersökning K 388.*

Hellström, F., Carlsäter Ekdahl, M. & Kero, L., 2012c: Bedrock map 27L Lansjärv SV, scale 1:50 000. *Sveriges geologiska undersökning K 389.*

Hellström, F., Carlsäter Ekdahl, M. & Kero, L., 2012d: Beskrivning till berggrundskartorna 27L Lansjärv NV, NO, SV & SO. *Sveriges geologiska undersökning K 387–390*, 1–27.

Hellström, F., Kathol, B. & Larsson, D., 2015: Age and chemical character of the Perthite monzonite suite in south-western Norrbotten, northern Sweden. *SGU-rapport 2015:38*, Sveriges geologiska undersökning, 23 pp.

Henderson, I.H.C., Viola, G. & Nasuti, A., 2015: A new tectonic model for the Palaeoproterozoic Kautokeino Greenstone Belt, northern Norway, based on high-resolution airborne magnetic data and field structural analysis and implications for mineral potential. *Norwegian Journal of Geology 95*, 339–363.

Henkel, H, 1987: Tectonic studies in the Lansjärv region. *SKB Technical Report 88-07*, 66 pp.

Henkel, H., 1991: Magnetic crustal structures in northern Fennoscandia. *Tectonophysics 192*, 57–79.

Herron, M.M., 1988: Geochemical classification of terrigenous sands and shales from core or log data. *Journal of Sedimentary Petrology 58*, 820–829.

Hietanen, A. 1975. Generation of potassium-poor magmas in the northern Sierra Nevada and the Svecofennian of Finland. *U.S. Geological Survey Journal of Research 3*, 631–645.

Hill, T., 1981: Allebuouda molybden – malmberäkning av "Stora malmen". *LKAB Prospektering AB PRO 8115*, 11 pp.

Högbom, A., 1931: Praktiskt-geologiska undersökningar inom Jokkmokks socken sommaren 1930. *Sveriges geologiska undersökning C 369*, 1–57.

Högbom, A., 1937: Skelleftefältet med angränsande delar av Västerbottens och Norrbottens län. *Sveriges geologiska undersökning C 389*, 1–122.

Holmqvist, A., Lundmark, C., Luppichini, E.-L., Niva, B., Sjöstrand, T. & Westfal. T., 1983: Rapport över wollastonit-prospektering vid Latanjarka, Jokkmokks kommun, intill 821201. *Sveriges Geologiska AB PRAP 83008*, 74 pp.

Holmqvist, P.J., 1906: Studien über die Granite von Schweden. *Bulletin of the Geological Institution of Uppsala VII*, 77–269.

Hölttä, P., Väisänen, M., Väänänen, J. & Manninen, T., 2007: Paleoproterozoic metamorphism and deformation in Central Lapland, Finland. *Geological Survey of Finland Special Paper 44*, 7–56.

Hübner, H. & Einarsson, Ö., 1980: Additional data on molybdenum and tungsten occurences in Northern and Central Sweden. *Sveriges geologiska undersökning BRAP 80538*, 62 pp.

Huhma, H., 1986: Sm-Nd, U-Pb and Pb-Pb isotopic evidence for the origin of the Early Proterozoic Svecokarelian crust in Finland. *Geological Survey of Finland, Bulletin 337*, 1–48.

Hyndman, R.D., Currie, C.A. & Mazzotti, S.P., 2005: Subduction zone backarcs, mobile belts, and orogenic heat. *GSA Today 15*, 4–10.

Ingram, R.L., 1954: Terminology for the thickness of stratification and parting units in sedimentary rocks. *Bulletin of the Geological Society of America 65*, 937–938.

Ishikawa, Y., Sawaguchi, T., Iwaya, S. & Horiuchi, M., 1976: Delineation of prospecting targets for Kuroko deposits based on modes of volcanism of underlying dacite and alteration haloes. *Mining Geology 26***,** 105–117.

Jensen, L. S., 1976: A new cation plot for classifying subalkalic volcanic rocks. *Ontario Division of Mines, Miscellaneous Papers 66,* 1–21.

Johansson, K.I. & Gustafsson, K., 1986: Nårvejaur 860101-861001. *LKAB S 8619*, 3 pp.

Johansson, R., 1980: Jokkmokksområdets järnmalmer – Geofysisk tolkning med malmberäkning. *Sveriges geologiska undersökning FM 8012*, 36 pp.

Jokkmokksprojektet, 1981: Basprospektering inom Jokkmokks kommun, slutrapport perioden 1979-06-05–1981-06-30. *Sveriges geologiska undersökning BRAP 81054*, 102 pp.

Jonasson, S. 1980: Besök hos Robertson & Ass, Toronto, Kanada 17–24 februari 1980. Diskussion av halter, tonnage och brytningsmetoder för Pleutajokk. *LKAB PRO 8043*, 16 pp.

Jonsson, E., 2008: Epigenetic REE-U-Th-anomalous Fe oxide mineralisation in the Narken area, NE Sweden. 33rd International Geological Congress, Abstracts, MRD-11.

Jonsson, E., 2010: Copper-gold-palladium mineralisation in the Korpilombolo area, NE Sweden. *In* H.A. Nakrem, A.O. Harstad & G. Haukdal (eds.): *29th Nordic Geological Winter Meeting, Oslo, January 11–13, NGF Abstracts and Proceedings of the Geological Society of Norway,* 87–88.

Jonsson, E. & Kero, L., 2013a: Bedrock map 27M Korpilombolo SO and 27N Svanstein SV, scale 1:50 000. *Sveriges geologiska undersökning K 394*.

Jonsson, E. & Kero, L., 2013b: Bedrock map 27M Korpilombolo NO and 27N Svanstein NV, scale 1:50 000. *Sveriges geologiska undersökning K 392*.

Jonsson, E. & Kero, L., 2013c: Bedrock map 27M Korpilombolo SV, scale 1:50 000. *Sveriges geologiska undersökning K 393*.

Jonsson, E. & Kero, L., 2013d: Beskrivning till berggrundskartorna 27M Korpilombolo NV, NO, SV, SO och 27N Svanstein NV, SV. *Sveriges geologiska undersökning K 391–394*, 1–20.

Kärki, A., Laajoki, K. & Luukas, J., 1993. Major Palaeoproterozoic shear zones of the central Fennoscandian Shield. *Precambrian Research 64*, 207–223.

Kathol, B. & Aaro, S., 2006a: Bedrock map 25I Stensund NO, scale 1:50 000. *Sveriges geologiska undersökning K 52.*

Kathol, B. & Aaro, S., 2006b: Bedrock map 25I Stensund SO, scale 1:50 000. *Sveriges geologiska undersökning K 54*.

Kathol, B. & Aaro, S., 2012: Bedrock map 25J Moskosel SV, scale 1:50 000. *Sveriges geologiska undersökning K 404.*

Kathol, B. & Hellström, F., 2015: U-Pb zircon age of a massive quartz monzonite from Lillraudok, c. 30 km north-west of Arjeplog, Norrbotten county, Sweden. *SGU-rapport 2015:16,* Sveriges geologiska undersökning, 14 pp.

Kathol, B. & Hellström, F., in press: U-Pb zircon age of a quartz monzonite from Sjávnjaluokta in the Sjaunjaätno massif in the central part of the Norrbotten County, northern Sweden – type area for the Perthite monzonite suite. *SGU-rapport,* Sveriges geologiska undersökning.

Kathol, B. & Jönberger, J., 2012a: Bedrock map 25K Harads NO, scale 1:50 000. *Sveriges geologiska undersökning K 407.*

Kathol, B. & Jönberger, J., 2012b: Bedrock map 25K Harads SO, scale 1:50 000. *Sveriges geologiska undersökning K 409.*

Kathol, B. & Persson, P.-O., 1997: U-Pb zircon dating of the Antak granite, northeastern Västerbotten County, northern Sweden. *In* Th. Lundqvist (ed.): Radiometric dating results 3, Division of Bedrock Geology, Geological Survey of Sweden. *Sveriges geologiska undersökning C 830*, 6–13.

Kathol, B. & Persson, P.-O., 2007a: U-Pb zircon age of a granodiorite from Övre Ljusselet in the Moskosel area, southern Norrbotten County, Sweden. *In* F. Hellström & J. Andersson (eds.): *Isotope analytical results 1. SGU-rapport 2007:28*, Sveriges geologiska undersökning, 20–22.

Kathol, B. & Persson, P.-O., 2007b: U-Pb zircon age of an ignimbritic rhyolite from Benbryteforsen in the area between Moskosel and Vidsel, southern Norrbotten County, Sweden. *In* F. Hellström & J. Andersson (eds.): *Isotope analytical results 1. SGU-rapport 2007:28*, Sveriges geologiska undersökning, 17–19.

Kathol, B. & Persson, P.-O., 2007c: Sm-Nd analysis of a felsic gneiss from Älvsborg in the area between Moskosel and Vidsel, southern Norrbotten County, Sweden. *In* F. Hellström & J. Andersson (eds.): *Isotope analytical results 1. SGU-rapport 2007*:28, Sveriges geologiska undersökning, 33.

Kathol, B. & Persson, P.-O., 2008a: Sm-Nd analysis of a quartz diorite from Sandträskberget, southern Norrbotten County, Sweden. *In* F. Hellström (ed.): Results from radiometric datings and other isotope analyses 2. *SGU-rapport 2008:27*, Sveriges geologiska undersökning, 31–32.

Kathol, B. & Persson, P.-O., 2008b: Sm-Nd analysis of a quartz monzodiorite from Gunnarberget at Harads, southern Norrbotten County, Sweden. *In* F. Hellström (ed.): Results from radiometric datings and other isotope analyses 2. *SGU-rapport 2008:27*, Sveriges geologiska undersökning, 29–30.

Kathol, B. & Persson, P.-O., 2008c: U-Pb zircon age of a massive granite from Spikberg, c. 14 km to the west of Harads, southern Norrbotten County, Sweden. *In* F. Hellström (ed.): Results from radiometric datings and other isotope analyses 2. *SGU-rapport,* Sveriges geologiska undersökning, *2008:28*, 27–28.

Kathol, B. & Rapp, C., 1996: Comagmatic origin of a granitic intrusion (Antak granite) and felsic volcanic rocks (Hej volcanites) in the Arvidsjaur district, Västerbotten–Norrbotten, Sweden. *GFF 118*, Jubilee Issue, A16–17.

Kathol, B. & Triumf, C.-A., 2004: Bedrock map 24J Arvidsjaur, scale 1:50 000. *Sveriges geologiska undersökning Ai 148–151.*

Kathol, B. & Weihed, P. (eds.), 2005: Description of regional geological and geophysical maps of the Skellefte District and surrounding areas. *Sveriges geologiska undersökning Ba 57*, 197 pp.

Kathol, B., Aaro, S. & Hartvig, F., 2006: Moskosel–Harads, baskartering berg. *In* H. Delin (ed.): Berggrundsgeologisk undersökning – sammanfattning av pågående verksamhet 2005. *Rapporter och meddelanden 123*, Sveriges geologiska undersökning, 21–27.

Kathol, B., Weihed, P., Antal Lundin, I., Bark, G., Bergman Weihed, J., Bergström, U., Billström, K., Björk, L., Claesson, L., Daniels, J., Eliasson, T., Frumerie, M., Kero, L., Kumpulainen, R.A., Lundström, H., Lundström, I., Mellqvist, C., Petersson, J., Skiöld, T., Sträng, T., Stølen, L.-K., Söderman, J., Triumf, C.-A., Wikström, A., Wikström, T. & Årebäck, H., 2005: Regional geological and geophysical maps of the Skellefte District and surrounding areas. Bedrock map. *Sveriges geologiska undersökning Ba 57:1.*

Kathol, B., Lundmark, C., Hellström, F. & Rimša, A., 2008a: U-Pb zircon age of a feldspar-porphyritic rhyodacite from the Trollforsen area, c. 20 km northwest of Moskosel, southern Norrbotten County, Sweden. *In* F. Hellström (ed.): Results from radiometric datings and other isotope analyses 2. *SGU-rapport 2008:27*, Sveriges geologiska undersökning, 33–35.

Kathol, B., Rimša, A. & Hellström, F., 2008b: U-Pb zircon age of a strongly deformed rhyolite from Danielstugan, c. 3.5 km north-north-east of Svartlå, southern Norrbotten County, Sweden. *In* F. Hellström (ed.): Results from radiometric datings and other isotope analyses 2. *SGU-rapport 2008:27,* Sveriges geologiska undersökning, *36–38*.

Kathol, B., Sadeghi, M., Aaro, S., Albrecht, L., Larsson, D. & Jönberger, J., 2010: Jäkkvik-Boden. *In* H. Delin (ed.): Berggrundsgeologisk undersökning – sammanfattning av pågående verksamhet 2009. *SGU-rapport 2010:2*, Sveriges geologiska undersökning, 17–42.

Kathol, B., Sadeghi, M., Aaro, S., Jönberger, J. & Larsson, D., 2011: Boden-Jäkkvik, berg, *In* S. Lundqvist (ed.), Berggrundsgeologisk undersökning. Sammanfattning av pågående verksamhet 2010. *SGU-rapport 2011:6*, Sveriges geologiska undersökning, 37–69.

Kathol, B., Aaro, S., Gustafsson, B. & Hartvig, F., 2012a: Beskrivning till berggrundskartorna 25J Moskosel NV, NO, SV & SO. *Sveriges geologiska undersökning K 402–405*, 1–33.

Kathol, B., Jönberger, J., Kumpulainen, R. & Larsson, D., 2012b: Beskrivning till berggrundskartorna 25K Harads NV, NO, SV & SO. *Sveriges geologiska undersökning K 406–409*, 1–33.

Kathol, B., Sadeghi, M., Triumf, C.-A. & Larsson, D., 2012c: Berggrundsgeologisk undersökning, Jäkkvik-Boden. *SGU-rapport 2012:5*, Sveriges geologiska undersökning, 1–39.

Kathol, B., Antal Lundin, I., Jönberger, J., Larsson, D., Morris, G. & Persson, L., 2014: Barentsprojektet 2013. Berggrundsgeologisk undersökning 25H Arjeplog, 26I Luvos SO, 26J Jokkmokk SV. *SGU-rapport 2014:12*, Sveriges geologiska undersökning, 32 pp.

Kathol, B., Antal Lundin, I., Jönberger, J., Larsson, D. & Morris, G., 2015: Berggrundsgeologisk undersökning, 26J Jokkmokk SO, 27J Porjus SO. *SGU-rapport 2015:28,* Sveriges geologiska undersökning, 51 pp.

Kathol, B., Hellström, F., Persson, P.-O. & Morris, G., in press: U-Pb zircon age of a granodioritic to tonalitic gneiss from Rimokojan at Stora Luleälven in the central part of the Norrbotten County, Northern Sweden. *SGU-rapport,* Sveriges geologiska undersökning.

Kautsky, G., 1957: Ein Beitrag zur Stratigraphie und dem Bau des Skelleftefeldes, Nordschweden. *Sveriges geologiska undersökning C 543*, 1–65.

Kerrick, D.M., (ed.) 1991: Contact metamorphism. *Mineralogical Society of America Reviews in Mineralogy 26*, 847 pp.

Koistinen, T., Stephens, M.B., Bogatchev, V., Nordgulen, Ø., Wennerström, M. & Korhonen, J., 2001: Geological map of the Fennoscandian Shield, scale 1:2 000 000. *Geological Surveys of Finland, Norway and Sweden and the North-West Department of Natural Resources of Russia*.

Kousa, J. & Lundqvist, Th., 2000a: Svecofennian domain. *In* Th. Lundqvist & S. Autio (eds): Description to the Bedrock Map of Central Fennoscandia (Mid-Norden). *Geological Survey of Finland, Special Paper 28*, 47–75.

Kousa, J. & Lundqvist, Th., 2000b: Meso- and Neoproterozoic cover rocks of the Svecofennian Domain. *In* Th. Lundqvist & S. Autio (eds): Description to the Bedrock Map of Central Fennoscandia (Mid-Norden). *Geological Survey of Finland, Special Paper 28*, 75–76.

Kresten, P., Åhman, E. & Brunfelt, A.O., 1981: Alcaline ultramafic lamprophyres and associated carbonatite dykes from the Kalix area, northern Sweden. *Geologische Rundschau 70*, 1215–1231.

Kresten, P., Rex, D.C. & Guise, P.G., 1997: 40Ar-39Ar ages of ultramafic lamprophyres from the Kalix area, northern Sweden. *In* Th. Lundqvist (ed.): Radiometric dating results 3. *Sveriges geologiska undersökning C 830*, 14–19.

Kulling, O., 1942: Grunddragen av fjällkedjerandens bergbyggnad inom Västerbottens län. *Sveriges geologiska undersökning C 445,* 1–320.

Kulling, O., 1955: Den kaledoniska fjällkedjans berggrund inom Västerbottens län. *In* S. Gavelin & O. Kulling (eds.): Beskrivning till berggrundskarta över Västerbottens län. *Sveriges geologiska undersökning Ca 37*, 101–296.

Kulling, O., 1972: The Swedish Caledonides. *In* T. Strand & O. Kulling (eds.): *Scandinavian Caledonides*. John Wiley & Sons Ltd., London, 147–285.

Kulling, O., 1982: Översikt över södra Norrbottensfjällens kaledonberggrund. *Sveriges geologiska undersökning Ba 26*, 1–295.

Kullman, F., 1984: Kvarnå-området – kortfattad beskrivning till berggrundsgeologisk karta i 1:50 000. *Sveriges Geologiska AB, IRAP 84123*, 9 pp.

Kumpulainen, R., 1980: Upper Proterozoic stratigraphy and depositional environments of the Tossåsfjället Group, Särv Nappe, southern Swedish Caledonides. *Geologiska Föreningens i Stockholm Förhandlingar 102*, 531–550.

Kumpulainen, R., 1982: The Upper Proterozoic Risbäck Group, northern Jämtland and southwestern Västerbotten, central Swedish Caledonides. *University of Uppsala, Department of Mineralogy and Petrology, Research Report 28*, 1–60.

Kumpulainen, R. A., 2003: Svecofennian sedimentary record of northern Sweden. *Final research report, SGU-project 03-1225/99*, Sveriges geologiska undersökning, 20 pp.

Kumpulainen, R., 2009: The Bothnian basin – its rocks, its age, its origin. *Final research report of SGU-project 60-1931/2005*, Sveriges geologiska undersökning, 27 pp.

Kumpulainen, R.A. (ed.), 2017: Guide for geological nomenclature in Sweden. *GFF 139*, 3–20.

Kumpulainen, R. & Nystuen, J.P., 1985: Late Proterozoic basin evolution and sedimentation in the westernmost part of Baltoscandia. *In* D.G. Gee & B.A. Sturt (eds.): *The Caledonian Orogen – Scandinavia and related areas*. John Wiley & Sons Ltd, 213–232.

Lager, I. & Loberg, B., 1990: *Sedimentologisk-bassänganalytisk malmprospekteringsmetodik inom norrbottniska grönstenbälten*. STU-Projekt 86-03967P, Slutrapport. Ekonomisk geologi, Högskolan i Luleå, 112 pp.

Lagerbäck, R., 1979: Neotectonic structures in northern Sweden. *Geologiska Föreningens i Stockholm Förhandlingar 100*, 263–269.

Lagerbäck, R. & Witschard, F., 1983: Neotectonics in northern Sweden – geological investigations. *SKBF KBS Technical Report 83–58*, 58 pp.

Lahtinen, R., Korja, A. & Nironen, M., 2005: Paleoproterozoic tectonic evolution. *In* M. Lehtinen, M., P.A. Nurmi & O.T. Rämö (eds.): *Precambrian Geology of Finland – Key to the Evolution of the Fennoscandian Shield.* Elsevier B.V., Amsterdam, 481–532.

Lahtinen, R., Korja, A., Nironen, M. & Heikkinen, P., 2009: Palaeoproterozoic accretionary processes in Fennoscandia. *In* P.A. Cawood & A. Kröner (eds.): *Earth Accretionary Systems in Space and Time. Geological Society London Special Publication 318*, 237–256.

Lahtinen, R., Huhma, H., Lahaye, Y., Jonsson, E., Manninen, T., Lauri, L.S., Bergman, S., Hellström, F., Niiranen, T. & Nironen, M., 2015a: New geochronological and Sm-Nd constraints across the Pajala shear zone of northern Fennoscandia: Reactivation of a Paleoproterozoic suture. *Precambrian Research 256*, 102–119.

Lahtinen, R., Sayab, M. & Karell, F., 2015b: Near-orthogonal deformation successions in the poly-deformed Paleoproterozoic Martimo belt: Implications for the tectonic evolution of Northern Fennoscandia. *Precambrian Research 270*, 22–38.

Larsson, J.-O., 1993: Tjåmotisområdet, ett framtida gruvcentrum i Jokkmokks kommun? *Sveriges geologiska undersökning MINK 96235*, 10 pp.

Larsson, W., 1943: Zur Kenntnis der alkalinen ultrabasischen Ganggesteine des Kalixgebietes, Nordschweden. *Sveriges geologiska undersökning C 456*, 1–41.

Laurikko, J., 1983a: Uranprospektering i Skuppesavonområdet 1979–82. *Sveriges Geologiska AB IRAP 83011,* 19 pp.

Laurikko, J., 1983b: Preliminär malmberäkning i Skuppesavon syd. *Sveriges Geologiska AB IRAP 83013*, 8 pp.

Le Bas, M.J., Le Maitre, R.W., Streckeisen, A. & Zanettin, B., 1986: A chemical classification of volcanic rocks based on the total alkali-silica diagram. *Journal of Petrology 27,* 745–750.

Lilljequist, R. 1973: Caledonian geology of the Laisvall area, Southern Norrbotten, *Swedish Lapland. Sveriges geologiska undersökning C 691*, 1–43.

Lindström, M., Lundqvist, J. & Lundqvist, Th., 2000: *Sveriges geologi från urtid till nutid.* Studentlitteratur, Lund, 491 pp.

Ljung, S., 1992: Tjuoiva 1992. *Sveriges Geologiska AB NSG 92030*, 10 pp.

Ljung, S. & Einarsson, Ö., 1990: Borrning Tjärrovare 1990. *NSG 90068*, 17 pp.

LKAB 2016: Olivinpellets gav LKAB högförädlad product. Accessed from <http://www.lkab.com/sv/om-oss/Historia/Innovationer/Olivinpellets/> 20 October 2016.

Löfvendahl, R. & Åberg, G., 1982: An isotope study of Swedish secondary U-Pb minerals. *Geologiska Föreningens i Stockholm Förhandlingar 103*, 331–342.

London, D., 2005: Granitic pegmatites: an assessment of current concepts and directions for the future. *Lithos 80*, 281–303.

Lovering, T., 1963: Epigenetic, diplogenetic, syngenetic, and lithogene deposits. *Economic Geology 58*, 315–331.

Lukkarinen, H. & Lundqvist, Th., 2000: Karelian domain. *In* Th. Lundqvist & S. Autio (eds.): Description to the Bedrock Map of Central Fennoscandia (Mid-Norden*). Geological Survey of Finland, Special Paper 28*, 26–47.

Lundberg, B., 1980: Aspects of the geology of the Skellefte field, northern Sweden. *Geologiska Föreningens i Stockholm Förhandlingar 102*, 156–166.

Lundh, J., Sadeghi, M. & Barker, A., 2014: Application of Rare Earth Elements in mapping: Implication on tracing mafic and ultramafic suites in Northern Sweden. ERES2014: 1st European Rare Earth Resources Conference; Greece.

Lundmark, C., 1983a: Sydöstra Tjåmotis – utvärdering. *Sveriges Geologiska AB PRAP 83090*, 43 pp.

Lundmark, C., 1983b: Sydöstra Tjåmotis resultat från fältsäsongen 1983. *Sveriges Geologiska AB PRAP 83137,* 12 pp.

Lundmark, C., 1984a: Kukkola, Resultat av diamantborrningen 1984. *Sveriges Geologiska AB PRAP 84122*, 15 pp.

Lundmark, C., 1984b: Vaikijaur Resultat av borrning 1983. *Sveriges Geologiska AB PRAP 84041*, 24 pp.

Lundmark, C. & Hålenius, U., 1984: Iekelvare-Guldanalysering. *Sveriges Geologiska AB PRAP 84040*, 7 pp.

Lundmark, C., Billström, K. & Weihed, P., 2005a: The Jokkmokk granitoid, an example of 1.88 Ga juvenile magmatism at the Archaean-Proterozoic border in northern Sweden. *GFF 127*, 83–98.

Lundmark, C., Stein, H. & Weihed, P., 2005b: The geology and Re–Os geochronology of the Palaeoproterozoic Vaikijaur Cu-Au-(Mo) porphyry-style deposit in the Jokkmokk granitoid, northern Sweden. *Mineralium Deposita 40*, 396–408.

Lundmark, C., Broman, C., Boyce, A. & Weihed, P., 2006: Vaikijaur Cu-Au-(Mo) deposit, northern Sweden: Preliminary results from fluid inclusion and (O, H) isotope studies. *Bulletin of the Geological Society of Finland, Special Issue 1*, 95.

Lundqvist, Th., Boe, R., Kousa, J., Lukkarinen, H., Lutro, O., Roberts, D., Solli, A., Stephens, M. & Weihed, P., 1996a: *Bedrock map of Central Fennoscandia. Scale 1:1 000 000.* Geological Surveys of Finland (Espoo), Norway (Trondheim) and Sweden (Uppsala).

Lundqvist, Th., Vaasjoki, M. & Skiöld, T., 1996b: Preliminary note on the occurrence of Archaean rocks in the Vallen–Alhamn area, northern Sweden. *Sveriges geologiska undersökning C 828*, 32–33.

Lundqvist, Th., Vaasjoki, M. & Persson, P.-O., 1998: U-Pb ages of plutonic and volcanic rocks in the Svecofennian Bothnian Basin, central Sweden, and their implications for the Palaeoproterozoic evolution of the Basin. *GFF 120*, 357–363.

Lundqvist, Th., Skiöld, T., & Vaasjoki, M. 2000: Archaean–Proterozoic geochronology of the Vallen–Alhamn area, northern Sweden. *GFF 122*, 273–280.

Lundström, I. & Persson, P.-O., 1999: The Brännbergsliden gneiss – an exotic block of a plastically deformed Arvidsjaur metavolcanic rock? Field geologic and radiometric dating results. *In* S. Bergman, (ed.): Radiometric dating results 4. *Sveriges geologiska undersökning C 831*, 42–51.

Lundström, I., Persson, P.-O. & Bergström, U., 1999: Indications of early deformational events in the northeastern parts of the Skellefte field. Indirect evidence from geologic and radiometric data from the Stavaträsk-Klintån area, Boliden map sheet. *In* S. Bergman (ed.): *Radiometric dating results 4. Sveriges geologiska undersökning C 831*, 52–69.

Luth, S., Lynch, E.P., Grigull, S., Thörnelöf, M., Berggren, R. & Jönberger, J., 2014: Geological and geophysical studies in the Harrijärvet, Vittangivaara and Akkiskera-Kuormakka key areas. *SGU-rapport 2014:09*, Sveriges geologiska undersökning, 24 pp.

Luth, S., Jönberger, J. & Grigull, S., 2018a: The Vakko and Kovo greenstone belts north of Kiruna: Integrating structural geological mapping and geophysical modelling. *In* S. Bergman (ed.): Geology of the Northern Norrbotten ore province, northern Sweden, *Rapporter och Meddelanden 141*, Sveriges geologiska undersökning, 287–309.

Luth, S., Jönsson, C., Jönberger, J., Grigull, S., Berggren, R., van Assema, B., Smoor, W. & Djuly, T., 2018b: The Pajala Deformation Belt in northeast Sweden: Structural geological mapping and 3D modelling around Pajala. *In* S. Bergman (ed.): Geology of the Northern Norrbotten ore province, northern Sweden, *Rapporter och Meddelanden 141*, Sveriges geologiska undersökning, 259–285.

Lynch, E.P., Bauer, T.E., Jönberger, J., Sarlus, Z., Morris, G.A. & Persson, P.-O., in 2018a: Petrology and and structural character of c. 1.88 Ga meta-volcanosedimentary rocks hosting iron oxide-copper-gold and related mineralisation in the Nautanen--Aitik area, northern Sweden. *In* S. Bergman (ed.): Geology of the Northern Norrbotten ore province, northern Sweden, *Rapporter och Meddelanden 141*, Sveriges geologiska undersökning, 107–149.

Lynch, E.P., Hellström, F.A., Huhma, H., Jönberger, J., Persson, P.-O. & Morris, G.A., 2018b: Geology, lithostratigraphy and petrogenesis of c. 2.14 Ga greenstones in the Nunasvaara and Masugnsbyn areas, northernmost Sweden. *In* S. Bergman (ed.): Geology of the Northern Norrbotten ore province, northern Sweden, *Rapporter och Meddelanden 141*, Sveriges geologiska undersökning, 19–77.

Magnusson, N.H., 1962: De prekambriska bergarterna utanför fjällkedjan. *In* N.H. Magnusson, P. Thorslund, F. Brotzen, B. Asklund & O. Kulling: Beskrivning till karta över Sveriges berggrund. *Sveriges geologiska undersökning Ba 16*, 5–110.

Markkula, H., 1977: Sedimentsynklinal mellan två graniter i Norvijaur, Norrbotten, Sverige. (unpublished pro gradu thesis), Åbo Academy, Finland, 59 pp.

Martinsson, O., 2004: Geology and metallogeny of the northern Norrbotten Fe-Cu-Au province. *In* R.L. Allen, O. Martinsson & P. Weihed (eds.): Svecofennian ore-forming environments: Volcanic-associated Zn-Cu-Au-Ag, intrusion associated Cu-Au, sediment-hosted Pb-Zn, and magnetite-apatite deposits in northern Sweden. *Society of Economic Geologists, Guidebook Series 33*, 131–148.

Martinsson, O. & Billström, K., 2006: Plume related MORB and high-Ti basalts in the Kalix greenstones, northern Sweden. *In* P. Peltonen & A. Pasanen (eds.): The 27th Nordic Geological Winter Meeting, Abstract volume. *Bulletin of the Geological Society of Finland, Special Issue 1*, p. 98.

Martinsson, O. & Perdahl, J.-A., 1995: Paleoproterozoic extensional and compressional magmatism in northern Sweden. *In* J.-A. Perdahl: Svecofennian volcanism in northern Sweden, *Doctoral thesis 1995:169D, Paper II,* 1–13. Luleå University of Technology.

Martinsson, O., Billström, K., Broman, C., Weihed, P. & Wanhainen, C., 2016: Metallogeny of the Northern Norrbotten Ore Province, northern Fennoscandian Shield with emphasis on IOCG and apatite-iron ore deposits. *Ore Geology Reviews 78*, 447–492.

Martyn, D., 1984: Airborne electromagnetic survey. Nämnden för statens gruvegendom. Jokkmokk area, northern Sweden. *Sveriges geologiska undersökning MINK 98066*, 21 pp.

Melezhik, V.A. & Fallick, A.E., 2010: On the Lomagundi-Jatuli carbon isotopic event: The evidence from the Kalix Greenstone Belt, Sweden. *Precambrian Research 179,* 165–190.

Mellqvist, C., 1999: Proterozoic Crustal Growth along the Archaean Continental Margin in the Luleå and Jokkmokk Areas, Northern Sweden. *Doctoral thesis 1999:24*, Luleå University of Technology, Sweden, 15 pp.

Mellqvist, C. & Aaro, S., 2006a: Bedrock map 25I Stensund NV, scale 1:50 000. *Sveriges geologiska undersökning K 51.*

Mellqvist, C. & Aaro, S., 2006b: Bedrock map 25I Stensund SV, scale 1:50 000. *Sveriges geologiska undersökning K 53.*

Mellqvist, C., Öhlander, B. & Skiöld, T., 1999a: Traces of Archaean crust in the Jokkmokk area, northern Sweden: a way of defining the Archaean-Proterozoic boundary. *In* C. Mellqvist: Proterozoic crustal growth along the Archaean continental margin in the Luleå and Jokkmokk areas, northern Sweden. *Doctoral thesis 1999:24*, Luleå University of Technology, Sweden, 1–24.

Mellqvist, C., Öhlander, B., Skiöld, T. & Wikström, A., 1999b: The Archaean–Proterozoic Palaeoboundary in the Luleå area, northern Sweden: field and isotope geochemical evidence for a sharp terrane boundary. *Precambrian Research 96*, 225–243.

Mellqvist, C., Öhlander, B., Weihed, P. & Schöberg, H., 2003: Some aspects on the subdivision of the Haparanda and Jörn intrusive suites in northern Sweden. *GFF 125*, 77–85.

Meschede, M., 1986: A method of discriminating between different types of mid-ocean ridge basalts and continental tholeiites with the Nb-Zr-Y diagram. *Chemical Geology 56*, 207–218

Middlemost, E.A.K., 1985: *Magmas and magmatic rocks: an introduction to igneous petrology*. Longman, London, 266 pp.

Morris, G. A. & Hellström, F., 2016: U-Pb zircon age of a Lina suite granite at the Archean-Proterozoic palaeoboundary south of Jokkmokk, northern Sweden. *SGU-rapport 2016:01*, Sveriges geologiska undersökning, 12 pp.

Morris, G.A., Hellström, F. & Kathol, B., 2015: U-Pb zircon age of an Arvidsjaur group rhyolite at Makkavare in the Arjeplog area, northern Sweden. *SGU-rapport 2015:17*, Sveriges geologiska undersökning, 14 pp.

Müllern, C.F., 1967: Slutrapport över 1966 års arbeten på kalkstråket vid Norvijaur. *Sveriges geologiska undersökning MINK 98064*, 9 pp.

Nabelek, P.I., Whittington, A.G. & Sirbescu, M.-L.C., 2010: The role of H2O in rapid emplacement and crystallization of granite pegmatites: resolving the paradox of large crystals in highly undercooled melts. *Contributions to Mineralogy and Petrology 160*, 313–325.

Nichols, G.T., Berry, R.F. & Green, D.H., 1992: Internally consistent gahnitic spinel-cordierite-garnet equilibria in the FMASHZn system: geothermobarometry and applications. *Contributions to Mineralogy and Petrology 111,* 362–377.

Nicolson, D., 1993: The paleoenvironmental setting and Au genesis of the early Proterozoic Holmtjärn volcanogenic massive sulphide deposit, Skellefte district, northern Sweden. Ph.D. thesis. University of Wales, College of Cardiff.

Nironen, M., 1997: The Svecofennian Orogen: a tectonic model. *Precambrian Research 86*, 21–44.

Nylund, B. & Nisca, D., 1981: Regionala tyngdkraftsmätningar och flygmagnetisk tolkning över Jokkmokks kommun. *Sveriges geologiska undersökning BRAP 81420*, 32 pp.

Nysten, P., Persson, S. & Triumf, C.-A., 2014: Berggrundsgeologisk undersökning 27I Tjåmotis NV och NO. *SGU-rapport 2014:11*, Sveriges geologiska undersökning, 30 p.

Nysten, P., Persson, S. & Triumf, C.-A., 2015: Barentsprojektet 2014. Berggrundsgeologisk undersökning 27H Kvikkjokk NO och SO, 27I Tjåmotis NV och NO samt 27J Porjus NV och NO. *SGU-rapport 2015:22*, Sveriges geologiska undersökning, 33 pp.

Nysten, P., Persson, P-O., Hellström, F. & Morris, G., in press: Age of the rhyolite hosting the Ultevis Mn-Fe-Ba-As mineralisation, northern Sweden. *SGU-rapport,* Sveriges geologiska undersökning.

Nysten, P., Persson, S., Triumf, C.-A., Persson, P.O., Hellström, F. & Morris, G., 2018: U-Pb zircon dating of granodiorite from the Muddus structure, northern Sweden. *SGU-rapport 2018:04*, Sveriges geologiska undersökning, 13 pp.

Ödman, O.H., 1942: Rapport över provtagning av molybdenmalmen i Druggegruvan vid Klubbudden i Jokkmokks socken. *Sveriges geologiska undersökning BRAP 00655*, 2 pp.

Ödman, O.H., 1943: Geology of the copper deposit at Laver, N. Sweden. *Sveriges geologiska undersökning C 452*, 1–35.

Ödman, O.H., 1947: Manganese mineralization in the Ultevis district, Jokkmokk, north Sweden. Part 1: Geology. *Sveriges geologiska undersökning C 487*, 1–90.

Ödman, O.H., 1957: Beskrivning till berggrundskarta över urberget i Norrbottens län. *Sveriges geologiska undersökning Ca 41*, 151 pp.

Ödman, O.H., Härme, M., Mikkola, A. & Simonen, A., 1949: Den svensk-finska geologiska exkursionen i Tornedalen sommaren 1948. *Geologiska Föreningens i Stockholm Förhandlingar 71*, 113–120.

Offerberg, J., 1967. Beskrivning till berggrundskartbladen Kiruna NV, NO, SV, SO. *Sveriges geologiska undersökning Af 1–4*, 146 pp. (English summary).

Öhlander, B., 1986: Proterozoic mineralizations associated with granitoids in northern Sweden. *Sveriges geologiska undersökning Ca 65*, 39 pp.

Öhlander, B. & Billström, K., 1989: Regional implications of U-Pb zircon dating of two Proterozoic granites associated with molybdenite mineralized aplites in northern Sweden. *Geologiska Föreningens i Stockholm Förhandlingar 111*, 229–238.

Öhlander, B. & Nisca, D.H., 1985: Tectonic control of Precambrian molybdenite mineralization in northern Sweden. *Economic Geology 80*, 505–512.

Öhlander, B. & Skiöld, T., 1994. Diversity of 1.8 Ga potassic granitoids along the edge of the Archaean craton in northern Scandinavia: a result of melt formation at various depths and from various sources. *Lithos 33*, 265–283.

Öhlander, B., Hamilton, P.J., Fallick, A.E. & Wilson, M.R., 1987a: Crustal Reactivation in northern Sweden: the Vettasjärvi Granite. *Precambrian Research 35*, 277–293.

Öhlander, B., Skiöld, T., Hamilton, P.J. & Claesson, L.-Å., 1987b: The western border of the Archaean province of the Baltic Shield: evidence from northern Sweden. *Contributions to Mineralogy and Petrology 95*, 437–450.

Öhlander, B., Lager, I., Loberg, B.E.H. & Schöberg, H., 1992: Stratigraphical position of Lower Proterozoic carbonate rocks from the Kalix Greenstone Belt, northern Sweden. *Geologiska Föreningens i Stockholm Förhandlingar 114*, 317–322.

Öhlander, B., Skiöld, T., Elming, S. Å., Claesson, S. & Nisca, D. H., 1993: Delineation and character of the Archaean-Proterozoic boundary in northern Sweden. *Precambrian Research 64*, 67–84.

Öhlander, B., Mellqvist, C. & Skiöld, T., 1999: Sm-Nd isotope evidence of a collisional event in the Precambrian of northern Sweden. *Precambrian Research 93*, 105–117.

Olesen, O. & Sandstad, J.S., 1993: Interpretation of the Proterozoic Kautokeino Greenstone Belt, Finnmark, Norway from combined geophysical and geological data. *Norges geologiske undersøkelse Bulletin 425*, 41–62.

Padget, P., 1966: The geology and mineralization of the Radnejaure area, Norrbotten County, Sweden. *Sveriges geologiska undersökning C 609*, 1–60.

Padget, P., 1971: Lulepottenmalmen. Rapport över SGUs undersökningar 1960–1971. *Sveriges geologiska undersökning Mink 96259*, 6 pp.

Patison, N.L, Korja, A., Lahtinen, R., Ojala, V.J. & the FIRE Working Group 2006: FIRE seismic reflection profiles 4, 4A and 4B: Insights into the Crustal Structure of Northern Finland from Ranua to Näätämö. *Geological Survey of Finland, Special Paper 43*, 161–222.

Pearce, J. A., 1982: Trace element characteristics of lavas from destructive plate boundaries. *In* R. S. Thorpe (ed.) Andesites: Orogenic Andesites and Related Rocks. John Wiley & Sons, Chichester, 525–548.

Pearce, J. A., 1983: Role of sub-continental lithosphere in magma genesis at active continental margins. Continental Basalts and Mantle Xenoliths. Shiva, Nantwich, 230–249

Pearce, J. A., 1996: A User's Guide to Basalt Discrimination Diagrams. *In* Wyman, D. A. (ed.) Trace Element Geochemistry of Volcanic Rocks: Applications for Massive Sulphide Exploration. *Geological Association of Canada, Short Course Notes 12*, 79–113

Perdahl, J.-A. & Einarsson, Ö., 1994: The marine-continental transition of the Early Proterozoic Skellefte-Arvidsjaur volcanic arc in the Bure area, northern Sweden. *GFF 116*, 133–138.

Perdahl, J.-A. & Frietsch, R., 1993: Petrochemical and petrological characteristics of 1.9 Ga old volcanics in northern Sweden. *Precambrian Research 64*, 239–252.

Persson, G., 1975: Luspevaratj sulfidmineralisering - rapport rörande SGU:s undersökningar under åren 1971–1974. *Sveriges geologiska undersökning BRAP 00629*, 18 pp.

Perttunen, V., 1985: On the Proterozoic stratigraphy and exogenic evolution of the Peräpohja area, Finland. *In* Proterozoic exogenic processes and related metallogeny: proceedings of the symposium held in Oulu, Finland, August 15–16, 1983. *Geological Survey of Finland Bulletin 331*. Espoo: Geologian tutkimuskeskus, 131–141.

Perttunen, V. & Hanski, E., 2003: Geological map of Finland 1:100 000. Explanation to the maps of Pre-quaternary rocks. Sheets 2631 Törmäsjärvi and 2633 Koivu, 88 pp.

Perttunen, V. & Vaasjoki, M., 2001: U-Pb geochronology of the Peräpohja Schist Belt, northwestern Finland. *In* M. Vaasjoki (ed.): Radiometric age determinations from Finnish Lapland and their bearing on the timing of Precambrian volcano-sedimentary sequences. *Geological Survey of Finland Special Paper 33,* 45–84.

Perttunen, V., Hanski, E. & Väänänen, J., 1995: Stratigraphical map of the Peräpohja Schist Belt, northern Finland. The 22nd Nordic Geological Winter Meeting 8–11 January 1996 in Turku – Åbo, Finland: abstracts of oral and poster presentations. Turun yliopisto/*Åbo Akademi,* Turku/Åbo 152.

Pettersen, K., 1878: Det nordlige Sveriges og Norges Geologi. *Archiv for Mathematik og Naturvidenskab 3*, 1–38.

Pettijohn, F.J., Potter, P.E. & Siever, R., 1972: *Sand and sandstone*. New York, Springer-Verlag, 618 pp.

Phillips, A. 2005: Continental Precious Minerals Inc.: Results of NI 43-101 Geological Report. 29th of July 2005. Accessed from <http://www.marketwired.com/press-release/continental-precious-minerals-inc-results-of-ni-43-101-geological-report-nex-board-czq.h-550222.htm> 26 October 2016.

Philpotts, J.A., Taylor, C.D., Tatsumoto, M. & Belkin, H.E., 1998: Petrogenesis of late-stage granites and Y-REE-Zr-Nb-enriched vein dikes of the Bokan Mountain stock, Prince of Wales Island, southeastern Alaska. *Open-File Report 98-459*, U.S. Geological Survey, 71 pp.

Pirajno, F., 2009: Hydrothermal Processes and Mineral Systems. *Springer,* 1250 pp.

Pollard, P.J., Taylor, R.G., Taylor, R.P. & Groves, D.I., 1991: Petrographic and geochemical evolution of pervasively altered Bushveld granites at the Zaaiplaats tin mine. *Economic Geology 86,* 1401–1433.

Rasilainen, K., Eilu, P., Halkoaho, T., Karinen, T., Konnunaho, J., Kontinen A. & Törmänen, T., 2016: Quantitative assessment of undiscovered resources in stratiform and podiform chromite deposits in Finland. *Geological Survey of Finland, Report of Investigation 226,* 186 pp.

Rehnström, E.F., 2003: Geochronology and petrology of the Tielma Magmatic Complex, northern Swedish Caledonides–results and tectonic implications. *Norwegian Journal of Geology 83*, 243–257.

Romer, R.L. & Smeds, S.-A., 1994: Implications of U-Pb ages of columbite-tantalites from granitic pegmatites for the Palaeoproterozoic accretion of 1.90–1.85 Ga magmatic arcs to the Baltic Shield. *Precambrian research 67*, 141–158.

Romer, R.L. & Wright, J.E., 1992: U-Pb dating of columbites: A geochronologic tool to date magmatism and ore deposits. *Geochimica et Cosmochimica Acta 56*, 2137–2142.

Rösholt, B., 1985a: Tallberget kobber- gull-mineraliseringer. *Sveriges geologiska undersökning MINK 96069*, 6 pp.

Rösholt, B., 1985b: Tjäula mineralization, Tjåmotis. *Sveriges geologiska undersöknig MINK 96123*, 34 pp.

Sadeghi, M. & Hellström, F., 2015: U-Pb zircon ages of ignimbrites and porphyritic metarhyolites in the Boden area, northern Sweden. *SGU-rapport 2015:15*, Sveriges geologiska undersökning, 15 pp.

Sadeghi, M. & Hellström, F., 2018a: Age of migmatisation in the Boden area, northern Sweden. *SGU-rapport 2018:02*, Sveriges geologiska undersökning, 13 pp.

Sadeghi, M. & Hellström, F., 2018b: U-Pb zircon age of an Archean granodioritic gneiss in the Boden area, northern Sweden. *SGU-rapport 2018:03*, Sveriges geologiska undersökning, 12 pp..

Sadeghi, M., Triumf, C.-A., Larsson, D., Kumpulainen, R. & Kathol, B., in press: Beskrivning till berggrundskartorna 25L Boden NV, NO, SV & SO. *Sveriges geologiska undersökning.*

Saintilan, N.J., Schneider, J., Stephens, M.B., Chiaradia, M., Kouzmanov, K., Wälle, M. & Fontboté, L., 2015: A Middle Ordovician Age for the Laisvall Sandstone-Hosted Pb-Zn Deposit, Sweden: A Response to Early Caledonian Orogenic Activity. *Economic Geology 110*, 1779–1801.

Saintilan, N.J., Spangenberg, J.E., Samankassou, E., Kouzmanov, K., Chiaradia, M., Stephens, M.B. & Fontboté, L., 2016: A refined genetic model for the Laisvall and Vassbo Mississippi Valley-type sandstone-hosted deposits, Sweden: constraints from paragenetic studies, organic geochemistry, and S, C, N, and Sr isotope data. *Mineralium Deposita 51*, 639–664.

Sammelin (Kontturi), M., Wanhainen, C. & Martinsson, O., 2011: Gold mineralogy at the Aitik Cu-Au-Ag deposit, Gällivare area, northern Sweden. *GFF 133*, 19–30.

Sandahl, K.-A., 1973: Lulepotten kopparmalmsfyndighet. Rapport rörande resultaten av SGUs undersökning under åren 1960–1971. *Sveriges geologiska undersökning BRAP 00585*, 5 pp.

Sandahl, K.-A., Ek, J. & Isaksson, H., 1981: Projekt Ballek Norra. *Sveriges geologiska undersökning BRAP 81562*, 19 pp.

Sarlus, Z., Bauer, T.E., Andersson, U.B., Wanhainen, C., Martinsson, O., Nordin, R. & Andersson, J., 2016: Age constraints on igneous rocks in the Gällivare area. *In* Z. Sarlus (ed.): Geochemical and geochronological constraints on 1.88 and 1.80 Ga magmatic events in the Gällivare area, northern Sweden. *Licentiate thesis,* Luleå University of Technology, 32 pp.

Seedorff, E., Barton, M.D., Stavast, W.J.A. & Maher, D.J., 2008: Root Zones of Porphyry Systems: Extending the Porphyry Model to Depth. *Economic Geology 103,* 939–956.

Senften, T., 2008: Dokumentation av gruvlämningar i Ruotevare, Jokkmokks kommun. *Länsstyrelsens rapportserie nr 1/2008*. Länsstyrelsen i Norrbottens län, 27 pp.

Seward, T.M., 1973: Thio complexes of gold and the transport of gold in hydrothermal ore solutions. *Geochimica et Cosmochimica Acta 37,* 379–399.

SGU, 2017: Berggrund – databas 1:1 000 000 –. Sgudb-bergdb-bena.

Shaikh, N.A., Kumpulainen, R., Riad, L., Snäll, S., Sundberg, A., Westlund, B. & Wik, N.-G., 1986: Industriella mineral och bergarter i Norrbottens län. *Sveriges geologiska undersökning BRAP 86006*, 128 pp.

Shaikh, N.A., Karis, L., Kumpulainen, R., Sundberg, A. & Wik, N.-G., 1989: Kalksten och dolomit i Sverige. Del 1. Norra Sverige. *Rapporter och meddelanden 54*, Sveriges geologiska undersökning, 380 pp.

Shand, S. J., 1943: *Eruptive rocks, 2nd edition*. John Wiley, New York, 444p.

Silvennoinen, A., Gustavson, M., Perttunen, V., Siedlecka, A., Sjöstrand, T., Stephens, M.B. & Zachrisson, E., 1987: *Geological map, Pre-Quaternary rocks, Northern Fennoscandia. Scale 1:1 000 000.* Geological Surveys of Finland, Norway and Sweden.

Sjöstrand, T., 1981: Kåtaberget, redovisning av grävningsarbeten utförda hösten 1980. *Sveriges geologiska undersökning BRAP 81041*, 7 pp.

Sjöstrand, T., Berndtsson, A. & Nisca, D., 1984: Berggrundsbeskrivning och flygmagnetisk tolkning för Överkalix. *Sveriges Geologiska AB PRAP 84014*, 1–64.

Skiöld, T., 1988: Implications of new U-Pb zircon chronology to early Proterozoic crustal accretion in northern Sweden. *Precambrian Research 38,* 147–164.

Skiöld, T. & Larsson, C., 1978: Age data on Proterozoic granitoids from the Norvijaur area of northern Sweden. *Geologiska Föreningens i Stockholm Förhandlingar 100*, 171–176.

Skiöld, T. & Öhlander, B., 1989: Chronology and geochemistry of late Svecofennian processes in northern Sweden. *Geologiska Föreningens i Stockholm Förhandlingar 11*1, 347–354.

Skiöld, T. & Rutland, R.W.R., 2006: Successive ~1.94 Ga plutonism and ~1.92 Ga deformation and metamorphism south of the Skellefte district, northern Sweden: Substantiation of the marginal basin accretion hypothesis of Svecofennian evolution. *Precambrian Research 148*, 181–204.

Skiöld, T., Öhlander, B., Vocke, R.D. Jr. & Hamilton, P.J., 1988. Chemistry of Proterozoic orogenic processes at a continental margin in northern Sweden. *Chemical Geology 69*, 193–207.

Skiöld, T., Öhlander, B., Markkula, H., Widenfalk, L. & Claesson, L.-Å., 1993: Chronology of Proterozoic orogenic processes at the Archaean continental margin in northern Sweden. *Precambrian Research 64*, 225–238.

Skyttä, P., Bauer, T.E., Tavakoli, S., Hermansson, T., Andersson, J. & Weihed, P., 2012: Pre-1.87 Ga development of crustal domains overprinted by 1.87 Ga transpression in the Palaeoproterozoic Skellefte district, Sweden. *Precambrian Research 206–207,* 109–136.

Smellie, J.A.T., 1982: Preliminary mineralogical investigation of the Skåpiesavon syd mineralisation, N. Norrland. *Sveriges geologiska undersökning BRAP 82006*, 12 pp.

Söderholm, K. & Inkinen, O. 1982: The Tornio layered intrusion – a recently discovered intrusion with chromitite horizons in Northern Finland. *Bulletin of the Geological Society of Finland 54*, 15–24.

Spear, F.S., 1993*: Metamorphic Phase Equilibria and Pressure-Temperature-Time Paths.* Mineralogical Society of America, Washington, D.C., 799 pp.

Stein, H. J., 2006: Low-rhenium molybdenite by metamorphism in northern Sweden: Recognition, genesis, and global implications. *Lithos 87*, 300–327.

Stephens, M.B., Ripa, M., Lundström, I., Persson, L., Bergman, T., Ahl, M., Wahlgren, C.-H., Persson, P.-O. & Wickström, L., 2009: Synthesis of the bedrock geology in the Bergslagen region, Fennoscandian Shield, south-central Sweden. *Sveriges geologiska undersökning Ba 58*, 259 pp.

Strömberg, A., 1955: Zum Gebirgsbau der Skanden im mittleren Härjedalen. *Bulletin of the Geological Institutions of the University of Uppsala 35*, 199–243.

Strömberg, A., 1961: On the tectonics of the Caledonides in the southwestern part of the county of Jämtland, Sweden. *Bulletin of the Geological Institutions of the University of Uppsala 39,* 92 pp.

Sun, S.S. & McDonough, W.F., 1989: Chemical and isotopic systematics of oceanic basalts: implications for mantle composition and processes. *In* A.D. Saunders & M.J. Norry (eds.): Magmatism in the ocean basins. *Geological Society, Special Publication 42*, 313–345.

Sundbergh, S., 1979: Uranmineraliseringen vid Manak. *Sveriges geologiska undersökning BRAP 79051*, 16 pp.

Sundius, N., 1952: Kvarts, fältspat och glimmer samt förekomster därav i Sverige. *Sveriges geologiska undersökning C 520*, 1–231.

Svenonius, F., 1915: Norrbottens läns kalkstensförekomster från praktisk och särskilt agrikulturell synpunkt. *Sveriges geologiska undersökning C 269*, 1–71.

Svensson, S., Troëng, B., Forsberg, L.-O., Kullman, F., Gustafsson, B., Laurikko, J & Gerlach, R., 1981: Uranium prospecting in Norrland interim report Nov. 1981. *Sveriges geologiska undersökning BRAP 81083*, 28 pp.

Talbot, C.J., 2001: Weak zones in Precambrian Sweden. *Geological Society, London, Special Publications 186,* 287–304.

Talbot, C., Munier, R. & Riad, L., 1989: Reactivations of Proterozoic shear zones. In G. Bäckblom & R. Stanfors (eds.): Interdisciplinary study of post-glacial faulting in the Lansjärv area Northern Sweden 1986–1988. *SKB Technical Report 89–31*, 17 pp.

Talga 2016: Raitajärvi. Accessed from <http://www.talgaresources.com/irm/content/raitaj-rvi.aspx?RID=286> 20 October 2016.

Thelander, T., 1982: The Torneträsk Formation of the Dividal Group, northern Swedish Caledonides. *Sveriges geologiska undersökning C 789*, 1–41.

Thelander, T., 2009a: Bedrock map The Caledonides in northern Sweden, scale 1:250 000. Soouthern part. *Sveriges geologiska undersökning K 222:2*.

Thelander, T., 2009b: Beskrivning till berggrundkartan Kaledoniderna i norra Sverige. *Sveriges geologiska undersökning K 222*, 1–51.

Thompson, A.F.B. & Thompson, J.F.H., (eds.) 1996: Atlas of alteration: A field and petrographic guide to hydrothermal alteration minerals. *Geological Association of Canada,* 119 pp.

Thunehed, H., 2000: Mapping and characterisation of Swedish bedrock by DC resistivity and transient-field electromagnetic measurement. *Doctoral Thesis 2000:17*, Luleå University of Technology, 169 pp.

Tollefsen, E., 2014: Thermal and chemical variations in metamorphic rocks in Nautanen, Gällivare, Sweden. Master thesis, University of Stockholm, Stockholm, Sweden. 50 pp.

Vaasjoki, M. & Sakko, M. 1988: The evolution of the Raahe-Ladoga zone in Finland: isotopic constraints. *Geological Survey of Finland Bulletin 343*, 7–32.

Vernon, R.H., 1998: Chemical and volume changes during deformation and prograde metamorphism of sediments. *In* P.J. Treloar & P.J. O'Brien (eds.): What drives metamorphism and metamorphic reactions? *Geological Society of London, Special Publications 138*, 215–246.

Walser, G. & Einarsson, Ö., 1982: The geological context of molybdenum occurrences in the southern Norrbotten region, northern Sweden. *Geologische Rundschau 71*, 213–229.
Wanhainen, C., Billström, K., Martinsson, O., Stein, H. & Nordin, R., 2005: 160 Ma of magmatic/hydrothermal and metamorphic activity in the Gällivare area: Re–Os dating of molybdenite and U-Pb dating of titanite from the Aitik Cu–Au–Ag deposit, northern Sweden. *Mineralium Deposita 40,* 435–447.
Wanhainen, C. Billström, K. & Martinsson, O., 2006: Age, petrology and geochemistry of the porphyritic Aitik intrusion, and its relation to the disseminated Aitik Cu-Au-Ag deposit, northern Sweden. *GFF 128*, 273–286.
Wanke, A. & Melezhik, V.A., 2005: Sedimentary and volcanic facies recording the Neoarchaean continent breakup and decline of the positive $\delta^{13}C_{carb}$ excursion. *Precambrian Research 140*, 1–35.
Ward, P., Härkönen, I., Nurmi, P.A. & Pankka, H.S., 1989: Structural studies in the Lapland greenstone belt, northern Finland and their application to gold mineralization. *Geological Survey of Finland, Special Paper 10*, 71–77.
Wasström, A., 1993: U-Pb zircon dating of a quartz-feldspar porphyritic dyke in the Knaften area; Västerbotten County; northern Sweden. *In* Th. Lundqvist (ed.): *Radiometric dating results 2. Sveriges geologiska undersökning C 828*, 34–40.
Wasström, A., 1996: The Knaften granitoids of Västerbotten County, northern Sweden. *In* Th. Lundqvist (ed.): *Radiometric dating results. Sveriges geologiska undersökning C 823*, 60–64.
Wasström, A., 2005: Petrology of a 1.95 Ga granite-granodiorite-tonalite-trondhjemite complex and associated extrusive rocks in the Knaften area, northern Sweden. *GFF 127*, 67–82.
Webber, K.L., Simmons, W.B., Falster, A.U. & Foord, E.E., 1999: Cooling rates and crystallization dynamics of shallow level pegmatite-aplite dikes, San Diego County, California. *American Mineralogist 84*, 708–717.
Weihed, P., Bergman, J. & Bergström, U., 1992: Metallogeny and tectonic evolution of the early Proterozoic Skellefte District, northern Sweden. *Precambrian Research 58*, 143–167.
Welin, E., 1979: Tabulation of recalculated radiometric ages published 1960–1979 for rocks and minerals in Sweden. *GFF 101*, 309–320.
Welin, E. & Blomqvist, G., 1964: Age measurements on radioactive minerals from Sweden. *GFF 86*, 33–50.
Widenfalk, L., Elming, S.-Å. & Enmark, T., 1985: A multidisiplinary investigation of the Notträsk Gabbro, northern Sweden. *Geologiska Föreningens i Stockholm Förhandlingar 107*, 109–126.
Wikström, A., 1993: Berggrundskartan 25M Kalix SV. *Sveriges geologiska undersökning Ai 81.*
Wikström, A., 1995: Berggrundskartan Kalix NV. *Sveriges geologiska undersökning Ai 79.*
Wikström, A., 1996: Berggrundskartan 25M Kalix NO. *Sveriges geologiska undersökning Ai 80.*
Wikström, A. & Persson, P.-O., 1997a: Two Haparanda type granodiorites with contrasting ages in the southeastern part of Norrbotten County, northern Sweden. *In* Th. Lundqvist (ed.): Radiometric dating results 3. *Sveriges geologiska undersökning C 830*, 73–80.
Wikström, A. & Persson, P.-O., 1997b: U -Pb zircon and monazite dating of a Lina type leucogranite in northern Sweden and its relationship to the Bothnian shear zone. *In* Th. Lundqvist (ed.): Radiometric dating results 3. *Sveriges geologiska undersökning C 830*, 81–87.
Wikström, A. & Söderman, J., 2000. Bedrock map 24L Luleå NO, scale 1:50 000. *Sveriges geologiska undersökning Ai 153.*
Wikström, A., Mellqvist, C. & Persson, P.O., 1996a: An Archaean megaxenolith and a Proterozoic fragment within the Bälinge magmatic breccia, Luleå, northern Sweden. *Sveriges geologiska undersökning C 828*, 48–56.
Wikström, A., Skiöld, T. & Öhlander, B., 1996b: The relationships between 1.88 Ga old magmatism and the Baltic-Bothnian shear zone in northern Sweden. *In* T.S. Brewer (ed.): Precambrian crustal evolution in the north Atlantic region. *Geological Society Special Publication 112*, 249–259.
Wilkinson, J.J., Stoffell, B., Wilkinson, C.C., Jeffries, T.E. & Appold, M.S., 2009: Anomalously metal-rich fluids form hydrothermal ore deposits. *Science 323,* 764–767.
Willdén, M.Y., 1980: Paleoenvironment of the autochthonous sedimentary rock sequence at Laisvall, Swedish Caledonides. *Stockholm Contributions in Geology 23,* 1–100.

Willdén, M., 2004: The Lasivall sandstone-hosted Pb-Zn deposit: Geological overview. *In* R.L. Allen, O. Martinsson & P. Weihed (eds.): Svecofennian Ore-Forming Environments – Volcanic-Associated Zn-Cu-Au-Ag, Intrusion-Associated Cu-Au, Sediment-Hosted Pb-Zn, and Magnetite-Apatite Deposits of Northern Sweden. *Society of Economic Geologists, Guidebook Series Vol. 33*, 115–127.

Wilson, M.R. & Åkerblom, G.V., 1982: Geological setting and geochemistry of uranium rich granites in the Proterozoic of Sweden. *Mineralogical Magazine 46*, 233–245.

Wilson, M.R., Hamilton, P.J., Fallick, A.E., Aftalion, M. & Michard, A., 1985: Granites and early Proterozoic crustal evolution in Sweden: evidence from Sm-Nd, U-Pb and O isotope systematics. *Earth and Planetary Science Letters 72*, 376–388.

Wilson, M.R., Claesson, L.-Å., Sehlstedt, S., Smellie, J.A.T., Aftalion, M., Hamilton, P.J. & Fallick., A.E., 1987: Jörn: An early Proterozoic intrusive complex in a volcanic arc environment, north Sweden. *Precambrian Research 36*, 201–225.

Winterhalter, B., 2000: Sedimentary rocks underlying the Gulf of Bothnia. *In* Th. Lundqvist & S. Autio (eds): Description to the Bedrock Map of Central Fennoscandia (Mid-Norden). *Geological Survey of Finland, Special Paper 28*, 76–79.

Witschard, F., 1970: Descriptions of the geological maps Lainio NV, NO, SV, SO. *Sveriges geologiska undersökning Ai 9–12*, 1–102.

Witschard, F., 1975: Descriptions of the geological maps Fjällåsen NV, NO, SV, SO. *Sveriges geologiska undersökning Ai 17–20*, 1–96.

Witschard, F., 1984: The geological and tectonic evolution of the Precambrian of northern Sweden – a case for basement reactivation? *Precambrian Research 23*, 273–315.

Witschard, F., 1996: Berggrundskartan 28K Gällivare SV 1:50 000. *Sveriges geologiska undersökning Ai 100*.

Witschard, F. & Zachrisson, E., 1995: Berggrundskartan 28I Stora Sjöfallet NO, 1:50 000, *Sveriges geologiska undersökning Ai 90.*

Yardley, B.W.D., 1993: An introduction to metamorphic petrology. *Longman Scientific & Technical, UK,* 248 pp.

Zachrisson, E., 1997: Berggrundskartorna 22F Risbäck, 1:50 000. *Sveriges geologiska undersökning Ai 102–105.*

Zachrisson, E., & Witschard, F., 1995a: Berggrundskartan 28I Stora Sjöfallet NV, 1:50 000, *Sveriges geologiska undersökning Ai 88.*

Zachrisson, E., & Witschard, F., 1995b: Berggrundskartan 28I Stora Sjöfallet SV, 1:50 000, *Sveriges geologiska undersökning Ai 89.*

Zezin Yu., D., Migdisov, A.A. & Williams-Jones, A.E., 2007: The solubility of gold in hydrogen sulfide gas: An experimental study. *Geochimica et Cosmochimica Acta 71*, 3070–3081.

MANUSCRIPTS IN PREPARATION

Bergman, T. & Hellström, F. in preparation: Inventory of mineral resources in the north-eastern part of the Norrbotten County, Sweden. *SGU-rapport*. Sveriges geologiska undersökning.

Bergström, U., Bergman, S. & Hellström, F., in preparation-a: Age of diatexites, Tallberg area. *SGU-rapport*. Sveriges geologiska undersökning.

Bergström, U., Bergman, S. & Hellström, F., in preparation-b: Age of volcanic intercalations in the Råneå Group. *SGU-rapport*. Sveriges geologiska undersökning.

Claeson, D., Antal Lundin, I. & Hellström., in preparation: Rhyolite to trachyte west of Lagmansgraven, 26J Jokkmokk NV. *SGU-rapport*. Sveriges geologiska undersökning.

Hellström, F., in preparation-a: Age of the rhyolitic host rock to the Skuppesavon uranium mineralisation in the Arjeplog area, Northern Sweden. *SGU-rapport.* Sveriges geologiska undersökning.

Hellström, F., in preparation-b: U-Pb SIMS zircon age of migmatisation in the Arjeplog area, northern Sweden. *SGU-rapport.* Sveriges geologiska undersökning.

Hellström, F., in preparation-c: U-Pb age of a quartz-feldspar porphyric rhyolite in the Arjeplog area, Northern Sweden. *SGU-rapport*. Sveriges geologiska undersökning.

Kathol, B., Triumf, C.-A., Larsson, D. & Jönberger, J., in prep: Beskrivning till berggrundskartorna 26H Jäkkvik NO, SV & SO. Sveriges geologiska undersökning.

Geological Survey of Sweden
Box 670
SE-751 28 Uppsala
Phone: +46 18 17 90 00
Fax: +46 18 17 92 10
www.sgu.se

Uppsala 2018
ISSN 0349-2176
ISBN 978-91-7403-410-3
Tryck: Elanders Sverige AB